2014-ENAM-0018

École doctorale n° 432 : Sciences des Métiers de l'Ingénieur

Doctorat ParisTech

T H È S E

pour obtenir le grade de docteur délivré par

l'École Nationale Supérieure d'Arts et Métiers

Spécialité " Automatique et Traitement du Signal "

présentée et soutenue publiquement par

Benjamin LAMOUREUX

le 30 juin 2014

Development of an Integrated Approach for PHM - Prognostics and Health Management - : Application to a Turbofan Fuel System

Directeur de thèse : **Philippe LORONG**
Co-encadrement de la thèse : **Nazih MECHBAL**

Jury

M. Albert BENVENISTE, Directeur de recherche, INRIA	Président
M. Christophe BERENGUER, Professeur des Universités, GIPSA Lab Grenoble	Rapporteur
M. Emanuele BORGONOVO, Professeur des Universités, Bocconi University	Rapporteur
M. Michael AZARIAN, Chercheur, CALCE, University of Maryland	Examinateur
M. Jean-Rémi MASSE, Expert Sénior, SAFRAN Snecma	Examinateur
M. Philippe LORONG, Professeur des Universités, PIMM, Arts et Métiers ParisTech	Examinateur
M. Nazih MECHBAL, Maître de conférences, PIMM, Arts et Métiers ParisTech	Examinateur
M. Thierry SCHMITT, Chef de Département, SAFRAN Snecma	Invité

T H È S E

Arts et Métiers ParisTech - Centre de Paris
PIMM - Procédés et Ingénierie en Mécanique et Matériaux

"Physics has more imagination than engineers".

Dr. Jean-Rémi Massé

Acknowledgement

First of all, I would like to thank SAFRAN Snecma for having supported this PhD thesis. In particular, I would like to express my gratitude to Jean-Rémi Massé, my industrial supervisor, for having proposed the subject and getting involved in the main decisions of the development of this very interesting thesis work. I also express my acknowledgment to Thierry Schmitt for having accepted the inviation as a Snecma representative during my defense.

I would also like to thank my supervisors from the PIMM laboratory, Philippe Lorong and Nazih Mechbal for their valuable comments on my presentations and publications and global involvment in my work. Beyond they supervisor role, they were colleagues with whom it was very pleasant and interesting to learn and share.

I would like to express my most sincere thanks to the other members of the jury, Albert Benveniste, Research Director at INRIA and president of the jury, Christophe Bérenguer, Professor at GIPSA Lab, Emanuele Borgonovo, Professor at Bocconi University and Michael Azarian, researcher at the university of Maryland for having agreed to read and comment my work because believe me, I am in the best position to know that reading what follows is not easy.

I would also like to send my regards to the other PhD students and researchers I had the chance to meet within the PIMM laboratory or in other conferences and with whom we could discuss scientific topics that have allowed me to advance in my work and most importantly to meet wonderful people.

My acknowledgment goes also to my former coworkers, in particular Guilhem, Xavier and François, former members of the “PHM dreamteam” for the precious time they have given me at the beginning. I also thank the all the people I had the chance to rub shoulders with in the famous site Villaroche. It would be too long to thank everyone independently, so I'll assume that if you are reading these lines, it means that you're part of the lot. I finally thank the Snecma basketball team because even in the defeat, it was always a pleasure to spend time with you, and all the urban soccer players for having accepted me despite my technical deficiencies.

For all my friends from different groups, thank you for having been able to distract me from my work when needed. I think especially to my longtime friends from school in Cholet, namely Khien, Paul, JD, Fred, Etienne and Matthias, my friends from Clémenceau and the “Terrasses”, in particular Kevin, Raph, Alain, Flo, Seb and Sarah and the group from Nice with the V and the twins.

Last but not least, I would like to thank my familly for all the emotional support they have given me during the past three years. To all the people part of my large familly, I have nothing else to say I am proud to have you by my side. To Romain (yes, I consider you part of the familly), thank you for those nice years spent together in our perch at Gare du Nord. To my parents, thank you for a countless number of things, and I know I do not tell you often enough. To my sisters, thank you for being so great, each in your style. Eventually, to the one who shares my life, Anne-Lise, I would like to say thank you for having managed to hold with a PhD student boyfriend for so long. In the end, you have your own doctor. It was worth the wait, wasn’t it?

TABLE OF CONTENTS

List of Figures **11**
List of Tables **15**
Author's Publications **1**
Acronyms and abbreviations **3**
Notations **7**

Résumé étendu en français

Introduction **11**
Chapitre 1: développement intégré du PHM **14**
Terminologie pour le PHM des moteurs d'avions *15*
Environnement et cadre fonctionnel du PHM *17*
Développement intégré du PHM *20*
Chapitre 2: développement des IS en phases de conception **22**
Selection des IS *23*
Normalisation des IS *25*
Validation des IS *30*
Chapitre 3: Krigeage pour la propagation des incertitudes **34**
Introduction générale au Krigeage *34*
Présentation du Krigeage SVR *37*
Validation et amélioration du Krigeage SVR *41*
Chapitre 4: application au système carburant d'un moteur d'avions **44**
Présentation du système carburant *44*
Sélection des indicateurs de santé et de service conforme *46*
Construction du modèle de Krigeage SVR *51*
Normalisation des IS *52*
Validation des IS *53*
Conclusion **54**

Complete document in english

General Introduction **57**

Chapter 1: Integrated development of prognostics and health management for aircraft engines

1.1 Introduction **68**
1.2 Proposed terminology for PHM of aircraft engines **69**
1.2.1 *Taxonomy of threats* *69*
1.2.2 *Extraction means* *73*
1.2.3 *Processing means* *76*
1.2.4 *Scheduling means* *78*
1.2.5 *The proposed global MRO strategy* *79*
1.3 Proposed scope and functions of PHM for aircraft engines **80**
1.3.1 *The scope of PHM systems for aircraft engines* *80*
1.3.2 *Architecture of a PHM system* *81*
1.3.3 *Architecture of the host system* *83*
1.3.4 *Architecture of the health monitoring system* *85*
1.3.5 *Architecture of the engine monitoring unit* *85*
1.3.6 *Architecture of the processing unit* *86*
1.4 Integrated Development of PHM **91**
1.4.1 *Current PHM systems development methodology* *91*
1.4.2 *Weaknesses of current PHM system development* *94*

1.4.3 The IDPHM methodology ... 94
1.5 Conclusion ... 97

Chapter 2: Development of the embedded extraction tasks during the design stages of aircraft engines

2.1 Introduction ... 100
2.2 Modeling and selection of HIs ... 102
2.2.1 Modeling formalism and representation ... 102
2.2.2 Uncertainties Management ... 107
2.2.3 Modeling implementation ... 108
2.2.4 Selection of HIs ... 108
2.3 Standardization of HIs ... 111
2.3.1 Sensitivity analysis ... 111
2.3.2 Support Vector Regression ... 119
2.3.3 SA and SVR for the standardization of HIs ... 122
2.4 Virtual implementation and validation of HIs ... 124
2.4.1 Definition of numerical key performance indicators ... 124
2.4.2 Virtual implementation ... 133
2.4.3 Validation of HIs ... 137
2.5 Conclusion ... 138

Chapter 3: Construction and use of Kriging models for the propagation of uncertainties

3.1 Introduction ... 142
3.2 The construction of Kriging models ... 144
3.2.1 General considerations about surrogate modeling construction ... 144
3.2.2 Latin hypercube sampling ... 146
3.2.3 Kriging ... 14650
3.3 SVR-Kriging approach ... 154
3.3.1 Description of the method ... 154
3.3.2 Presentation of the test models ... 155
3.3.3 Performance Metrics ... 157
3.3.4 Assessment of SVR-Kriging performances ... 159
3.3.5 Proposition of enhancements for the θ optimization algorithm ... 163
3.4 Validation of SVR-Kriging ... 164
3.4.1 Introduction to sequential learning ... 164
3.4.2 Proposition of a new selection criterion ... 166
3.4.3 Validation of sequential learning on test models ... 169
3.4.4 Final numerical experiments plan ... 170
3.4.5 Computational issues ... 171
3.5 Conclusion ... 173

Chapter 4: Application to the development of a PHM solution for a generic aircraft engine fuel system

4.1 Introduction ... 176
4.2 Introduction to aircraft engines fuel systems ... 177
4.2.1 Introduction to aircraft engines ... 177
4.2.2 The fuel system ... 178
4.2.3 Level 2 subsystems of the fuel system ... 181
4.2.4 Level 1 subsystems of the fuel system ... 185
4.3 Selection of HIs and CSIs ... 191
4.3.1 Level 2 subsystems of the fuel system ... 191
4.3.2 Level 1 subsystems of the fuel system ... 195
4.3.3 Level 0: fuel system ... 202
4.3.4 Parameters ... 203
4.4 Construction and validation of the surrogate model ... 206
4.4.1 Designs of experiments ... 206
4.4.2 SVR-Kriging modeling and validation ... 206
4.5 Standardization of HIs ... 209
4.5.1 Computation of Sobol indices ... 209
4.5.2 Examples of standardization effects ... 209

4.6 Validation of HIs 210
4.6.1 Specifications 210
4.6.2 NKPIs of real HIs for fleet models 211
4.6.3 NKPIs of standardized HIs for fleet models 213
4.6.4 NKPIs of real HIs for individual models 213
4.6.5 NKPIs of virtual HIs 213
4.7 Conclusion 214
General Conclusion 217

Appendices

Appendix I. Line replaceable units association matrix 234
Appendix II. active channel selection 235
Appendix III. Computation of selected measures 236
Appendix IV. PID controllers for closed-loops 237
Appendix V. Actuation faults detection 238
Appendix VI. Targeted compliant service threats for the fuel metering valve loop 239
Appendix VII. Targeted ompliant service threats for the fuel metering unit 240
Appendix VIII. Compliant service threats for the main fuel pump 241
Appendix IX. Compliant service threats for the main fuel filter 242
Appendix X. Compliant service threats for the variable stator vane 243
Appendix XI. Compliant service threats for the variable stator vane 244
Appendix XII. Compliant service threats for the flowmeter 245
Appendix XIII. Complete list of parameters 246
Appendix XIV. Complete list of degradation modes 248
Appendix XV. Complete list of health indicators 250
Appendix XVI. Complete list of compliant service indicators. 253
Appendix XVII. Initial uncertainties quantification 254
Appendix XVIII. Complete results of the Morris method 255
Appendix XIX. List of potential cause degradation modes 257
Appendix XX. List of degradation modes and associated median limit values. 258
Appendix XXI. Performance metrics for the SVR models of HIs and CSIs 261
Appendix XXII. Performance metrics for the first set of SVR-Kriging models 262
Appendix XXIII. Performance metrics for the second set of SVR-Kriging models 263
Appendix XXIV. Detection NKPIs for the fleet models with real HIs 264
Appendix XXV. Identification NKPIs for the raw set of HIs 268
Appendix XXVI. Localization NKPIs for the raw set of HIs 269
Appendix XXVII. Prognostics NKPIs for the raw set of HIs 270
Appendix XXVIII. List of Sobol indices of order 1 271
Appendix XXIX. List of total Sobol indices 277
Appendix XXX. Detection NKPIs for standardized HIs 283
Appendix XXXI. Identification NKPIs standardized HIs 287
Appendix XXXII. Localization NKPIs for standardized HIs 288
Appendix XXXIII. Prognostics NKPIs for the standardized HIs 289
Appendix XXXIV. Detection NKPIs for individual models 290
Appendix XXXV. Identification NKPIs for individual models 294
Appendix XXXVI. Localization NKPIs for individual models 295
Appendix XXXVII. Prognostics NKPIs for individual models 296
Appendix XXXVIII. Detection NKPIs for virtual HIs 297
Appendix XXXIX. Identification NKPIs for virtual HIs 301
Appendix XL. Localization NKPIs for virtual HIs 302
Appendix XLI. Prognostics NKPIs for virtual HIs 303

List of Figures

Figure R.1 Classification des modes de dégradation et environnement du PHM. 16
Figure R.2 Etape du processus OAS-CBM et définitions de health monitoring et supervision. 18
Figure R.3 Représentations fonctionnelle hiérarchique (à gauche) et structurelle hiérarchique (à droite). 18
Figure R.4 Architecture d'un agent de health monitoring. 19
Figure R.5 Cycles de développement actuels des systèmes hôte et de PHM. 21
Figure R.6 Cycles de développement futurs des systèmes hôte et de PHM. 22
Figure R.7 Modèle en V de la partie embarquée seule. 23
Figure R.8 Schéma du modèle déterministe $\mathcal{M}$ avec extraction des IS et ISC. 24
Figure R.9 Schéma du modèle déterministe à entrées temporelle constantes $\mathcal{MU}$. 24
Figure R.10 Estimation SVR pour un cas non-linéaire. 29
Figure R.11 Point de conformité (compliance point) et courbe COR pour un cas de non-conformité (gauche) et un cas de conformité (droite). 31
Figure R.12 Schéma de principe de la validation des IS. 34
Figure R.13 Méthodologie pour la construction d'un métamodèle. 35
Figure R.14 Proposed classification of Kriging techniques. 37
Figure R.15 Procédure pour la construction d'un modèle de Krigeage SVR. 38
Figure R.16 Fonctions analytiques test : SISO (en haut à gauche), DISO (en haut à droite) et Ishigami. 39
Figure R.17 Schéma de l'apprentissage séquentiel proposé. 42
Figure R.18 Schéma global du plan d'expériences numérique. 43
Figure R.19 Réprésentation fonctionnelle du système carburant. 45
Figure R.20 Schéma du système carburant avec ses URL. 46
Figure R.21 Représentation structurelle hiérarchique du système carburant. 46
Figure R.22 Extraction des courbes brute et lissées de gain en vitesse pour la FMV. 47
Figure R.23 Indicateurs de santé pour la boucle FMV. 47
Figure R.24 Indicateurs de santé pour la SOV. 48
Figure R.25 Extraction des courbes brute et lissées de gain en vitesse pour la VSV. 49
Figure R.26 Indicateurs de santé pour la boucle VSV. 49
Figure R.27 Extraction des courbes brute et lissées de gain en vitesse pour la VBV. 49
Figure R.28 Indicateurs de santé pour la boucle VSV. 50
Figure R.29 Distribution de l'IS $\boldsymbol{FmvHyst0A}$ pour le MD $\boldsymbol{DEFmvStic_Pos}$. 52
Figure i.1 PHM enhanced dependability management strategy. 60
Figure i.2 Different levels of representativeness. 63
Figure 1.1 Guiding thread hydraulic system for the illustration of definitions. 71
Figure 1.2 Example of a precursors' evolution for DEM $\boldsymbol{c}$ from healthy state to $\boldsymbol{1\text{-}PRc}$. 76
Figure 1.3 The big picture of MRO management in aircraft engines. 80
Figure 1.4 Classification of CST with highlight on the PHM scope. 80
Figure 1.5 Classification of degradation modes with highlight on the PHM scope. 81
Figure 1.6 The OSA-CBM process. 82
Figure 1.7 Classification of the OSA-CBM steps. 82
Figure 1.8 Supervised system architecture. 83
Figure 1.9 Typical functional breakdown representation of a complex system. 84
Figure 1.10 Typical structural breakdown representation of a complex system. 84
Figure 1.11 Structuration of the health monitoring system. 85
Figure 1.12 Functional architecture of the EMU. 86
Figure 1.13 Classes of architecture for the processing unit: rectangles are HM agents and circles are equipments. 86
Figure 1.14 Hierarchical agent-based architecture for the processing unit. 87
Figure 1.15 Structure of a HM agent. 88
Figure 1.16 Binary classification performances indicators. 88
Figure 1.17 V-model for the host system's development. 91
Figure 1.18 Current V-model for the PHM system's development. 92

Figure 1.19 Current interactions between the host system V-model and the PHM system V-model. 93
Figure 1.20 The V2-model for the development of PHM systems. 95
Figure 1.21 The V3-model for the development of PHM systems. 95
Figure 1.22 Future interactions between the host system V-model and the PHM system V3-model. 96
Figure 2.1 Standalone V-model of the EMU development process. 100
Figure 2.2 Classification of parameters. 103
Figure 2.3 Scheme of the numerical model interfaces. 104
Figure 2.4 Scheme of the deterministic model $\boldsymbol{\mathcal{M}}$ with extraction of HIs and CSIs. 105
Figure 2.5 Scheme of the constant temporal inputs model $\boldsymbol{\mathcal{MU}}$. 106
Figure 2.6 Low dimension representation of the modeling formalism for the detection issue. 106
Figure 2.7 Low dimension representation of the modeling formalism for the identification issue. 107
Figure 2.8 Matlab-AMESim cosimulation scheme. 108
Figure 2.9 Graph of the HIs selection process. 109
Figure 2.10 Example of Morris method graphical representation. 114
Figure 2.11 Sensitivity analysis for uncertainties management. 118
Figure 2.12 SVR estimation for a linear case accounting for slack variables. 120
Figure 2.13 SVR estimation for a nonlinear case accounting for slack variables. 121
Figure 2.14 Construction of the SVR standardization model. 123
Figure 2.15 Example of ROC curve (right) drawn from two distributions defined by their histograms (top-left) and empirical density functions (bottom-left). 125
Figure 2.16 Compliance Point and ROC curve for non-compliant HI (left) and compliant HI (right). 126
Figure 2.17 Detection margin and minimal detectable intensity. 131
Figure 2.18 Schematic overview of the NKPIs and criteria for the validation of HIs. 133
Figure 2.19 Global scheme of the uncertainty propagation methodology. 136
Figure 2.20 Graph of the HIs validation process. 138
Figure 3.1 Computation time costs of the total uncertainty propagation. 143
Figure 3.2 Principle steps of a surrogate model construction. 145
Figure 3.3 Graphical representation of a LH(10,2) 147
Figure 3.4 Graphical representation of a high discrepancy LH(10,2) 147
Figure 3.5 Transformation of a LH into a LHSDOE 148
Figure 3.6 Influence of hyperparameters values on the shape of the exponential-Gaussian function. 150
Figure 3.7 Non exhaustive classification of Kriging methods. 151
Figure 3.8 Kriging estimations for the regression part (top left) alone, a complete Kriging model with high (top right) and low(bottom) values of $\boldsymbol{\theta}$. 153
Figure 3.9 The global methodology to build SVR-Kriging models. 155
Figure 3.10 SISO analytical test function. 156
Figure 3.11 DISO analytical test function. 157
Figure 3.12 The 2D Ishigami function restricted to its two first input variables. 157
Figure 3.13 Example of cross-validation curve. 158
Figure 3.14 Results of ordinary Kriging (top right), universal Kriging (bottom left) and SVR-Kriging (bottom right) for the estimation of SISO model. 160
Figure 3.15 Results of ordinary Kriging (top right), universal Kriging (bottom left) and SVR-Kriging (bottom right) for the estimation of DISO model. 161
Figure 3.16 Results of ordinary Kriging (top right), universal Kriging (bottom left) and SVR-Kriging (bottom right) for the estimation of the 2D Ishigami function. 162
Figure 3.17 Scheme of a typical sequential learning process. 165
Figure 3.18 Scheme of the proposed sequential learning process. 167
Figure 3.19 Sequential learning process for multiple outputs. 168
Figure 3.20 Graphical results of the sequential learning process for (α,β)=(1,0) 169
Figure 3.21 Results of the sequential learning process for (α,β)=(1,1). 170
Figure 3.22 Global scheme of the numerical experiments plan. 171
Figure 4.1 Functioning scheme of a two-stages turbofan 177
Figure 4.2 Position of the valves and vanes on benchmark turbofan architecture. 179
Figure 4.3 Functional breakdown representation of the fuel system. 179
Figure 4.4 Fuel system scheme with emphasis on LRUs. 180
Figure 4.5 Structural breakdown representation of the fuel system. 181
Figure 4.6 Representation of the FMV subsystem. 181
Figure 4.7 Block diagram of the closed loop regulation of FMV displacement. 182
Figure 4.8 Representation of the SOV subsystem. 183
Figure 4.9 Block diagram of the open loop regulation of SOV displacement. 183

Figure 4.10 Characteristic of the fuel recirculation loop. 184
Figure 4.11 Representation of the SOV subsystem. 184
Figure 4.12 Representation of the FMU subsystem. 185
Figure 4.13 Representation of the LPP subsystem (image issued from http://www.wermac.org/). 185
Figure 4.14 Representation of the MFP subsystem (image issued from http://processprinciples.com/). 186
Figure 4.15 Mechanical structure of the VSV subsystem. 187
Figure 4.16 Representation of the VSV subsystem. 187
Figure 4.17 Detailed scheme of a two stages flapper nozzle servovalve. 187
Figure 4.18 Detailed scheme of a VSV actuator. 188
Figure 4.19 Block diagram of the VSV displacement regulation loop. 188
Figure 4.20 Mechanical structure of the VBV subsystem. 189
Figure 4.21 Block diagram of the VBV displacement regulation loop. 189
Figure 4.22 Mechanical structure of the TBV subsystem. 190
Figure 4.23 Representation of the TBV subsystem. 190
Figure 4.24 Block diagram of the TBV displacement regulation loop. 191
Figure 4.25 Mechanical structure of the flowmeter. 191
Figure 4.26 Health Indicators from the smoothed velocity gain curve for the FMV loop. 193
Figure 4.27 Real HIs for the HPSOV. 194
Figure 4.28 Extraction of $\boldsymbol{\omega SOV}$. 197
Figure 4.29 Extraction of the raw and smoothed velocity gain curves for the VSV loop. 199
Figure 4.30 Health Indicators from the smoothed velocity gain curve for the VSV loop. 199
Figure 4.31 Extraction of the raw and smoothed velocity gain curves for the VBV loop. 200
Figure 4.32 Health Indicators from the smoothed velocity gain curve for the VBV loop. 201
Figure 4.33 Morris graphical representation for HIs. 204
Figure 4.34 Morris graphical representation for CSIs. 205
Figure 4.35 Distribution of HI $\boldsymbol{FmvHyst0A}$ for DEM $\boldsymbol{DEFmvStic_Pos}$. 209
Figure 4.36 Distribution of HI $\boldsymbol{MffSlpN2DP}$ for DEM $\boldsymbol{DEMffFlowRate_Neg}$. 209
Figure 4.37 Healthy distribution of HI $\boldsymbol{VsvMAErr}$ for raw and standardized cases. 210
Figure A.1 Command fault status calculation. 235
Figure A.2 Computation of selected measures. 236
Figure A.3 Controller logic for actuation loops. 237
Figure A.4 Actuation fault status computation. 238
Figure A.5 Theoretical maximum and minimum values computation. 238

List of Tables

Tableau R.1 Classification des types de dispatch. 15
Tableau R.2 Matrice d'association des URL. 18
Tableau R.3 Résumé des spécificités liées à l'application aux moteurs d'avions. 35
Tableau R.4 Résultats comparés des méthodes de Krigeage pour les trois fonctions tests. 40
Tableau R.5 Amélioration des performances avec itération de l'algorithme d'optimisation. 41
Tableau R.6 Liste des paramètres épistémiques pour le système carburant. 50
Tableau R.7 Exemple de causes potentielles d'occurrence d'un ISC. 51
Tableau R.8 Parameters for the SVR-Kriging learning. 52
Tableau R.9 Liste des spécifications pour le jeu d'IS. 53
Tableau R.10 53
Table 1.1 Dispatch types classification 70
Table 1.2 Comparison between the BITE system and the PHM system. 79
Table 1.3 Example of LRU association matrix. 84
Table 2.1 Parameters definition and classification for the guiding thread example. 104
Table 2.2 Advantages, drawbacks and main utilization of global and screening methods. 118
Table 2.3 Different types of kernel functions for SVR. 121
Table 2.4 Specifications for the development of the EMU. 137
Table 3.1 Summary of the particularities related to the intended application. 146
Table 3.2 Different types of correlation models for Kriging. 149
Table 3.3 Comparison of Kriging performances for the SISO model. 160
Table 3.4 Comparison of Kriging performances for the DISO model. 161
Table 3.5 Comparison of Kriging performances for the 2D Ishigami function. 162
Table 3.6 Comparison of Kriging performances for the 3D Ishigami function. 162
Table 3.7 Performances of the anisotropic estimation for the 3D Ishigami function. 163
Table 3.8 Performances of the $\boldsymbol{\theta}$ optimization iteration for the 3D Ishigami function. 164
Table 3.9 Results of the sequential learning process for (α,β)=(1,0). 169
Table 3.10 Results of the sequential learning process for (α,β)=(1,1). 170
Table 4.1 List of degradation modes for the FMV loop. 192
Table 4.2 List of HIs for the FMV loop. 193
Table 4.3 List of degradation modes for the HPSOV. 194
Table 4.4 List of HIs for the HPSOV. 194
Table 4.5 List of degradation modes for the Bypass valve. 195
Table 4.6 List of HIs for the bypass valve. 195
Table 4.7 List of HIs for the FMU. 196
Table 4.8 List of degradation modes for the LPP. 196
Table 4.9 List of HIs for the FMU. 196
Table 4.10 List of degradation modes for the MFP. 196
Table 4.11 List of HIs for the MFP. 197
Table 4.12 List of degradation modes for the MFF. 197
Table 4.13 List of HIs for the MFP. 198
Table 4.14 List of degradation modes for the VSV loop. 198
Table 4.15 List of HIs for the VSV loop. 199
Table 4.16 List of degradation modes for the VBV loop. 200
Table 4.17 List of HIs for the VBV loop. 201
Table 4.18 List of degradation modes for the Bypass valve. 201
Table 4.19 List of HIs for the TBV. 202
Table 4.20 List of degradation modes for the Flowmeter. 202
Table 4.21 List of HIs for the Flowmeter. 202
Table 4.22 List of degradation modes for the fuel system. 202
Table 4.23 List of HIs for the fuel system. 203
Table 4.24 List of context parameters for the fuel system. 203
Table 4.25 List of epistemic parameters for the fuel system. 203

Table 4.26 List of uncertain parameters. 205
Table 4.27 Example of potential cause degradation parameter for two compliant service indicators (CSIs). 206
Table 4.28 Parameters for the SVR. 206
Table 4.29 Example of performance metrics for the SVR model for HIs. 207
Table 4.30 Example of MLVs for two degradation modes learning. 207
Table 4.31 Parameters for the SVR-Kriging learning. 208
Table 4.32 List of specifications for the HIs set. 210
Table 4.33 Example of compliant detectability values. 211
Table 4.34 Example of compliant identifiability values. 212
Table 4.35 Final results of criteria computation for different HIs configurations. 214
Table A.1 LRU association matrix for the fuel system. 234
Table A.2 List of models parameters for FMV, VSV and VBV loops. 238
Table A.3 List of targeted compliant service threats for the FMV loop. 239
Table A.4 List of targeted compliant service threats for the FMU. 240
Table A.5 List of targeted compliant service threats for the MFP. 241
Table A.6 List of targeted compliant service threats for the MFF. 242
Table A.7 List of targeted compliant service threats for the VSV loop. 243
Table A.8 List of targeted compliant service threats for the VBV loop. 244
Table A.9 List of targeted compliant service threats for the WFM. 245
Table A.10 Complete list of parameters. 247
Table A.11 Complete list of degradation modes. 249
Table A.12 Complete list of health indicators. 252
Table A.13 Complete list of compliant service indicators. 253
Table A.14 Initial coarse uncertainties quantification. 254
Table A.15 Morris method results. 256
Table A.16 List of potential cause degradation parameter for each compliant service indicator (CSI). 257
Table A.17 MLV matrix and mlv vector for the degradation modes of the fuel system. 260
Table A.18 Q2 index of the SVR model for HIs and CSIs. 261
Table A.19 Performance metrics of the SVR-Kriging model for HIs. 262
Table A.20 Performance metrics of the SVR-Kriging model for HIs 263
Table A.21 Detection NKPIs for the set of raw health indicators. 267
Table A.22 Identification NKPIs for the set of raw health indicators. 268
Table A.23 Localization NKPIs for the set of raw health indicators. 269
Table A.24 Detection NKPIs for standardized HIs. 286
Table A.25 Identification NKPIs for standardized HIs. 287
Table A.26 Localization NKPIs for standardized HIs. 288
Table A.27 Detection NKPIs for individual models. 293
Table A.28 Identification NKPIs for individual models. 294
Table A.29 Localization NKPIs for individual models. 295
Table A.30 Detection NKPIs for virtual HIs. 300
Table A.31 Identification NKPIs for virtual HIs.. 301
Table A.32 Localization NKPIs for virtual HIs. 302

Author's Publications

International journals with peer review process:

Lamoureux, B., Massé, J. R., & Mechbal, N. (2014). Improving Aircraft Engines Prognostics and Health Management via Anticipated Model-Based Validation of Health Indicators. *Prognostics Journal, 2*(1), 18-38. Available at http://prognosticsjournal.com/

Lamoureux, B., Mechbal, N., & Massé, J.-R. (2014, DOI: 10.1016/j.ress.2014.03.007). A Combined Sensitivity Analysis and Kriging Surrogate Modeling for Early Validation of Health Indicators. *Reliability Engineering and System Safety*.

International conferences proceedings with peer review process:

Lamoureux, B., Massé, J. R., & Mechbal, N. (2012). An Approach to the Health Monitoring of a Pumping Unit in an Aircraft Engine Fuel System. *First European Conference of the Prognostics and Health Management Society*, (pp. 23-29). Dresden,.

Lamoureux, B., Massé, J. R., & Mechbal, N. (2012). An Approach to the Health Monitoring of the Fuel System of a Turbofan. *Prognostics and Health Management (PHM), 2012 IEEE Conference on*, (pp. 1-6). Denver (CO),.

Lamoureux, B., Massé, J. R., & Mechbal, N. (2012). Methodology for the Diagnosis of Hydromechanical Actuation Loops in Aircraft Engines. *Control \& Automation (MED), 2012 20th Mediterranean Conference on*, (pp. 972-977). Barcelona, Spain,.

Lamoureux, B., Massé, J.-R., & Mechbal, N. (2013). Diagnostics of an aircraft engine pumping unit using a hybrid approach based-on surrogate modeling. *Prognostics and Health Management (PHM), 2013 IEEE Conference on*, (pp. 1-8).

Lamoureux, B., Mechbal, N., & Massé, J. R. (2013). Selection and Validation of Health Indicators in Prognostics and Health Management System Design. *2nd International Conference on Control and Fault-Tolerant Systems, SysTol'13.* Nice,.

Massé, J., Lamoureux, B., & Boulet, X. (2011). Prognosis and Health Management in system design. Prognostics and Health Management (PHM), 2011 IEEE Conference on, (pp. 1-5). Denver, CO,.

International patents:

Massé, J.-R. A., Lamoureux, B. P., Idrissi, H. J., Marquisseau, F., & Sif, A. (2012, #dec#~3). Method for monitoring a control device of a fuel metering valve of a turbojet engine. *Method for monitoring a control device of a fuel metering valve of a turbojet engine*. Google Patents.

Massé, J.-R., Lamoureux, B., Aurousseau, C., Deldalle, R., Michel, P., Flandrois, X., & Sif, A. (2012, April). Method and device for monitoring a feedback loop of a variable-geometry actuator system of a jet engine. *Method and device for monitoring a feedback loop of a variable-geometry actuator system of a jet engine(WO Patent 2.012.052.696)*. Geneva, Switzerland: World Intellectual Property Organization,.

Acronyms and abbreviations

$ACARS$	Aircraft Communications Addressing and Reporting System
$ACMS$	Aircraft Condition Monitoring System
ACU	Actuation Control Unit
AS	Analyse de Sensibilité
ATP	Acceptance Test Procedure
AUC	Area Under the Curve
$BITE$	Built-In Test Equipment
BYV	Bypass Valve
CD	Compliant Detectability
CI	Compliant Identificability
CL	Compliant Localizability
CSI	Conform Service Indicator
CST	Conform Service Threat
COR	Caractéristiques Opérationnelles de Réception
CV	Cross-Validation
$D\&C$	Delays and Cancellations
$D\&P$	Diagnostic and Prognostic
DEM	Degradation Mode
$DISO$	Dual Inputs Single Output
DMC	Direct Maintenance Costs
DOE	Design Of Experiments
$EASA$	European Aviation Safety Agency
ECU	Engine Control Unit
EEC	Electronic Engine Controller
EIS	Entry Into Service
EMU	Engine Monitoring System
FAA	Federal Aviation Administration
$FADEC$	Full Authority Digital Engine (or Electronics) Control
$FMEA$	Failure Modes and Effects Analysis
FMU	Fuel Metering Unit
FMV	Fuel Metering Valve
FP	False Positive rate
FTC	Fault Tolerance Control
GD	Global Detectability

GI	Global Identificability
GL	Global Localizability
HI	Health Indicator
HM	Health Monitoring
$HPSOV\ or\ SOV$	High Pressure Shut Off Valve or Shut Off Valve
HS	Health Status
$IDPHM$	Integrated Development of Prognostics and Health Management
$IEEE$	Institute of Electrical and Electronics Engineering
$IFSD$	In-Flight Shut Down
IS	Indicateur de Santé
ISC	Indicateur de Service Conforme
LH	Latin Hypercube
LHS	Latin Hypercube Sampling
$LHSDOE$	Latin Hypercube Sampling Design Of Experiments
LPP	Low Pressure Pump
LRU	Line Replaceable Unit
$LVDT$	Linear Variable Differential Transformer
MD	Mode de Dégradation
MDC	Mode de Dégradation Cible
MDI	Minimal Detectable Intensity
MFF	Main Fuel Filter
MFP	Main Fuel Pump
MII	Minimal Identifiable Intensity
MLI	Minimal Localizable Intensity
MLV	Mean Limit Value
MSC	Menace au Service Conforme
$MSCC$	Menace au Service Conforme Cible
MRO	Maintenance, Repair and Operations
NFF	No Fault Found
$NKPI$	Numerical Key Performance Indicators
$OSA-CBM$	Open-System Architecture for Condition Based Maintenance
PDE	Partial Derivative Equations
PDF	Probability Density Function
PE	Plan d'Expériences
PHM	Prognostics and Health Management
PID	Proportional Integrator Derivative controller
RBF	Radial Basis Function
ROC	Receiver Operating Characteristics
RTC	Real Time Clock

RUL	Remaining Useful Lifetime
SA	Sensitivity Analysis
SE	Systems Engineering
$SISO$	Single Input Single Output
SVR	Support Vector Regression
TBV	Transient Bleed Valve
$TCST$	Targeted Conform Service Threat
$TDEM$	Targeted Degradation Mode
TP	True Positive rate
URL	Unité Remplaçable en Ligne
$V\&V$	Verification and Validation
VBV	Variable Bleed Valve
VLM	Valeur Limite Médiane
VSV	Variable Stator Vane
WFM	Weight Flow Meter

NOTATIONS

Mathematics

a	Scalar variable
$\underline{b}$	Column vector
$\boldsymbol{A}$	Matrix
$\boldsymbol{A^T}, \underline{b}^T$	Transpose of matrix $\boldsymbol{A}$ and vector $\underline{b}$
$\boldsymbol{A^{-1}}$	Inverse of matrix $\boldsymbol{A}$
δ_{ij}	Kronecker delta

Numerical key performance indicators

i	Index of health indicators (HIs)
j	Index of degradation modes
k	Value of the intensity
T_i^0	Healthy empirical distribution of HI i
$T_{i,j}^k$	Empirical distribution of HI i for degradation mode j of intensity k
TP_{SPEC}	Specified minimal true positive rate
FP_{SPEC}	Specified maximal false positive rate
α_{SPEC}	Specified minimal angle
MDI^j, MII^j, MLI^j	Minimal detectable, identifiable and localizable intensities for DEM j
MLV^j	Mean limit value for DEM j

Sensitivity analysis

$E_i^{(k)}$	Elementary effect i of iteration k for the Morris method
μ_i	Mean of elementary effects i for the Morris method
μ_i^*	Absolute mean of elementary effects i for the Morris method
σ_i	Standard deviation of elementary effects i for the Morris method
$\mu_{i,j}$	Mean of elementary effects i on output j
$\mu_{i,j}^*$	Absolute mean of elementary effects i on output j
$\sigma_{i,j}$	Standard deviation of elementary effects i on output j
T_i	Total effect index of input i
N_i	Nonlinearity index of input i
$D_{i,j}$	Direction index of input i on output j
$\not{f}$	Function studied by sensitivity analysis
$Var(y)$	Variance of output y
$V_i, V_{ij}, \ldots$	First order, second order, etc… effects coefficient of variance

$\mathbb{E}(y\|x_i), \mathbb{E}(y\|x_i x_j), \ldots$	Conditional expected values of y
$S_i, S_{ij}, \ldots$	First order, second order, etc… Sobol indices
S_{Ti}	Total Sobbol sensitivity index

Support vector regression

s	Function to be estimated
$\mathcal{H}$	Estimation via the support vector regression
$\underline{x_i}, i = 1, \ldots, n$	Support vectors
$\underline{\xi}$	Hyperparameters vector for the kernel function
$k\left(\underline{\xi}, \underline{x_i}, \underline{x_j}\right)$	Kernel function computed between vectors $\underline{x_i}$and $\underline{x_j}$
$\underline{y}$	Matrix of the responses at learning points
$\boldsymbol{G}$	Matrix of the kernel function values at learning points
$\underline{v}(\underline{s})$	Vector of the kernel function values a new point $\underline{s}$
$\underline{\alpha}$	Vector of the regression coefficients

Modeling formalism

f	Deterministic physics-based model black-box function
$\boldsymbol{U}$	Matrix of temporal inputs
$\boldsymbol{Y}$	Matrix of temporal outputs
$\rho_1, \ldots, \rho_p$	List of parameters
$\gamma_1, \ldots, \gamma_e$	List of epistemic parameters
$\lambda_1, \ldots, \lambda_c$	List of context parameters
$\omega_1, \ldots, \omega_d$	List of degradation parameters
$\underline{\omega}^0$	Nominal condition
$\delta \underline{e_j^{\mathcal{D}}}$	Degradation mode $\underline{e_j^{\mathcal{D}}}$ of value δ
$\varphi_1, \ldots, \varphi_h$	List of HIs
$\psi_1, \ldots, \psi_o$	List of OIs
g	Extraction function for HIs
h	Extraction function for OIs
$\mathcal{M}_{\boldsymbol{U}}$	Constant temporal inputs model
$\mathcal{M}_{\boldsymbol{U}}^j$	Constant temporal inputs model for output *j*
$\mathcal{MF}_{\boldsymbol{U}}^j$	Constant temporal inputs fleet model for output *j*
$\mathcal{MI}_{\boldsymbol{U}}^j$	Constant temporal inputs individual model for output *j*
$\underline{\rho}^*$	Fixed parameters
$\underline{\rho}^{ni}, \underline{\rho}^{li}$	Nonlinear and linear influential parameters
$\underline{\rho_j}^{np}, \underline{\rho_j}^{lp}$	Nonlinear and linear principal parameters for output *j*
$\underline{\rho_j}^{na}, \underline{\rho_j}^{la}$	Nonlinear and linear ancillary parameters for output *j*
$\underline{\rho_j}^{ns}, \underline{\rho_j}^{ls}$	Nonlinear and linear standardization parameters for output *j*
$\underline{\rho_j}^{nu}, \underline{\rho_j}^{lu}$	Nonlinear and linear unknown parameters for output *j*

$\underline{\pi_j}$	Standardization parameters for HI j
$\mathcal{T}_c$	Performance function for DEM c
$\mathcal{G}_c$	Median performance function for DEM c

Kriging

$\mathbb{k}$	Function to be estimated
$\mathcal{K}$	Estimation via the SVR-Kriging
$\mathcal{R}$	Regression part of the Kriging model (SVR)
$\mathcal{G}$	Gaussian process part of the Kriging model
σ^2	Kriging variance
$\underline{\theta}$	Hyperparameters vector for the correlation function
$k(\underline{\theta}, \underline{x_i}, \underline{x_j})$	Correlation function computed between vectors $\underline{x_i}$ and $\underline{x_j}$
$\underline{y}$	Matrix of the responses at learning points
$\underline{\widehat{y_{\mathcal{R}}}}$	Matrix of the estimation at learning points by the regression function
$\boldsymbol{R}$	Matrix of the correlation function values at learning points
$\underline{r}(\underline{s})$	Vector of the correlation function values a new point $\underline{s}$
$\underline{\gamma}$	Vector of the gaussian process coefficients
$\boldsymbol{F}$	Matrix of the kernel function values at learning points
$\underline{f}(\underline{s})$	Vector of the kernel function values a new point $\underline{s}$
$\underline{\beta}$	Vector of the regression coefficients
e_{-i}	Cross-validation error at learning point i
$\mathcal{K}_{-i}$	SVR-Kriging model learned without point i
$Q2$	Value of the $Q2$ index
μ_{CV}	Mean of the cross-validation errors
σ_{CV}	Standard deviation of the cross-validation errors
σ_y	Standard deviation of output y
$\mathbb{f}_{SISO}$	Single input single output (SISO) analytical test function
$\mathbb{f}_{MISO}$	Dual input single output (DISO) analytical test function
$\mathbb{f}_{ISHIGAMI}$	Ishigami analytical test function
OC	Optimization criterion for the DACEFIT iteration
SC	Selection criterion for the sequential learning
p_i	Assignation probability of model i
(α, β)	Weighting coefficient for the selection criterion computation
n_{optT}	Number of influential parameters included in the DACEFIT algorithm
n_{CV}	Step for the computation of cross-validation error based criteria
n_{par}	Number of parallel model evaluation for sequential learning

Résumé étendu en français

Introduction

Au sein du groupe SAFRAN, Snecma est un des leaders mondiaux dans la conception et la réalisation de moteurs d'avions. Il y a une dizaine d'années, ses conseillers scientifiques ont commencé à s'intéresser à la surveillance prédictive des systèmes, plus connue sous le terme PHM pour prognostics and health management. Par la suite, les experts et ingénieurs de Snecma ont développé des algorithmes de PHM pour les moteurs d'avions. Cependant, même si ces derniers sont détenteurs de la connaissance du comportement physique des systèmes, ils rencontrent des difficultés lorsqu'il s'agit de définir et d'appliquer un processus de développement pour le PHM. Le contexte de ces travaux de thèse en découle. Il est le résultat d'une demande de Snecma d'élaborer une approche pour améliorer le développement du PHM.

Dans de nombreux domaines, la performabilité des systèmes est au cœur des préoccupations (Meyer, 1992). Elle est composée de deux volets: la performance et la sûreté de fonctionnement. Les travaux de thèse présentés ici se focalisent sur le second volet. Telle que définie par Avizienis et Laprie (Avizienis, et al., 2000), la sûreté de fonctionnement englobe trois caractéristiques: les attributs sur lesquels elle repose, les menaces qu'elle cible et les moyens quelle utilise. Dans l'aéronautique, les attributs sont typiquement la sûreté, la fiabilité, la disponibilité et la maintenabilité, les menaces sont les fautes, les erreurs et les défaillances et les moyens sont la suppression, la prévention, la tolérance et la prévision.

Pour les constructeurs de moteurs d'avions comme Snecma, les contraintes liées à la sûreté de fonctionnement proviennent principalement des autorités de certification. Pour répondre à ces contraintes, la stratégie utilisée est basée sur la suppression et la prévention, caractérisées respectivement par les opérations de maintenance corrective et préventive. Les premières consistent à supprimer une faute ou une défaillance après son occurrence et les secondes à remplacer les équipements de manière périodique et systématique pour prévenir leur apparition. Comme en témoigne la très faible occurrence des accidents dans l'aviation civile, cette stratégie est efficace pour assurer les certifications en matière de sûreté et de fiabilité. Cependant, la disponibilité n'est pas aussi bien assurée, comme en témoignent la fréquence des retards et annulations et les nombreux arrêts opérationnels pour la maintenance préventive. Cela entraîne des surcoûts très importants qui font que la disponibilité est petit à petit devenue un défi majeur pour les compagnies aériennes.

Pour améliorer la disponibilité, la première solution est la tolérance qui consiste à autoriser un appareil à prolonger son utilisation après l'apparition d'une faute. Ces logiques de tolérance sont définies par le "dispatch". Cependant, du fait du nombre limité de fautes autorisant un dispatch, ce n'est pas suffisant. C'est dans ce contexte que les premiers travaux sur la prédiction sont apparus il y a une dizaine d'années. L'idée de base est d'utiliser les données disponibles pour surveiller l'évolution de l'état de santé d'un système afin d'anticiper l'occurrence de fautes ou de défaillances. Au cours de la dernière décennie, une nouvelle communauté scientifique dédiée à la prédiction s'est rapidement imposée: le health monitoring (**HM**). Le HM réalise idéalement les tâches de diagnostic (Isermann, 1997; Patterson-

Hine, et al., 2005) et de pronostic (Kalgren, et al., 2006; Roemer, et al., 2007). La première consiste à détecter les anormalités, identifier les précurseurs de menaces au service conforme et localiser les unités remplaçables en ligne (**URL**) incriminées. La seconde consiste à évaluer l'intensité du mode de dégradation identifié et d'en prédire son évolution. Le HM repose sur l'extraction de variables reflétant l'état de santé du système appelés indicateurs de santé (**IS**). Le lien entre le HM et la maintenance peut se faire par exemple par l'intermédiaire du prognostics and health management (**PHM**). Cette discipline est apparue récemment, mais elle gagne progressivement en importance. L'idée de base du PHM est d'utiliser les sorties du HM comme entrées d'un processus de supervision basé sur les maintenances conditionnelles et prédictives (Ben-Daya, et al., 2009). Pratiquement, le PHM pourrait permettre: une réduction des coûts liés aux retards et annulations, une amélioration de l'efficacité des opérations de maintenance, une diminution et une réduction de la taille des flottes ainsi que des stocks de pièces détachées. Pour ces raisons, il est en passe de devenir un argument de vente majeur pour les avionneurs et leurs équipementiers, a fortiori quand on considère la généralisation des contrats à l'heure de vol dans l'aéronautique.

Dans ce contexte industriel, Snecma développe des systèmes de PHM pour ses moteurs. Cependant, ce développement n'est pour le moment pas suffisamment adapté aux spécificités du domaine. En effet, le PHM est actuellement vendu pour être performant au plus tôt trois ans après l'entrée en service. La conséquence à court terme est que la partie intégrée de PHM algorithmes qui sont sur le point d'être implémentés dans les contrôleurs n'ont fait l'objet d'aucune évaluation quantitative de performance. Ainsi, il pourrait s'avérer que l'ensemble des indicateurs de la santé est inefficace. Les conséquences sont alors : (1) l'obligation de modifier la partie embarquée du PHM pour étendre le jeu d'IS, ce qui entraîne des surcoûts important ; (2) la non prise en charge des crises de jeunesse et des campagnes de retrofit par le PHM car ce dernier n'est pas opérationnel au moment des premiers essais moteur et enfin (3) la perte de réputation du point de vue des compagnies aériennes et des opérateurs de maintenance à cause d'un PHM qui ne tient pas ses promesses. Pour éviter cela, le développement du PHM doit être amélioré : la conception et la validation du PHM et en particulier de la partie embarquée doivent être effectués simultanément et en interaction avec le système hôte. Ainsi, l'objectif final serait de supprimer les trois ans de délai pour avoir un système PHM opérationnel dès l'entrée en service du moteur. La complexité des systèmes rencontrés, illustrée par l'application du Chapitre 4, fait qu'il est nécessaire de formaliser une approche systématique pour ce nouveau type de développement du PHM. Puisqu'aucune mesure n'est disponible pendant les phases de conception, des modèles numériques doivent être utilisés, ce qui implique une incertitude liée à la qualité de la modélisation. Par conséquent, la nouvelle approche doit permettre d'évaluer le niveau de précision des modèles. Après un état de l'art, trois problématiques principales se sont détachées et sont traitées, respectivement, dans les chapitres 1 à 3. Le chapitre 4 étant, quant à lui, dédié à l'application des méthodes et outils développés.

La première problématique, traitée dans le premier chapitre, concerne le développement du PHM. Plus particulièrement, on cherche à développer simultanément et interactivement les systèmes hôtes et de PHM. Trois sous-problèmes ont été identifiés. Ils concernent, respectivement, la terminologie du PHM, son cadre fonctionnel et son processus de développement. Au niveau de la terminologie, l'objectif est d'identifier un ensemble de définitions pour le PHM compatible avec les pratiques industrielles actuelles de Snecma. Au vu de l'état de l'art actuel, il est difficile de trouver une terminologie générique pour cette discipline, comme l'illustre l'éventail d'appellations existantes (ISHM, IVHM, HUMS, etc….) (Johnson, et al., 2011). Ainsi, un cadre terminologique spécifique à l'application du PHM aux

moteurs d'avions, s'inspirant de définitions issues d'ouvrages scientifiques, est proposé. Au niveau du cadre fonctionnel du PHM, le problème est de définir l'environnement du PHM ainsi que ses fonctions principales. Là encore, la communauté scientifique ne propose pas de solution générique adaptée aux moteurs d'avions. C'est pourquoi nous proposons une nouvelle définition de l'environnement à partir de la notion spécifique de dispatch. Les fonctions principales du PHM sont, quant à elles, définies sur les bases de la terminologie introduite au préalable. Finalement, le point le plus important concerne le développement du PHM. Il apparaît que la méthodologie adoptée actuellement n'est pas adaptée aux spécificités du PHM pour les moteurs d'avions. En particulier, le PHM n'est pas un système unique, mais une interaction entre trois systèmes : une partie embarquée chargée d'extraire les indicateurs et deux parties au sol chargées, respectivement, de les traiter et de superviser les tâches de maintenance. Ces trois systèmes doivent faire l'objet de processus de développement séparés. En réponse, un nouveau processus appelé approche intégrée pour le développement du PHM est introduit. Il est basé sur un modèle original appelé modèle V3, issu de la subdivision du PHM en trois entités : l'unité d'extraction, l'unité de traitement et l'unité de supervision. Les interactions entre ce V3-modèle et le V-modèle du système hôte sont mises en exergue et formalisées.

La seconde problématique concerne un aspect bien spécifique du V3-modèle : le développement de la partie embarquée chargée de l'extraction des indicateurs de santé. En effet, dans ce modèle, cette partie est conçue et validée pendant les phases de conception. L'objectif du second chapitre est d'expliquer comment ce développement peut être réalisé alors qu'aucune mesure n'est disponible. L'idée centrale est d'utiliser des modèles physiques pour générer des données. La méthode est subdivisée en trois points : la sélection des IS, leur normalisation et leur validation. Dans un premier temps, l'approche pour la modélisation des systèmes est présentée. Elle est basée sur une représentation des paramètres sous forme d'espaces vectoriels et utilise des signaux d'entrée constants d'une évaluation à l'autre. La méthode de sélection des IS est ensuite introduite. Elle suit les étapes suivantes : (1) présélection des IS via analyse des documents de spécifications, des procédures de tests d'acceptation des équipements et des built-in test (**BIT**) ; (2) prototypage sur modèles partiels des équipements et (3) validation du jeu d'IS par des experts. Le processus de normalisation consiste à évaluer les effets du premier ordre dû à des paramètres disponibles en vol et à retirer ces effets aux IS mesurés (Lacaille, 2009). Cela permet de diminuer l'écart type des IS et donc d'améliorer les performances en détection. Une nouvelle méthode de normalisation basée sur l'analyse de sensibilité et la régression par vecteurs support est proposée. Enfin, le processus de validation des IS en phase de conception est basé sur le calcul de métriques de performance et de critères de validation. Ces métriques, appelées indicateurs numériques de performances (**NKPI**), sont calculées pour plusieurs configurations des IS pour déterminer le jeu optimal répondant aux spécifications. Les NKPI sont définis à partir des courbes de caractéristiques opérationnelles de réception (**COR**) qui nécessitent de connaître les distributions des IS aux états sains et dégradés. Les modèles disponibles étant déterministes, une méthode de propagation d'incertitudes est utilisée pour introduire un aspect stochastique. Ce type de méthodes nécessite un grand nombre d'évaluations du modèle de sorte que le temps de simulation total peut rapidement s'avérer rédhibitoire. Pour diminuer la complexité des calculs, il est proposé d'utiliser des métamodèles, fonctions permettant d'estimer les sorties d'un modèle par une fonction mathématique de faible coût de calcul. En particulier, nous avons choisi d'utiliser le Krigeage pour ses bonnes propriétés en grande dimension et son côté stochastique (processus gaussien).

Le chapitre 3 est dédié à la problématique suivante : comment construire et utiliser un modèle de Krigeage pour obtenir les distributions nécessaires à la validation des IS ? Le développement de ce chapitre se divise en trois parties : une introduction au Krigeage (Forrester, et al., 2009), la présentation d'une nouvelle technique appelée Krigeage SVR adaptée aux spécificités de l'application aux moteurs d'avions et enfin le développement d'une méthode de validation et d'amélioration du modèle. L'état de l'art sur le Krigeage présente les points suivants : la construction du plan d'expériences (**PE**) (Iman, 2008) d'apprentissage, l'estimation des hyperparamètres du modèle et sa validation. La technique du Krigeage est également introduite de manière théorique et une classification des techniques existantes est proposée. À partir de celle-ci, il apparaît que les méthodes actuelles ne sont pas adaptées aux spécificités suivantes des comportements rencontrés dans les moteurs d'avions : non-linéarité, monotonie, discontinuités locales et faibles interactions entre paramètres. La nouvelle technique nommée Krigeage SVR proposée se base sur l'idée suivante : puisque les effets du premier ordre sont prépondérants, ils sont modélisés précisément par des régressions par vecteurs supports (**SVR**) (Smola, et al., 2004) sur chacune des dimensions. Ensuite, le processus gaussien du Krigeage est utilisé pour affiner le modèle en considérant les effets dus aux interactions. La pertinence du Krigeage SVR est testée sur des fonctions analytiques représentatives des comportements rencontrés. Les critères utilisés pour l'évaluation des performances sont le $Q2$ (basé sur la comparaison avec un second plan d'expériences) et l'erreur de validation croisée. Enfin, pour s'assurer de la précision du modèle, une méthode d'apprentissage séquentiel (Bichon, et al., 2008) est définie autour d'un critère de validation construit à partir de la variance du Krigeage et des erreurs de validation croisée. La méthode de modélisation globale est alors d'utiliser comme PE initial un ensemble de vecteurs d'apprentissage mono dimensionnels puis d'améliorer itérativement la précision du Krigeage jusqu'à atteindre le critère de validation spécifié. Afin de gérer le fait que de nombreuses sorties sont estimées à partir du même ensemble de points d'apprentissage, un modèle cible est désigné à chaque itération.

Finalement, le chapitre 4 est dédié à l'application de la méthode et des outils proposés au système carburant d'un moteur d'avion (Moir, et al., 2008). Ce système est chargé de réguler la quantité de carburant injectée dans la chambre de combustion pour fournir la poussée demandée. Il est composé de nombreuses unités fonctionnelles telles que les boucles de régulation des géométries variables et les pompes. Sa criticité ainsi que les nombreux évènements opérationnels qui peuvent l'affecter en font un bon candidat pour tester le développement intégré du PHM. Par ailleurs, la complexité de son modèle physique en fait également un bon candidat pour tester le Krigeage SVR. Le chapitre 4 se divise en 5 parties : la présentation du système carburant, la sélection des IS et des indicateurs de service conforme (**ISC**), la construction du modèle de Krigeage SVR, la normalisation des IS et enfin leur validation. À chaque étape, les résultats sont présentés, critiqués et, le cas échéant, des pistes d'amélioration sont proposées.

Chapitre 1 : développement intégré du PHM

Ce premier chapitre a pour but d'introduire le PHM et les particularités liées à son application aux moteurs d'avions. La première section vise à proposer une nouvelle terminologie à la fois inspirée de définitions extraites de documents scientifiques et adaptée aux pratiques industrielles de Snecma. La seconde section est dédiée à la présentation du cadre fonctionnel du PHM. En particulier, son environnement est clairement défini à l'aune des notions particulières au domaine de l'aéronautique et

les verrous technologiques majeurs sont identifiés. Finalement, la troisième section présente les lacunes du processus de développement actuel du PHM et proposer une nouvelle démarche dont la caractéristique principale est de permettre le développement complet de la partie embarquée en phase de conception. Ce nouveau processus est conçu pour permettre un développement systématique du PHM pour les systèmes aéronautiques complexes tels que celui présenté dans le Chapitre 4.

Terminologie pour le PHM des moteurs d'avions

Dans cette première section, les principaux éléments d'un système PHM sont définis. Ces définitions sont classées selon cinq catégories : les menaces opérationnelles, les menaces physiques, les vecteurs d'observation, les outils de traitement et les outils de planification.

Le **service conforme** d'un système est défini comme sa capacité à se maintenir en condition fonctionnelle, en accord avec les spécifications demandées. À partir de cette notion, les **menaces au service conforme** sont définies comme des évènements observables liés à des changements externes et constatables du système. Trois types de menaces opérationnelles sont proposées : les **défaillances**, les **fautes** et les **défauts**. Les défaillances sont des observations en ligne de la perte d'opérabilité d'un système. Les fautes sont des observations en ligne d'une différence entre une caractéristique et sa spécification, cette différence excédant les limites d'acceptabilité. Les fautes sont caractérisées par leur niveau de **dispatch** qui indique le nombre d'heures supplémentaires qu'un appareil est autorisé à fonctionner avant d'être envoyé vers un centre de maintenance. Les six niveaux de dispatch existants sont présentés dans le Tableau R.1.

Dispatch Level	Dispatch	Availability
A	No-Go	Vol non autorisé. Maintenance immédiate.
A GO IF	Go-If	Vol non autorisé sauf sur décision du pilote.
Beta	Dispatch à long terme puis No-Go	**Dispatch C** lorsqu'une faute sur un capteur apparaît puis **dispatch A** si une faute sur le second capteur apparaît (valable pour capteurs redondés)
B	Dispatch à court terme	150 heures de vol autorisées
C	Dispatch à long terme	250 heures de vol autorisées
D	Dispatch infini	Pas de limitation

Tableau R.1 *Classification des types de dispatch.*

Seules les fautes de dispatch A, A Go-if et Beta sont impactantes pour la disponibilité puisque les autres types autorisent des heures de vol supplémentaires permettant d'organiser la maintenance. Les défauts sont l'équivalent des fautes pour des observations hors ligne réalisées lors d'opérations de maintenance. Ils n'ont pas d'impact direct sur l'opérabilité donc pas d'intérêt pour la disponibilité, mais permettent d'améliorer la maintenabilité en donnant des informations sur le niveau de dégradation des équipements surveillés. Finalement, le **périmètre du PHM** peut se caractériser de la manière suivante : il doit intégrer la surveillance des défaillances, des fautes de dispatch A, A Go-if et Beta et les défauts. Ce sont les **menaces au service conforme cible**s (**MSCC**).

Les **menaces physiques** sont des évènements non observables liés à des changements internes et cachés du système. Une **dégradation** est une menace physique définie comme une modification d'une ou plusieurs valeurs des paramètres structurels du système. Pour restreindre l'étendue des menaces

physiques prises en compte, les **modes de dégradation** (**MD**) sont considérés. Ces derniers sont définis comme l'altération d'un unique paramètre susceptible de se produire dans le système. Ils sont typiquement identifiés par expertise ou retour d'expérience. Les modes de dégradation sont classés en fonction de leurs effets. Seuls ceux qui peuvent entraîner des défaillances, des fautes de dispatch A, A Go-if et Beta et les défauts sont inclus dans l'environnement du PHM. Ce sont les **modes de dégradation cibles** (**MDC**), comme présentés dans la Figure R.1.

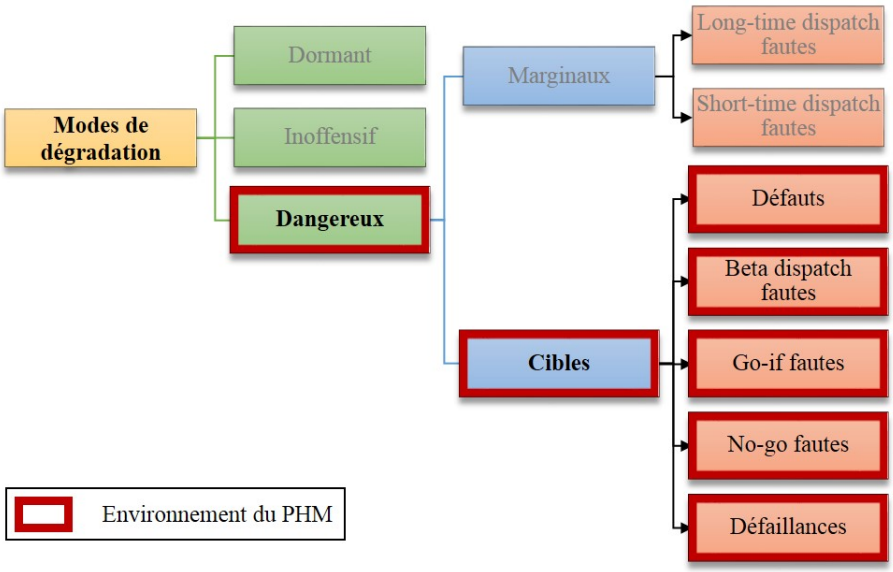


Figure R.1 *Classification des modes de dégradation et environnement du PHM.*

Pour un mode de dégradation donné, la **valeur limite médiane (VLM)**, équivalente à la dose létale médiane en pharmacologie, est définie comme la valeur d'un paramètre de dégradation pour laquelle une menace opérationnelle est atteinte avec une probabilité supérieure à 0.5. L'**intensité** d'un mode de dégradation est alors définie comme le ratio de la valeur courante de la dégradation sur la valeur limite médiane.

Les **vecteurs d'observation** sont des variables traduisant l'évolution des menaces opérationnelles et physiques au sein d'un système. Deux types d'indicateurs sont définis : les **indicateurs de service conforme** (**ISC**) et les **indicateurs de santé** (**IS**). Les premiers sont définis comme des variables traduisant directement l'évolution des MSCC dans le système. Par construction, ils sont proches des **fonctions de performance** issues du domaine de la fiabilité structurelle : les ISC sont des fonctions décroissantes du paramètre de dégradation auquel ils sont associés, prenant des valeurs positives lorsque le système est sain et des valeurs négatives lorsque le MSCC est atteint. La VLM est alors calculée comme la valeur du paramètre de dégradation pour laquelle l'ISC est égal à 0. Ces indicateurs ont deux défauts : (1) ils se limitent à surveiller les conséquences des modes de dégradations, mais ne permettent pas de connaître leur mécanisme d'évolution pour capitaliser de l'expérience et (2) ils ne sont que très **rarement mesurables en service** du fait que les capteurs nécessaires ne sont souvent pas disponibles. L'idée est alors de trouver une méthode indirecte pour les surveiller. En fait, quitte à développer une approche indirecte, il a été décidé de surveiller non pas les MSCC, mais leurs causes, à savoir les modes de dégradation. En pratique, ces derniers ne sont pas mesurables non plus. Par conséquent, des variables reflétant indirectement leur évolution sont utilisées : ce sont les IS. À partir de ces variables, les **symptômes** sont définis comme des variables traduisant la variation d'un IS par rapport à sa distribution

nominale. Un **syndrome** est un vecteur contenant tous les symptômes à un instant donné. Une **anormalité** est définie comme une observation d'un symptôme au-delà d'un seuil défini par l'utilisateur. Un **précurseur** est un syndrome de référence traduisant la présence d'un mode de dégradation. Il est associé à un niveau d'intensité en pourcentage. Typiquement, on considère les précurseurs à 25, 50, 75 et 100%.

Les outils de traitement associés au **health monitoring** (**HM**) ont pour but l'évaluation de **l'état de santé** des systèmes. Ce dernier est défini comme l'ensemble des informations relatives à l'évolution des modes de dégradation au sein du système. Typiquement, les états de santé courant et futur d'un système sont respectivement évalués et prédits par le **diagnostic** (Ribot, 2009) et le **pronostic** (Ly, et al., 1999). Le diagnostic contient trois tâches principales : la **détection** qui consiste à reconnaître les anormalités, l'**identification** qui consiste à classifier les syndromes par rapport à une base de données de précurseurs et enfin la **localisation** qui consiste à associer le précurseur à l'**unité remplaçable en ligne** (**URL**) endommagée. Le pronostic consiste à évaluer la sévérité du précurseur et prédire l'occurrence d'une MSCC à partir du diagnostic et des données historiques. Dans le cas des moteurs d'avions, le pronostic est de type horizon fixe, c'est-à-dire basé sur l'estimation de la probabilité d'atteindre une MSCC dans un horizon temporel fixé, généralement entre 10 et 100 vols.

Les outils de planification sont des leviers permettant d'agir directement sur la maintenance. Trois outils sont définis : les **alarmes**, les **avertissements,** les **mises en garde** et les **alertes**. Les alarmes sont des messages envoyés en vol au pilote pour l'informer de l'apparition d'une faute. Les avertissements sont des messages envoyés au sol aux opérateurs du PHM pour les informer de la détection d'une anormalité. À terme, les avertissements pourraient être utiles par exemple pour déclencher une surveillance plus fine. Les mises en garde et les alertes sont des messages envoyés au sol aux opérateurs de maintenance pour les informer respectivement de l'apparition d'un défaut et que la probabilité d'occurrence d'un MSCC sur l'horizon fixé a dépassé le seuil spécifié. La supervision est définie comme l'ensemble des tâches suivantes : gestion des envois d'avertissements, de mises en garde et d'alertes, assurance de la disponibilité des états de santé de chacun des moteurs à tout moment, maintenance et mise à jour de la base de précurseurs, gestion des données historiques par flotte ou par moteur et gestion des interfaces entre les acteurs du PHM. Finalement, le PHM peut être défini comme la combinaison entre HM et supervision.

Environnement et cadre fonctionnel du PHM

Un système de PHM est avant tout un processus allant de l'extraction d'IS jusqu'à l'aide à la maintenance. Parmi tous les moyens possibles pour mener à bien ce processus, le schéma **OSA-CBM** (Swearingen, et al., 2007; OSA) pour *open-system architecture for condition based maintenance* s'est progressivement imposé, entre autres à Snecma. Il est composé de sept étapes : (1) l'acquisition des données ; (2) la manipulation des données ; (3) la détection d'anormalités ; (4) l'évaluation de l'état de santé ; (5) le pronostic ; (6) l'aide à la décision et (7) la présentation des résultats. La Figure R.2 présente et détaille ces étapes en indiquant la correspondance avec les définitions proposées pour les tâches de HM et de supervision. À noter la subdivision du HM en deux sous-tâches : l'**extraction** et le **traitement** des SI.

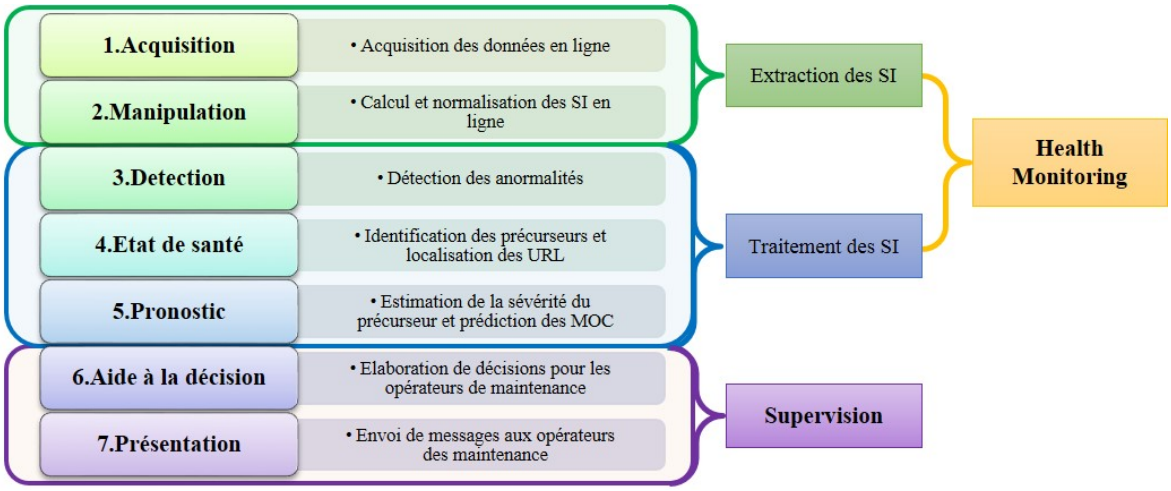


Figure R.2 *Etape du processus OAS-CBM et définitions de health monitoring et supervision.*

L'architecture d'un système hôte est définie de deux manières différentes : la **représentation fonctionnelle hiérarchique** et la **représentation structurelle hiérarchique**. La première est basée sur une segmentation en unités fonctionnelles (sous-systèmes et équipements) et la seconde sur une segmentation en unités structurelles (URL et équipements), comme schématisées sur la Figure R.3. Les **équipements** sont définis comme des entités qui sont à la fois unité fonctionnelle et unité structurelle.

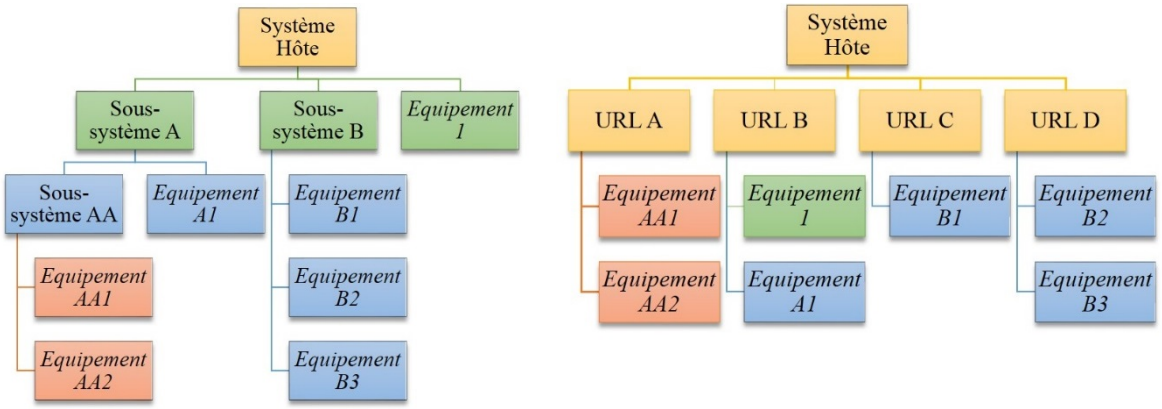


Figure R.3 *Représentations fonctionnelle hiérarchique (à gauche) et structurelle hiérarchique (à droite).*

À partir de ces deux représentations, généralement issues des documents de spécification du système hôte, la matrice d'association des URL est définie de la manière suivante : ses coefficients sont égaux à 1 si d'équipement appartient à l'URL et à 0 sinon. Ceci est illustré dans le Tableau R.2 qui correspond aux représentations données Figure R.3.

	URL A	***URL B***	***URL C***	***URL D***
Équipement AA1	**1**	0	0	0
Équipement AA2	**1**	0	0	0
Équipement A1	0	**1**	0	0
Équipement B1	0	0	**1**	0
Équipement B2	0	0	0	**1**
Équipement B2	0	0	0	**1**
Équipement 1	0	**1**	0	0

Tableau R.2 *Matrice d'association des URL.*

Comme mentionné précédemment, un système de PHM est un système de systèmes divisé entre le système de HM et le système de supervision. Dans le cadre des travaux présentés ici, seul le premier est abordé. Dans le cas des moteurs d'avions, toutes les tâches de HM ne peuvent pas être effectuées en vol. Ainsi, les tâches d'extraction et de traitement des SI sont séparées : la première est réalisée en vol par l'unité d'extraction ou EMU pour engine monitoring unit alors que la seconde est exécutée au sol par l'unité de traitement. L'unité d'extraction est le siège des calculs embarqués liés aux tâches de HM, à savoir l'enregistrement des données, la construction des IS et leur normalisation (Lacaille, 2009). L'unité de traitement est le siège des calculs liés à la détection, l'identification, la localisation et le pronostic. L'architecture des unités de traitement peut varier en fonction des applications. Dans le cas présent, on considère une architecture hiérarchique à base d'agents, dans laquelle chaque unité fonctionnelle est liée à un agent de HM qui communique avec les autres pour établir un diagnostic et un pronostic global par fusion. L'architecture d'un agent de HM est présentée Figure R.4.

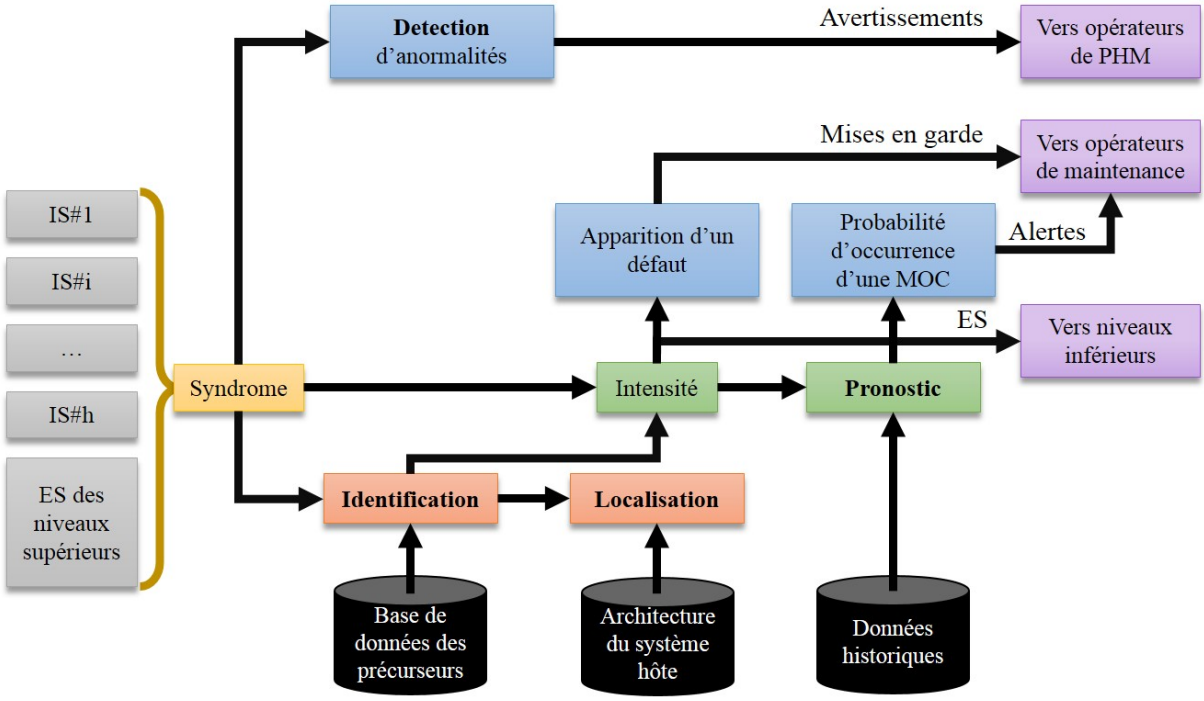


Figure R.4 *Architecture d'un agent de health monitoring.*

La définition du processus de détection des anormalités consiste en une classification binaire entre état anormal et état dégradé. Elle est effectuée par comparaison entre la valeur prise par l'IS à un instant donné et un seuil d'anormalité, la difficulté étant alors de définir la valeur de ce seuil. Les performances de la détection entre deux distributions se mesurent par les taux de vrai positif (**TP**) ou $P(\text{détection}|\text{anormal})$ et de faux positif (**FP**) ou $P(\text{détection}|\text{sain})$. Lorsque ces performances sont trop faibles pour tous les seuils possibles, il est possible de diminuer l'écart type en ajoutant une étape de confirmation. Par exemple, on peut confirmer sur k vols consécutifs, ou sur k parmi n vols. Le processus d'identification consiste à de la reconnaissance de formes, en général une classification entre le syndrome courant et la base de données des précurseurs. À Snecma, la classification est faite en calculant les probabilités de correspondance avec chaque précurseur à partir de l'angle avec le syndrome courant. Les précurseurs sont ensuite hiérarchisés suivant leur probabilité. La méthode de classification étant adoptée, la difficulté majeure restante est la construction de la base de données. En effet, l'efficacité de l'identification augmente avec la qualité et la quantité des données relatives aux précurseurs. Les

approches proposées par la communauté scientifique sont en général : les approches basées sur des modèles, les approches guidées par des mesures et les approches basées sur la connaissance (Mokhtari, 2007). Actuellement, la connaissance sert à déterminer a priori et de manière quantitative l'allure des précurseurs et les mesures en service permettent de générer leur base de données de manière quantitative pendant la phase de maturation. Comme évoqué précédemment, cette approche peut nécessiter de nombreuses années. La proposition est d'utiliser, dans le cadre de l'approche intégrée, les modèles pour alimenter de manière quantitative la base de données des précurseurs pendant les phases de conception puis de les recaler au fur et à mesure pendant la phase opérationnelle. La localisation consiste uniquement à associer les précurseurs identifiés à l'URL à laquelle ils appartiennent par la matrice d'association des URL (c.f. Tableau R.2). Finalement, le pronostic consiste à prédire l'évolution de l'intensité du mode de dégradation le plus probable. La difficulté est alors d'estimer l'allure de cette évolution en fonction du temps. Là encore, trois approches sont possibles selon que l'on se base sur l'expérience, sur les mesures ou sur les modèles (Jardine, et al., 2006). N'ayant pas de modèle de l'évolution temporelle des dégradations, l'approche choisie par les ingénieurs de Snecma est basée sur les mesures et consiste à extrapoler une tendance à partir des données historiques relatives aux IS (Lacaille, et al., 2013). Il apparaît que le développement des systèmes de PHM doit faire face à des problématiques de natures très variées nécessitant des interactions fortes avec les concepteurs du système hôte. La question du développement de ces systèmes est le sujet de la section suivante.

Approche intégrée de PHM

Dans l'industrie, et en particulier à Snecma, le développement des systèmes hôte suit le modèle en V défini par l'ingénierie des systèmes. La première branche du modèle en V correspond aux activités de conception. La seconde inclut les activités de vérification et validation (**V&V**). Ce modèle peut s'appliquer à la fois aux systèmes physiques et aux logiciels. Actuellement, le développement du PHM suit également, à l'instar du système hôte, le modèle en V. Dans la logique actuelle, les interactions entre les cycles de développement des systèmes hôte et de PHM sont limitées à quelques données clefs. La Figure R.5 schématise les modèles en V des deux systèmes. Trois données clefs sont représentées : (1) la mise à disposition des spécifications du système hôte pour définir les spécifications du PHM ; (2) l'envoi des spécifications des équipements pour la conception du PHM et (3) l'implémentation du système de PHM qui se fait au plus tard au moment de l'intégration finale du système hôte. La phase de **maturation** (Massé, et al., 2012) est définie comme le laps de temps nécessaire à récolter les données statistiques pour la validation du PHM.

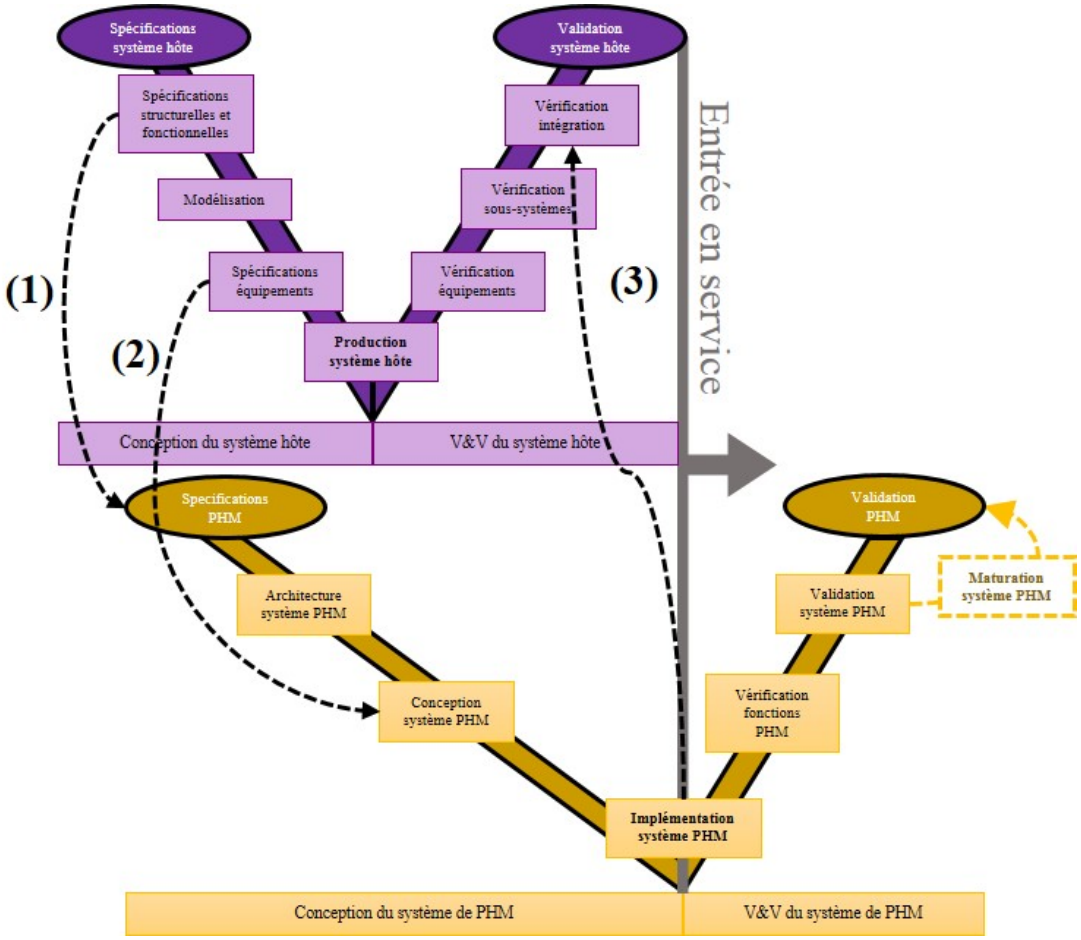


Figure R.5 *Cycles de développement actuels des systèmes hôte et de PHM.*

Dans la solution actuelle, les modèles ne sont pas utilisés, en partie parce que non adaptés aux besoins du PHM et qu'au moment de la mise en service, aucun élément du système de PHM n'ont été validés. Les problèmes liés à ce processus de développement sont les suivants :

- Il n'est pas possible, actuellement, de quantifier les effets des paramètres de contexte avant la disponibilité des premières mesures. Par conséquent, la normalisation risque d'être inefficace.
- Avant l'apparition de toutes les menaces au service conforme, la base de données des précurseurs est incomplète et l'identification risque d'être impossible.
- Sans mesure, il est impossible de calculer les valeurs limites médianes (VLM) et donc d'évaluer l'intensité des modes de dégradation.
- Il n'y a actuellement aucun moyen d'évaluer la qualité du jeu d'IS avant l'apparition de toutes les menaces au service conforme. De plus, ces dernières doivent avoir eu lieu plusieurs fois pour permettre une analyse statistique. Ce processus peut nécessiter plusieurs années.

Dans le but d'améliorer le développement du PHM, nous proposons un nouveau processus basé sur une ségrégation entre les tâches relatives à l'extraction des IS, au traitement des IS et à la supervision. Chacune fait l'objet d'un cycle en V distinct. Ces trois processus de développement indépendants sont ensuite imbriqués pour former le V3 modèle présenté en Figure R.6.

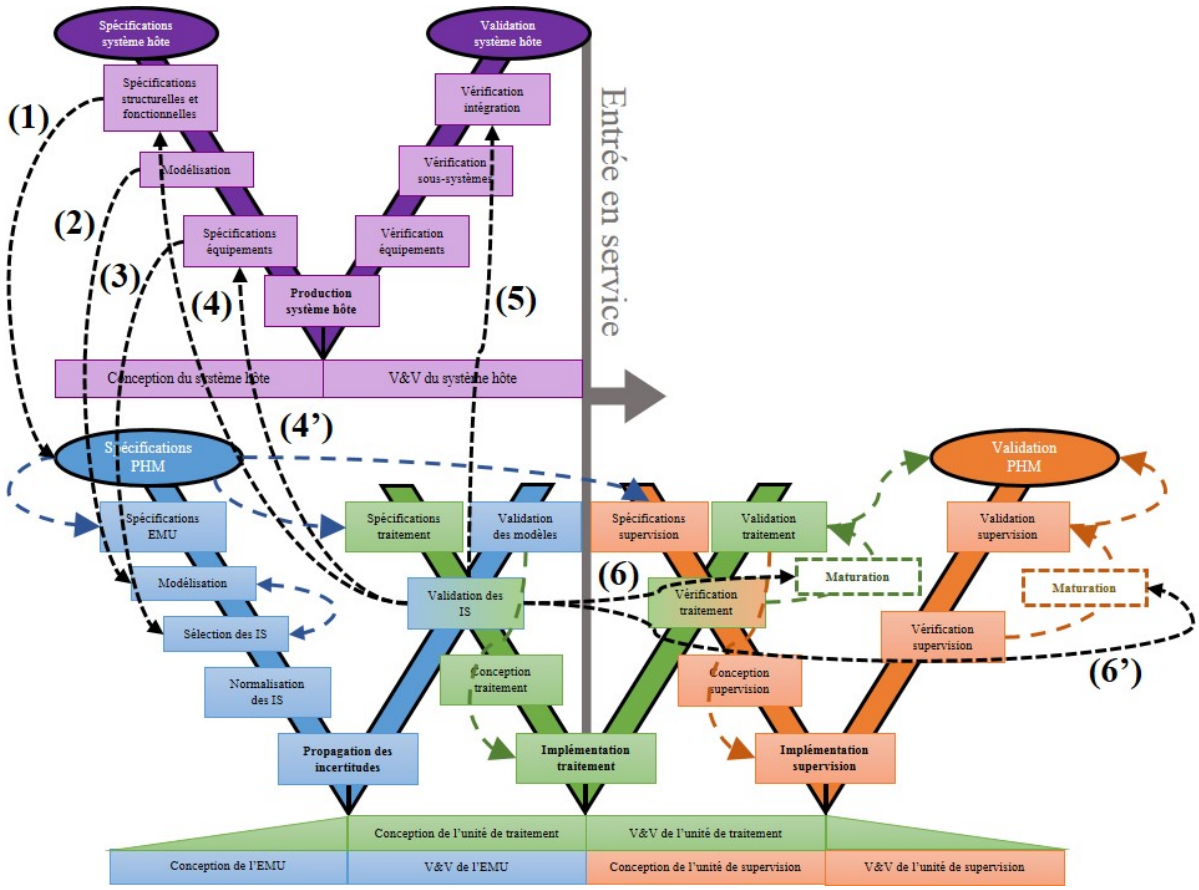


Figure R.6 *Cycles de développement futurs des systèmes hôte et de PHM.*

Les données clefs du V3 modèle présenté sur la Figure R.6 sont les suivantes : (1) les spécifications du système de PHM sont dérivées de celles du système hôte ; (2) les modèles utilisés pour le système hôte sont utilisés par les concepteurs du PHM ; (3) la sélection des IS est réalisée principalement à partir des spécifications des équipements ; (4a) et (4b) la validation des IS avant la mise en service permet un feed-back sur la conception du système hôte, par exemple pour ajouter des capteurs ou en modifier les caractéristiques ; (5) la validation du système hôte doit débuter après que les IS ont été validés et (6a) et (6b) la validation des IS permet à la fois de compléter la base de données des précurseurs et de calculer les VLM en amont de la mise en service, ce qui permet de réduire la durée de la phase de maturation.

Finalement, ce premier chapitre a permis d'introduire en détail les spécificités du PHM appliqué aux moteurs d'avion. Une nouvelle terminologie en phase avec les pratiques industrielles actuelles a été proposée. De plus, l'environnement du PHM dédié aux moteurs d'avions ainsi que le cadre fonctionnel ont été définis. Finalement, une nouvelle approche de développement appelé développement intégré a été proposée afin de combler certaines lacunes de l'approche actuelle. En particulier, cette approche intégrée incorpore une ségrégation entre tâches embarquées et tâches réalisées au sol. Son atout majeur est de permettre le développement complet, incluant la validation, des IS dès les phases de conception du système hôte.

Chapitre 2 : développement des IS en phases de conception

Ce second chapitre est dédié au développement de la partie embarquée, ou de l'extraction des indicateurs de santé. Ainsi, seul le premier V du modèle V3 est considéré. Il est présenté sur la Figure

R.7. Le modèle en V complet doit être réalisé pendant les phases de conception, exception faite de la validation du modèle qui est réalisée à partir d'un recalage par rapport aux premières mesures disponibles. Cette dernière partie n'est pas traitée dans le cadre de cette thèse.

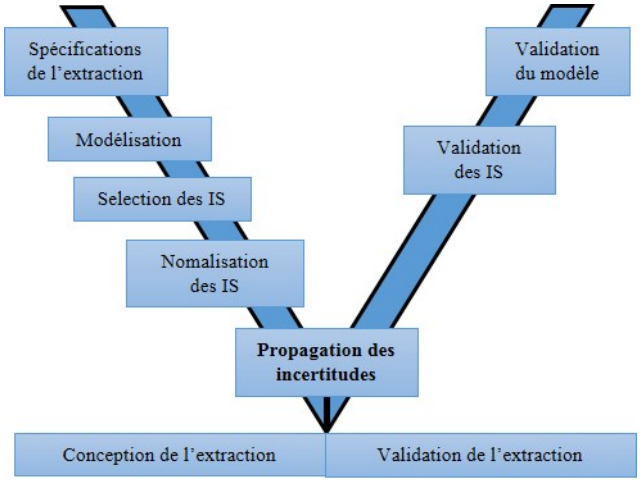


Figure R.7 *Modèle en V de la partie embarquée seule.*

La première section est dédiée à la sélection des IS. Elle propose en premier lieu un formalisme mathématique pour la modélisation adapté aux spécificités des modèles utilisés. La méthodologie de sélection est ensuite présentée. Elle est fondée principalement sur les connaissances relatives au système hôte et sur la modélisation. La seconde section est dédiée à la normalisation des IS. Elle propose une nouvelle approche utilisant à la fois l'analyse de sensibilité (**AS**) et la régression par vecteur supports (**SVR**). Enfin, la dernière section est centrée sur le processus de validation des IS en phases de conception. Sa contribution majeure est de proposer un ensemble d'indicateurs numériques de performances (**NKPI**) pour évaluer l'efficacité *a priori* des IS pour les tâches de détection, identification, localisation et pronostic.

Sélection des IS

La sélection des IS consiste à déterminer un ensemble de variables ayant une forte sensibilité aux modes de dégradation et une faible sensibilité aux variations dues aux incertitudes de contexte ou dimensionnelles. Comme la méthodologie de sélection des IS présentée par la suite nécessite de simuler la réactivité des IS aux différents modes de dégradation, le premier point abordé dans cette section est le formalisme mathématique des modèles physiques. Les modèles sont représentés par la fonction déterministe $\mathbb{f}$ suivante :

$$\boldsymbol{Y} = \mathbb{f}(\boldsymbol{U}, \rho_1, \dots, \rho_p) \qquad \textbf{(r.1)}$$

où $\boldsymbol{U}$ et $\boldsymbol{Y}$ sont, respectivement, les matrices des signaux temporels d'entrée et de sortie et $\rho_1, \dots, \rho_p$ sont les paramètres du modèle. Dans le but de clarifier cette représentation, l'ensemble des paramètres est divisé en trois catégories : les paramètres de contexte, épistémiques et de dégradation. Sous cette hypothèse, l'équation **(r.1)** peut être écrite :

$$\boldsymbol{Y} = \mathbb{f}\left(\boldsymbol{U}, \underline{\gamma}, \underline{\lambda}, \underline{\omega}^0 + \underline{\delta}\right) \qquad \textbf{(r.2)}$$

où $\underline{\gamma}$ et $\underline{\lambda}$ sont les vecteurs des paramètres, respectivement, épistémiques et de contexte, $\underline{\omega}^0$ est la condition nominale du système et $\underline{\delta}$ est le vecteur des paramètres de dégradation. Dans le cadre de ces

travaux, on ne considère que des dégradations simples, c'est-à-dire n'affectant qu'un paramètre de dégradation à la fois. On définit alors le mode et la valeur d'une dégradation de la manière suivante :

$$\text{Mode}(\underline{\delta}) = \frac{\underline{\delta}}{\|\underline{\delta}\|^{\mathcal{D}}}, \text{Valeur}(\underline{\delta}) = \|\underline{\delta}\|^{\mathcal{D}} \qquad \textbf{(r.3)}$$

Nous proposons ensuite de définir les espaces des vecteurs des indicateurs de santé $\underline{\varphi} = |\varphi_1 \quad \cdots \quad \varphi_h|^T$ et des indicateurs de service conforme $\underline{\psi} = |\psi_1 \quad \cdots \quad \psi_o|^T$ comme les images de la matrice de sortie $\boldsymbol{Y}$ par les fonctions d'extraction $\mathcal{g}$ et $\mathcal{h}$ telles que :

$$\begin{cases} \underline{\varphi} = \mathcal{g}(\boldsymbol{Y}) \\ \underline{\psi} = \mathcal{h}(\boldsymbol{Y}) \end{cases} \qquad \textbf{(r.4)}$$

Le modèle déterministe $\mathcal{M}$ schématisé sur la Figure R.8, est défini par la fonction suivante :

$$\left(\underline{\varphi}, \underline{\psi}\right) = \mathcal{M}(\boldsymbol{U}, \underline{\rho}) \qquad \textbf{(r.5)}$$

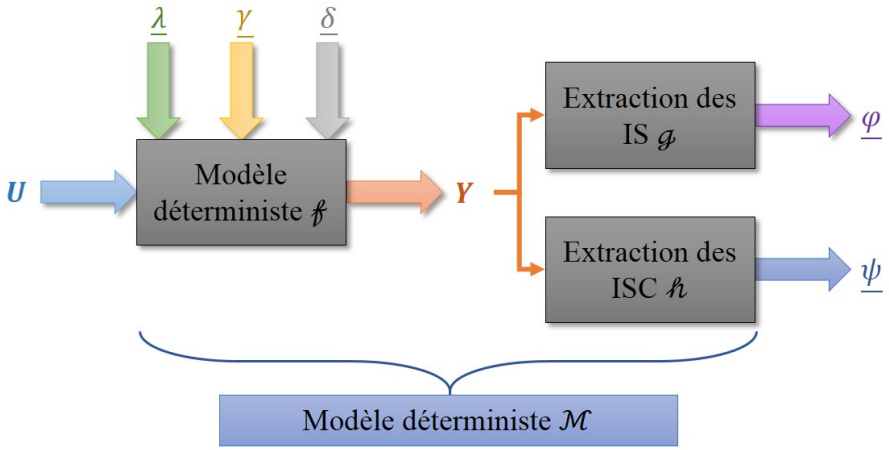


Figure R.8 *Schéma du modèle déterministe $\mathcal{M}$ avec extraction des IS et ISC.*

Dans le cadre de ces travaux, l'étude est limitée aux impacts des paramètres sur les indicateurs. Ainsi, l'impact du profil des signaux d'entrée n'est pas considéré. Nous avons donc choisi de déterminer un unique profil caractéristique pour chacune des entrées temporelles à partir de retour d'expérience sur des moteurs similaires. Ce profil sera ensuite constant d'une simulation à l'autre. Le modèle finalement obtenu est appelé modèle à entrées temporelles constantes et est défini de la manière suivante :

$$\underline{\chi} = \mathcal{M}_{\boldsymbol{U}}(\underline{\rho}) \qquad \textbf{(r.6)}$$

où $\underline{\chi} = |\underline{\varphi} \quad \underline{\psi}|^{\boldsymbol{t}}$ est le vecteur des indicateurs. Le modèle à entrées temporelles constantes est schématisé sur la Figure R.9.

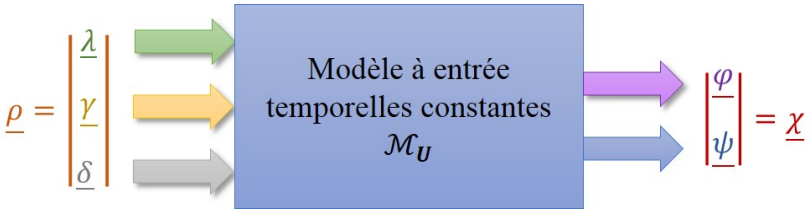


Figure R.9 *Schéma du modèle déterministe à entrées temporelles constantes $\mathcal{M}_{\boldsymbol{U}}$.*

Dans le cas de systèmes soumis à des conditions opérationnelles réelles, les paramètres sont rarement déterministes. La plupart sont associés à des incertitudes qui peuvent être définies sous forme de densités de probabilité (**PDF**). La gestion des incertitudes se fait en deux étapes (De Rocquigny, et al., 2007). Dans un premier temps, la localisation des incertitudes consiste à déterminer la liste des paramètres incertains. Dans un second temps, la quantification des incertitudes consiste à définir les PDF de chacun des paramètres incertains. Cette seconde étape peut être très coûteuse en temps et en argent dans les cas où une grande quantité d'information est nécessaire pour caractériser les PDF. Pour le modèle à entrées temporelles constantes considéré, la manière de gérer les incertitudes dépend du type de paramètre considéré :

- **Paramètres de contexte** : comme le contexte est assez similaire entre deux moteurs, des données issues de retours d'expériences sont utilisées.
- **Paramètres épistémiques** : ce sont en majorité des paramètres dimensionnels dont les intervalles de variations peuvent être déterminés à partir des spécifications des équipements.
- **Paramètres de dégradation** : ils sont fixes pour l'évaluation d'une distribution donnée, mais varient entre deux ensembles de Monte-Carlo.

La sélection des IS est effectuée de manière hiérarchique à partir du niveau équipement jusqu'au niveau système. La procédure de sélection se fait, pour chaque unité fonctionnelle cible, en 5 étapes : (1) énumération des menaces au service conforme cibles et définition des indicateurs de service conforme associés ; (2) inventaire des modes de dégradation cibles ; (3) construction des indicateurs de santé ; (4) prototypage sur modèles physiques pour évaluer la sensibilité des IS aux différents modes de dégradation et (5) présentation aux experts pour approbation du jeu d'indicateur initial.

La sélection se fait à partir de plusieurs sources d'informations appelées données clefs. Ainsi, la définition des unités fonctionnelles cibles se fait à partir des spécifications du système hôte. La liste des menaces au service conforme cibles est établie principalement à partir des spécifications des built-in tests et des analyses des modes de défaillance, de leurs effets et de leur criticité (**AMDEC**) (Megill, 1984). Concernant les modes de dégradation cibles, ils sont identifiés par retour d'expériences, expertises ou considérations basées sur la physique du système. Enfin, la construction des IS à proprement parler peut être supervisée par l'analyse des procédures de tests d'acceptation (**ATP**) des équipements. Par ailleurs, ces tests étant utilisés pendant les opérations de maintenance, ils sont déjà utilisés et maîtrisés par les opérateurs de maintenance. En phase opérationnelle, la construction des IS utilise des variables disponibles en temps réel. Ce sont des indicateurs de santé réels. Cependant, pendant les phases de conception, il est possible de définir des indicateurs de santé virtuels qui sont construits à partir de variables simulées dont la disponibilité n'est pas prévue. Cela permet d'opérer un retour d'expérience vers la conception du système hôte pour spécifier une modification de la configuration des capteurs dans le but d'améliorer le jeu d'IS en y ajoutant les ISV.

Normalisation des IS

L'objectif de la normalisation des IS est de réduire leur variabilité pour améliorer les performances en détection. Le principe est de soustraire les effets dus aux paramètres de contexte et épistémiques mesurables lors du calcul des IS. La normalisation se fait en deux étapes : l'identification des paramètres de normalisation et la modélisation des effets. Pour l'application présente, une nouvelle approche basée sur l'AS et la SVR est proposée.

L'analyse de sensibilité consiste à étudier la variabilité des sorties d'un modèle ou d'un système par rapport aux incertitudes sur les entrées (Iooss, 2011). Elle consiste en général à mesurer des indices de sensibilité. Dans le cadre de ces travaux de thèse, ces indices permettent de classer les paramètres en fonction de leur effet sur les sorties. Ainsi, les **paramètres influentials** sont définis comme des paramètres ayant un effet significatif sur au moins une des sorties du modèle. À l'inverse, les **paramètres marginaux** ont un effet négligeable sur toutes les sorties et sont considérés comme déterministes. Ces derniers sont ainsi fixés à leur valeur nominale. La différence entre significatif et négligeable est généralement définie par un seuil sur un indice de sensibilité. Certaines méthodes d'AS comme la méthode de Morris (Morris, 1991) définie plus loin permettent d'évaluer le niveau de linéarité des effets et de séparer les paramètres influentials entre **paramètres linéaires** et **paramètres non linéaires**. Les premiers ont un effet linéaire par rapport à toutes les sorties alors que les seconds ont un effet non linéaire par rapport à au moins une des sorties. Cette distinction permet d'alléger le nombre de points de calcul nécessaire puisque dans le cas des paramètres linéaires deux points suffisent. Enfin, une distinction est également faite, pour chaque sortie, entre les **paramètres principaux** et les **paramètres auxiliaires**. Ils sont définis comme l'ensemble des paramètres influentials ayant les effets, respectivement, les plus et les moins importants sur la sortie considérée. Sous ce formalisme, un modèle $\mathcal{M}_{\boldsymbol{U}}^{j}$ est défini pour chacune des sorties $j = 1, \dots, h + o$ (IS et ISC), elles mêmes définies de la sorte :

$$\chi_j = \mathcal{M}_{\boldsymbol{U}}^{j}\left(\underline{\rho}_j^{np}, \underline{\rho}_j^{lp}, \underline{\rho}_j^{na}, \underline{\rho}_j^{la}, \underline{\rho}^{*}\right), \qquad j = 1, \dots, h + o \qquad \textbf{(r.7)}$$

avec $\underline{\rho}_j^{np}$ et $\underline{\rho}_j^{lp}$ les paramètres principaux, respectivement non linéaires et linéaires, $\underline{\rho}_j^{na}$ et $\underline{\rho}_j^{la}$ les paramètres auxiliaires, respectivement non linéaires et linéaires et $\underline{\rho}^{*}$ les paramètres fixes. Enfin, les paramètres de normalisation sont définis pour chacun des IS comme des paramètres influentials et mesurables. La normalisation ne touchant pas les ISC, on peut écrire :

$$\varphi_j = \mathcal{M}_{\boldsymbol{U}}^{j}\left(\underline{\rho}_j^{ns}, \underline{\rho}_j^{ls}, \underline{\rho}_j^{nu}, \underline{\rho}_j^{lu}, \underline{\rho}_j^{na}, \underline{\rho}_j^{la}, \underline{\rho}^{*}\right), \qquad j = 1, \dots, h \qquad \textbf{(r.8)}$$

où $\left(\underline{\rho}_j^{ns}, \underline{\rho}_j^{ls}\right)$ sont les paramètres de normalisation non-linéaires et linéaires et $\left(\underline{\rho}_j^{nu}, \underline{\rho}_j^{lu}\right)$ sont les paramètres inconnus non linéaires et linéaires pour la sortie j.

Il existe deux principaux types d'approche pour l'analyse de sensibilité : les méthodes locales (Saltelli, et al., 2000) et globales. Les premières sont basées sur le calcul de dérivées partielles. Elles visent à examiner des petites perturbations sur des zones précises de l'espace des entrées. Les secondes ont pour but d'étudier les effets des entrées sur la totalité de l'espace. Dans le cadre de ces travaux de thèse, seules les méthodes globales sont utilisées car on souhaite caractériser l'influence des paramètres sur les HIs sur l'ensemble de leurs domaines de variation. Elles sont subdivisées en deux catégories : les méthodes de criblage, typiquement utilisées pour gérer un très grand nombre d'entrées (atour de cent ou plus) et les méthodes quantitatives, principalement basées sur la décomposition de la variance. Pour chacune de ces approches, une méthode est présentée en détail : la méthode de Morris (Morris, 1991) pour le criblage et le calcul des indices de Sobol (Sobol, 1993) pour les approches quantitatives.

- **La méthode de Morris :**

Elle est généralement utilisée pour effectuer une exploration rapide, mais assez grossière d'un modèle de grande dimension. Le principe est de répéter plusieurs fois un plan d'expérience one-at-a-time (OAT). Un PE OAT consiste à faire varier chaque paramètre indépendamment en tirant

aléatoirement le point initial et la progression séquentielle. Pour chacune des r répétitions, on calcule un effet élémentaire $E_i^{(k)}$ comme la différence entre deux sorties successives. À partir de ces $E_i^{(k)}$, les variables suivantes sont obtenues :

$$\mu_i = \sum_{i=1}^{r} E_i^{(k)} \; ; \; \mu_i^* = \sum_{i=1}^{r} \left| E_i^{(k)} \right| ; \; \sigma_i \; = \sqrt{\frac{\sum_{k=1}^{r} \left(E_i^{(k)} - \mu_i \right)}{r}} \qquad \textbf{(r.9)}$$

où $\mu_i = \sum_{k=1}^{r} E_i^{(k)}$, μ_i^* et σ_i sont, respectivement, la moyenne, la moyenne absolue et l'écart type. Les résultats sont alors classés en trois catégories : les paramètres aux effets négligeables (μ_i^* et σ_i proche de zéro), ceux ayant des effets linéaires (μ_i^* avec valeur non négligeable et σ_i proche de zéro) et ceux ayant des effets non linéaires ou avec interactions (μ_i^* et σ_i non négligeables). Dans le but d'apporter un aspect quantifiable, on peut utiliser les indices DGSM (derivative-based global sensitivity measures) (Sobol, et al., 2009) ν_j qui peuvent être estimés à partir des effets élémentaires de la manière suivante :

$$\widehat{\nu_j} = \frac{1}{r} \sum_{r=1}^{n} \left(\frac{\partial \ell(E_i^{(r)})}{\partial x_j} \right)^2 , \qquad j = 1, \dots, n \qquad \textbf{(r.10)}$$

Dans le but de gérer l'aspect multi sorties des modèles utilisés dans le cadre de cette thèse, deux indices de sensibilité basés sur les variables introduites ci-dessus sont utilisées : l'indice d'effet total Tot_i reflétant l'importance du paramètre i sur l'ensemble des sorties et l'indice de linéarité Lin_i traduisant le niveau de linéarité moyen de ses relations avec les sorties. Il sont définis de la sorte :

$$\begin{aligned} Tot_i &= \frac{\sum_{j=1}^{m} \hat{v}_{i,j}}{M_i} \in [0\,,1] \text{ avec } M_i = \max_j \left\{ \sum_{j=1}^{m} \hat{v}_{i,j} \right\} \\ Lin_i &= 1 - \frac{\sum_{j=1}^{h} \sigma_{i,j}}{A_i} \in [0\,,1] \text{ avec } A_i = \max_j \left\{ \sum_{j=1}^{m} \sigma_{i,j} \right\} \end{aligned} \qquad \textbf{(r.11)}$$

où $\hat{v}_{i,j}$ et $\sigma_{i,j}$ sont définis, respectivement, comme l'estimation de l'indice DGSM et l'écart type des effets élémentaires calculés pour le couple (entrée i/sortie j). Ces indices sont utilisés dans la procédure de normalisation introduite par la suite.

- **Indices de Sobol :**

Les indices de Sobol sont basés sur la décomposition fonctionnelle de la variance qui peut être exprimée de la manière suivante (Sobol, 1993) :

$$Var(y) = \sum_{i=0}^{n} V_i(y) + \sum_{i<j}^{n} V_{ij}(y) + \sum_{i<j<k}^{n} V_{ijk}(y) + \dots + V_{12\dots n}(y) \qquad \textbf{(r.12)}$$

avec $V_i(y) = Var[\mathbb{E}(y|x_i)], V_{ij}(y) = Var\left[\mathbb{E}\left(y|x_i x_j\right)\right] - V_i(y) - V_j(y)$, *etc*… Les indices de Sobol sont alors définis de la manière suivante :

$$S_i = \frac{Var[\mathbb{E}(y|x_i)]}{Var(y)} = \frac{V_i(y)}{Var(y)} \qquad S_{ij} = \frac{V_{ij}(y)}{Var(y)} \qquad S_{ijk} = \frac{V_{ijk}(y)}{Var(y)} \quad \dots \qquad \textbf{(r.13)}$$

Pour chacun de ces indices de Sobol, la somme sur le nombre d'entrées est égal à 1. Pour exprimer l'effet global d'une entrée sur une sortie, on peut utiliser les indices totaux définis de la sorte :

$$S_{Ti} = S_i + \sum_{j \neq i}^{n} S_{ij} + \sum_{j \neq i, k \neq i, j<k}^{n} S_{ijk} + \ldots = \sum_{l \in \#i} S_l \qquad \textbf{(r.14)}$$

où $\#i$ désigne l'ensemble des sous-espaces indices contenant i. En pratique, quand la dimension est élevée, on calcule juste les indices de premier ordre S_i et les indices totaux. Les indices des Sobol peuvent être estimés par une méthode dite de Monte-Carlo présentée en section 2.3.1.6. L'inconvénient de cette méthode est qu'elle nécessite un très grand nombre d'évaluations du modèle (environ 10 000 pour atteindre une précision de 10%). Ainsi, dans les cas où le modèle a un temps de simulation conséquent, cette approche n'est pas envisageable. Une des solutions à ce problème est d'utiliser des métamodèles, fonctions analytiques à faible temps de calcul approximant les sorties d'un modèle. Ils sont présentés en détail dans le chapitre 3.

Finalement, du fait de son faible coût en temps de calcul, la méthode de Morris est utilisée en premier pour identifier les paramètres influentials et déterminer ceux qui sont linéaires. Les indices de Sobol sont ensuite calculés à partir d'un métamodèle et utilisés pour différentier les paramètres principaux des paramètres auxiliaires.

La régression par vecteurs de supports, ou SVR, est une méthode de régression basée sur la théorie des machines à vecteurs de support (Vapnik, et al., 1997). Le principe de base de la SVR est de trouver une fonction $\mathcal{S}$ avec au plus une déviation ε par rapport à chacun des points d'apprentissage. Dans le cas linéaire, l'estimation par SVR $\mathcal{S}$ d'une fonction au point $\underline{s}$ est donnée par (Smola, et al., 2004) :

$$\mathcal{S}(\underline{s}) = \langle \underline{w} \cdot \underline{s} \rangle + b \qquad \textbf{(r.15)}$$

où $\langle \underline{a} \cdot \underline{b} \rangle$ est le produit scalaire entre les vecteurs $\underline{a}$ et $\underline{b}$. Par ailleurs, on souhaite que $\mathcal{S}$ soit la plus platte possible. La platitude signifie en l'occurrence une petite valeur pour $\underline{w}$. Cela suppose l'existence d'une fonction capable d'estimer tous les couples avec une précision ε, ce qui n'est pas garanti. Pour relâcher cette contrainte, on définit les variables η_i et η_i^* destinées à introduire une marge d'erreur. Il vient le problème d'optimisation suivant :

$$\text{Minimiser } \frac{1}{2} \left|\underline{w}\right|^2 + C \sum_{i=1}^{k} (\eta_i + \eta_i^*)$$

$$\text{sous contraints de } \begin{cases} y_i - \langle \underline{w} \cdot \underline{x_i} \rangle - b \leq \varepsilon + \eta_i \\ \langle \underline{w} \cdot \underline{x_i} \rangle + b - y_i \leq \varepsilon + \eta_i^* \\ \eta_i, \eta_i^* \geq 0 \end{cases} \qquad \textbf{(r.16)}$$

où $C > 0$ est un coefficient déterminant le poids entre la platitude et le degré avec lequel les déviations supérieures à η_i (en positif) ou η_i^* (en négatif) sont tolérées. L'estimateur par SVR à un point $\underline{s}$ s'exprime finalement comme une combinaison linéaire de produits scalaires avec les vecteurs supports, ces derniers étant définis comme les points utilisés effectivement pour l'apprentissage de l'estimateur SVR. Dans le cas présent, les modèles utilisés étant déterministes, tous les points d'apprentissage sont des vecteurs supports. Dans le cas où le problème est non-linéaire, une fonction noyau est utilisée pour le

transposer dans un espace de dimension supérieure où il devient linéaire. Finalement, l'estimation SVR $\mathcal{S}(\underline{s})$ à un point $\underline{s}$ est exprimée de la manière suivante :

$$\mathcal{S}(\underline{s}) = \sum_{i=1}^{k} \alpha_i k\left(\underline{\xi}, \underline{x}_i, \underline{s}\right) \qquad \textbf{(r.17)}$$

avec $\underline{x}_i$ les vecteurs supports, κ la fonction noyau et α_i les coefficients de régression. Ces derniers peuvent être estimés par moindres carrés via :

$$\underline{\alpha} = (\boldsymbol{G^t G})^{-1} \boldsymbol{G^t} \underline{y} \qquad \textbf{(r.18)}$$

où $\underline{y} = [y_1 \quad \cdots \quad y_n]^T$ est le vecteur des réponses du modèle pour les vecteurs supports. Un exemple d'estimation par SVR pour un problème non linéaire est donné en Figure R.10.

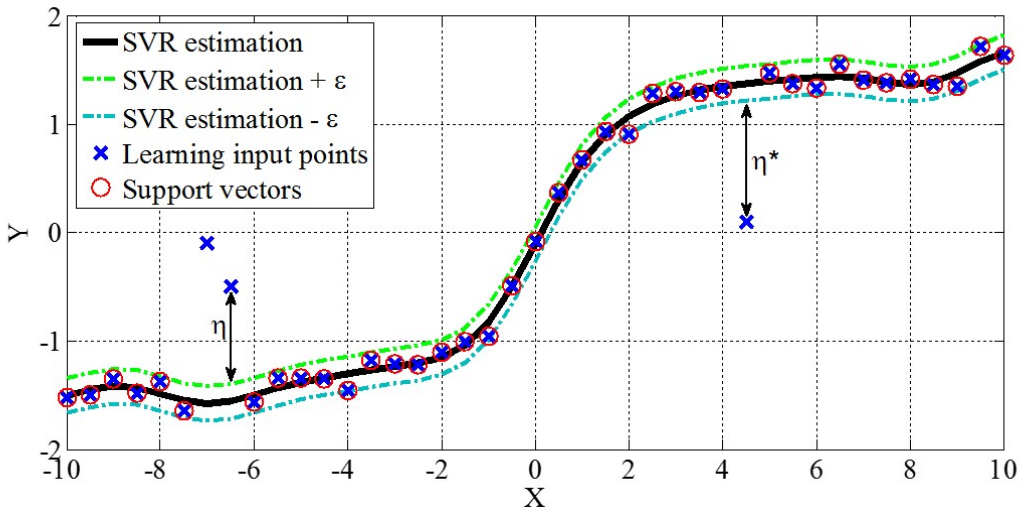


Figure R.10 *Estimation SVR pour un cas non linéaire.*

L'avantage majeur de la SVR est qu'elle permet une estimation de comportements non linéaire sans nécessiter de connaissance *a priori* sur la forme de la fonction. En contrepartie, cette estimation n'est possible que sur le domaine couvert par les points d'apprentissage, ce qui implique d'avoir bien défini les plages de variation des entrées.

Finalement, la procédure de normalisation consiste à déterminer, pour chaque indicateur de santé (IS) φ_j, l'ensemble des paramètres de normalisation puis à apprendre les modèles SVR de normalisation $\mathcal{S}^j$ estimant les valeurs de φ_j. Les valeurs normalisées des IS sont alors les résidus entre les mesures réelles et leur estimation par les modèles de normalisation :

$$\varphi_j^{sTd} = \varphi_j - \hat{\varphi}_j^{svr}, \qquad j = 1, \ldots, h \qquad \textbf{(r.19)}$$

Par hypothèse, les effets d'interaction entre paramètres sont faibles. On choisit donc d'utiliser des SVR mono dimensionnelles. Ainsi, seuls les effets du premier ordre sont modélisés. L'estimé $\hat{\varphi}_j^{svr}$ est alors calculé de la manière suivante :

$$\hat{\varphi}_j^{svr} = \mathcal{S}_1^j(\rho_{j1}^{ns}) + \ \ldots + \mathcal{S}_{a_j}^j\left(\rho_{ja_j}^{ns}\right) + \mathcal{S}_{a_j+1}^j(\rho_{j1}^{ls}) + \ \ldots + \ \mathcal{S}_{c_j}^j\left(\rho_{jb_j}^{ls}\right), j = 1, \ldots, h \qquad \textbf{(r.20)}$$

où $\underline{\rho_j^{ns}} = \left[\rho_{j,1}^{ns} \quad \cdots \quad \rho_{j,a_j}^{ns}\right]^T$, $\underline{\rho_j^{ls}} = \left[\rho_{j,1}^{ls} \quad \cdots \quad \rho_{j,b_j}^{ls}\right]^T$, a_j, b_j sont les nombres de paramètres de normalisation, respectivement, non-linéaires et linéaires pour le $j^{ème}$ IS, les $\mathcal{S}_i^j, (i,j) \in [\![1; c_j]\!] \times [\![1; h]\!]$ sont les modèles SVR individuels associés à chaque dimension et $c_j = a_j + b_j$. Finalement, pour chaque couple (i,j), l'estimation $\mathcal{S}_i^j(\underline{s})$ s'écrit :

$$\mathcal{S}_i^j(\underline{s}) = \left[k_i(\xi_i, x_i^1, \underline{s}) \quad \cdots \quad k_i(\xi_i, x_i^{l_i}, \underline{s})\right]\underline{\alpha_{ij}} \qquad \textbf{(r.21)}$$

où $k_i, i = 1, \dots, n$ sont les fonctions noyaux et $\underline{x_i} = \left[x_i^1 \cdots x_i^{l_i}\right]^T, i = 1, \dots, n$ sont les vecteurs d'apprentissage pour chaque dimension.

Nous proposons d'utiliser les valeurs de Lin_i pour superviser le choix des fonctions noyaux et des tailles l_i des vecteurs d'apprentissage. Ainsi, pour des valeurs élevées de Lin_i, on choisira un nombre restreint de points d'apprentissage, par exemple 3, suffisant pour estimer un comportement linéaire, et un noyau linéaire. À l'inverse, pour des valeurs faibles de Lin_i, on choisira plus de points, par exemple 5, et un noyau RBF (radial basis functions).

Validation des IS

Afin de valider les IS, nous proposons un ensemble de métriques appelées NKPI pour numerical key performance indicators. Ils permettent d'évaluer les performances des IS pour détecter les anormalités, identifier les précurseurs, localiser les URL et pronostiquer les menaces au service conforme.

- **NKPI pour la détection :**

Deux NKPI sont définis pour la détection : la **détectabilité globale** et la **détectabilité conforme**. Ils sont tous les deux calculés à partir des courbes de caractéristiques opérationnelles de réception (**COR**) nécessitant de connaître les distributions des IS aux états sains et dégradés. On suppose dans cette section que ces distributions sont disponibles. On notera T_i^0 la distribution saine associée au $i^{ème}$ IS et $T_{i,j}^k$ la distribution de cet IS pour le $j^{ème}$ mode de dégradation d'intensité k. Pour deux distributions quelconques T et T', la détectabilité globale (**GD**) est définie de la manière suivante :

$$GD(T, T') = 2 \times AUC(ROC(T, T')) - 1 \qquad \textbf{(r.22)}$$

où $ROC(.)$ est la fonction définissant la courbe COR entre deux distributions et $AUC(.)$ est la fonction calculant l'aire sous la courbe (Bradley, 1997). La matrice de détectabilité globale $\boldsymbol{GDx}$ est ensuite définie de la sorte :

$$\boldsymbol{GDx} = \begin{vmatrix} GD\left(T_1^0, T_{1,1}^1\right) & \dots & GD\left(T_h^0, T_{h,1}^1\right) \\ \vdots & \ddots & \vdots \\ GD\left(T_1^0, T_{1,d}^1\right) & \dots & GD\left(T_h^0, T_{h,d}^1\right) \end{vmatrix} \in [0; 1]^{d \times h} \qquad \textbf{(r.23)}$$

Dans le cadre du développement intégré, les spécifications portent sur le taux minimal de bonnes détections (**TP**) et le taux maximal de fausses alarmes (**FP**), notés respectivement TP_{SPEC} et FP_{SPEC}. On définit alors le point de conformité comme le point ayant pour coordonnées (FP_{SPEC}, TP_{SPEC}). La détectabilité conforme (**CD**) est définie par :

$$CD(T, T') = \begin{cases} 1 \; si \; ROC(T, T') \; est \; au \; dessus \; du \; point \; de \; conformité \\ 0 \; si \; ROC(T, T') \; est \; en \; dessous \; du \; point \; de \; conformité \end{cases} \qquad \textbf{(r.24)}$$

La Figure R.11 présente deux courbes COR avec le point de conformité pour un cas où $CD = 0$ (à gauche) et un cas ou $CD = 1$ (à droite).

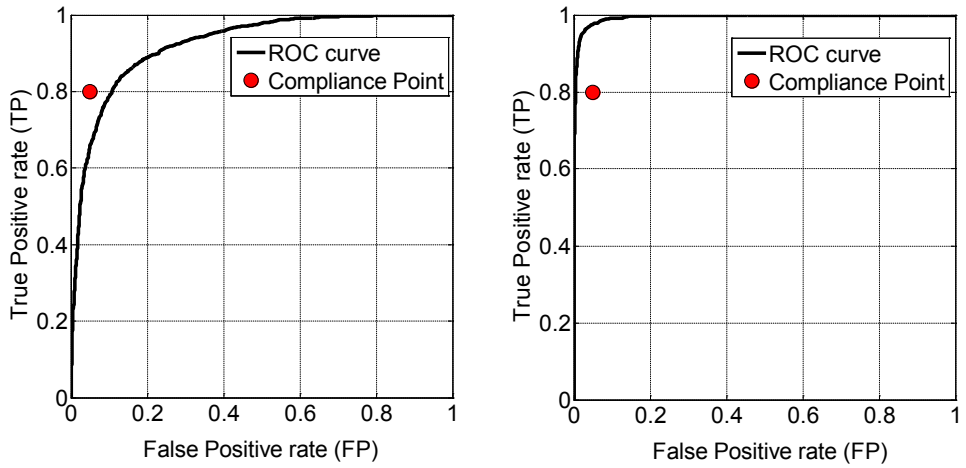


Figure R.11 *Point de conformité (compliance point) et courbe COR pour un cas de non-conformité (gauche) et un cas de conformité (droite).*

La matrice de détectabilité conforme est finalement définie par :

$$\boldsymbol{CDx} = \begin{vmatrix} CD\left(T_1^0, T_{1,1}^1\right) & \dots & CD\left(T_h^0, T_{h,1}^1\right) \\ \vdots & \ddots & \vdots \\ CD\left(T_1^0, T_{1,d}^1\right) & \dots & CD\left(T_h^0, T_{h,d}^1\right) \end{vmatrix} \in \{0,1\}^{d \times h} \quad \textbf{(r.25)}$$

Un mode de dégradation (**MD**) est dit *a priori* détectable si la ligne associée de $\boldsymbol{CDx}$ est non nulle. Nous définissons alors le critère de détectabilité $DTDEM_{\%}$ comme le ratio du nombre de MD *a priori* détectables sur le nombre total de MD.

- **NKPI pour l'identification :**

Dans le cas de l'identification, on définit tout d'abord la matrice de variation $\boldsymbol{V}_k$:

$$\boldsymbol{V}_k = \begin{vmatrix} s\left(m\left(T_{1,1}^k\right) - m\left(T_1^0\right)\right) GD\left(T_1^0, T_{1,1}^k\right) & \cdots & s\left(m\left(T_{h,1}^k\right) - m\left(T_h^0\right)\right) GD\left(T_h^0, T_{h,1}^k\right) \\ \vdots & \ddots & \vdots \\ s\left(m\left(T_{1,d}^k\right) - m\left(T_1^0\right)\right) GD\left(T_1^0, T_{1,d}^k\right) & \cdots & s\left(m\left(T_{h,d}^k\right) - m\left(T_h^0\right)\right) GD\left(T_h^0, T_{h,d}^k\right) \end{vmatrix} \in [-1;1]^{d \times h} \quad \textbf{(r.26)}$$

où $m(.)$ est la fonction médiane, $s(.)$ est la fonction signe et $\underline{v}_k^j$ est définie comme la $j^{ème}$ ligne of $\boldsymbol{V}_k$. Ce dernier est appelé vecteur de variation et correspond au $j^{ème}$ mode de dégradation d'intensité k. L'identifiabilité globale (**GI**) est définie par :

$$GI(j,q,k,k') = \frac{1}{\pi} \arccos\left(\frac{\langle \underline{v}_k^{j^t} \cdot \underline{v}_{k'}^q \rangle}{\|\underline{v}_k^j\|_s \|\underline{v}_{k'}^q\|_s}\right) \quad \textbf{(r.27)}$$

Dans le cas de l'identification, on propose de spécifier l'angle minimal α_{SPEC} entre les vecteurs de variation. Cette valeur est aussi utilisée pour la localisation. À partir de là, on définit l'identifiabilité conforme (**CI**) comme :

$$CI(j,q,k,k') = \begin{cases} 1 \; if \; GI(j,q,k,l) \geq \alpha_{SPEC} \\ 0 \; if \; GI(j,q,k,l) < \alpha_{SPEC} \end{cases} \quad \textbf{(r.28)}$$

Les matrices d'identifiabilité globale $\boldsymbol{GIx}$ et conforme $\boldsymbol{CIx}$ sont définies de la manière suivante :

$$\boldsymbol{GIx} = \begin{vmatrix} GI(1,1,1,1) & \dots & GI(1,d,1,1) \\ \vdots & \ddots & \vdots \\ GI(d,1,1,1) & \dots & GI(d,d,1,1) \end{vmatrix} ; \; \boldsymbol{CIx} = \begin{vmatrix} CI(1,1,1,1) & \dots & CI(1,d,1,1) \\ \vdots & \ddots & \vdots \\ CI(d,1,1,1) & \dots & CI(d,d,1,1) \end{vmatrix} \quad \textbf{(r.29)}$$

Un MD est dit *a priori* identifiable si la ligne à laquelle il est associé dans $\boldsymbol{CIx}$ ne présente que des 1 pour les coefficients hors diagonales. Le critère d'identifiabilité $ITDEM_{\%}$ est ensuite défini comme le ratio des MD *a priori* identifiables sur le nombre total de MD.

- **NKPI pour la localisation :**

Pour la localisation, on rappelle que la matrice d'association des URL est définie par :

$$\boldsymbol{U} = \begin{vmatrix} u(1,1) & \dots & u(1,l) \\ \vdots & \ddots & \vdots \\ u(d,1) & \dots & u(d,l) \end{vmatrix} \in \{0;1\}^{d \times l} \quad \textbf{(r.30)}$$

où l est le nombre d'URL composant le système et $u(j,r)$ est égal à 1 si le MD j affecte l'URL r et égal à 0 sinon. À partir de là, la matrice de localisabilité globale $\boldsymbol{GLx}$ est définie par :

$$\boldsymbol{GLx} = \boldsymbol{U^T CIx U} \in [0;1]^{l \times l} \quad \textbf{(r.31)}$$

On propose ensuite de définir la localisabilité conforme (**CL**) de la manière suivante :

$$CL(a,b) = \begin{cases} \begin{cases} 1 \; if \; \boldsymbol{GLx}(a,b) = \boldsymbol{Nb}(a,b) \\ 0 \; if \; \boldsymbol{GLx}(a,b) < \boldsymbol{Nb}(a,b) \end{cases} & if \; a \neq b \\ 0 \; if \; a = b \end{cases} \quad \textbf{(r.32)}$$

avec $\boldsymbol{Nb}$ la matrice donnant le nombre de couples de MD entre deux URL. La matrice de localisabilité conforme est enfin définie par :

$$\boldsymbol{CLx} = \begin{vmatrix} CL(1,1) & \dots & CL(1,l) \\ \vdots & \ddots & \vdots \\ CL(l,1) & \dots & CL(l,l) \end{vmatrix} \in [0;1]^{d \times d} \quad \textbf{(r.33)}$$

Une URL est dite *a priori* localisable si la ligne à laquelle elle est associée dans $\boldsymbol{CLx}$ ne présente que des 1 pour les coefficients hors diagonale. Le critère d'identifiabilité $LLRU_{\%}$ est ensuite défini comme le ratio des URL *a priori* localisables sur le nombre total d'URL.

- **NKPI pour le pronostic :**

On définit l'intensité minimale de détection (**MDI**) comme l'intensité pour laquelle un MD est *a priori* détectable par au moins un IS. Par ailleurs, les intensités minimales d'identification (**MII**) et de localisation (**MLI**) sont les intensités pour lesquelles le mode de dégradation ou l'URL considérée sont, respectivement, *a priori* identifiables et *a priori* localisables. Les marges de détection $\delta D(j)$, identification $\delta I(j)$ et localisation $\delta L(j)$ pour le $j^{ème}$ MD sont alors respectivement définies comme les différences entre la valeur limite médiane et les MDI, MDI et MLI :

$$\delta D(j) = 1 - MDI^j \; ; \; \delta I(j) = 1 - MII^j \; ; \; \delta L(j) = 1 - MLI^j \qquad \textbf{(r.34)}$$

Une menace au service conforme cible (MSCC) est dite *a priori* pronosticable si tous les modes de dégradation qui peuvent la causer ont des marges de détection, identification et localisation positives. Le critère de pronosticabilité $PCST_{\%}$ est ensuite défini comme le ratio des MSCC *a priori* pronosticables sur le nombre total de MSC.

Pour calculer ces NKPI à partir d'un modèle déterministe, on utilise la propagation d'incertitudes. Pour ce faire, on remplace les vecteurs déterministes des paramètres de contexte et épistémiques incertains par des vecteurs aléatoires. On a alors :

$$\begin{aligned} \Phi_j &= \mathcal{M}_{\boldsymbol{U}}^j \left(\underline{\Gamma}_j^p, \underline{\Gamma}_j^a, \underline{\Lambda}_j^p, \underline{\Lambda}_j^a, \underline{\delta}^i, \underline{\rho}^* \right) \\ \Psi_j &= \mathcal{M}_{\boldsymbol{U}}^j \left(\underline{\Gamma}_j^p, \underline{\Gamma}_j^a, \underline{\Lambda}_j^p, \underline{\Lambda}_j^a, \underline{\delta}^i, \underline{\rho}^* \right) \end{aligned} \qquad \textbf{(r.35)}$$

où Φ_j et Ψ_j sont les variables aléatoires caractérisant les valeurs, respectivement, des IS et des ISC, $\underline{\Gamma}_j^p, \underline{\Gamma}_j^a$ sont les variables aléatoires des paramètres principaux et auxiliaires épistémiques et $\underline{\Lambda}_j^p, \underline{\Lambda}_j^a$ ceux des paramètres de contexte. Le modèle flotte est issu de la propagation des incertitudes liées aux paramètres épistémiques et de contexte alors que le modèle individuel consiste à propager uniquement celles liées au contexte. Dans le second cas, la variabilité des IS due aux incertitudes de fabrication n'est pas prise en compte. On peut calculer les valeurs limites médianes à partir de l'équation **(r.35)**. La méthode est expliquée à la section 0.

Finalement, la méthodologie de validation à proprement parler se compose des étapes suivantes représentées sur la Figure R.12 : (1) calcul des NKPI pour les IS réels et un modèle flotte ; (2) si les performances ne sont pas validées, on calcule des NKPI pour les IS réels normalisés ; (3) si la validation n'est toujours pas acquise, on passe au calcul des NKPI pour des modèles individuels ; (4) si les critères sont toujours non validés et si le cycle de développement le permet, on peut calculer des NKPI pour les IS virtuels et enfin (5) si la validation n'est toujours pas effective, le jeu d'IS doit être modifié.

Finalement, la méthodologie de développement de la partie embarqué du PHM proposée est basée sur la propagation d'incertitudes dans des modèles physiques. Celle-ci est indispensable, en phase de conception, pour obtenir le jeu de distributions nécessaire au calcul des NKPI. Cependant, elle peut rapidement nécessiter un nombre rédhibitoire d'évaluations du modèle complet. Dans ce cas, on propose d'utiliser des métamodèles pour réduire les temps de calcul. Ce sont des fonctions mathématiques avec un temps de simulation réduit qui estiment les sorties d'un modèle numérique. Dans cette thèse, nous avons choisi d'utiliser le Krigeage, une technique de métamodélisation issue du domaine de la géostatistique. Ce choix a été guidé par le fait que le Krigeage est bien adapté aux problèmes de grande dimension. De plus, l'aspect stochastique du Krigeage est bien compatible avec les problèmes traités dans ces travaux.

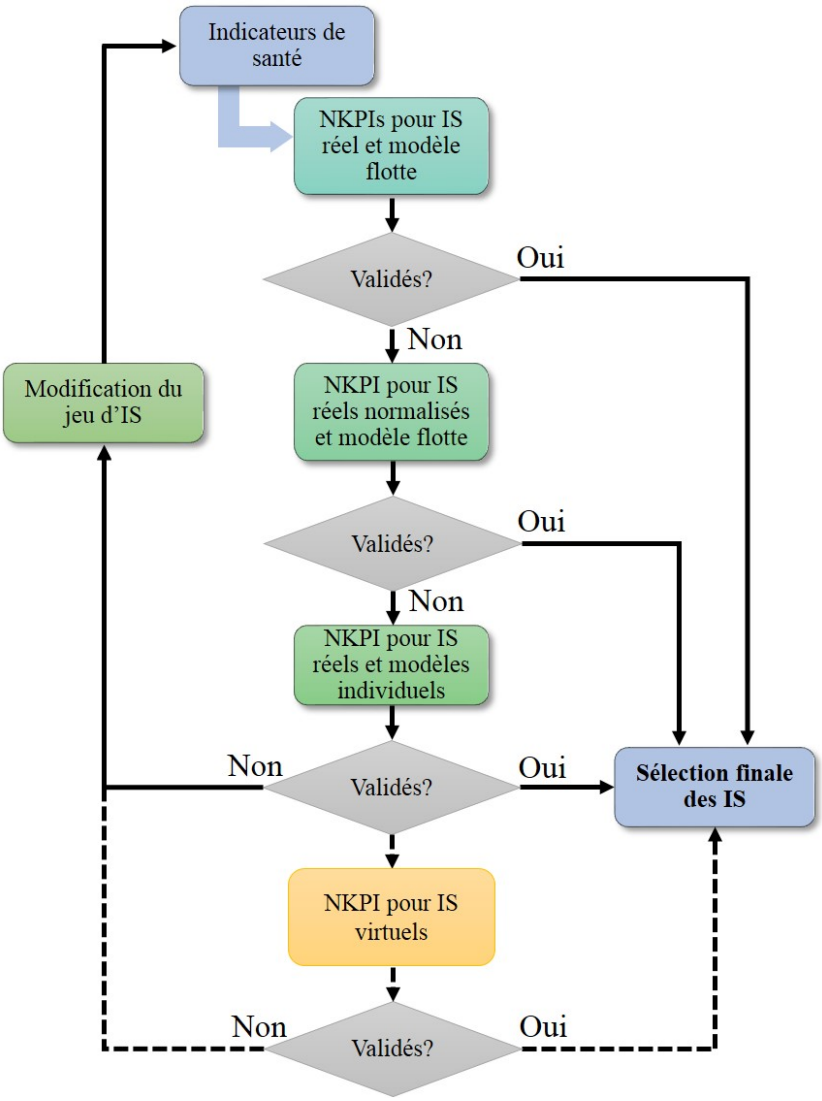


Figure R.12 *Schéma de principe de la validation des IS.*

Chapitre 3 : Krigeage pour la propagation des incertitudes

Dans ce chapitre, l'objectif est de présenter une solution pour la construction et l'utilisation d'un métamodèle de Krigeage adapté aux spécificités de l'application aux moteurs d'avions. Le chapitre est scindé en trois sections : l'introduction générale au Krigeage, la présentation d'une nouvelle technique appelée Krigeage SVR et la méthodologie pour la validation ou l'amélioration de ce type de métamodèles.

Introduction générale au Krigeage

Le principe général de construction d'un métamodèle consiste en trois étapes (voir Figure R.13) : (1) définition des plages de variation des paramètres ; (2) construction du plan d'expérience (**PE**) d'apprentissage et (3) apprentissage du métamodèle, généralement par estimation des hyperparamètres.

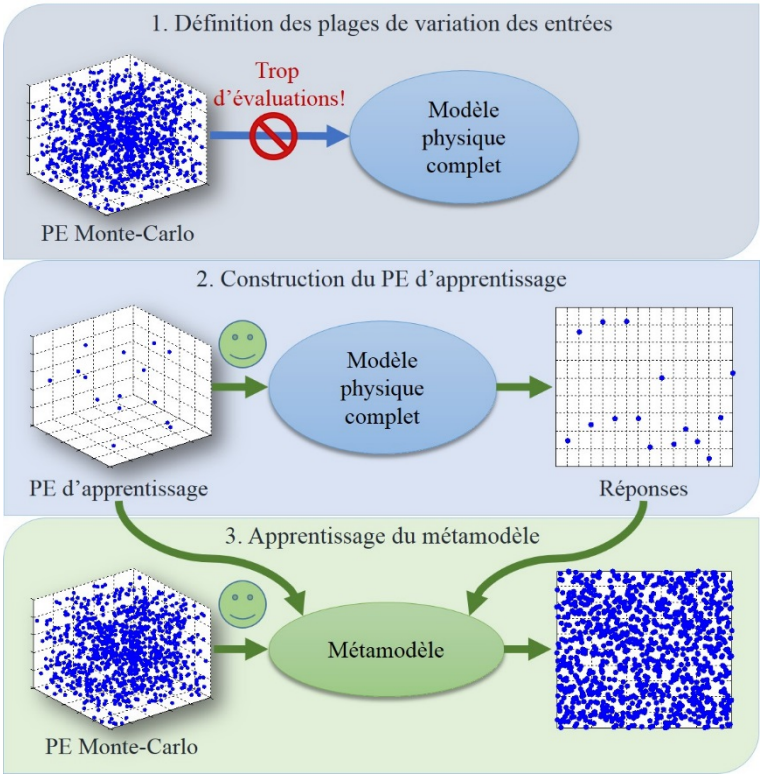


Figure R.13 *Méthodologie pour la construction d'un métamodèle.*

Les spécificités liées à l'application aux moteurs d'avions sont présentées dans le Tableau R.3.

Caractéristiques des modèles	Comportements physiques	Spécifications liées à l'application
Grande dimension de l'espace des entrées (≈ 100)	Non-linéarité	Calculs sur un ordinateur de bureau →moins de 1000 évaluations du modèle
Faibles interactions entre les entrées	Platitude et monotonie	Grande précision requise pour la modélisation des effets du premier ordre
Temps de simulation important ($\approx 5h$)	Discontinuités locales	Les discontinuités peuvent être modélisées par des fonctions continues

Tableau R.3 *Résumé des spécificités liées à l'application aux moteurs d'avions.*

La définition des plages de variation résulte de la phase de quantification des incertitudes sur les paramètres incertains introduite précédemment. Pour la construction du PE d'apprentissage, nous avons choisi de nous focaliser sur les hypercubes latins pour les bonnes propriétés de remplissage d'espace qu'ils présentent même avec un nombre de points réduit. Ainsi, seul ce type de PE est introduit. Enfin, le Krigeage a été sélectionné pour son aspect stochastique, ses points communs avec la SVR présentée au chapitre précédent, sa capacité à gérer de grandes dimensions et enfin sa bonne compatibilité avec les méthodes d'apprentissage séquentiel. L'échantillonnage par hypercubes latins et le Krigeage sont tous deux introduits dans les points qui suivent.

- **Échantillonnage par hypercubes latins :**

La construction d'un hypercube Latin (**LH**) de p points en dimension n, noté $LH(p,n)$ consiste à discrétiser les n dimensions en p intervalles et à générer une matrice de permutation de la manière suivante (McKay, et al., 2000) :

$$LH(p,n) = \begin{vmatrix} \sigma^1(1) & \cdots & \sigma^n(1) \\ \vdots & & \vdots \\ \sigma^1(p) & \cdots & \sigma^n(p) \end{vmatrix} \quad \textbf{(r.36)}$$

où $\sigma^1, \dots, \sigma^n$ sont des permutations aléatoires sur l'intervalle d'entiers $[\![1; p]\!]$. Afin d'assurer de bonnes propriétés de remplissage de l'espace des entrées, on utilise l'approche suivante : un grand nombre de HL est tiré aléatoirement et on choisit le meilleur par rapport à un critère de sélection (Marrel, 2008). Le critère de sélection choisi est le critère *maximin*. On suppose qu'un hypercube latin $LH(p,n)$ a été choisi. On suppose également que chacune des entrées est sujette à une incertitude représentée par les PDF $\mathcal{p}_1, \dots, \mathcal{p}_n$. Les plans d'expériences issus de l'échantillonnage par $LH(p,n)$, noté $LHSDOE(p,n)$ est alors obtenu en divisant la plage de variation de chaque entrée en p sous-intervalles de même probabilité $\mathcal{I}_i^1, \dots, \mathcal{I}_i^p$ et en construisant la matrice suivante :

$$LHSDOE(p,n) = \begin{vmatrix} rand(\mathcal{I}^1_{\sigma^1(1)}) & \cdots & rand(\mathcal{I}^p_{\sigma^p(1)}) \\ \vdots & \ddots & \vdots \\ rand(\mathcal{I}^1_{\sigma^1(n)}) & \cdots & rand(\mathcal{I}^p_{\sigma^p(n)}) \end{vmatrix} \quad \textbf{(r.37)}$$

où $rand(\mathcal{I}_i^j)$ est la fonction tirant aléatoirement une valeur dans l'intervalle $\mathcal{I}_i^j$ suivant la PDF $\mathcal{p}_i$.

- **Introduction au Krigeage :**

Développé originalement pour des problématiques de géostatistique (Matheron, 1963), le Krigeage est une méthode d'estimation combinant une régression classique avec un processus gaussien (Kleijnen, 2009). Ainsi, un modèle de Krigeage $\mathcal{K}$ pour l'estimation d'une fonction $\mathcal{k}$ peut s'écrire :

$$\mathcal{K}(\underline{x}) = \mathcal{R}(\underline{x}) + \mathcal{G}(\underline{x}) \quad \textbf{(r.38)}$$

avec $\mathcal{R}$ et $\mathcal{G}$ les parties, respectivement, régression et processus gaussiens du modèle. Quelque soit le type de $\mathcal{R}$, $\mathcal{G}$ est un processus gaussien de moyenne nulle avec la fonction de covariance $\mathcal{C}$ suivante :

$$\mathcal{C}\big(\mathcal{G}(\underline{x_i}), \mathcal{G}(\underline{x_j})\big) = \sigma^2 k(\underline{\theta}, \underline{x_i}, \underline{x_j}) \quad \textbf{(r.39)}$$

où σ^2 est la variance du processus et k est le modèle de corrélation définie par les hyperparamètres $\underline{\theta}$. Pour les points d'apprentissage $\underline{x}_1, \dots, \underline{x}_k$ et un point $\underline{s}$ quelconque, la matrice $\boldsymbol{R}$ et le vecteur $\underline{r}(\underline{s})$ sont définis de la manière suivante :

$$\begin{aligned} R_{ij} &= k(\underline{\theta}, \underline{x_i}, \underline{x_j}), \quad i,j = 1, \dots, n \\ \underline{r}(\underline{s}) &= \begin{bmatrix} k(\underline{\theta}, \underline{x}_1, \underline{s}) & \cdots & k(\underline{\theta}, \underline{x}_k, \underline{s}) \end{bmatrix}^{\boldsymbol{t}} \end{aligned} \quad \textbf{(r.40)}$$

L'estimation par le processus gaussien seul est alors exprimée de la sorte :

$$\mathcal{G}(\underline{s}) = \underline{r}(\underline{s})^T \boldsymbol{R}^{-1} \left(\underline{y} - \underline{\hat{y}}_{\mathcal{R}}\right) \quad \textbf{(r.41)}$$

avec $\underline{y} = \begin{bmatrix} y_1 & \cdots & y_n \end{bmatrix}^T$ les réponses aux points d'apprentissage et $\underline{\hat{y}}_{\mathcal{R}} = \begin{bmatrix} \mathcal{R}(\underline{x}_1) & \cdots & \mathcal{R}(\underline{x}_k) \end{bmatrix}^T$. L

Les différentes techniques de Krigeage se distinguent principalement par le type de régression $\mathcal{R}$ qu'elles utilisent. Nous proposons ici une classification basée sur cinq grands types d'approche pour l'apprentissage de la partie régression (Moyeed, et al., 2002; Rivoirard, 1994; Liu, 2003; Omre, 1987; Myers, 1982). Elle est présentée en Figure R.14.

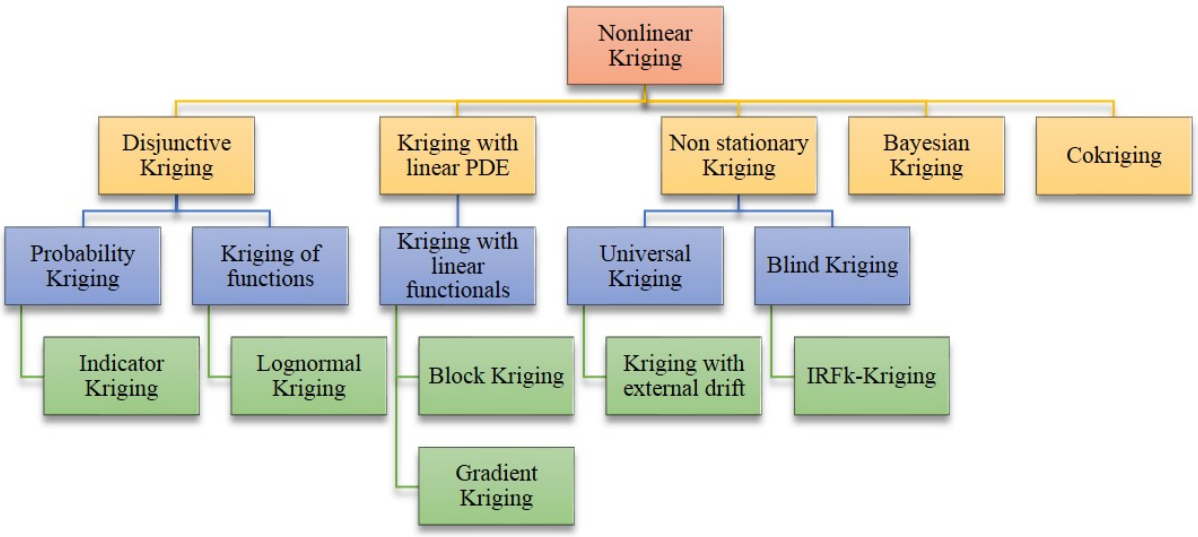


Figure R.14 *Proposed classification of Kriging techniques.*

Dans le cadre de ces travaux de thèse, le type d'approche le plus adapté aux problèmes rencontrés est le Krigeage non stationnaire qui consiste à utiliser un ensemble de fonctions linéaires ou non $g_1, \dots, g_p$ comme base pour modéliser les effets dus aux non-stationnarités par une combinaison linéaire. Ainsi, on définit la matrice $\boldsymbol{F}$ par :

$$\boldsymbol{F} = \begin{vmatrix} g_1(\underline{x}_1) & \cdots & g_p(\underline{x}_1) \\ \vdots & \ddots & \vdots \\ g_1(\underline{x}_k) & \cdots & g_p(\underline{x}_k) \end{vmatrix} \in \mathbb{R}^{k \times p} \qquad \textbf{(r.42)}$$

L'estimation par la régression $\mathcal{R}$ au point $\underline{s}$ peut alors s'exprimer de la manière suivante :

$$\mathcal{R}(\underline{s}) = \underline{f}(\underline{s})^T \underline{\beta} \qquad \textbf{(r.43)}$$

avec $\underline{f}(\underline{s}) = \begin{bmatrix} g_1(\underline{s}) & \cdots & g_p(\underline{s}) \end{bmatrix}^T$ et $\underline{\beta}$ estimé par moindres carrés généralisés :

$$\underline{\beta} = \left(\boldsymbol{F^t R^{-1} F}\right)^{-1} \boldsymbol{F^t R^{-1}} \underline{y} \qquad \textbf{(r.44)}$$

Au final, on obtient l'expression de l'estimateur du Krigeage :

$$\mathcal{K}(\underline{s}) = \underline{f}(\underline{s})^T \underline{\beta} + \underline{r}(\underline{s}) \boldsymbol{R^{-1}} \left(y - \boldsymbol{F}\underline{\beta}\right) \qquad \textbf{(r.45)}$$

Le Krigeage à la propriété intéressante d'être à la fois le meilleur estimateur linéaire non biaisé et un estimateur exact sur les points d'apprentissage. Il est également capable d'estimer l'erreur quadratique moyenne de ses estimations par la formule suivante (Lophaven, et al., 2002) :

$$MSE(\mathcal{K}(\boldsymbol{s})) = \sigma^2 \left(1 - \begin{bmatrix} f^T(\underline{s}) & r^T(\underline{s}) \end{bmatrix} \begin{bmatrix} \boldsymbol{0} & \boldsymbol{F^t} \\ \boldsymbol{F} & \boldsymbol{R} \end{bmatrix} \begin{bmatrix} f(\underline{s}) \\ r(\underline{s}) \end{bmatrix}\right) \qquad \textbf{(r.46)}$$

Présentation du Krigeage SVR

Comme mentionnées précédemment, les entrées des modèles considérés sont peu corrélées. De plus, les spécifications demandent à ce que les effets du premier ordre soient modélisés avec une précision importante. C'est dans ce but que le Krigeage SVR a été développé. L'idée générale est d'utiliser la

régression par vecteur support (**SVR**) pour la partie régression du modèle de Krigeage et d'utiliser le processus gaussien pour modéliser les effets d'interaction résiduels. Pour évaluer les performances, le Krigeage SVR est comparé avec les approches classiques de Krigeage ordinaire et universel sur des fonctions analytiques.

L'estimateur du Krigeage SVR consiste à remplacer $\underline{f}, \underline{\beta}$ et $\boldsymbol{F}$ par, respectivement, $\underline{v}, \underline{\alpha}$ et $\boldsymbol{G}$ dans **(r.45)** pour obtenir l'expression suivante :

$$\mathcal{K}(\underline{s}) = v(\underline{s})^T \underline{\alpha} + r(\underline{s}) \boldsymbol{R}^{-1} \left(\underline{y} - \boldsymbol{G} \underline{\alpha} \right) \qquad \textbf{(r.47)}$$

De même que pour la normalisation des IS, on choisit d'utiliser des SVR mono dimensionnelles pour se focaliser sur les effets du premier ordre. De plus, on supervise là aussi le choix du nombre de points d'apprentissage et le type de fonction noyau pour chaque dimension par la valeur des indices de linéarité. La méthodologie globale de construction d'un modèle de Krigeage SVR, schématisée Figure R.15, est la suivante : (1) définition du jeu de paramètre initial ; (2) quantification sommaire des incertitudes (PDF uniformes) ; (3) analyse de sensibilité par la méthode de Morris : calcul des Lin_i et identification des paramètres influentials ; (4) hiérarchisation des paramètres influentials ; (5) construction des vecteurs d'apprentissage pour chaque dimension ; (6) estimation des modèles SVR mono dimensionnels et (7) estimation des hyperparamètres du processus gaussien.

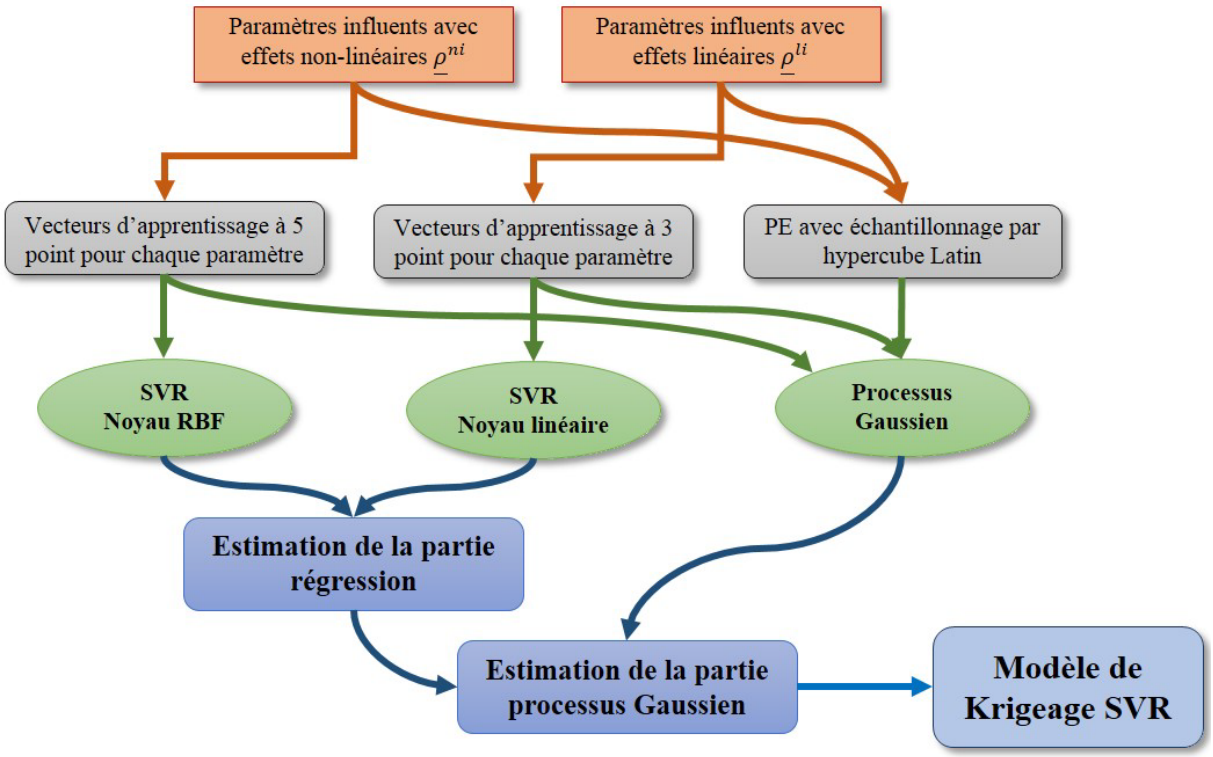


Figure R.15 *Procédure pour la construction d'un modèle de Krigeage SVR.*

Les performances du Krigeage SVR sont évaluées pour trois fonctions analytiques tests à partir de trois métriques.

- **Fonctions analytiques tests :**

Les trois fonctions analytiques utilisées pour tester le Krigeage SVR sont : une fonction SISO (single input single outout), une fonction DISO (dual inputs single output) et la fonction d'Ishigami. Ces trois

fonctions sont représentées sur la Figure R.16. À noter que les fonctions SISO et DISO sont représentatives de comportements couramment rencontrés dans le cas des moteurs d'avions (non linéarité, discontinuité et faible interaction). La fonction d'Ishigami est, quant à elle, un exemple commun dans le domaine de l'analyse de sensibilité. Sur la Figure R.16, c'est sa restriction aux deux premières variables qui est représentée, car elle est normalement définie pour trois dimensions.

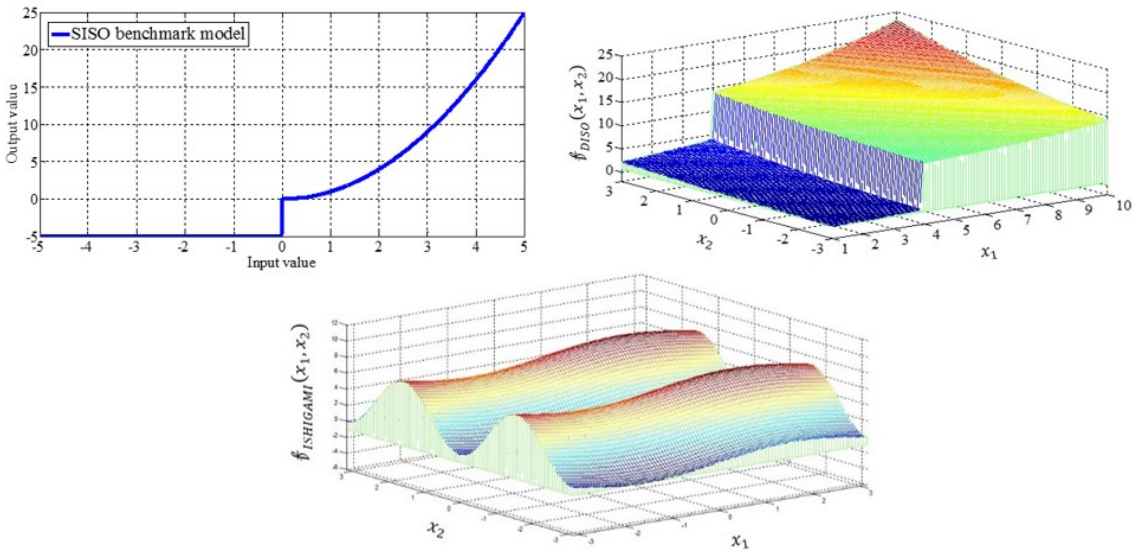


Figure R.16 *Fonctions analytiques tests : SISO (en haut à gauche), DISO (en haut à droite) et Ishigami.*

- **Métriques pour l'évaluation des performances :**

Sur les trois critères d'évaluation des performances utilisés, deux sont dérivés du calcul de l'erreur de validation croisée e_{-i} définie de la manière suivante :

$$e_{-i} = y_i - \mathcal{K}_{-i}(\underline{x_i}) \tag{r.48}$$

où y_i est la valeur exacte du modèle au point d'apprentissage $\underline{x_i}$ et $\mathcal{K}_{-i}$ est le modèle de Krigeage appris sans le point d'apprentissage $\underline{x_i}$. La valeur de e_{-i} indique l'importance relative de chaque point d'apprentissage $\underline{x_i}$ dans l'estimation des hyperparamètres du modèle de Krigeage. À partir de e_{-i}, deux métriques sont définies :

$$\begin{aligned} \mu_{CV} &= \frac{\sum_{i=1}^{n} e_{-i}}{n}\left(\frac{1}{3\sigma_y}\right) \\ \sigma_{CV} &= \sqrt{\frac{\sum_{i=1}^{n}(e_{-i} - \mu_{CV})^2}{n}}\left(\frac{1}{3\sigma_y}\right) \end{aligned} \tag{r.49}$$

avec n le nombre de points d'apprentissage et σ_y l'écart type de la sortie y calculée à partir de ces points. L'avantage de ces métriques est qu'elles ne nécessitent pas de point additionnel. Cependant, elles permettent essentiellement de quantifier le degré de cohérence de la fonction de corrélation. Ainsi, une troisième métrique est utilisée pour évaluer la précision globale : l'indice de $Q2$. Ce dernier correspond au coefficient de détermination R^2 Pour un échantillon test. Il est défini de la sorte :

$$Q2\left(\underline{y},\mathcal{K}\left(\underline{x}\right)\right) = 1 - \frac{\sum_{i=1}^{a}\left(y_i - \mathcal{K}\left(\underline{x}_i\right)\right)^2}{\sum_{i=1}^{a}\left(\bar{\underline{y}} - y_i\right)^2} \quad \textbf{(r.50)}$$

où $\underline{x}$ représente les a points de l'échantillon test, $\underline{y}$ les réponses associées et $\mathcal{K}\left(\underline{x}\right)$ l'estimation par le modèle de Krigeage.

Le Tableau R.4 présente les résultats comparatifs pour l'estimation des trois fonctions tests par Krigeage ordinaire, universel et SVR. Pour que les résultats soient robustes vis-à-vis d'un changement de PE initial, l'estimation a été itérée 100 fois avec des PE initiaux aléatoires et on présente la moyenne et l'écart type des trois métriques sur toutes les itérations.

Fonction SISO			
Technique	**Moyenne et écart type de μ_{CV}**	**Moyenne et écart type de σ_{CV}**	**Moyenne et écart type de Q2**
Krigeage ordinaire	$(1.6e^{-4}; 0.007)$	$(0.16; 0.03)$	$(0.93; 0.03)$
Krigeage universel	$(-0.006; 0.016)$	$(0.20; 0.04)$	$(0.92; 0.04)$
Krigeage SVR	$(-4.7e^{-4}; 0.029)$	$(0.09; 0.05)$	$(0.89; 0.05)$
Fonction DISO			
Technique	**Moyenne et écart type de μ_{CV}**	**Moyenne et écart type de σ_{CV}**	**Moyenne et écart type de Q2**
Krigeage ordinaire	$(0.003; 0.01)$	$(0.19; 0.04)$	$(0.95; 0.02)$
Krigeage universel	$(0.006; 0.02)$	$(0.24; 0.06)$	$(0.93; 0.03)$
Krigeage SVR	$(-0.003; 0.007)$	$(0.11; 0.03)$	$(0.95; 0.008)$
Fonction d'Ishigami en 3 dimensions			
Technique	**Moyenne et écart type de μ_{CV}**	**Moyenne et écart type de σ_{CV}**	**Moyenne et écart type de Q2**
Krigeage ordinaire	(−0.005;0.01)	(0.28;0.05)	(0.42;0.09)
Krigeage universel	(−0.004;0.02)	(0.41;009)	(0.12;0.27)
Krigeage SVR	(−0.001;0.02)	(0.16;0.04)	(0.66;0.09)

Tableau R.4 *Résultats comparés des méthodes de Krigeage pour les trois fonctions tests.*

Les résultats montrent que le Krigeage SVR donne de meilleurs résultats que les deux autres techniques pour l'estimation des fonctions DISO et Ishigami. En fait, on observe que plus la dimension est élevée, plus il est intéressant d'utiliser le Krigeage SVR.

Dans le but d'améliorer la méthode d'estimation du vecteur des hyperparamètres $\underline{\theta}$, deux améliorations sont proposées : l'utilisation d'une fonction de corrélation exponentielle-gaussienne avec un exposant anisotropique et l'itération de l'algorithme d'optimisation de $\underline{\theta}$. La fonction de corrélation exponentielle-gaussienne s'écrit $k\left(\underline{\theta},\underline{x_i},\underline{x_j}\right) = exp\left(-\theta_1\left|x_j - x_i\right|^{\theta_2}\right)$. Typiquement, θ_1 dépend de la dimension considérée alors que θ_2 est isotropique. On propose ici d'utiliser un θ_2 anisotropique. Cette approche est testée sur la fonction d'Ishigami en 3 dimensions et démontre une légère amélioration de la précision des estimations.

La seconde amélioration consiste à estimer $\underline{\theta}$ pour différentes valeurs initiales $\underline{\theta}^{init}$ et à choisir le modèle associé à la plus grande valeur du critère d'optimisation OC calculé de la manière suivante :

$$OC = \begin{cases} \dfrac{Q2}{|\sigma_{CV}\,\mu_{CV}|}, & Q2 > 0 \\ Q2|\sigma_{CV}\,\mu_{CV}|, & Q2 \leq 0 \end{cases} \quad \textbf{(r.51)}$$

L'inconvénient de cette méthode est qu'elle nécessite un échantillon test pour calculer le $Q2$. Cependant, les résultats présentés sur le Tableau R.5 montrent un gain significatif de précision pour un nombre d'itérations supérieur à 50. On utilisera donc cette technique avec 50 itérations par la suite.

Estimation technique	Mean and standard deviation of μ_{CV}	Mean and standard deviation of σ_{CV}	Mean and standard deviation of Q2
Single DACEFIT	$(-0.002; 0.017)$	$(0.15; 0.04)$	$(0.66; 0.06)$
Multiple:10 iterations	$(-0.004; 0.017)$	$(0.15; 0.04)$	$(0.66; 0.08)$
Multiple : 20 iterations	$(-0.003; 0.013)$	$(0.14; 0.04)$	$(0.69; 0.08)$
Multiple : 50 iterations	$(-0.003; 0.012)$	$(0.14; 0.04)$	$(0.72; 0.08)$
Multiple : 100 iterations	$(-0.001; 0.012)$	$(0.12; 0.44)$	$(0.73; 0.08)$

Tableau R.5 *Amélioration des performances avec itération de l'algorithme d'optimisation.*

Validation et amélioration du Krigeage SVR

Pour valider et améliorer les modèles de Krigeage SVR, on propose d'utiliser une approche d'apprentissage séquentiel (Jin, et al., 2002; Scheidt, 2006; Bichon, et al., 2008). Cela consiste à ajouter itérativement des points d'apprentissage dans les zones les plus pertinentes de l'espace des entrées. Une méthode d'apprentissage séquentiel est définie par un critère de validation et un critère de sélection.

- **Critère de validation :**

Le critère de validation est utilisé pour déterminer si le modèle construit est assez précis. Le cas échéant, les itérations sont stoppées. Dans le cas présent, on définit un ensemble de trois critères de validation :

$$\begin{cases} Q2 > Q2^{min} \\ |\mu_{CV}| < \mu_{CV}^{max} \\ \sigma_{CV} < \sigma_{CV}^{max} \end{cases} \quad \textbf{(r.52)}$$

où $Q2^{min}, \mu_{CV}^{max}$ and σ_{CV}^{max} sont, respectivement, la valeur minimale acceptable pour $Q2$, la valeur absolue maximale acceptable pour μ_{CV} et la valeur maximale acceptable pour σ_{CV}. Ces valeurs doivent être définies par les concepteurs du système de PHM.

- **Critère de sélection :**

Pour les applications de ces travaux, on propose de définir un critère de sélection SC basé à la fois sur l'erreur quadratique moyenne du Krigeage SVR et sur l'erreur de validation croisée. Il s'exprime de la manière suivante :

$$SC\colon \mathbb{R}^n \longrightarrow [0;1]$$
$$\underline{x} \longmapsto \alpha\left(\frac{\|MSE(\underline{x})\|}{\max\limits_{x\in\mathbb{R}^n} MSE(\underline{x})}\right) + \beta\left(\frac{\|\hat{e}(\underline{x})\|}{\max\limits_{x\in\mathbb{R}^n} \hat{e}(\underline{x})}\right) \quad \textbf{(r.53)}$$

avec MSE et $\hat{e}$, respectivement, l'erreur quadratique moyenne et l'estimation de l'erreur de validation croisée. Le premier terme apporte un aspect local à la recherche du meilleur point d'apprentissage en pointant vers les zones les plus significatives pour l'estimation des hyperparamètres. Le second terme apporte un aspect global en indiquant les zones où la densité de points d'apprentissage est la plus faible. Les coefficients (α, β) sont des poids permettant de définir l'importance relative des aspects local et global. L'estimation $\hat{e}$ est obtenue par un modèle de Krigeage ordinaire avec une corrélation Gaussienne. Finalement, le schéma de principe de l'apprentissage séquentiel est présenté sur la Figure R.17.

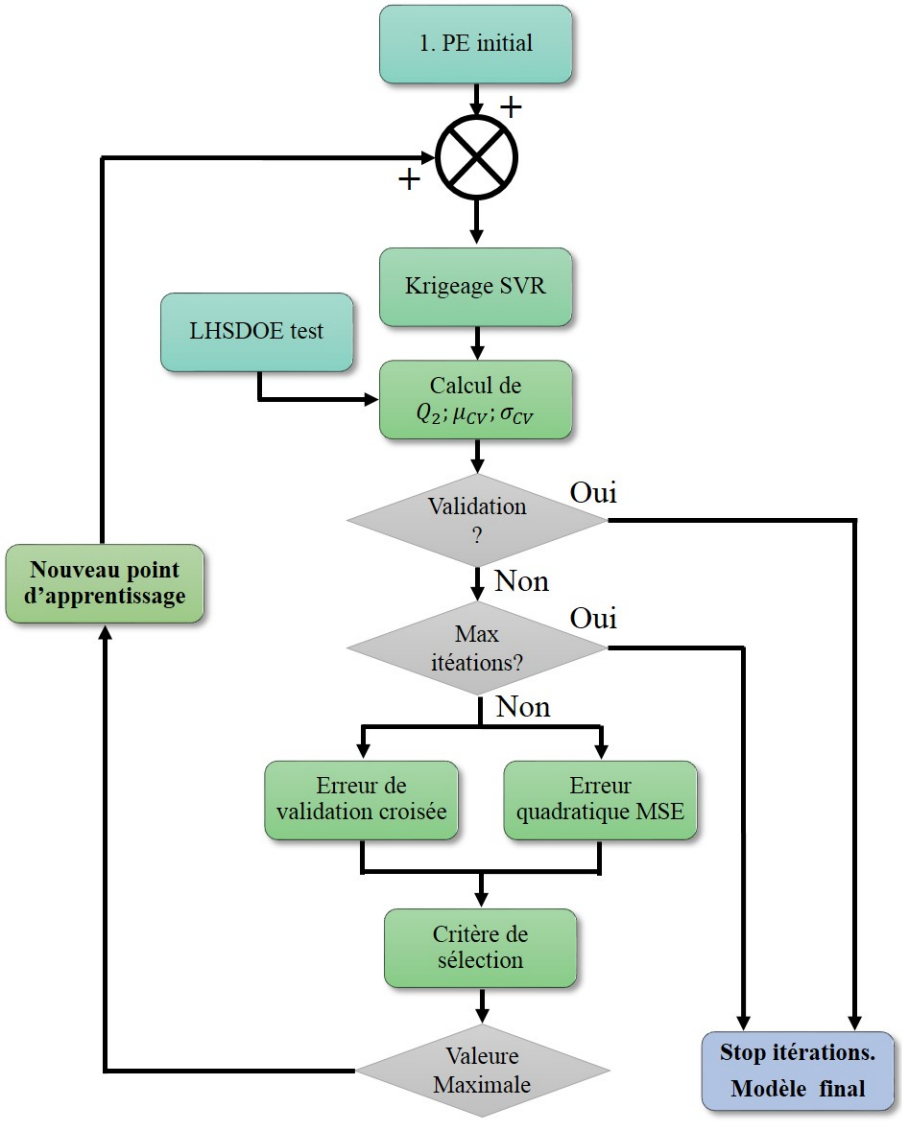


Figure R.17 *Schéma de l'apprentissage séquentiel proposé.*

Les résultats confirment que l'apprentissage séquentiel est performant. On propose même d'utiliser uniquement les vecteurs d'apprentissage mono dimensionnels de la SVR comme PE initial et de lancer

l'apprentissage séquentiel sans utiliser de LHSDOE additionnel. La procédure finale est représentée sur la Figure R.18

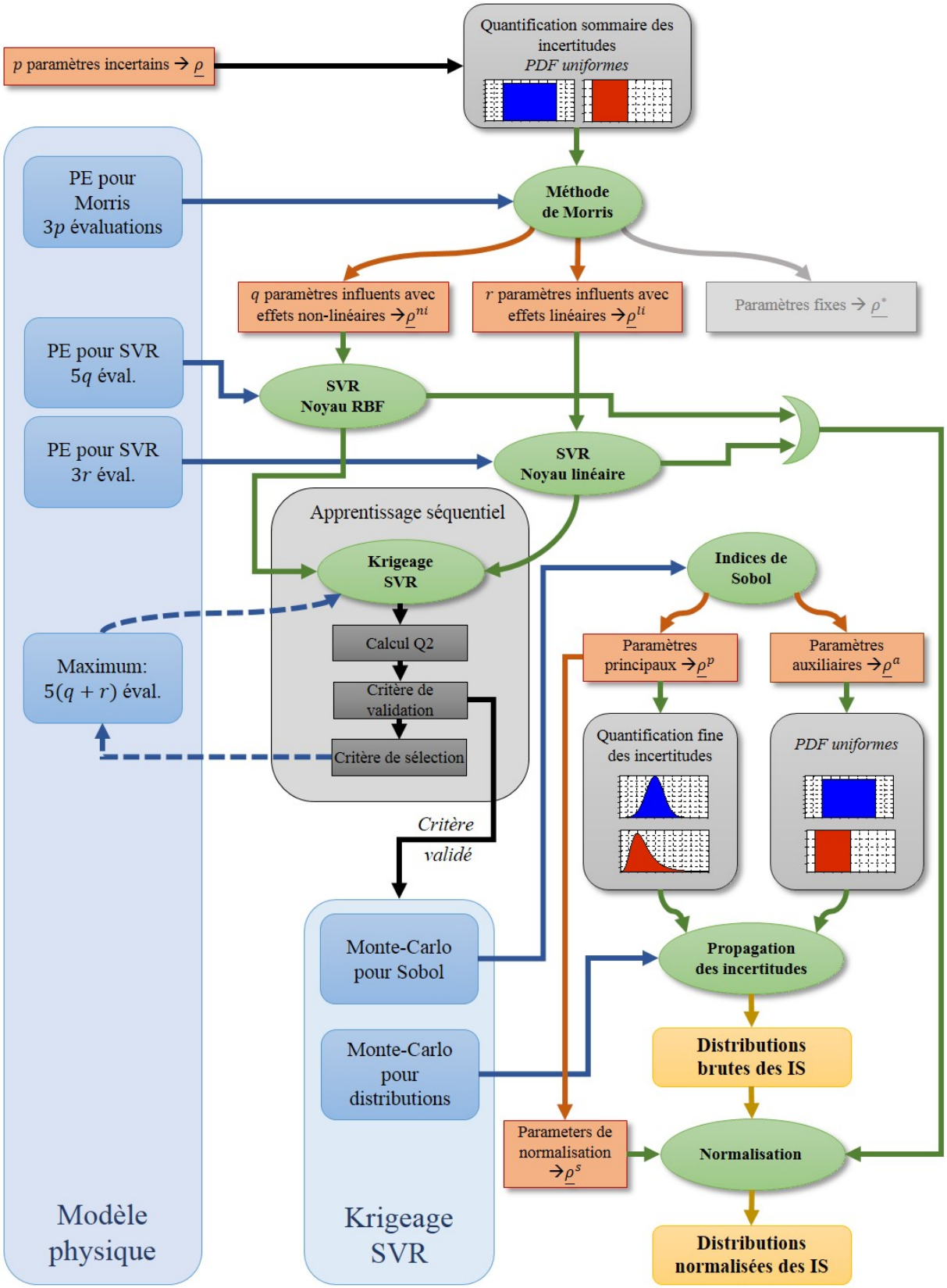


Figure R.18 *Schéma global du plan d'expériences numérique.*

Finalement, ce chapitre a permis de définir une méthodologie pour la construction, l'utilisation et la validation d'un nouveau type de métamodèle appelé Krigeage SVR, particulièrement adapté aux particularités des moteurs d'avions. Ce modèle est destiné à être utilisé pour la propagation des incertitudes nécessaire au calcul des NKPI pour la validation des IS. Dans le chapitre suivant, tous les développements précédents sont appliqués et évalués sur un système réel : le système carburant d'un moteur d'avion.

Chapitre 4 : application au système carburant d'un moteur d'avions

L'ensemble des méthodes et outils développés dans cette thèse est appliqué au développement d'un ensemble d'indicateurs de santé pour la surveillance du système carburant. Ce dernier est un bon candidat pour deux raisons : il est sujet à un grand nombre de modes de dégradations et de menaces au service conforme et son modèle physique génère un temps de simulation important (environ 5h) qui justifie l'utilisation d'un métamodèle.

Présentation du système carburant

La fonction principale du système carburant pour un moteur d'avion (Moir, et al., 2008) est de réguler la quantité de carburant injectée dans la chambre de combustion. Ses fonctions secondaires sont de refroidir l'huile de lubrification et d'actionner les géométries variables. À partir des spécifications fonctionnelles, on peut définir les unités fonctionnelles suivantes :

- **Low pressure pump (LPP) :** pompe centrifuge de gavage.
- **Main fuel pump (MFP) :** pompe à engrenages principale.
- **Main fuel filter (MFF) :** filtre à particules principal.
- **Fuel metering unit (FMU) :** sous-système chargé de l'injection du carburant. Il se compose des unités fonctionnelles suivantes :
  - ***Fuel metering valve loop (FMV) :*** pour réguler la position de la valve de dosage.
  - ***High Pressure Shut-Off Valve (HPSOV) :*** pour assurer une pression minimale dans le circuit et couper ou activer l'injection.
  - ***bypass valve (BYV) :*** pour recirculer l'excès de carburant généré par la MFP.
- **Variable stator vane loop (VSV) :** boucle de régulation de la position angulaire des aubes du stator du compresseur HP et optimiser le rendement.
- **Variable bleed valve loop (VBV) :** boucle de régulation de l'ouverture de trappes situées entre les compresseurs BP et HP pour diminuer la quantité d'air dans la chambre de combustion.
- **Transient bleed valve loop (TBV) :** valve provoquant une décharge à l'entrée de la chambre de combustion si nécessaire.
- **WFM :** débitmètre mesurant le débit injecté dans la chambre.

La représentation fonctionnelle du système est donnée en Figure R.19.

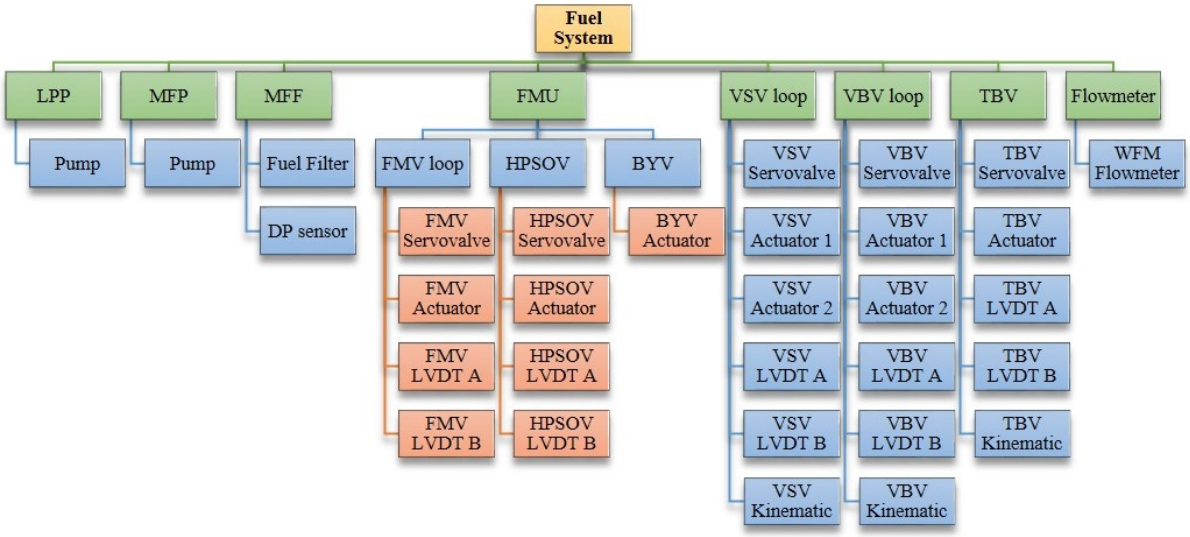


Figure R.19 *Représentation fonctionnelle du système carburant.*

La structure du système carburant est divisée en 8 unités remplaçables en ligne (**URL**) :

- **Pumping unit :** contient les équipements de pompage, c.-à-d. la LPP et la MFP.
- **Fuel filter :** contient le MFF et un capteur de pression différentielle (deltaP) redondé.
- **Actuation control unit (ACU) :** contient les servovalves pour les boucles de régulation.
- **FMU :** contient la FMV, deux capteurs LVDT redondés, la servovalve FMV et la HPSOV avec deux proximètres redondés.
- **VSV actuation unit :** contient deux actionneurs équipés chacun d'un capteur LVDT et la chaîne cinématique.
- **VBV actuation unit :** comme la VSV actuation unit, contient deux actionneurs équipés chacun d'un capteur LVDT et la chaîne cinématique.
- **TBV actuation unit :** contient deux actionneurs équipés chacun d'un capteur LVDT et la chaîne cinématique. Dans le cas de la TBV, le capteur LVDT est utilisé comme un proximètre, à savoir qu'il donne un booléen indiquant si la valve est ouverte ou fermée.
- **Flowmeter :** contient le débitmètre avec deux circuits de mesure redondés.

Ces URL sont représentées sur la Figure R.20 et la représentation hiérarchique structurelle est donnée sur la Figure R.21. La matrice d'association des URL est donnée en Appendix I.

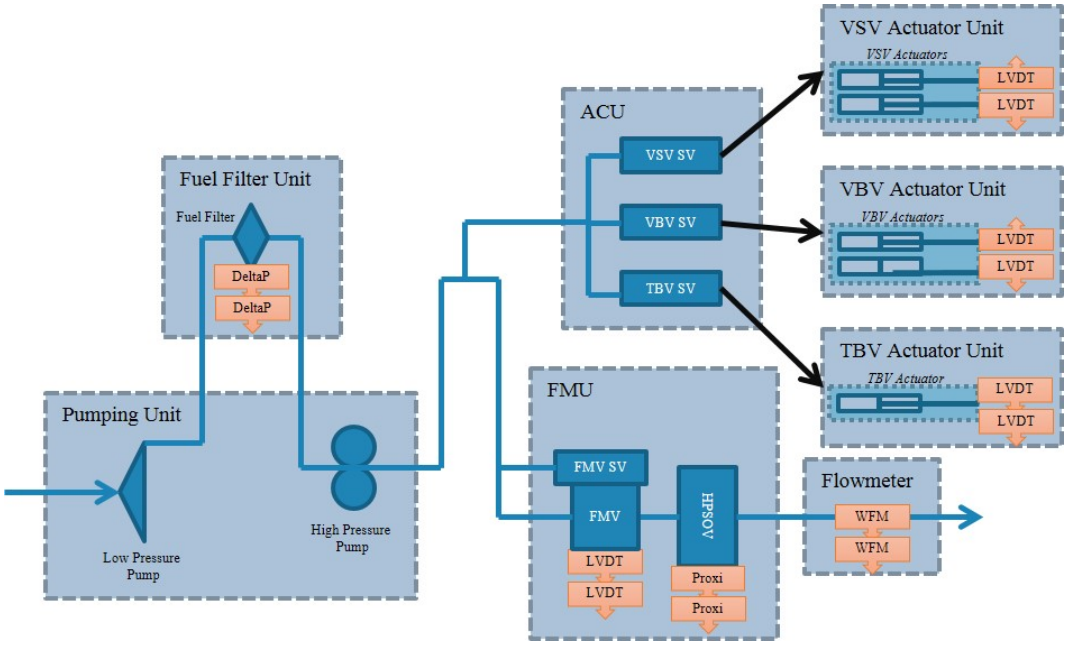


Figure R.20 *Schéma du système carburant avec ses URL.*

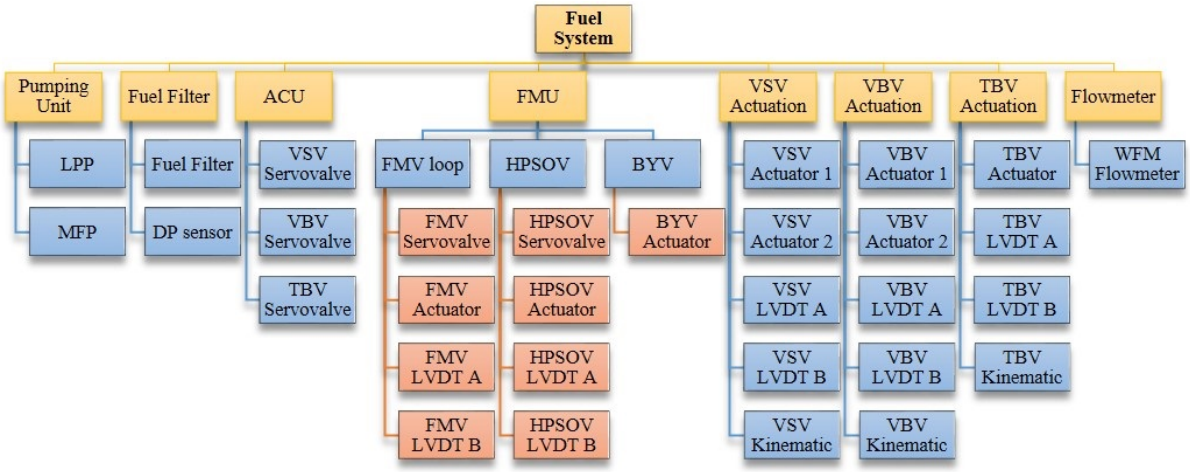


Figure R.21 *Représentation structurelle hiérarchique du système carburant.*

Sélection des indicateurs de santé et de service conforme

En accord avec la méthodologie proposée pour le développement intégré du PHM, la sélection des IS et des ISC se fait pour chacune des unités fonctionnelles à partir des niveaux inférieurs jusqu'au niveau 0 (niveau système). On ne présentera ici que les indicateurs de santé et uniquement ceux qui sont réels. Pour les modes de dégradation, les éléments hydrauliques sont principalement sujets à des augmentations de frottements visqueux ou statiques, à des abrasions causant des fuites internes ou de la cokéfaction provoquant des colmatages d'orifices. Dans le cas des éléments électriques, les modes de dégradation principaux sont des dérives de mesure des capteurs et des dérives de courant d'équilibre sur les servovalves.

- **IS pour les unités fonctionnelles de niveau 2 :**

Dans le cas du système carburant, on a trois unités fonctionnelles de niveau 2 : la boucle FMV, la valve bypass et la HPSOV. Pour la boucle FMV, nous avons défini des nouveaux indicateurs de santé à

partir de l'étude des tests d'acceptation des équipements. En effet, ces derniers utilisent la courbe de gain en débit pour caractériser la conformité ou non des servovalves des boucles FMV. La courbe de gain en débit représente les débits de sortie d'une servovalve en fonction de son courant de commande. Cependant, la mesure directe du débit n'est pas disponible en vol donc nous en avons cherché une mesure indirecte. La solution retenue a été de considérer la vitesse de l'actionneur, disponible via les capteurs LVDT, qui est théoriquement proportionnelle au débit suivant la relation suivante :

$$Q = VS \tag{r.54}$$

avec Q le débit de sortie de la servovalve, S la section dans l'actionneur et V la vitesse de l'actionneur. La courbe de la vitesse en fonction du courant de commande est appelée courbe de gain en vitesse. À cause de l'hystérésis de la cinématique, la version brute de cette courbe a une grande dispersion qu'on diminue via un algorithme de lissage basé sur des moyennes locales afin d'obtenir un profil exploitable comme montré sur la Figure R.22.

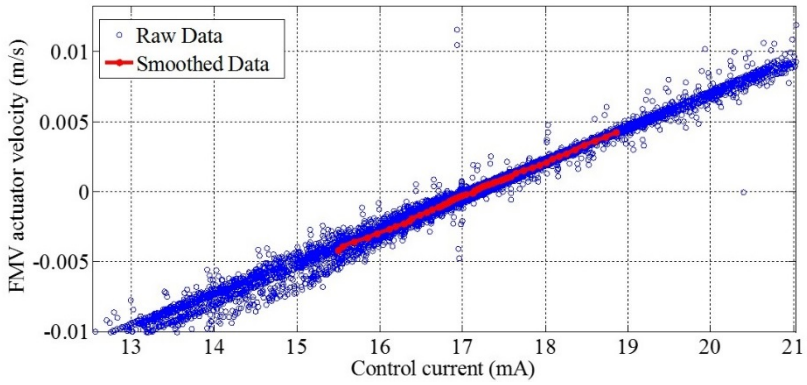


Figure R.22 *Extraction des courbes brutes et lissées de gain en vitesse pour la FMV.*

À partir de cette courbe, on définit ensuite quatre IS : l'hystérésis du courant pour les points à vitesse nulle $FmvHyst0$, la pente de la courbe $FmvSlp$, le courant d'équilibre $FmvCEqu$ et l'échelle complète de la courbe en abscisse $FmvScale$. Les trois derniers sont représentés graphiquement Figure R.23.

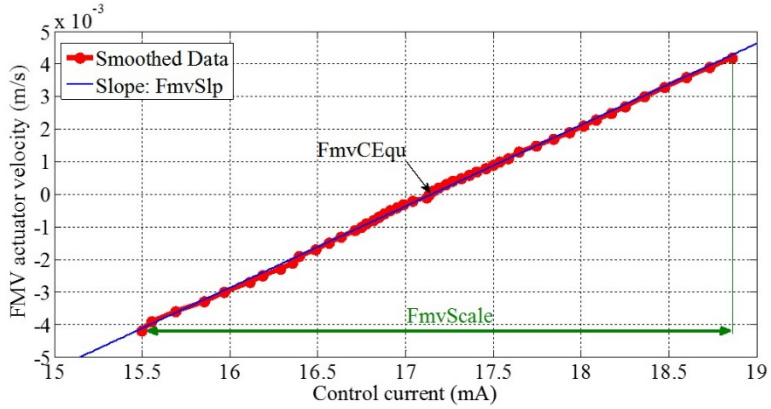


Figure R.23 *Indicateurs de santé pour la boucle FMV.*

On définit également des IS à partir des positions mesurées par les capteurs LVDTs redondants. Quatre d'entre eux sont définis comme les valeurs maximales et minimales des positions mesurées sur chacun des capteurs. Quatre autres sont construits comme les valeurs maximale et minimale des écarts types et moyennes de l'écart de position entre les deux mesures. Enfin, un dernier IS est défini comme la valeur moyenne de la valeur absolue de l'erreur de régulation sur un vol complet. Tous ces IS sont

calculés pour les voies A et B ainsi que pour la voie sélectionnée (ici, on suppose que c'est la moyenne des positions mesurées par les voies A et B), ce qui fait 21 IS au total.

Pour la HPSOV (ou SOV), un seul capteur est disponible. Il indique si la valve est ouverte ou fermée. On dispose également de l'information de commande du contrôleur. Pendant la phase de démarrage, l'ouverture de la SOV est demandée à 5% du régime de rotation $N2$ dans le cadre d'un built-in test. Sa fermeture est ensuite exigée à 10%. À environ 20% du régime, l'ouverture est de nouveau requise pour l'injection du carburant. Finalement, la SOV doit changer de statuts à trois reprises. Trois IS sont alors définis : le délai de la première ouverture $SOVdelop1$, le délai de la fermeture à $10\%N2$ $SOVdelclo$ et le second délai d'ouverture $SOVdelop2$. Ces IS sont présentés sur la Figure R.24.

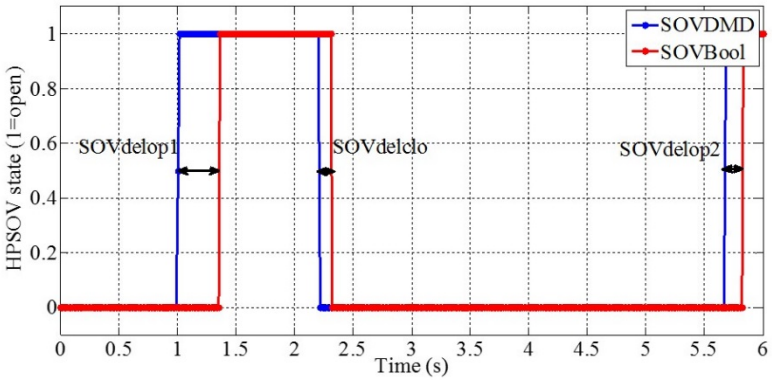


Figure R.24 *Indicateurs de santé pour la SOV.*

Pour la valve bypass, aucune mesure n'est disponible donc aucun IS réel n'est défini.

- **IS pour les unités fonctionnelles de niveau 1 :**

Pour le FMU, deux IS sont définis en plus de ceux construits pour ses sous-systèmes : $FmuSlpFW$ et $FmuR2FW$ qui sont, respectivement, la pente et le coefficient de détermination R^2 de la régression linéaire de degré 0 sur la courbe $log(WFMSEL)$ en fonction de $FMVSEL$ avec $WFMSEL$ le débit injecté mesuré et $FMVSEL$ la position FMV sélectionnée.

Pour la pompe MFP, il n'y a pas de mesure directe de son rendement. Dans le but de construire un IS capable de traduire l'occurrence d'une perte de rendement, une technique de surveillance indirecte doit donc être développée. L'idée est de trouver des variables images de la puissance hydraulique de la pompe pendant la phase de démarrage. Il apparaît que le régime $N2$ à l'ouverture des valves SOV et TBV peut être un bon indicateur de cette puissance hydraulique. En effet, elles ne peuvent s'ouvrir que lorsque le circuit hydraulique a atteint une pression suffisante. En suivant ce régime d'ouverture d'un vol à l'autre, on devrait donc pouvoir détecter une baisse de rendement de la pompe. Finalement, les IS suivants, approuvés par des experts sont définis : ω_{SOV} et ω_{TBV} les régimes $N2$ à l'ouverture de, respectivement, la SOV et la TBV.

Dans le cas du filtre MFF, les IS suivants sont définis : $MffSlpN2DP$ la pente de la régression linéaire sur la courbe $\sqrt{DeltaP}$ en fonction de $N2$ et $MffR2N2DP$ le coefficient de détermination R^2 de cette régression avec $DeltaP$ la pression différentielle mesurée aux bornes du filtre.

Concernant la boucle de régulation VSV, des indicateurs de santé sont définis à partir de la courbe de gain en vitesse, obtenue de la même manière que pour la boucle FMV. Un exemple de courbe de gain en vitesse pour la boucle VSV est présenté Figure R.25.

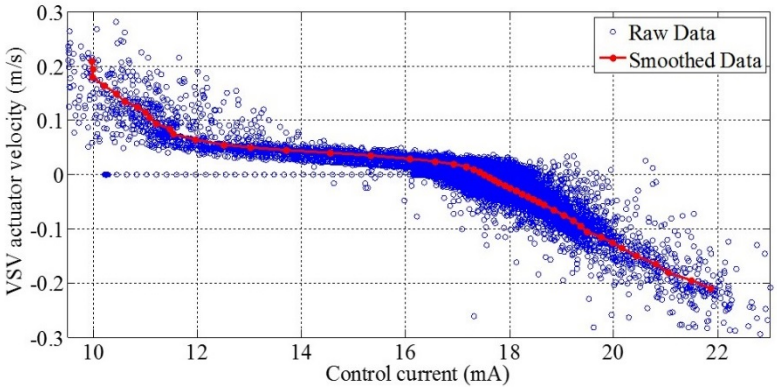


Figure R.25 *Extraction des courbes brutes et lissées de gain en vitesse pour la VSV.*

Dix IS sont extraits de cette courbe : l'hystérésis à vitesse nulle $VsvHyst0$, les pentes des parties gauche $VsvSlpLeft$, centrale $VsvSlpNull$ et droite $VsvSlpRight$, le courant d'équilibre $VsvCEqu$, les coordonnées du point central de la zone de recouvrement $VsvCNullX$ et $VsvCNullY$, la largeur du recouvrement en abscisse $VsvOverlapX$ et en ordonnée $VsvOverlapY$ et l'échelle en abscisse de la courbe $VsvScale$. Les neuf derniers sont illustrés sur la Figure R.26. De même que pour la boucle FMV, on définit également des IS à partir des positions données par les deux capteurs LVDT. Au final, 39 IS sont définis pour la boucle VSV.

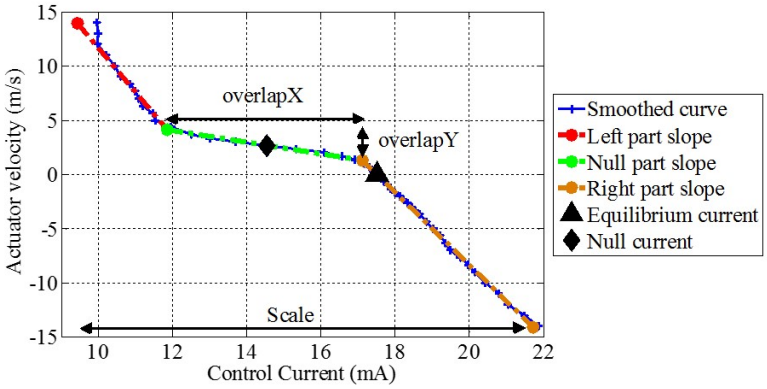


Figure R.26 *Indicateurs de santé pour la boucle VSV.*

Le cas de la boucle VBV est très similaire à celui de la boucle VSV. La différence principale est que les valeurs du courant de commande ne sont pas assez basses pour faire apparaître la partie gauche de la courbe, si bien que la courbe de gain en vitesse est celle présentée sur la Figure R.27.

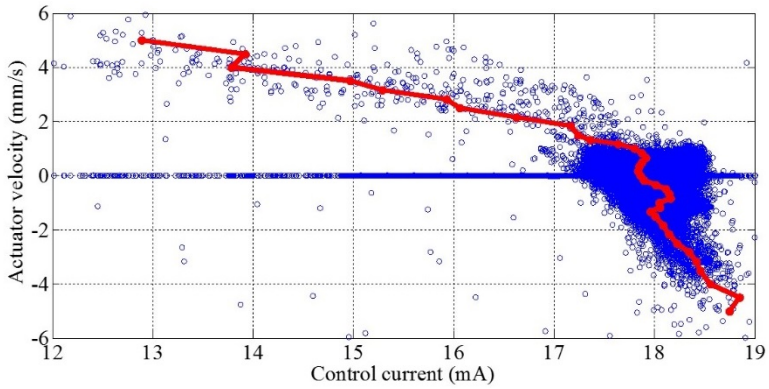


Figure R.27 *Extraction des courbes brutes et lissées de gain en vitesse pour la VBV.*

Il n'ensuit qu'uniquement 7 IS sont définis à partir de cette courbe : $VbvHyst0$, $VbvSlpNull$, $VbvSlpRight$, $VbvCEqu$, les coordonnées du point de changement de pente $VbvXchg$ et $VbvYchg$ et l'échelle $VbvScale$. L'extraction de ces IS est illustrée sur la Figure R.28.

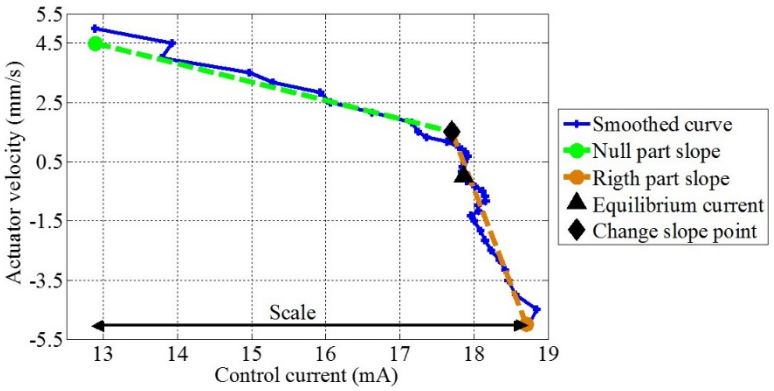


Figure R.28 *Indicateurs de santé pour la boucle VSV.*

Pour le débitmètre, les 8 IS définis sont inspirés du cas de la surveillance des mesures LVDT de la boucle FMV. Ils sont définis à partir des positions mesurées par les capteurs de débit redondants. Quatre d'entre eux sont définis comme les valeurs maximales et minimales des débits mesurées sur chacun des capteurs. Quatre autres sont construits comme les valeurs maximale et minimale des écarts types et moyennes de l'écart de débit entre les deux mesures.

Finalement, pour la pompe LPP et la boucle TBV, aucun IS n'est défini.

- **IS pour les unités fonctionnelles de niveau 0 :**

Pour le circuit carburant complet, aucun IS spécifique n'est défini. L'ensemble des IS est la fusion de tous les IS définis pour chacun de ses sous-systèmes.

- **Modélisation finale du système :**

Au final, on obtient un total de 105 IS réels et 22 ISC répertoriés, respectivement, dans les annexes Appendix XV et Appendix XVI. Pour la modélisation du système, on définit les paramètres incertains suivants : un paramètre de contexte, à savoir la température carburant T_{fuel}, 12 paramètres épistémiques listés dans le Tableau R.6 et 67 paramètres de dégradation, listés en Appendix XIII. À partir des 67 paramètres de dégradation, 85 modes de dégradation sont définis et listés dans l'Appendix XIV.

Nom	Paramètre épistémique	Nom	Paramètre épistémique
Mfp_{Dis}	1.Cylindrée de la MFP	Tbv_{Pop}	2.Pression d'ouverture de la TBV
$Tbv_{Ostroke}$	3.Course d'ouverture de la TBV	Byv_{Drod}	4. Diamètre de la tige bypass
Byv_{Dpist}	5. Diamètre de la valve bypass	Byv_{Ulp}	6.Recouvrement de la bypass
Sov_{Dpist}	7. Diamètre du piston SOV	Sov_{Ulp}	8. Recouvrement de la SOV
$Sov_{Ostroke}$	9. Course d'ouverture de la SOV	Fmv_{ChLg}	10.Longueur de la chambre FMV
Fmv_{Dpist}	11. Diamètre du piston FMV	Sta_{law}	12.Coefficient du profil de la loi de démarrage

Tableau R.6 *Liste des paramètres épistémiques pour le système carburant.*

- **Quantification initiale des incertitudes :**

Initialement, la quantification des incertitudes est faite de manière sommaire sous forme de PDF uniformes. Les valeurs sont données en annexe Appendix XVII. Une méthode de Morris à 3 répétitions est ensuite exécutée pour calculer les valeurs de Tot_i et Lin_i pour chaque paramètre $i = 1, \dots, 80$. On a donc $3 \times 80 = 240$ évaluations du modèle. Les résultats complets sont donnés en Appendix XVIII. À partir de cette analyse de sensibilité sur les IS, la liste des paramètres influentials a été réduite à 59 parmi lesquels 11 sont linéaires. Par extension, la liste des modes de dégradation a été réduite à 71. Les résultats sur les ISC, quant à eux, permettent une première identification des causes potentielles de chacune des menaces au service conforme. Par exemple, le Tableau R.7 montre un exemple de causes potentielles pour un ISC. Ainsi, il apparaît qu'un bypass du filtre carburant (MFF) est susceptible d'apparaître suite à une dérive du capteur de pression différentielle de ce même filtre. Le reste de ces résultats est donné en Appendix XIX.

ISC	Cause potentielle (mode de dégradation)
$DPMFF$	$DEMffSenO$

Tableau R.7 *Exemple de causes potentielles d'occurrence d'un ISC.*

Construction du modèle de Krigeage SVR

Pour la construction du modèle de Krigeage SVR, le PE initial est composé uniquement de vecteurs mono dimensionnels. Dans le cas du circuit carburant, on a donc $11 \times 3 + 48 \times 5 = 273$ évaluations. On utilise également un PE par échantillonnage de type hypercube latin pour le calcul du $Q2$ composé de $4 \times 59 = 236$ évaluations. Finalement, pour l'apprentissage séquentiel, on limite le nombre d'itérations de sorte que leur nombre total ne dépasse pas 1000. Les valeurs pour le critère de validation du modèle sont les suivantes :

$$\begin{cases} Q2^{min} = 0.5 \\ \mu_{CV}^{max} = 0.05 \\ \sigma_{CV}^{max} = 0.25 \end{cases} \quad \textbf{(r.55)}$$

Finalement, on a, au maximum, 973 évaluations du modèle, ce qui est bien en dessous de la valeur limite spécifiée de 1000.

- **Modèles SVR :**

Les modèles SVR sont construits pour chaque IS et ISC en utilisant 3 points d'apprentissage et une fonction noyau linéaire pour les paramètres linéaires et 5 points d'apprentissage et une fonction noyau RBF avec $\gamma = 10$ pour les paramètres non linéaires. Pour l'évaluation des performances, seul le $Q2$ peut être utilisé. Les résultats sont donnés en Appendix XXI. En supposant que les SVR sont très précises, les valeurs de $Q2$ très différentes de 1 indiquent des effets d'interaction importants.

- **Calcul des valeurs limites médianes :**

Les valeurs limites médianes (**VLM**) peuvent être calculées à partir des modèles SVR des ISC. La méthode est détaillée en section 0. Elles indiquent, pour chacun des 71 modes de dégradation, la valeur pour laquelle chaque menace au service conforme est atteinte. Pour un mode de dégradation donné, la VLM est la valeur minimale des VLM associées à chacune des menaces au service conforme. Les résultats complets du calcul des VLM pour chaque mode de dégradation sont donnés en Appendix XX.

- **Modèles de Krigeage SVR :**

Pour l'apprentissage du Krigeage SVR, on utilise le paramétrage proposé dans le Tableau R.8.

Type de fonction de corrélation	Exponential-Gaussian
Nombre d'itérations pour l'optimisation de $\underline{\theta}$	50
Valeur initiale de $\underline{\theta}$: $\underline{\theta}^{init}$	$\underline{\theta_1}^{init} = [1e^{x_1} \quad \cdots \quad 1e^{x_{59}}]^T$; $\underline{\theta_2}^{init} = [y_1 \quad \cdots \quad y_{59}]^T$ with $x_1 \sim \mathcal{U}(-8\,;2), \ldots, x_{59} \sim \mathcal{U}(-8\,;2)$ and $y_1 \sim \mathcal{U}(1\,;2), \ldots, y_{59} \sim \mathcal{U}(1\,;2)$
Valeur minimale de $\underline{\theta}$: $\underline{\theta}^{lb}$	$\underline{\theta_1}^{lb} = [1e^{-8} \quad \cdots \quad 1e^{-8}]^T$; $\underline{\theta_2}^{lb} = [1 \quad \cdots \quad 1]^T$
Valeur maximale de $\underline{\theta}$: $\underline{\theta}^{ub}$	$\underline{\theta_1}^{ub} = [100 \quad \cdots \quad 100]^T$; $\underline{\theta_2}^{ub} = [2 \quad \cdots \quad 2]^T$

Tableau R.8 *Parameters for the SVR-Kriging learning.*

Les valeurs de μ_{CV} et σ_{CV} calculées pour ces modèles sont présentées dans l'annexe Appendix XXIII. Elles montrent que parmi l'ensemble des modèles de Krigeage SVR appris, 35 ne sont pas validés pour μ_{CV} et 35 ne le sont pas pour σ_{CV}. Pour des applications futures, l'apprentissage séquentiel devrait permettre d'atteindre la précision escomptée.

- **Exemple de distribution d'IS :**

La propagation d'incertitudes est réalisée sur les modèles de Krigeage SVR à partir d'un PE de type Monte-Carlo composé de 1000 échantillons pour l'état sain et trois intensités de dégradation pour chacun des modes de dégradation (**MD**). La Figure R.29 montre un exemple de distribution de l'IS FmvHyst0A pour le MD DEFmvStic_Pos. On peut noter que pour une intensité égale à 0.33, le recouvrement entre les distributions saine et dégradée est important, ce qui présage de mauvaises performances pour la détection. Cependant, pour les intensités 0.66 et 1, ce recouvrement est très réduit et les performances en détection devraient être validées.

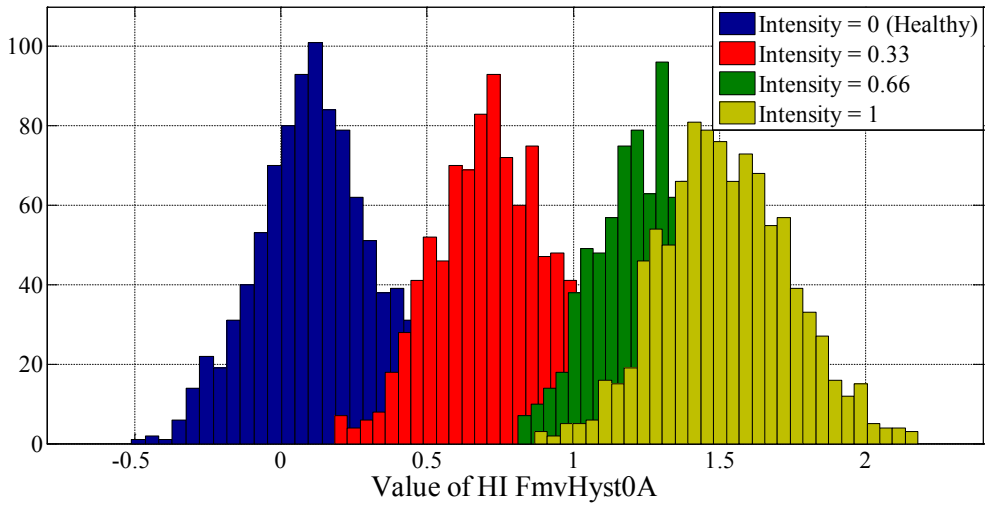


Figure R.29 *Distribution de l'IS FmvHyst0A pour le MD DEFmvStic_Pos.*

Normalisation des IS

Afin de normaliser les IS, on commence par calculer les indices de Sobol. Pour ce faire, on utilise la méthode de Monte-Carlo à partir de deux PE de 10 000 points construits à partir d'hypercubes latins.

On calcule les indices de premier ordre et totaux dont les valeurs sont données, respectivement, en annexes Appendix XXVIII et Appendix XXIX.

Validation des IS

Pour la validation des IS, on définit les spécifications telles que présentées dans le Tableau R.9.

Type	Spécification
Détection	$(TP_{SPEC}, FP_{SPEC}) = (0.80, 0.05)$ et $DTDEM_{\%} = 80\%$
Identification	$\alpha_{SPEC} = 60° \ (1.04\ rad)$ et $ITDEM_{\%} = 80\%$
Localisation	$LLRU_{\%} = 100\%$
Pronostic	$POT_{\%} = 80\%$

Tableau R.9 *Liste des spécifications pour le jeu d'IS.*

Les valeurs calculées des NKPI pour un modèle flotte avec le jeu d'IS brut sont données en Appendix XXIV, Appendix XXV, Appendix XXVI et Appendix XXVII pour les performances attendues, respectivement, en détection, identification, localisation et pronostic. Les résultats montrent que seulement 41 modes de dégradation sur 71 sont détectables avec le jeu d'IS brut. Par conséquent, $DTDEM_{\%} = 57.7\%$, ce qui est en dessous des spécifications requises. Au niveau de l'identification, 15 MDs sur 71 ne sont pas identifiables ce qui donne $ITDEM_{\%} = 78.9\%$. Là encore, c'est en dessous des spécifications. Pour la localisation, on a $LLRU_{\%} = 37.5\%$ et pour le pronostic, $PCST_{\%} = 0\%$. Finalement, aucun des critères n'est validé. Par la suite, on calcule les NKPI pour les indicateurs de santé normalisés puis pour des modèles individuels. Les résultats sont donnés dans le Tableau R.10. Ces résultats montrent que la normalisation induit une légère amélioration pour tous les critères sauf $LLRU_{\%}$. Si cette normalisation est peu efficace, c'est principalement à cause du petit nombre de paramètres de contexte. Le passage aux modèles individuels, quant à lui, entraîne une amélioration significative du critère $DTDEM_{\%}$, ce qui traduit une sensibilité accrue des IS. Cependant, l'accroissement de cette sensibilité produit en contrepartie une baisse des performances de l'identification. Il faudrait supprimer les IS qui sont sensibles à un grand nombre de modes de dégradation pour augmenter la valeur de $ITDEM_{\%}$. Finalement, les propriétés en localisation sont moyennement bonnes parce que beaucoup de modes de dégradation sont encore non *a priori* détectables. Par extension, les mauvaises propriétés du pronostic sont une conséquence des faibles performances en localisation qui induisent des marges de localisation nulles.

Configuration des IS	$DTDEM_{\%}$	$ITDEM_{\%}$	$LLRU_{\%}$	$PCST_{\%}$
IS bruts pour un modèle flotte	57.7%	78.9%	37.5%,	0%
IS normalisés pour un modèle flotte	61.9%	80.3%	37.5%,	1.4%
IS bruts pour des modèles individuels	85.9%	67,6%	50%	1.4%

Tableau R.10 *Configurations testées pour les IS.*

Finalement, ce chapitre a permis de prouver l'efficacité de la méthodologie développée pour définir un jeu d'IS et le valider. On notera tout de même que les critères calculés pour l'application présente ne sont pas conformes aux exigences et que le jeu d'indicateurs proposé nécessite une amélioration. Si cette amélioration n'est pas envisageable, il faudra assouplir les spécifications.

Conclusion

Dans l'introduction générale, le contexte de ces travaux de thèse a été introduit de la manière suivante : Snecma s'intéresse de plus en plus au PHM mais ses ingénieurs rencontrent des difficultés pour définir et appliquer un processus de développement adéquat. Une solution à ce problème industriel a été développée et illustrée tout au long des quatre chapitres.

La contribution principale du premier chapitre a été de formaliser une nouvelle approche de développement intégrée pour le PHM. Dans le but de dérouler cette approche sur des bases solides, une terminologie originale, compatible avec les pratiques industrielles de Snecma, a été proposée, basée sur la dualité entre les menaces au service conforme et les menaces physiques. Les principaux objets sont les indicateurs de santé (IS) et les indicateurs de service conforme (ISC). De plus, l'environnement et le cadre fonctionnel du PHM pour les moteurs d'avions ont été clairement définis. La nouveauté majeure est d'inclure les soi-disant défauts dans l'environnement du PHM, dans le but d'améliorer le processus de troubleshooting en maintenance. À partir de là, les problématiques du développement du PHM ont été soulignées et les fondements de la nouvelle approche intégrée ont été présentés. Cette approche est basée sur le modèle V3, constitué d'une imbrication de 3 modèles en V relatifs à, respectivement, la partie d'extraction des IS, la partie traitement des IS et la partie supervision. Dans cette thèse, l'accent a été mis sur la première partie qui permet de développer complètement la partie embarquée du PHM pendant les phases de conception du système hôte, ce qui permet des gains de temps, d'argent et de réputation.

Dans le second chapitre, la méthodologie pour le développement de cette partie embarquée a été traitée. L'idée principale est que l'absence de données mesurées en phase de conception nécessite l'utilisation de modèles. La méthodologie de développement se base sur trois étapes : la sélection, la normalisation et la validation des IS. Pour la modélisation physique du système hôte, un formalisme mathématique a été proposé, basé sur la classification des paramètres en trois catégories : de contexte, épistémiques et de dégradation. Pour la sélection des IS, un ensemble de données clefs est proposé et la méthodologie se base sur une association de prototypage et d'expertise. Pour la normalisation, une nouvelle approche est proposée. Elle consiste à utiliser l'analyse de sensibilité pour identifier les paramètres de normalisation et la régression par vecteurs supports (**SVR**) pour modéliser les effets des de ces paramètres sur les IS. Enfin, la validation est basée sur des métriques appelées NKPI qui permettent de quantifier les performances d'un jeu d'IS pour la détection, l'identification, la localisation et le pronostic. Ces NKPI sont calculés à partir de distributions des IS qui sont elles-mêmes obtenues par propagation des incertitudes. Finalement, la méthodologie de validation consiste à évaluer des critères associés à ces NKPI pour différentes configurations du jeu d'IS.

Le troisième chapitre apporte une contribution théorique dans le but de répondre à la problématique suivante : dans les cas où le modèle physique nécessite un temps de simulation important impliquant un temps de calcul rédhibitoire pour la propagation des incertitudes, comment faire pour obtenir les distributions des IS ? La solution proposée est d'utiliser un métamodèle de Krigeage. Dans un premier

temps, la construction d'un modèle de Krigeage dans le cas général est présentée. Dans un second temps, une nouvelle technique alliant SVR et Krigeage appelée Krigeage SVR est proposée. Pour évaluer la précision de cette méthode, ses estimations sont comparées à des techniques classiques pour différentes fonctions analytiques sur la base de critères couramment utilisés. Les résultats montrent que le Krigeage SVR est d'autant plus intéressant que la dimension de l'espace des entrées est importante. Enfin, une approche d'apprentissage séquentiel pour améliorer et valider le modèle de Krigeage SVR est développée. Elle s'appuie sur un critère de sélection inédit combinant l'erreur quadratique moyenne du Krigeage avec l'erreur de validation croisée. L'efficacité de cette approche a été prouvée pour l'estimation des fonctions analytiques.

Le quatrième chapitre propose une application de la méthode au système carburant d'un moteur d'avion. La fonction principale de ce système est de réguler le débit injecté dans la chambre de combustion. Il est composé de 12 unités fonctionnelles et 8 unités remplaçables en ligne. Des indicateurs de santé sont définis principalement à partir de caractéristiques extraites des courbes de gain en vitesse et de valeurs statistiques calculées à partir de capteurs redondants. Les modes de dégradation surveillés sont principalement des fuites, des colmatages, des augmentations de frottement et des dérives de capteurs. Le modèle est défini par 105 IS et 80 paramètres incertains. À partir d'une analyse de sensibilité, 59 paramètres influentials sont dégagés. Si, en l'état actuel, les modèles de Krigeage SVR n'ont pas la précision escomptée, on s'attend à ce que l'apprentissage séquentiel permette de l'atteindre dans le futur. Cependant, pour des raisons de temps de calcul trop important, cette approche n'a pas pu être testée pour le moment. Nous avons donc évaluer les performances à partir d'un plan d'expériences de type hypercube Latin uniquement. Les résultats du calcul des NKPIs montrent qu'aucun des jeux d'IS testés n'est conforme aux spécifications. Il est important de savoir si cela est dû à une mauvaise configuration des points d'apprentissage ou à un jeu d'indicateurs de santé insuffisant. Si la seconde cause est identifiée, il faudra rapidement soit définir de nouveaux indicateurs de santé afin d'améliorer les performances ou en dernier recours assouplir les spécifications.

General Introduction

Snecma[1] is one of the worldwide leaders in aircraft engine manufacturing. Approximately 10 years ago, its scientific advisors began to take an interest in prognostics and health management (PHM). The first applications are implemented on existing and new engines. The present PhD thesis work focuses on this trend. The growing interest from both academics and industrials for this discipline has led to the emergence of several projects, dedicated conferences and journals. However, the interest of PHM is still not obvious in the light of current maintenance-based business models. Before getting into the heart of the matter, the industrial background is introduced to justify the interest of developing PHM solutions for aircraft engines.

The industrial background

In many industrial fields, the system lifecycles are governed by the concept of performability. This term first appeared in the 1950s, but the concept was later formalized, mostly by the work of Meyer (Meyer, 1992). According to Bertolino *et al.* (Bertolino, et al., 2011), performability is defined as the *"ability to accomplish a service in the presence of faults over a specified period of time"*. Originally, it was dedicated to computing systems (Meyer, 1980), but its framework can be extended to any type of systems (Johnson, et al., 2011). Performability consists of two aspects: performance and dependability. Performance is defined as the *"ability to accomplish service within given constraints"*, and dependability is defined as the *"ability to deliver service that can justifiably be trusted"*. At the beginning of the industrial era, the performance aspect was clearly privileged, mostly because the systems were not notably efficient and little involved research expenses could lead to high-performance gains. Currently, the situation has changed: the ratio of performance improvement over involved research costs is becoming increasingly less interesting because the performances are getting closer to their optimum. On the contrary, the same ratio becomes increasingly more appealing when it is applied to dependability; thus, there is growing interest for this discipline in the industrial world, particularly in aeronautics.

The concept of dependability was introduced in the mid-1980s by Jean-Claude Laprie (Laprie, 1985). Then, his collaboration with Avizienis (Avizienis, et al., 2000) resulted in the formalism of the concept based on three features: attributes (safety, reliability, maintainability and availability), threats (faults, errors and failures) and means (removal, prevention, tolerance and forecasting). The prominence of dependability management has grown over the last decades and is currently deeply rooted in engineering practices, as evidenced by the existence of international standards that provide systematic methods and tools[2]. For aircraft engines manufacturer such as Snecma, dependability constraints are primarily safety

1 Snecma S.A. is a French multinational aircraft engines manufacturer headquartered in Courcouronnes, France. Snecma is a subsidiary of Safran Group.

2 For example the IEC 60300-X series, an international standard for dependability management published by the International Electrotechnical Commission.

and reliability. They are imposed by certification authorities such as FAA[3] of EASA[4], and each newly manufactured aircraft engine is subjected to a series of test to determine whether it is sufficiently safe and reliable to enter service. To ensure the minimum required levels, removal and prevention are used. Removal consists of suppressing faults and failures after they occur via corrective maintenance, repair and operations (**MRO**). Prevention acts in two methods. First, it is at the origin of fault definition. Faults are operating events that occur as forerunner of failures to prevent them from occurring. They are generally the result of positive built-in test equipment (**BITE**). The second role of prevention is to limit the appearance of faults or failures in the system by scheduling preventive MRO to send every engine of the fleet to a maintenance center at regular time intervals based on the equipment reliability considerations. Concerning maintainability, a minimal level is necessary to optimize the MRO costs. It is provided by prevention, mostly under the form of modular design, which allows for more MRO effectiveness even with the increasing complexity of aircraft engine architectures. As evidenced by the low number of aircraft accidents and the MRO effectiveness, these three means-based strategies are efficient in ensuring minimum safety, reliability and maintainability levels.

However, the same cannot be said for availability. Indeed, faults that are defined by prevention induce numerous delays and cancellations (**D&Cs**) for corrective MRO. Moreover, preventive MRO limits the operational time of aircraft engines by systematically getting them out of service at periodic time intervals. Finally, despite its efficiency, the troubleshooting procedure during MRO often requires a substantial time to perform. The cost of this lack of availability is a major drawback. Indeed, D&Cs are notably expensive in terms of both costs and reputation. For example, in the United States, the FAA estimates that flight delays cost airlines $22 billion yearly (Rapajic, 2009). Furthermore, the European legislation states that flight delays for over three hours or cancellations entitle passengers to a compensation of up to €600 from the airline. The costs are even higher when the airlines are required to pay for the lodging of passengers or when aircrafts are forced to stay on ground in an isolated and poorly equipped airport and require the delivery of spare parts and labor force. A reduced number of D&Cs can lead to significant savings. Furthermore, direct maintenance costs (DMCs) for corrective and preventive MRO were quantified at $42 billions in 2011 and expected to be up to $65 billions in 2015 (IATA, 2011). They mostly occur because of the price of infrastructures, the purchase of spare parts and the payment of labor force. Even if it is not conceivable to suppress these costs, they can be decreased by optimizing both the time interval between systematic MROs and the duration of operations, which involves an optimization of the troubleshooting procedure. In addition, the insufficient availability forces airlines to oversize the dimension of their fleets, the stock of spare parts and the number of MRO infrastructures. Finally, considering previous observations, it is not surprising that the availability of aircraft has become a key challenge for airline companies.

To improve the availability, the first solution that aircraft manufacturers and suppliers adopt was the fault tolerance, which was enabled by the appearance of FADEC[5]. The basic idea of fault tolerance is that instead of immediately sending the aircraft to MRO when a fault is declared, it is preserved in

3 Federal Aviation Administration. The national aviation authority of the United States of America, which was created by the Federal Aviation Act of 1958.

4 European Aviation Safety Agency. The European Union (EU) agency with regulatory and executive tasks in the field of civilian aviation safety. It is based in Cologne, Germany and was created on 15 July 2003.

5 Full authority digital engine (or electronics) control is a system that consists of a digital computer, which is called an electronic engine controller (EEC) or engine control unit (ECU), and its related accessories that control all aspects of aircraft engine performance.

operating conditions and allowed to fly in additional missions fusing tolerance logics. However, even if it allows a gain of availability, this solution is obviously not sufficient because the number of D&Cs remains significant today. The main reasons are probably that tolerance logics are only set for equipment or sensors that propose a physical or analytical redundancy, which does not represent a large proportion of the engine, and many faults are associated with no-go dispatch logics to limit the tolerance effectiveness. A new approach that has rapidly emerged during the last 10 years is to use forecasting.

The basic idea of forecasting is to use measured data to monitor the evolution of a system's state of health to predict the occurrence of faults or failures. Over the past decade, a new scientific community dedicated to forecasting has emerged: the health monitoring (**HM**) community. Ideally, HM performs diagnostics and prognostics. The former consists of detecting abnormalities, identifying the precursors of the compliant service threats and localizing the incriminated line replaceable unit (**LRU**). The latter consists of assessing the intensity of the occuring degradation mode and predicting its evolution from historical data. HM relies on variables that reflect the state of health of the host system, which are called health indicators (**HIs**) in the present case. HM only emerges lately because it is based on statistical analysis, and both computational and data-storage capabilities were not sufficient before the advent of the *big data* era. Currently, computer power and the miniaturization of electrical components allow complex real-time on-board mathematical processing, whereas large-scale networks allow the high-speed remote management of large volumes of data. Eventually, HM is currently enabled for large fleets of systems.

To establish the relationship between HM and MRO, PHM is gradually emerging as the inevitable solution. This trend is evidenced by the multiplication of conferences dedicated to PHM such as the one sponsored by the Institute of Electrical and Electronics Engineering[6] (**IEEE**) or the one sponsored by the PHM society[7]. PHM is also gaining importance in terms of publicationx, as evidenced by the recent creation of journals such as the *International Journal of Prognostics and Health Management*[8], the online Prognostics Journal[9] and the PHM special issue of the IEEE Transactions on Reliability. Within the PHM community, research is oriented along two main axes: the development of mathematical and algorithmic solutions for diagnostic (Isermann, 1997; Patterson-Hine, et al., 2005) and prognostic (Kalgren, et al., 2006; Roemer, et al., 2006) and the formalization of new PHM-based maintenance strategies such as condition-based maintenance, predictive maintenance (Ben-Daya, et al., 2009) and e-maintenance (Muller, et al., 2008). In terms of applications, diagnostics and prognostics algorithms have already shown some results for notably simple applications for bearings monitoring (Roemer, et al., 2007), battery end-of-life prediction (Saha, et al., 2008) or turbine blade creeping (Baraldi, et al., 2012). Note that aeronautics is a common application field for PHM (Johnson, et al., 2011).

The basic idea of PHM is to use HM outputs as inputs for a supervision process based on two new types of maintenance: condition-based maintenance and predictive maintenance. The former is based on diagnostic information and allows the replacement or repair of a given equipment only when it is in an advanced degraded state. The latter is based on prognostics and allows the scheduling of the maintenance of the system before faults or failures occur. Practically, the major advantage of condition-based and predictive maintenace is that they theoretically reduce the number of D&Cs and consequently

6 http://www.phmconf.org/
7 https://www.phmsociety.org/
8 ISSN 2153-2648
9 ISSN 2167-4167

decrease their associated costs. The secondary impact of PHM should be to improve the troubleshooting process by sending informations about the equipments health status to MRO operators. Furthermore, it can even decrease the frequency of preventive MRO. Moreover, for long-term potential, a combination of PHM with fault tolerance logic can limit the number of false alarms by cross checking of information. Finally, from previous considerations, the stock of spare parts, size of fleets and number of MRO infrastructures can be limited. The final scheme of enhanced dependability management of PHM in aeronautics is proposed in Figure i.1, where the negative effects of prevention on the availability are compensated by the joint action of forecasting and tolerance.

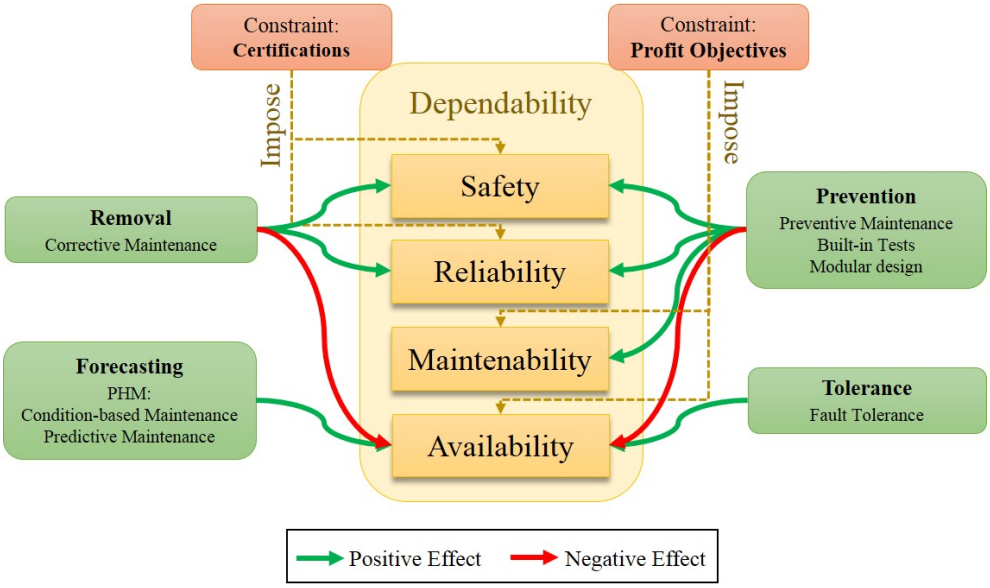


Figure i.1 *PHM enhanced dependability management strategy.*

Because of all cited advantages, PHM can be a real asset for aircraft manufacturers such as Snecma. However, it must face this fundamental issue: until now, no one has been able to establish either a business model or a return on investment for the using of PHM. Furthermore, business models of aeronautical suppliers are often based on the profits generated by corrective and preventive MRO. One question is why one should use PHM for this type of industry. The answer to that question is critical because it justifies the development of PHM. In fact, the answer is two-fold. The first reason to develop PHM in aircraft engine manufacturing is that airline companies are currently under the same economic constraints as engine manufacturers, which includes the rapid increase of operating costs. Consequently, they believe that PHM can be a great source of savings. Indeed, after PHM proves its efficiency, companies will be interested in purchasing it as an option, which implies that it is important to immediately start working on PHM to prepare the imminent transition when it becomes a key selling feature. The second reason is that, in the coming years, all aircraft engine contract will be flight hour contracts. For example, the recent contract between Safran and Dassault aviation[10] to motorize the Falcon 5X is a flight hour contract. Moreover, the maintenance contracts of the future LEAP of CFM International[11] provides that every cost of D&Cs will be the responsibility of the engine manufacturer.

10 The Dassault Aviation Group is a French aircraft manufacturer of military and business jets, subsidiary of Dassault Group.

11 CFM International is a joint venture between GE Aviation, a division of General Electric of the United States and Snecma, a division of Safran of France. The joint venture was formed to build and support the CFM56 series.

Therefore, when these new types of contracts are available and standard, a new business plan will be required and a mature PHM technology will be a great asset if not the keystone.

The PhD thesis work

The motivation of the present work arises from the following observation: the development of systems PHM in Snecma is not sufficiently driven by proven performance at entry into service. Currently, the performance proof is forecasted three years after the entry into service. The practical short term consequence is that the embedded part of the PHM algorithms that are soon implemented in the controllers have not been subject to any performance assessment. At that time, the set of health indicators (HIs) may appear inefficient. The consequences are: (1) costly and perhaps inapplicable changes of the embedded system, (2) youth crisis and retrofits that are not covered by PHM HIs and (3) poor reputation in the mind of MRO operators and airliners. The design and validation should be done concurrently and interactively for the PHM and the host system. From this observation, three levels of issues have been identified and are addressed in the first three chapters. The fourth chapter is devoted to the application. The content of each chapter is introduced below.

Chapter 1: the general issue - improving the development of PHM for aircraft engines.

The general issue derives from the following question: how to efficiently, concurrently and interactively develop the PHM and the host system for aircraft engines? From this question, three sub-issues are identified, which are related to the PHM terminology, the PHM functional framework and the development of PHM systems.

Regarding the PHM terminology, the problem is to identify a set of definitions to be used. Because no existing terminology is fully compatible with the specificities of aircraft engines, a new original one is proposed. It must be consistent with the current industrial practices and coherent with the existing terminologies such as those found in (Sheppard, et al., 2009) or (Johnson, et al., 2011). For more clarity, the definitions are divided into four classes: (1) the threats - events that are likely to be monitored by the PHM system, (2) the extraction means - elements to compress the on-board information with limited loss of information, (3) the processing means - elements to assess the health status of the system from extraction means and (4) the supervision means - elements that support the MRO scheduling from health status information. For each class, the definitions are illustrated on a guiding thread example. In particular, the keystones are the health indicators (HIs), which are variables that are measured online and reflect the health status of the host system. Their construction is a crucial PHM task.

Regarding the PHM functional framework, the challenge is to define the scope and the principal functions of PHM. The PHM scope with application to aircraft engines remains fuzzy regarding the complexity of the considered systems. Therefore, a precise definition of the scope must be proposed with respect to the MRO specificities for aircraft engines and the previously introduced terminology. Moreover, the classical functional architectures of PHM are not compatible with the intended applications. The limited embedded storage and computation capacities make it impossible to perform the entire set of PHM tasks online. Thus, a specific functional framework that accounts for this split between in-flight and on-ground tasks is proposed. It is consistent with the OSA-CBM architecture (Swearingen, et al., 2007). In particular, two tasks are introduced in details: the extraction and the

processing of HIs. For the extraction task, the main issue and the main useful sources of knowledge are presented. For the processing task, the main functions, *i.e.*, the detection, identification, localization and prognostics, are introduced, and their main implementation issues are addressed.

Regarding the development of PHM systems, the main problem is to identify the major milestones of the process and their interaction with the lifecycle of the host system. The current development process of PHM systems of aircraft engines suffers from several obvious shortcomings mainly because the V-model is used and the interactions with the host system lifecycle are undefined and insufficient. From the criticism of the current practices, this thesis work proposes a new development process based on the V3-model. This original type of model is issued from the imbrication of three Vs with multiple development milestones for the standalone developments of the embedded extraction unit, processing unit and supervision unit. This segregation allows a more precise definition of the interactions between the PHM and the host system. In particular, the needs for models, risk analysis results and specifications can be associated with the milestones of the V3-model. Because the approach is mainly to integrate the development of the PHM system into the host system lifecycle, the name "Integrated Development of Prognostic and Health Management" (**IDPHM**) is proposed.

Finally, the IDPHM methodology with its underlying terminology and functional framework proposes a solution to the general issue. From these considerations, a specific issue arises regarding the first V of the V3-model: how to design and validate the embedded extraction before the entry into service.

Chapter 2: The specific issue – developing the embedded extraction in the design stages.

The specific issue derives from the following question: how to develop the embedded extraction in design stages? The answer is fundamental as it is the key to assess the performances of HIs before the entry into service. The major stakes are avoidance of unplanned retrofits and preventive support in cases of youth crisis. The problem can be divided into three principal sub-issues relative to, respectively, the selection, the standardization and the validation of HIs.

Regarding the selection of HIs, the challenge is to formalize a procedure to define a suitable set of HIs during the design stages, *i.e.*, before the availability of measured data. Currently, it is principally performed from data that are retrieved from experience feedback on other engines under the assumption that the new one behaves similarly. However, this restrictive approach is not appropriate when the targeted host system has a new architecture. Moreover, this subject is almost unaddressed in the scientific community. Therefore, a new selection process is proposed, which consists of hierarchically defining a set of HIs for each functional unit from the equipment to the global host system. This process is strongly based on modeling. A specific formalism to aircraft engine physics-based models for PHM applications is proposed based on a constant temporal input representation and an original classification of the input parameters. The proposed selection procedure consists of an iteration for each functional unit of the following sequential steps: identify the prior relevant HIs, assess the HI sensitivity by prototyping the individual models and submit to engineering judgment.

The standardization process consists of subtracting the effects from the HI values that are attributable to known and influential parameters, which are called standardization parameters. Thus, the standard deviation is reduced, and the performances should improve. In this process, the challenge is to identify the standardization parameters and models. Until now, the former are only identified using engineering

judgment, and the latter are estimated using nonlinear regression based on analytical functions (Lacaille, 2009). In this thesis work, it is first proposed to add a quantifiable aspect to the identification of standardization parameters using a sensitivity analysis (**SA**), which allows one to assess and hierarchize the effects of the parameters on the HIs. Moreover, an alternative to the nonlinear regression is proposed: the support vector regression (**SVR**). This method is chosen for its good results in modeling non-linear behaviors without prior knowledge about the shapes of the modeled behaviors. Eventually, a standardization procedure that combines SA and SVR is presented.

Regarding the validation of HIs, the major issue is to define the metrics and criteria. Until now, no metric has been defined to validate the HIs in the design stages in industrial practices and the literature. The validation of PHM is addressed in some papers, but it is dedicated to the prognostic aspect (Saxena, et al., 2008; Saxena, et al., 2010). In this thesis work, numerical key performance indicators (**NKPIs**) are proposed as metrics to assess the detection, identification, localization and prognostic performances. Associated criteria are also suggested. Finally, a procedure to validate the HIs for the intended application is defined based on the assessment of the HI set performances for different configurations. Three configurations are tested: (1) raw HIs with a fleet model; (2) if (1) is not efficient, standardized HIs with a fleet model are tested; (3) if (1) and (2) are not sufficient, standardized HIs with individual engine models. An additional and optional step is added when the sensors are concurrently selected with the design of the host system.

Finally, the proposed approach to validate the HIs relies on NKPIs, which are computed from the HI distributions. To obtain these distributions in the design stages, uncertainty propagation is used. However, because the physics-based models are time-demanding and defined by numerous parameters, the necessary simulation time makes it unrealistic. Therefore, surrogate models, particularly Kriging models, are proposed, which are low-computation-time mathematical functions to estimate the outputs of a complex model (see Figure i.2).

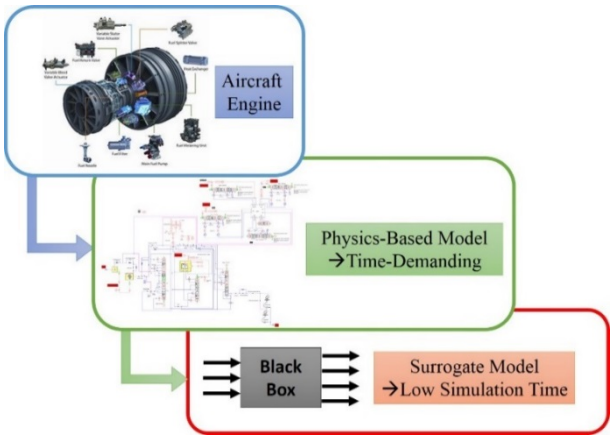


Figure i.2 *Different levels of representativeness.*

Chapter 3: The mathematical issue - constructing Kriging models.

The mathematical issue derives from the following question: how to build and use an accurate Kriging model to estimate the aircraft engine physics-based models? The answer is the key to enable the necessary uncertainty propagation to validate the HIs. Three sub-issues have been identified: how to construct a Kriging model in the general case? How to adapt it to the specificities of the intended applications? How to validate or improve the accuracy?

Regarding the construction of Kriging models, three main steps are commonly identified: determine the variation ranges of the input parameters, construct the learning design of experiment (**DOE**) and estimate the hyperparameters for the Kriging model (Forrester, et al., 2009). The first step relies on the quantification of uncertainty ranges. In the second step, the main challenge is to find a method to construct a learning DOE that combines good space-filling properties and a limited number of samples. The Latin hypercube sampling (**LHS**) (Iman, 2008) is proposed. However, this type of sampling methods yields DOE with notably heterogeneous qualities. Therefore, a random draw of several LHSs that are associated with a selection criterion is used to ensure the good space-filling properties, which is inspired by (Marrel, 2008). The learning of the model is introduced through a theoretical presentation of the Kriging technique. An extended state of the art on such techniques is proposed with a focus on non-stationary Kriging issues that are determinant for the intended applications.

From experiences feedback on existing engines, it appears that for the intended applications, the encountered behaviors are notably monotonic and subject to strong local nonlinearities. Moreover, the second- and higher-order effects, due to interactions, are limited. Moreover, the input parameters are weakly correlated. Therefore, regression is used to model the first-order effects. Support vector regression (SVR) is used for the good performances and robustness in modeling nonlinearities (Smola, et al., 2004). In addition, the Kriging technique addresses the residual interaction effects. The proposed technique is termed “SVR-Kriging”. Because it is a new approach, it is compared with ordinary and universal Krigings for three types of example models of various dimensions. For the comparison, three criteria, which are inspired from the literature, are used: the Q2 index (Marrel, 2008), which is based on the comparison with an additional test sample, the mean and the standard deviation of the cross-validation error (Davis, 1987). Finally, computation techniques are proposed to better estimate the Kriging hyperparameters.

To assess the SVR-Kriging accuracy, a set of three validation criteria based on the Q2 index and the cross-validation error are proposed. If the accuracy of the surrogate model is not validated at the first estimation, a sequential learning procedure is proposed. This common approach (Jones, et al., 1998; Bichon, et al., 2008) consists of iteratively adding some well-chosen points and re-estimating the model hyperparameters. The well-chosen points are identified with respect to a new selection criterion based on a combination of the Kriging variance and the cross-validation error. However, there are as many SVR-Kriging models as the number of outputs. Consequently, there are as many new potential learning points as the number of outputs. Therefore, a combination of the three validation criteria allows one to choose a single learning point. Finally, computational issues are addressed, and three techniques are proposed to reduce the computation time of the sequential learning.

This new technique of SVR-Kriging is compared with other Kriging approaches to estimate the simple analytical functions. It shows better accuracy than ordinary and universal Kriging. The last chapter is devoted to an actual and time-demanding physics-based model.

Chapter 4: the application – monitoring a generic aircraft engine fuel system.

The complete developed methodology is finally applied to the development of a PHM solution to monitor a generic aircraft engine fuel system (Moir, et al., 2008). The main function of the fuel system is to regulate the fuel supply of the combustion chamber. In the scope of the present thesis work, only the development of the HI extraction is addressed. Indeed, to develop a complete PHM solution for this

complex system was a too time-demanding work and we chose to focus on the first task chronologically. This system has been chosen because it has numerous potential threats and its physics-based model is complex, which makes it a good candidate for the specific issue and the mathematical issue, respectively.

First, the system architecture is introduced via its functional and structural representations. The former includes several functional units such as pumps, filters, fuel metering devices and locally controlled inlet air variable geometries. The former contains LRUs such as an actuation control unit, actuators and sensors. Each functional unit is presented in details.

Second, the selection of HIs and for the PHM of the fuel system is addressed. For each functional unit, the compliant service threats and degradation modes are identified. From these elements, the lists of HIs and compliant service indicators are determined. Both real and virtual HIs are defined to handle the case where the existing sensors are insufficient.

Third, the construction of the SVR-Kriging to estimate the fuel system model is presented. The initial quantification of uncertainties is introduced, and the sets of influential and linear parameters are computed from the sensitivity analysis. Then, the SVR-Kriging model is constructed, and the sequential learning process is performed to attain the desire final accuracy.

Fourth, the standardization procedure is applied. A more precise sensitivity analysis is performed to determine the standardization parameters, and the standardization models are estimated using the SVR. The effect of standardization on the HI distribution is illustrated using several examples.

Finally, the HIs are validated. The uncertainty propagation is performed on the SVR-Kriging model. The compliance with detection, identification, localization and prognostics criteria are computed and criticized for different sets of HIs.

1

Integrated development of prognostics and health management for aircraft engines

Abstract: In current practices, the development of PHM for aircraft engines is not well-integrated in the host system's lifecycle. Indeed, the current development process of PHM, based on the V-model, has a major drawback: the process addresses PHM as a single system, whereas PHM is composed of three different tasks types: the embedded in-flight extraction, the on-ground processing and the maintenance support service. Each of these should be developed following a standalone process. In particular, concerning the development of the embedded extraction task, it should be designed and validated concurrently and interactively with the host system. However, this requirement is not currently well-addressed. In fact, the selection of HIs is performed in an unstructured manner, and their validation occurs long after the entry into service, which is too late or too expensive to update in missing HI cases. To propose enhancements for the PHM development process, both a terminology and a functional framework are necessary. However, the literature does not provide any that are suitable for the specificities of the intended application. Therefore, specific sets of definitions, clearly expressed scope and systems representation formalism are provided. Next, the integrated development of PHM, termed IDPHM, is proposed, based on the V3-model. The latter is composed of three imbricated generic V models corresponding to the three mentioned tasks. The first V of this V3 is run concurrently with the V of the host system. The design and validation of the HIs set is performed with physics-based models coupled with control laws. This approach allows both the definition and validation of the right set of HIs and also the estimation the following elements before the entry into service: the standardization parameters and models, the precursors of compliant service threats and the median limit values of each degradation mode.

Overview

1.1 Introduction 68
1.2 Proposed terminology for PHM of aircraft engines 69
1.2.1 Taxonomy of threats 69
1.2.2 Extraction means 73
1.2.3 Processing means 76
1.2.4 Scheduling means 78
1.2.5 The proposed global MRO strategy 79
1.3 Proposed scope and functions of PHM for aircraft engines 80
1.3.1 The scope of PHM systems for aircraft engines 80
1.3.2 Architecture of a PHM system 81
1.3.3 Architecture of the host system 83
1.3.4 Architecture of the health monitoring system 85
1.3.5 Architecture of the engine monitoring unit 85
1.3.6 Architecture of the processing unit 86
1.4 Integrated Development of PHM 91
1.4.1 Current PHM systems development methodology 91
1.4.2 Weaknesses of current PHM system development 94
1.4.3 The IDPHM methodology 94
1.5 Conclusion 97

1.1 Introduction

As mentioned in the general introduction, the purpose of this chapter is to propose a solution to the efficient development, concurrently and interactively, of PHM and the host systems for aircraft engines. The underlying issues are of three types: the definition of PHM, the functions of PHM and the development of PHM systems.

The first section is dedicated to the proposition of a novel terminology for PHM with application to aircraft engines. Indeed, as neither a generic set of definitions nor a standard exist for PHM, the solution adopted is to define a specific terminological framework. In this manner, the basic terms are in line with Snecma's current practices. Furthermore, they also fall in the line with the PHM community as the major part of proposed definitions are inspired by papers or books published in the field, such as (Johnson, et al., 2011) or (Kalgren, et al., 2006). They are divided into four classes: the threats, the extraction means, the processing means and the supervision means. The main original feature of these definitions is the distinction between compliant service indicators (**CSIs**) and HIs. The global MRO strategy for aircraft engines issued from this novel terminology is finally proposed.

The second section is devoted to the proposition of a scope and a functional framework for the PHM of aircraft engines. Indeed, the current objectives and targeted items are unclear with regard to the specificities and the complexity of present applications. In this thesis work, a precise scope, taking into account the notion of dispatch and based on the previous terminology, is proposed to reduce this fuzziness. It is consistent with the OSA-CBM architecture (Swearingen, et al., 2007). Consequently, the targeted degradation modes and compliant service threats are highlighted. Moreover, as the existing

functional architectures are incompatible with intended applications, an original architecture is proposed, based on the distinction between the HM and the supervision systems. The HM system is described in detail, and a solution based on a hierarchical agent-based architecture is proposed. It is subdivided into the HI extraction and the HI processing tasks. The former is introduced through the architecture of the embedded functions, the latter through its encompassed tasks, *i.e.*, the detection, the identification, the localization and the prognostics and their principal independent issues.

The third section is centered on the proposition of an innovative development process dedicated to aircraft engines PHM systems. Indeed, after having introduced and criticized the current practices, the following observation is compiled: the present-day V-model is not suitable for the intended applications. Its principal weaknesses are the undefined and insufficient interactions with the host system's lifecycle. Therefore, this thesis work proposes a novel development scheme for aircraft engine PHM systems based on the original V3-model, issued from the imbrication of three V-models for, respectively, the development of the engine monitoring unit, the processing unit and the supervision unit. The scheme allows a clearer definition of interactions between the PHM and the host system. As the primary idea is that the developments of the PHM system must be integrated into the host system's lifecycle, the name integrated development of prognostic and health management (**IDPHM**) is proposed.

1.2 Proposed terminology for PHM of aircraft engines

Browsing the scientific literature, it is difficult to find a common terminology recognized by the entire community. For example, the term PHM itself is not standardized. The same concept can be found under the name SHM for system health management (Johnson, et al., 2011), ISHM for integrated system health management and IVHM for integrated vehicle health management of HUMS for health and usage monitoring systems. Their associated terminological frameworks are devoted to particular applications and rarely enlargeable to others. Moreover, according to the point of view of the recent IEEE standardization group (Sheppard, et al., 2009), if a standard for PHM is to be published, its normative features must be reduced. As a consequence, a terminological framework specific to aircraft engines is proposed. The definitions are divided into four classes: the threats, the extraction means, the processing means and the supervision means.

1.2.1 Taxonomy of threats

Threats are usually defined as feared events that have a negative effect on a system's dependability. In (Avizienis, et al., 2004), three types of threats are defined: faults, errors and failures. Both faults and failures are classified with respect to numerous features found in (Avizienis, et al., 2000). Despite its popularity, this taxonomy is not adaptable to PHM for aircraft engines because the notion of fault has a completely different meaning. Moreover, this taxonomy does not make a clear distinction between the effects and the causes of threats. Consequently, a novel taxonomy of threats is proposed, based on the distinction between compliant service threats and physical threats.

1.2.1.1 *Compliant service threats*

Before defining compliant service threats, the notion of compliant service should be introduced. It is an extension of the notion of availability, with the added restriction concerning the compliance with specifications. Indeed, a system can be available without being compliant with all the specifications. It is defined as follows:

DEFINITION 1 (**Compliant service**). *Compliant service is the ability to keep a system available, in compliance with all the specifications.*

Compliant service threats (**CST**) are observable threats related to external and apparent changes of the system. They have a direct impact on compliant service. In this work, three types of compliant service threats, namely failures, faults and defects are considered. The proposed definition of failure is very close to the classical one, as found in (Avizienis, et al., 2000):

DEFINITION 2 (**Failure**). *A failure is an online observation of a loss of a system's functionality.*

Failures result in operational interruptions that require immediate corrective maintenance operations. The most common failure for aircraft engines is the in-flight shut down (**IFSD**). This failure can be either commanded by the FADEC or triggered by the pilot to prevent the engine from reaching a worse state, for example, a fire or an explosion. Some other failures, such as a loss of blade or a bearing breakage, can also occur, although they are much rarer. Because of safety concerns, a great portion of potential failures identified by reliability and safety studies are protected by built-in test equipment (BITE) embedded in the controller. BITE is defined by the control system designers based on specifications of reliability and safety engineers. The idea is that critical failures must be protected by a BITE triggering a fault as a forerunner. The occurrence of faults are then communicated to both the pilot via alarms and to the maintenance crew via the ACARS[12] system. Faults can be defined as follows:

DEFINITION 3 (**Fault**). *A fault is an online observation of a difference between the actual value of a variable measured by built-in test equipment and the specified value, with this difference exceeding the limits of specifications.*

Faults are associated with tolerance logic aimed at allowing the aircraft engine to extend its operating lifetime. Those extensions are governed by the notion of dispatch. Dispatch indicates how many extra hours an aircraft engine is allowed to fly before being sent to a maintenance center for fault removal. Their definition depends on the type of engine. For example, for the SaM146[13], the principal types of dispatch are presented in Table 1.1.

Dispatch level	Type of dispatch	Availability
A	no-go dispatch	Prohibited flight, repair or replacement is to be performed immediately on site.
A GO IF	go-if dispatch	Prohibited flight, except for some particular cases on pilot decision.
Beta (C then A)	beta dispatch	For physical redundant sensors. Fault for which level increases from C to A with the following combination: $\{local\ channel\ faulT + cross\ channel\ similar\ faulT\}$.
B	short-time dispatch	150 h authorized flight hours.
C	long-time dispatch	250 h authorized flight hours.
D	infinite dispatch	Unlimited.

Table 1.1 *Dispatch types classification*

[12] In aviation, ACARS (Aircraft Communications Addressing and Reporting System) is a digital datalink system for transmission of short, relatively simple messages between aircraft and ground stations via radio or satellite.

[13] The SaM146 is a turbofan engine produced by the PowerJet joint venture between Snecma and NPO Saturn of Russia. It was certified by the EASA on 23 June 2010.

Therefore, from an availability point of view, faults with no-go dispatch are the most feared ones because they systematically result in D&Cs for immediate corrective operations. Faults with go-if or beta dispatch also produce D&Cs in certain configurations. However, the other types of faults associated with short-time, long-time or infinite dispatch have almost no effect on compliant service. Indeed, the authorized delays give maintenance managers the time to organize the delivery of spare parts to the right location, to prepare infrastructures and to mobilize crews. Defects are the last type of compliant service threat. They are defined as follows:

DEFINITION 4 (**Defect**). *A defect is an offline observation of a difference between the actual value of a variable measured by dedicated offline test procedures and the specified value, with this difference exceeding the limits of specifications.*

The dedicated offline procedures can be based, for example, on NDT[14] or on hydraulic installations provided with sensors unavailable online. Because they are not related to any embedded functions, defects have no direct impact on availability. However, they do have a direct impact on compliant service as they induce non-compliance to specifications. Typically, the monitoring of defects can be used for improving the troubleshooting procedure during MRO by focusing on equipment that is defective.

To illustrate the taxonomy of threats, the system presented in Figure 1.1 is considered. Throughout the remainder of this work, it plays the role of the guiding thread example for the deployment of the proposed terminology and framework. It is a hydraulic system composed of four elements:

- A simple two position-two port hydraulic servovalve
- A simple effect jack with embedded feedback spring
- A mobile mass mechanically linked to the rod of the jack
- A displacement sensor
- A controller of type proportional, integrator derivative (PID).

The system is defined by a single input, the displacement demand X_{dmd}. Concerning the outputs, two signals are measured: the displacement of the rod X and the control current from the PID I_c. At initial time $T = 0$, the rod is at $X = 0$. The displacement demand signal X_{dmd} is a step equal to 0 at $T = 0$ that switches to 1 at $T = T_{sw}$.

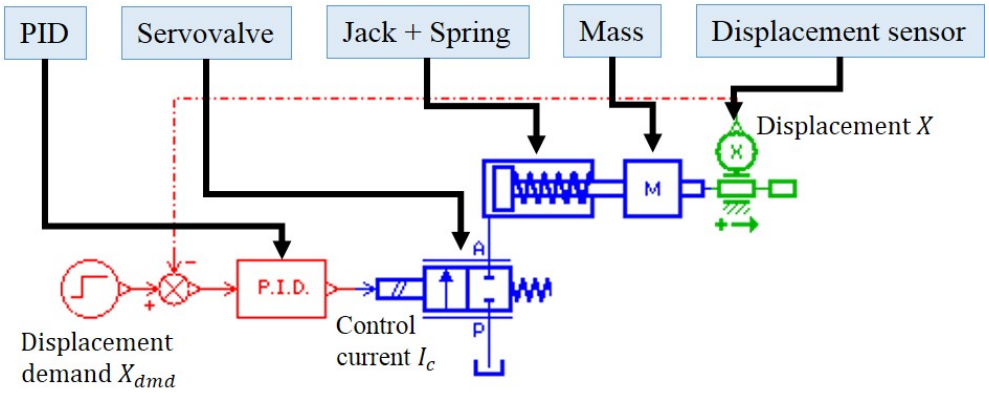


Figure 1.1 *Guiding thread hydraulic system for the illustration of definitions.*

[14] Nondestructive testing or Non-destructive testing (NDT) is a wide group of analysis techniques used in science and industry to evaluate the properties of a material, component or system without causing damage.

It is supposed here that the main function of this system is to activate a valve for the discharge of a compressor. A malfunction of this system can provoke stalling, which is a critical failure. To prevent stalling from occurring, a BITE associated with a fault should be defined. The actuation error is defined as the absolute difference between X_{dmd} and X. It is supposed that experts have analyzed that stalling is likely to occur with a non-acceptable probability if the actuation error of the system is above $1\ mm$ for ten consecutive samples. Consequently, the associated fault is defined as the following event: ten consecutive values of $|X_{dmd} - X|$ are over the maximal value $\Delta X_{max} = 1\ mm$. Concerning defects, it is supposed that the servovalve must comply with the following specification: the maximal loss of pressure through the servovalve must be under $\Delta P_{max} = 1\ bar$. This value is not measurable on-line because no pressure sensors are available in the system. However, it can be measured via a dedicated test procedure during MRO. During this test, if the measured value is above $1\ bar$, it is a defect.

1.2.1.2 *Physical threats*

Physical threats are unobservable threats related to internal and hidden changes of the system. Two types of compliant service threats are defined: degradations and degradation modes. Degradations are defined as follows:

DEFINITION 5 (**Degradation**). *A degradation is the alteration of one or several values of the host system's parameters exceeding the boundaries of the nominal case.*

In the present case, only single degradations are considered. This means that a given degradation is the outcome of a unique parameter's alteration. For the guiding thread example (see Figure 1.1), the considered degradations are issued from the alteration of following parameters: the static friction coefficient μ of the shaft with respect to its bore and the diameter of the bore D_b. Considering that the nominal values of μ and D_b are specified to belong to, respectively, the intervals $[0\ N; 10\ N]$ and $[0.9\ mm; 1.1\ mm]$, a value of either of these parameters outside of its nominal range is a degradation. However, not all the parameters are likely to be subject to alterations. This is the reason why degradation modes are defined as follows:

DEFINITION 6 (**Degradation mode**). *A degradation mode (**DEM**) is an alteration of a parameter likely to occur in the system. Degradation modes can be defined by expertise, experience feedback or physical reasoning.*

Parameters at the origin of degradation modes are termed degradation parameters. Because only degradation modes are considered in this work, physical threats and degradation modes are equivalent. Thus, DEMs are used instead of physical threats.

Returning to the guiding thread example (see Figure 1.1), suppose that the analysis of experience feedback and expertise has revealed that the alteration of the degradation parameter D_b is not likely to happen. On the contrary, another analysis has shown that the value of μ is capable of increasing beyond its nominal boundaries. Indeed, from a physical point of view, the ageing of the system could induce a release of particles into the hydraulic fluid that are likely to get stuck between the seal and the bore. The manifestation of this phenomenon at the macroscopic scale could most likely be an increase of the static friction coefficient μ. Thus, of the two considered parameters, only the increase of μ is a DEM. The degradation parameter carrying this DEM is μ. For a given DEM, its direction is positive if the degradation parameter increases and negative if it decreases. In cases where it can go both ways, two different DEMs are defined. The difference between degradations and a DEM is very important for the

upcoming modeling steps because only the seconds are to be modeled. For a DEM, two features are defined: median limit value (**MLV**) and intensity.

DEFINITION 7 (**Median limit value**). *The Median Limit Value (**MLV**) of a DEM is the minimal value of the degradation parameter for which an associated compliant service threat is reached with a probability of 0.5.*

The definition of the MLV is derived from the definition of the limit state issued from the reliability engineering field (Echard, et al., 2011). For a given system, the limit state is the hyperplane of the input space separating healthy states from states associated with failures. For a couple (DEM/compliant service threat), the limit value of the degradation parameter δ is defined as the distribution containing all the values of δ belonging to the limit state. The MLV is then the median of this distribution. Considering the DEM c and the compliant service threat j, the associated MLV is written $\delta_{c,j}^{MLV}$. The MLV of DEM c, written δ_c^{MLV}, is then the minimum of the set of MLVs:

$$\delta_c^{MLV} = \min_j \{\delta_{c,j}^{MLV}\} \quad \textbf{(1.1)}$$

Note that this definition is equivalent to the median lethal dose (LD50) of the pharmacology field. The cases where the compliant service threat j cannot be reached by DEM c are written $\delta_{c,j}^{MLV} = \infty$.

DEFINITION 8 (**Intensity**). *For a given DEM, the intensity is the ratio of the current value of the associated degradation parameter over its MLV.*

Eventually, the definitions of compliant service threats proposed above are far from those introduced in the Avizienis-Laprie concept (Avizienis, et al., 2004). It is obvious that their terminology is not appropriate in the present context because of all the specificities to be considered for the particular case of PHM with application to aircraft engines. The main feature to be remembered is the segregation between compliant service threats and physical threats, allowing taking into account physics-based considerations.

1.2.2 Extraction means

Extraction means are objects or functions aimed at reflecting the evolution of operating and physical threats within a system. Two principal types of objects are defined: compliant service indicators (**CSIs**) devoted to the monitoring of compliant service threats and health indicators (**HIs**) devoted to the monitoring of DEMs. CSIs are defined as follows:

DEFINITION 9 (**Compliant service indicators**). *Compliant service indicators (CSIs) are decreasing functions reflecting directly the evolution of CSTs within the system; a negative value of a CSI means that the associated CST has been reached.*

In practice, CSIs are defined to be equivalent to performance functions inspired by the structural reliability field. CSIs are used among other things to compute MLVs. Thus, for the computation of the MLV for the couple (DEM c/compliant service threat j), the function of the values of CSI j versus the values of the degradation parameter δ associated with DEM c is considered, all the other parameters being fixed to their nominal values. The MLV $\delta_{c,j}^{MLV}$ is the value of δ for which the CSI j takes a negative value. The definition of CSIs is quite easy for faults and defects that occur at a deterministic value defined either by the BITE or the equipment specification documents. However, it is often more complex for failures as they do not occur at a given theoretical threshold. Actually, the definition of CSIs for

failures cannot be performed in design stages because it requires a large amount of actual data to characterize the occurrence conditions. Consequently, only faults and defects are associated with a CSIs.

In the guiding thread example (see Figure 1.1), a fault is declared if the actuation error of the loop is greater than ΔX_{max} for ten consecutive samples. The CSI associated to this fault can then be defined as the following value:

$$\mathrm{CSI}_1 = \min_{i=10,\dots,n}(\{\Delta X(k), k \in [\![i-9; i]\!]\}) \quad \textbf{(1.2)}$$

where $\Delta X(k)$ is the actuation error measured at sample k, and n is the number of samples for the considered mission. It can be verified that this value is positive as long as the fault is unreached and becomes negative when it occurs. Moreover, a defect is declared when the pressure drop within the servovalve reaches $\Delta P_{max} = 1\ bar$. An associated CSI can be defined as follows:

$$\mathrm{CSI}_2 = \frac{1}{n}\sum_{i=1}^{n}(P_{in}(i) - P_{ouT}(i)) \quad \textbf{(1.3)}$$

where $P_{in}(i)$ and $P_{ouT}(i)$ are, respectively, the inlet and outlet pressures of the servovalve at sample i. Obviously, direct monitoring of the CSIs would be an efficient way to assess the evolution of compliant service threats. However, this approach depends on the availability of required sensors. For the guiding thread example (see Figure 1.1), if the computation of CSI_1 is effectively feasible online via the displacement sensor, the CSI_2 is not measurable because the necessary pressure sensors are not provided with the system. Actually, in practice, CSIs are rarely directly computable.

The idea is then the following: if it is impossible to evaluate directly CSIs, a roundabout way to monitor CST should be found. It is proposed to monitor their causes, *i.e.,* DEMs. In practice, DEMs are generally not measurable either. Thus, some variables indirectly reflecting their evolution are defined by aggregating observations from other sources: health indicators (**HI**). The advantage of this approach is that it provides information about the propagation mechanisms and the origin of CSTs and consequently a good capitalization on the experience. These physics-based concerns are one of the added-values of PHM.

DEFINITION 10 (**Health indicators**). *Health Indicators (HIs) are variables reflecting the evolution of DEMs within the system. HIs are issued from a combination of measures, control values, models or other sources of knowledge available on-line that reflect the health status of a system.*

In the particular case of aircraft engines, a constraint for HIs is to compress information because online storage capacities are limited. This compression must keep as much information as possible about degradation modes. For example, for the guiding thread example, considering the degradation mode "increase of the static friction", it is not possible to measure directly the static friction. Looking at the whole system, it appears that the only available information are the displacement of the rod and the control current of the valve. Thus, a HI to monitor indirectly the static friction from the displacement and control current information only is to be constructed. A potential solution is to define the HI ΔT as the time elapsed between T_{sw} and the beginning of the rod displacement T_{dis}. Indeed, based on physical reasoning, an increase of static friction should delay the displacement and increase the value of ΔT.

As actual systems are subject to uncertainties, HIs values are not deterministic. They are considered as stochastic objects defined by a nominal value and a probability distribution. Moreover, as the nominal value is not systematically equal to zero, symptoms are considered. They are defined as follows:

DEFINITION 11 (**Symptom**). *A symptom is a value indicating a variation of a health indicator value relative to its nominal distribution.*

A symptom can be expressed as follows:

$$sym_x = z(HI_x, \theta_{HI}) \quad \textbf{(1.4)}$$

where Sym_x is the value of the symptom; HI_x is the current value of the HI and θ_{HI} is a set of parameters characterizing the nominal distribution of the HI learnt on healthy data. The function z is called the score function. Among score functions, Snecma's PHM designers use the Z_score defined as follows (Lacaille, et al., 2010):

$$Z_score(HI_x, \mu_{HI}, \sigma_{HI}) = \frac{HI_x - \mu_{HI}}{\sigma_{HI}} \quad \textbf{(1.5)}$$

with μ_{HI} is the healthy mean value of the distribution of the HI, and σ_{HI} its healthy standard deviation of the normal distribution. Resuming the guiding thread example (see Figure 1.1), suppose that for the healthy state, *i.e.,* for a null value of the degradation parameter μ, the HI ΔT follows a normal distribution $\mathcal{N}(2s, 0.5s)$. The Z_score symptom associated to a measured value $\Delta T = 3s$ is then as follows:

$$Z_score(3,2,0.5) = 2$$

The score is expressed in numbers of standard deviations from the nominal value. The score presents natural variations around zero due to uncertainties but when these variations exceed a certain value, it is considered abnormal. This value is termed the abnormality threshold. The local abnormality threshold is determined by the PHM engineer from the characterization of the nominal distribution of symptoms and physical reasoning. A local abnormality threshold is defined for each symptom. Abnormalities are then defined as follows:

DEFINITION 12 (A**bnormality**). *An abnormality is an observation of a symptom that crosses its abnormality threshold. It traduces the global health status of a system.*

When multiple HIs are defined, which is generally the case, syndromes are considered instead of individual symptoms. They are defined as follows:

DEFINITION 13 (**Syndrome**). *A syndrome is a vector concatenating all the symptoms' values.*

Computing syndromes requires a comparison with a database with DEMs. Finally, abnormality thresholds are used for detecting DEMs, whereas syndromes are used for identification by comparison with a precursors' database. Precursors are defined as follows:

DEFINITION 14 (**Precursor**). *A precursor is a reference syndrome indicating the presence of a particular DEM. A precursor is associated to the level of intensity of the running DEM.*

A precursor of DEM c of intensity k is written $\underline{P_c^k}$. Typically, precursors are considered for $k = 0.25, 0.5, 0.75$ and 1. Note that for DEM c, the $\underline{P_c^1}$ indicates a state where the considered CST has a 0.5 probability to occur because the intensity is equal to the MLV.

In the guiding thread example (see Figure 1.1), a single DEM and two CST are defined. It is supposed that the first CST "actuation error" is reached for $\delta_{1,1}^{MLV} = 200\ N$. It is also supposed that the second CST "high servovalve pressure drop" is never reached with the considered DOE. Thus, the associated MLV is $\delta_{1,2}^{MLV} = \infty$. The MLV of DEM c is then $\delta_{1}^{MLV} = 200\ N$. Considering that for values of the static friction equal to $50\ N, 100\ N, 150\ N$ and $200\ N$, it is supposed that the HI ΔT is equal to $2.2\ s, 2.6\ s, 3.4\ s$ and $5\ s$, respectively. Under this assumption, the precursors for intensities $k = 0.25, 0.5, 0.75$ and 1 are

$$\underline{P_c^{0.25}} = 0.4$$

$$\underline{P_c^{0.5}} = 1.2$$

$$\underline{P_c^{0.75}} = 2.8$$

$$\underline{P_c^{1}} = 6$$

For a PHM system with multiple HIs and by extension multiple symptoms, precursors can be represented via bar plots. The following Figure 1.2 shows the evolution of a precursor associated with DEM c for a PHM system composed of 4 HIs. It can be noticed from this figure that the $\underline{P_c^1}$ precursor is equivalent to the definition of signatures as introduced in (Lacaille, 2009).

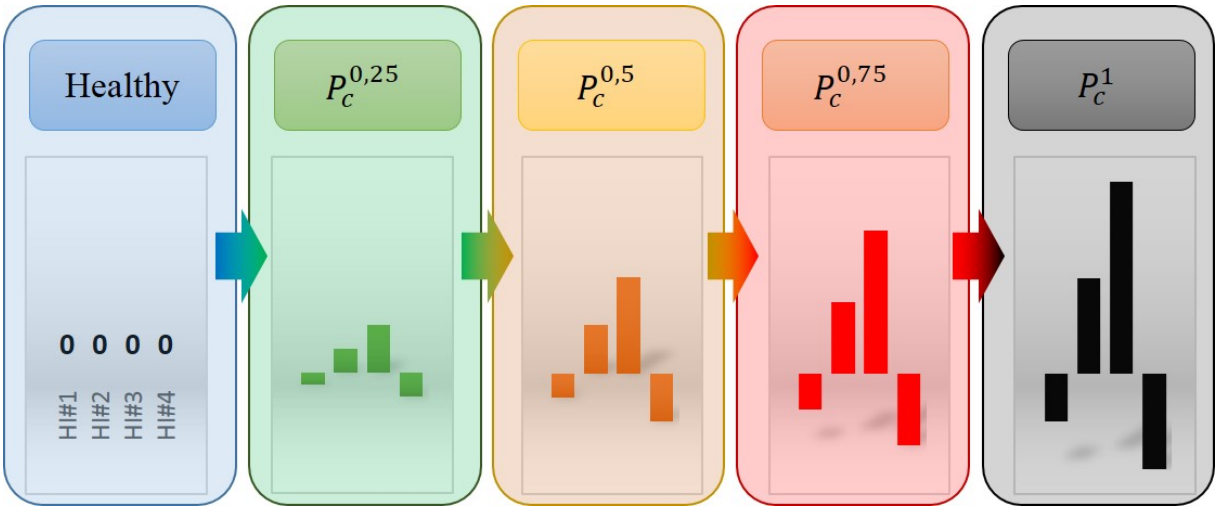


Figure 1.2 *Example of a precursors' evolution for DEM c from healthy state to* $\underline{P_c^1}$.

1.2.3 Processing means

Processing means are related to the notion of health monitoring (**HM**). HM appeared originally in the context of Structural Health Monitoring (Diamanti, et al., 2010). Then, it expanded to other fields, including systems health monitoring. The equivalent term condition monitoring can also be found in the literature. HM is based on the notion of health status, defined as follows:

DEFINITION 15 (**Health status**). *Health Status (**HS**) is the set of information related to the DEMs occurring in a system.*

The following definition of HM, inspired by (Ly, et al., 1999), is defined from the HS:

DEFINITION 16 (**Health monitoring**). *Health Monitoring (**HM**) is the application of the appropriate sensors (data), analysis (knowledge) and reasoning (context) to assess the current and future HS of a host system.*

Typically, HM performs diagnostics and prognostics functions. The former is aimed at assessing current HS, whereas the latter is devoted to the prediction of future HS. The words diagnostics and prognostics can sometimes be found written, respectively, diagnosis and prognosis. In terms of the literature, there is no fundamental difference between the two versions except that the terms diagnosis and prognosis are mostly used in the medical field. Within the present framework, the difference will not be considered. From (Ribot, 2009) and (Ly, et al., 1999), diagnostics and prognostics are defined as follows:

DEFINITION 17 (**Diagnostics**). *Diagnostics is the set of operations performed to detect abnormalities, identify CST precursors and localize incriminated structural unit.*

Diagnostics is currently a proven discipline, with a prolific number of review papers such as (Isermann, 2005; Jardine, et al., 2006; Patterson-Hine, et al., 2005; Wang, et al., 2009). There are numerous sets of definitions for diagnostics, where it sometimes encompasses only identification purposes and sometimes detection, identification and localization purposes. The second point of view will be adopted, considering that diagnostics includes detection, identification and localization, which are defined as follows:

DEFINITION 18 (**Detection**). *Detection is the observation of an abnormality of symptoms.*

To limit the occurrence of false alarms, a confirmation step can be added to the detection. The confirmation process is addressed in 1.3.4.

DEFINITION 19 (**Identification**). *Identification is the classification of the observed syndrome with respect to the precursor database to determine the most probable type of DEM.*

Classification of syndromes can be performed via numerous different solutions. It is actually on of the most prolific scientific fields related to PHM. Classification issues with application to diagnostics are addressed in 1.3.4. The classification tasks outputs the list of DEMs sorted according to their probability, from the highest to the lowest. The one at the top of the list is the most probable DEM.

DEFINITION 20 (**Localization**). *Localization is the determination of the structural unit that is affected by the most probable DEM.*

In the present logic, the localization is performed after the identification. In the case of aircraft engines, the structural units are the LRUs. The LRUs are components or sets of components that can be replaced in a single MRO task performed without disassembling the entire engine.

DEFINITION 21 (**Prognostics**). *Prognostics is the set of operations performed to evaluate the intensity of the most probable DEM from current diagnostic, estimate its future evolution based on available historical data and predict the occurrence of CSTs.*

There are two major families of prognostics. On the one hand, fixed horizon prognostics involve estimating the probability of reaching a CST within a fixed horizon (in number of missions or flight hours). On the other hand, variable horizon prognostics involve estimating of the remaining horizon (in number of missions or flight hours) before the occurrence of a CST. This horizon is generally called the

remaining useful lifetime (RUL). For most industrial applications, the principal objective of prognostics is to evaluate the RUL (Baraldi, et al., 2012; Tran, et al., 2012; Miao, et al., 2012). However, in the field of aircraft engine PHM, fixed horizon prognostics are addressed. The fixed horizon is defined by airline companies and is generally between 10 and 100. Airline companies also specify the probability threshold above which an alert must be sent to maintenance operators.

Finally, the processing means introduced above are used to detect abnormalities, identify the most probable DEM, localize the LRU and prognosticate CSTs. Based on this information, the final purpose of PHM is to update the MRO plan. This task is enabled by scheduling means.

1.2.4 Scheduling means

Scheduling means are levers aimed at allowing an enhancement of the MRO schedule. They are principally messages sent to PHM or MRO operators. In this work, these messages are divided into three classes: warnings, notifications and alerts. They are the basis of the supervision process.

DEFINITION 22 (**Warning**). *A warning is a message sent on ground from the EMU to the PHM operators to inform about the detection of an abnormality.*

Warnings have **no** direct effect on neither availability no maintainability. They inform PHM engineers whenever an abnormality is confirmed to launch further investigations into the phenomenon. For now, warnings do not generate much interest because the amount of recorded data is limited, but ultimately, they could allow an on-condition analysis of signals to understand the origin of the abnormality.

DEFINITION 23 (**Notifications**). *A notification is a message sent on ground to the MRO operators to inform about the appearance of a defect.*

Notifications have a maintainability-related purpose. They inform the MRO crew about the occurrence of a defect that makes a subsystem or equipment not compliant with its specifications. The long-term idea is then to use notifications to support the trouble shooting process during MRO, for example by orienting the investigations toward defects. At term, the fault isolation manuals could be updated to take into account notifications.

DEFINITION 24 (**Alert**). *An alert is a message sent on ground to the MRO operators to inform them when the probability of the occurrence of a CST within the fixed horizon is above the defined threshold.*

Alerts have an availability purpose. They inform the MRO crew of the probable occurrence of a CST. Alerts are the most important scheduling means. Indeed, they enable both condition-based and predictive MRO strategies. Finally, the supervision task can be defined as follows:

DEFINITION 25 (**Supervision**). S*upervision is a set of tasks aimed at scheduling and optimizing the MRO of a system based on health status informations. The main tasks of supervision are as follows:*

- To manage warnings, notifications and alerts
- To keep the health status of all the engines updated and available for maintenance operators at any time in cases where a compliant service threat occurs without forerunner precursor

- To manage the precursors database and the historical data of the fleet or engines
- To manage the interfaces between the different actors.

Finally, the proposed definition of prognostics and health management is elaborated from HM and supervision. This definition is specific to the current use of PHM. Indeed, as PHM is a recently developed discipline, many other definitions can be found, for example in (Kalgren, et al., 2006).

DEFINITION 26 (**Prognostics and health management**). *Prognostics and Health Management (**PHM**) is the combination of HM with supervision.*

Finally, the PHM system can be observed as an additional part of the MRO strategy. Therefore, its operating implementation requires that its specific tasks are clarified with respect to other systems, mostly the BITE system.

1.2.5 The proposed global MRO strategy

Initially, the MRO strategy principally consisted of defining the periodicity of preventive check-ups from reliability information and managing spare parts stocks, MRO infrastructures and labor force. With the advent of the BITE system enabled by the FADEC, a novel aspect was added to the MRO: the management of alarms that are defined as follows:

DEFINITION 27 (**Alarm**). *An alarm is a message sent in flight from the FADEC to the pilot to inform them about the occurrence of a fault in the engine.*

When an alarm is declared online, the on-ground MRO crew is also informed via ACARS. Alarms have safety and reliability purposes. They prevent the engine from reaching a failure state. The BITE system is in charge of the sending of alarms and the activation of tolerance logic when it exists. It was already mentioned in the general introduction that the BITE and the PHM systems do not have the same purpose. Indeed, the former is mainly safety and reliability oriented, whereas the latter is devoted to availability and maintainability. Moreover, Table 1.2 summarizes all the main differences between them.

	BITE system	**PHM system**
Objective	Safety and reliability	Availability and maintainability
Target	Faults	No-go, go-if, beta faults and failures
Localization	Secondary	Essential (LRU targeting)
Criticality	High	Low
Messages	Alarms to pilot	Warnings, notifications and alerts
Periodicity	Real-time → at sampling rate	Periodic → at the end of each mission
Location	Embedded	Embedded + on-ground

Table 1.2 *Comparison between the BITE system and the PHM system.*

To conclude in regards to the MRO strategy, the BITE and the PHM systems should work together to optimize MRO. The following summary can be made: PHM is a process acting on precursors as a non-critical first defense dealing with physical threats to prevent CST, whereas the BITE provides a highly critical second defense aimed at reducing the effects of CST. The big picture is schematized in Figure 1.3.

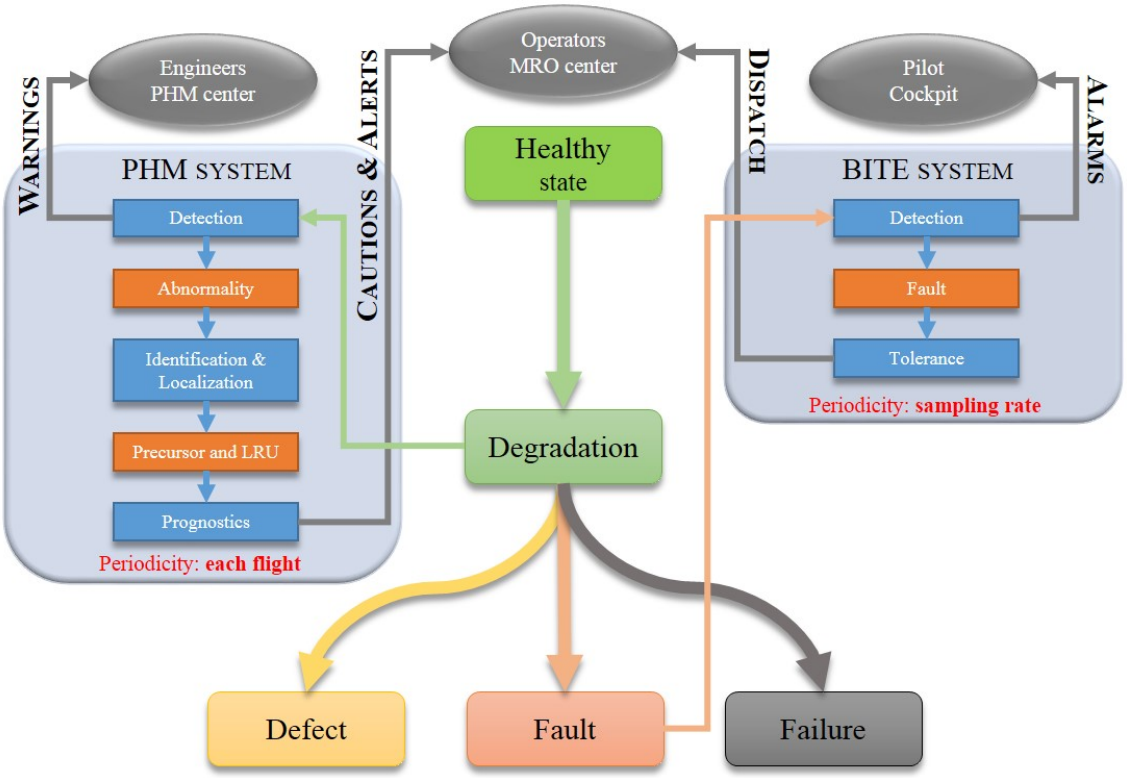


Figure 1.3 *The big picture of MRO management in aircraft engines.*

1.3 Proposed scope and functions of PHM for aircraft engines

The set of definition introduced in the terminology now provides the basis for the introduction of the scope and functions of PHM.

1.3.1 The scope of PHM systems for aircraft engines

As well as the terminology, the scope of the PHM system can vary from one application to another. In the case of aircraft engines, it is proposed to encompass all the CST that are likely to affect directly either the availability or the maintainability. Therefore, the scope is defined with failures, no-go, go-if and beta dispatch faults and defects, as presented in Figure 1.4. By extension, the objective of PHM is to predict their occurrence. The CST belonging to the PHM scope are termed targeted CST (**TCST**).

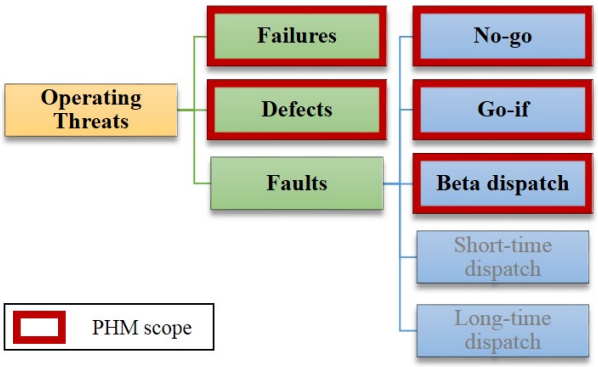


Figure 1.4 *Classification of CST with highlight on the PHM scope.*

For the classification of DEMS, the following taxonomy, based on their consequences, is proposed:

- Dormant DEM: lead to no CST
- Harmless DEM: lead to infinite dispatch faults (type D)
- Hazardous DEM:
  - Marginal DEM: lead to long-time or short-time dispatch faults (types B and C).
  - **Targeted DEM (TDEM): lead to targeted compliant service threats (TCSTS).**

Figure 1.5 presents the DEMs classification. The degradation modes incorporated into the PHM scope are circled in red. Among these degradation modes, some have been proven, i.e., they have already occurred in similar systems, and some are potential, *i.e.*, experts suppose that they are likely to appear (Cocheteux, et al., 2007). In the framework of this work, the difference will not be taken into account. However, note that for future development, it could be interesting to define a type of confidence index aimed at indicating the likelihood of occurrence for each degradation mode.

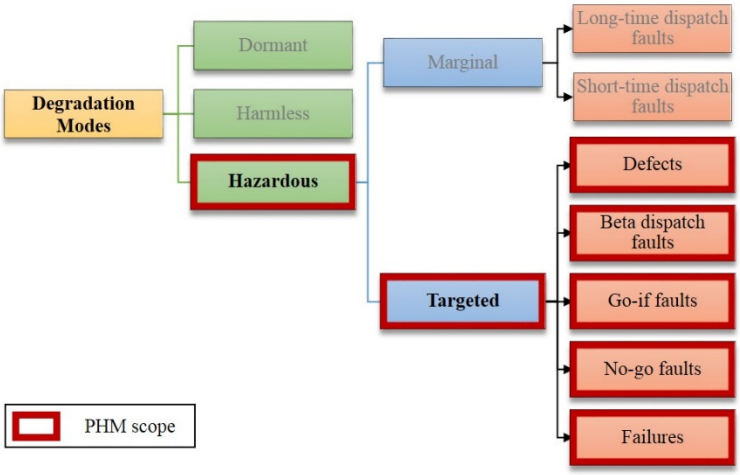


Figure 1.5 *Classification of degradation modes with highlight on the PHM scope.*

Although only TDEMs enter the PHM scope, it is necessary to consider all the other types of DEM for identification matters because even if they are not dangerous for the system, they can be detected and cause erroneous diagnostics. In the present framework, a given DEM can lead to multiple types of CST and a given CST can be the result of different DEMs. Sometimes expertise and experience feedback can be insufficient to determine if a DEM should be targeted or not. In these cases, numerical simulations combined with sensitivity analysis can provide a good alternative. This assertion will be demonstrated in practice in chapters 2 and 3.

1.3.2 Architecture of a PHM system

1.3.2.1 *The PHM process*

A PHM system encompasses several functions from the extraction of HIs to the MRO support. One of the potential solutions has progressively imposed itself over the last decade: the open-system architecture for condition based maintenance (**OSA-CBM**) (OSA). To be consistent with the whole PHM community, the PHM systems developed by Snecma follow the OSA-CBM process and so does the present work. This process is based on seven steps listed and detailed in Figure 1.6.

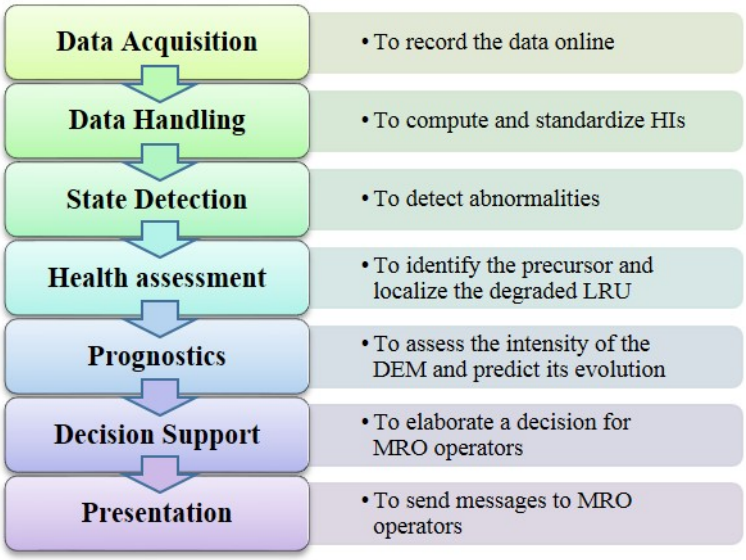


Figure 1.6 *The OSA-CBM process.*

Among the steps of the OSA-CBM, two main families can be identified with respect to the definitions proposed in the previous section: the steps relative to health monitoring and those relative to supervision. Among the former family, a distinction is also made between two subfamilies: HI extraction steps and HI processing steps. This classification is shown in Figure 1.7.

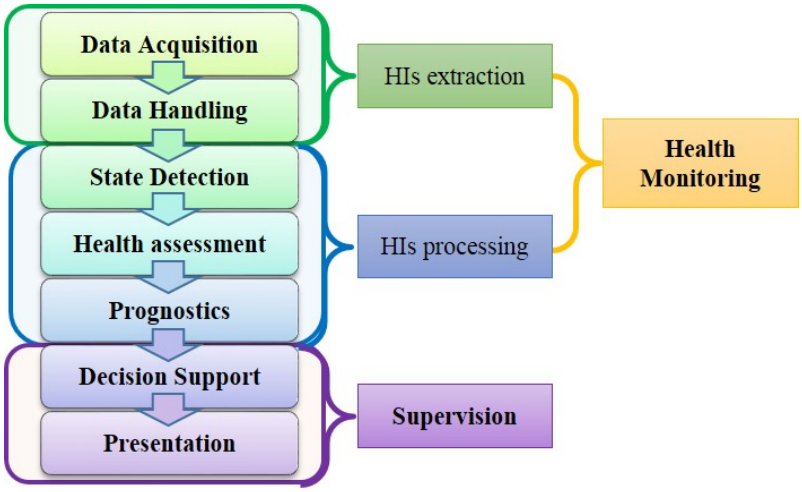


Figure 1.7 *Classification of the OSA-CBM steps.*

1.3.2.2 *Architecture of a supervised system*

The PHM is composed of two interacting systems: the HM system and the supervision system. Combined with the host system, it is part of a larger system of systems (Jamshidi, 2011), which is proposed to be designated the supervised system. The aircraft engine interacts with the HM system via a combination of sensors and the EMU[15]. The HM system communicates with the supervision system via the sending of HM reports, containing health status and messages to maintenance operators such as cautions and alerts. The whole architecture of a supervised system is presented in Figure 1.8.

[15] The Engine Monitoring Unit (EMU) is an aircraft engine controller dedicated to the monitoring functions. Another controller, the Electronic Engine Controller (EEC) is in charge of the regulation functions.

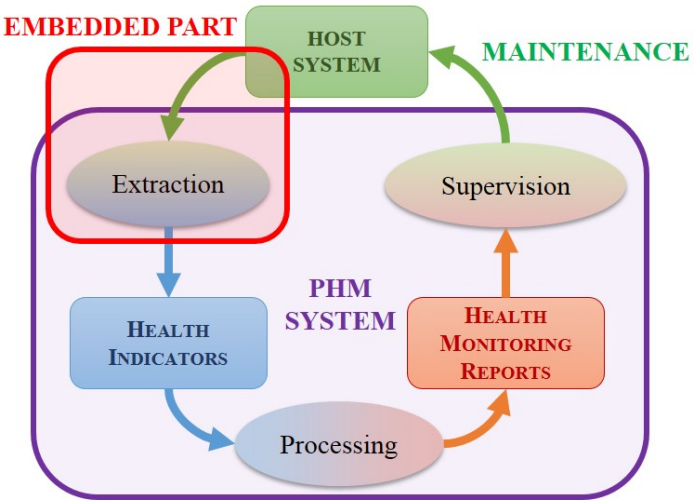


Figure 1.8 *Supervised system architecture.*

1.3.3 Architecture of the host system

In a supervised system, the host system is the main actor. Defining and formalizing a generic architectural representation for it is essential for further PHM purposes. This is particularly true in cases where the host system is complex. The following definition, inspired by (Kempowsky, 2004) for complex systems is proposed.

DEFINITION 28 (**Complex system**). *A complex system is a structured set of related heterogeneous entities that are connected and communicate with each other to perform a function.*

According to this definition, aircraft engines are complex systems, with multiple imbricated regulation loops. There are several possible formalisms for representing complex systems. For example, those presented in (Ribot, 2009) or (Cocheteux, 2010) or (Khalil, et al., 2012) with their hypergraph theory could be cited. A complex system is defined by different types of knowledge (Ly, et al., 1999; Desforges, et al., 2012):

- The structural knowledge describing the topology of the system
- The behavioral knowledge describing the physical behavior of the system
- The functional knowledge describing the intended functions of the system
- The teleological knowledge describing the goal of the system.

In this work, the teleological knowledge is not used and the behavioral knowledge is one objective of PHM. Concerning the functional knowledge and the structural knowledge, they are used for representing complex systems via, respectively, the functional and structural breakdown. The former is based on a segmentation into functional units (subsystems and equipment) and the latter on a segmentation into structural units (LRU and equipment). Note that in the present logic, the following definition of equipment is proposed:

DEFINITION 29 (**Equipment**). *Equipment is an entity of the system that is at the same time a functional and a structural unit.*

An example of typical functional breakdown is given in Figure 1.9 for a complex system with 2 functional levels. The complex system is level 0. The green boxes are level 1, the blue ones level 2 and the red ones level 3.

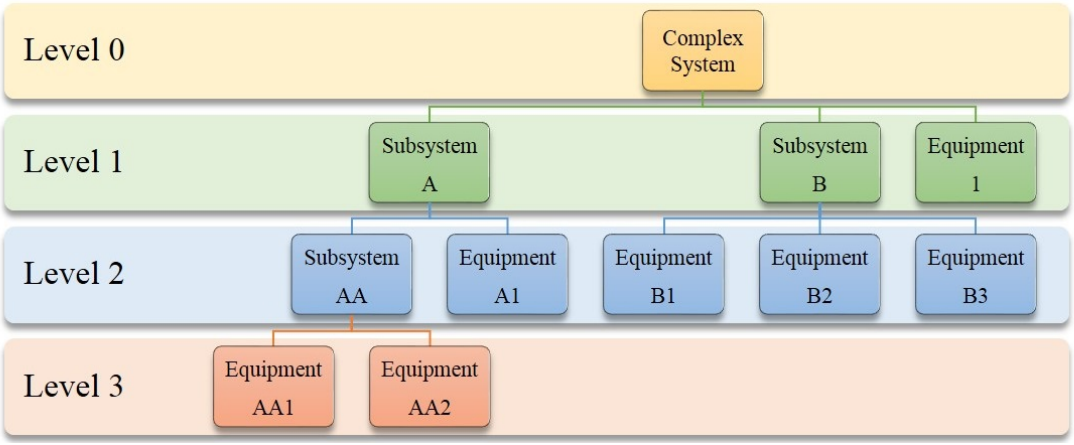


Figure 1.9 *Typical functional breakdown representation of a complex system.*

An example of structural breakdown representation associated with the same complex system is shown in Figure 1.10. The structural analysis consists of associating each equipment to an LRU. Eventually, for PHM objectives, sets of health indicators are defined for each subsystem, with the concern of their associate physical meaning. The objective of health monitoring is to identify the equipment when the degradation mode is occurring. The structural breakdown is then used for localizing the associated LRU.

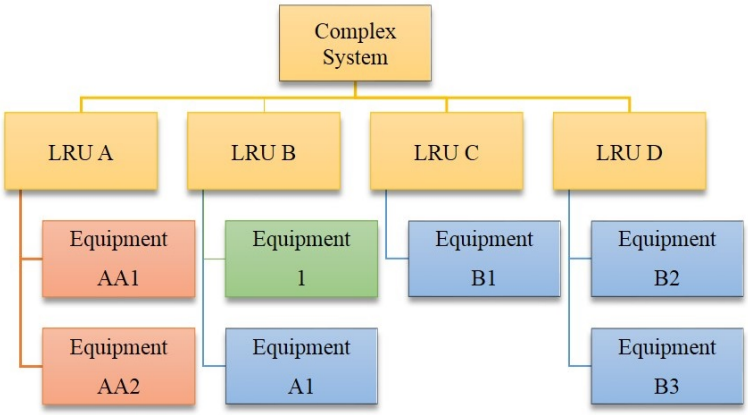


Figure 1.10 *Typical structural breakdown representation of a complex system.*

From both the functional and structural breakdown structures, it is possible to construct an LRU association matrix whose coefficient are equal to 1 if the equipment belongs to the LRU it and equal to 0 if not. The LRU association matrix for the example system is given in Table 1.3.

	LRU A	***LRU B***	***LRU C***	***LRU D***
Equipment AA1	**1**	0	0	0
Equipment AA2	**1**	0	0	0
Equipment A1	0	**1**	0	0
Equipment B1	0	0	**1**	0
Equipment B2	0	0	0	**1**
Equipment B2	0	0	0	**1**
Equipment 1	0	**1**	0	0

Table 1.3 *Example of LRU association matrix.*

1.3.4 Architecture of the health monitoring system

Whereas health monitoring problems are of the physical and mathematical type, supervision problems are rather managerial and statistical. Because dealing with both was too time-demanding for this thesis work, it was decided that the work would be focused on the HM system. As a result, supervision issues will not be addressed. If the reader is interested in that subject, he can refer to (Cocheteux, 2010; Dragomir, et al., 2009; Muller, 2005; Zemouri, 2003).

In the majority of cases, all the tasks of the health monitoring system are performed via online embedded computing, whereas supervision tasks are performed offline by remote computer or human reasoning. However, in the aerospace field, the embedded computing capabilities are limited. Therefore, the extraction task is separated from the processing task: HIs are collected online by the ECU and transmitted to a remote processing unit at the end of each flight, for example, by satellite communication or ACMS. Then, the processing unit performs diagnostic and prognostic tasks whose results are summarized through computation of HM reports. Finally, the health monitoring system is structured as shown in Figure 1.11.

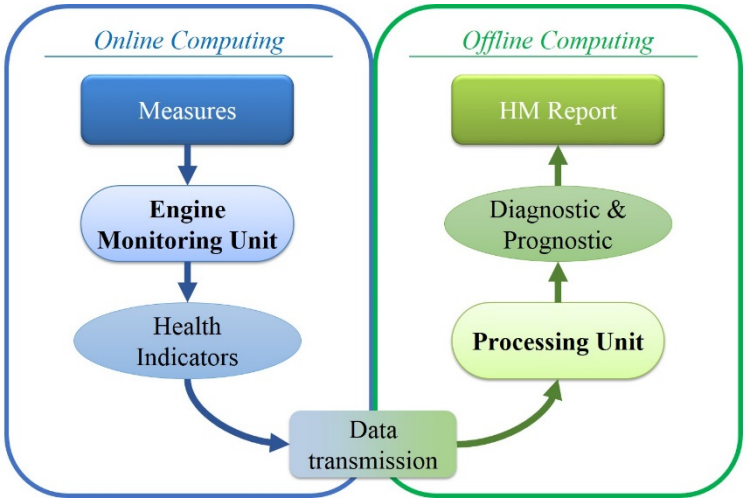


Figure 1.11 *Structuration of the health monitoring system.*

1.3.5 Architecture of the engine monitoring unit

The EMU is in charge of the online computation of HIs. This computation is performed using various sources of knowledge available online. These sources can be for example, measures from sensors (raw or preprocessed) or control variables from the controller. Then, these sources of knowledge are combined and fused to create HIs with relevant physical meaning. In cases where HIs are very sensitive to environmental context randomness and/or manufacturing variability between engines, they are standardized with respect to environment and/or structural information (Lacaille, 2009). This standardization step is aimed at reducing the standard deviation of HI and allowing better detection performance. It will be introduced in detail in chapter 2. Finally, the functional architecture of the EMU can be summarized as presented in Figure 1.12.

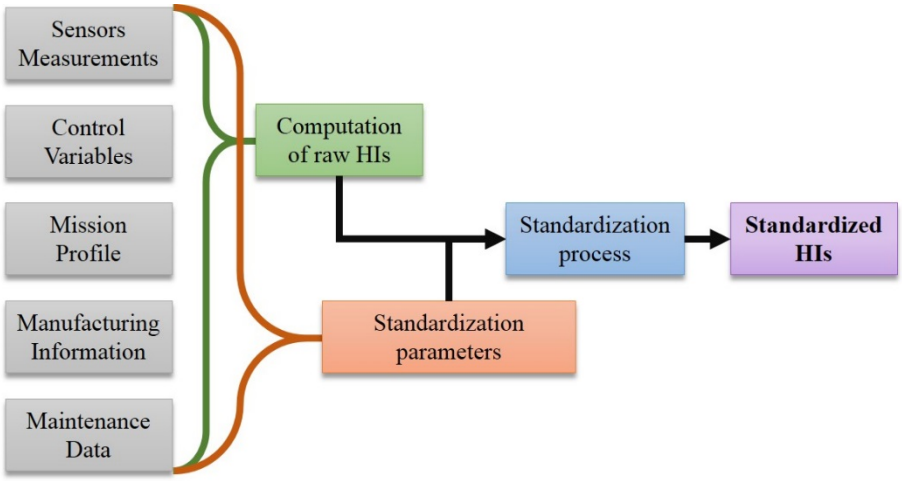


Figure 1.12 *Functional architecture of the EMU.*

1.3.6 Architecture of the processing unit

The processing unit is in charge of building HM reports from the reception of HIs. In cases where the host system is composed of several hierarchical levels, defining an architecture for the processing unit can be a difficult task. Indeed, the dilemma is to choose either to centralize the processing task, *i.e.,* to define a set of HIs for the whole system and to perform a global monitoring or to distribute to several independent HM units. These independent units are termed HM agents. Actually, when browsing the scientific literature, different types of architectures between the centralized and distributed types can be found. For example, an overview of these different types of architectures is presented in (Boufaied, 2003). The main five architectures are presented in Figure 1.13.

- **Centralized architecture:** A central HM agent processes the whole set of HIs for the system (Rana, et al., 1988). Its main flaw is a lack of reliability in case of central agent failure.
- **Hierarchical architecture:** Several levels of agents process the set of HIs for each functional unit. These HM agents communicate with the ones of the upper level. Its main flaw is that a problem affecting an agent affects all the lower level agents.
- **Oligarchical architecture:** A type of hierarchical architecture where HM agents of the same level can communicate together.
- **Half-heterarchical architecture:** A type of hierarchical architecture where HM agents of a given level do not communicate with agents of the same level or of other levels.
- **Heterarchical architecture:** Or distributed architecture. HM agents perform the processing of local sets of HIs for equipment. They do not communicate with any other agent.

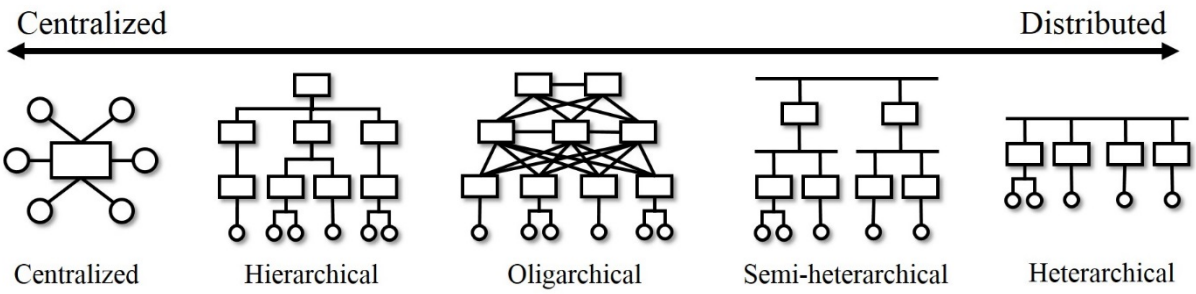


Figure 1.13 *Classes of architecture for the processing unit: rectangles are HM agents and circles are equipment.*

The choice of the processing unit architecture depends on the one of the host system. If the latter is designed according to a hierarchical scheme, with well-defined functional subsystems, then it is often also suitable to use a hierarchical model for the processing unit. For aircraft engines, it has been observed that the heterogeneousness and the complexity of subsystems necessitate that the design of the whole system is presented as a hierarchical model. A hierarchical architecture is used for the processing unit. This means that the diagnostics and prognostics are performed by many HM agents communicating together. For each hierarchical level, HM agents receive a set of HIs from the EMU and Status Indicators (SI) from lower levels HM agents. SI can be of many different forms. For example, they can be computed as the severity of the most probable degradation mode of the level. The advantage of using a hierarchical architecture is that the HIs are grouped with respect to the subsystem they are related to and, consequently, the syndromes include fewer symptoms' values. This reduction of syndrome length enhances the identification performance. An example of hierarchical architecture for the processing unit is shown in Figure 1.14.

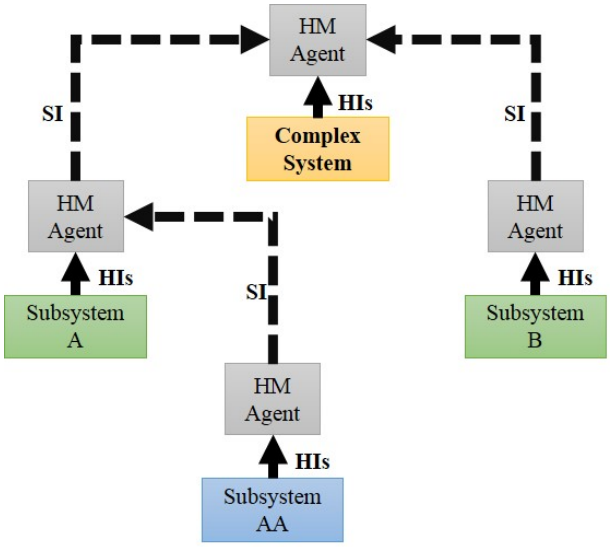


Figure 1.14 *Hierarchical agent-based architecture for the processing unit.*

Note that this type of agent-based architecture necessitates that HIs are defined chronologically from the highest levels to level 0. Note also that the number of HM agents is equal to the total number of subsystems plus one (due to the complex system).

Let us consider a single HM agents and how it is organized in the inside. A HM agent is a sequence of six steps: (1) the syndrome computation and the research for local abnormality, (2) the reduced syndrom computation and the research for global abnormality, (3) the identification of the most probable degradation from a database of precursors, (4) the computation of the severity, (5) the localization of the degrading unit from the knowledge of the host system's structural and functional architectures, and (6) the evaluation of the severity, the prognostic of the degradation mode evolution and the research for threshold crossing of the threat occurrence probability in the fixed horizon. These steps are graphically presented in Figure 1.15.

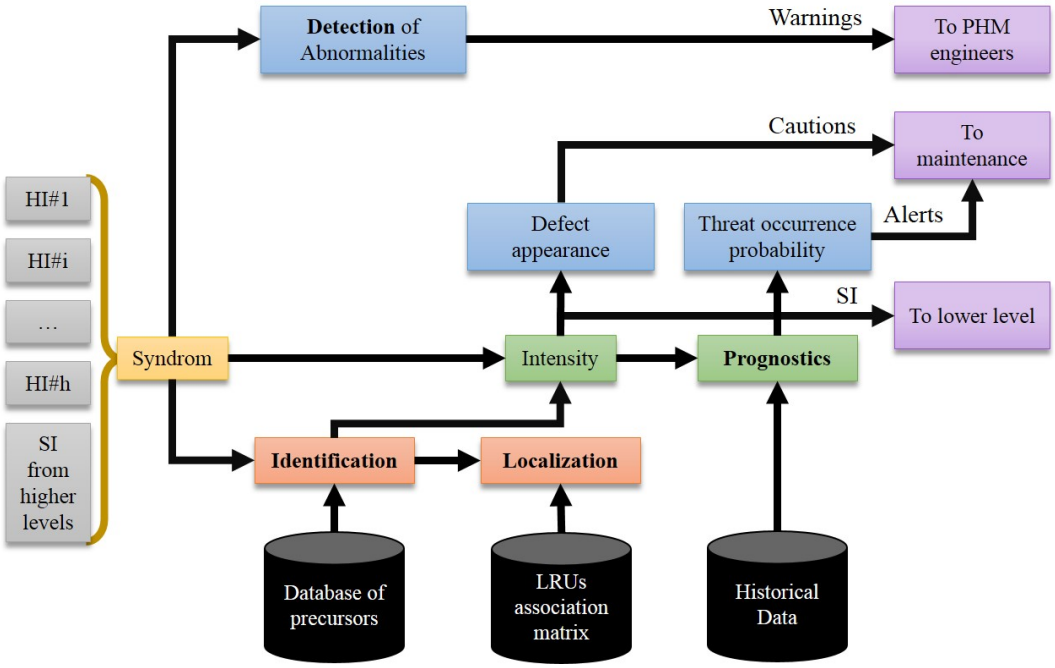


Figure 1.15 *Structure of a HM agent.*

For the coming subsections, the focus is on the four tasks of the processing unit, namely the detection, the identification, the localization and the prognostics. For each of these, the main issues are addressed and a solution that suits aircraft engines specificities is proposed.

1.3.6.1 *The detection task*

The detection task consists of a binary classification between the normal and abnormal states. For further theoretical considerations concerning the detection, the reader can refer to (Wickens, 2002) or (Hwang, et al., 2010) for a more recent review. The binary classification is performed through the comparison of the value of a variable with an abnormality threshold. If this value is greater than the threshold, it indicates an abnormality. The required detection performances are commonly specified in terms of minimal true positive rate (**TP**) and maximal false positive rate (**FP**). TP is the probability of abnormality detection knowing that the system is abnormal or $P(\text{detection}|\text{abnormal})$, and the FP is the probability of abnormality detection knowing that the system is healthy or $P(\text{detection}|\text{healthy})$, as represented in Figure 1.16.

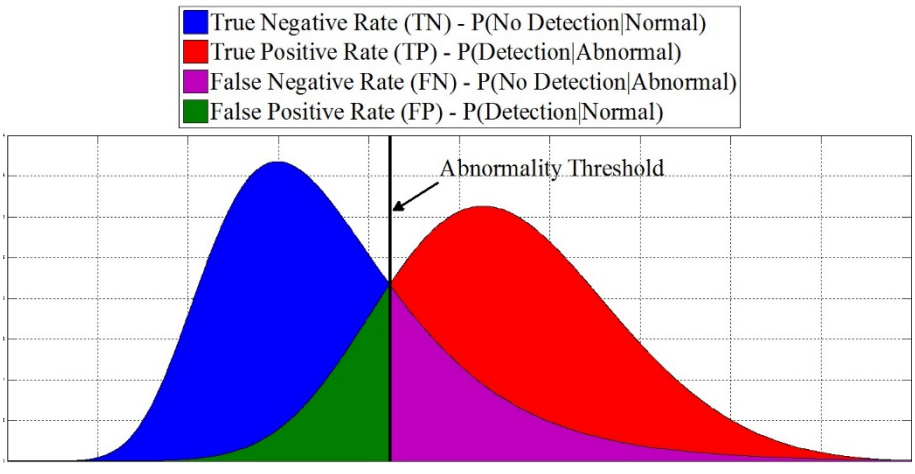


Figure 1.16 *Binary classification performances indicators.*

As presented in Figure 1.16, the values of TP and FP depend on the position of the abnormality threshold. Actually, the main difficulty of detection is the tuning of this threshold. Indeed, changing its position modifies both the values of TP and FP with contrary effects on performances. Finally, the set of compliant abnormality threshold are searched. It is defined as follows:

DEFINITION 30 (**Compliant abnormality threshold**). *It is a threshold for which the couple (TP, FP) is compliant with the specifications of minimal TP and maximal FP.*

In some cases, the distributions of Figure 1.16 overlap so much that it is impossible to find an abnormality threshold that fits the specifications. In those cases, this overlapping is decreased by adding a confirmation step. This confirmation step consists globally in considering several consecutive values to limit the impact of extreme values and decrease the standard deviation of the distributions. This confirmation can be performed via different techniques, for example, sliding average or k among n. The latter has been developed for applications on Snecma's engines and is presented in (Hmad, et al., 2013).

1.3.6.2 *Identification*

The identification process consists of pattern recognition, more particularly multiclass classification between a syndrome and a database of precursors. There are many available techniques to perform multiclass classification. For a complete review of the field, the reader can refer to (Bishop, et al., 2006). Among these classification techniques, the most commonly used for PHM applications are artificial neural networks (Sick, 2002) and support vector machine (Hsu, et al., 2002). In Snecma's framework, the multiclass classification consist first of computing the syndrome of the collected HIs by using the Z-score function (see 1.2.2), as introduced in (Lacaille, et al., 2010). The second step consists of calculating the probability of matching with each precursor. Thus far, this classification is limited to the precursors with intensities equal to 1. The probability of matching $P_c^1(syn)$ between syndrome $\underline{syn} = [s_1 \quad \cdots \quad s_h]^T$ and precursor $\underline{P_c^1} = [p_1 \quad \cdots \quad p_h]^T$ corresponding to the DEM c with intensity 1 is

$$P_c^k(\underline{syn}) = 1 - \left(\frac{1}{\pi\Sigma} \arccos\left(\frac{\underline{syn}^T \cdot \underline{P_c^1}}{\left\|\underline{syn}\right\| \left\|\underline{P_c^1}\right\|} \right) \right) \tag{1.6}$$

with Σ a normalization coefficient for the probabilities to range between 0 and 1, defined as follows:

$$\Sigma = \sum_{c=1}^{d} \left(1 - \left(\frac{1}{\pi} \arccos\left(\frac{\underline{syn}^T \cdot \underline{P_c^1}}{\left\|\underline{syn}\right\| \left\|\underline{P_c^1}\right\|} \right) \right) \right) \tag{1.7}$$

Where d is the number of DEMs.

The third step is the multiclass classification that consists of sorting the precursors by highest probability of matching. One of the difficulties of the classification is to manage newties, i.e. syndrom that do match with none of the references of the database. In these cases, another class must be created, but this topic will not be addressed here.

The hardest aspect of implementing identification for aircraft engines PHM is the construction of the precursor database. Indeed, the efficiency of the identification process depends both on the quality and the quantity of precursor-related data. Several approaches for the construction of this database can be

found in the scientific community, for example in (Kempowsky, 2004; Patterson-Hine, et al., 2005; Narvaez, 2007). In this work, the one presented by Mokhtari (Mokhtari, 2007) will be considered. He proposes three method groups for the construction of the precursor database: data-driven approaches, knowledge-based approaches and model-based approaches. See (Mokhtari, 2007) and references therein for further details. The first group provides the most precise dataset, as it naturally integrates uncertainties effects. However, it necessitates waiting for multiple occurrences of every operating and physical threats to build a useful database, which is costly and above all time-demanding. The second group provides a very rapid and inexpensive dataset. However, they are generally based on qualitative expertise, so the quality and precision of data are often low. Finally, the third approach is more reliable than the second and less expensive in both time and money than the first one. Hence, this is the one that will be used in this work. Actually, it is a type of hybrid approach of the three methods because models are recalibrated with respect to the actual data and built thanks to experts' knowledge.

1.3.6.3 *Localization*

The localization process consists of isolating the most probable degradation line replaceable unit (LRU). In the present case, this task consists of associating the most probable identified degradation mode with the LRU it belongs to from the LRU association matrix (see Table 1.3).

1.3.6.4 *Prognostics*

The prognostic process consists of estimating the intensity of the most likely degradation mode and its future evolution in a given horizon. The hard part of prognostic is to make a forecast about the temporal evolution of the intensity, which necessitates estimating the function of the degradation parameters' values versus time. According to (Jardine, et al., 2006), there are three types of solutions to evaluate these functions: experience-based methods, data-driven methods and model-based methods. Experience-based methods are based on qualitative formulation of degradation mechanisms. They yield imprecise estimations of evolution functions as they are rarely relevant about the quantification. However, they are not expensive to perform. Data-driven methods are used when both healthy and degraded data are available, but the degradation mechanisms are unknown. They typically rely on statistical trend analysis to perform prognostic. They are more precise than experience-based methods but more expensive and complex. Finally, the model-based approaches are based on an analytical characterization of the degradation mechanisms. They are extremely costly, but the most precise of the three methods. Indeed, the knowledge of the physical changes mechanisms provided, for example, by finite elements modeling allows a more trusting prognostic over a larger horizon. In the present application, **physics-based degradation models are not available,** so that a data-driven prognostics is adopted. It uses historical data to draw a trend curve from a given number of past flights as presented in (Lacaille, et al., 2013). The trend is then projected over future flights to determine the upcoming evolution of health indicators. The two major families, namely fixed horizon and variable horizon prognostics, have already been introduced.

The issues specific to the supervision system have not been addressed. In the litterature, it appears that they mostly consist of searching solutions for the implementation of condition-based and predictive maintenances for actual industrial cases. For example, Barros *et al.* addressed the issue of optimizing the replacement times using imperfect monitoring in (Barros, et al., 2003). In (Bérenguer, et al., 1997), maintenance strategy was developped in order to limit the costs due to preventive maintenance and unexpected breakdowns. The problem was modeled by a stochastic semi-Markov decision process. In the framework of this thesis work, the supervision process will not be addressed further as it is not part

of the objectives. Finally, this second section was aimed at proposing a specific scope and specific functions for PHM with application to aircraft engines. This whole formalism was elaborated from Snecma's practices. It appears that the issues for the development of PHM are of very different natures and need specific interactions with the host system's designers. The issue of PHM systems development is addressed in the next section through the criticism of the current solution and the proposition of a new approach termed the IDPHM approach.

1.4 Integrated Development of PHM

The Integrated Development of Prognostics and Health Management system, abbreviated IDPHM, is the core of the present methodological contribution to PHM development. The previous section provide the basis around which the IDPHM unfolds. Before introducing the IDPHM methodology, the current practice in PHM systems development are introduced and criticized.

1.4.1 Current PHM systems development methodology

1.4.1.1 *Development model for the host system*

In the industry and especially in the aerospace industry, the development of host systems usually follows the V-model (Clark, 2009). The V-model is composed of two branches: the one on the left corresponding to sequential design tasks and the one on the right with verification and validation (**V&V**) tasks. According to (Dzakowic, et al., 2007), verification and validation can be defined as follows:

DEFINITION 31 (**Verification**). *Verification is the process of determining that a technology accurately represents the developer's conceptual description as a function of the design specifications.*

DEFINITION 32 (**Validation**). *Validation is the process of determining the degree to which the technology achieves the performance specifications within the system constraints and provides accurate results in the operational environment.*

Note that for customers, the validation is the most important aspect because it reflects the level of compliance of the system with respect to specified performances. For the development of aircraft engines, the following scheme for the V-model of the host system is proposed. It is composed of the nine steps presented in Figure 1.17.

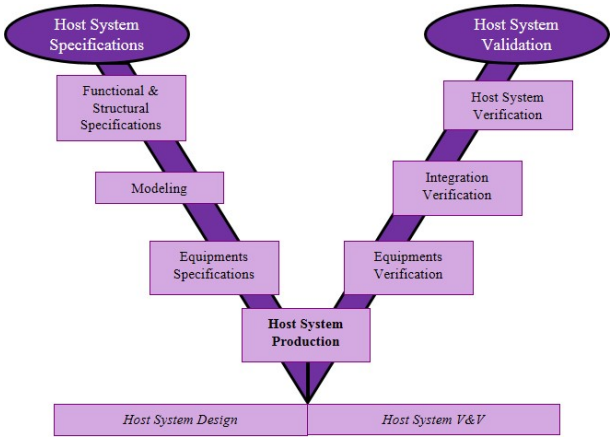


Figure 1.17 *V-model for the host system's development.*

This type of model can also be used for software development. In this case, the software architecture is not considered and equipment instead of subfunctions are specified. Moreover, the production is replaced by implementation.

1.4.1.2 *Current development model for the PHM system*

Currently, the development of the PHM system also follows the V-model. Indeed, as explained above, the V-model can be used for software development and PHM systems can be considered as software. Thus, the development of PHM systems can be divided into seven steps: (1) listing the specifications from customers, (2) defining the PHM architecture, (3) designing the PHM system, (4) implementing the system, (5) verifying the system's functions, (6) validating the system's functions and (7) validating the whole PHM solution. The V-model for the PHM system is presented in Figure 1.18.

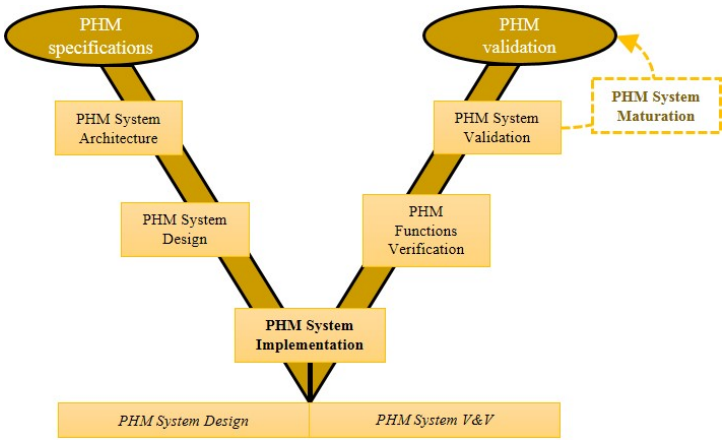


Figure 1.18 *Current V-model for the PHM system's development.*

Note the presence of a maturation step between the verification and the validation of the PHM system's functions. This maturation process (Massé, et al., 2012) can be assimilated to a data collecting phase. It consists of waiting for the host system to have witnessed all of the compliant service threats several times to have a large enough database for validating the PHM process. Although part of the development of every type of PHM system, it is particularly significant for highly reliable systems such as aircraft engines. Indeed, it is obvious that when threats occurrence probabilities are around 10^{-6} per flight hour, and it takes a very long time to collect all the necessary data.

1.4.1.3 *Interactions between host system and the PHM system developments*

In the past, the development of PHM systems was considered as a marginal task. Indeed, as mentioned in the general introduction, within the former socio-techno-economic context, the importance of PHM was reduced because it was used against the MRO profit-based business model. It is then easily understandable that maximizing the availability of aircraft engines was not a priority at that time. As a consequence, although some PHM solutions were developed, the priority was systematically given to the development of the host system so that no resources were allocated to the implementation of PHM during the design stages. Eventually, although some PHM solutions have been developed here and there, they are never actually used because no effort has been made to define their development process. Currently, the situation has changed with the progressive introduction of flight hours' contracts and contracts stipulating the costs of D&Cs because engines are the supplier's responsibility. Within this new context, availability has become an important aspect and PHM a major asset in the making. Thus, PHM is receiving increasing credit from the aircraft engine industry's scientific advisers. Therefore, its

development process is now a matter of concerns. The main issue in defining the PHM development process is to identify its interaction with the host system lifecycle to integrate it into the current practices. These interactions are manifested in the form of key data defined as follows:

DEFINITION 33 (**Key data**). *Data about the host system that is relevant for and transmitted to the PHM system designers.*

Key data can be a document, a scheme, an expertise or any other type of information about the host system. The current development process of the PHM is undertaken during the upstream design stages, as presented in Figure 1.19.

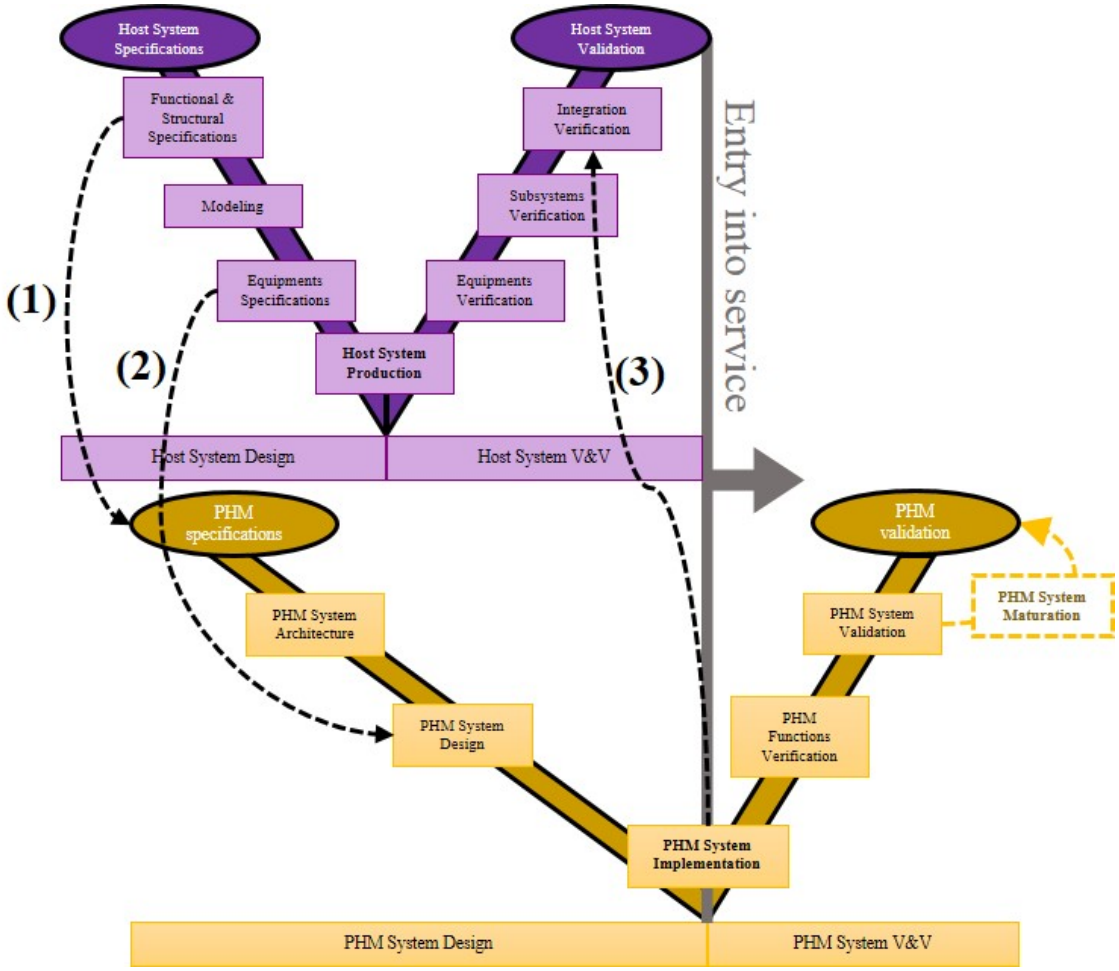


Figure 1.19 *Current interactions between the host system V-model and the PHM system V-model.*

Note that there are three key data in the scheme depicted in Figure 1.19: (1) PHM requirements are derived from those of the host system; (2) the design of the PHM system depends on the equipment specifications; (3) the PHM system must be implemented before or at least simultaneously with the host system production. The main feature to be remembered about the current practice is that the verification and validation branch of the PHM development process is undertaken after the final validation of the host system, *i.e.,* after the entry into service of the engine. Indeed, as models are presently unused, the only method to obtain the necessary data for the validation is to rely on operating data.

1.4.2 Weaknesses of current PHM system development

Despite its enhancements compared with former practices, the current PHM development process still displays imperfections in some particular points. Its main weakness concerns its global organization that does not make the distinction between the development of EMU, processing unit and supervision unit despite their intrinsic difference. Therefore, each should be the object of a standalone development process. Under this assumption, the specific weaknesses of the EMU development process are mostly due to two factors. The first one is the lack of data in upstream design stages. Indeed, when models are unused, which is currently the case, the development of PHM relies only on expertise and experience feedback. However, these sources of knowledge are not quantifiable data, so it is impossible to assess performance with respect to specifications. Thus, there is no other solution than waiting for the entry into service to begin the V&V of the PHM system (see Figure 1.19). The second factor, related to the first one, is originated in the high level of reliability of aircraft engines: even after the entry into service, it takes years or even decades for all the compliant service threats to occur, specifically in the aerospace industry. Finally, the following principal weaknesses for the development of the EMU can be listed:

- It is currently impossible to quantify the effects of context before data are available. Consequently, the standardization of HIs produces important retrofit costs and the detection is likely to be inefficient for a period during the calibration of the standardization model.
- Until the occurrence of every compliant service threat, the precursor database is uncompleted and the identification is likely to be inefficient for a period during the data collection phase.
- With no data, it is neither possible to assess the MLV of DEMs before the occurrence of every CST nor to assess their intensity. As a result, the prognostics are also likely to be inefficient during the data collecting phase.
- There is currently no way to evaluate the quality of HIs before the occurrence of every single CST. This means that PHM designers could possibly find out after many months or years that the set of HIs they defined were not efficient. In this case, additional costs for the development of palliative actions are to be expected, especially if after many years the designers of the original PHM solutions are not available anymore. Moreover, a loss of reputation with airline companies is also anticipated if the PHM options do not fulfill their purpose.

Finally, to obtain a solution to those weaknesses, a new development scheme is proposed in this thesis work. It is based on the discrimination of the PHM development process into 3 standalone V-models, one of them being dedicated to the EMU. For the specific case of EMU, the development process is based on the generation of data from physics-based models during the design stages of the host system.

1.4.3 The IDPHM methodology

1.4.3.1 *The V2-model*

The new methodology is based on the following observation: a supervised system is an interaction of three systems of different nature: the host system, the health monitoring system, and the supervision system (see Figure 1.8). If the host system is considered apart, why not do the same with the others? Then, the development of the PHM system can be divided into two tasks: the development of the health

monitoring system and the development of the supervision system. From this observation, the V2-model is proposed, as presented in Figure 1.20:

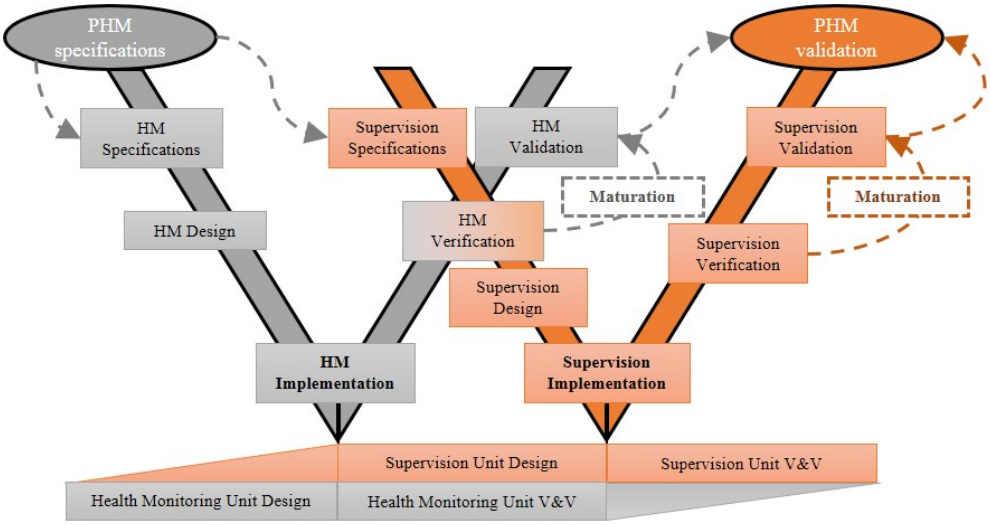


Figure 1.20 *The V2-model for the development of PHM systems.*

1.4.3.2 *The V3-model*

The second observation is that the development of the health monitoring system can be divided into the development of the EMU and the development of the processing unit (see Figure 1.11). From this observation, the V3-model is proposed, as presented in Figure 1.21:

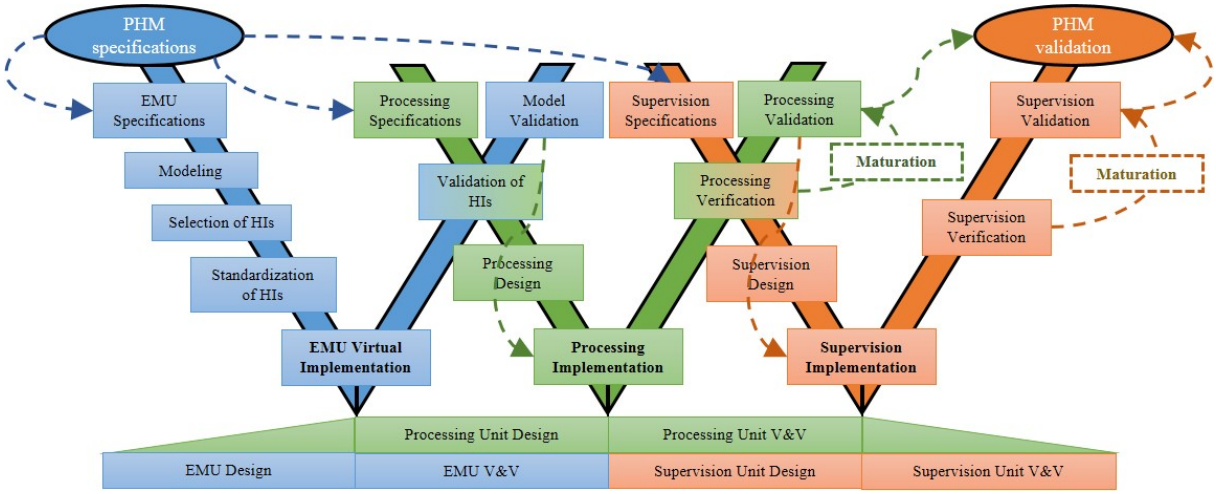


Figure 1.21 *The V3-model for the development of PHM systems.*

In Figure 1.21, the specifications of each standalone V-models are derived from those of the whole PHM system. From this V3-model, the following relationships are derived: the processing implementation starts after the model validation and the supervision implementation starts after the processing validation. This method avoids propagating errors from one unit to the others. In the next chapter, the focus is on the first V-model, the one associated with the development of the EMU, and particularly the selection, standardization and validation of HIs. Note that in the logic of this model, the processing implementation must wait for the models to be validated and the final complete. Moreover, the validation of the PHM system is now effective after two maturation processes, one for the processing unit and one for the supervision unit.

1.4.3.3 *Interactions between host system V-model and the PHM system V3-model*

This V3-model being made to replace the former V-model, it must, in turn, be integrated into the host system lifecycle. In this thesis work, the scheme of interactions of Figure 1.22 is proposed. The key data are organized as follows: (1) the PHM specifications are derived from those of the host system; (2) the models of the host system are used by PHM designers for their specific applications; (3) the selection of HIs is mostly based on equipment specifications; (4a) and (4b) the early validation of HIs allows a feedback from PHM designers about the host system's design, for example, to ask for additional sensors, different equipment specifications, in particular characteristics or even revised manufacturing tolerance; (5) the validation of the host system occurs after the set of HIs has been validated; (6a) and (6b) the validation of HIs provides both an estimation of precursors database and MLVs that allow drastically reducing the duration of the maturation phases.

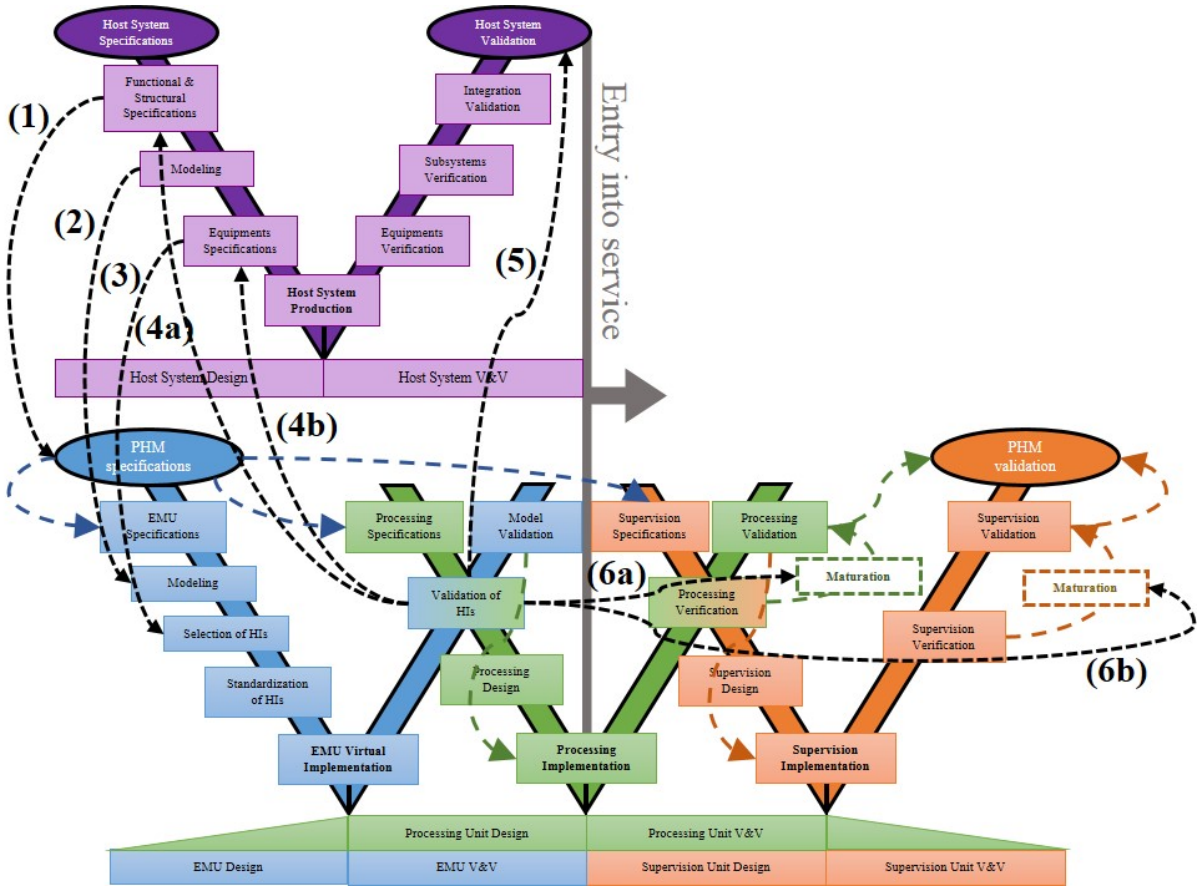


Figure 1.22 *Future interactions between the host system V-model and the PHM system V3-model.*

As this method is aimed at enhancing the integration of the PHM development process in the lifecycle of the host system, this approach is termed the integrated development of PHM (**IDPHM**). The IDPHM proposes standalone development processes for each of the main PHM units. It allows a better specific treatment of each one of them. In particular, the model-based standalone development of the EMU is the main novelty of this approach and is the subject of the next chapter. This new approach allows solving some of the drawbacks of the former approach:

- It is now possible to quantify the effects of context on HIs and to both define the standardization parameters and estimate the standardization models during the design stages.

- It is now possible to build a model-based database of precursors because simulations allow injecting a DEM to provoke defects and faults *ad libitum*.
- For the same reason, the MLV can now be estimated during design stages. Hence, the intensity can be evaluated as soon as the first functioning hours of the host system.
- It is now possible to quantify the expected performances of the HIs set before the entry into service of the host system.

Finally, the objective of this last section was to show the weaknesses of the current development process for PHM system and to propose a novel approach based on the V3-model, called IDPHM. The central idea is to use physics-based models to generate the standalone V-model of the EMU before the entry into service of the host system. This allows significant savings of time and money.

1.5 Conclusions

The main feature to be remembered is that a novel approach for the development of PHM dedicated to aircraft engines has been proposed. It is termed IDPHM and based on the V3-model. Taking into account the methodological construction of this approach, the present thesis work has made three major contributions to the field of PHM.

The first contribution of this chapter is the brand new terminology for PHM with application to aircraft engines. For more clarity, the definitions are divided into four classes. The first original feature of the proposed definitions concerns the taxonomy of threats. Indeed, they are divided into compliant service threats (**CSTs**) and degradation modes (**DEMs**). On the one hand, the CSTs are observable threats affecting the compliant service of engines. On the other hand, the DEMs are non-observable threats affecting the behavior of the engines likely to cause CSTs. Another novelty, arising for the first one, is the discrimination between compliant service indicators (**CSIs**) and health indicators (**HIs**). The former are devoted to the direct monitoring of CSTs and generally not measurable except on models, whereas the latter are dedicated to the indirect monitoring of measurable DEMs. The third original feature is the definition of the median limit value (MLV) for couples (DEMs/CSTs), as the value of the degradation parameter for which the CST is reached with a probability of 0.5. It is equivalent to the median lethal dose. MLVs are computed from the CSIs. The last novelty is the proposition of several supervision tools aimed at completing the current MRO strategy, namely the warnings, the notifications and the alerts. Finally, the PHM is defined as the combination of health monitoring (HM) with supervision.

The second contribution is the definition of both the scope and the functional framework for PHM of aircraft engines. The first newty is the scope itself, taking into account the notion of dispatch to define the following CST as targeted ones (**TCSTs**): failures, no-go, go-if and beta dispatch faults and noticeably the defects, a potential interesting source of information for the troubleshooting process of MRO. Another originality is the proposed representation of the complex host system, based on both the hierarchical functional and hierarchical structural representation and above all the LRU association matrix to link them. These are to be used in the second chapter. The third newty is the hierarchical agent based solution proposed for the HM system. It is based on the use of HM agents communicating with lower levels in order to perform global diagnostic and prognostic at the system level. The last originality is the segregation of the PHM system into the HM and the supervision system, the former being itself

subdivided into the embedded HI extraction tasks and the on-ground HI processing tasks. The extraction is performed by the engine monitoring unit (**EMU**) while the processing is performed by the processing unit. As far as the latter is concerned, it is based on four tasks, namely the detection of abnormalities, the identification of precursors, the localization of LRUs and the prognostic of TCSTs. For each of this task, possible solutions have been addressed.

The third and main contribution of this chapter is the proposition of a new approach for the development process of aircraft engines PHM systems, termed integrated development of PHM (IDPHM). It is intended to fill gaps in the current V-model. It is based on the proposed terminology and functional frameworks. The first originality of IDPHM is to propose a new development model adapted to the specificities of PHM system in aircraft engines, *i.e.*, the discrimination between the embedded and the on-ground tasks. This is performed through the introduction of an innovative development model called V3-model based on the subdivision of the PHM development process into three standalone Vs for the EMU, the processing unit and the supervision unit. Their principal milestones are highlighted with focus on the importance of the maturation process in the global validation process. The second newty brought by the IDPHM is the formalism of the interactions between the V3-model and the host system's lifecycle. Thus, key data are defined as knowledge to be exchanged between both processes in order to facilitate the design of the PHM system and enhance its capabilities. The two fundamental points is the use of physics-based models to create the necessary data for the V-model of the EMU before the entry into service and the possibility of feedback from the PHM to the host system's designers.

Lastly, the focus is on the first V of the V3-model, *i.e.*, the standalone development of the EMU, because of the imminent issue of the selection, standardization and validation of HIs which is happening when approaching the actual implementation of PHM. Indeed, it could be a real asset as it allows quantifying the effects of context, building a model-based precursors' database, estimating MLVs and quantifying expected performances of the HIs set and all that during the design stages of the host system. Thus, for the remainder of the document, only the standalone development process of the EMU is considered.

2

Development of the embedded extraction tasks during the design stages of aircraft engines

Abstract: The present chapter is devoted to the definition of the standalone development process of the embedded extraction tasks, *i.e.*, the first V of the V3-model. To the best of our knowledge, this issue is still an unaddressed topic in the literature. The process consists of three model-based steps: the selection, standardization and validation of HIs. For the representation of physics-based models, three types of uncertainty sources are considered: context parameters, epistemic parameters and degradation parameters accounting for, respectively, the environment randomness, manufacturing variability and degradation intensity. The selection of HIs is prioritized from equipment to systems and is based on key data such as FMECA, ATPs and BITE specifications, prototyping on partial models and engineering judgment. The standardization process is based on sensitivity analysis, which allows one to identify the influent parameters impacting the HIs, quantify and sort their effects and assess the nonlinear relationships between the inputs and outputs. Support vector regression is used to model the first-order effects for the physics-based models. These models are subsequently used for the standardization. To validate the HIs, metrics called numerical key performance indicators (NKPIs) are defined. The first proposed class of metrics is relative to the degradation modes' detectability, and these metrics are computed from receiver operating characteristics curves. The second and third classes of metrics are dedicated to precursors' identification and LRUs' localization capability, and these metrics are based on the angular gap between the vectors of HIs. The last class of metrics is devoted to the prognostic capability of compliant service threats and is based on the gaps between the minimal detectable, identifiable and localizable degradation intensities and the median limit value. These NKPIs rely on the HIs' distributions. Although physics-based models allow one to establish the NKPIs via the propagation of influent parameters, this approach is highly time-demanding.

Overview

2.1 Introduction 100
2.2 Modeling and selection of HIs 102
2.2.1 Modeling formalism and representation 102
2.2.2 Uncertainties Management 107
2.2.3 Modeling implementation 108
2.2.4 Selection of HIs 108
2.3 Standardization of HIs 111
2.3.1 Sensitivity analysis 111
2.3.2 Support Vector Regression 119
2.3.3 SA and SVR for the standardization of HIs 122
2.4 Virtual implementation and validation of HIs 124
2.4.1 Definition of numerical key performance indicators 124
2.4.2 Virtual implementation 133
2.4.3 Validation of HIs 137
2.5 Conclusion 138

2.1 Introduction

In the previous chapter, the framework of IDPHM was introduced as a means to improve the development of PHM systems. As we explained, IDPHM is based on a distinction between the interacting developments of the embedded extraction tasks (EMU), the processing unit and the supervision unit. This chapter is dedicated to the development of the embedded extraction tasks corresponding to the first V of the V3-model, which is based on the seven steps given in the V-model of Figure 2.1.

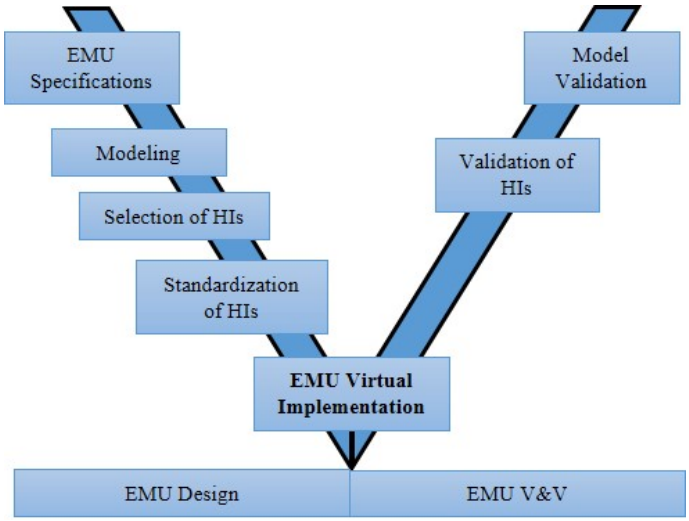


Figure 2.1 *The standalone V-model of the EMU development process.*

The topic of this second chapter is the development of the embedded extraction tasks the during design stages. Recall that the final objective is to be able to assess the performances of the defined set of health indicators (**HIs**) before their entry into service (**EIS**). Indeed, PHM algorithms are presently

sold to airline companies with specified performances guaranteed at the EIS plus three years. Advantageously, a PHM system is considered efficient as soon as the EIS could reduce the costs of application software changes. Indeed, in cases where the embedded part is not satisfactory, costly coding modifications are to be expected. Moreover, a PHM system effective at the EIS could avoid the loss of reputation among airline companies and enable additional support for immediate crises.

The first section is devoted to the selection of HIs in the design phases. The selection task consists of identifying the relevant measured variables that are likely to be sensitive to single degradation modes with a limited sensitivity to the others. Then, HIs are constructed from these variables. In this thesis work, the proposed selection process involves defining hierarchically a set of HIs for each functional unit from the equipment to the global host system. First, because models are needed for the selection tasks, a modeling formalism specific to aircraft engines' PHM applications is proposed. This formalism is based on the constant temporal input representation and a classification of the input parameters with respect to the type of their uncertainty. The selection is then presented through the definition of key data to be exchanged with the host system's designers. The selection procedure is finally introduced, and it consists of iterating the following sequential steps for each functional unit: identifying *a priori* relevant HIs from feedback experiences and specification documents and testing the HIs' sensitivity via prototyping on partial models and submission to experts for approval before the standardization step.

The second section addresses the problem of standardization. The standardization process is defined as a method aimed at reducing the standard deviation of the HIs by subtracting the effects from the known and influential parameters, which are termed the standardization parameters. The two principal difficulties in this process are identifying the so-called standardization parameters and estimating the model of their effect on the HIs, which is called the standardization model. In this thesis, both issues are treated independently with particular statistical and mathematical tools. Concerning the identification of the standardization parameters, we propose to use sensitivity analysis (**SA**) to assess and prioritize the effects of the parameters on the HIs. Generalities about SA are introduced, and two techniques are developed in detail: the Morris method and the computation of Sobol indices. These techniques are combined to determine the standardization parameters. For the estimation of standardization models, the use of support vector regression (**SVR**) is proposed. This regression technique is preferred for its good properties in modeling non-linear behaviors. Finally, a standardization procedure combining SA and SVR is introduced.

The third and last section is devoted to the validation of HIs in the design stages. The main challenge of the validation process is to define the performance metrics and criteria. However, whereas the definition of metrics for the validation of the global PHM system is a well-addressed subject, the equivalent definition for the validation of HIs is to the best of our knowledge a novel field of research. Therefore, in this thesis a set of numerical key performance indicators (**NKPIs**) are proposed as metrics for assessing the performances of a given set of HIs that are intended for detecting abnormalities, identifying precursors, localizing LRUs and predicting compliant service threats. A list of associated criteria is also suggested. Finally, a validation procedure adapted to the particularities of aircraft engines is proposed; this procedure is based on the assessment of the HIs' performances for different configurations until its validation is effective. Three configurations are tested: raw HIs with a fleet model, standardized HIs with a fleet model and standardized HIs with individual models. An optional step can be added in cases where virtual HIs are also defined.

2.2 Modeling and selecting HIs

The selection of HIs consists of defining variables with a high sensitivity to DEMs and a low sensitivity to context variations and dimensional uncertainties. This selection is performed concurrently with the modeling of the host system. The initial selection of HIs is supervised by some prototyping on the physics-based model via simple simulations aimed at capturing their behavior. Therefore, the first subsection will present both the formalism and the representation adopted for the modeling of the host system.

2.2.1 Formalism and representation of the model

2.2.1.1 *Inputs and outputs*

The numerical model considered in this section is represented by a deterministic function $\not{f}$ so that:

$$\boldsymbol{Y} = \not{f}(\boldsymbol{U}, \rho_1, \dots, \rho_p) \tag{2.1}$$

where $\boldsymbol{U}$ is the matrix of the model inputs, $\boldsymbol{Y}$ is the matrix of the model outputs and $\rho_1, \dots, \rho_p$ are the model parameters. The parameters are variables that are considered constant during a single simulation but can vary between two different runs. As the numerical model is a discrete system, by considering a sample period equal to T and a simulation of k samples ($k \in \mathbb{N}$), the input and output matrix can be written as follows:

$$\boldsymbol{U} = \begin{vmatrix} u_1(0) & \dots & u_n(0) \\ u_1(T) & \dots & u_n(T) \\ \vdots & & \vdots \\ u_1\big((k-1)T\big) & \dots & u_n\big((k-1)T\big) \\ u_1(kT) & \dots & u_n(kT) \end{vmatrix} \in \mathbb{R}^{k \times n}$$

$$\boldsymbol{Y} = \begin{vmatrix} y_1(0) & \dots & y_m(0) \\ y_1(T) & \dots & y_m(T) \\ \vdots & & \vdots \\ y_1((k-1)T) & \dots & y_m((k-1)T) \\ y_1(kT) & \dots & y_m(kT) \end{vmatrix} \in \mathbb{R}^{k \times m} \tag{2.2}$$

where n and m are the respective numbers of input and output signals. For an aircraft engine, the mission profiles are very similar one to each other, and the majority of both the control and environmental variables are stationary during the cruise, which is the longest part of a flight. In parallel, HIs are generally defined as variables reflecting the average behavior of the system over a complete mission. Because of this observation, we decided to use real signals retrieved and adapted from other, older engines as inputs to the model.

2.2.1.2 *Classification of the parameters*

The following formalism is proposed for the classification of the parameters $\rho_1, \dots, \rho_p$: they are divided into two types: the context parameters $\lambda_1, \dots, \lambda_c$ $(c \leq p)$ that account for the environmental variations and the structural parameters $\beta_1, \dots, \beta_s$ $(s \leq p)$ that account for the manufacturing variability. The structural parameters set is subdivided into epistemic parameters $\gamma_1, \dots, \gamma_e$, $(e \leq s)$ that are stationary for a given engine and degradation parameters $\delta_1, \dots, \delta_d$, $(d \leq s)$ that can evolve in time. A parameter can be simultaneously considered epistemic and degradation. The classification of the parameters is schematized in Figure 2.2.

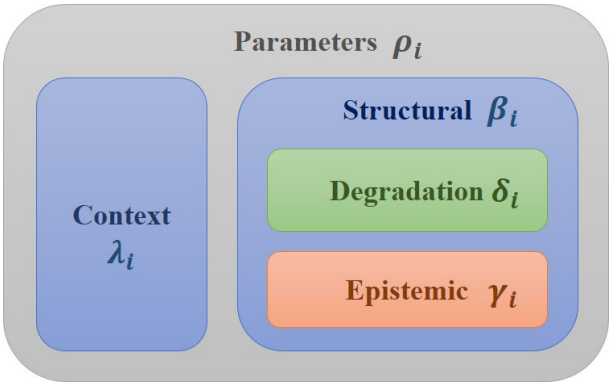


Figure 2.2 *Classification of the parameters.*

To give a mathematical framework to the modeling of the host systems, the following formalism based on vector spaces is proposed:

- **Parameterizations' space**

The parameterizations' space is defined as a Euclidian vector space of dimension p provided with the canonical base $\left(\underline{e_1^{\mathcal{P}}}, \ldots, \underline{e_p^{\mathcal{P}}}\right)^T$ and the Euclidian norm $\|\cdot\|^{\mathcal{P}}$. A parameterization vector $\underline{\rho}$ is defined as $\underline{\rho} = |\rho_1 \quad \cdots \quad \rho_p|^T$, and the nominal parameterization vector $\underline{\rho}^0$ is defined for the nominal values of the parameters as $\underline{\rho}^0 = \left|\rho_1^0 \quad \cdots \quad \rho_p^0\right|^T$.

- **Configurations' space**

The configurations' space $\mathcal{E}$ is defined as a subspace of $\mathcal{P}$ of dimension e with the inherited canonical base $\left(\underline{e_1^{\mathcal{E}}}, \ldots, \underline{e_e^{\mathcal{E}}}\right)^T$ and Euclidian norm $\|\cdot\|^{\mathcal{E}}$. A configuration vector $\underline{\gamma}$ is defined as $\underline{\gamma} = |\gamma_1 \quad \cdots \quad \gamma_e|^T$. Furthermore, the nominal configuration vector $\underline{\gamma}^0$ is defined for the nominal values of the parameters as $\underline{\gamma}^0 = |\gamma_1^0 \quad \cdots \quad \gamma_e^0|^T$.

- **Contexts' space**

The contexts' space $\mathcal{C}$ is defined as a subspace of $\mathcal{P}$ of dimension c with the inherited canonical base $\left(\underline{e_1^{\mathcal{C}}}, \ldots, \underline{e_c^{\mathcal{C}}}\right)^T$ and Euclidian norm $\|\cdot\|^{\mathcal{K}}$. A context vector $\underline{\lambda}$ is defined as $\underline{\lambda} = |\lambda_1 \quad \cdots \quad \lambda_c|^T$, and the nominal context vector $\underline{\lambda}^0$ is defined for the nominal values of the parameters as $\underline{\lambda}^0 = |\lambda_1^0 \quad \cdots \quad \lambda_c^0|^T$.

- **Conditions' space**

The conditions' space Q is defined as a subspace of $\mathcal{P}$ of dimension d with the inherited canonical base $\left(\underline{e_1^{Q}}, \ldots, \underline{e_d^{Q}}\right)^T$ and Euclidian norm $\|\cdot\|_Q$. A condition vector $\underline{\omega}$ is defined as $\underline{\omega} = |\omega_1 \quad \cdots \quad \omega_d|^T$, and the nominal condition vector $\underline{\omega}^0$ is defined for the nominal values of the parameters as $\underline{\omega}^0 = |\omega_1^0 \quad \cdots \quad \omega_d^0|^T$.

- **Degradations' space**

The degradations' space $\mathcal{D}$ is defined as an affine subspace of Q with origin $\underline{\omega}^0$ and the same dimension, base and norm. A degradation vector $\underline{\delta} = |\delta_1 \quad \cdots \quad \delta_d|^T$ is a non-null vector of $\mathcal{D}$. Such a vector is characterized by its mode and value, which are defined as follows:

$$\text{Mode}(\underline{\delta}) = \frac{\underline{\delta}}{\|\underline{\delta}\|^{\mathcal{D}}}, \qquad \text{Value}(\underline{\delta}) = \|\underline{\delta}\|^{\mathcal{D}} \tag{2.3}$$

It is easy to verify that if $\underline{\delta} = 0$, then the system is in a healthy state. In this work, only single degradation modes (DEMs) are considered. Thus, DEMs are defined as vectors of the canonical base, *i.e.*, $\underline{\delta} = \delta \underline{e}_j^{\mathcal{D}}$ where $\underline{e}_j^{\mathcal{D}}$ is the degradation mode and δ is the value of the associated degradation parameter.

Finally, the model can be expressed by (2.4) and its general representation is given in Figure 2.3:

$$\boldsymbol{Y} = \mathbb{f}\left(\boldsymbol{U}, \underline{\gamma}, \underline{\lambda}, \underline{\omega}^0 + \underline{\delta}\right) \tag{2.4}$$

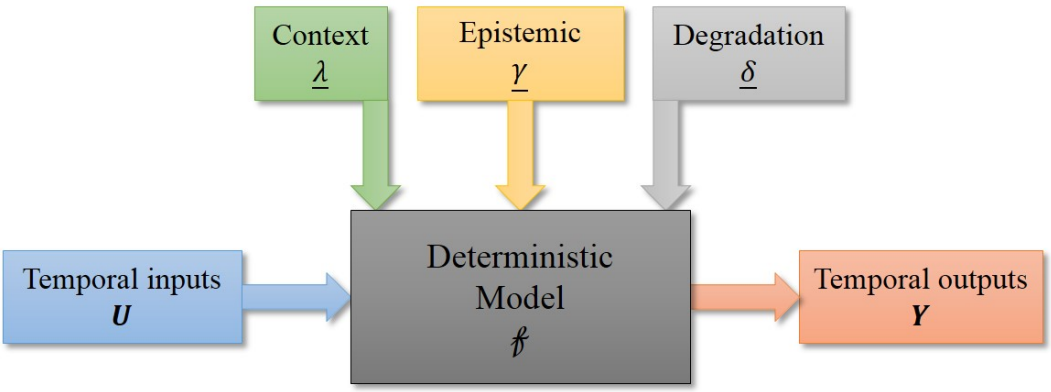


Figure 2.3 *The scheme of the numerical model interfaces.*

Resuming the guiding thread example of chapter 1, the acting parameters are defined and classified as presented in Table 2.1.

Context parameters	Epistemic parameters	Degradation parameters
Fluid temperature T_{fluid} Fluid inlet pressure P_{fluid}	Actuator's head diameter D Feedback stiffness K Mass of the rod M	Static friction coefficient μ

Table 2.1 *The parameters' definitions and the classification for the guiding thread example.*

2.2.1.3 *Compliant service indicators and health indicators*

In this section, the HIs are denoted $\varphi_1, \ldots, \varphi_h$ and the compliant service vectors are denoted $\psi_1, \ldots, \psi_o$. It is proposed to define the health space $\mathcal{H}$ as a Euclidian vector space of dimension h provided with the canonical base $\left(\underline{e}_1^{\mathcal{H}}, \ldots, \underline{e}_h^{\mathcal{H}}\right)^T$ and Euclidian norm $\|\cdot\|_{\mathcal{H}}$. An HIs vector $\underline{\varphi}$ is defined as $\underline{\varphi} = |\varphi_1 \quad \cdots \quad \varphi_h|^T$.

Similarly, we define the compliant service space $\mathcal{O}$ as a Euclidian vector space of dimension o provided with the canonical base $\left(\underline{e}_1^{\mathcal{O}}, \ldots, \underline{e}_o^{\mathcal{O}}\right)^T$ and Euclidian norm $\|\cdot\|_{\mathcal{O}}$. A compliant service indicators

(CSIs) vector $\underline{\psi}$ is defined as $\underline{\psi} = |\psi_1 \quad \cdots \quad \psi_o|^T$. Both the HIs' and the CSIs' vectors are computed from the output matrix of the model by the extraction functions $\mathcal{g}$ and $\mathcal{h}$, which are defined as follows:

$$\begin{aligned} \mathcal{g}&: \mathbb{R}^{k\times m} \longrightarrow \mathcal{H} \\ \boldsymbol{Y} &\longmapsto \underline{\varphi} = \mathcal{g}(\boldsymbol{Y}) \end{aligned} \tag{2.5}$$

$$\begin{aligned} \mathcal{h}&: \mathbb{R}^{k\times m} \longrightarrow \mathcal{O} \\ \boldsymbol{Y} &\longmapsto \underline{\psi} = \mathcal{h}(\boldsymbol{Y}) \end{aligned} \tag{2.6}$$

Subsequently, $\underline{\varphi}$ and $\underline{\psi}$ can be expressed as functions of $\boldsymbol{U}$ and $\underline{\rho}$, where $\circ$ is the operator for the composition of functions:

$$\begin{aligned} \underline{\varphi} &= (\mathcal{g} \circ \mathcal{f})\left(\boldsymbol{U}, \underline{\rho}\right) \\ \underline{\psi} &= (\mathcal{h} \circ \mathcal{f})\left(\boldsymbol{U}, \underline{\rho}\right) \end{aligned} \tag{2.7}$$

The nominal HIs and CSIs vectors, *i.e.*, $\underline{\varphi}^0$ and $\underline{\psi}^0$ are defined as the images of the nominal parameterization through the extraction functions $\mathcal{g}$ and $\mathcal{h}$:

$$\begin{aligned} \underline{\varphi}^0 &= (\mathcal{g} \circ \mathcal{f})\left(\boldsymbol{U}, \underline{\rho}^0\right) \\ \underline{\psi}^0 &= (\mathcal{h} \circ \mathcal{f})\left(\boldsymbol{U}, \underline{\rho}^0\right) \end{aligned} \tag{2.8}$$

The deterministic model $\mathcal{M}$ can then be expressed as follows:

$$\begin{aligned} \mathcal{M}&: \mathbb{R}^{k\times n} \times \mathcal{P} \longrightarrow \mathcal{H} \times \mathcal{O} \\ \boldsymbol{U} &\longmapsto \left(\underline{\varphi}, \underline{\psi}\right) = \mathcal{M}(\boldsymbol{U}, \underline{\rho}) \end{aligned} \tag{2.9}$$

The representation of this model is given in Figure 2.4.

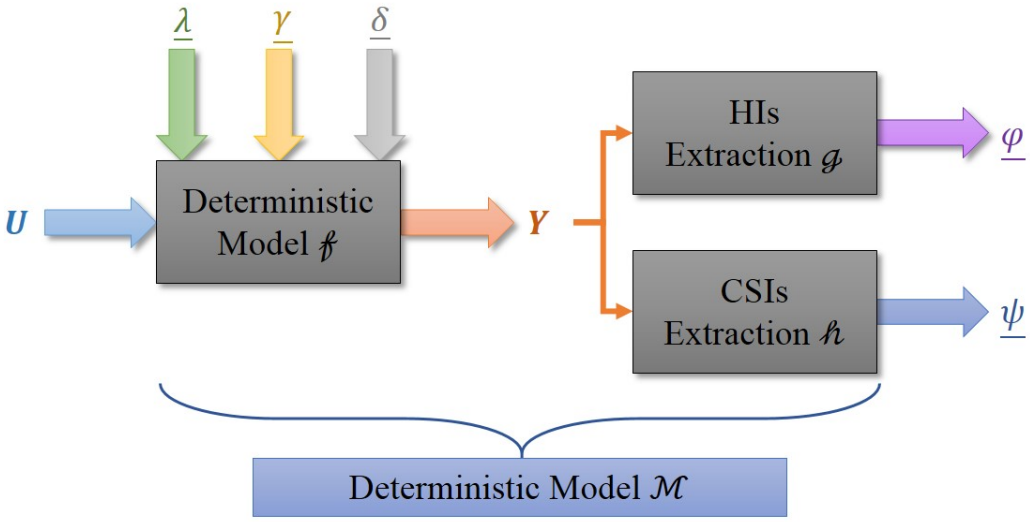


Figure 2.4 *A scheme of the deterministic model $\mathcal{M}$ with the extraction of HIs and CSIs.*

2.2.1.4 *The constant temporal inputs representation*

Because only the effects of the parameters and not of the inputs are considered in the present work, a new model $\mathcal{M}_{\mathbf{U}}$, which is termed the constant temporal inputs model, has been defined. This model

uses the same set of inputs **U** for every simulation; this set of inputs is determined from the feedback from other, similar engines. Finally, the inputs of the physics-based model are parameterizations, its outputs are HIs and CSIs and it is expressed as follows:

$$\begin{aligned} \mathcal{M}_{\boldsymbol{U}}&: \mathcal{P} \longrightarrow \mathcal{Y} \\ \underline{\rho} &\longmapsto \underline{\chi} = \mathcal{M}_{\boldsymbol{U}}(\underline{\rho}) \end{aligned} \tag{2.10}$$

where $\mathcal{Y} = \mathcal{H} \cup \mathcal{O}$, $\underline{\rho} = |\underline{\gamma} \quad \underline{\lambda} \quad \underline{\delta}|^{\boldsymbol{t}}$ and $\underline{\chi} = |\underline{\varphi} \quad \underline{\psi}|^{\boldsymbol{t}}$. The constant temporal inputs' representation is given in Figure 2.5.

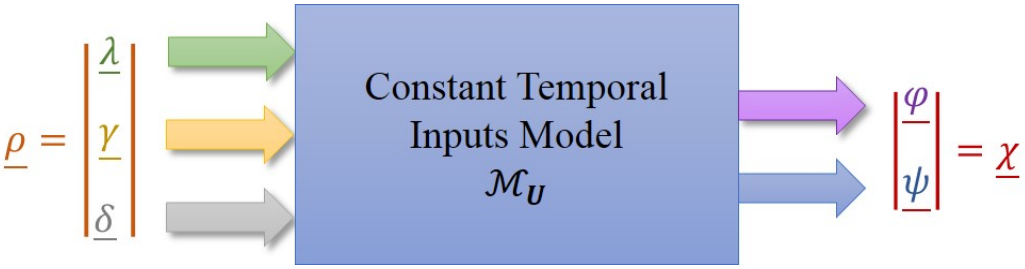


Figure 2.5 *A scheme of the constant temporal inputs model $\mathcal{M}_{\boldsymbol{U}}$.*

The purpose is to have values of $\underline{\chi}$ that are sensitive to $\underline{\delta}$ with a limited responsiveness to $\underline{\lambda}$ and $\underline{\gamma}$. The modeling formalism can be graphically represented for low dimensions. Figure 2.6 shows the first example, which includes three parameters (one context, one epistemic and one degradation parameter) and two indicators (one HI and one CSI). The issue of detection is clear from this scheme: it consists of estimating the value of $\underline{\delta}$ from the measurement of $\underline{\varphi}$ without knowing either $\underline{\gamma}$ or $\underline{\lambda}$.

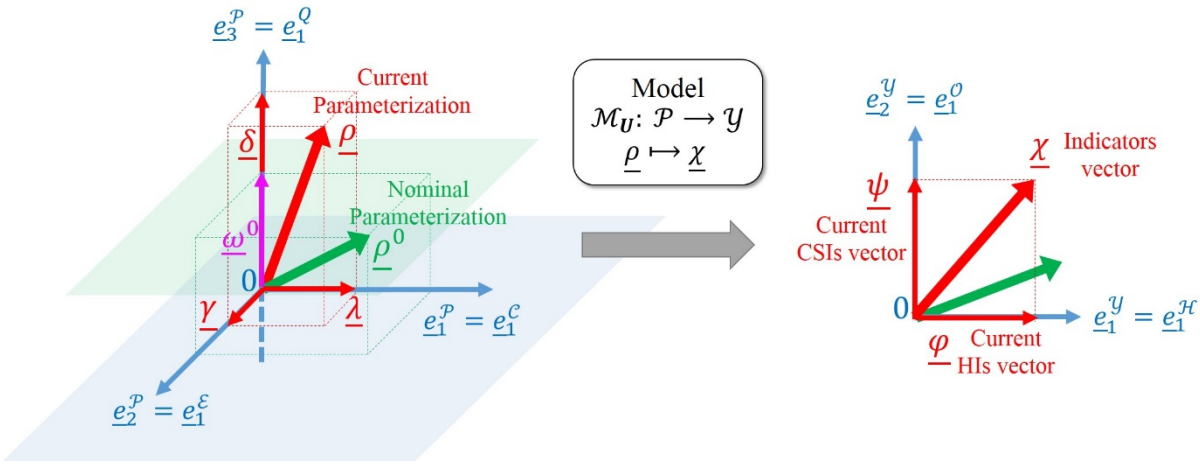


Figure 2.6 *A low-dimension representation of the modeling formalism for the detection issue.*

The second graphical example is aimed at illustrating the identification problem. The representation of Figure 2.7 corresponds to a system with two degradation parameters and one context parameter as inputs and two HIs as outputs. From this representation, the issue of identification can be summarized as follows: the current HIs vector $\underline{\varphi}$ is to be classified between $\underline{\varphi^1}$ and $\underline{\varphi^2}$ from the values of α_1 and α_2. The vectors $\underline{\varphi^1}$ and $\underline{\varphi^2}$ correspond, respectively, to the reference parameterizations $\underline{\rho^1}$ and $\underline{\rho^2}$. In this example, $\underline{\varphi^1}$ and $\underline{\varphi^2}$ are deterministic because $\underline{\lambda^0}$ is fixed. However, for actual applications, $\underline{\varphi^1}$ and $\underline{\varphi^2}$are stochastic because $\underline{\lambda^0}$ is random and unknown. As a result, the identification is more difficult.

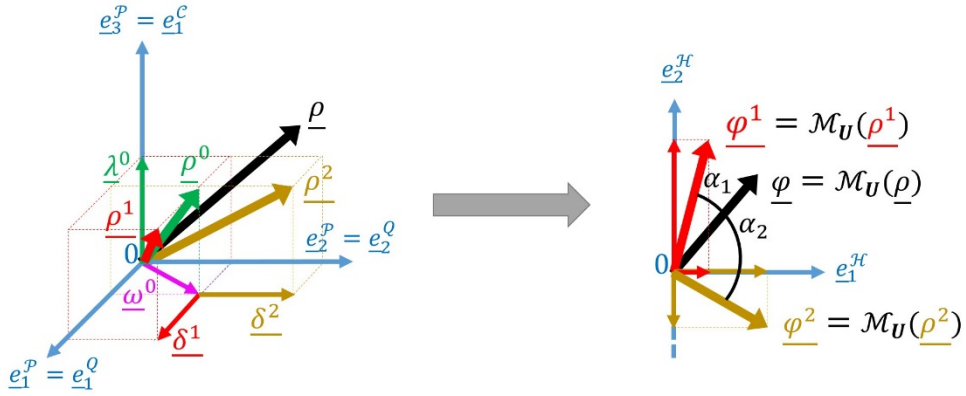


Figure 2.7 *A low-dimension representation of the modeling formalism for the identification issue.*

Finally, for the example of the previous chapter 1, one HI and two CSIs are defined. Then, the constant temporal inputs model of this system can be expressed as follows:

$$\begin{vmatrix} \Delta T \\ \mathrm{CSI}_1 \\ \mathrm{CSI}_2 \end{vmatrix} = \mathcal{M}_{\boldsymbol{U}} \left(\begin{vmatrix} T_{fluid} \\ P_{fluid} \\ \mathrm{D} \\ K \\ M \\ \mu \end{vmatrix} \right) \tag{2.11}$$

2.2.2 Uncertainties Management

For multi-physics complex systems subject to actual operating conditions, the set of parameters is rarely deterministic. Many parameters are associated with uncertainties that must be managed to model the system's behavior over its full operating range. In the present work, two types of uncertainties are considered: random uncertainties derived from the environmental variations and affecting the context parameters and systematic uncertainties derived from the manufacturing variability and affecting the epistemic parameters (De Rocquigny, et al., 2007). Managing the uncertainties of a deterministic model consists of identifying the probability density functions (**PDFs**) of its parameters, which are usually defined by the type of their distribution (normal, uniform, generalized extreme values, etc.) and their parameter vector $\underline{\theta}$. For example, $\Lambda_3 \sim \mathcal{N}(\underline{\theta})$ with $\underline{\theta} = [\mu \ \sigma]$ means that the uncertainty on Λ_3 is defined by a Gaussian distribution of mean μ and standard deviation σ. Note that other possible formalisms than PDFs, such as intervals arithmetic (Moore, et al., 1979), can be adopted. However, in the present case, intervals arithmetic is not adopted because it necessitates an analytical expression of the model that is not available.

Uncertainties management is typically performed in two steps (De Rocquigny, et al., 2007). The first step is uncertainties localization, which consists of establishing the initial list of uncertain parameters. The second step is the uncertainties' quantification, wherein the determination of their PDFs is performed. It has to be noticed that for cases where the number of uncertain parameters is large and the knowledge is not easily accessible, this step could be very expensive in terms of time and cost if a high level of accuracy is required for the PDFs. The level of completeness of this quantification is at the discretion of the user. The way the quantification of uncertainties is performed depends on the type of parameter:

- **Context parameters:** because the context is very similar between different types of engines, data from other engines are generally used to determine the empirical PDF. If these data are not in sufficient quantity, bootstrap techniques can be implemented (Efron, et al., 1993).
- **Epistemic parameters:** they are mostly dimensional parameters whose values and uncertainty intervals can be found in equipment specifications. Usually, the specified uncertainty interval is modeled by a uniform PDF.
- **Degradation parameters:** the case of degradation parameters is peculiar. Although these parameters are fixed during a given Monte-Carlo simulation set, they vary between two sets. Their variation range is characterized by their nominal and maximal values.

2.2.3 Modeling implementation

The modeling of host systems is performed with the commercial software AMESim™ (2003). AMESim[16] is a proven tool for the simulation and analysis of multi-domain systems. Models are described by nonlinear analytical equations that represent the system's hydraulic, pneumatic, thermal, electric or mechanical behavior. The main advantage of this type of simulation is that it allows one to capture the system's behavior before detailed computer-aided design geometry is available. Hence, it is particularly useful in the upstream development stages of a host system. As both the construction of configurations' DOEs and the extraction of HIs and CSIs algorithms are coded in Matlab™, the cosimulation scheme of Figure 2.8 is used to take advantage of both Matlab's generic functionalities and the AMESim solver.

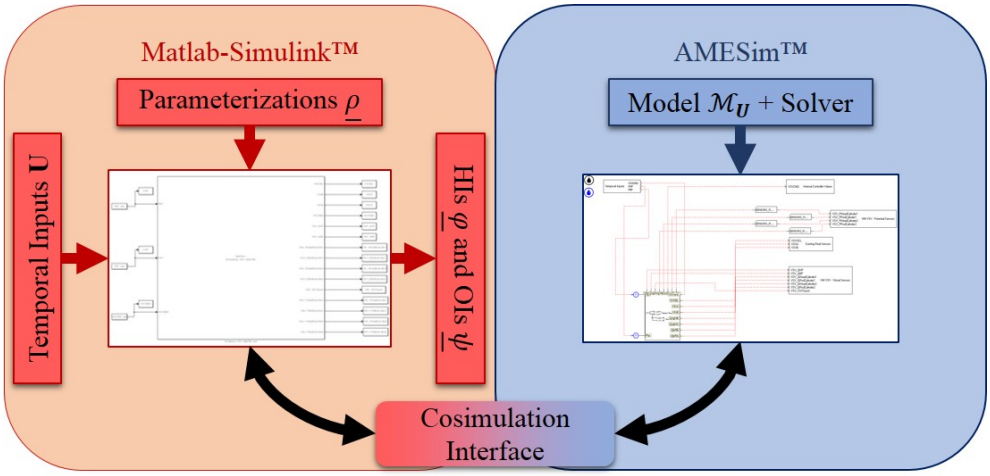


Figure 2.8 *A Matlab-AMESim cosimulation scheme.*

Note that even if a good representativeness is suitable for the model, its quality is not critical for ensuring the efficiency of the IDPHM approach. Indeed, the idea is to assess the behavior of HIs and CSIs with respect to the nominal state when the parameters' values change. Hence, even if the model is not perfectly calibrated, the provided information is not less valuable because only relative variations are studied. The only problem is that an inaccurate model will populate a biased precursors' database. However, this drawback may be circumscribed by a post EIS recalibration of the model and hence of the precursors' database from the first actual data retrieved at the beginning of the in-service life.

[16] The version used in this thesis work is AMESim Rev 11, v1100.

2.2.4 The selection of HIs

The HIs' selection is principally a matter of physics-based reasoning that amounts to anticipating what measured variable or combination of measured variables is likely to be sensitive to a given degradation mode with a limited sensitivity to the other modes. The initial step for the selection of health indicators is to list the targeted functional units, *i.e.,* the subsystems and equipment, for each hierarchical level. Then, for each defined functional unit from the highest hierarchical level to level zero, the selection process is based on five steps: (1) the determination of the targeted compliant service threats and the definitions of the associated CSIs, (2) the determination of the targeted physical threats, (3) the construction of HIs with respect to the list of physical threats to monitor and the CSIs, (4) prototyping on physics-based models of either separated equipment or the complete system to perform a first crude evaluation of the HIs' sensitivity to DEMs and (5) the presentation of the prototyping results to experts for the solution's evaluation. If the selection is both confirmed by prototyping and approved by experts, the selection of the HIs is completed. The logical scheme is represented in Figure 2.9.

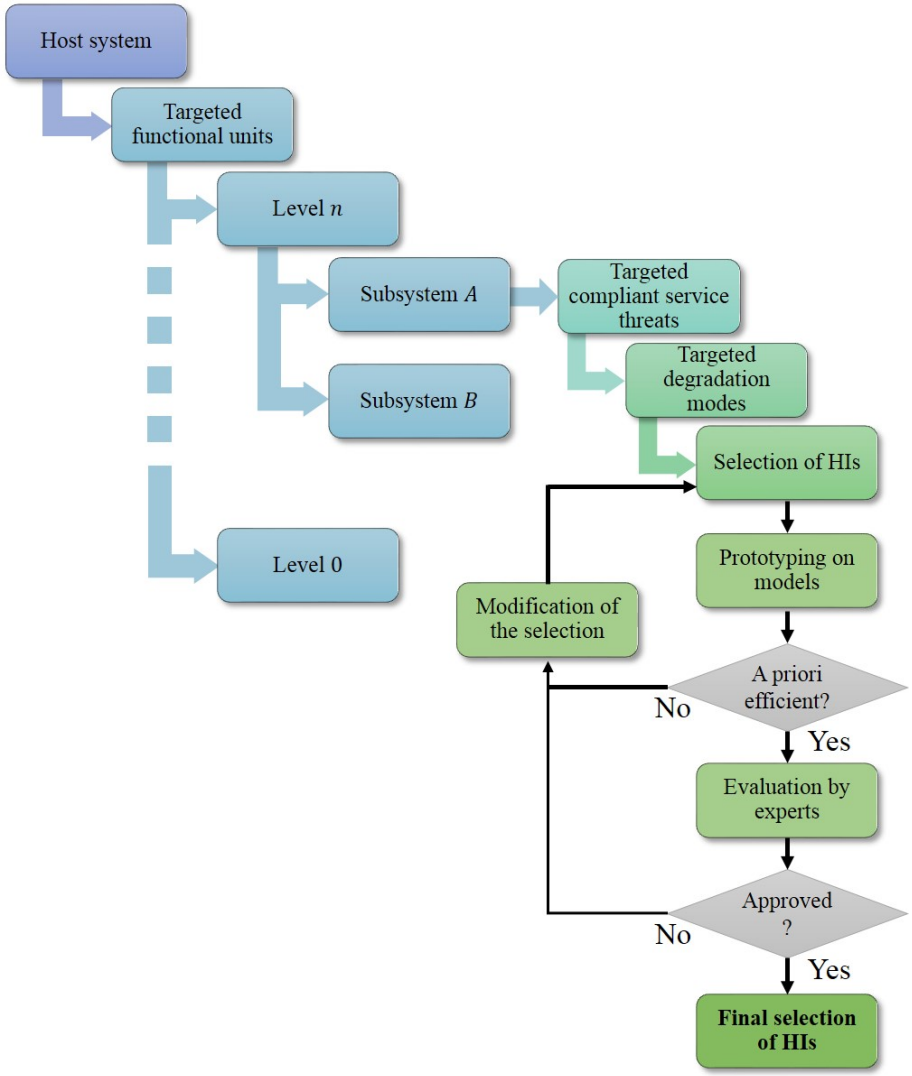


Figure 2.9 *Graph of the HIs selection process.*

The main difficulty in selecting HIs is generally to collect the knowledge from the host system. Indeed, in cases where this system has a complex design involving multiple disciplines located in different offices, it can take a long time to retrieve the necessary documents. In addition, the information

PHM designers need could possibly be unavailable. This possibility is particularly likely, as PHM is considered as a marginal task. In the first chapter, the notion of key data was introduced, and it was mostly issued from functional and structural specifications documents and equipment specifications. The link between this key data and the steps of the HIs' selection is addressed in detail in the following subsections.

2.2.4.1 *Targeted functional units*

To define the targeted functional units for the different hierarchical levels, a functional breakdown representation of the system is needed. Typically, it can be found in the functional specifications of the host system, which is one of the first edited documents.

2.2.4.2 *Targeted compliant service threats*

To determine the list of compliant service threats, both functional and equipment specifications are needed. More precisely, equipment specifications typically provide failure modes and effects analysis (**FMEA**) (Megill, 1984), whose purpose is to identify the potential failure modes, their causes and their effects. Hence, for PHM purposes, the FMEA of the host system's equipment allows the listing of failures. Note that the FMEA itself is principally performed from experience-based feedback and expertise. Because fault detection and tolerance logics are implemented in the controller, the list of no-go, go-if and beta dispatch faults can be found in the EEC specifications. Finally, the list of defects is identified from the equipment specifications. Indeed, these specifications provide lists of requirements, which can be of structural type (e.g., lengths, diameters, or stiffness) or of functional type (e.g., minimum flow, response time, maximum gap, *etc*.).

2.2.4.3 *Targeted physical threats*

The list of TDEMs is defined from the list of compliant service threats via a combination of expertise, feedback and physics-based reasoning. The list of other DEMs is determined from the model of the system using the list of degradation parameters that are likely to degrade over time. From the knowledge of DEMs, the list of CSIs can be defined.

2.2.4.4 *The construction of raw HIs*

Even if the construction of HIs is principally performed through physics-based reasoning, some orientations can be found in the equipment specifications and especially in acceptance test procedures (**ATPs**) descriptions. ATPs are series of tests run on equipment or subsystems received from suppliers to check if they comply with the needed specifications to allow them to enter into service. The same tests are also used during maintenance check-ups. Thus, ATPs are a valuable source of ideas that can help define HIs. Beyond the precious information they give, the importance of using ATPs is that they are already used and mastered by maintenance operators so that HIs based on ATPs will be more quickly understood and implemented. Generally, the construction of HIs uses variables that are actually measured. However, it is also possible to use some variables that are available in the model but are not measurable. Finally, two types of HIs can be constructed:

DEFINITION 34 (**Real HIs**). Real HIs (**RHIs**) are HIs constructed from only measured variables.

DEFINITION 35 (**Virtual HIs**). Virtual HIs (**VHIs**) are HIs constructed from variables available in the model that are not necessarily actual measured variables.

In cases where the set of real HIs is not compliant with the specifications, it is possible to define virtual ones to enrich the total set. Then, one can operate a feedback on the host system's design to ask for new locations or different characteristics for the sensors.

2.3 Standardization of HIs

Among the selected HIs, some are likely to have a significant variability that jeopardizes their performances. To reduce this variability, one solution is to standardize the HIs as proposed in (Lacaille, 2009). The standardization involves globally subtracting the effects of some known parameters of the HIs. Thus, the standardized HIs become residuals that only account for unknown effects, and hence, their standard deviation is reduced. The standardization consists of two steps: first, the identification of the standardization parameters, and then, the estimation of standardization models. For the present application, SA is used for the first step and SVR is used for the second one. The next subsection introduces SA in outline form.

2.3.1 Sensitivity analysis

2.3.1.1 *Classification of the parameters according to their effects on the outputs*

Sensitivity analysis is the study of how the variability in the outputs of a model or system can be apportioned to the different sources of uncertainties in its inputs. In the present case with the constant input model formalism, the inputs are parameters. According to De Rocquigny *et al.* (De Rocquigny, et al., 2007), the parameters of a given model can be either uncertain or fixed, and whereas the former are parameters whose values are subject to uncertainties and represented by stochastic variables such as probability density functions, the latter are parameters whose values are known and deterministic. The purpose of SA is to study the effects of the uncertain parameters on the outputs. In the present thesis, SA is used first to identify the influential parameters from the marginal parameters, which are, respectively, defined as follows:

DEFINITION 36 (**Influential parameter**). *Influential parameters are parameters that have significant effects on at least one of the outputs of the model.*

DEFINITION 37 (**Marginal parameter**). *Marginal parameters are parameters that have negligible effects on the whole set of outputs. They are considered as fixed parameters.*

These definitions account for the multidimensional nature of the output space. The classification between influential and marginal parameters depends on some criteria provided by SA tools that will be introduced in section 2.3.1.4. With such knowledge, the user can define the selection thresholds depending on the number of influential parameters that can be handled by the computational device. Under this assumption, the model $\mathcal{M}_{\boldsymbol{U}}$ can be rewritten as follows:

$$\underline{\chi} = \mathcal{M}_{\boldsymbol{U}}\left(\underline{\rho}^{\boldsymbol{i}}, \underline{\rho}^{*}\right) \tag{2.12}$$

where $\underline{\rho}^{\boldsymbol{i}}$ is the vector of influential parameters and $\underline{\rho}^{*}$ is the vector of fixed parameters. The fixed values of $\underline{\rho}^{*}$ are equal to the nominal values of the parameters. Some sensitivity analysis methods such as the Morris method (Morris, 1991), which will be introduced later, also provide information about the level of linearity associated with each influent parameter's effect. Actually, these parameters are classified either as linear or as nonlinear and/or with interactions (Iooss, 2011). For the present application, the

purpose is to identify the linear parameters for the supervision of SVR (see section 2.3.3). Hence, influential parameters are classified either as linear ones or nonlinear ones according to the following definitions:

DEFINITION 38 (**Linear parameter**). *Linear parameters are parameters that have linear relations with respect to the whole set of outputs.*

DEFINITION 39 (**Nonlinear parameter**). *Nonlinear parameters are parameters that have at least one nonlinear relations and/or a relation with interactions with at least one output.*

The model $\mathcal{M}_{\boldsymbol{U}}$ can then be rewritten as follows:

$$\underline{\chi} = \mathcal{M}_{\boldsymbol{U}}\left(\underline{\rho}^{ni}, \underline{\rho}^{li}, \underline{\rho}^{*}\right) \tag{2.13}$$

where $\underline{\rho}^{\boldsymbol{ni}}$ are the nonlinear influential parameters and $\underline{\rho}^{\boldsymbol{li}}$ are the linear influential parameters. Among the set of influential parameters, it is generally observed that a few of them own the major part of the effects on the outputs. Another purpose of uncertainties analysis is to sort the influential parameters according to the importance of their effects on the outputs. Subsequently, the distinction can be made between principal and secondary parameters, which are defined as follows:

DEFINITION 40 (**Principal parameter**). *For a given output, principal parameters encompass the set of influential parameters that have the most important effects on the output.*

DEFINITION 41 (**Ancillary parameter**). *For a given output, ancillary parameters encompass the set of influential parameters that have the less important effects on the output.*

The proportion of principal and ancillary parameters is at the discretion of the user with respect to the specificities of the intended application. Hence, if the number of influential parameters is large and the model is complex, a reduced proportion of principal parameters should be chosen. On the contrary, for a simple model with few influential parameters, this proportion can be larger. In the present application, the models have multiple outputs. It is probable that the principal parameters are different for each output, so that as many models as the number of outputs need to be considered. These models, which are denoted $\mathcal{M}_U^j$, are defined as follows:

$$\chi_j = \mathcal{M}_{\boldsymbol{U}}^{j}\left(\underline{\rho}_j^{np}, \underline{\rho}_j^{lp}, \underline{\rho}_j^{na}, \underline{\rho}_j^{la}, \underline{\rho}^{*}\right), \qquad j = 1, \dots, h+o \tag{2.14}$$

where $\left(\underline{\rho}_j^{np}, \underline{\rho}_j^{lp}\right)$ are the nonlinear and linear principal parameters for output j and $\left(\underline{\rho}_j^{na}, \underline{\rho}_j^{la}\right)$ are the nonlinear and linear ancillary parameters for output j. For the purposes of the present application, the principal parameters are subdivided into standardization and unknown parameters, which are defined as follows:

DEFINITION 42 (**Standardization parameter**). *For a given output, standardization parameters are principal parameters that are measurable.*

DEFINITION 43 (**Unknown parameter**). *For a given output, unknown parameters are principal parameters that are not measurable.*

Standardization parameters are defined only for HIs because CSIs are not directly measurable. In the framework of the present modeling formalism, the models $\mathcal{M}_{\boldsymbol{U}}^{j}$ for the HIs can be rewritten as follows:

$$\varphi_j = \mathcal{M}_{\boldsymbol{U}}^{j}\left(\underline{\rho}_j^{ns}, \underline{\rho}_j^{ls}, \underline{\rho}_j^{nu}, \underline{\rho}_j^{lu}, \underline{\rho}_j^{na}, \underline{\rho}_j^{la}, \underline{\rho}^{*}\right), \qquad j = 1, \dots, h \tag{2.15}$$

where $\left(\underline{\rho}_j^{ns}, \underline{\rho}_j^{ls}\right)$ are the nonlinear and linear standardization parameters and $\left(\underline{\rho}_j^{nu}, \underline{\rho}_j^{lu}\right)$ are the nonlinear and linear unknown parameters for output j. To determine the lists of these different types of parameters, SA methods are used.

2.3.1.2 *Classifications of sensitivity analysis methods*

According to (Iooss, 2011), there are two principal types of sensitivity analysis methods: local methods and global methods. Local methods are based on the computation of partial derivatives, and they do not attempt to fully explore the input space, as they examine small perturbations. This examination typically occurs one variable at a time. Local methods will not be described further, as they are not used in this work (please refer to (Saltelli, et al., 2000) for more details on the subject). Global methods are aimed at determining the influence of the parameters over the whole input space, and they are subdivided into two classes: screening methods and quantitative methods. Screening methods are intended to deal with a large number of variables, which are typically on the order of tens or hundreds. An example of a screening method is the Morris method (Morris, 1991), which allows a coarse estimation of the main effects from a reduced number of model evaluations. Despite its advantages, the Morris method is not capable of computing precisely the sensitivity indices associated with the interactions between inputs. Quantitative methods are mainly based on the decomposition of the output variance, which leads to the so-called variance-based methods and Sobol sensitivity indices (Sobol, 1993). These methods allow the computation of both the main and the total effects of each input variable as well as the precise interaction effects. However, for functions with nonlinear and interaction effects, the estimation of Sobol indices is particularly time-demanding and generally limited to models with a reduced number of input variables (on a smaller order than tens). In the following subsections, both the Morris method and the Sobol indices are introduced. For a review on uncertainty importance measurment, the reader is invited to refer to (Borgonovo, 2006).

2.3.1.3 *The Morris method*

The Morris method (Morris, 1991) is generally used to perform a fast but rather coarse exploration of the output behavior of a high-simulation-runtime model with numerous inputs, which are typically on the order of tens or hundreds. The principle is to perform multiple one-at-a-time designs of experiments (OAT-DOEs) with various properties. An OAT-DOE consists of varying each parameter independently with both the initial point and the sequential progression drawn randomly. If a sequence of r OAT-DOEs is used for the Morris method, each repetition k, $k \in [\![1, r]\!]$[17] gives an elementary effect $E_i^{(k)}$ (the difference between two successive points) for each parameter $i, i \in [\![1, p]\!]$. The r repetitions provide an r-sample of the effects for each parameter i from which the following variables are calculated:

[17] The mathematical notation $k \in [\![1, r]\!]$ means that k belongs to the set of integers from 1 to r. It is equivalent to $k \in [1, r] \cap \mathbb{N}$.

$$\mu_i = \sum_{i=1}^{r} E_i^{(k)}$$
$$\mu_i^* = \sum_{i=1}^{r} \left| E_i^{(k)} \right| \qquad \textbf{(2.16)}$$
$$\sigma_i = \sqrt{\frac{\sum_{k=1}^{r} \left(E_i^{(k)} - \mu_i \right)}{r}}$$

where $\mu_i = \sum_{k=1}^{r} E_i^{(k)}$, μ_i^* and σ_i are, respectively, the mean, absolute mean and standard deviation effect of $E_i^{(k)}, k \in [\![1; r]\!]$. Then, the results are then classified into three classes:

- The parameters with negligible effects *i.e.,* both $\boldsymbol{\mu_i^*}$ and $\boldsymbol{\sigma_i}$ are almost null.
- The parameters with linear effects if $\boldsymbol{\mu_i^*}$ is different from zero and $\boldsymbol{\sigma_i}$ is almost null.
- The parameters with nonlinear and/or interactions effects if both $\boldsymbol{\mu_i^*}$ and $\boldsymbol{\sigma_i}$ are different from zero.

The information given by the Morris method about nonlinearity is meaningful only for cases where the studied behaviors are monotonic (Ravalico, et al., 2005). For applications to aircraft engines, this monotonicity hypothesis is almost systematically verified. Therefore, the Morris method can be used for assessing nonlinearity. The variables μ_j^* and σ_j are generally plotted on a graph where each input is represented by a point with coordinate (μ_j^*, σ_j), as shown in Figure 2.10, which contains results for 9 input parameters. The sensitivity analysis results show that parameters 1 to 3 are fixed parameters, parameters 4 to 6 are nonlinear parameters and parameters 7 to 9 are linear parameters. Finally, the Morris method gives coarse results, but it is useful to compute the main effects of the model input variables at a reduced calculation runtime.

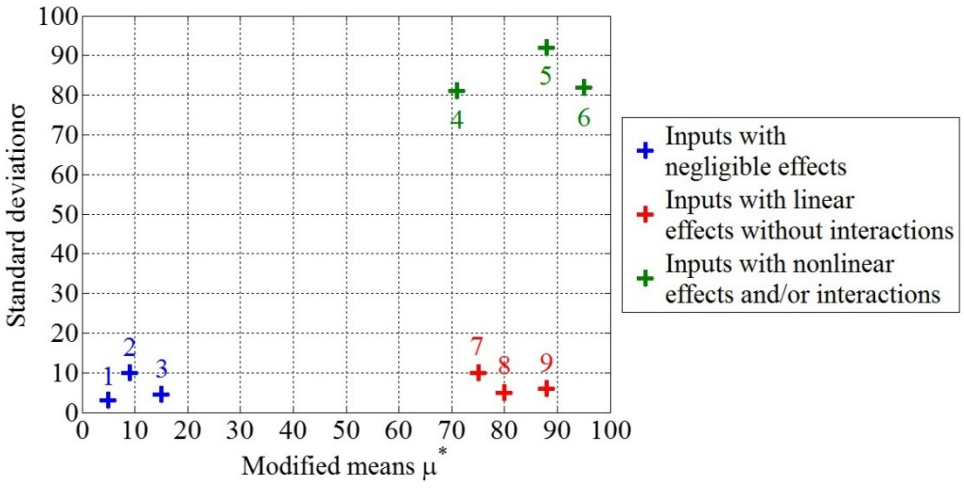


Figure 2.10 *An example of a Morris method graphical representation.*

In light of the present application, the Morris method has two main drawbacks. First, its graphical representation is not suitable in cases where the number of inputs is very large (more than one hundred). This limitation can be resolved by using sensitivity indices, which allow for a quantification of the input variables' effects on the whole set of outputs. To compute these indices, we intend to use derivative-

based global sensitivity measures (**DGSM**s) (Sobol, et al., 2009), which can be observed as a type of generalization of the Morris screening method (Lamboni, et al., 2013). The second drawback is that for models with a large number of outputs, the amount of information rapidly becomes unmanageable. Thus, we propose to use two new sensitivity indices that compress information about the outputs and are easily interpretable. One is used for the identification of influential parameters (see Definition 36) and the other is meant for the identification of linear parameters (see Definition 38).

2.3.1.4 *Total sensitivity indices from DGSMs*

The basis of DGSMs is to use the second moment of the model derivatives as an importance measure. Hence, significant variation of the model output is expected when the variables are perturbed. According to (Lamboni, et al., 2013), for a model output $y = \ell(\underline{x})$ with $\underline{x} = |x_1 \quad \cdots \quad x_n|^t$, the DGSM indices are defined as follows:

$$\nu_j = \mathbb{E}\left[\left(\frac{\partial \ell(\underline{x})}{\partial x_j}\right)^2\right], \qquad j = 1, \dots, n \tag{2.17}$$

Additionally, a classical estimator for the DGSM indices is the empirical one defined as follows from the elementary effect of the Morris method:

$$\hat{\nu}_j = \frac{1}{r}\sum_{r=1}^{n}\left(\frac{\partial \ell(E_i^{(r)})}{\partial x_j}\right)^2, \qquad j = 1, \dots, n \tag{2.18}$$

These indices allow an upper bound for the total Sobol indices.

Consider a model with i parameters and j outputs, where $\hat{\nu}_{i,j}$ and $\sigma_{i,j}$ are defined as the estimation of the DGSM index and the standard deviation effect computed for the pair (i, j), respectively. From these variables, two original sensitivity indices that account for the effects on the whole set of outputs are proposed. The total effect index Tot_i reflects the importance of parameter i, and the linearity index Lin_i indicates the level of linearity of the effect of parameter i on the total set of outputs. These indices are defined as follows:

$$\begin{aligned} Tot_i &= \frac{\sum_{j=1}^{m}\hat{\nu}_{i,j}}{M_i} \in [0,1] \text{ with } M_i = \max_j\left\{\sum_{j=1}^{m}\hat{\nu}_{i,j}\right\} \\ Lin_i &= 1 - \frac{\sum_{j=1}^{h}\sigma_{i,j}}{A_i} \in [0,1] \text{ with } A_i = \max_j\left\{\sum_{j=1}^{m}\sigma_{i,j}\right\} \end{aligned} \tag{2.19}$$

To conclude, the computation of Toy_i and Lin_i allows the identification of influent and linear parameters. Still, the results of the Morris method are not capable of computing precisely the second and higher-order effects or the total effects. Moreover, the evaluation of the main effects provided by the Morris method is not trustworthy enough to be used for anything other than the identification of influent and linear parameters. For other applications, Sobol indices are used.

2.3.1.5 *Variance-based Sobol indices*

For the single-dimension outputs space model $y = \ell(\underline{x})$ with $\underline{x} = |x_1 \quad \cdots \quad x_n|^t$, it is possible to estimate precisely the importance of the parameters' effects on the output y by decomposing ℓ into a sum of elementary functions (Hoeffding, 1948):

$$\ell(\rho_1, \dots, \rho_n) = \ell_0 + \sum_{i=0}^{n} \ell_i(x_i) + \sum_{i<j}^{n} \ell_{ij}(x_i, x_j) + \dots + \ell_{12\dots n}(x_1, \dots, x_n) \quad \textbf{(2.20)}$$

where ℓ is integrable on $\mathbb{R}^n$. This decomposition was then extended to SA by Sobol (Sobol, 1993), and he proved that this decomposition is unique. If the x_i are independent random variables, the functional variance decomposition of y or the functional analysis of the variance representation can be written as follows:

$$Var(y) = \sum_{i=0}^{n} V_i(y) + \sum_{i<j}^{n} V_{ij}(y) + \sum_{i<j<k}^{n} V_{ijk}(y) + \dots + V_{12\dots n}(y) \quad \textbf{(2.21)}$$

with $V_i(y) = Var[\mathbb{E}(y|x_i)], V_{ij}(y) = Var\left[\mathbb{E}\left(y|x_i x_j\right)\right] - V_i(y) - V_j(y)$, *etc*. Some sensitivity indices can then be defined as follows:

$$S_i = \frac{Var[\mathbb{E}(y|x_i)]}{Var(y)} = \frac{V_i(y)}{Var(y)} \qquad S_{ij} = \frac{V_{ij}(y)}{Var(y)} \qquad S_{ijk} = \frac{V_{ijk}(y)}{Var(y)} \quad \dots \quad \textbf{(2.22)}$$

These coefficients are called variance-based importance measures or Sobol indices (Sobol, 1993). Because these indices range from 0 to 1, they are quite easy to interpret, which explains their popularity. For example, index S_{ij} reduces the model sensitivity to the interaction between parameters x_i and x_j; the sum of these indices is equal to 1. When the parameters space dimension n increases, the number of Sobol indices grows exponentially (it is equal to 2^{n-1}). Homma and Saltelli (Homma, et al., 1996) introduced the notion of the total sensitivity index to express the whole effect of a given input on output y, and thus, to simplify their interpretation:

$$S_{Ti} = S_i + \sum_{j\neq i}^{n} S_{ij} + \sum_{j\neq i, k\neq i, j<k}^{n} S_{ijk} + \dots = \sum_{l\in \#i} S_l \quad \textbf{(2.23)}$$

where $\#i$ stands for all of the indices' subsets containing index i. Thus, $\sum_{l\in \#i} S_l$ is the sum of all of the Sobol indices involving i. In practice, when n is large, only the main indices and total indices are computed. If their values are close, the considered input does not interact with the others. In the contrary case, the interactions are strong. Sobol indices are computed via the Monte-Carlo method, which is explicated in the next subsection. The reader should be notified that in terms of uncertainty analysis, the Sobol indices and more generally variance-based global SA a limited by the fact that they focus on just one moment of the output distribution and thus cannot represent the whole decision-maker state of knowledge. To overcome this shortcoming, Borgonovo proposed a new uncertainty importance measure in (Borgonovo, 2007).

2.3.1.6 *The computation of Sobol indices via the Monte-Carlo method*

The Monte-Carlo method for SA was developed by Sobol and Saltelli (Saltelli, et al., 2000), and it consists of the following steps: consider an a-sample $\underline{x}_{(a)} = (x_{k1}, \dots, x_{kn})_{k=1,\dots,a}$ of realizations of uncertain parameters $x_1, \dots, x_n$. The expected value of the output $y, \mathbb{E}(y) = \ell_0$, and its variance $Var(y) = V$ are estimated via these formulas:

$$\hat{\ell}_0 = \frac{1}{a}\sum_{k=1}^{a} \ell\,(x_{k1}, \dots, x_{kn}) \quad \text{and} \quad \hat{V} = \frac{1}{a}\sum_{k=1}^{a} \ell^2\,(x_{k1}, \dots, x_{kn}) - \hat{\ell}_0^2 \quad \textbf{(2.24)}$$

The Sobol indices are then computed as follows:

$$S_i = \frac{\hat{V}_i}{\hat{V}} = \frac{\hat{U}_i - \hat{\ell}_0^2}{\hat{V}} \tag{2.25}$$

Sobol explains how to compute the estimation $\hat{U}_i$ in (Sobol, 1993) based on 2 samples of realizations of inputs, which he named $\underline{x}^1_{(a)}$ and $\underline{x}^2_{(a)}$:

$$\hat{U}_i = \frac{1}{a}\sum_{k=1}^{a} \ell\left(x^1_{k1}, \dots, x^1_{ki}, \dots, x^1_{kn}\right) \ell\left(x^2_{k1}, \dots, x^2_{k(i-1)}, x^1_{ki}, x^2_{k(i+1)}, \dots, x^2_{kn}\right) \tag{2.26}$$

Higher orders of indices can be computed recursively. The details of their calculation are not presented in this work, but can be found in (Sobol, 1993). Total indices can be computed directly via

$$S_{Ti} = 1 - \frac{V_{\sim i}}{V} = 1 - \frac{\hat{U}_{\sim i} - \hat{\ell}_0^2}{\hat{V}} \tag{2.27}$$

where $\sim i$ designates all of the indexes except i and $\hat{U}_{\sim i}$ is calculated similarly to $\hat{U}_i$:

$$\hat{U}_{\sim i} = \frac{1}{a}\sum_{k=1}^{a} \ell\left(x^1_{k1}, \dots, x^1_{ki}, \dots, x^1_{kn}\right) \ell\left(x^1_{k1}, \dots, x^1_{k(i-1)}, x^2_{ki}, x^1_{k(i+1)}, \dots, x^1_{kn}\right) \tag{2.28}$$

The main drawback of the Monte-Carlo method for the computation of Sobol indices is that the number of model evaluations needed for each realization of the inputs is equal to approximately 10,000 to reach approximately 10% precision. Consequently, in cases where the model is time-demanding, this method is impracticable. Numerous techniques are available to reduce the computational cost, such as high-dimensional model representation (Li, et al., 2001) and the Fourier amplitude sensitivity test (McRae, et al., 1982), but they still need a consequent number of evaluations of the model.

For the present application on aircraft engine models, the number of input parameters is very large, and typically about a hundred. Moreover, one evaluation of the considered physics-based models can take several hours. Obviously, the 10,000 evaluations needed for computing the Sobol indices is unrealistic. To overcome these computational issues, the use of a surrogate model is a common approach (Shahsavani, et al., 2011). Surrogate models, which are also known as metamodels, are mathematical functions that estimate almost instantaneously the outputs of a time-demanding model (Simpson, et al., 2001). The idea is to replace complete models by surrogates for the computation of Sobol indices. A state of the art discussion of surrogate models is provided in the following chapter 3.

2.3.1.7 *Application of SA techniques*

Finally, from our practical experience and the comparative studies proposed in (Ravalico, et al., 2005) and (Li, et al., 2013), the advantages, drawbacks and main utilization of the Morris method and the Sobol indices are summarized in Table 2.2.

	Advantages	**Drawbacks**	**Utilization**
Sobol Indices	Good precision Computation of the main effects, total effects and interaction effects	Need a very large number of model evaluations Surrogate models are often needed	Fine SA
Morris Method	Limited model evaluations	Lack of precision	Crude SA

	Computation of the main effects and evaluation of linearity	Not capable of computing the total effects or the interaction effects	

Table 2.2 *The advantages, drawbacks and main utilization of global and screening methods.*

For the present application, both the Morris method and the computation of Sobol indices are used complementarily. The former method is aimed at identifying influential parameters and differentiating linear from nonlinear ones, whereas the latter method is used for the prioritization of influential parameters and the definition of principal and ancillary ones.

For the present application, the proposed sensitivity analysis strategy is divided into 4 steps: (1) an uncertainties localization is carried out to determine the initial list of uncertain parameters $\underline{\rho}$, (2) the Morris method is performed on the physics-based model for the whole set of uncertain parameters $\underline{\rho}$ to determine $\underline{\rho}^*, \underline{\rho}^{ni}$ and $\underline{\rho}^{li}$, (3) a Sobol indices computation is performed on a surrogate model for the set of influential parameters $\underline{\rho}^i$ to determine $\underline{\rho}^{np}, \underline{\rho}^{lp}, \underline{\rho}^{na}$ and $\underline{\rho}^{la}$ and (4) the identification of actual measurable data from knowledge about the host system allows the determination of $\underline{\rho}^{ns}, \underline{\rho}^{ls}, \underline{\rho}^{nu}$ and $\underline{\rho}^{lu}$. This process is represented in Figure 2.11.

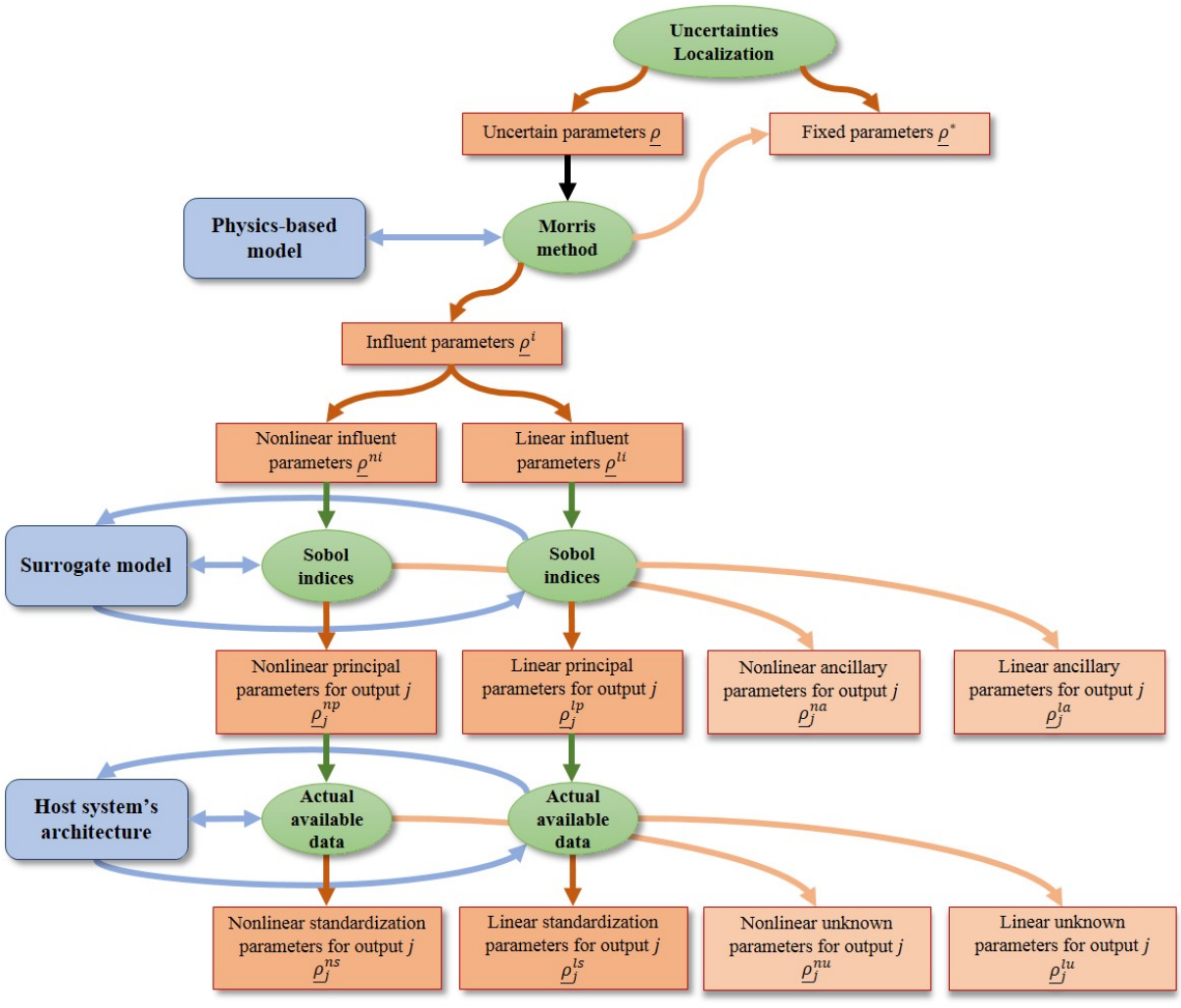


Figure 2.11 *Sensitivity analysis for uncertainties management.*

2.3.2 Support Vector Regression

2.3.2.1 *Introduction to support vector machines*

Support vector machines are a set of supervised learning methods aimed at solving discrimination and regression problems. They appeared in the 1990s from the theoretical considerations of Vapnik (Vapnik, et al., 1997), and they were rapidly adopted by the scientific community, in particular for their powerful generalization properties in classification problems (Hsu, et al., 2003). These machines' use was then extended to regression problems with support vector regression (**SVR**) (Smola, et al., 2004). In this work, only the regression aspect of support vector machines is addressed. For examples of practical applications of SVR to engineering problems, the reader is invited to refer to (Clarke, et al., 2005). To introduce SVR, the following unknown function $\mathcal{s}$ is considered:

$$\begin{aligned} \mathcal{s}&: \mathbb{R}^n \longrightarrow \mathbb{R}^m \\ &\underline{x} \longmapsto y = \mathcal{s}(\underline{x}) \end{aligned} \tag{2.29}$$

where n is the dimension of the inputs space. To construct an estimator of $\mathcal{s}$, a set of learning points is needed. Suppose that $\mathcal{s}$ has been evaluated for k training input vectors $\underline{x}_1, \dots, \underline{x}_k$. The associated output values are denoted $y_1, \dots, y_k$. The objective is to estimate the function $\mathcal{s}$ by an SVR estimate $\mathcal{S}$ defined as follows:

$$\begin{aligned} \mathcal{S}&: \mathbb{R}^n \longrightarrow \mathbb{R} \\ &\underline{x} \longmapsto \hat{y} = \mathcal{S}(\underline{x}) \end{aligned} \tag{2.30}$$

2.3.2.2 *Support vector regression model*

The basic aim of SVR is to find the function $\mathcal{S}$ that has at most ε deviations from each of the training input vectors. For the linear case, the estimation of $\mathcal{S}$ as a new point $\underline{s}$ is given by

$$\mathcal{S}(\underline{s}) = \langle \underline{w} \cdot \underline{s} \rangle + b \tag{2.31}$$

where $\langle \underline{a} \cdot \underline{b} \rangle$ is the dot product between vectors $\underline{a}$ and $\underline{b}$.

Moreover, we would like $\mathcal{S}$ to be as flat as possible, where flatness means there is a small value for $\underline{w}$. This second objective is important in the formulation of the following optimization problem relative to the construct of the SVR:

$$\begin{aligned} &\text{Minimize } \frac{1}{2} \left|\underline{w}\right|^2 \\ &\text{subject to } \begin{cases} y_i - \langle \underline{w} \cdot \underline{x}_i \rangle - b \leq \varepsilon \\ \langle \underline{w} \cdot \underline{x}_i \rangle + b - y_i \leq \varepsilon \end{cases} \end{aligned} \tag{2.32}$$

This solution is valuable under the assumption that a function $\mathcal{S}$ capable of estimating all pairs $(\underline{x}_i, y_i)$ with ε precision actually exists. To relax this constraint, slack variables η_i and η_i^* are defined, and they are meant to allow error for the following new formulation of the optimization problem:

$$\text{Minimize } \frac{1}{2} \left|\underline{w}\right|^2 + C \sum_{i=1}^{k} (\eta_i + \eta_i^*) \tag{2.33}$$

$$\text{subject to } \begin{cases} y_i - \langle \underline{w} \cdot \underline{x}_i \rangle - b \leq \varepsilon + \eta_i \\ \langle \underline{w} \cdot \underline{x}_i \rangle + b - y_i \leq \varepsilon + \eta_i^* \\ \eta_i, \eta_i^* \geq 0 \end{cases}$$

where $C > 0$ is a coefficient determining the balance between the flatness and the degree to which a gap larger than η_i (positively) or η_i^* (negatively) are tolerated. This type of SVR is referred to as the ε-insensitive loss function (Vapnik, et al., 1997). The estimation is then performed from a set of so-called support vectors whose deviation is smaller than η_i or η_i^*. Figure 2.12 show an example of SVR for a linear case that incorporates slack variables.

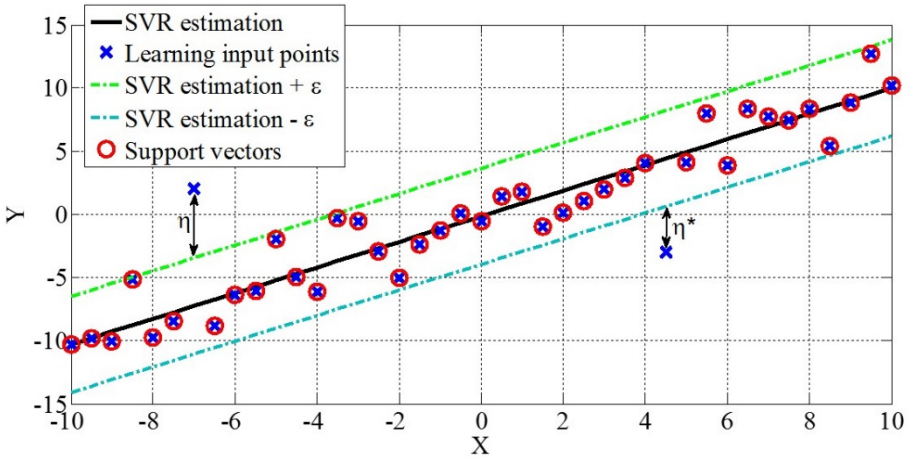


Figure 2.12 *SVR estimation for a linear case that includes slack variables.*

The idea of SVR is then to estimate the output of function $\mathcal{S}$ as a weighted linear combination of a scalar product between support vectors and the point where estimation is demanded (Smola, et al., 2004). In non-linear problems, a kernel trick is used to transpose the problem into a higher-dimension space such that it becomes linear. For details on the theoretical aspects of this process, please refer to (Smola, et al., 2004) and the references in it. As proposed in (An, et al., 2007), the resolution of SVR is achieved by the use of least squares estimation[18]. Finally, the estimation $\mathcal{S}(\underline{s})$ at point $\underline{s}$ can be expressed as follows:

$$\mathcal{S}(\underline{s}) = \sum_{i=1}^{k} \alpha_i \kappa(\underline{x}_i, \underline{s}) \tag{2.34}$$

where $\underline{x}_i$ are the support vectors, κ is the kernel function and α_i are the regression coefficients. A kernel function κ can be written as follows:

$$\kappa(\underline{x}_i, \underline{x}_j) = k\left(\underline{\xi}, \underline{x}_i, \underline{x}_j\right) \tag{2.35}$$

where $\underline{\xi}$ is the hyperparameters vector that defines the shape of the kernel function. Some examples of kernel functions from (Hsu, et al., 2003) are given in Table 2.3.

[18] A toolbox for least square SVR is available for Matlab™, and it is named LS-SVMlab.

Correlation Type	Configuration of $\underline{\xi}_d$	$k(\underline{\xi}, \underline{x}_i, \underline{x}_j)$
Linear	-	$\underline{x}_i{}^T \underline{x}_j$
Radial basis function (RBF)	$\underline{\xi}_d = \gamma$	$\exp\left(-\gamma \left\| \underline{x}_i{}^T \underline{x}_j \right\|^2\right), \gamma > 0$
Sigmoid	$\underline{\xi}_d = [\gamma \ r]^T$	$\tanh(\gamma \underline{x}_i{}^T \underline{x}_j + r)$
Polynomial	$\underline{\xi}_d = [\gamma \ r \ d]^T$	$(\gamma \underline{x}_i{}^T \underline{x}_j + r)^d, \gamma > 0$

Table 2.3 *Different types of kernel functions for SVR.*

For the set of learning points $\underline{x}_1, \ldots, \underline{x}_k$, the following matrix $\boldsymbol{G}$ is defined:

$$\boldsymbol{G} = \begin{vmatrix} k\left(\underline{\xi}, \underline{x}_1, \underline{x}_1\right) & \cdots & k\left(\underline{\xi}, \underline{x}_1, \underline{x}_k\right) \\ \vdots & \ddots & \vdots \\ k\left(\underline{\xi}, \underline{x}_k, \underline{x}_1\right) & \cdots & k\left(\underline{\xi}, \underline{x}_k, \underline{x}_k\right) \end{vmatrix} \in \mathbb{R}^{k \times k} \tag{2.36}$$

Moreover, for an input vector $\underline{s} = [s_1 \ \cdots \ s_n]^{\boldsymbol{t}}$, the vector $\boldsymbol{v}$ is defined as follows:

$$\underline{v}(\underline{s}) = \left[k(\underline{\xi}, \underline{x}_1, \underline{s}) \ \cdots \ k(\underline{\xi}, \underline{x}_k, \underline{s})\right]^T \tag{2.37}$$

Then, the estimation of the model outputs for input $\underline{s}$ via SVR can be written as follows:

$$\mathcal{S}(\underline{s}) = \underline{v}(\underline{s})^T \underline{\alpha} \tag{2.38}$$

where $\boldsymbol{\alpha}$ is estimated via regular least square estimation from the learning points:

$$\underline{\alpha} = (\boldsymbol{G}^{\boldsymbol{t}} \boldsymbol{G})^{-1} \boldsymbol{G}^{\boldsymbol{t}} \underline{y} \tag{2.39}$$

In the above formula, $\underline{y} = [y_1 \ \cdots \ y_n]^T$ is the vector of the responses of model $\mathcal{F}$ at the support vector, *i.e.*, the learning points for the present application. An example of SVR estimation for a nonlinear function from an RBF kernel with $\gamma = 5$ is presented in Figure 2.13.

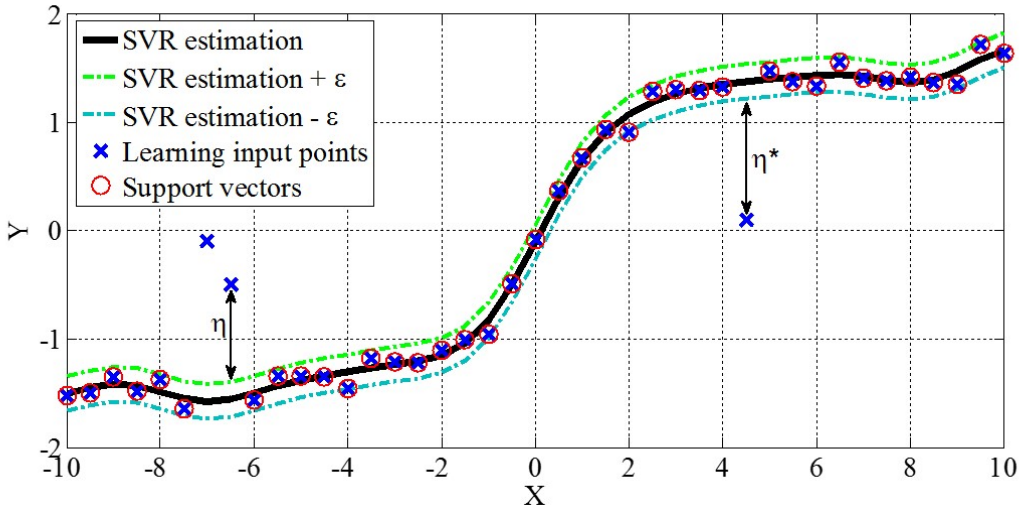


Figure 2.13 *SVR estimation for a nonlinear that includes slack variables.*

The advantage of SVR is that it is a nonlinear estimator that does not need *a priori* knowledge about the shape of the function. However, the main drawback of SVR is that it is not capable of making an

estimation beyond the boundaries of its learning samples. Consequently, for an efficient regression, the boundaries of the inputs must be defined properly and included in the learning samples. In this work, SVR is used for two applications: first, in the next subsection, we use it jointly with SA to estimate the standardization model for HIs (Lacaille, 2009); then, in the next chapter, we use it jointly with Kriging to build a surrogate model.

2.3.3 SA and SVR for the standardization of HIs

In this section, it is supposed that both the Morris method and the Sobol indices computations have been performed so that the standardization parameters have been identified. Notice that the standardization process concerns only the HIs.

The idea of standardization is to evaluate the SVR standardization models $\mathcal{S}^j$ that estimate the values of φ_j from the associated standardization parameters only. Then, the standardized values of the HIs are the residuals between the actual values and the estimated values. The actual value can be either the value obtained from the physics-based model during the design phases or the actual measured value during the operating phases. As the present chapter is dedicated to the development of the EMU in the design phases, the first case is considered. The SVR standardization models of the HIs are expressed as follows:

$$\hat{\varphi}_j^{svr} = \mathcal{S}^j(\underline{\pi}),\ j = 1, \dots, h \quad \text{with} \quad \underline{\pi} = \begin{vmatrix} \underline{\rho}_j^{ns} \\ \underline{\rho}_j^{ls} \end{vmatrix} \tag{2.40}$$

where $\underline{\rho}_j^{ns} = \left[\rho_{j,1}^{ns} \quad \cdots \quad \rho_{j,a_j}^{ns}\right]^T$, $\underline{\rho}_j^{ls} = \left[\rho_{j,1}^{ls} \quad \cdots \quad \rho_{j,b_j}^{ls}\right]^T$ and a_j, b_j are the numbers of, respectively, nonlinear and linear standardization parameters for the j^{th} HI. The standardized value φ_j^{sTd} of φ_j is then computed as the residual between φ_j and its estimation from the SVR standardization model:

$$\varphi_j^{sTd} = \varphi_j - \hat{\varphi}_j^{svr}, \qquad j = 1, \dots, h \tag{2.41}$$

Even if the SVR is capable of estimating models with multiple inputs, we decided to use a combination of single-dimension input SVRs. The goal is to model only the first-order effects of each standardization parameter on the HIs. This choice is motivated by the fact that higher-order effects due to the interactions between inputs should not be included in the model. Moreover, it is interesting and appreciated in an industrial environment to capture the expected behavior of the parameters independently to derive a better physical understanding of the system. The mentioned individual SVR models are written $\mathcal{S}_i^j, (i,j) \in [\![1; c_j]\!] \times [\![1; h]\!]$, where $c_j = a_j + b_j$. Then, the estimated values $\hat{\varphi}_j^{svr}$ are the sums of the estimations from the individual models:

$$\hat{\varphi}_j^{svr} = \mathcal{S}_1^j(\rho_{j1}^{ns}) + \dots + \mathcal{S}_{a_j}^j\left(\rho_{ja_j}^{ns}\right) + \mathcal{S}_{a_j+1}^j(\rho_{j1}^{ls}) + \dots + \mathcal{S}_{c_j}^j\left(\rho_{jb_j}^{ls}\right), j = 1, \dots, h \tag{2.42}$$

For the construction of individual SVR models $\mathcal{S}_i^j$, the function to be estimated is $\mathcal{M}_{\boldsymbol{U}}^{i,j}$, which is defined as the restriction of $\mathcal{M}_{\boldsymbol{U}}^j$ to the i^{th} standardization parameter with the other parameters fixed to their nominal values:

$$\begin{aligned} \mathcal{M}_{\boldsymbol{U}}^{i,j} &: \mathbb{R} \longrightarrow \mathbb{R} \\ \underline{\pi}_i &\longmapsto \mathcal{M}_{\boldsymbol{U}}^j\left(\underline{\pi}_i, \underline{\rho}^*\right) \end{aligned} \tag{2.43}$$

where $\underline{\rho}^*$ includes all of the parameters except $\underline{\pi}_i$, which are fixed at their nominal values. For each standardization parameter i, the learning vector $\underline{x}_i$ is written as follows:

$$\underline{x}_i = \left[x_i^1 \ \cdots \ x_i^{l_i}\right]^T \tag{2.44}$$

where l_i is the number of points of the learning vector and lb_i, ub_i are, respectively, the upper and lower bounds of the standardization parameter i. In the case of non-uniform PDFs, it is proposed to define lb_i and ub_i as, respectively, the 0.1 percent and 99.9 percent quantiles. Note that because the SVR is relevant only between its lower and upper learning points, lb_i and ub_i must belong to the learning DOE, so that $\left(x_i^1, x_i^{l_i}\right) = (lb_i, ub_i)$. According to subsection 2.3.2.2, The SVR estimation $\mathcal{S}_i^j$ at a new point s is expressed as follows:

$$\mathcal{S}_i^j(s) = \left[k_i(\xi_i, x_i^1, s) \quad \cdots \quad k_i(\xi_i, x_i^{l_i}, s)\right]\underline{\alpha}_{ij} \tag{2.45}$$

In the above formula, k_i is the kernel function, ξ_i is the hyperparameters vector and $\underline{\alpha}_{ij}$ is the vector of regression coefficients, which is computed via the following least square estimation:

$$\underline{\alpha}_{ij} = \left(\boldsymbol{G_{ij}}^t \boldsymbol{G_{ij}}\right)^{-1} \boldsymbol{G_{ij}}^t \underline{y}_{ij} \tag{2.46}$$

where $\underline{y}_{ij}$ is the vector of the $\mathcal{M}_U^{i,j}$ values at learning points x_i and $\boldsymbol{G_{ij}}$ is the matrix defined as follows:

$$\boldsymbol{G_{ij}} = \begin{vmatrix} k_i(\xi_i, x_i^1, x_i^1) & \cdots & k_i(\xi_i, x_i^1, x_i^{l_i}) \\ \vdots & \ddots & \vdots \\ k_i(\xi_i, x_i^{l_i}, x_i^1) & \cdots & k_i(\xi_i, x_i^{l_i}, x_i^{l_i}) \end{vmatrix} \tag{2.47}$$

The global SVR standardization model for the j^{th} HI is finally expressed as follows:

$$\hat{\varphi}_j^{svr}(\underline{s}) = \sum_{i=1,..,c_j} \left[k_i(\xi_i, x_i^1, s_i) \quad \cdots \quad k_i(\xi_i, x_i^{l_i}, s_i)\right]\underline{\alpha}_{ij} \tag{2.48}$$

The selection of learning points is supervised by the result of the Morris method and the identification of nonlinear parameters. Thus, for linear standardization parameters, a few sampling points and a linear kernel are selected, whereas for nonlinear ones, a larger number of sampling points and an RBF kernel are chosen. Because the model is deterministic, all of the vectors of the learning sample are support vectors. The final scheme of the SVR standardization model's construction is presented in Figure 2.14.

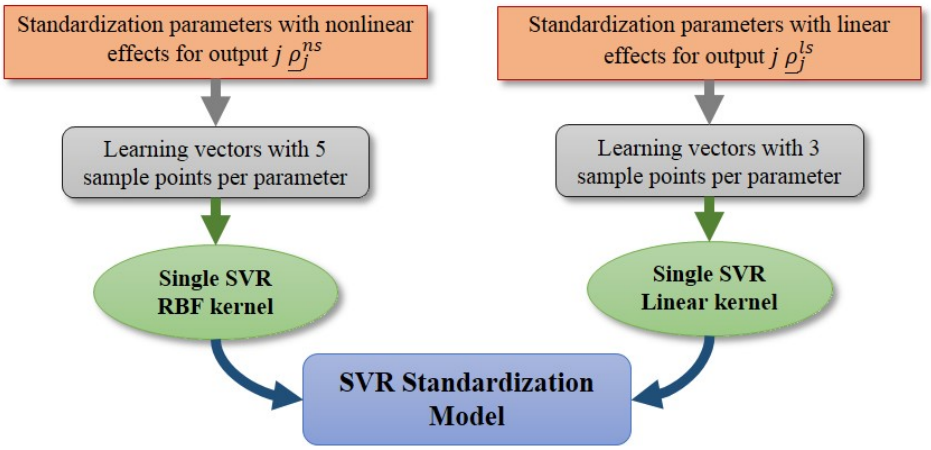


Figure 2.14 *Construction of the SVR standardization model.*

2.4 Virtual implementation and validation of the HIs

In this section, both the virtual implementation and the validation of the HIs are addressed. Whereas the virtual implementation is based on uncertainties propagation, the validation is based on original performance metrics aimed at evaluating the ability of the HIs set to detect abnormalities, identify precursors, localize LRUs and prognosticate compliant service threats.

2.4.1 Definition of numerical key performance indicators

The purpose of this subsection is to propose some performance metrics termed numerical key performance indicators (**NKPIs**). Their purpose is to quantify the potential of the set of HIs for meeting the specifications relative to detection, identification, localization and prognostics. In the scientific community, the definition of metrics for validating PHM is not a novel idea. For example, the recent works of Saxena (Saxena, et al., 2008), Roemer (Roemer, et al., 2007) or Dzakowic (Dzakowic, et al., 2007) can be cited. However, these metrics are computed after the entry into service and are systematically dedicated to prognostication. In contrast, in the IDPHM framework, metrics are needed as soon as the design stages to validate the potential of the HIs set not only for prognostication but also for detection, identification and localization. Therefore, it has been decided to define new metrics, which are termed numerical key performance indicators (NKPIs), and these indicators are specific to IDPHM requirements. The main particularity of these NKPIs is that they can be computed during the design phases. Indeed, their calculation only needs HIs data for healthy and faulty conditions, which can be obtained via numerical simulations.

2.4.1.1 *Receiver Operating Characteristics Curves*

NKPIs are defined from receiver operating characteristics (**ROC**) curves, which are a well-known graphical tool in signal detection theory to illustrate the performance of a binary classifier (Wickens, 2002). ROC curves are created by plotting the rate of False Positives (**FP**) versus the rate of True Positives (**TP**) for varying discrimination thresholds. In terms of conditional probabilities, FP is $P(DeTecTion|HealThy)$ and TP is $P(DeTecTion|Degraded)$. In the present case, ROC curves are drawn from two distributions of a given HI. Consider the i^{th} HI: the first distribution always reflects the nominal state of the system and is denoted T_i^0, and the second distribution reflects a degraded state of the system resulting from degradation mode j with intensity k. This second distribution is denoted $T_{i,j}^k$. Empirical distribution functions are used to represent the stochastic data. The following Figure 2.15 presents an example of a ROC curve that was computed for a random selection of 2000 points following normal laws of respective means 3 and 5 and the same standard deviation 2.

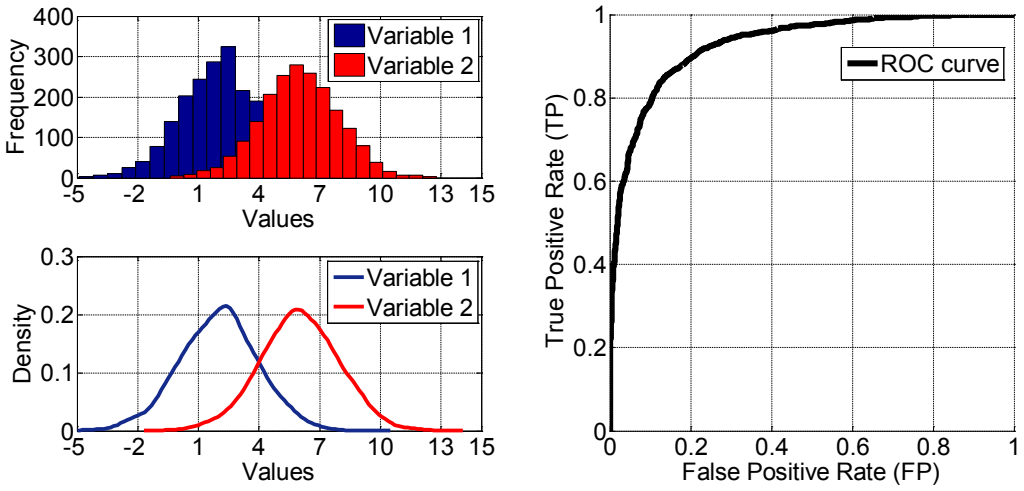


Figure 2.15 *An example of a ROC curve (right) drawn from two distributions defined by their histograms (top-left) and empirical density functions (bottom-left).*

2.4.1.2 *NKPIs and criteria for detection*

For a given degradation mode, global detectability (**GD**) quantifies the potential of an HI for the detection of this degradation mode regardless of the specifications of TP and FP. It is defined as a function calculated from the Area under the curve (**AUC**) (Bradley, 1997). The closer the GD's value is to one, the higher the detection potential is. In fact, GD is equivalent to the Gini coefficient, which is a well-known tool to measure income inequality within a country (Gini, 1997). For any two distributions T and T', the global detectability is computed as follows:

$$GD(T, T') = 2 \times AUC(ROC(T, T')) - 1 \qquad \textbf{(2.49)}$$

where $ROC(.)$ is the function plotting the ROC curve of two discrete distributions and $AUC(.)$ is the function computing the AUC of a ROC curve. GD is computed for couples $\left(T_i^0, T_{i,j}^1\right)$, $(i,j) \in [\![1; \mathrm{h}]\!] \times [\![1; \mathrm{d}]\!]$ where h is the number of HIs and d is the number of DEMs. Note that $T_{i,j}^1$ is computed for the maximal value of the degradation mode intensity. For a given degradation mode, the global detectability matrix $\boldsymbol{GDx}$ is defined as the matrix whose coefficients are the values of GD for every type of HI. For example, the global detectability matrix of degradation mode j is computed as follows:

$$\boldsymbol{GDx} = \begin{vmatrix} GD\left(T_1^0, T_{1,1}^1\right) & \dots & GD\left(T_h^0, T_{h,1}^1\right) \\ \vdots & \ddots & \vdots \\ GD\left(T_1^0, T_{1,d}^1\right) & \dots & GD\left(T_h^0, T_{h,d}^1\right) \end{vmatrix} \in [0;1]^{d \times h} \qquad \textbf{(2.50)}$$

In the framework of IDPHM, some specifications relative to the required minimal TP and maximal FP must be provided to estimate the quality of the HIs for a given detection problem. The minimal TP and maximal FP are denoted TP_{SPEC} and FP_{SPEC}, respectively. For a given ROC curve, the compliance point is defined as the point of coordinates (FP_{SPEC}, TP_{SPEC}), as shown in Figure 2.16.

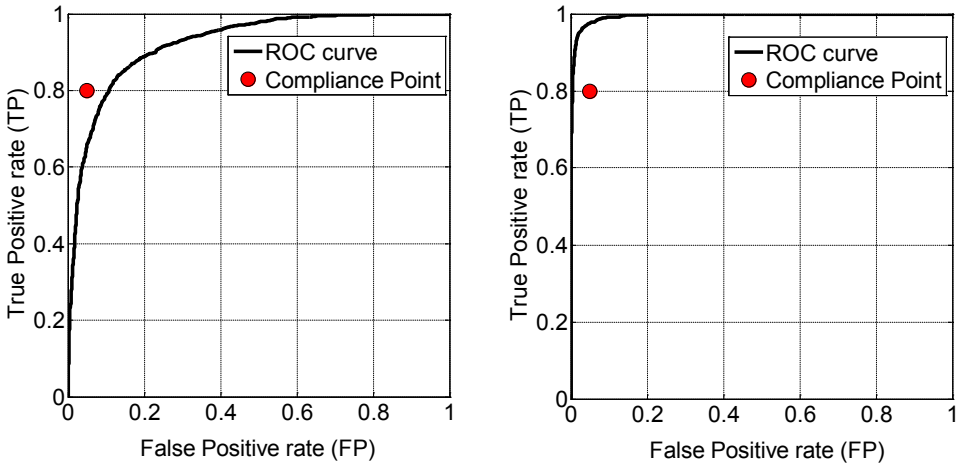


Figure 2.16 *The compliance Point and ROC curve for a non-compliant HI (left) and a compliant HI (right).*

The compliant detectability (**CD**) is defined as follows:

$$CD(T,T') = \begin{cases} 1 \; if \; ROC(T,T') \; is \; above \; the \; compliance \; point \\ 0 \; if \; ROC(T,T') \; is \; under \; the \; compliance \; point \end{cases} \quad \textbf{(2.51)}$$

If the specifications on FP are very restrictive, it is hard to see the compliance point on the curve. In this case, it is possible to use the semi-logarithmic ROC curve with a logarithmic scale in the abscissa for the FP, which provides more clarity to the curve. The purpose of CD is to give information about the potential of the set of HIs for detecting each degradation mode with respect to the specifications. This potential is evaluated for an intensity equal to 1. Therefore, CD is computed for each pair $\left(T_i^0, T_{i,j}^1\right)$, $(i,j) \in [\![1;\mathrm{h}]\!] \times [\![1;\mathrm{d}]\!]$ to construct the following CD matrix $\boldsymbol{CDx}$:

$$\boldsymbol{CDx} = \begin{vmatrix} CD\left(T_1^0, T_{1,1}^1\right) & \dots & CD\left(T_h^0, T_{h,1}^1\right) \\ \vdots & \ddots & \vdots \\ CD\left(T_1^0, T_{1,d}^1\right) & \dots & CD\left(T_h^0, T_{h,d}^1\right) \end{vmatrix} \in \{0,1\}^{d \times h} \quad \textbf{(2.52)}$$

It is now possible to propose a definition for the **a priori detectability** of a degradation mode and for the **a priori detection relevance** of health indicators.

DEFINITION 44 (***A priori*** **detectability**). *A degradation mode is a priori detectable if its associated line in the compliant detectability matrix is non-null.*

DEFINITION 45 (***A priori*** **detection relevance**). *A health indicator is a priori relevant for detection if its associated column in the compliant detectability matrix is non-null.*

$DTDEM_{\%}$ is defined as the ratio of *a priori* detectable TDEMs to the total number of TDEMs, and it is expressed as a percentage:

$$DTDEM_{\%} = \frac{\text{number of } a\ priori \text{ detectable TDEMs}}{\text{total number of TDEMs}} \times 100 \quad \textbf{(2.53)}$$

The set of HIs is validated for the detection task if the value of $DTDEM_{\%}$ is greater than the minimal specified one. At best, this percentage is equal to 100, but in practice, perfection is hardly reachable. Therefore, the specifications allow a margin of error, and they generally request 80% or 90%. If the $DHDEM_{\%}$ is under the specifications, it is necessary to define additional HIs or to modify the existing ones, for example, by improving their standardization.

$RDHI_{\%}$ is defined as the ratio of HIs that are *a priori* relevant to the detection to the total number of HIs, and it is also expressed as a percentage:

$$RDHI_{\%} = \frac{\text{number of } a\ priori \text{ detection relevant HIs}}{\text{total number of HIs}} \times 100 \quad \textbf{(2.54)}$$

The set of HIs is optimized for the detection task if the value of $RDHI_{\%}$ is equal to 100. In the contrary case, the non-relevant HIs can be withdrawn from the initial set, as they have no added value.

2.4.1.3 *NKPIs and criteria for identification*

First, we define the variation matrix $\boldsymbol{V}_k$ of intensity k as follows:

$$\boldsymbol{V}_k = \begin{vmatrix} s\left(m\left(T_{1,1}^k\right) - m\left(T_1^0\right)\right) GD\left(T_1^0, T_{1,1}^k\right) & \cdots & s\left(m\left(T_{h,1}^k\right) - m\left(T_h^0\right)\right) GD\left(T_h^0, T_{h,1}^k\right) \\ \vdots & \ddots & \vdots \\ s\left(m\left(T_{1,d}^k\right) - m\left(T_1^0\right)\right) GD\left(T_1^0, T_{1,d}^k\right) & \cdots & s\left(m\left(T_{h,d}^k\right) - m\left(T_h^0\right)\right) GD\left(T_h^0, T_{h,d}^k\right) \end{vmatrix} \in [-1;1]^{d\times h} \quad \textbf{(2.55)}$$

where $m(.)$ is the function computing the median of a distribution and $s(.)$ is the sign function. $\underline{v}_k^j$ is defined as the j^{th} row of $\boldsymbol{V}_k$, and it is the variation vector associated to degradation mode j for intensity k.

The global identifiability (**GI**) quantifies the potential of an HIs set for identification. We define the global identifiability GI as the ratio of the angular deviation between the variation vectors over the optimal angular deviation for identification, i.e., π rad or 180°. For a pair of degradation modes (j, q) of respective intensities (k, k'), GI is expressed as follows:

$$GI(j, q, k, k') = \frac{1}{\pi}\arccos\left(\frac{\langle \underline{v}_k^{j\,t} \cdot \underline{v}_{k'}^q \rangle}{\left\|\underline{v}_k^j\right\|_s \left\|\underline{v}_{k'}^q\right\|_s}\right) \quad \textbf{(2.56)}$$

The global identifiability is computed for each pair of degradation modes $(j, q) \in [\![1; \mathrm{d}]\!]^2$ with intensities k and k' equal to 1 to construct the following global identifiability symmetric matrix $\boldsymbol{GIx}$.

$$\boldsymbol{GIx} = \begin{vmatrix} GI(1,1,1,1) & \ldots & GI(1,d,1,1) \\ \vdots & \ddots & \vdots \\ GI(d,1,1,1) & \ldots & GI(d,d,1,1) \end{vmatrix} \in [0;1]^{d\times d} \quad \textbf{(2.57)}$$

For the development of PHM systems, some specifications relative to the required minimal angle between the variation vectors must be provided to estimate the quality of the HIs for a given problem of identification. This minimal angle is denoted α_{SPEC}, and it will also be applicable to localization. For a pair of degradation modes (j, q) of respective intensities (k, k'), the compliant identifiability (**CI**) is defined as follows:

$$CI(j, q, k, k') = \begin{cases} 1\ if\ GI(j,q,k,k') \geq \alpha_{SPEC} \\ 0\ if\ GI(j,q,k,k') < \alpha_{SPEC} \end{cases} \quad \textbf{(2.58)}$$

The compliant identifiability is computed for each pair of degradation modes $(j, q) \in [\![1; \mathrm{d}]\!]^2$ with k and l equal to 1 to construct the compliant identifiability symmetric matrix $\boldsymbol{CIx}$.

$$\boldsymbol{CIx} = \begin{vmatrix} CI(1,1,1,1) & \dots & CI(1,d,1,1) \\ \vdots & \ddots & \vdots \\ CI(d,1,1,1) & \dots & CI(d,d,1,1) \end{vmatrix} \in [0;1]^{d \times d} \quad \textbf{(2.59)}$$

It is now possible to propose a definition for the **a priori identifiability** of a degradation mode and for the **a priori identification relevance** of health indicators.

DEFINITION 46 (***A priori* identifiability**). *A degradation mode is a priori identifiable by a set of health indicators if its associated line in the compliant identifiability matrix has only non-zero values for its non-diagonal coefficients.*

DEFINITION 47 (***A priori* identification relevance**). *A health indicator h is a priori relevant for identification if the norm of $\boldsymbol{GIx}$ computed for the whole set of HIs is strictly superior to the norm of $\boldsymbol{GIx}$ computed for the set of HIs without h.*

$ITDEM_{\%}$ is defined as the ratio of *a priori* identifiable TDEMs among the total number of TDEMs, and it is expressed as a percentage:

$$ITDEM_{\%} = \frac{\text{number of } a\ priori \text{ identifiable TDEMs}}{\text{total number of TDEMs}} \times 100 \quad \textbf{(2.60)}$$

Commonly, it is reasonable to specify a minimal value for $ITDEM_{\%}$ that is between 80% and 90%. Then, the set of HIs is validated for identification if $ITDEM_{\%}$ is superior to this value. In the contrary case, it is necessary to define additional HIs or to improve the existing ones.

$RIHI_{\%}$ is defined as the ratio of HIs that are *a priori* relevant to the identification process among the total number of HIs.

$$RIHI_{\%} = \frac{\text{number of } a\ priori \text{ identification relevant HIs}}{\text{total number of HIs}} \times 100 \quad \textbf{(2.61)}$$

The set of HIs is optimized for the identification task if the value of $RIHI_{\%}$ is equal to 100. In the contrary case, the non-relevant HIs can be withdrawn from the initial set, if they do not affect the detectability performances.

2.4.1.4 *NKPIs and criteria for localization*

Before introducing the localizability matrix, we recall that the LRU association matrix links each degradation mode to the LRU it belongs to. Furthermore, this matrix allows localization of the degraded LRU from the identified degradation mode. The LRU association matrix is defined as follows:

$$\boldsymbol{U} = \begin{vmatrix} u(1,1) & \dots & u(1,l) \\ \vdots & \ddots & \vdots \\ u(d,1) & \dots & u(d,l) \end{vmatrix} \in \{0;1\}^{d \times l} \quad \textbf{(2.62)}$$

where l is the number of LRUs composing the system and $u(j,r)$ is equal to 1 if the degradation mode j affects LRU r and equal to 0 otherwise.

The global localizability matrix $\boldsymbol{GLx}$ is linked to the compliant localizability matrix $\boldsymbol{CIx}$ by the LRU association matrix $\boldsymbol{U}$ through the following relation:

$$\boldsymbol{GLx} = \boldsymbol{U^T CIx U} \in [0;1]^{l \times l} \quad \textbf{(2.63)}$$

For two LRUs a and b, the corresponding coefficient of the $\boldsymbol{GLx}$ matrix gives an integer representing the number of DEM couples between the two LRUs that are *a priori* identifiable. For a pair of LRUs (a, b), the compliant localizability (**CL**) is defined as follows:

$$CL(a,b) = \begin{cases} \begin{cases} 1 \; if \; \boldsymbol{GLx}(a,b) = \boldsymbol{Nb}(a,b) \\ 0 \; if \; \boldsymbol{GLx}(a,b) < \boldsymbol{Nb}(a,b) \end{cases} & if \; a \neq b \\ 0 \; if \; a = b \end{cases} \quad \textbf{(2.64)}$$

where $\boldsymbol{Nb}$ is the matrix giving the number of DEM couples between two LRUs. This matrix is defined as follows:

$$\boldsymbol{Nb} = \begin{vmatrix} nb(1)\,nb(1) & \dots & nb(1)\,nb(l) \\ \vdots & \ddots & \vdots \\ nb(l)\,nb(1) & \dots & nb(l)\,nb(l) \end{vmatrix} \in \mathbb{N}^{l \times l} \quad \textbf{(2.65)}$$

with $nb(a)$ being the function giving the number of DEMs affecting LRU a. The compliant localizability is computed for each couple $(a, b) \in [\![1; l]\!]^2$ of LRUs to build the compliant localizability symmetric matrix $\boldsymbol{CLx}$.

$$\boldsymbol{CLx} = \begin{vmatrix} CL(1,1) & \dots & CL(1,l) \\ \vdots & \ddots & \vdots \\ CL(l,1) & \dots & CL(l,l) \end{vmatrix} \in [0;1]^{d \times d} \quad \textbf{(2.66)}$$

Note that the coefficients of the diagonal of $\boldsymbol{CLx}$ are null by construction. It is now possible to propose a definition for the **a priori localizability** of an LRU and for the **a priori localization relevance** of health indicators.

DEFINITION 48 (***A priori* localizability**). *A LRU is a priori localizable by a set of health indicators if its associated line in the compliant localizability matrix has only non-zero values for its non-diagonal coefficients.*

DEFINITION 49 (***A priori* localization relevance**). *A health indicator h is a priori relevant for localization if the norm of $\boldsymbol{CLx}$ computed for the whole set of HIs is strictly superior to the norm of $\boldsymbol{CLx}$ computed for the set of HIs without h.*

$LLRU_{\%}$ is defined as the ratio of *a priori* localizable LRUs among the total number of LRUs. It is expressed as a percentage:

$$LLRU_{\%} = \frac{\text{number of } a\ priori \text{ localizable LRUs}}{\text{total number of LRUs}} \times 100 \quad \textbf{(2.67)}$$

The set of HIs is validated for the localization task if the value of $LLRU_{\%}$ is greater than the minimal specified one. If $LLRU_{\%}$ is under the specifications, it is necessary to modify the HIs set.

$RLHI_{\%}$ is defined as the ratio of HIs that are *a priori* relevant to the localization among the total number of HIs.

$$RLHI_{\%} = \frac{\text{number of } a\ priori \text{ localization relevant HIs}}{\text{total number of HIs}} \times 100 \quad \textbf{(2.68)}$$

The set of HIs is optimized for the localization task if the value of $RLHI_{\%}$ is equal to 100. In the contrary case, the non-relevant HIs can be withdrawn from the initial set if they do not affect the detectability or the identifiability processes' performances.

2.4.1.5 *NKPIs and criteria for prognostic*

Before introducing the localizability matrix, the CST association matrix is defined as the matrix that links each DEM to the CSTs it can possibly cause. The CST association matrix is defined as follows:

$$\boldsymbol{C} = \begin{vmatrix} c(1,1) & \dots & c(1,w) \\ \vdots & \ddots & \vdots \\ c(d,1) & \dots & c(d,w) \end{vmatrix} \in \{0;1\}^{d \times w} \quad \textbf{(2.69)}$$

where w is the number of CSTs affecting the system and $c(j,z)$ is equal to 1 if the degradation mode j can cause the CST z and equal to 0 otherwise.

It is also necessary to define the notion of minimal detectable intensity (**MDI**). For a given degradation mode, the MDI is defined as follows:

DEFINITION 50 (**Minimal detectable intensity**). *The minimal detectable intensity (**MDI**) of a degradation mode is the minimal value of the intensity for which at least one of the HIs has a compliant detectability equal to 1.*

For a degradation mode j, the MDI is written MDI^j. To find the MDIs, the CD is computed for pairs $\left(T_i^0, T_{i,j}^k\right)$, $(i,j,k) \in [\![1;\mathrm{h}]\!] \times [\![1;\mathrm{d}]\!] \times \mathbb{R}$ where h is the number of HIs, d is the number of degradation modes, and k is the value of the degradation mode's intensity. The vector of intensities $\underline{i}$ is defined as a vector with coefficients of growing values ranging from 0 to the upper bound of the degradation parameter. The MDI of the degradation mode j for a vector of intensities $\underline{i}$ is computed as follows:

$$MDI^j = \min_{\substack{i=1,\dots,h \\ k \in [\![1;s]\!]}} \left\{ k / CD\left(T_i^0, T_{i,j}^{\underline{i}(k)}\right) = 1 \right\} \quad \textbf{(2.70)}$$

where s is the number of coefficients of vector $\underline{i}$ and $\underline{i}(k)$ is the k^{th} coefficient of $\underline{i}$. Then, the detection margin vector $\underline{\Delta D}$ is equal to:

$$\underline{\Delta D} = |\delta D(1) \quad \dots \quad \delta D(d)|^T \in [0;1]^d \quad \textbf{(2.71)}$$

with each coefficient $\delta D(j)$ defined for a degradation mode $j \in [\![1;\mathrm{d}]\!]$ as follows:

$$\delta D(j) = 1 - MDI^j \quad \textbf{(2.72)}$$

An example of a detection margin computation with respect to the minimal detectable intensity is given in Figure 2.17.

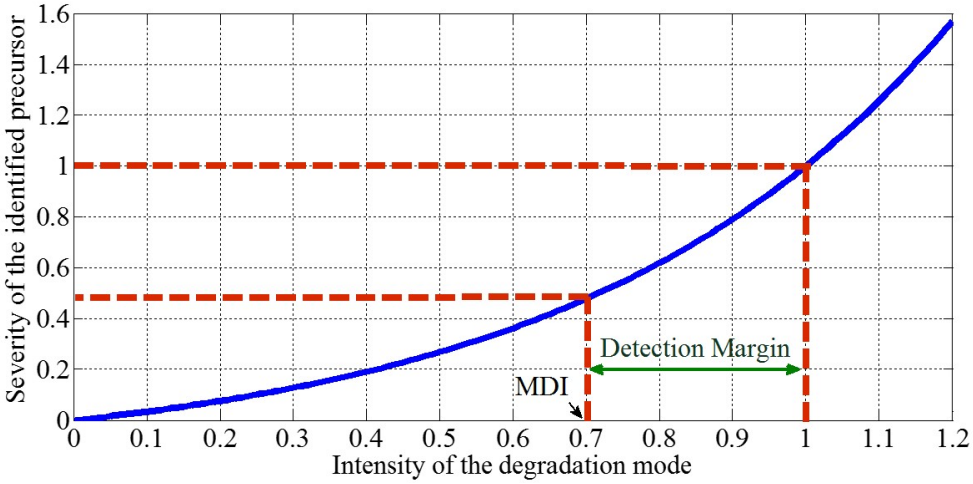


Figure 2.17 *The detection margin and the minimal detectable intensity.*

For a given degradation mode, the minimal identifiable intensity is defined as follows:

DEFINITION 51 (**Minimal identifiable intensity**). *The minimal identifiable intensity (**MII**) of a degradation mode is the minimal value of the intensity for which the CI is equal to 1.*

For degradation mode j, the MII is written MII^j. To calculate the MIIs, the CI is computed for pairs $\left(T_{i,j}^k, T_{i',j'}^{k'}\right)$, $(i, i', j, j', k, k') \in [\![1; \mathrm{h}]\!]^2 \times [\![1; \mathrm{d}]\!]^2 \times \mathbb{R}^2$. The MII of degradation mode j for a vector of intensities $\underline{i}$ is computed as follows:

$$MII^j = \min_{k \in [\![1;s]\!]} \left\{ k / \forall q \in [\![1; \mathrm{d}]\!], q \neq j, CI(j, q, \underline{i}(k), \underline{i}(k)) = 1 \right\} \quad \textbf{(2.73)}$$

Then, the identification margin vector $\underline{\Delta I}$ is equal to:

$$\underline{\Delta I} = |\delta I(1) \quad \dots \quad \delta I(d)|^{\boldsymbol{T}} \in [0; 1]^d \quad \textbf{(2.74)}$$

with each coefficient $\delta I(j)$ defined for a degradation mode j $\in [\![1; \mathrm{d}]\!]$ as follows:

$$\delta I(j) = 1 - MII^j \quad \textbf{(2.75)}$$

For a given degradation mode, the minimal localizable intensity is defined as follows:

DEFINITION 52 (**Minimal localizable intensity**). *The minimal localizable intensity (**MLI**) of a degradation mode is the minimal value of the intensity for which the compliant localizability of its home LRU is equal to 1.*

For degradation mode j, the MLI is written MLI^j. To calculate the MLIs, the CL is computed for pairs $\left(T_{i,j}^k, T_{i,j}^k\right)$, $(i, j, k) \in [\![1; \mathrm{h}]\!] \times [\![1; \mathrm{d}]\!] \times [0; 1]$. Supposing that the DEM j belongs to LRU a, its MLI for a vector of intensities $\underline{i}$ is computed as follows:

$$MLI^j = \min_{k \in [\![1;s]\!]} \left\{ k / \forall b \in [\![1; \mathrm{l}]\!], b \neq a, \boldsymbol{L}_{\underline{i}(\boldsymbol{k})}(a, b) = \boldsymbol{Nb}(a, b) \right\} \quad \textbf{(2.76)}$$

where the matrix $\boldsymbol{L_k}$ is defined as follows:

$$\boldsymbol{L_k} = \boldsymbol{U}^{\boldsymbol{T}} \begin{vmatrix} CI(1,1,k,k) & \dots & CI(1,d,k,k) \\ \vdots & \ddots & \vdots \\ CI(d,1,k,k) & \dots & CI(d,d,k,k) \end{vmatrix} \boldsymbol{U} \in [0; 1]^{l \times l} \quad \textbf{(2.77)}$$

Then, the localization margin vector $\underline{\Delta L}$ is equal to

$$\underline{\Delta L} = |\delta L(1) \quad \dots \quad \delta L(d)|^{\boldsymbol{T}} \in [0;1]^d \tag{2.78}$$

with each coefficient $\delta L(j)$ defined for a degradation mode j ∈ ⟦1; d⟧ in this way:

$$\delta L(j) = 1 - MLI^j \tag{2.79}$$

Then, the prognosticability P of a DEM j is defined as follows:

$$P(j) = \begin{cases} 1 \; if \; \delta D(j) > 0 \; and \; \delta I(j) > 0 \; and \; \delta L(j) > 0 \\ \\ 0 \; if \; \delta D(j) = 0 \; or \; \delta I(j) = 0 \; or \; \delta L(j) = 0 \end{cases} \tag{2.80}$$

and the vector of prognosticability $\underline{p}$ is :

$$\underline{p} = |P(1) \quad \cdots \quad P(d)|^T \tag{2.81}$$

The number of prognosticable cause DEMs for each TCST $\underline{NP}$ is then given by:

$$\boldsymbol{NP} = \boldsymbol{C}^{\boldsymbol{T}}\underline{p} \tag{2.82}$$

and the vector of compliant prognosticability (**CP**), written $\underline{cpv}$, is computed as follows:

$$\underline{cpv}(z) = \begin{cases} 1 \; if \; \boldsymbol{NP}(z) = \boldsymbol{Ncst}(z) \\ \\ 0 \; if \; \boldsymbol{NP}(z) = \boldsymbol{Ncst}(z) \end{cases} \tag{2.83}$$

with $\boldsymbol{Ncst}(z)$ the total number of cause DEMs for the TCST z.

It is now possible to propose a definition for the **a priori prognosticability** of a TCST and for the **a priori prognostic relevance** of health indicators.

DEFINITION 53 (***A priori*** **prognosticability**). *A targeted compliant service threat is a priori prognosticable by a set of HIs if the value of its compliant prognosticability is equal to 1.*

DEFINITION 54 (***A priori*** **prognostic relevance**). *A health indicator h is a priori relevant for prognostic if the number of a priori prognosticable TCSTs computed with h is strictly superior to the number of a priori prognosticable TCSTs computed for the set of HIs without h.*

Note that the previous margins are defined in terms of the intensity. If the models of the temporal evolution of the intensities were available, these margins could be transformed to be expressed as functions of time, which would be more relevant for prognostics. However, this practice is currently not in use.

$PCST_{\%}$ is defined as the ratio of *a priori* prognosticable compliant service threats among the total number of compliant service threats. This quantity is expressed as follows:

$$PCST_{\%} = \frac{\text{number of prognosticable compliant service threats}}{\text{total number of compliant service threats}} \times 100 \tag{2.84}$$

The set of HIs is validated for the prognostic task if the value of $POT_{\%}$ is greater that the minimal specified one. If the $PCST_{\%}$ is under the specifications, it is necessary to modify the HI set.

$RPHI_{\%}$ is defined as the ratio of HIs that are a priori relevant to the prognostication among the total number of HIs.

$$RPHI_{\%} = \frac{\text{number of } a\ priori \text{ prognostic relevant HIs}}{\text{total number of HIs}} \times 100 \qquad \textbf{(2.85)}$$

The set of HIs is optimized for the prognostic task if the value of $RPHI_{\%}$ is equal to 100. In the contrary case, the non-relevant HIs can be withdrawn from the initial set if they do not affect the detectability, the identifiability or the localizability performances.

Finally, we describe the performance metrics for the validation of HIs for the four main tasks of the PHM. Two or three NKPIs are associated with each of the tasks from which the final criteria are computed, as summarized in Figure 2.18.

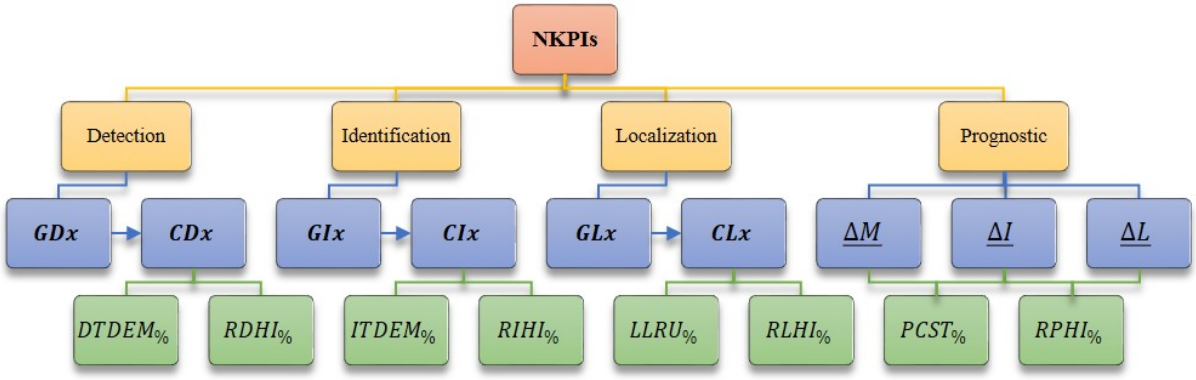


Figure 2.18 *A schematic overview of the NKPIs and the criteria for the validation of HIs.*

2.4.2 Virtual implementation

2.4.2.1 *Uncertainty propagation*

The virtual implementation is based on uncertainties propagation (De Rocquigny, et al., 2007), which consists of computing the distributions of HIs from a deterministic model by randomly sampling the influential parameters according to their PDFs. These distributions are computed for different values of $\boldsymbol{\delta}$ to calculate all of the necessary distributions for the validation of HIs. For example, if a degradation mode is modeled by the increase of the parameter δ_a, the values of the HIs are computed for growing values of δ_a up to the upper boundary of the parameter. Many tools are available for uncertainties propagation, but the most famous and proven one is Monte-Carlo simulation (Metropolis, et al., 1949). The procedure consists of replacing the deterministic vectors that are associated with influential parameters by random vectors. The model is then called several times with random selections of these vectors. We resume the model $\mathcal{M}_{\boldsymbol{U}}^{j}$ introduced in section 2.3.1.1:

$$\chi_j = \mathcal{M}_{\boldsymbol{U}}^{j}\left(\underline{\rho}_j^{np}, \underline{\rho}_j^{lp}, \underline{\rho}_j^{na}, \underline{\rho}_j^{la}, \underline{\rho}^{*}\right), \qquad j = 1, \dots, h+o \qquad \textbf{(2.86)}$$

For the uncertainty propagation, the distinction between linear and nonlinear parameters is not useful. The total sets of principal and ancillary parameters are written $\underline{\rho}_j^{p}$ and $\underline{\rho}_j^{a}$, respectively. By decomposing these parameters into context, epistemic and degradation ones, we obtain the following:

$$\chi_j = \mathcal{M}_{\boldsymbol{U}}^{j}\left(\underline{\gamma}^{p}{}_j, \underline{\gamma}^{a}{}_j, \underline{\lambda}_j^{p}, \underline{\lambda}_j^{a}, \underline{\delta}^{i}, \underline{\rho}^{*}\right), \qquad j = 1, \dots, h+o \qquad \textbf{(2.87)}$$

Note that for the degradation parameters, the distinction between principal and ancillary parameters is not useful. Uncertainties propagation consists of replacing the deterministic vectors $\underline{\gamma}_j^{p}, \underline{\gamma}_j^{a}, \underline{\lambda}_j^{p}, \underline{\lambda}_j^{a}$ by

random vectors $\underline{\Gamma}_j^p, \underline{\Gamma}_j^a, \underline{\Lambda}_j^p, \underline{\Lambda}_j^a$. In addition, $\underline{\delta}^i$ is fixed for a given Monte-Carlo run so that it remains a deterministic vector. Including the stochasticity in the model, the output vectors become:

$$\begin{aligned} \Phi_j &= \mathcal{M}_{\boldsymbol{U}}^j \left(\underline{\Gamma}_j^p, \underline{\Gamma}_j^a, \underline{\Lambda}_j^p, \underline{\Lambda}_j^a, \underline{\delta}^i, \underline{\rho}^*\right) \\ \Psi_j &= \mathcal{M}_{\boldsymbol{U}}^j \left(\underline{\Gamma}_j^p, \underline{\Gamma}_j^a, \underline{\Lambda}_j^p, \underline{\Lambda}_j^a, \underline{\delta}^i, \underline{\rho}^*\right) \end{aligned} \quad \textbf{(2.88)}$$

where Φ_j and Ψ_j are the random variable obtained via uncertainties propagation of the HIs and CSIs, respectively. If $\underline{\delta}^i = \underline{0}$, then the healthy distributions are computed.

2.4.2.2 *Computations of MLVs for DEMs*

For prognostic, the computation of the intensity necessitates knowing the MLV of the associated DEM. As mentioned in chapter 1, the MLV of a DEM c, which is written δ_c^{MLV}, is the minimum value of the set of MLVs for pairs (DEM c/CSI j), which is written $\delta_{c,j}^{MLV}$. For a degradation parameter c, the performance function $\mathcal{T}_c^j$ is defined as follows:

$$\begin{gathered} \mathcal{T}_c^j : \mathcal{E} \times \mathcal{C} \times \mathbb{R} \longrightarrow \mathbb{R} \\ (\underline{\Gamma}_{h+j}^p, \underline{\Gamma}_{h+j}^a, \underline{\Lambda}_{h+j}^p, \underline{\Lambda}_{h+j}^a, \delta) \mapsto \mathcal{M}_{\boldsymbol{U}}^{h+j} \left(\underline{\Gamma}_{h+j}^p, \underline{\Gamma}_{h+j}^a, \underline{\Lambda}_{h+j}^p, \underline{\Lambda}_{h+j}^a, \delta \underline{e}_c^{\mathcal{D}}, \underline{\rho}^*\right) \end{gathered} \quad \textbf{(2.89)}$$

This performance function characterizes the response of the system: a negative value means that a failure has occurred and a positive one implies that the system is safe in this configuration. The border between the negative and positive domains is called the limit state[19] (Echard, et al., 2011). Because of uncertainties, the value of the performance function as it is currently defined does not rely exclusively on the value of the degradation parameter; instead, it also relies on the values of $\underline{\Gamma}_{h+j}^p, \underline{\Gamma}_{h+j}^a, \underline{\Lambda}_{h+j}^p$ and $\underline{\Lambda}_{h+j}^p$. The limit value is defined as the set of values for which the limit state is reached, and the limit value is a random variable. To transform the problem into a deterministic type of problem, the median values are considered by fixing the epistemic and context parameters to their nominal values while varying δ. The median performance function $\mathcal{G}_c^j$ is defined as the value of $\mathcal{M}_{\boldsymbol{U}}^{h+j}$, and it is a function of δ with all of the other parameters at their nominal values:

$$\begin{gathered} \mathcal{G}_c^j : \mathbb{R} \longrightarrow \mathbb{R} \\ \delta \mapsto \mathcal{M}_{\boldsymbol{U}}^{h+j} \left(\underline{\gamma}^{i^0}, \underline{\lambda}^{i^0}, \delta \underline{e}_c^{\mathcal{D}}, \underline{\rho}^*\right) \end{gathered} \quad \textbf{(2.90)}$$

where $\underline{\gamma}^{i^0}$ and $\underline{\lambda}^{i^0}$ are the nominal vectors of the influent epistemic and context parameters, respectively. The MLV of DEM c for CSI j is finally found by solving the following equation:

$$\delta = \delta_{c,j}^{MLV} \Leftrightarrow \mathcal{G}_c^j(\delta) = 0 \quad \textbf{(2.91)}$$

Because the model $\mathcal{M}_{\boldsymbol{U}}^{h+i}$ is considered as a black box, SVR is used to estimate the median performance functions $\mathcal{G}_c^j$. Similarly to the standardization process, the estimation is of the individual input type, and sensitivity analysis results are used to perform a supervised selection of the number of learning points and the type of kernel function for each DEM. By analogy, the inputs are the influent degradation parameters and the outputs are the CSIs.

[19] The term limit state comes from the structural reliability field. It is defined as the condition of a structure beyond which it no longer fulfills the relevant design criteria.

For each degradation parameter c, the learning vector $\underline{x_c}$ is defined as $\underline{x_c} = \left[x_c^1 \cdots x_c^{l_c}\right]^T, i \in [\![1; d^u]\!]$, where d^u is the number of influent degradation parameters and l_c is the length of the vector. The lower and upper boundaries of the degradation parameter c, which are denoted lb_c and ub_c, respectively, must belong to the learning vector so that $\left(x_c^1, x_c^{l_c}\right) = (lb_c, ub_c)$. The SVR estimation at the degradation value δ of $\mathcal{G}_c^j$ is written as

$$\mathcal{G}_c^j(\delta) = \left[k_c(\underline{\xi_c}, x_c^1, \delta) \quad \cdots \quad k_c(\underline{\xi_c}, x_c^{l_c}, \delta)\right]\underline{\alpha_{cj}} \tag{2.92}$$

where k_c is the kernel function, $\underline{\xi_c}$ is the hyperparameters vector and $\underline{\alpha_{cj}}$ is the vector of regression coefficients computed via the following least square estimation:

$$\underline{\alpha_{cj}} = \left(\boldsymbol{H_{cj}}^{\boldsymbol{t}}\boldsymbol{H_{cj}}\right)^{-1}\boldsymbol{H_{cj}}^{\boldsymbol{t}}\underline{y_{cj}} \tag{2.93}$$

In the above equation, $\underline{y_{cj}}$ is the vector of the $\mathcal{G}_c^j$ values at learning points $\underline{x_c}$ and $\boldsymbol{H_{cj}}$ is the matrix defined as follows:

$$\boldsymbol{H_{cj}} = \begin{vmatrix} k_c(\underline{\xi_c}, x_c^1, x_c^1) & \cdots & k_c(\underline{\xi_c}, x_c^1, x_c^{l_c}) \\ \vdots & \ddots & \vdots \\ k_c(\underline{\xi_c}, x_c^{l_c}, x_c^1) & \cdots & k_c(\underline{\xi_c}, x_c^{l_c}, x_c^{l_c}) \end{vmatrix} \tag{2.94}$$

Typically, for degradation parameters with a high nonlinearity index, we choose the number of learning points equal to five and an RBF kernel, and for those with a low nonlinearity index, we choose three learning points and a linear kernel. For input parameters in common with those of the SVR standardization model estimation, the learning vectors used are the same so as not to perform redundant simulations. The matrix $\boldsymbol{MLV}$ is defined as the matrix whose coefficients are the $\delta_{c,j}^{MLV}, (c,j) \in [\![1; d^u]\!] \times [\![1; o]\!]$:

$$\boldsymbol{MLV} = \begin{vmatrix} \delta_{1,1}^{MLV} & \cdots & \delta_{1,o}^{MLV} \\ \vdots & \ddots & \vdots \\ \delta_{d^u,1}^{MLV} & \cdots & \delta_{d^u,o}^{MLV} \end{vmatrix} \in \mathbb{R}^{d^u \times o} \tag{2.95}$$

In cases where the equation $\mathcal{G}_c^j(\delta) = 0$ does not admit a solution on the interval (lb_c, ub_c), the MLV is defined as infinite, i.e., $\delta_{c,j}^{MLV} = \infty$. The MLV vector $\underline{mlv}$ containing the values δ_c^{MLV} is finally defined as follows:

$$\underline{mlv} = \begin{bmatrix} \min\limits_{j \in [\![1;o]\!]} \delta_{1,j}^{MLV} \\ \vdots \\ \min\limits_{j \in [\![1;o]\!]} \delta_{d^u,j}^{MLV} \end{bmatrix} \in \mathbb{R}^{d^u} \tag{2.96}$$

2.4.2.3 *Fleet model and individual model*

In many cases, PHM is not restricted to the monitoring and supervision of a single host system but is extended to a whole family of systems, which is called a fleet. Considering a fleet, uncertainties come from two sources: the randomness of contexts and the variability of configurations. Thus, the question is the following: When the precursors' database is learnt, is it better to consider systems as a family or as individuals? Actually, it depends on the initial variability of HIs because taking into account structural uncertainties unavoidably entails additional variability.

In the fleet model $\mathcal{MF}_{\boldsymbol{U}}^{j}$, both contexts and configurations are stochastic. It is defined as follows:

$$\begin{aligned} \Phi_j &= \mathcal{MF}_{\boldsymbol{U}}^{j}\left(\underline{\Gamma}_j^p, \underline{\Gamma}_j^a, \underline{\Lambda}_j^p, \underline{\Lambda}_j^a, \underline{\delta}^i, \underline{\rho}^*\right), \qquad j = 1, \ldots, h \\ \Psi_j &= \mathcal{MF}_{\boldsymbol{U}}^{j}\left(\underline{\Gamma}_j^p, \underline{\Gamma}_j^a, \underline{\Lambda}_j^p, \underline{\Lambda}_j^a, \underline{\delta}^i, \underline{\rho}^*\right), \qquad j = h+1, \ldots, o \end{aligned} \tag{2.97}$$

In the individual model $\mathcal{MI}_{\boldsymbol{U}}^{j}$, contexts are stochastic but configurations are set at their nominal deterministic value and incorporated in the fixed parameters vector $\underline{\rho}^*$. It is defined as follows:

$$\begin{aligned} \Phi_j &= \mathcal{MI}_{\boldsymbol{U}}^{j}\left(\underline{\Lambda}_j^p, \underline{\Lambda}_j^a, \underline{\delta}^i, \underline{\rho}^*\right), \qquad j = 1, \ldots, h \\ \Psi_j &= \mathcal{MI}_{\boldsymbol{U}}^{j}\left(\underline{\Lambda}_j^p, \underline{\Lambda}_j^a, \underline{\delta}^i, \underline{\rho}^*\right), \qquad j = h+1, \ldots, o \end{aligned} \tag{2.98}$$

The advantage of using an individual model is that the HIs distributions are narrower. The drawback is that it needs many more storage devices to perform individual monitoring per engine. During the validation step, the performances of the two approaches are evaluated. If the fleet system shows relevant performances, then it is privileged. However, if its performances are not satisfying, then individual models are used. Finally, the global scheme of the uncertainty propagation methodology is given in Figure 2.19.

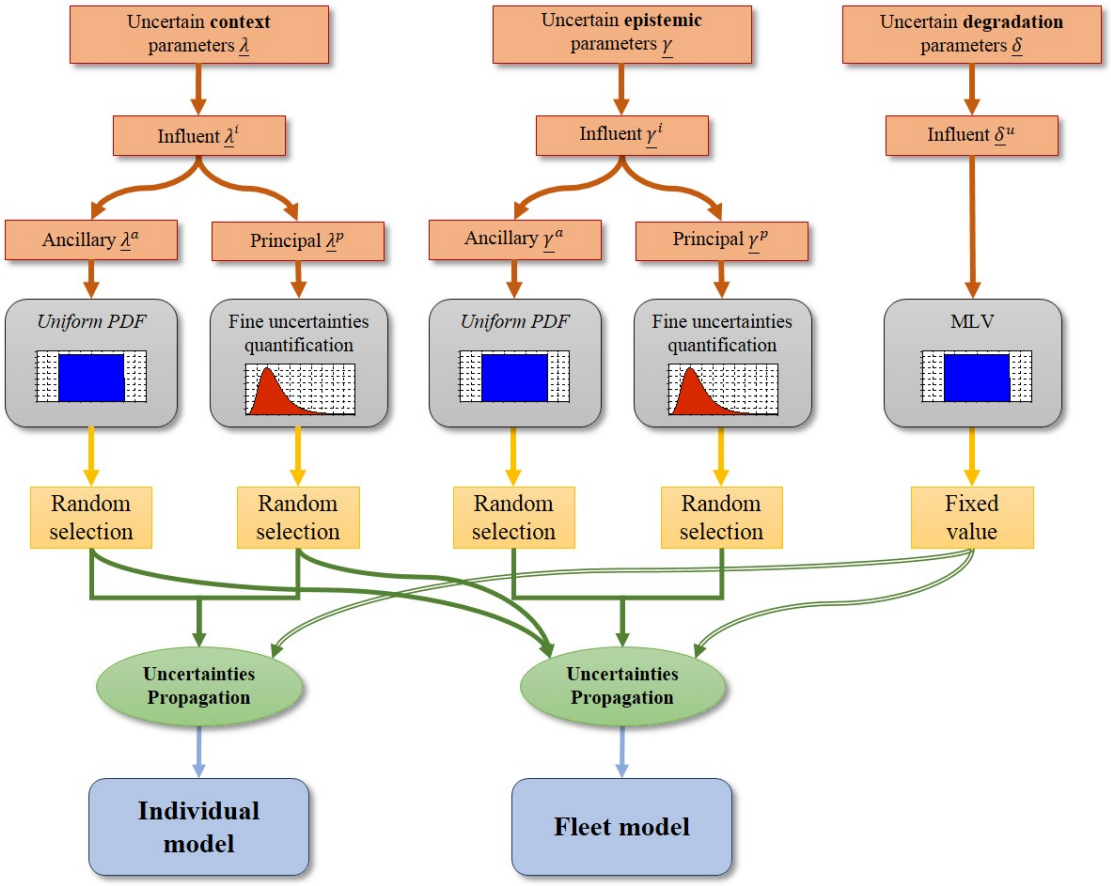


Figure 2.19 *Global scheme of the uncertainty propagation methodology.*

2.4.3 Validation of HIs

2.4.3.1 *Specifications for the set of HIs*

As mentioned in the previous chapter, the IDPHM declines the PHM system specifications into independent specifications for the EMU. Now that the NKPIs and criteria have been introduced in 0, the associated specifications are proposed in Table 2.4.

Type	Common Specifications
Targeted system	Subsystems and equipment encompassed in the PHM scope
Detection performance	Required couple (TP_{SPEC}, FP_{SPEC})
	Minimum rate of detectable TDEM: $DTDEM_{\%}$
	Minimum rate of relevant detection HIs: $RDHI_{\%}$
Identification performance	Required minimal angle α_{SPEC}
	Minimum rate of identifiable TDEM: $ITDEM_{\%}$
	Minimum rate of relevant identification HIs: $RIHI_{\%}$
Localization performance	Required minimal angle α_{SPEC}
	Minimum rate of localizable LRU: $LLRU_{\%}$
	Minimum rate of relevant localization HIs: $RLHI_{\%}$
Prognostics performance	Minimum rate of prognosticable compliant service threats: $POT_{\%}$
	Minimum rate of relevant prognostic HIs: $RPHI_{\%}$

Table 2.4 *Specifications for the development of the EMU.*

2.4.3.2 *Computation of NKPIs*

The core of the HI validation process consists of computing the NKPIs. The methodology is as follows: NKPIs are first computed for real HIs and the fleet model. If the results are not satisfactory, standardization is performed and NKPIs are evaluated again. If the validation criteria are still unsatisfactory, the individual model is considered. In cases where this latter step is not sufficient, the set of HIs must be updated. When accepted by the host system designers, it is also possible to add an additional step consisting of the computation of NKPIs with virtual HIs. All these steps are summarized in Figure 2.20.

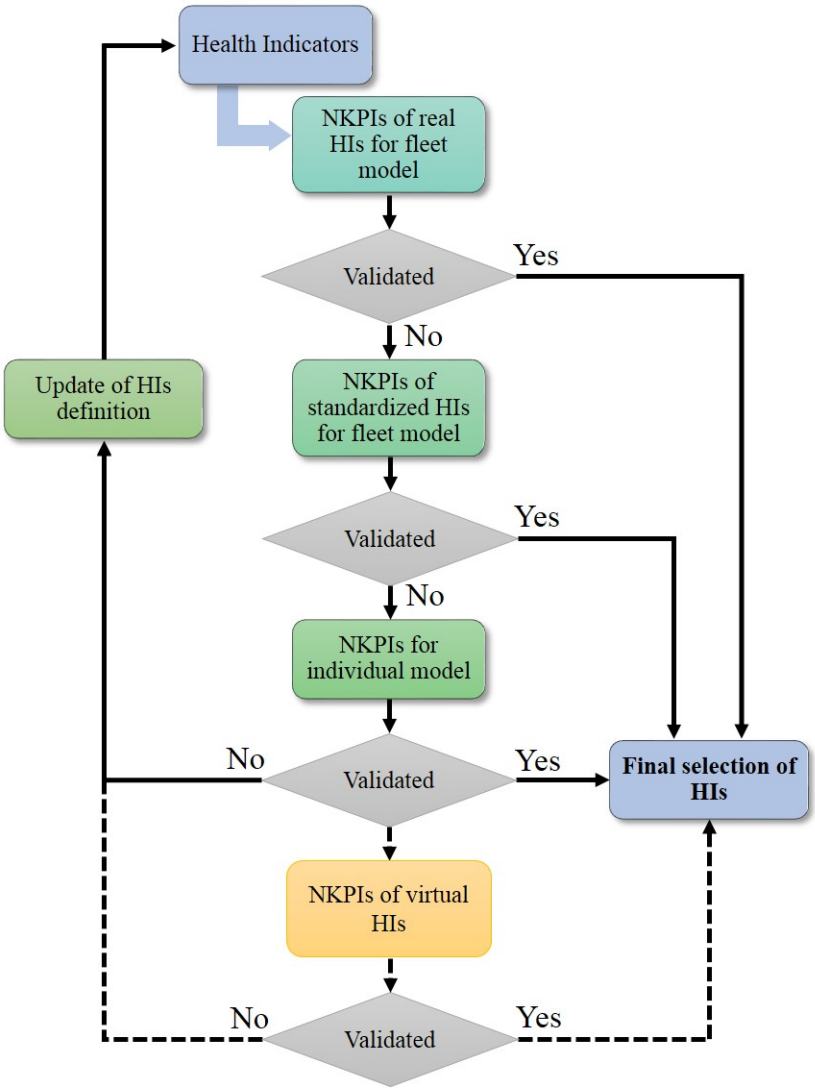


Figure 2.20 *Graph of the HIs validation process.*

This virtual implementation step is aimed at computing both the MLVs and the distributions of HIs for the fleet and individual models. The following validation step allows for assessing the performances of the defined HIs set and proposes a process to improve performance, if needed. The selection of HIs and CSIs for the fuel system is introduced in the next section.

2.5 Conclusion

To conclude this second chapter, the main feature to be remembered is that an innovative approach for the development of the embedded extraction tasks of PHM dedicated to aircraft engines has been proposed. The present chapter has made major contributions to the definition of processes for the selection, standardization and validation of HIs in design stages.

The first contribution of this chapter concerns the selection of HIs. The first novelty proposed by this thesis work is related to the modeling formalism. Indeed, the parameters are divided into three classes according to their uncertainty types: context, epistemic and degradation parameters. A vector space-based representation associated with this representation is developed to provide the mathematical basis for the models. This formalism is extended to the definition of two vector spaces related to HIs and

CSIs. Finally, the original constant temporal input representation, dedicated to the specific application of PHM development on aircraft engine models, is presented. Its main feature is utilizing non-temporal variables as inputs and outputs. The former are parameters, and the latter are HIs and CSIs. The physics-based models are built with AMESim, and a co-simulation interface is used to manage the simulations and process the results. The second originality concerning this first section is the proposition of a strategy for supervising the selection of HIs. This strategy consists of first identifying the hierarchical functional representation of the host system from its architectural specification documents. Next, for each functional unit from equipment to level 0, the CSTs and DEMs are defined from FMEAs, equipment specifications and BITE definition documents. Finally, the selection is performed through an iterative approach consisting of the following steps: (1) selection of a set of HIs from a fusion of experience feedback on other engines, ATP specifications and physical considerations; (2) testing of the HI sensitivity to DEMs via prototyping of models of equipment or subsystems; and (3) submission to expert judgment for final approval. If approved, the set of HIs is selected and sent to the standardization step, but if not, the initial selection is to be reconsidered.

The second contribution of this chapter is related to the standardization step of HIs. In this thesis work, the standardization if defined as a process aiming at modeling the effects of known influent context and epistemic parameters, termed standardization parameters, on HIs to subtract them from the actual measured values. This will attempt to reduce the standard deviation of the HIs distributions. The proposed standardization approach is divided into two steps: the identification of the standardization parameters and the estimation of the standardization models. The first originality of the approach is to use sensitivity analysis methods to identify standardization parameters. Standardization parameters are defined as influent, principal and measurable epistemic or context parameters. It is proposed to use original sensitivity indices inspired by the Morris method and adapted to models with multiple outputs to determine influential parameters. In contrast, Sobol indices are computed via the Monte Carlo method to identify the influent ones. The second novelty of the proposed approach is to use support vector regression to model the effects of the standardization parameters on outputs. The present use of SVR is original in two aspects. First, multiple output models are considered, but single-dimension SVR models are computed. This allows an easier verification of the simulated behavior of each individual output with respect to the expected physical one. Moreover, it is proposed to supervise the estimation of single SVR models with a sensitivity index indicating the level of non-linearity of each relation I/O. These sensitivity indices are computed from the Morris method. It allows a reduction of the number of needed sample and a supervision of the kernel function selection.

The third contribution concerns the validation of HIs during the design stages. The first originality of this process is to propose a set of metrics called numerical key performance indicators (**NKPIs**). These NKPIs are, to the best of our knowledge, the first of their kind. They are divided into four classes corresponding to the four main tasks of PHM: detection, identification, localization and prognostics. Two detection NKPIs are defined, based on the computation of receiver operating characteristic (**ROC**) curves between distributions of HIs obtained via uncertainty propagation: the global and the compliant detectability. They indicate the detection potential of the HI set for each DEM, regardless and with respect to false-positive and true-positive specifications. As far as identification is concerned, the global identifiability is computed from the angular gap between two variation vectors and indicates the identification potential between two DEMs. The compliant identifiability determines if the angular gaps are greater than the specified threshold. For the localization, global localizability and compliant

localizability are defined from the global identifiability and the LRU association matrix. They show the localization potential of HIs for couples of LRUs. As far as prognostics is concerned, detection, identification and localization margins are defined. They reflect the gap between intensity 1 and, respectively, the minimal detection, identification and localization intensities. Finally, some criteria issued from the NKPIs are proposed and destined to be the basis of future specifications for the specifications of the embedded extraction tasks. The second novelty proposed by this section is a process for the validation of HIs. It is based on the computation of NKPIs for different configurations of the HIs set. Thus, they are first calculated for the raw HIs for a fleet model, then for the standardized HIs with the same model and, finally, for individual models. The set of HIs is validated after all the defined criteria are checked.

Finally, the proposed approach for the development of the embedded extraction tasks relies on uncertainty propagation to create the necessary data for the computation of NKPIs. However, for the intended applications, the physics-based models are too time-demanding. To solve this problem, surrogate modeling has been chosen.

3

Construction and use of Kriging models for the propagation of uncertainties

Abstract: Because the Monte Carlo-based uncertainty propagation needed for the computation of NKPIs is too time consuming, surrogate models are used. The SVR models developed in the previous chapter are insufficient because they do not consider the correlations between the input parameters. Therefore, we propose to use Kriging, a well proven tool that is particularly efficient for estimating models that have a large number of input parameters. Kriging is based on a classical linear regression with a Gaussian process that takes into account the interactions. However, physics-based models of aircraft engines are often monotonic and non-linear with little interaction between the parameters. Therefore, a novel SVR-Kriging technique is proposed to address these characteristics. This technique combines single dimension SVRs that account for first order effects with a Gaussian process to model the interaction effects. The efficiency of the approach is demonstrated with tests that include nonlinear analytical functions of various dimensions. For this comparison, three criteria are evaluated: the Q2 index, the accuracy of the SVR-Kriging model compared to witness samples and the mean and standard deviation of the cross-validation error. The results are compared to ordinary and universal kriging. SVR-Kriging has better accuracy than the other techniques, particularly for large dimension models. To comply with the industrial need for model validation, a sequential learning process aimed at iteratively increasing the model accuracy is defined. The selection strategy for the novel learning sample takes into account the weighted sum of the cross validation error and the Kriging variance. For a given number of samples, iterative SVR-Kriging appears to be better than the non-iterative approach.

Overview

3.1 Introduction 142
3.2 The construction of Kriging models 144
3.2.1 *General considerations about surrogate modeling construction 144*
3.2.2 *Latin hypercube sampling 146*
3.2.3 *Kriging ..... **Erreur ! Signet non défini.***
3.3 SVR-Kriging approach 154
3.3.1 *Description of the method 154*
3.3.2 *Presentation of the test models 155*
3.3.3 *Performance Metrics 157*
3.3.4 *Assessment of SVR-Kriging performances 159*
3.3.5 *Proposition of enhancements for the θ optimization algorithm 163*
3.4 Validation of SVR-Kriging 164
3.4.1 *Introduction to sequential learning 164*
3.4.2 *Proposition of a new selection criterion 166*
3.4.3 *Validation of sequential learning on test models 169*
3.4.4 *Final numerical experiments plan 170*
3.4.5 *Computational issues 171*
3.5 Conclusion 173

3.1 Introduction

Forecasting and assessing the effectiveness of health indicators in a complex system is often complicated for two main reasons. First, an actual degradation database is rarely available. Second, the physical system is modeled analytically in an attempt to reproduce the real response, and analytical (numerical) models tend to become more time-intensive as their complexity is increased to improve accuracy and to consider all of the parameter uncertainties for different severities and for all outputs. As a result, a large number of model computations cannot be performed to assess the propagation of uncertainties. Figure 3.1 shows the partitioning of the necessary evaluations of a model. In an industrial context, where the user of the proposed methodology can evaluate, reassess and propose indicators without depending on a dedicated computing center, we consider the following example that runs on a classical desktop computer with 4 GB of RAM and a 2.5 GHz CPU. The system is composed of 100 HIs and 100 computations for 5 growing intensities, and the average runtime is equal to approximately 5 hours. Without parallelized calculations, the entire uncertainty propagation of 2000 Monte Carlo evaluations of the model would take more than 50,000 years. With 1000 parallel processors, the process would still take more than 50 years, which is obviously unrealistic.

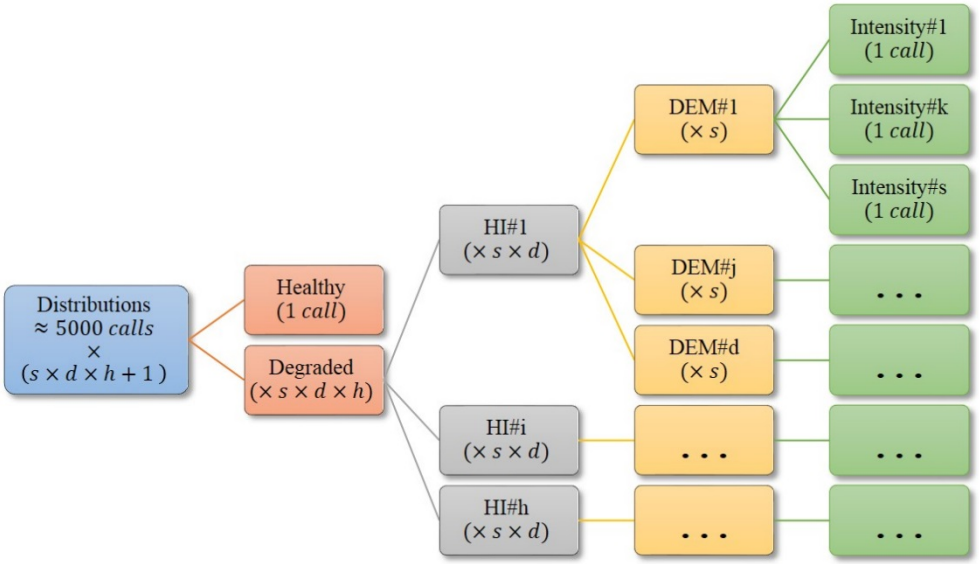


Figure 3.1 *Computation time costs of the uncertainty propagation.*

In these cases, where the model runtime is a fundamental issue, it is common to use surrogate modeling. This approach approximates computationally intensive functions with simple analytical models. The simple models are often called metamodels, and the process of constructing a metamodel is called metamodeling. This study focuses on Kriging (or Gaussian process regression), whose efficiency has been demonstrated in fields related to structural reliability, such as uncertainty propagation and global sensitivity analysis. In the case of systems, the choice of Kriging is also justified by the different inherent properties of the Kriging models in light of the target application. In this study, the stochastic aspect of Kriging, its ability to include physical insights and its good mathematical properties for sequential learning are suitable characteristics for the intended application.

The purpose of this chapter is to propose a solution to construct and use efficient Kriging models that are adapted to the specificities of the intended applications. The problem is subdivided into the construction of Kriging models, the adaptation to PHM systems and the validation or improvement of the model accuracy. Each section of the chapter is devoted to one of these topics.

The first section focuses on the construction of general Kriging models. Three major steps are identified from a literature review: the determination of the ranges of variation of the input parameters, the construction of the learning design of experiment (DOE) and the estimation of the hyperparameters. For the ranges of variation of the inputs, the reader may refer to the previous chapter, where issues of uncertainties were addressed. For the construction of the learning DOE, the Latin hypercube sampling (LHS) technique is introduced. To ensure their good space filling properties, a random sampling of several LHSs associated with a selection criterion is used. Lastly, the state of the art of Kriging is described, including a classification of existing methods, focusing on the class of non-stationary Kriging techniques that appears to be the most suitable for the intended application.

The second section is dedicated to the adaptation of non-stationary Kriging to the specifics of applications to aircraft engines models. The first particularity is that the behaviors of the variables are relatively monotonic and often contain strong nonlinearities. Moreover, the input parameters typically have low correlations, so the second and higher-order effects have a limited influence on the outputs. The approach proposes to use Kriging with support vector regression as the deterministic part. This

combination was chosen because of the similarities between Kriging and SVR (Vazquez, et al., 2003). This novel technique, called SVR-Kriging, is introduced through theoretical considerations. Because it is a new approach, it is compared with classical ordinary and universal Krigings in several pedagogical analytical functions of various dimensions. Three common criteria are used for this comparison: the Q2 index (based on a comparison with an additional test sample) and the mean and standard deviation of the cross-validation error. Computational techniques aimed at improving the estimation of the Kriging hyperparameters are also proposed. Lastly, the results of the estimation of the example models are presented and critiqued.

The third and last section focuses on validating and improving the accuracy of the SVR-Kriging model. Because the model is intended for industrial use, validation of the model is required by the customers. This validation is performed using a set of three criteria that are also based on the Q2 index and the cross-validation error. In cases where the first estimation of the surrogate model is not accurate enough, a sequential learning procedure is proposed. This method consists of iteratively adding well-chosen points and reestimating the model's hyperparameters to increase its accuracy. In this way, the specified accuracy can be attained. The points are chosen using a selection criterion that is based on a combination of the Kriging variance and the cross-validation error over the entire input space. An ordinary Kriging model is used to estimate the cross-validation error over the entire space. For the present application, one SVR-Kriging model is constructed for each HI from the learning DOE. To choose the model to which it is most desirable to add a sampling point, a method based on a probability assignment is developed. Lastly, computational issues are addressed, and two techniques aimed at reducing the computation time of the estimation of the SVR-Kriging hyperparameters and the sequential learning are proposed.

3.2 Construction of the Kriging models

3.2.1 General considerations about surrogate model construction

In our case of HIs evaluation, computationally intensive problems are common if we want to guarantee that all of the possible degradations and uncertainties are considered. Surrogate modeling techniques are often used to address this type of problem. Surrogate models are also called metamodels or emulators. They are aimed at estimating complex numerical models via mathematical functions. Surrogate modeling is often used to solve optimization problems with time-consuming models (Forrester, et al., 2009). For example, in the aerospace field, surrogate modeling has been applied to the optimization of airfoil aerodynamics (Arias-Montano, et al., 2012) and the shape of axial compressor blades (Samad, et al., 2008). Recently, it was also used for uncertainty assessment in aviation environmental system models (Allaire, et al., 2010). A surrogate model is typically constructed using the following steps (Figure 3.2):

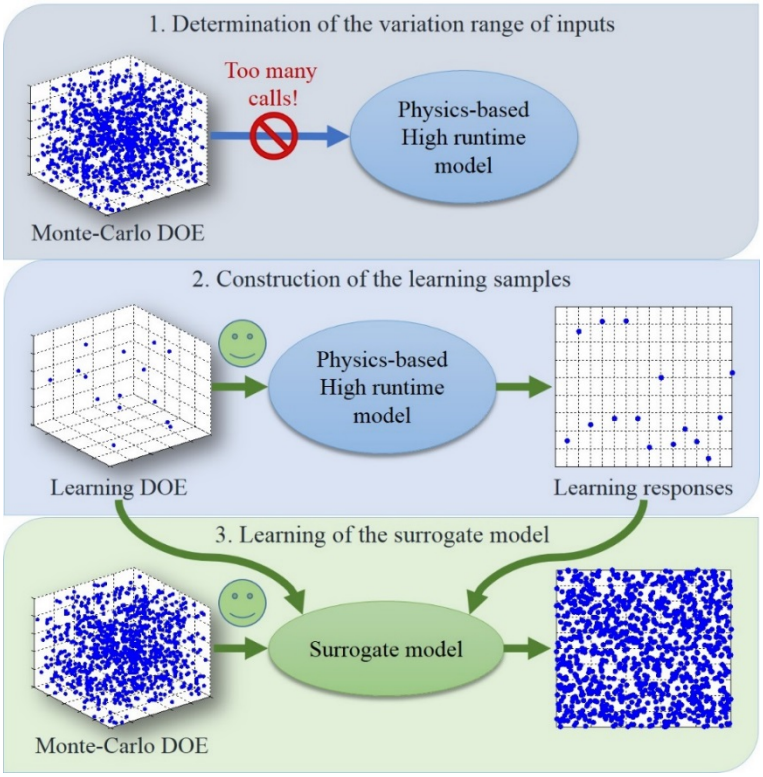


Figure 3.2 *Principle steps in the construction of a surrogate model.*

1. Determination of the ranges of variation of the input parameters and construction of the Monte Carlo DOE. The ranges of variation are generally identified from an uncertainty analysis that is performed by expertise and experience feedback.
2. Construction of the learning design of experiment (DOE) and computation of the associated outputs. The issues of the learning sampling design choice will be introduced later.
3. Learning of the surrogate model and propagation of the Monte Carlo DOE. Surrogate models are often parametric; therefore, the learning step consists of an estimation of the hyperparameters from the set of learning samples.

The learning DOE is a fundamental feature of an efficient surrogate model. Numerous types of DOE have been presented in the literature. The most famous type is the factorial experiment, which consists of defining multiple levels for each input (generally two: a lower value and an upper value) and computing the model responses for each possible combination of values. This approach requires 2^n evaluations of the model. Consequently, although it can be efficient for low input space dimensions, it rapidly becomes unfeasible for dimensions greater than 10. Therefore, another technique for generating DOEs is needed. Ideally, the technique should use a limited number of learning points while ensuring good input space filling properties[20]. In this study, we use Latin hypercube sampling (**LHS**) (Iman, 2008). LHS is introduced in detail in section 3.2.2. The idea of using LHS for the learning of the surrogate model was introduced by McKay *et al.* (McKay, et al., 2000).

Surrogate modeling is a recent discipline that was developed with the first time-consuming computer codes. A brief review of the scientific literature shows that there are many surrogate modeling techniques

[20] This is sometimes called a low discrepancy DOE.

with various levels of complexity. The most basic type is linear regression. Other types are polynomial response surfaces (Rajashekhar, et al., 1993), multivariate adaptive regression splines (Friedman, 1991), support vector machines (Guo, et al., 2009), artificial neural networks (Rayas-Sanchez, 2004), radial basis functions (Yee, et al., 2001), chaos polygons (Fisher, et al., 2011) and Kriging (Kleijnen, 2009). Note that Goel *et al.* (Goel, et al., 2007) proposed using an ensemble of surrogates and combining their results an alternative to choosing one surrogate modeling type. The basic idea of this approach is interesting, but although multiple surrogates generate more information, they require tuning more hyperparameters and may produce more sources of errors. For these reasons, this method is not addressed. The choice of the surrogate model type depends on three factors: (1) the characteristics of the models (dimension, computation time), (2) the physical behaviors of the variables (linearity, monotonicity, continuity) and (3) the specifications of the intended application (computational power available, required accuracy). The characteristics of the intended application for these three factors are summarized in Table 3.1.

Physics-based models characteristics	Physical behaviors of variables	Specifications of the intended application
Large dimension of inputs space (≈ 100)	Nonlinear behaviors	Computation on a desktop computer →Less than 1000 model evaluations
Weak interactions between inputs	Flat and monotonic shapes	First order effects must be modeled with high levels of accuracy
Time-consuming model evaluation ($\approx 5h$)	Possible local discontinuities	The modeling of discontinuity effects is not required. Approximations by continuous functions are allowed

Table 3.1 *Summary of the characteristics of the intended application.*

Examples of comparative studies of surrogate models can be found in (Jin, et al., 2001), (Peter, et al., 2008) and (Chowdhury, et al., 2010). In these papers and our experience, only Kriging and neural networks are able to handle the size of the considered input space. This study focuses on Kriging for three reasons. First, traditional neural network approaches are black box tools that are often criticized for lacking the ability to provide or include physical insights. The second reason is that the Gaussian process that is included in the Kriging technique (see section 3.2.3) provides a statistical framework that suits both the final purpose of estimating the distributions of HIs and the use of support vector regression (SVR) as introduced in chapter 2. Indeed, the kernel function of SVR is similar to the correlation function of the Kriging Gaussian process. The relationship between these methods was demonstrated in (Vazquez, et al., 2003). Lastly, Kriging was chosen over neural networks because of two mathematical properties: it is able to estimate the variance of its own precision error, and it is an exact interpolator on learning points. Both properties allow easier and more efficient sequential learning than other surrogate modeling techniques, which ensures the accuracy of the estimations (Jin, et al., 2002). The theoretical aspects of Kriging and sequential learning will be introduced in detail in section 3.2.3 and section 3.4.1, respectively.

3.2.2 Latin hypercube sampling

3.2.2.1 *Simple Latin hypercube*

Latin hypercubes (**LH**) are commonly used in several applications, such as reliability analysis (Shu, et al., 2011) and geostatistics (Lin, et al., 2011). Consider a model with n inputs. The construction of a

LH with p learning points, denoted $LH(p,n)$, consists of a discretization of the n dimensions into p intervals and the creation of a permutation matrix. This permutation matrix is computed as follows:

$$LH(p,n) = \begin{vmatrix} \sigma^1(1) & \cdots & \sigma^n(1) \\ \vdots & & \vdots \\ \sigma^1(p) & \cdots & \sigma^n(p) \end{vmatrix} \quad \textbf{(3.1)}$$

where $\sigma^1, \ldots, \sigma^n$ are random permutations of $[\![1; p]\!]$. For example, assuming that $n = 2$ and $p = 10$, the example of $LH(10,2)$ proposed by Marrel (Marrel, 2008) is the following:

$$\begin{vmatrix} 8 & 2 & 10 & 7 & 4 & 3 & 6 & 9 & 5 & 1 \\ 5 & 6 & 9 & 1 & 4 & 2 & 10 & 8 & 3 & 7 \end{vmatrix}^t \quad \textbf{(3.2)}$$

This LH can be represented in its graphical form as shown in Figure 3.3.

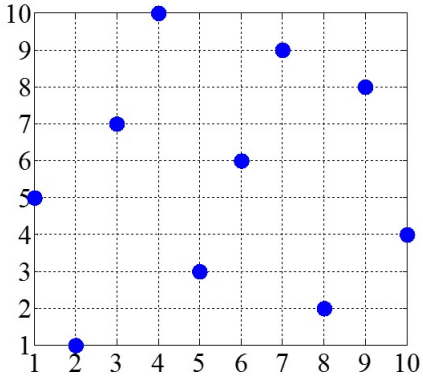


Figure 3.3 *Graphical representation of a LH(10,2).*

The quality of a LH depends on the random selection of permutation functions and sometimes results in good space filling properties, but sometimes does not. For example, the LH represented in Figure 3.4 includes large unsampled areas and will not be efficient.

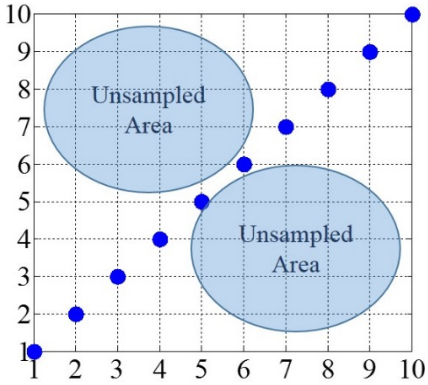


Figure 3.4 *Graphical representation of a high discrepancy LH(10,2).*

To avoid generating a LH with bad space filling properties, particular types of LH that guarantee good space filling properties can be used, such as U-sampling (Tang, 1998) or orthogonal Latin hypercubes (Ye, 1998). In this study, we use an approach that optimizes LH according to a selection criterion.

3.2.2.2 *Optimized Latin hypercube*

Many publications have focused on optimization, such as (Jin, et al., 2005), (Liefvendahl, et al., 2006) and (Johnson, et al., 1990). Marrel (Marrel, 2008) listed several types of criteria, including

correlation, *maximin* and *minimax*, maximal volume and wrap-around discrepancy. Once the criterion is chosen, LH can be optimized in two ways:

- Generate a large number of LHs and select the one with the best value for the criterion.
- Use a probabilistic metaheuristic; for example, simulated annealing (Marrel, 2008).

In this study, we use the first technique. Even though it requires the generation of numerous LHs, the associated computation time must be put into perspective with the model runtime; the optimization of a $LH(500,50)$ with 10,000 iterations takes approximately $126\,s$ to compute, which is negligible compared with the runtime of a single simulation of the fuel system model. The maximin will be retained as the selection criterion because its efficiency has been demonstrated (Marrel, 2008).

Suppose that the Latin hypercube $L = LH(p,n)$ was constructed from n variables and p learning samples and that the uncertainty of each of the n inputs is represented by a probability density function $\wp_1, \dots, \wp_n$. The associated Latin hypercube sampling design of experiments (**LHSDOE**) is obtained by dividing the range of variation of each input $i, i = 1, \dots, n$ into p sub-intervals of the same probability $\mathcal{I}_i^1, \dots, \mathcal{I}_i^p$ and computing the following matrix:

$$\textbf{LHSDOE} = \begin{vmatrix} rand(\mathcal{I}_{\sigma^1(1)}^1) & \cdots & rand(\mathcal{I}_{\sigma^p(1)}^p) \\ \vdots & \ddots & \vdots \\ rand(\mathcal{I}_{\sigma^1(n)}^1) & \cdots & rand(\mathcal{I}_{\sigma^p(n)}^p) \end{vmatrix} \tag{3.3}$$

where $rand(\mathcal{I}_i^j)$ is a function that randomly selects a value in the interval $\mathcal{I}_i^j$ according to the PDF $\wp_i$. For input uncertainties, uniform PDFs are commonly used; therefore, the intervals $\mathcal{I}_i^1, \dots, \mathcal{I}_i^p$ have the same lengths. Figure 3.5 shows an example of the transformation from $LH(10,2)$ to $LHSDOE(10,2)$. In this example, the two inputs are represented by uniform PDFs of the parameters $(1;5)$ and $(-2;1)$.

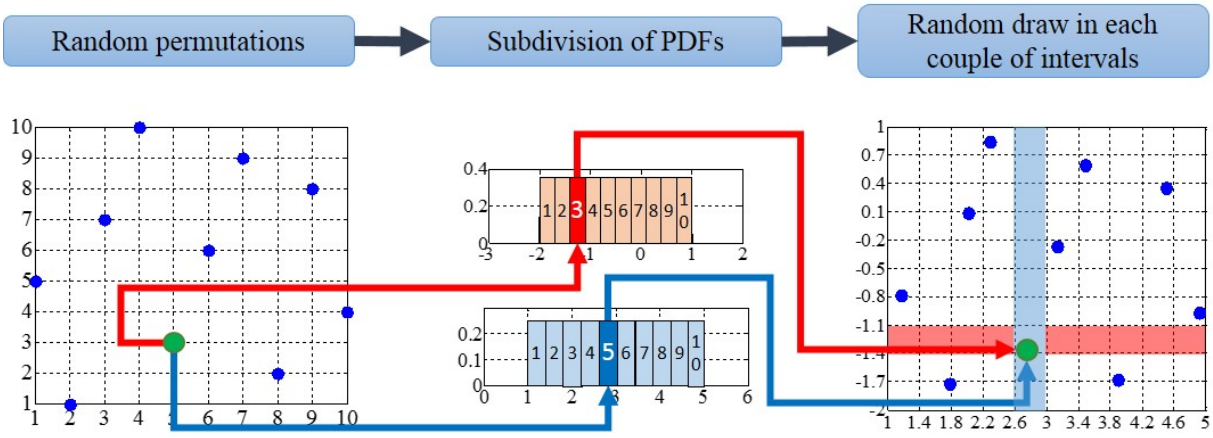


Figure 3.5 *Transformation of a LH into a LHSDOE.*

3.2.3 Kriging

3.2.3.1 *Introduction to Kriging*

First, consider a model $\mathcal{k}$ that is assumed to be a black box and is defined as follows:

$$\begin{aligned} \mathcal{k}&: \mathbb{R}^n \longrightarrow \mathbb{R}^m \\ \underline{x} &\longmapsto \underline{y} = \mathcal{k}(\underline{x}) \end{aligned} \tag{3.4}$$

where n and m are the dimensions of the input and the output spaces, respectively, and $\underline{x}$ and $\underline{y}$ are the input and output vectors, respectively. In the sequel, only the single output case will be considered; *i.e.*, $m = 1$. A set of learning points is needed to construct an estimator of $\mathscr{k}$. Suppose that the model was evaluated for k input vectors $\underline{x}_1, \dots, \underline{x}_k$. The associated output values are denoted $y_1, \dots, y_k$.

Kriging is a type of regression model that includes a Gaussian process; thus, it is also called Gaussian process regression. It was originally developed by the mining engineer Daniel Krige for interpolation in geostatistics problems and was formalized by Matheron (Matheron, 1963). The idea of applying Kriging to estimate the outputs of a numerical model was proposed recently (Sacks, et al., 1989; Jones, et al., 1998; Simpson, et al., 2001); (Kleijnen, 2009) provides a recent and complete survey of the topic. A Kriging model that estimates $\mathscr{f}$ is a function $\mathcal{K}$ that can be written as follows:

$$\begin{aligned} \mathcal{K}\colon \mathbb{R}^n &\longrightarrow \mathbb{R}^m \\ \underline{x} &\longmapsto \underline{\hat{y}} \end{aligned} \tag{3.5}$$

The function $\mathcal{K}$ can be expressed as a combination of a deterministic regression function and a stochastic Gaussian process (Rasmussen, 2006) as follows:

$$\mathcal{K}(\underline{x}) = \mathcal{R}(\underline{x}) + \mathcal{G}(\underline{x}) \tag{3.6}$$

This expression can be interpreted as a regression model $\mathcal{R}$ with an error term that is approximated by a Gaussian process $\mathcal{G}$.

3.2.3.2 *The stochastic correlation model*

In every regression function $\mathcal{R}$, $\mathcal{G}$ is always a Gaussian process with a mean of zero and the following covariance function $\mathcal{C}$ between $\mathcal{G}(\underline{x}_i)$ and $\mathcal{G}(\underline{x}_j)$:

$$\mathcal{C}\big(\mathcal{G}(\underline{x}_i), \mathcal{G}(\underline{x}_j)\big) = \sigma^2 k(\underline{\theta}, \underline{x}_i, \underline{x}_j) \tag{3.7}$$

where σ^2 is the Gaussian process variance to be estimated, and k is a correlation model (kernel function) of the hyperparameters $\underline{\theta}$. The function $k(\underline{\theta}, \underline{x}_i, \underline{x}_j)$ is the product of the functions $k_1, \dots, k_n$ defined for each dimension of the input space:

$$k(\underline{\theta}, \underline{x}_i, \underline{x}_j) = \prod_{d=1}^{n} k_d(\underline{\theta}_d, x_{id}, x_{jd}) \tag{3.8}$$

The parameter vectors $\underline{\theta}_d$ define the shape of the correlation functions for dimension $d \in [\![1; n]\!]$. Examples of correlation functions are given in Table 3.2.

Correlation Type	Configuration of $\underline{\theta}_d$	$k_d(\underline{\theta}_d, x_{id}, x_{jd})$
Exponential	$\underline{\theta}_d = \theta_d$	$exp(-\theta_d \lvert x_{jd} - x_{id} \rvert)$
Gaussian	$\underline{\theta}_d = \theta_d$	$exp\left(-\theta_d \lvert x_{jd} - x_{id} \rvert^2\right)$
Exponential - Gaussian	$\underline{\theta}_d = [\theta_{d1}\ \ \theta_{d2}]^t$	$exp\left(-\theta_{d1} \lvert x_{jd} - x_{id} \rvert^{\theta_{d2}}\right), 0 < \theta_{d2} \leq 2$
Linear	$\underline{\theta}_d = \theta_d$	$max\{0, 1 - \theta_d \lvert x_{jd} - x_{id} \rvert\}$

Table 3.2 *Different types of correlation models for Kriging.*

The influence of θ_{d1} and θ_{d1} on the shape of the correlation for the exponential-Gaussian function is shown in Figure 3.6.

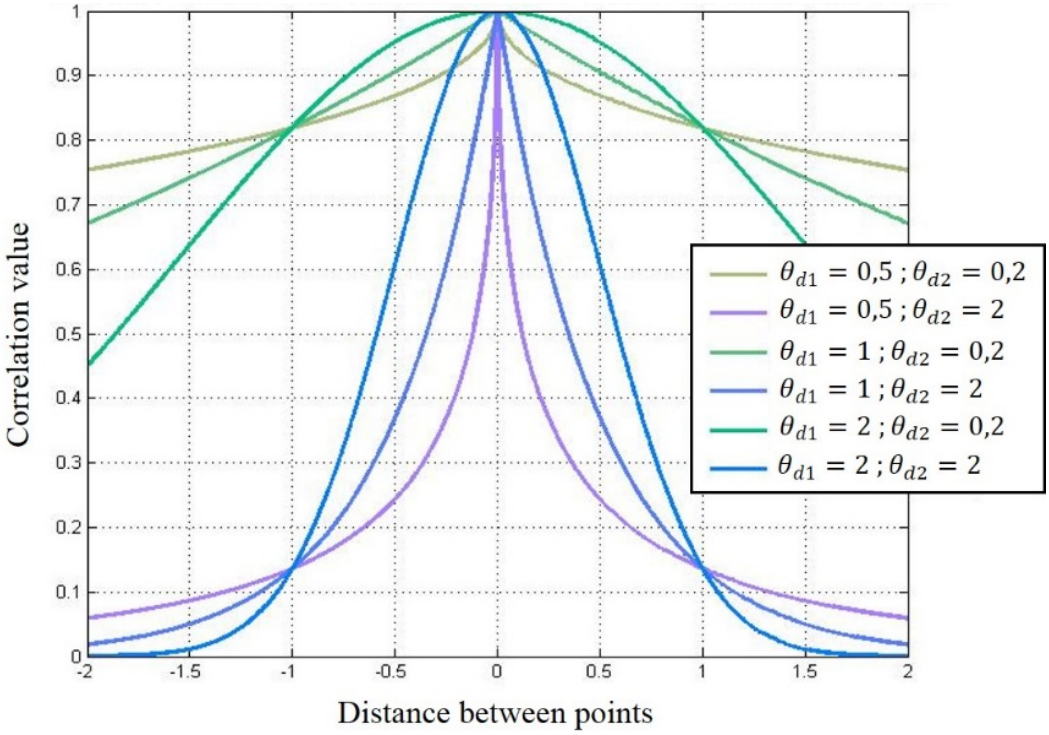


Figure 3.6 *Influence of the hyperparameter values on the shape of the exponential-Gaussian function.*

For the set of learning points $\underline{x}_1, \ldots, \underline{x}_k$, $\boldsymbol{R}$ is a matrix whose coefficients R_{ij} are defined as follows:

$$R_{ij} = k(\underline{\theta}, \underline{x}_i, \underline{x}_j), \quad i,j = 1, \ldots, n \tag{3.9}$$

For the input vector $\underline{s} = [s_1 \quad \cdots \quad s_n]^t$, we define the following function r in the following way:

$$\underline{r}(\underline{s}) = \left[k(\underline{\theta}, \underline{x}_1, \underline{s}) \quad \cdots \quad k(\underline{\theta}, \underline{x}_k, \underline{s})\right]^{\boldsymbol{t}} \tag{3.10}$$

The estimation of the Gaussian process for the input $\boldsymbol{s}$ can be written as follows (Lophaven, et al., 2002):

$$\mathcal{G}(\underline{s}) = \underline{r}(\underline{s})^t \underline{\gamma} \tag{3.11}$$

where $\underline{\gamma}$ is estimated via the generalized least square residuals relative to the regression estimations:

$$\underline{\gamma} = \boldsymbol{R}^{-1}\left(\underline{y} - \underline{\hat{y}}_{\mathcal{R}}\right) \tag{3.12}$$

where $\underline{y} = [y_1 \quad \cdots \quad y_n]^t$ is the matrix of model responses values at the learning points and $\underline{\hat{y}}_{\mathcal{R}} = \left[\mathcal{R}(\underline{x}_1) \quad \cdots \quad \mathcal{R}(\underline{x}_k)\right]^t$ is the estimation of the regression function $\mathcal{R}$ at these points.

3.2.3.3 *Kriging techniques*

Basic Kriging uses a constant μ for the regression function and is called simple Kriging. When the constant is computed as the mean of the responses at the learning points so that $\mu = \sum_{i=1}^{n} y_i/n$, the method is called ordinary Kriging (Cressie, 1990). Many novel techniques have emerged from these historical methods over the past several decades for specific applications. As a result, numerous Kriging

techniques have been described in the literature. A non-exhaustive classification of these methods is proposed in Figure 3.7. The most generic form of Kriging is nonlinear Kriging (Moyeed, et al., 2002). The first level of our classification includes five classes. Disjunctive Kriging (Rivoirard, 1994) consists of estimating an ancillary variable instead of directly estimating the outputs of the model. For example, in geostatistics, one can choose to estimate the probability that a material density is greater than a determined threshold at a location instead of predicting the value of the density. The advantage of this is a simplification of the computation tasks. The second class includes Kriging techniques that use information about derivatives, such as partial differential equations (**PDEs**) (Hon, et al., 1999) or gradients (Liu, 2003). The third class is composed of techniques that try to model the non-stationarity of models by improving the regression function. Among these techniques, universal Kriging uses a polynomial regression for the deterministic part of Kriging to model its non-stationary trend. Lastly, Bayesian Kriging (Omre, 1987) considers the uncertainties of the hyperparameters to improve its precision, and CoKriging (Myers, 1982) uses correlations between the output variables in multi-output models to increase the knowledge without adding learning points.

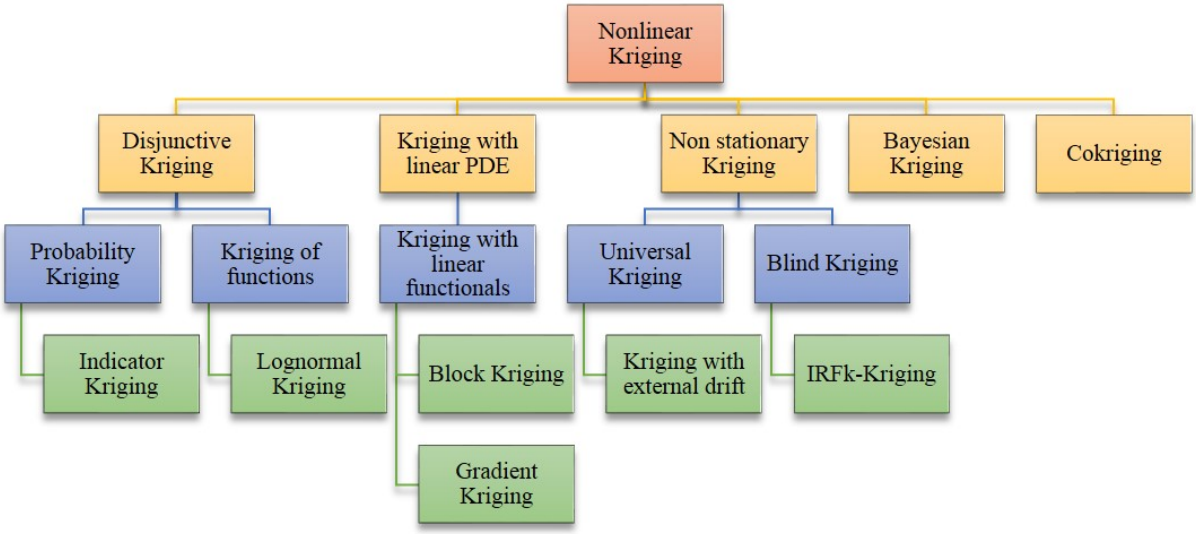


Figure 3.7 *Non-exhaustive classification of Kriging methods.*

Considering all of these different techniques and the requirements of our application, we decided to use a non-stationary Kriging method. Recall that our purpose is to estimate the distributions of HIs. Hence, a direct estimation of the model outputs is needed, so disjunctive Kriging cannot be used. The model outputs do not need to be correlated, so the co-Kriging technique is not applicable. In addition, PDEs are not pertinent because the model is supposed to be a black box; this eliminates the second class of techniques. Bayesian Kriging is still a possible technique and would be interesting for our work. However, the fundamental issue is that this study deals with thermal, hydraulic, mechanical and aerodynamic behaviors that are characterized by monotonic functions with potentially abrupt changes due to saturation and threshold effects. Therefore, the importance of the regression function directed the choice of the Kriging technique towards the non-stationary methods. The next subsection introduces the regression function in a non-stationary Kriging framework in detail.

3.2.3.4 *The deterministic regression model*

In non-stationary Kriging, the regression function uses a set of linear or nonlinear functions $g_1, \dots, g_p$ as a base for a linear combination to model the effects of non-stationarity. For the set of learning points $\underline{x_1}, \dots, \underline{x_k}$, the matrix $\boldsymbol{F}$ is defined as follows:

$$\boldsymbol{F} = \begin{vmatrix} g_1(\underline{x_1}) & \cdots & g_p(\underline{x_1}) \\ \vdots & \ddots & \vdots \\ g_1(\underline{x_k}) & \cdots & g_p(\underline{x_k}) \end{vmatrix} \in \mathbb{R}^{k \times p} \tag{3.13}$$

For the input vector $\underline{s} = [s_1 \quad \cdots \quad s_n]^{\boldsymbol{t}}$, the function $\underline{f}$ is also defined as follows:

$$\underline{f}(\underline{s}) = \begin{bmatrix} g_1(\underline{s}) & \cdots & g_p(\underline{s}) \end{bmatrix}^T \tag{3.14}$$

In this case, the estimation of $\mathcal{R}$ at $\underline{s}$ can be written as (Lophaven, et al., 2002):

$$\mathcal{R}(\underline{s}) = \underline{f}(\underline{s})^T \underline{\beta} \tag{3.15}$$

where $\underline{\beta}$ can be computed via least squares estimation as follows:

$$\underline{\beta} = \left(\boldsymbol{F^T F}\right)^{-1} \boldsymbol{F^T} \underline{y} \tag{3.16}$$

The least squares estimation is appropriate in cases where there is no correlation between the learning points. In the opposite case, generalized least squares estimation can be used:

$$\underline{\beta} = \left(\boldsymbol{F^T R^{-1} F}\right)^{-1} \boldsymbol{F^T R^{-1}} \underline{y} \tag{3.17}$$

Lastly, for non-stationary Kriging, the final estimate at a new point $\underline{s}$ is the following:

$$\mathcal{K}(\underline{s}) = \underline{f}(\underline{s})^T \underline{\beta} + \underline{r}(\underline{s}) \boldsymbol{R^{-1}} \left(y - \boldsymbol{F}\underline{\beta}\right) \tag{3.18}$$

The principle of Kriging estimation is illustrated for a one dimensional case in Figure 3.8. The effect of the Gaussian process is clearly visible; it reshapes the estimation to fit the real values on the learning points exactly. It may be noted that for a high value of θ, the correlation function has less influence and affects the model estimation in narrow neighborhoods around the learning points. The influence of the correlation function extends further for low values of θ. High values are well suited to cases where the model is subject to noise and erroneous data, while the latter case is more suitable for deterministic models with flat and monotonic behaviors. Therefore, referring to Table 3.1, low values of θ will be used for the application to aircraft engines.

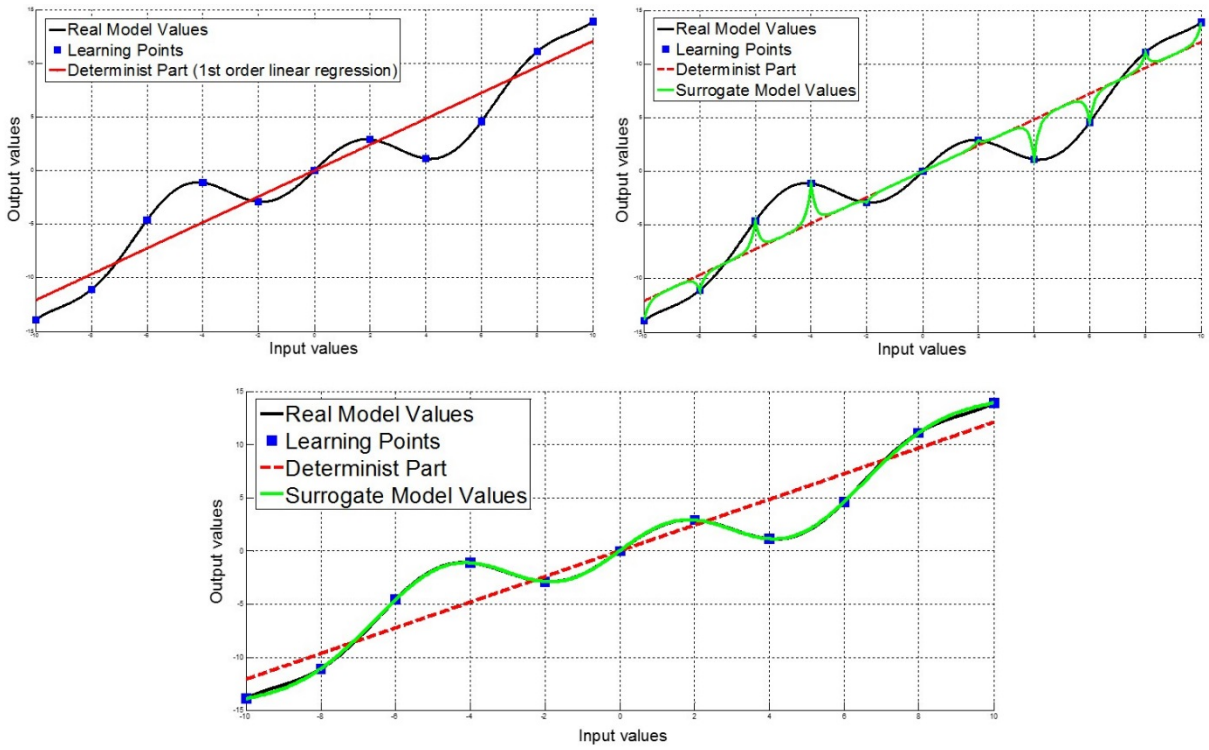


Figure 3.8 *Kriging estimations for the regression part (top left) alone and complete Kriging model with high (top right) and low(bottom) values of θ.*

Universal Kriging is probably the most commonly used non-stationary approach. It uses a polynomial regression of order z as the regression function and a set of functions. For example, considering a second order polynomial, the functions $g_1, \ldots, g_5$ for $\underline{s} = [s_1 \quad s_2]^t$ are as follows:

$$\begin{aligned} g_1(\boldsymbol{s}) &= 1 \\ g_2(\boldsymbol{s}) &= s_1 \\ g_3(\boldsymbol{s}) &= s_2 \\ g_4(\boldsymbol{s}) &= {s_1}^2 \\ g_5(\boldsymbol{s}) &= {s_2}^2 \end{aligned} \tag{3.19}$$

This list can be composed of several functions. This approach has two main issues. First, it is difficult to choose relevant functions for each input independently. If the dimension of the input space is important and each independent input has a different influence on the outputs, this task can be very time consuming and difficult to perform. The second issue is that the number of learning points needed for the generalized least squares estimation of $\underline{\beta}$ in the case of multiple inputs is prohibitively large. In section 0, a technique to solve both issues is proposed: SVR-Kriging.

3.2.3.5 *Kriging properties*

This subsection reviews some of the basic properties of Kriging. If $\underline{s}$ is replaced by $\underline{x_i}, i \in [\![1; k]\!]$ where $\underline{e_i}^T = \left|\delta_{ij}\right|_{j=1,\ldots,k}$ with δ_{ij} the Kronecker delta:

$$\begin{aligned}\mathcal{K}(\underline{x_i}) &= \underline{f}(\underline{x_i})^T\underline{\beta} + \underline{r}(\underline{x_i})\boldsymbol{R}^{-1}\left(\underline{y} - \boldsymbol{F}\underline{\beta}\right)\\ \mathcal{K}(\underline{x_i}) &= f(\underline{x_i})^T\underline{\beta} + \underline{e_i}^T\left(\underline{y} - \boldsymbol{F}\underline{\beta}\right)\\ \mathcal{K}(\underline{x_i}) &= f(\underline{x_i})^T\underline{\beta} + y_i - \underline{e_i}^T\boldsymbol{F}\underline{\beta}\\ \mathcal{K}(\underline{x_i}) &= y_i\end{aligned} \quad \textbf{(3.20)}$$

Hence, by its construction, Kriging is an exact interpolator on learning points; actually, it is the best linear unbiased predictor. According to (Lophaven, et al., 2002), the variance σ^2 can be expressed as follows:

$$\sigma^2 = \frac{1}{n}\left(\underline{y} - \boldsymbol{F}\underline{\beta}\right)\boldsymbol{R^{-1}}\left(\underline{y} - \boldsymbol{F}\underline{\beta}\right) \quad \textbf{(3.21)}$$

Note that this variance can also be computed via bootstrap approaches (for additional details, see (Den Hertog, et al., 2006)). From σ^2, it is possible to calculate the mean square error of the prediction $\mathcal{K}(\underline{s})$ at any point $\underline{s}$:

$$MSE(\mathcal{K}(\boldsymbol{s})) = \sigma^2\left(1 - \begin{bmatrix} f^T(\underline{s}) & r^T(\underline{s})\end{bmatrix}\begin{bmatrix}\boldsymbol{0} & \boldsymbol{F^T}\\ \boldsymbol{F} & \boldsymbol{R}\end{bmatrix}\begin{bmatrix} f(\underline{s})\\ r(\underline{s})\end{bmatrix}\right) \quad \textbf{(3.22)}$$

It can be verified that if $\underline{s} = \underline{x_i}, i \in [\![1; k]\!]$, then $MSE(\mathcal{K}(\underline{s})) = 0$. The Kriging predictor has three main advantages: it is a best linear unbiased predictor, it is an exact interpolator on design sites, and it is capable of estimating its own prediction mean square error. The last point is an interesting characteristic for sequential learning purposes (c.f. Section 3.4.1).

3.3 The SVR-Kriging approach

As shown in Table 3.1, the input parameters of the physics-based models considered in our application are weakly correlated. Moreover, the specifications require that the first order effects be modeled with high levels of accuracy. To comply with these requirements, a novel Kriging technique, termed SVR-Kriging, is developed. Its main idea is to use support vector regression as the deterministic part of the technique. To evaluate its performance, SVR-Kriging is compared with both ordinary and universal Kriging based on three analytical functions that are considered as black boxes and three criteria taken from the literature.

3.3.1 Description of the method

The SVR-Kriging estimator uses support vector regression for the deterministic part, which replaces $\underline{f}, \underline{\beta}$ and $\boldsymbol{F}$ by $\underline{v}, \underline{\alpha}$ and $\boldsymbol{G}$, respectively, as follows:

$$\mathcal{K}(\underline{s}) = v(\underline{s})^T\underline{\alpha} + r(\underline{s})\boldsymbol{R}^{-1}\left(\underline{y} - \boldsymbol{G}\underline{\alpha}\right) \quad \textbf{(3.23)}$$

The idea of non-stationary Kriging is to make the deterministic part account for a large amount of the model variation to ensure an accurate estimation of the first order effects. Under these conditions, the Gaussian process essentially acts as an error term that covers the interaction effects, which are assumed to be weak (see Table 3.1). In the present applications, the first order effects are often nonlinear and potentially have local discontinuities, so we propose using support vector regression (SVR) for their estimation. The main advantage of SVR is that it does not need *a priori* knowledge about the shapes of

the functions. However, its principal drawback compared with linear regression is that it is relevant only within the boundaries defined by the learning DOE, which means that the learning DOE must contain the limits of the ranges of variation of the inputs that are defined by uncertainty analyses.

Even if the SVR is capable of dealing with multiple input models, in the intended application, the effect of each input parameter is modeled independently using single input SVRs. This one dimensional approach for SVR is similar to the approach that was developed in the previous chapter for the standardization (see section 2.3.3) and has two main advantages. First, it allows the model to be checked independently to determine if it is coherent with respect to the expected physical behavior of each parameter. It also allows a more intelligent selection of the initial sampling points and kernel functions. Therefore, for parameters that have a linear influence on the outputs, only a few sampling points and a linear kernel will be chosen, while those with a non-linear influence will be associated with a greater number of design points and a more complex kernel function, such as the RBF. Several common points can be identified with the correlation function of the Gaussian process using kernel functions. However, these methods differ in their utilization; while the SVR is used to model the principal effects, the correlation function is used to model the residual effects.

The global methodology, which is summarized in Figure 3.9, includes the following steps: (1) definition of the initial set of input parameters, (2) coarse quantification of the uncertainties (defined by uniform PDFs), (3) sensitivity analysis based on the Morris method and the identification of the influential parameters, (4) classification of the influential parameters with respect to their degree of nonlinearity, (5) construction of the SVR learning vectors (which contain the limits of the ranges of variation of the parameters) and choosing the hyperparameters for SVRs, (6) estimation of the single dimension SVR functions, and (7) estimation of the hyperparameters of the Gaussian process.

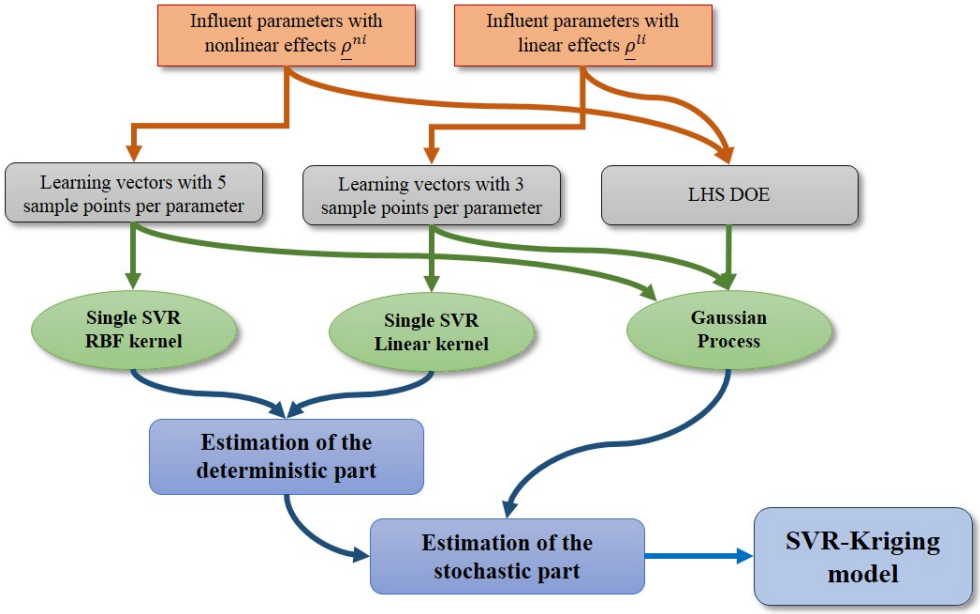


Figure 3.9 *The global methodology used to build SVR-Kriging models.*

A set of analytical test functions is used to assess the accuracy of SVR-Kriging. Two functions are designed to represent the classical behavior of aircraft engine models. Thus, they are nonlinear and have a local discontinuity. The third analytical function is called the Ishigami function and is commonly used in sensitivity analyses.

3.3.2 Presentation of the test models

3.3.2.1 *The SISO function*

The first proposed analytical test function f_{SISO} is a single input single output (SISO) function. Its principal features are that it is nonlinear (quadratic), monotonic and contains a discontinuity. As described in Table 3.1, it represents the typical behavior of an aircraft engine variable. The SISO analytical test function f_{SISO} is defined as follows:

$$f_{SISO}: [-5;5] \longrightarrow [-5;25]$$

$$x \quad \longmapsto \quad y = f_{SISO}(x) = \begin{cases} -5, & for\ x < 0 \\ x^2, & for\ x \geq 0 \end{cases}$$

A graphical representation of this model in its defined interval is shown in Figure 3.10.

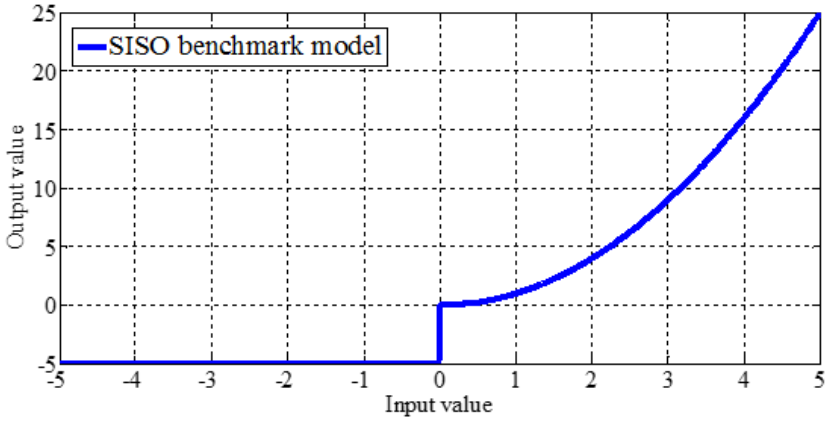


Figure 3.10 *SISO analytical test function.*

The discontinuity at zero is a type of behavior that is commonly observed and is principally due to threshold effects. For example, it could represent the displacement of a valve that unlocks when a pressure reaches a threshold and allows the valve to relieve the load. As described previously, the discontinuity does not need to be modeled precisely; it can be modeled by a continuous function.

3.3.2.2 *The DISO model*

The second analytical test function f_{DISO} is a dual input single output (DISO) function that represents a typical behavior of two correlated aircraft engine variables. It is defined as follows:

$$f_{DISO}: [1;10] \times [-3;3] \longrightarrow [0;25]$$

$$(x_1, x_2) \quad \longmapsto \quad y = f_{DISO}(x_1, x_2) = \begin{cases} \exp\big(0.2(x_1 + x_2)\big), & x_1 < 4 \\ 10 + \exp\big(0.2(x_1 + x_2)\big), & x_1 \geq 4 \end{cases}$$

A graphical representation of this model in its defined interval is given in Figure 3.11.

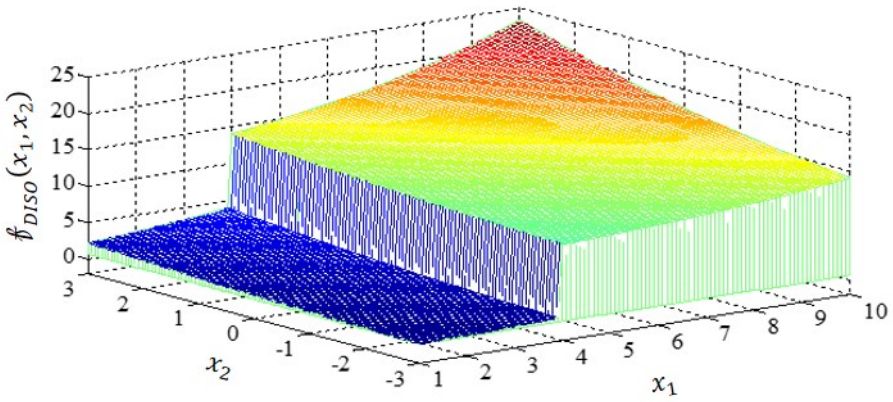


Figure 3.11 *DISO analytical test function.*

Note that this model is nonlinear in x_1 at the value of 4 and that x_1 and x_2 are correlated.

3.3.2.3 *The Ishigami function*

The Ishigami function, which is denoted $\mathcal{f}_{ISHIGAMI}$, is a well-known function that is commonly used in the field of sensitivity analysis because of its strong nonlinearities and correlations. It is defined as follows (Saltelli, et al., 2000):

$$\mathcal{f}_{ISHIGAMI}: [-\pi; \pi]^3 \longrightarrow [0; 25]$$

$$(x_1, x_2, x_3) \mapsto \quad y = \mathcal{f}_{ISHIGAMI}(x_1, x_2, x_3) = \sin(x_1) + a\sin(x_2)^2 + b{x_3}^4\sin(x_1)$$

We generally assume that $a = 7$ and $b = 0.1$. This Ishigami function will be used under two forms: the 2D form, which only considers the impact of the two first dimensions by assuming that $x_3 = 0$ (Figure 3.12), and the classical 3D form.

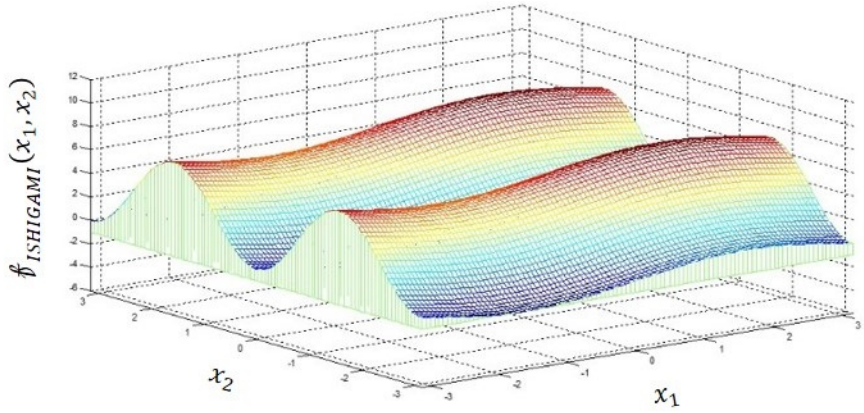


Figure 3.12 *The 2D Ishigami function, which is restricted to its first two input variables.*

3.3.3 Performance Metrics

The precision of the surrogate models is evaluated using indices that are based on cross-validation (Davis, 1987) and the Q_2 index (Marrel, et al., 2008).

3.3.3.1 *Cross-validation related indices*

The cross validation (CV) is based on the computation of the modeling error e_{-i}, which is defined as follows:

$$e_{-i} = y_i - \mathcal{K}_{-i}(\underline{x_i}) \tag{3.24}$$

where y_i is the exact model output value at the learning point $\underline{x_i}$, and $\mathcal{K}_{-i}$ is the Kriging model that is learned without the design point $\underline{x_i}$. The value e_{-i} globally indicates the relative importance of the learning point $\underline{x_i}$ in the estimation of the hyperparameters of the Kriging model. If a learning point is associated with a high value of e_{-i}, the sampling is probably not dense enough around this point. Two types of indicators can be defined from e_{-i}. The first indicator is graphical; the cross validation curve is defined as the curve of $\mathcal{K}_{-i}(\underline{x_i})$ versus y_i. A scatterplot that is similar to the curve $\mathcal{K}_{-i}(\underline{x_i}) = y_i$ introduces a more accurate Kriging model. An example of a cross-validation curve is shown in Figure 3.13.

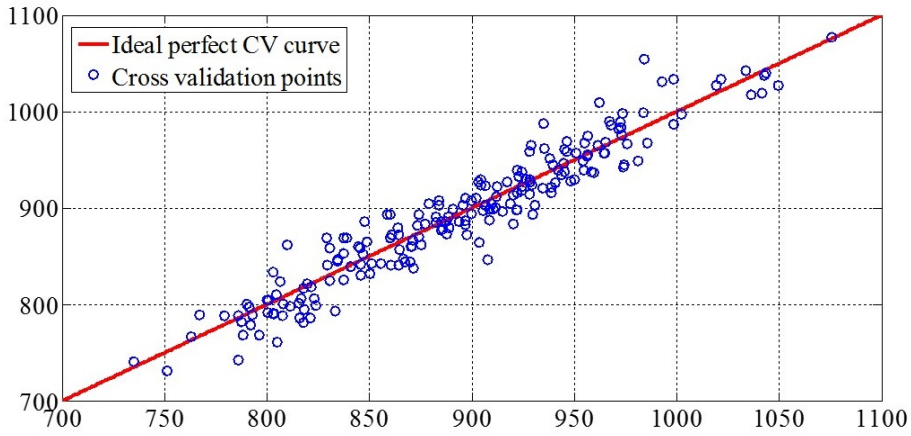


Figure 3.13 *Example of a cross-validation curve.*

The second type of indicator is composed of metrics that are computed from the CV curve. We propose using the mean μ_{CV} of the error e_{-i} and its standard deviation σ_{CV}, which are computed as follows:

$$\begin{aligned} \mu_{CV} &= \frac{\sum_{i=1}^{n} e_{-i}}{n}\left(\frac{1}{3\sigma_y}\right) \\ \sigma_{CV} &= \sqrt{\frac{\sum_{i=1}^{n}(e_{-i} - \mu_{CV})^2}{n}}\left(\frac{1}{3\sigma_y}\right) \end{aligned} \tag{3.25}$$

where n is the number of learning points, and σ_y is the standard deviation of the considered output y. The quality of the surrogate model is evaluated according to these two metrics. The average μ_{CV} indicates whether the estimation of a model is biased or not; it should be equal to zero if it is not biased. The standard deviation σ_{CV} indicates the level of coherence of a model. The lower the σ_{CV} value is, the better the surrogate model is. The main advantage of the cross-validation is that is does not require computing additional sampling points. However, $\underline{\beta}$ and $\underline{\gamma}$ are estimated at each iteration for the computation of e_{-i}, whereas $\underline{\theta}$ is fixed. Hence, μ_{CV} and σ_{CV} principally gives information about the quality of the correlation map. Therefore, another metric must be used to correctly assess the global performance of the model.

3.3.3.2 *The Q2 index*

The $Q2$ index corresponds to the classical coefficient of determination R^2 for a test sample (Marrel, et al., 2008) and is defined as follows:

$$Q2\left(\underline{y},\mathcal{K}\left(\underline{x}\right)\right)=1-\frac{\sum_{i=1}^{a}\left(y_i-\mathcal{K}\left(\underline{x}_i\right)\right)^2}{\sum_{i=1}^{a}\left(\bar{\underline{y}}-y_i\right)^2} \quad \textbf{(3.26)}$$

where $\underline{x}$ denotes the a points of the test set, $\underline{y}$ is the associated responses of the physics-based model at these points, and $\mathcal{K}\left(\underline{x}\right)$ is the estimation given by the Kriging model. If $Q2=1$, all of the estimations are exactly equal to the real values. Unlike the cross-validation index, this index indicates the global quality of a Kriging model. However, its major drawback is that it requires an extra set of sampling points.

We propose to combine the CV and Q2 indices to maximize the confidence in the quality of the surrogate model. The former is particularly useful for assessing the quality of the standalone correlation function, while the latter is used to evaluate the global accuracy of Kriging.

3.3.4 Assessment of the performance of SVR-Kriging

3.3.4.1 *SISO function*

In this section, the performance of SVR-Kriging is assessed and compared to the performance of the ordinary and universal Kriging techniques. The universal Kriging model is computed for a second order linear regression function, and the SVR uses a RBF kernel $exp\left(-\gamma\left\|\underline{x_i}^T\underline{x_j}\right\|^2\right)$, where $\gamma=10$. The same exponential-Gaussian correlation function $k_d\left(\underline{\theta_d},x_{id},x_{jd}\right)=exp\left(-\theta_{d1}\left|x_{jd}-x_{id}\right|^{\theta_{d2}}\right)$, where d is the considered dimension of the input space, is used for the Gaussian process to compare the three Kriging approaches for the estimation of the SISO function. In the SISO model, $d=1$. The parameter $\underline{\theta}$ is estimated via an optimization algorithm with constraints relative to the possible variation boundaries. The optimization problem requires an a priori value of $\underline{\theta}$, which is denoted $\underline{\theta}^{init}$, and its lower and upper boundaries $\underline{\theta}^{lb}$ and $\underline{\theta}^{ub}$, which are defined by the user. For clarity, the estimation $\hat{\underline{\theta}}$ is written $\underline{\theta}$, which is a common simplification in the field. This optimization problem can be solved by the DACEFIT[21] algorithm (Nielsen, et al., 2002). In the SISO function, the chosen values are $\underline{\theta}^{init}=[1\quad 1.5]^T$, $\underline{\theta}^{lb}=[1e^{-8}\quad 1]^T$ and $\underline{\theta}^{ub}=[100\quad 2]^T$. The same number of learning samples is used for each technique. The ordinary and universal Kriging techniques use a monodimensional LHSDOE with 9 points, while the SVR-Kriging technique uses the combination of a 4 point monodimensional LHSDOE and a 5 point learning vector for the SVR.

An example of the results is shown in Figure 3.14. The difference between the regression function and the Kriging estimation, which indicates the impact of the Gaussian process, is less important in SVR-Kriging. The results are satisfactory because the global objective was to reduce the influence of the Gaussian process in favor of the regression. In addition, the behavior of SVR-Kriging at the border of the input space is better because the tangent of the estimation is closer to the real value than the other models; this is because the lower and upper values of the input parameter are included in its learning vector.

[21] DACE (Design and Analysis of Computer Experiments) is a Matlab™ toolbox for working with Kriging approximations to computer models. This toolbox contains an algorithm for estimating Kriging hyperparameters and computing Kriging predictions with associated mean square errors.

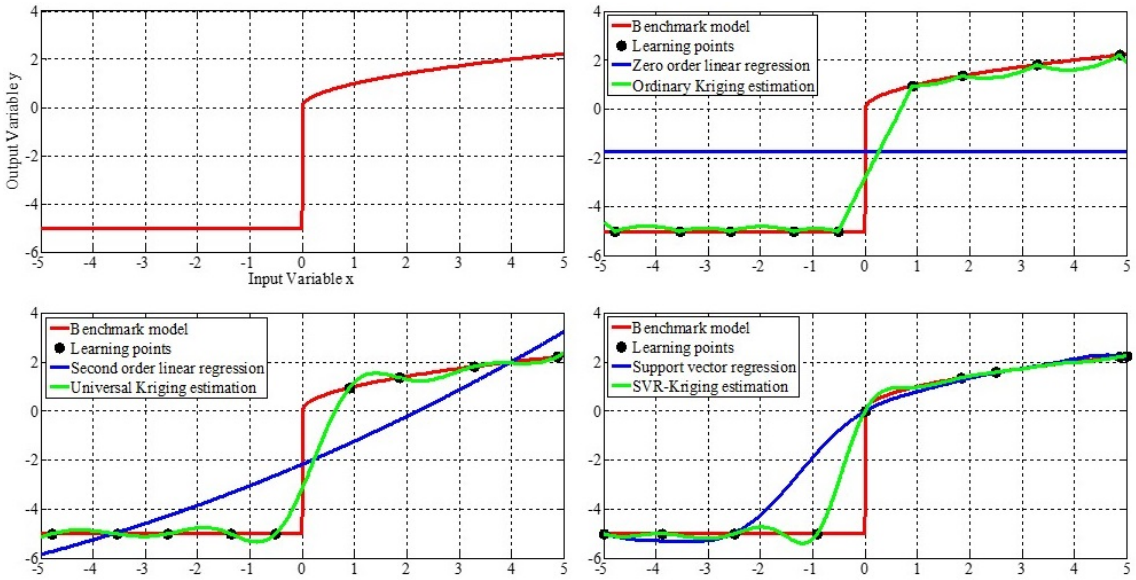


Figure 3.14 *Results of ordinary Kriging (top right), universal Kriging (bottom left) and SVR-Kriging (bottom right) for the estimation of the SISO model.*

To determine the performance of each technique, the values of the cross-validation and $Q2$ indices are computed. The $Q2$ indices are computed from a test sample of 100 points that are distributed equidistantly. To compare the performances, the means and standard deviations of these indices are calculated for 100 Kriging models that are trained with different initial LHSDOEs. The results are given in Table 3.3 and demonstrate that the qualities of the three models are almost equivalent for this example. It appears that SVR-Kriging provides better results for the σ_{CV} index. However, the other two Kriging techniques are better for the $Q2$ index. Universal Kriging induces more bias in the values of μ_{CV} than the other techniques. Lastly, it is not possible to determine the best Kriging technique for this model. As a result, SVR-Kriging is restrictive and insufficient for this monodimensional application.

Kriging Technique	Mean and standard deviation of μ_{CV}	Mean and standard deviation of σ_{CV}	Mean and standard deviation of Q2
Ordinary Kriging	$(1.6e^{-4};\ 0.007)$	$(0.16;\ 0.03)$	$(0.93;\ 0.03)$
Universal Kriging	$(-0.006;\ 0.016)$	$(0.20;\ 0.04)$	$(0.92;\ 0.04)$
SVR-Kriging	$(-4.7e^{-4};\ 0.029)$	$(0.09;\ 0.05)$	$(0.89;\ 0.05)$

Table 3.3 *Comparison of Kriging performances for the SISO model.*

3.3.4.2 *DISO function*

For this application, a second order regression is used for the universal Kriging, and a RBF kernel with $\gamma = 10$ is used for the SVR-Kriging. The correlation function is the exponential-Gaussian function $k_d(\underline{\theta}_d, x_{id}, x_{jd}) = exp\left(-\theta_{d1}\left|x_{jd} - x_{id}\right|^{\theta_{d2}}\right), d \in [\![1; 2]\!]$ in which $\underline{\theta}_d$ is defined as follows:

$$\begin{aligned} \underline{\theta_1}^{init} &= [1 \quad 1]^T;\ \underline{\theta_2}^{init} = 1.5 \\ \underline{\theta_1}^{lb} &= [1e^{-8} \quad 1e^{-8}]^T;\ \underline{\theta_2}^{lb} = 1 \\ \underline{\theta_1}^{ub} &= [100 \quad 100]^T;\ \underline{\theta_2}^{ub} = 2 \end{aligned} \tag{3.27}$$

A two dimensional LHSDOE with 18 points is used for the ordinary and universal Kriging, and a combination of an 8 point two dimensional LHSDOE and two 5 point learning vectors for one dimensional SVRs is used for the SVR-Kriging. An example of the results is shown in Figure 3.15 and demonstrations that the estimation provided by SVR-Kriging is most similar to the simple test DISO model.

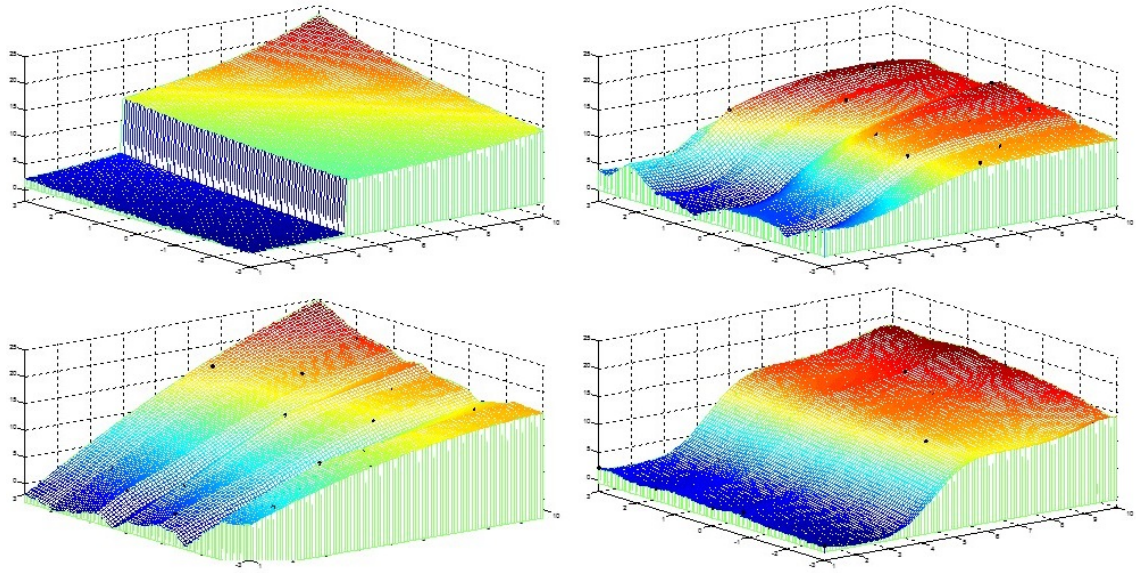


Figure 3.15 *Results of ordinary Kriging (top right), universal Kriging (bottom left) and SVR-Kriging (bottom right) for the estimation of the DISO model.*

The performance indices are also computed for this second test model. As in the SISO model, the Kriging models are constructed for 100 random LHSDOEs. The means and standard deviations of the results are given in Table 3.4.

Kriging Technique	Mean and standard deviation of μ_{CV}	Mean and standard deviation of σ_{CV}	Mean and standard deviation of Q2
Ordinary Kriging	$(0.003;\ 0.01)$	$(0.19;\ 0.04)$	$(0.95;\ 0.02)$
Universal Kriging	$(0.006;\ 0.02)$	$(0.24;\ 0.06)$	$(0.93;\ 0.03)$
SVR-Kriging	$(-0.003;\ 0.007)$	$(0.11;\ 0.03)$	$(0.95;\ 0.008)$

Table 3.4 *Comparison of Kriging performances for the DISO model.*

Table 3.4 shows that for a two dimensional function, the SVR-Kriging technique performs better; while its associated Q2 index is equal to that in the other techniques, it has a better σ_{CV} index. Hence, it is slightly better, although this difference is not significant enough to fully justify its use.

3.3.4.3 *Ishigami function*

Figure 3.16 shows an example of the 2D Ishigami function using the same parameterization as the DISO model. Again, SVR-Kriging appears to provide a better estimation of the Ishigami function for the same number of learning points.

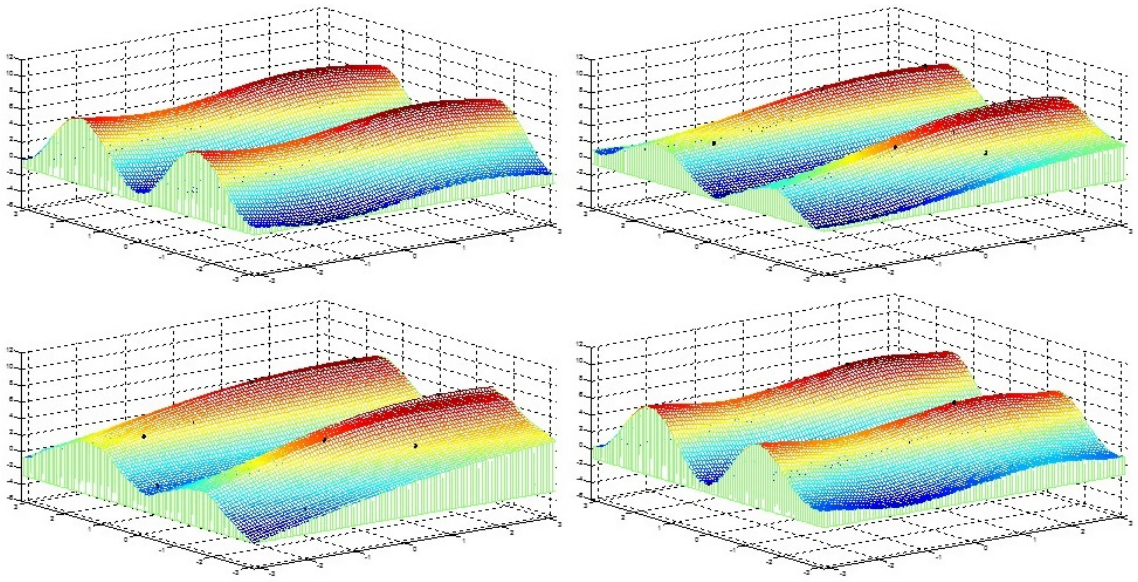


Figure 3.16 *Results of ordinary Kriging (top right), universal Kriging (bottom left) and SVR-Kriging (bottom right) for the estimation of the 2D Ishigami function.*

The means and standard deviations of the performance indices are computed for the same number of iterations and are presented in Table 3.5.

Kriging Technique	Mean and standard deviation of μ_{CV}	Mean and standard deviation of σ_{CV}	Mean and standard deviation of Q2
Ordinary Kriging	$(-0.005;\ 0.007)$	$(0.10;\ 0.04)$	$(0.93;\ 0.04)$
Universal Kriging	$(-0.003;\ 0.011)$	$(0.13;\ 0.03)$	$(0.90;\ 0.09)$
SVR-Kriging	$(-0.001;\ 0.001)$	$(0.02;\ 0.003)$	$(0.99;\ 0.001)$

Table 3.5 *Comparison of Kriging performances for the 2D Ishigami function.*

The results shown in Table 3.5 confirm and reinforce the conclusions of the previous section. The results provided by the SVR-Kriging technique for the evaluation of the 2D Ishigami function are clearly better than those from ordinary and universal Kriging for both the cross-validation and Q2 indices. Moreover, the standard deviations of these indices are reduced, which also indicates good repeatability of the results. The performance of SVR-Kriging is finally tested on the estimation of the 3D Ishigami function for the same hyperparameter values to analyze the influence of the dimension size. A three dimensional LHSDOE with 27 points is used for the ordinary and universal Kriging, while the SVR-Kriging uses a combination of a 12 point three dimensional LHSDOE and three 5 point learning vectors for a single dimension SVR. The results are presented in Table 3.6.

Kriging Technique	Mean and standard deviation of μ_{CV}	Mean and standard deviation of σ_{CV}	Mean and standard deviation of Q2
Ordinary Kriging	$(-0.005;\ 0.01)$	$(0.28;\ 0.05)$	$(0.42;\ 0.09)$
Universal Kriging	$(-0.004;\ 0.02)$	$(0.41;\ 009)$	$(0.12;\ 0.27)$
SVR-Kriging	$(-0.001;\ 0.02)$	$(0.16;\ 0.04)$	$(0.66;\ 0.09)$

Table 3.6 *Comparison of Kriging performances for the 3D Ishigami function.*

Table 3.6 shows that the conclusions drawn from the 2D functions are even better with a higher dimension. The results show that the larger the dimension of the input space is, the better the performance of SVR-Kriging compared to the other techniques. It can be explained by the fact that interactions are weak and that for each new dimension, the SVR estimates each parameter's behavior independently and accurately while other techniques estimate the global behavior.

3.3.5 Proposed enhancements for the $\underline{\theta}$ optimization algorithm

Beyond the selection of the learning DOE and the Kriging method itself, the estimation of the hyperparameters has important impacts on the final quality of the surrogate model. In the previous subsection, the results were obtained using an optimization algorithm to estimate the hyperparameter $\underline{\theta}$ with a Gaussian-exponential correlation function. For the remainder of this chapter, this algorithm will be termed the $\underline{\theta}$ optimization algorithm. There are many ways to improve this algorithm (Marrel, 2008). In this study, two techniques are proposed: the use of non-isotropic correlation hyperparameters and the iteration of the $\underline{\theta}$ optimization algorithm.

3.3.5.1 *Anisotropic exponential-Gaussian correlation functions*

The first proposed technique to improve the precision of the estimations of the hyperparameters is to use an anisotropic exponential-Gaussian correlation. Hence, for $k(\underline{\theta}, \underline{x_i}, \underline{x_j}) = exp\left(-\theta_1 \left|x_j - x_i\right|^{\theta_2}\right)$, the value of θ_2 can vary with the dimension, while the classical approach is to consider it isotropic. The idea is to add several hyperparameters to provide more degrees of freedom for the model fitting. We reuse the previous example test, the 3D Ishigami function, which is now estimated by SVR-Kriging with an anisotropic exponential-Gaussian correlation function. The initial hyperparameters are equal to:

$$\begin{gathered} \underline{\theta_1}^{init} = [1 \quad 1 \quad 1]^T;\ \underline{\theta_2}^{init} = [1.5 \quad 1.5 \quad 1.5]^T \\ \underline{\theta_1}^{lb} = [1e^{-8} \quad 1e^{-8} \quad 1e^{-8}]^T;\ \underline{\theta_2}^{lb} = [1 \quad 1 \quad 1]^T \\ \underline{\theta_1}^{ub} = [100 \quad 100 \quad 100]^T;\ \underline{\theta_2}^{ub} = [2 \quad 2 \quad 2]^T \end{gathered} \tag{3.28}$$

The technique is compared with the classical isotropic approach for a set of 100 random learning DOEs. The results are given in Table 3.7.

Estimation Technique	Mean and standard deviation of μ_{CV}	Mean and standard deviation of σ_{CV}	Mean and standard deviation of Q2
Isotropic	$(-0.002;\ 0.017)$	$(0.15;\ 0.04)$	$(0.64;\ 0.09)$
Anisotropic	$(-0.002;\ 0.017)$	$(0.15;\ 0.04)$	$(0.66;\ 0.06)$

Table 3.7 *Performances of anisotropic estimation for the 3D Ishigami function.*

Table 3.7 shows that the results of the anisotropic approach are slightly better than those of the isotropic approach. This approach will be used because it provides more degrees of freedom for the fitting of the correlation function.

3.3.5.2 *Multiple iterations of the $\underline{\theta}$ optimization algorithm*

The second proposed technique to improve the precision of the estimation of the hyperparameters is to use multiple iterations of the $\underline{\theta}$ optimization algorithm with random initial parameterizations. The chosen value for $\underline{\theta}^{init}$ is that associated with the highest optimization criterion OC calculated as follows:

$$OC = \begin{cases} \dfrac{Q2}{|\sigma_{CV}\,\mu_{CV}|}, & Q2 > 0 \\ Q2|\sigma_{CV}\,\mu_{CV}|, & Q2 \leq 0 \end{cases} \tag{3.29}$$

The drawback of this technique is that it requires a set of test points to compute Q2. Consequently, more evaluations of the model are needed. Because these test points will be necessary to validate the SVR-Kriging model anyway, this technique will be used. It is tested for 10, 20, 50 and 100 iterations of the $\underline{\theta}$ optimization algorithm and for the hyperparameters defined as follows:

$$\begin{gathered} \underline{\theta_1}^{init} = [1e^{x_1} \quad 1e^{x_2} \quad 1e^{x_3}]^T;\ \underline{\theta_2}^{init} = [y_1 \quad y_2 \quad y_3]^T \\ \underline{\theta_1}^{lb} = [1e^{-8} \quad 1e^{-8} \quad 1e^{-8}]^T;\ \underline{\theta_2}^{lb} = [1 \quad 1 \quad 1]^T \\ \underline{\theta_1}^{ub} = [100 \quad 100 \quad 100]^T;\ \underline{\theta_2}^{ub} = [2 \quad 2 \quad 2]^T \end{gathered} \tag{3.30}$$

where x_1, x_2, x_3, y_1, y_2 and y_3 are random variables that are determined according to the following PDFs:

$$\begin{gathered} x_1 \sim \mathcal{U}(-8\,;2);\ x_2 \sim \mathcal{U}(-8\,;2);\ x_3 \sim \mathcal{U}(-8\,;2) \\ y_1 \sim \mathcal{U}(1\,;2);\ y_2 \sim \mathcal{U}(1\,;2);\ y_3 \sim \mathcal{U}(1\,;2) \end{gathered} \tag{3.31}$$

where $\mathcal{U}(a\,;b)$ is the uniform distribution with a lower bound a and an upper bound b. To give meaningful results, the values of the μ_{CV}, σ_{CV} and $Q2$ indices are computed for 100 random LHSDOEs; their means and standard deviations are presented in Table 3.8.

Estimation Technique	Mean and standard deviation of μ_{CV}	Mean and standard deviation of σ_{CV}	Mean and standard deviation of Q2
Single DACEFIT	$(-0.002;\ 0.017)$	$(0.15;\ 0.04)$	$(0.66;\ 0.06)$
Multiple:10 iterations	$(-0.004;\ 0.017)$	$(0.15;\ 0.04)$	$(0.66;\ 0.08)$
Multiple: 20 iterations	$(-0.003;\ 0.013)$	$(0.14;\ 0.04)$	$(0.69;\ 0.08)$
Multiple: 50 iterations	$(-0.003;\ 0.012)$	$(0.14;\ 0.04)$	$(0.72;\ 0.08)$
Multiple: 100 iterations	$(-0.001;\ 0.012)$	$(0.12;\ 0.44)$	$(0.73;\ 0.08)$

Table 3.8 *Performances of multiple iterations of the $\underline{\theta}$ optimization for the 3D Ishigami function.*

Table 3.8 shows a significant improvement of the Q2 index and a small decrease of μ_{CV} with more than 20 iterations. There is no performance gain for 10 iterations of the $\underline{\theta}$ optimization. Moreover, the difference between 50 and 100 iterations is insignificant. Consequently, because of runtime limitations, 50 iterations will be used. This idea is inspired by Bayesian Kriging, which uses a random variable for $\underline{\theta}$ with a prior distribution (Omre, 1987).

3.4 Validation of SVR-Kriging

The construction of surrogate models is a complex task, primarily because of the numerous choices (e.g., input representations, emulator type, DOE type, a priori values of the hyperparameters) that must be made at each step. If one choice is not appropriate, the surrogate model may provide aberrant results.

Because of the relative fragility of its estimation, a surrogate model must be validated before being used. This validation is the subject of this section.

3.4.1 Introduction to sequential learning

The computation of performance metrics for surrogate models was addressed in section 3.3.3. The next question is how to improve the model if its values are not accurate? This study proposes using sequential learning to iteratively enhance the quality of the surrogate model by adding learning points at suitable locations. Approaches based on Kriging are well suited to sequential learning because they can use information about the error variance to identify the relevant samples at which the model should be evaluated. The fact that Kriging is an exact interpolator on learning points is also a good property for sequential learning.

Sequential learning methods are typically divided into the following steps (Jin, et al., 2002): (1) construction of the initial learning DOE, (2) building the surrogate model, (3) computation of the selection criterion over the entire input space, (4) determining the input point that corresponds to the maximum or minimum of this selection criterion and (5) addition of this new learning point to the learning DOE and iteration of the process. The computation ends when either the maximum number of iterations or the validation criteria threshold value has been reached. The entire framework is shown in Figure 3.17.

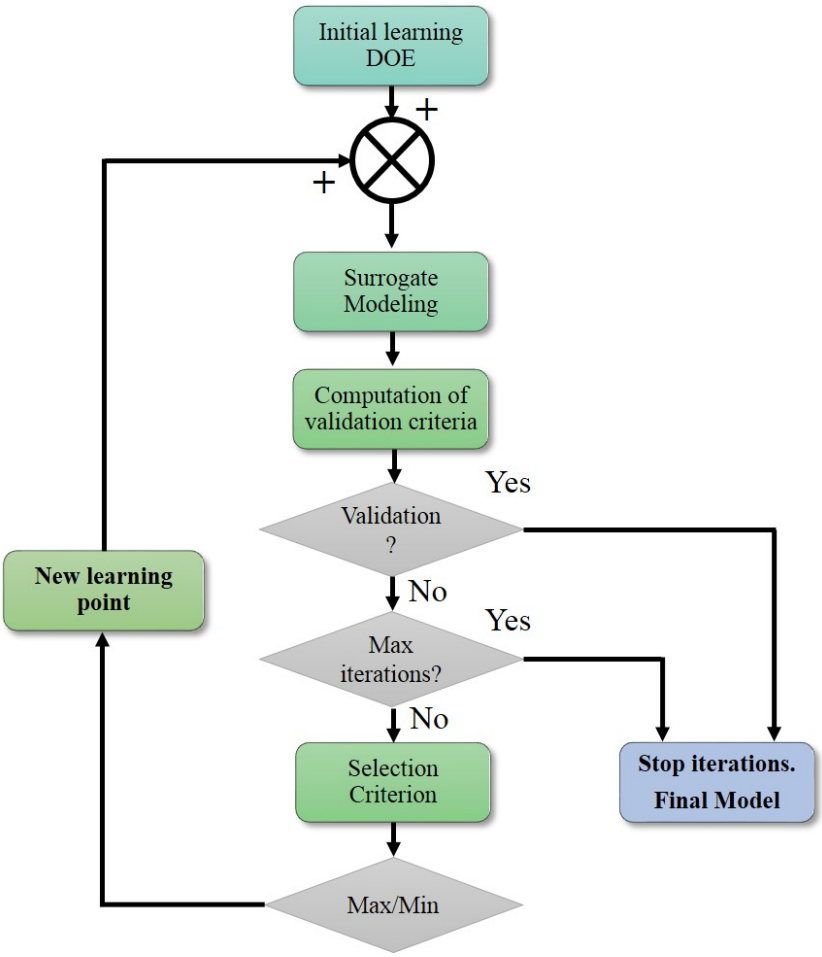


Figure 3.17 *Schematic of a typical sequential learning process.*

Sequential learning is widely used in the scientific community (Scheidt, 2006; Marrel, 2008; Forrester, et al., 2009) and references therein. The main difficulty of these methods is to define the selection criterion for identifying suitable new sampling locations. These criteria can differ from one application to another. One general idea is to encompass both global and local optimization aspects. For example, Jones *et al.* (Jones, et al., 1998) used sequential learning to maximize or minimize a function with a Kriging model. The criterion they defined was the expected improvement, which is a combination of the Kriging variance and the difference from the best current solution. The use of Kriging variance ensures a global optimization aspect, while the use of the gap between the outputs and the best solution at each point guarantees a local optimization aspect. Similarly, Bichon *et al.* (Bichon, et al., 2008) applied sequential learning to the computation of failure probabilities and defined a selection criterion based on local and global optimization in which the global aspect was also provided by the Kriging variance. The present application has a different objective, so it requires a novel selection criterion.

3.4.2 Proposal of a new selection criterion

In this study, the objective of the sequential learning is to improve the quality of the model. The validation criterion will be defined as a combination of three conditions:

$$\begin{cases} Q2 > Q2^{min} \\ |\mu_{CV}| < \mu_{CV}^{max} \\ \sigma_{CV} < \sigma_{CV}^{max} \end{cases} \tag{3.32}$$

where $Q2^{min}, \mu_{CV}^{max}$ and σ_{CV}^{max} are the minimum acceptable value of the Q2 index, the maximum acceptable absolute value of μ_{CV} and the maximum acceptable value of σ_{CV}, respectively. Note that as in the optimization criterion defined in section 3.3.5.2, this validation criterion requires a test learning DOE, which is expensive in terms of computation time. Therefore, the same test DOE that was used in section 3.3.5.2 will be used.

The proposed selection criterion is based on both the Kriging variance and the modeling errors that are computed by cross-validation (c.f. section 0). The SVR-Kriging mean square error provides the global aspect by indicating the location with the lowest density of learning points, and the modeling error provides the local aspect by showing areas where these learning points are the most significant for the SVR-Kriging model. The selection criterion SC is defined as follows:

$$\begin{aligned} &SC\colon \mathbb{R}^n \longrightarrow [0;1] \\ &\underline{x} \longmapsto \alpha\left(\frac{\|MSE(\underline{x})\|}{\max\limits_{x\in\mathbb{R}^n} MSE(\underline{x})}\right) + \beta\left(\frac{\|\hat{e}(\underline{x})\|}{\max\limits_{x\in\mathbb{R}^n} \hat{e}(\underline{x})}\right) \end{aligned} \tag{3.33}$$

where MSE and $\hat{e}$ are the SVR-Kriging mean square error and the estimation of the cross-validation modeling error, respectively, defined at each point of the input space $x \in \mathbb{R}^n$, and (α, β) are weighting coefficients for the global and local aspects. The combination of global and local considerations limits the nugget effects that appear when two learning points are too close. The cross-validation modeling error at each point of the input space is estimated by the construction of a surrogate model from the learning couples $(x_i\,;e_{-i})$, $i \in [\![1\,;k]\!]$, where k is the number of learning points. The surrogate model

is chosen as ordinary Kriging with a Gaussian correlation that has a relatively smooth estimation map. Its hyperparameter vectors $\underline{\eta}^{init}, \underline{\eta}^{lb}$ and $\underline{\eta}^{ub}$ are defined as follows:

$$\begin{aligned} \underline{\eta}^{init} &= [0.1 \quad 0.1 \quad 0.1]^T \\ \underline{\eta}^{lb} &= [0.01 \quad 0.01 \quad 0.01]^T \\ \underline{\eta}^{ub} &= [1 \quad 1 \quad 1]^T \end{aligned} \tag{3.34}$$

To find the best new learning sample, the maximum value of the SC function must be found. Classical optimization algorithms such as the DIRECT method (Björkman, et al., 1999) can be used to solve this problem. However, for large input space dimensions, this can be a complex computational task. To avoid this problem and following the approach presented in (Echard, et al., 2011), we computed the CV at a large sample of points, such as with Monte Carlo, an Important Sampling or a large dimension LHS DOE. The problem of finding the maximum of a continuous function will then be transformed into the simpler problem of finding the maximum value of a discrete set of points. The final sequential learning process is graphically presented in Figure 3.18.

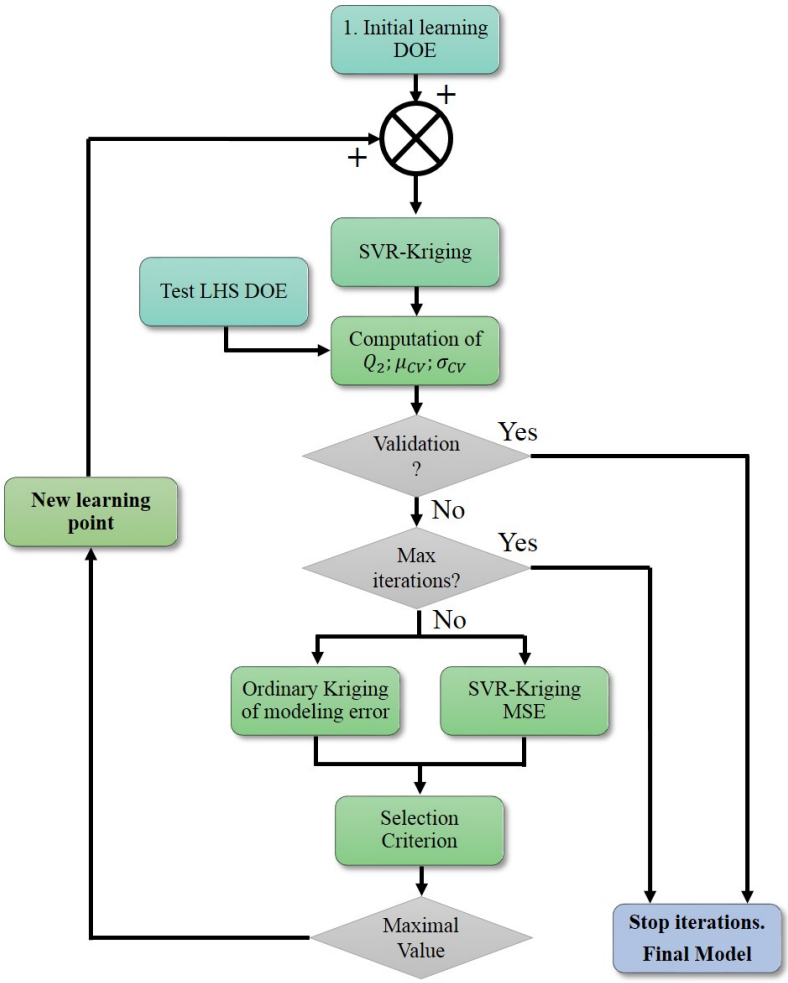


Figure 3.18 *Schematic of the proposed sequential learning process.*

Note that in the multiple outputs configuration, the SVR-Kriging model is built for each output, but they share both the same input space and the same learning sets so as to limit the computational costs.

The validation criteria are calculated for each SVR-Kriging model $i, i \in [\![1\,;h]\!]$. The iterations finish either when all of the models are validated or when the number of iterations is greater than $4u$, where u is the number of uncertain parameters. One value of selection criterion is then computed for each model so that h new learning points are proposed. The point is chosen via random selection according to the probabilities $p_1, \dots, p_h$ assigned to each SVR-Kriging model. This probability assignment is performed as follows:

$$p_i = \frac{\max\limits_{i=1,\dots,h} OC_i - OC_i}{\sum_{i=1}^{h}\left(\max\limits_{i=1,\dots,h} OC_i - OC_i\right)}, i = 1, \dots, h \tag{3.35}$$

where OC_i is the optimization criterion defined in section 3.3.5.2 computed for the SVR-Kriging model i. The final multi-output sequential learning process is graphically presented in Figure 3.19. For the initial learning DOE, we propose to use the learning vectors relative to the single dimension SVRs.

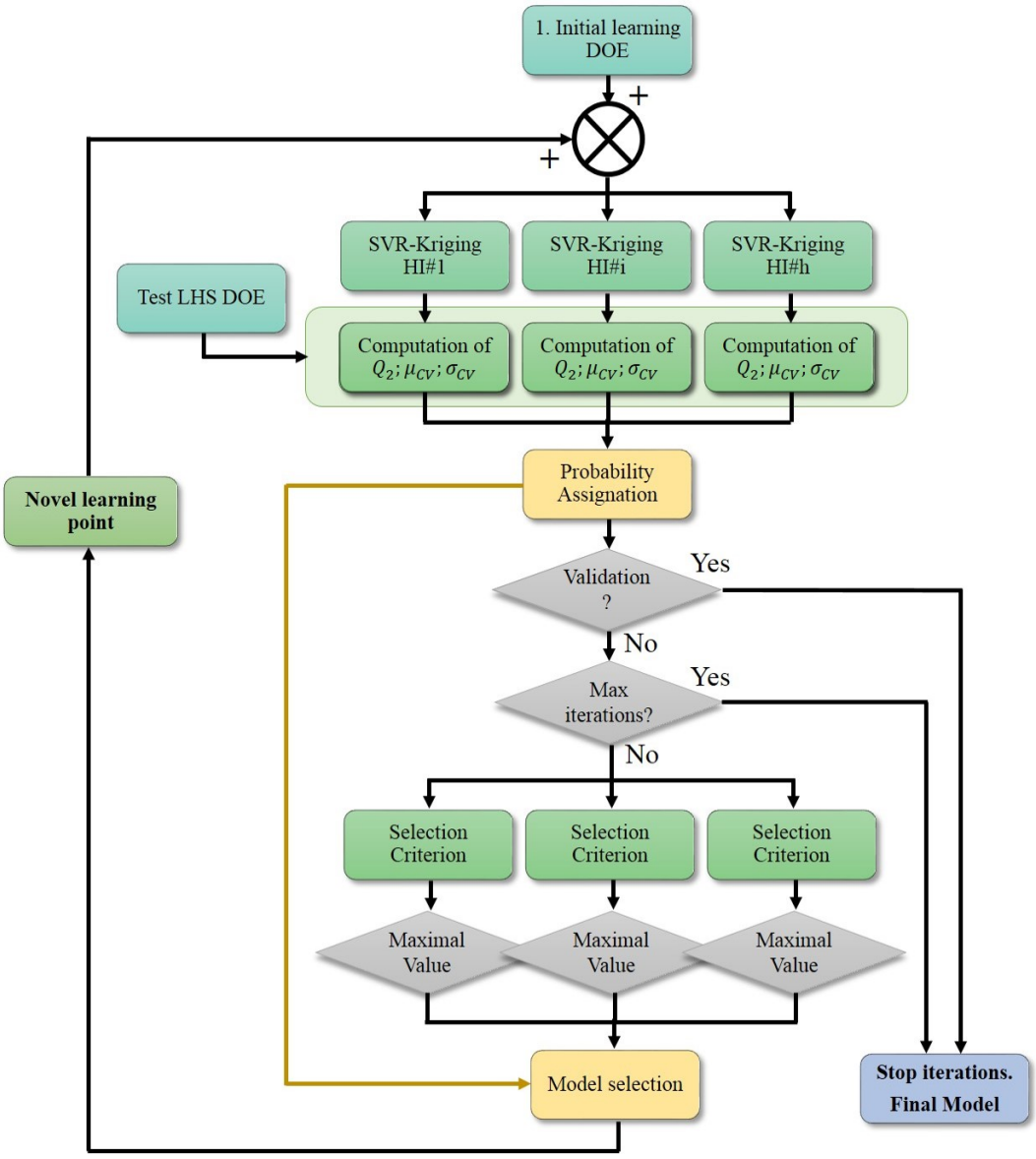


Figure 3.19 *Sequential learning process for multiple outputs.*

3.4.3 Validation of sequential learning on test models

To validate the efficiency of sequential learning for improving the accuracy of SVR-Kriging, the algorithm is tested on the 3D Ishigami functions. The indices of μ_{CV}, σ_{CV} and $Q2$ are computed for 15 iterations of the sequential learning algorithm for two set of values (α, β). The first case is the control case and only uses the MSE information for the selection criterion so that $(\alpha, \beta) = (1,0)$. The second case uses $(\alpha, \beta) = (1,1)$ and is aimed at demonstrating the benefits of using the CV information. For both cases, the sequential learning process is iterated 50 times with random initial learning LHSDOEs. The LHSDOE is composed of only two points. The results for the first case are graphically presented in Figure 3.20.

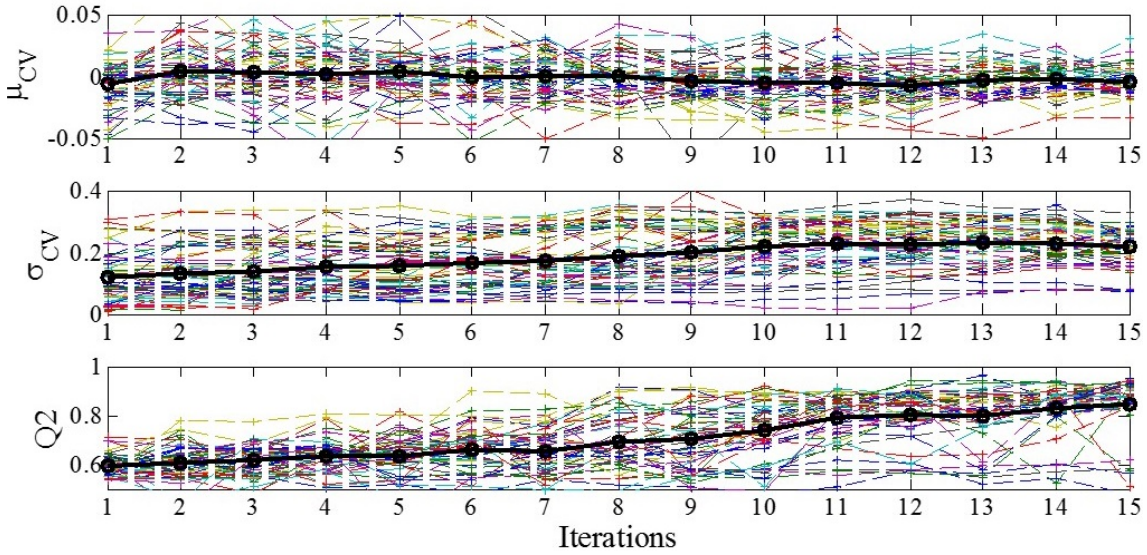


Figure 3.20 *Graphical results of the sequential learning process for (α,β)=(1,0).*

The results in Figure 3.20 show that for $(\alpha, \beta) = (1,0)$, the values of $Q2$ increase constantly, which is a good result. However, the σ_{CV} index also increases constantly, which indicates a decrease of performance. In parallel, the values of μ_{CV} are globally constant. These results can be compared with those in Table 3.8. Because the results in Table 3.8 were obtained for 12 learning points in the LHSDOE, they are compared with those of the 10th iteration in Table 3.9.

Iteration	Mean and standard deviation of μ_{CV}	Mean and standard deviation of σ_{CV}	Mean and standard deviation of Q2
Iteration 1	$(-0.005;\ 0.013)$	$(0.12;\ 0.04)$	$(0.60;\ 0.08)$
Iteration 5	$(0.004;\ 0.013)$	$(0.16;\ 0.04)$	$(0.64;\ 0.08)$
Iteration 10	$(-0.005;\ 0.011)$	$(0.22;\ 0.03)$	$(0.74;\ 0.08)$
Results of Table 3.8 for 50 $\underline{\theta}$ optimization iterations	$(-0.003;\ 0.012)$	$(0.14;\ 0.04)$	$(0.72;\ 0.08)$
Iteration 15	$(-0.004;\ 0.009)$	$(0.22;\ 0.03)$	$(0.85;\ 0.11)$

Table 3.9 *Results of the sequential learning process for (α,β)=(1,0).*

The comparison of Table 3.7 and Table 3.9 shows that when only the MSE is used, the results obtained by sequential learning are worse than those provided by a global learning LHSDOE. The values

of $Q2$ are slightly better, but σ_{CV} is significantly worse; this is because for relatively low dimensions, the unsampled areas are narrow. The results for the second case are graphically presented in Figure 3.21.

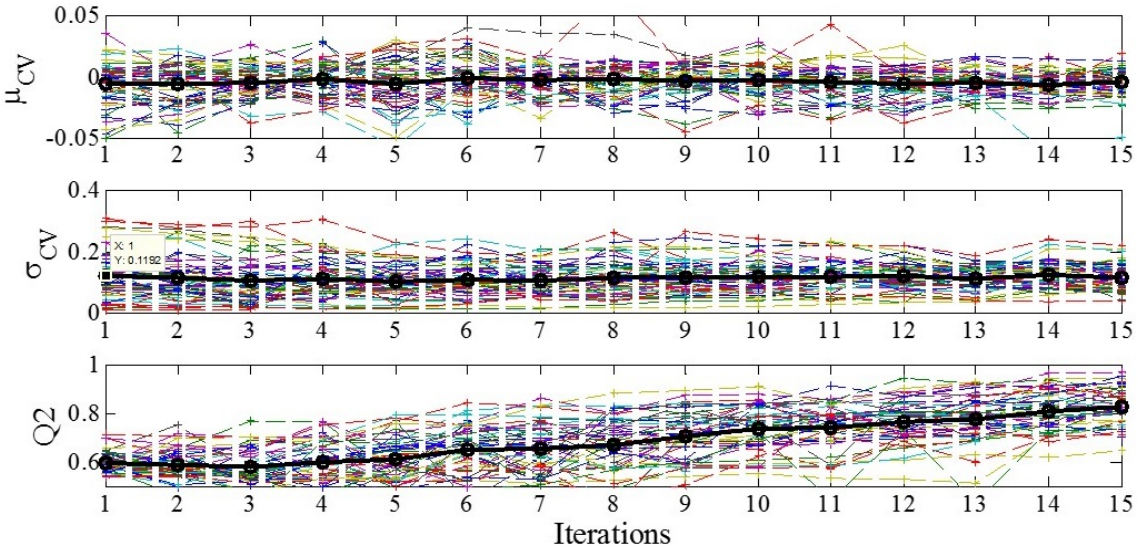


Figure 3.21 *Results of the sequential learning process for (α,β)=(1,1).*

The main difference from the first case is that σ_{CV} is globally constant, while $Q2$ increases. The results of Table 3.10 indicate that the values of both σ_{CV} and $Q2$ are better than those obtained for the learning DOE without sequential learning.

Iteration	Mean and standard deviation of μ_{CV}	Mean and standard deviation of σ_{CV}	Mean and standard deviation of Q2
Iteration 1	$(-0.006;\ 0.013)$	$(0.12;\ 0.04)$	$(0.60;\ 0.08)$
Iteration 5	$(-0.006;\ 0.012)$	$(0.10;\ 0.04)$	$(0.61;\ 0.08)$
Iteration 10	$(-0.003;\ 0.010)$	$(0.11;\ 0.03)$	$(0.74;\ 0.08)$
Results of Table 3.8 for 50 $\underline{\theta}$ optimization iterations	$(-0.003;\ 0.012)$	$(0.14;\ 0.04)$	$(0.72;\ 0.08)$
Iteration 15	$(-0.004;\ 0.008)$	$(0.11;\ 0.02)$	$(0.82;\ 0.07)$

Table 3.10 *Results of the sequential learning process for (α,β)=(1,1).*

Even though the efficiency of the sequential learning algorithm with the novel selection criterion was demonstrated with quantifiable results, the gain in performance with respect to the normal learning DOE without iterations is not significant in this example. However, the results indicate that the performance increases with the dimension of the input space, so this method will be used for the application.

3.4.4 Final plan of the numerical experiment

Figure 3.22 summarizes the plan of the entire numerical experiment.

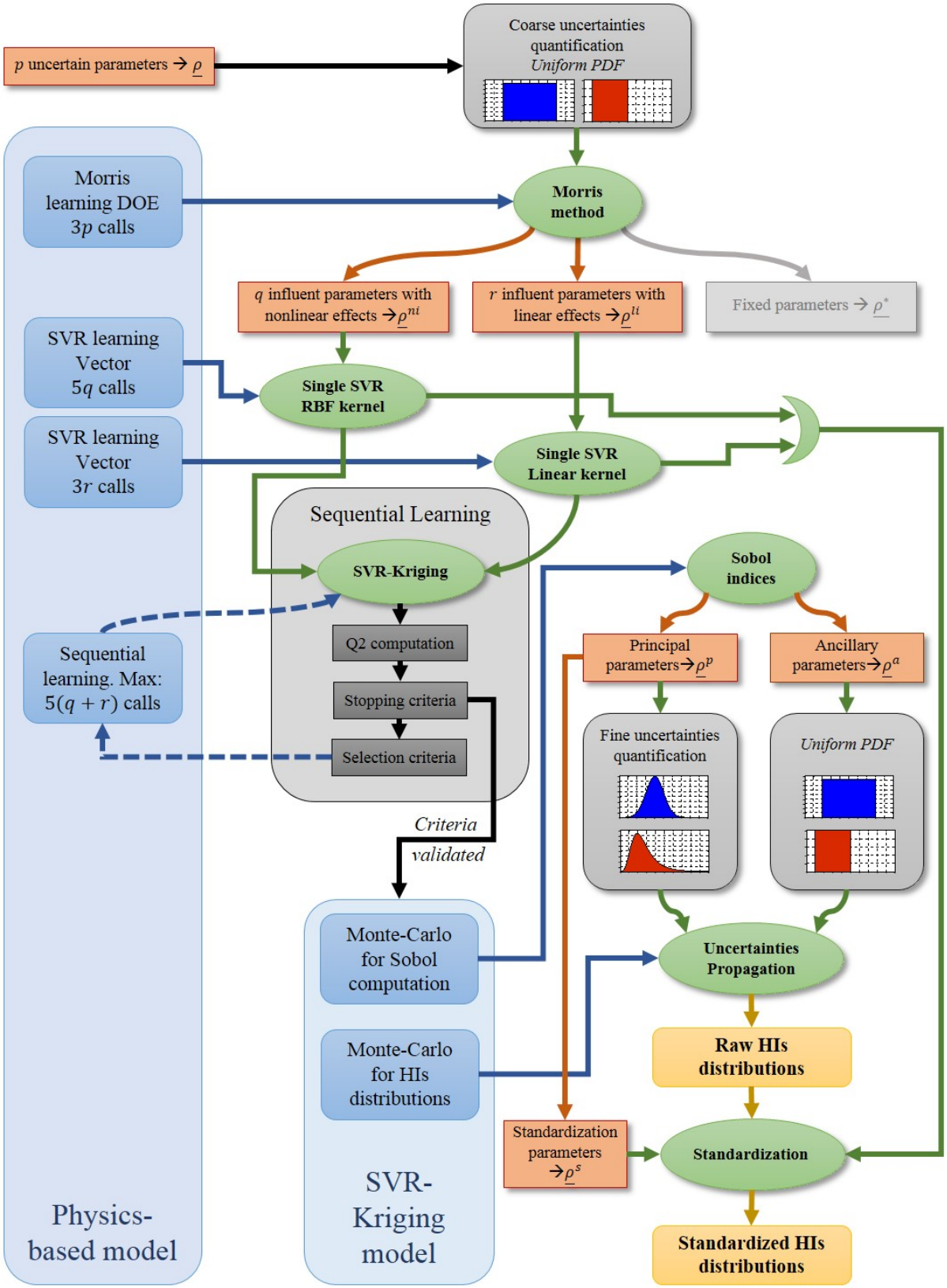


Figure 3.22 *Global schematic of the numerical experiment.*

3.4.5 Computational issues

Three types of computational issues are encountered in applications of the SVR-Kriging technique to multiple output physics-based models with a large number of dimensions: the duration of the

$\underline{\theta}$ optimization algorithm, the computation time of the cross-validation and the length of the sequential learning step. The proposed solutions are to supervise the $\underline{\theta}$ optimization algorithm using the sensitivity analysis results, to perform only partial cross-validation computation and to add multiple learning points in parallel for the sequential learning.

3.4.5.1 *Sensitivity analysis-supervised $\underline{\theta}$ optimization algorithm*

In cases where the dimension of the parameters space is large (typically greater than 20), estimating the SVR-Kriging hyperparameter vector $\underline{\theta}$ using the $\underline{\theta}$ optimization algorithm can take a very long time on a classical desktop computer. For a model with 20 parameters, determining the best value of $\underline{\theta}$ using an exponential-Gaussian correlation function with anisotropic values of the superscripts requires simultaneously optimizing a set of 40 values. This complex process can take a significant amount of time. The proposed solution is to constrain the optimization problem of the hyperparameter vector $\underline{\theta}$ to only a well-chosen proportion of the parameters. The selection of the parameters to be optimized is supervised by the results of the Morris method, which allows sorting a hierarchy of parameters according to the importance of their effect on the i^{th} HIs. Subsequently, the n_{opt} parameters with the most important effects can be chosen. The $\underline{\theta}$ optimization algorithm is then run to optimize only the coefficient associated to the n_{opt} chosen parameters. The value of n_{opt} is chosen by the user and is dependent on the available computational capabilities. For example, considering the 3D Ishigami model and assuming that only the first and second parameters are taken into account for the $\underline{\theta}$ optimization algorithm, $\underline{\theta}$ can be parameterized as follows:

$$\begin{aligned} \underline{\theta_1}^{init} &= [1e^x \quad 1e^x \quad 1e^x]^T;\ \underline{\theta_2}^{init} = [y \quad y \quad y]^T \\ \underline{\theta_1}^{lb} &= [1e^{-8} \quad 1e^{-8} \quad 1e^x]^T;\ \underline{\theta_2}^{lb} = [1 \quad 1 \quad y]^T \\ \underline{\theta_1}^{ub} &= [100 \quad 100 \quad 1e^x]^T;\ \underline{\theta_2}^{ub} = [2 \quad 2 \quad y]^T \end{aligned} \tag{3.36}$$

where x and y are random variables that are selected according to the following PDFs:

$$\begin{aligned} x &\sim \mathcal{U}(-8;2) \\ y &\sim \mathcal{U}(1;2) \end{aligned} \tag{3.37}$$

Note that in contrast to the parameterization in section 3.3.5.2, the random selection of $\underline{\theta_1}^{init}$ and $\underline{\theta_2}^{init}$ is isotropic; this is because the anisotropic case requires more random selections, which entails an additional computational cost.

3.4.5.2 *Partial cross-validation computation*

For a SVR-Kriging model that is developed from n learning samples, the computation of the cross-validation errors requires learning n SVR-Kriging models. To limit the computation time, we propose computing the cross validation for only a small sample of the entire set of learning points. In practice, we propose considering only one point out of n_{CV} for the computation of the cross-validation error. Under this assumption, the parameters μ_{CV} and σ_{CV} introduced in section 3.3.1 are computed as follows:

$$\mu_{CV} = \frac{\sum_{i=5k,k=1,\dots,\lfloor n/n_{CV} \rfloor} e_{-i}}{\lfloor n/n_{CV} \rfloor}\left(\frac{1}{3\sigma_y}\right)$$
$$\sigma_{CV} = \sqrt{\frac{\sum_{i=5k,k=1,\dots,\lfloor n/n_{CV} \rfloor}(e_{-i} - \mu_{CV})^2}{\lfloor n/n_{CV} \rfloor}}\left(\frac{1}{3\sigma_y}\right) \quad \textbf{(3.38)}$$

where $\lfloor a \rfloor$ is the minimum value of a. As for the selection of n_{opt}, the choice of n_{CV} is at the discretion of the user; in the next chapter, for example, n_{CV} is chosen to be equal to 5.

3.4.5.3 *Parallel sequential learning*

The last source of computational issues is the sequential learning process. The iterative aspect of this technique evaluates the physics-based models one after the other because the results of the previous step are needed to compute the selection criterion for the current step. To reduce the computation time, we propose running n_{par} physics-based model evaluations in parallel. Thus, the total computation time is divided by n_{par}. The suitable new learning points are then selected by randomly drawing a set of n_{par} suitable models with respect to the probability assignments (c.f. Figure 3.19). The choice of n_{par} is also at the discretion of the user with the constraint that n_{par} must be greater than the number of HIs.

The use of these tools to reduce the computational load is at the discretion of the user. If time is limited, it is necessary to decrease the computation complexity, but in the contrary case or when a supercomputer is available, these solutions are not necessary.

3.5 Conclusion

The main result of this chapter is that a novel Kriging technique was developed for the estimation of aircraft engines physics-based models. This technique, which is called SVR-Kriging and is adapted to the specifics of the present application, provided promising results compared with classical approaches.

The first contribution of this chapter is a review of the construction of Kriging models. The chapter begins with a general introduction of the principles of surrogate modeling. Subsequently, the state of the art of the construction of learning DOE is described. Several approaches are reviewed, particularly the use of Latin hypercube sampling with a random generation and the *maximin* criterion-based selection, which is aimed at ensuring good space filling properties. Lastly, the theoretical aspects of Kriging are presented, and a classification of all of the techniques in the literature is proposed. The classification distinguishes between non-stationary Kriging, disjunctive Kriging, Bayesian Kriging, Kriging with linear partial differential equations and CoKriging and emphasizes the non-stationary methods.

The second contribution is the proposal of a novel Kriging technique, called SVR-Kriging that is adapted to the specifics of aircraft engine models. The principle of this technique is to use single dimension SVR as the deterministic part of Kriging. Thus, the first order effects are modeled precisely, even in cases of nonlinearities. The Gaussian process of Kriging is then used to model the interaction effects. This approach is better adapted to the estimation of aircraft engine models than typical Kriging techniques. To demonstrate this assertion, the accuracy of SVR-Kriging is compared with ordinary and universal Kriging for the estimation of three simple models that are representative of the typical behaviors of the models encountered in this field: a one dimensional analytical function that is strongly nonlinear, a two dimensional model with nonlinearities and weak interaction effects and the well-known Ishigami function. The comparisons are based on both the $Q2$ index and the mean μ_{CV} and standard

deviation σ_{CV} of the cross-validation error. SVR-Kriging shows promising results because its estimations of the test functions are better than other techniques; in fact, the larger the input space is, the better the results of SVR-Kriging are. Two techniques are proposed to improve the estimation of the hyperparameters by the $\underline{\theta}$ optimization algorithm. First, the model is computed for several random initial selections for the value of $\underline{\theta}$, and the best model is selected; thus, the robustness to the initial conditions is ensured. The second technique is to use a configuration that is heterogeneous with respect to the dimensions for the exponent of the exponential-Gaussian correlation function so that more degrees of freedom are available. These improvements are tested on the test models and increase the accuracy of the SVR-Kriging estimation.

The last contribution is to validate and improve the SVR-Kriging technique. An original set of validation criteria based on the Q2 index and the cross-validation error is defined. A novel sequential learning procedure is proposed for cases where the set of criteria has not been validated. The procedure is based on the selection criterion SC, which is computed as the weighted sum of the Kriging variance and the cross validation error. The latter is estimated by an ordinary Kriging model using the same inputs as SVR-Kriging. The idea is that the Kriging variance provides a global aspect to the selection process of the novel learning point, which allows targeting the areas where the sampling density is the lowest, while the cross-validation error provides a local aspect that allows focusing on areas where the sampling points have the most significant effects on the model precision. Because the considered physics-based models have multiple outputs, the last aspect of the sequential learning process is proposing a solution to manage this particularity. This involves choosing the one model from the set that is most desirable to add a sampling point from a probability assignment. For each model, the selection probability is assigned with respect to the current accuracy of the model; the less accurate models have higher probabilities. Lastly, original computational improvements are proposed to reduce the computation time for estimating the SVR-Kriging hyperparameters and for the sequential learning procedure. The former consists of supervising the choice of correlation parameters using the Morris method results, and the latter consists of adding novel learning points in batches using parallel model evaluations.

An efficient method to estimate the outputs of complex physics-based models of aircraft engines is now available. Moreover, it is possible to evaluate the accuracy of this surrogate model and to improve it if necessary. However, it has been tested only for simple pedagogical models; it still must demonstrate its efficiency in actual applications.

4

Application to the development of a PHM solution for a generic aircraft engine fuel system

Abstract: For the application of both the approaches proposed in the first chapter and the tools developed in chapters 2 and 3, the considered host system is a generic aircraft engine fuel system. In particular, the considered engine is a turbofan for which the thrust is generated by the fan rotation transmitted from turbines that are powered by the combustion of a gas and air mixture after compressors have increased the air pressure upstream. The mechanical link between turbines and compressors ensures the continuous rotation. The fuel system is in charge of metering the amount of fuel to be injected in the combustor. It includes multiple functional units such as pumps, filters, fuel metering devices and locally controlled inlet air variable geometries and several LRUs, such as actuation control units, actuators and sensors. Each of its subsystems can be affected by different degradations, leading to various compliant service threats. However, there is currently no global solution for monitoring. Therefore, the fuel system is a good candidate for the application of the IDPHM approach. One evaluation of its associated physics-based model for the simulation of a single flight hour is approximately 5 hours long. For monitoring, 22 compliant service indicators and 116 health indicators are defined. In parallel, 80 uncertain parameters are identified. Considering this large number of parameters and the simulation time of the model, this system is also a good candidate for the developed mathematical tools. The application of the Morris method allows identifying 59 influent parameters, among which 11 are linear. An SVR-Kriging model is trained using monodimensional learning vectors with a 2-point Latin hypercube sampling DOE, and a sequential learning process allows reaching the required accuracy. The distributions of the defined health indicators are then computed via uncertainty propagation for 71 degradation modes with six growing intensities. The NKPIs are then computed, and associated criteria are compared with specified ones. The results reveal that the defined raw health indicators set for a fleet model do not comply with the expectations. The standardization process increases the performances, and the set of health indicators is validated only for individual models.

Overview

4.1 Introduction 176
4.2 Introduction to aircraft engines fuel systems 177
4.2.1 Introduction to aircraft engines 177
4.2.2 The fuel system 178
4.2.3 Level 2 subsystems of the fuel system 181
4.2.4 Level 1 subsystems of the fuel system 185
4.3 Selection of HIs and CSIs 191
4.3.1 Level 2 subsystems of the fuel system 191
4.3.2 Level 1 subsystems of the fuel system 195
4.3.3 Level 0: fuel system 202
4.3.4 Parameters 203
4.4 Construction and validation of the surrogate model 206
4.4.1 Designs of experiments 206
4.4.2 SVR-Kriging modeling and validation 206
4.5 Standardization of HIs 209
4.5.1 Computation of Sobol indices 209
4.5.2 Examples of standardization effects 209
4.6 Validation of HIs 210
4.6.1 Specifications 210
4.6.2 NKPIs of real HIs for fleet models 211
4.6.3 NKPIs of standardized HIs for fleet models 213
4.6.4 NKPIs of real HIs for individual models 213
4.6.5 NKPIs of virtual HIs 213
4.7 Conclusion 214

4.1 Introduction

In this chapter, the complete developed methodology is applied to the development of a PHM solution to monitor a generic aircraft engine fuel system (Moir, et al., 2008). The main function of the fuel system is to regulate the fuel supply of the combustion chamber. Its secondary functions are to cool the lubrication oil and to drive variable geometries. This system has been chosen because it is a good candidate for several reasons. It contains numerous potential threats. It is a complex system, and the physics-based model is time-demanding on available computers.

First, the architecture of the system is introduced via its functional and structural breakdowns. The former includes several functional units such as pumps, filters, fuel metering devices and locally controlled inlet air variable geometries. The latter contains LRUs such as actuation control unit, actuators and sensors. Each of the functional units is presented in detail so that the following steps are more easily understood. Note that the scope of this application does not consider degradation modes affecting harnesses, hydraulic pipes or the engine control unit.

Second, the selection of health indicators (**HIs**) for the PHM of the fuel system is addressed. For each functional unit, the compliant service threats (**CSTs**) and degradation modes (**DEMs**) are

identified. From these elements, the lists of HIs and compliant service indicators (**CSIs**) are determined. Both real and virtual HIs are built to handle the case where existing sensors are insufficient.

Third, the construction of the SVR-Kriging for the estimation of the model of the fuel system is addressed. The initial characterization of uncertainties is presented, and the sets of influent and linear parameters are computed from sensitivity analysis. First, models with monodimensional support vector regressions (**SVRs**) only are trained to compute the median limit values (**MLVs**) of DEMs. The accuracy of these SVR models are compared with those of the SVR-Kriging models trained with the same points to prove the efficiency of the proposed modeling approach. The sequential learning process is then performed to reach the desired final accuracy.

Fourth, the standardization procedure is applied. A more precise sensitivity analysis based on the Sobol indices is performed to determine the standardization parameters. The standardization models are then estimated by SVR. The effect of standardization on the distribution of HIs is illustrated through several examples.

Finally, the uncertainties propagation is run on the SVR-Kriging model, and the validation of HIs is performed. Numerical key performance indicators (**NKPIs**) are computed for different configurations. The compliance with detection, identification, localization and prognostics criteria are computed and criticized for different set of HIs. Operational impacts from an industrial point of view are eventually highlighted.

4.2 Introduction to aircraft engines fuel systems

4.2.1 Introduction to aircraft engines

Aircraft engines are complex systems whose main role is to generate mechanical power. It is part of the aircraft propulsion system with the nacelle. For large commercial aircraft, engines are currently either of turbofan or turboprop types. In this work, only turbofan engines will be considered. In this type of engines, the propulsive properties are provided by the velocity difference between the inlet and outlet. During the functioning, the compressors increase the air pressure for the combustion. After the combustion, gas is ejected and drives the turbines. Because turbines and compressors are on the same shaft, continuous rotation is ensured (see Figure 4.1).

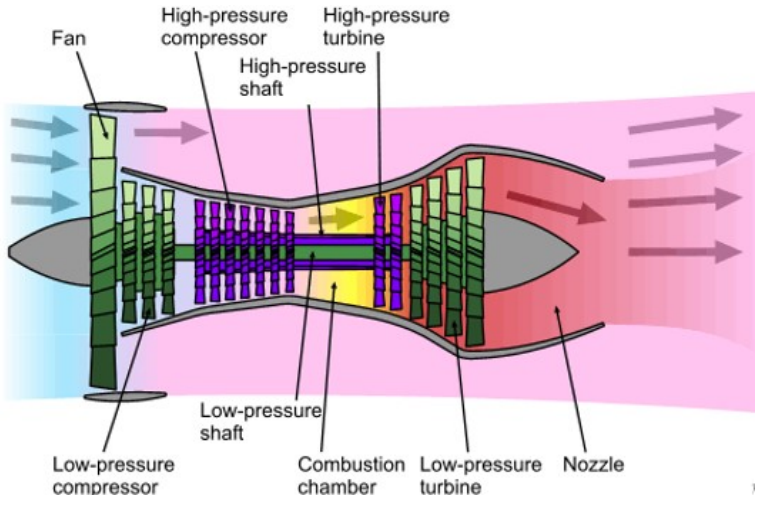


Figure 4.1 *Functioning scheme of a two-stages turbofan*

The good functioning of turbofans relies on an interaction of various subsystems (Moir, et al., 2008). For example, the breakdown architecture of the SaM146 is composed of the following: the electric control and protection system, oil and power transmission system, pneumatic system, electrical system, fuel system and starter system. Then, all of these principal subsystems are divided into other entities. In the scope of this work, the study will be limited to the monitoring of the fuel system and its underlying entities. As mentioned, aircraft engines architecture can vary. Therefore, it is useful to choose a benchmark architecture for the application of IDPHM. The chosen architecture of the fuel system is similar to the one of the SaM146. Note that this engine is already certified, so it is actually not possible to apply the IDPHM. However, to simulate real development conditions, it will be supposed that access to in-service data is not possible for the selection and validation of HIs.

4.2.2 The fuel system

4.2.2.1 *System's functional analysis*

The main function of the fuel system is to regulate the fuel supply of the combustion chamber. Its secondary functions are to cool the lubrication oil and to drive variable geometries. It is possible to define the functional units or subsystems of the fuel systems from the specification documents.

- **Low pressure pump (LPP):** boosting centrifugal pump to provide the minimal pressure at the inlet of the main fuel pump to avoid cavitation.
- **Main fuel pump (MFP):** positive displacement gear pump to provide the flow to downstream equipment.
- **Main fuel filter (MFF):** to retain particles from the fuel circuit to protect the main fuel pump and metering organs.
- **Fuel metering unit (FMU):** subsystem aimed at regulating the amount of fuel injected into the combustion chamber. It is composed of the following:
  - ***Fuel metering valve loop (FMV):*** to regulate the position of the metering valve.
  - ***High Pressure Shut-Off Valve (HPSOV):*** to ensure a minimal pressure in the circuit.
  - ***A bypass valve (BYV):*** to recirculate the excess of fuel provided by the MFP with respect to the injection command.
- **Variable stator vane loop (VSV):** to regulate the angular position of the stator blades of the high pressure compressor aimed at optimizing the global efficiency of the gas turbine.
- **Variable bleed valve loop (VBV):** to regulate the opening of hatches located between the low pressure and high pressure compressors aimed at decreasing the amount of air of the number of particles reaching the combustion chamber.
- **Transient bleed valve loop (TBV):** to provoke a discharge of the airflow at the inlet of the combustion chamber if necessary.
- **WFM:** to measure the injected fuel flow.

Figure 4.2 shows the locations of the variable geometries' actuators. The variable geometries' actuators are those of the VSV, VBV and TBV systems. Their functions will be presented with further details in the following subsections.

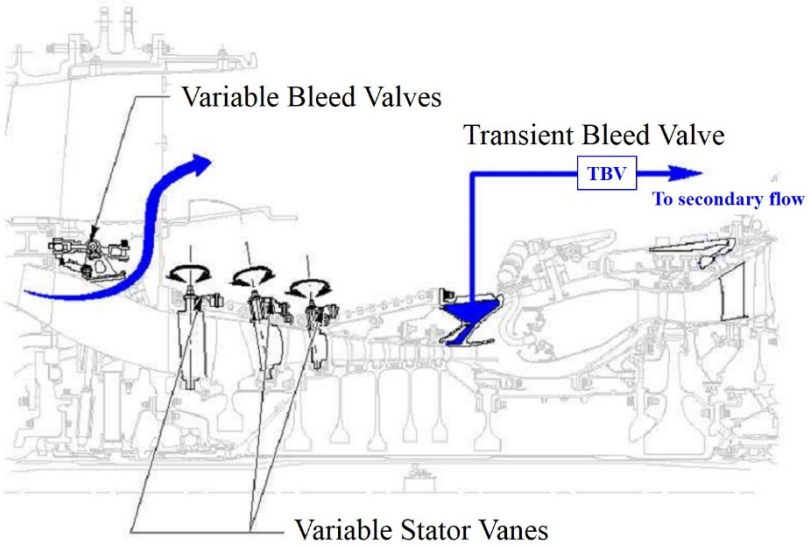


Figure 4.2 *Position of the valves and vanes on benchmark turbofan architecture.*

Finally, the functional breakdown representation of the fuel system from its subsystems presented above is given in Figure 4.3. The further presentation of each subsystems with detailed explanations about the equipment will be provided in following subsections.

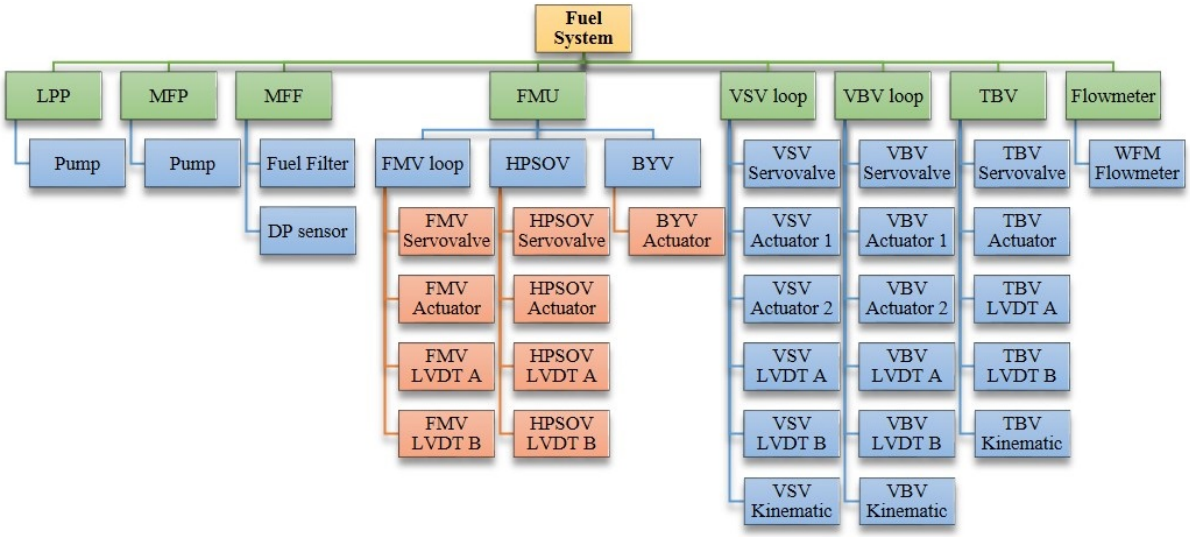


Figure 4.3 *Functional breakdown representation of the fuel system.*

4.2.2.2 *System structural analysis*

Given the specification documents, mostly those about maintenance or assembly, it is possible to define 8 LRUs that are represented in the scheme of the fuel system of Figure 4.4.

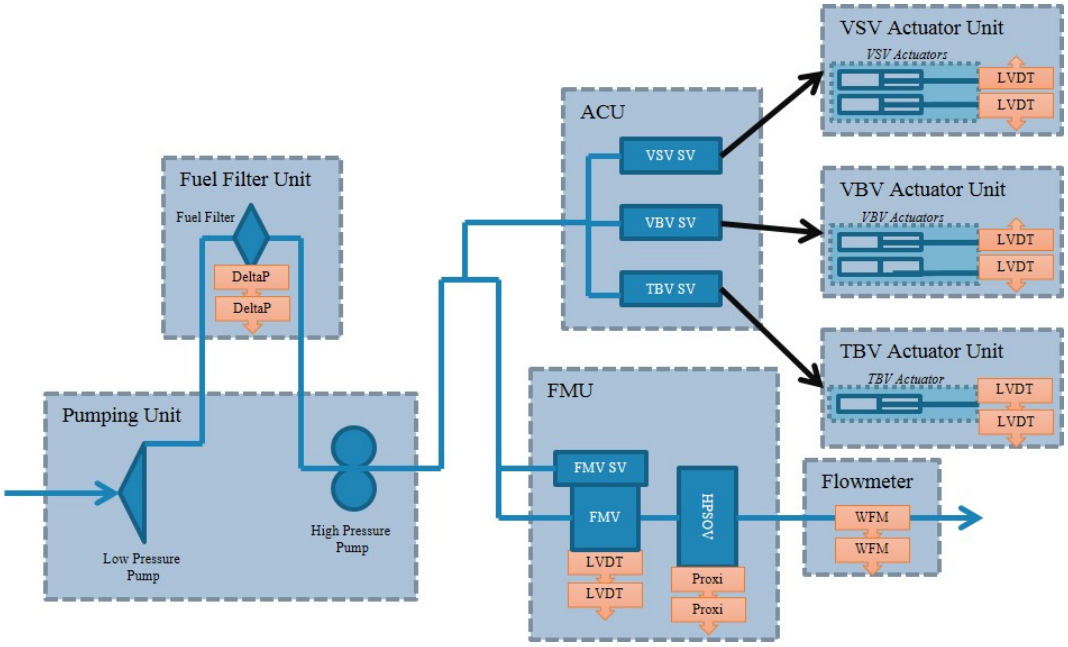


Figure 4.4 *Fuel system scheme with emphasis on LRUs.*

The LRUs presented on Figure 4.4 are organized as follows:

- **Pumping unit:** contains the pumping devices, i.e. the LPP and the MFP.
- **Fuel filter:** contains the MFF and a delta pressure sensor (DP sensor) measuring the pressure difference between its inlet and outlet.
- **Actuation control unit (ACU):** contains the servovalve providing the necessary fuel flow to the variable geometries' actuators.
- **FMU:** contains the FMV, its servovalve and the HPSOV.
- **VSV actuation unit:** contains the two VSV actuators and two linear variable differential transformers (LVDTs) to measure the positions of each one of them independently. It also contains the kinematic chain driven by the actuators.
- **VBV actuation unit:** contains the two VBV actuators and two LVDTs to measure the positions of each one of them independently. It also contains the kinematic chain driven by the actuators.
- **TBV actuation unit:** contains the TBV actuator and two redundant LVDTs to measure its position. Actually, the calculated measure is a Boolean value indicating whether the valve is open (1) or close (0).
- **Flowmeter:** contains a flowmeter to measure the value of WFM, the flow injected in the combustion chamber.

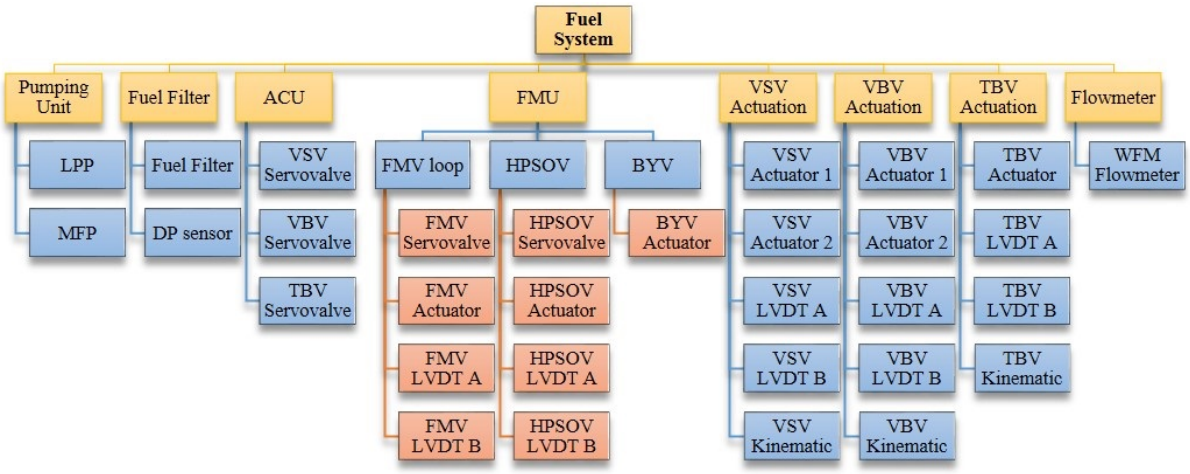


Figure 4.5 *Structural breakdown representation of the fuel system.*

From Figure 4.3 and Figure 4.5, it is possible to construct the LRU association matrix for the fuel system. This matrix is presented in Appendix I.

Finally, in this subsection, the functional and structural analyses of the fuel system have been introduced. As mentioned before, the monitoring of the whole fuel system will be performed via a hierarchical architecture. Therefore, it is level 0 of the architecture. HIs are then defined for every subsystem, starting by the highest architectural level. As presented above, there are 3 subsystems at level 2: the FMV loop, the HPSOV and the Bypass and 8 subsystems at level 1: LPP, MFP, MFF, FMU, VSV loop, VBV loop, TBV and flowmeter.

4.2.3 Level 2 subsystems of the fuel system

4.2.3.1 *Fuel metering valve regulation loop*

The principal function of the FMV regulation loop is to control the displacement of the fuel metering actuator. Then, the position of the spool is associated to an opening section determining the amount of fuel flowing to the downstream circuit. The FMV subsystem is represented in Figure 4.6.

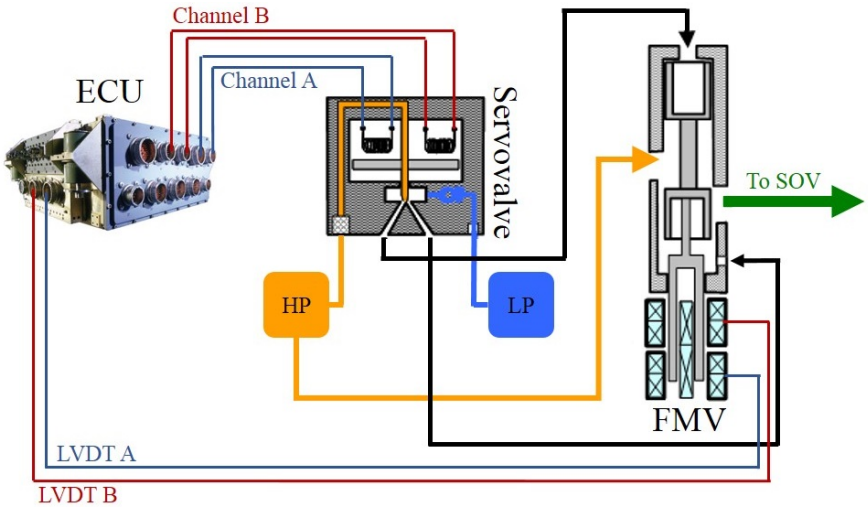


Figure 4.6 *Representation of the FMV subsystem.*

As presented in Figure 4.6, the FMV subsystem is composed of the following equipment:

- **FMV servovalve:** single stage servovalve (torque motor) whose outlet flows are determined by its control current $\boldsymbol{FMVCMD}$. The servovalve can be controlled by either channel A or B. The selection of the active channel is presented in Appendix II. To simplify the study, for the whole chapter, only channel A will be considered as used for every control loop.
- **FMV actuator:** metering spool with an opening section varying with its displacement according to an exponential law.
- **FMV LVDT A&B:** redundant LVDTs measuring the displacement of the FMV actuator. They relate physical quantities into voltages transmitted to the ECU which converts them into discrete values. A LVDT is structured as follows: a primary winding, powered by an alternator with voltage $\boldsymbol{V_p}$ generates a magnetic field. This magnetic field induces voltages $\boldsymbol{V_{s1}}$ and $\boldsymbol{V_{s2}}$ in the secondary windings. The values $\boldsymbol{V_{s1}}$ and $\boldsymbol{V_{s2}}$ depend on the displacement of the core, fixed to the rod. The displacement of the rod is finally proportional to the value of the output voltage $\boldsymbol{V_{out}} = \frac{\boldsymbol{V_{s1}} - \boldsymbol{V_{s2}}}{\boldsymbol{V_{s1}} + \boldsymbol{V_{s2}}}$.
- **ECU:** controller elaborating the $\boldsymbol{FMVCMD}$ in function of the selected value of the FMV spool displacement $\boldsymbol{FMVSEL}$ and its demanded value $\boldsymbol{FMVDMD}$. The selected value $\boldsymbol{FMVSEL}$ is computed from the preprocessed values from LVDTs A and B named respectively $\boldsymbol{FMVA}$ and $\boldsymbol{FMVB}$. The preprocessing consists mostly of filtering and denoising. The computation of $\boldsymbol{VSVSEL}$ is performed according to the sensor measure selection presented in Appendix III. The architecture of the controller is presented in Appendix IV. The sampling rate of the FMV loop is $\boldsymbol{0.015\ ms}$ (1 RTC). Its block diagram is given in Figure 4.7.

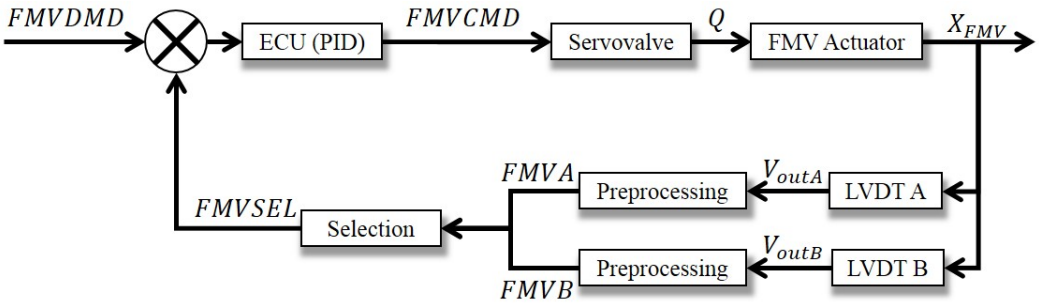


Figure 4.7 *Block diagram of the closed loop regulation of FMV displacement.*

In Figure 4.7, Q is the flow generated by the servovalve and transmitted to the FMV actuator; X_{FMV} is the actual value of the FMV actuator displacement, and V_{outA} and V_{outB} are the output voltages sent to the ECU by, respectively, LVDTs A and B.

4.2.3.2 *High-pressure shut-off valve (SOV)*

The high-pressure shut-off valve, abbreviated SOV, has two principal functions: to cut or activate the injection of fuel in the combustion chamber and to regulate the pressure difference between the high pressure and the low pressure circuits. The SOV subsystem is represented in Figure 4.8.

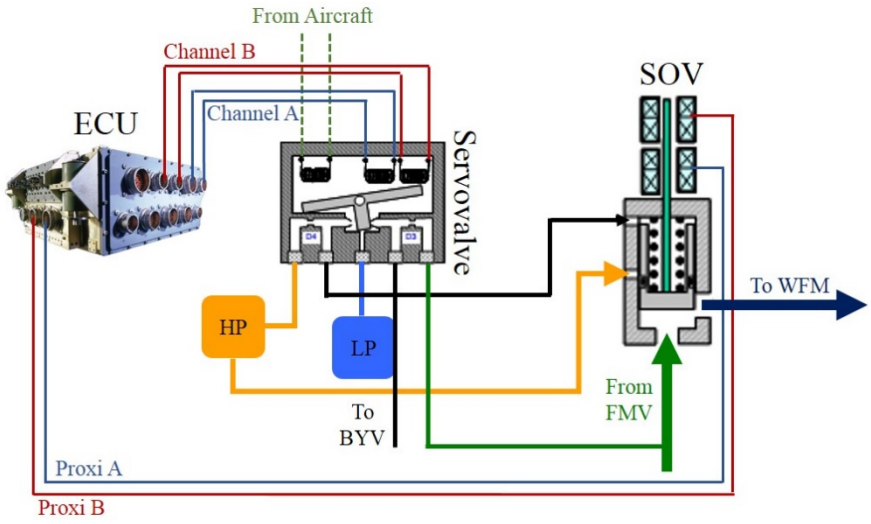


Figure 4.8 *Representation of the SOV subsystem.*

As presented in Figure 4.8, the SOV subsystem is composed of the following equipment:

- **SOV servovalve:** single-stage servovalve whose outlet flows are determined by its control current $\boldsymbol{SOVCMD}$. In this subsystem, the servovalve is commanded in all or nothing. In Figure 4.8, it is in open configuration and the SOV is open too. When it is in close configuration, the HP is sent to the SOV actuator, and the valve is closed.
- **SOV actuator:** spool with an opening section to downstream circuit appearing at a given displacement. This spool is manufactured as a pressure regulator. The spring it contains is aimed at maintaining a pressure difference of $\boldsymbol{20bars}$ between the high- and the low-pressure circuits.
- **SOV Proximeters A&B:** redundant proximeters measuring if the SOV actuator has reached a certain displacement value $\boldsymbol{O_{SOV}}$. They transform physical quantities into voltages and transmit them to the ECU. Then, the ECU converts these voltages into a Boolean value equal to 1 if the displacement is above $\boldsymbol{O_{SOV}}$ and to 0 if it is under.
- **ECU:** controller elaborating the $\boldsymbol{SOVCMD}$ in function of the demanded value $\boldsymbol{SOVDMD}$. It is an open loop system. The ECU computes the Boolean $\boldsymbol{SOVStatus}$ returning the position open/close of the SOV from $\boldsymbol{SOVA}$ and $\boldsymbol{SOVB}$. The sampling rate of the SOV loop is $\boldsymbol{0.03\ s}$ (2 RTC). The block diagram of the SOV loop is given in Figure 4.9.

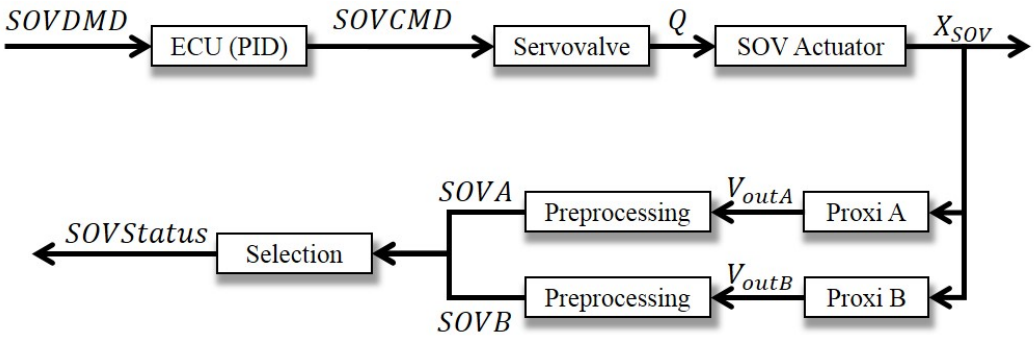


Figure 4.9 *Block diagram of the open loop regulation of SOV displacement.*

In Figure 4.9, Q is the flow generated by the servovalve and transmitted to the SOV actuator; X_{SOV} is the actual value of the SOV actuator displacement, and V_{outA} and V_{outB} are the output voltage sent to the ECU by, respectively, proximeters A and B.

4.2.3.3 *Bypass valve (BYV)*

The principal function of the bypass valve, abbreviated as BYV, is to recirculate the excess of fuel provided by the MFP with respect to the injection command. The characteristic of this recirculation is shown in Figure 4.10. The BYV subsystem is represented in Figure 4.11.

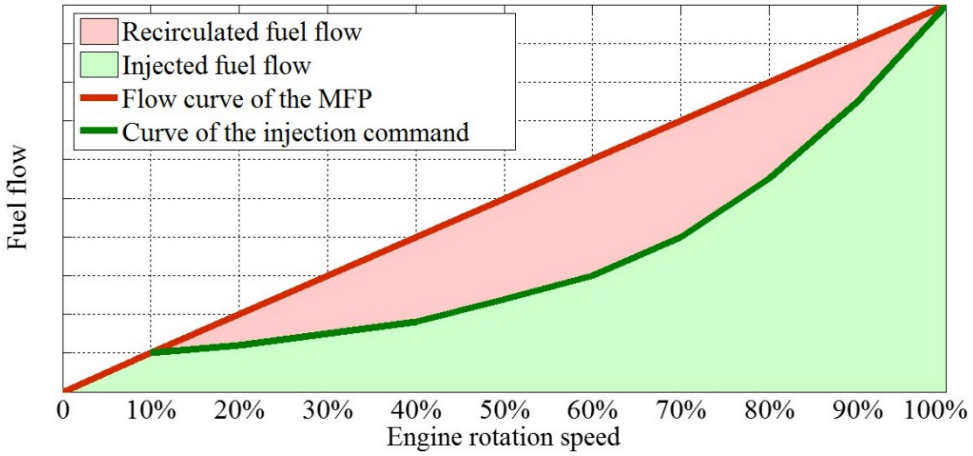


Figure 4.10 *Characteristics of the fuel recirculation loop.*

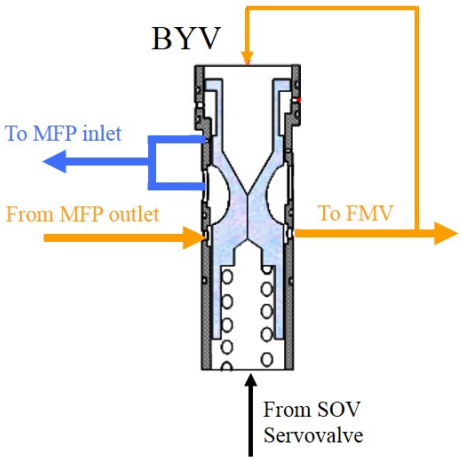


Figure 4.11 *Representation of the SOV subsystem.*

As presented in Figure 4.11, the SOV subsystem is composed of the following equipment:

- **BYV actuator:** spool with a varying opening section between MFP outlet and inlet. This section's function involves regulating the pressure difference between the FMV inlet and the pressure from the SOV servovalve. In cases where the SOV is opened, this pressure is the outlet pressure of the FMV. Thus, in this configuration, the BYV acts in conjunction with the SOV to maintain a constant pressure difference between the FMV outlet and inlet. In the considered generic fuel system, this difference is specified to be equal to $\mathbf{4}\ \boldsymbol{bars}$.

4.2.4 Level 1 subsystems of the fuel system

4.2.4.1 *Fuel metering unit*

The main function of the FMU is to control the amount of fuel flowing to the combustion chamber with a high level of precision. Based on section 0, it is possible to construct the architecture of the whole fuel metering unit subsystem, as represented in Figure 4.12.

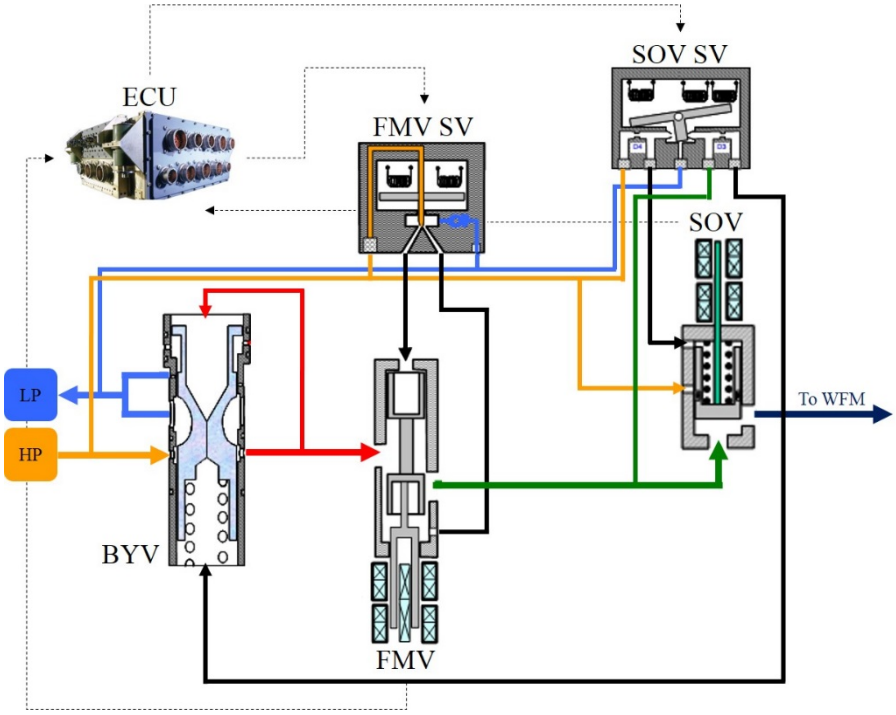


Figure 4.12 *Representation of the FMU subsystem.*

The equipment of the FMU has already been introduced during the presentation of it subsystems (c.f., 0). Let us now look at the other level 1 subsystems of the fuel system.

4.2.4.2 *Low-pressure pump*

The main function of the LPP subsystem is to provide a pressure increase between the aircraft fuel tank pump and the MFP. This pressure increase is aimed at limiting cavitation. The outlet pressure of the LPP defines the pressure of the LP circuit. It is composed of the **LPP device**, a centrifugal pump with outlet pressure ranging from 2 $bars$ to approximately 15 $bars$.

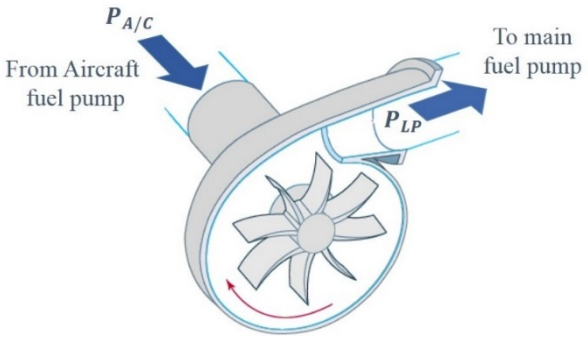


Figure 4.13 *Representation of the LPP subsystem (image issued from http://www.wermac.org/).*

In Figure 4.13, $P_{A/C}$ is the pressure at the inlet of the LPP device, generated from the aircraft fuel pump, and P_{LP} is the pressure of the LP circuit at its outlet.

4.2.4.3 *Main fuel pump*

The main function of the MFP subsystem is to provide the necessary amount of fuel flow to the downstream circuit. The outlet pressure of the MFP defines the pressure of the HP circuit. This subsystem is composed of the **MFP device**, a gear pump with outlet pressure ranging from 2 $bars$ to approximately 60 $bars$.

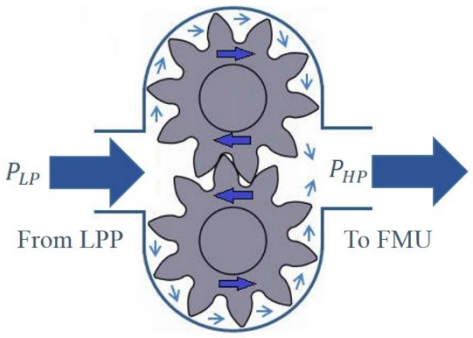


Figure 4.14 *Representation of the MFP subsystem (image issued from http://processprinciples.com/).*

In Figure 4.14, P_{LP} is the pressure from the outlet of the LPP device, and P_{HP} is the pressure of the HP circuit at the outlet of the MFP.

4.2.4.4 *Main fuel filter*

The MFF has two main functions: to filter particles in the fuel system circuit and to measure its own degree of clogging via a DeltaP sensor. This subsystem is composed of the following equipment:

- **MFF device:** fuel filter with orifices that are $\boldsymbol{32\ \mu m}$ in diameter.
- **DeltaP sensor:** sensor measuring the pressure difference between two circuits. It is composed of a non-metallic diaphragm on which the high and low pressures are applied on both sides. The rod displacement is proportional to the pressure difference. It is induced by a force balance between the diaphragm and the negative slope of a Belleville washer used as a reference load.

4.2.4.5 *Variable stator vane regulation loop*

The principal function of the VSV regulation loop is to control the angle of the high-pressure compressor stator blade to optimize the airflow and avoid stalling. This angle is controlled by two linear actuators driven by a single servovalve. These actuators are, respectively, located at the top and bottom of the engine. Both actuators are mechanically linked to a group of three actuation rings transmitting efforts to rotate the blades. The whole mechanical structure is shown in Figure 4.15.

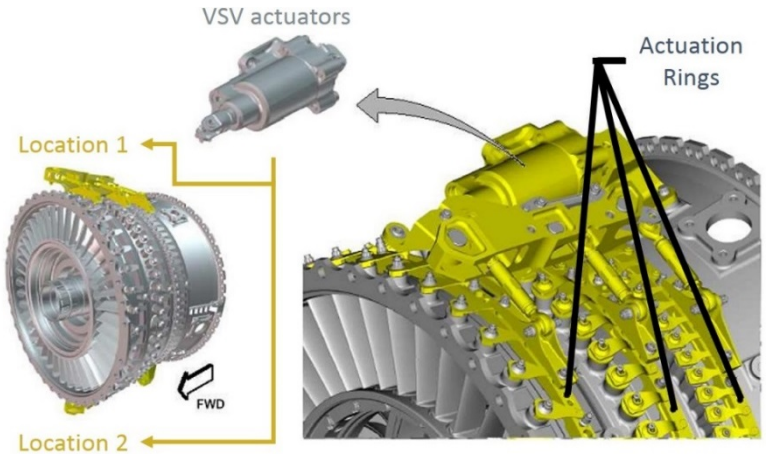


Figure 4.15 *Mechanical structure of the VSV subsystem.*

The VSV subsystem is represented in Figure 4.16.

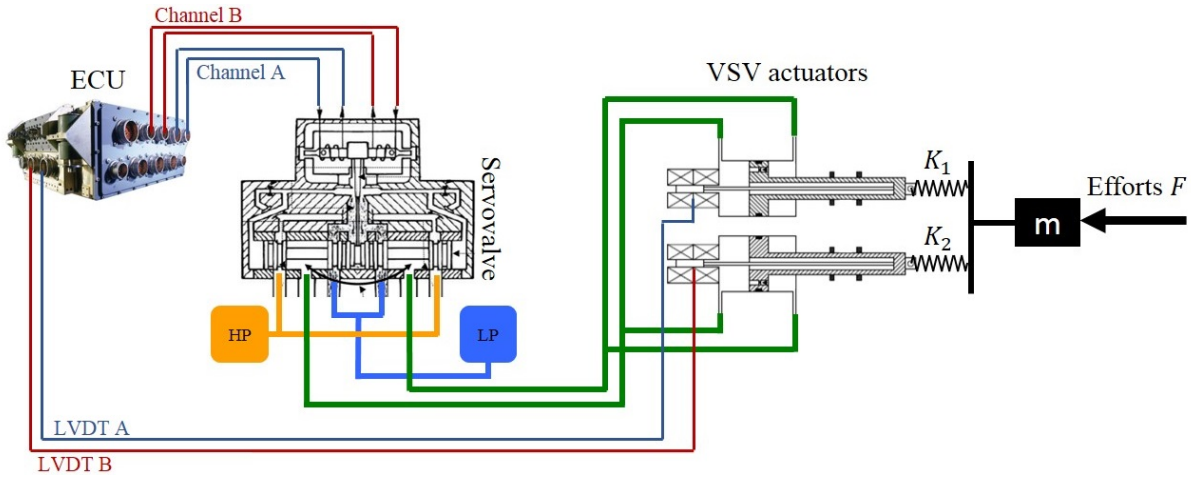


Figure 4.16 *Representation of the VSV subsystem.*

As presented in Figure 4.16, the VSV subsystem is composed of the following equipments:

- **VSV servovalve:** two-stage flapper nozzle servovalve whose outlet flows are determined by control current $\boldsymbol{VSVCMD}$. The architecture of the VSV servovalve is presented in Figure 4.17.

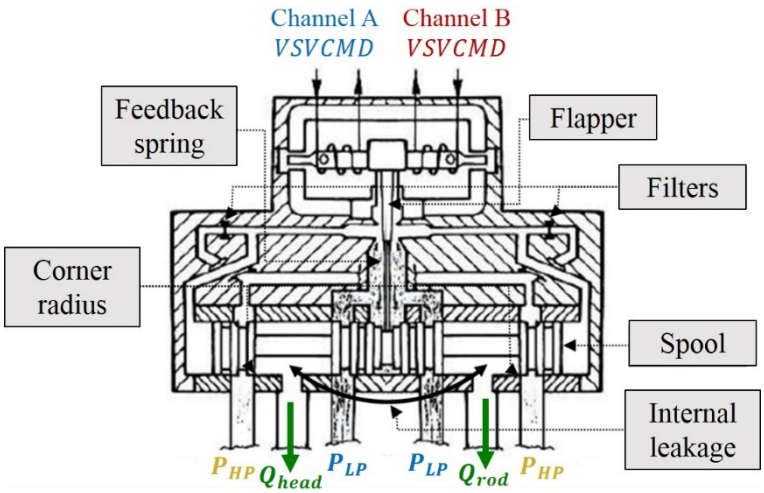


Figure 4.17 *Detailed scheme of a two stages flapper nozzle servovalve.*

- **VSV actuators:** dual-effect cylinders with a cooling orifice between the rod and head chambers. Both actuators are equipped with a LVDT and mechanically linked to the actuation rings. The detailed scheme for a single cylinder is given in Figure 4.18.

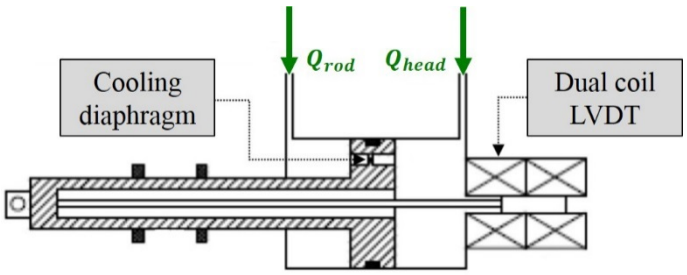


Figure 4.18 *Detailed scheme of a VSV actuator.*

- **VSV LVDT A&B:** LVDTs measuring the displacement of each of the VSV actuators.
- **VSV kinematics:** the three actuation rings are represented by a moving mass $\boldsymbol{m}$ subject to load $\boldsymbol{F = F_{fric} + F_{aero}}$ where $\boldsymbol{F_{fric}}$ is the mechanical effort due to the kinematic friction, and $\boldsymbol{F_{aero}}$ is the aerodynamic effort due to the air pressure on the blades. The mechanical link between actuators and actuation rings is modeled by springs of stiffnesses $\boldsymbol{K_1}$ and $\boldsymbol{K_2}$. Because of the size of actuation rings, it is likely that $\boldsymbol{K_1 \neq K_2}$.
- **ECU:** controller elaborating the $\boldsymbol{VSVCMD}$ in function of the selected value of the VSV actuators displacement $\boldsymbol{VSVSEL}$ (see Appendix III) and its demanded value $\boldsymbol{VSVDMD}$. The sampling rate of the VSV loop is $\boldsymbol{0.015\ s}$ (1 RTC). Its block diagram is given in Figure 4.19.

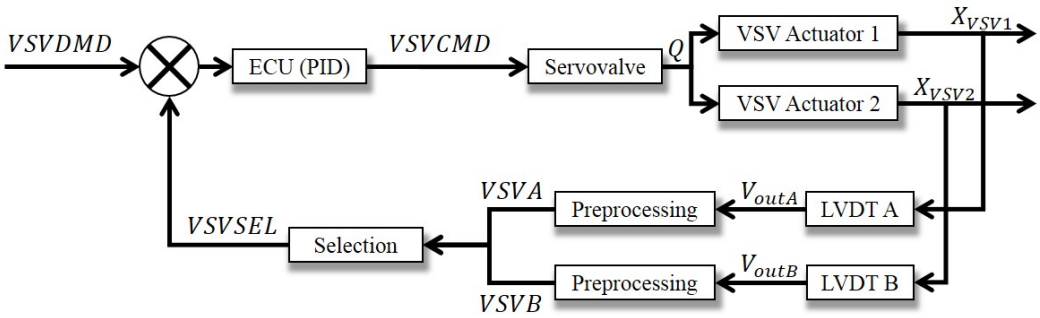


Figure 4.19 *Block diagram of the VSV displacement regulation loop.*

In Figure 4.19, Q is the flow generated by the servovalve and transmitted to the VSV actuators. X_{VSV1} and X_{VSV2} are the actual values of the VSV actuators 1 and 2 displacements, respectively, and V_{outA} and V_{outB} are the voltages sent to the ECU by LVDTs A and B, respectively.

4.2.4.6 *Variable bleed valve regulation loop*

The principal function of the VBV regulation loop is to control the opening of the hatch between the low-pressure and high-pressure compressors aimed at decreasing the amount of air of the number of particles reaching combustion chamber. This opening is controlled by two linear actuators driven by a single servovalve. These actuators are located at the top and bottom of the engine. Both actuators are mechanically linked to an actuation ring transmitting efforts to open or close the hatches. The whole mechanical structure is shown in Figure 4.20.

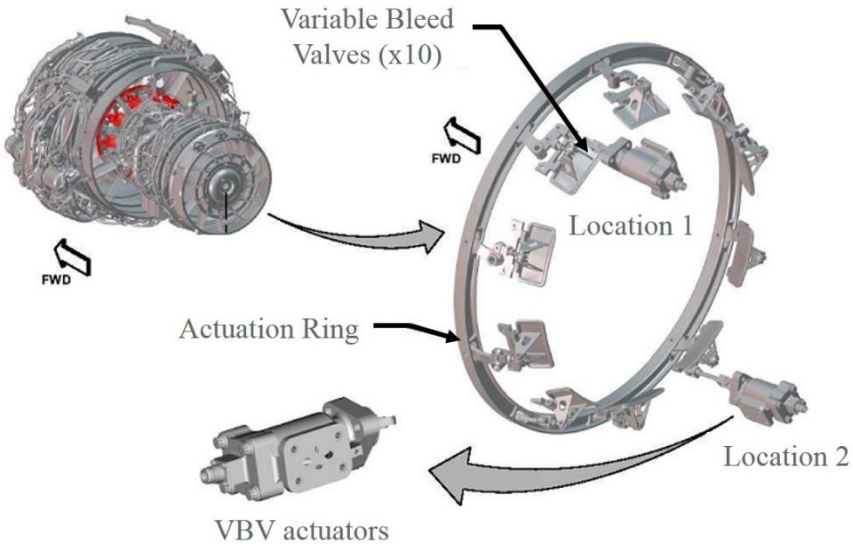


Figure 4.20 *Mechanical structure of the VBV subsystem.*

The VBV subsystem is very similar to the VSV subsystem. Actually, in the scope of this work, all of the equipment will be modeled identically. Only their parameters will vary. For example, the diameters of the cylinders are not the same, and the stiffness of the spring does not follow the same function. Because of this similarity, the reader is invited to refer to section 4.2.4.5 for more details. The sampling rate of the VBV loop is 0.03 s (2 RTC). The block diagram of the close-loop VBV subsystem is provided in Figure 4.21.

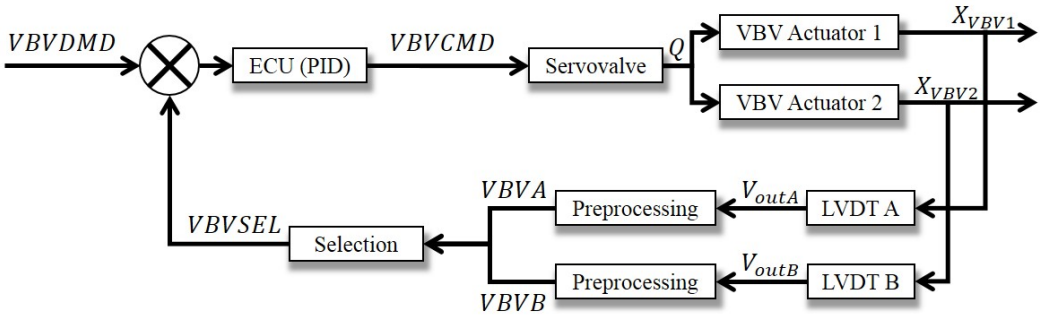


Figure 4.21 *Block diagram of the VBV displacement regulation loop.*

In Figure 4.21, Q is the flow generated by the servovalve and transmitted to the VBV actuators, X_{VBV1} and X_{VBV2}, which are the actual values of the VBV actuators 1 and 2 displacements, respectively, and V_{outA} and V_{outB} are the currents sent to the ECU by LVDTs A and B, respectively.

4.2.4.7 *Transient bleed valve*

The main function of the TBV is to provoke a discharge of the airflow at the inlet of the combustion chamber if necessary. The whole mechanical structure is shown in Figure 4.22.

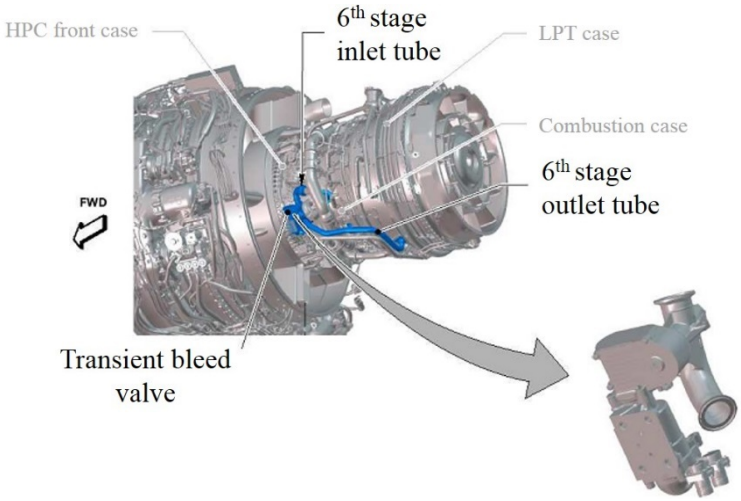


Figure 4.22 *Mechanical structure of the TBV subsystem.*

The TBV subsystem is represented in Figure 4.23.

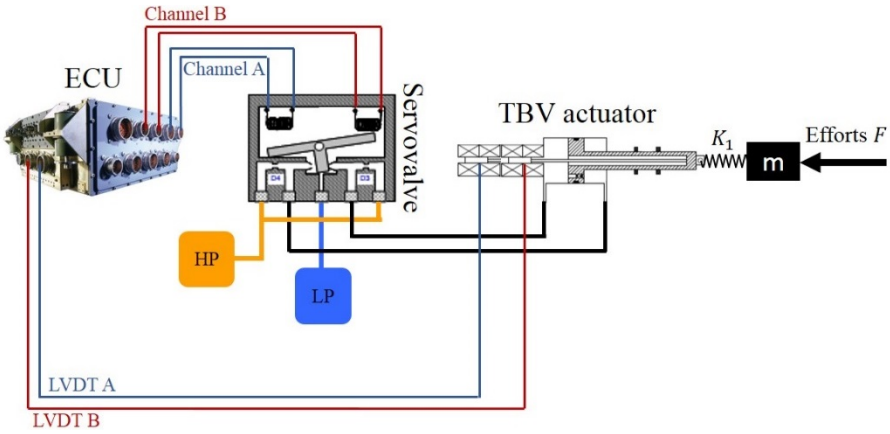


Figure 4.23 *Representation of the TBV subsystem.*

As presented in Figure 4.23, the TBV subsystem is composed of the following equipments:

- **TBV servovalve:** single-stage servovalve (torque motor) whose outlet flows are determined by its control current $\boldsymbol{TBVCMD}$. In this subsystem, the servovalve is commanded all or nothing. In Figure 4.23, it is in open configuration and the TBV is open (rod out).
- **TBV actuator:** dual-effect cylinder with a cooling orifice between rod and head chambers.
- **TBV LVDTs A&B:** redundant LVDTs measuring the displacement of the TBV actuator. For the TBV, the ECU converts these currents into a Boolean value equal to 1 if the displacement is above $\boldsymbol{O_{TBV}}$ and to 0 if it is under.
- **TBV kinematics:** in this work, the kinematic chain of the TBV is represented by a moving mass $\boldsymbol{m}$ subject to load $\boldsymbol{F = F_{fric} + F_{aero}}$. The mechanical link between the actuator and the mass is modeled by a spring of stiffness $\boldsymbol{K}$.
- **ECU:** controller elaborating the $\boldsymbol{TBVCMD}$ in function of the demanded value $\boldsymbol{TBVDMD}$. This system is in open loop. The ECU computes the Boolean value $\boldsymbol{TBVStatus}$ returning the

position open/close of the TBV (see Appendix III). The sampling rate of the TBV loop is 0.03s (2 RTC). Its block diagram is given in Figure 4.24.

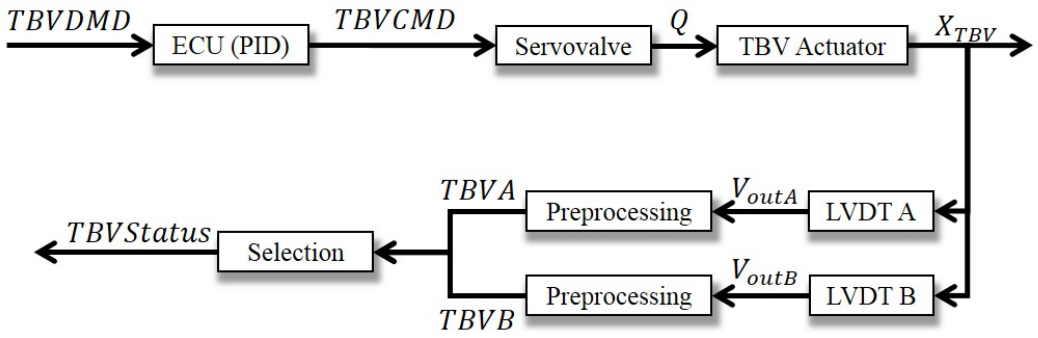


Figure 4.24 *Block diagram of the TBV displacement regulation loop.*

In Figure 4.24, Q is the flow generated by the servovalve and transmitted to the TBV actuator, X_{TBV} is the actual value of the TBV actuator displacement, and V_{outA} and V_{outB} are the output voltage sent to the ECU by LVDTs A and B, respectively.

4.2.4.8 *Flowmeter*

The main function of the flowmeter is to measure the amount of flow injected into the combustion chamber WFM. This subsystem is composed of the following equipment:

- **WFM flowmeter:** mass flowmeter with redundant coil magnets computing voltages $\boldsymbol{V_A}$ and $\boldsymbol{V_B}$, as presented in Figure 4.25.
- **ECU:** computes the values of $\boldsymbol{WFMSEL}$ from $\boldsymbol{WFMA}$ and $\boldsymbol{WFMB}$.

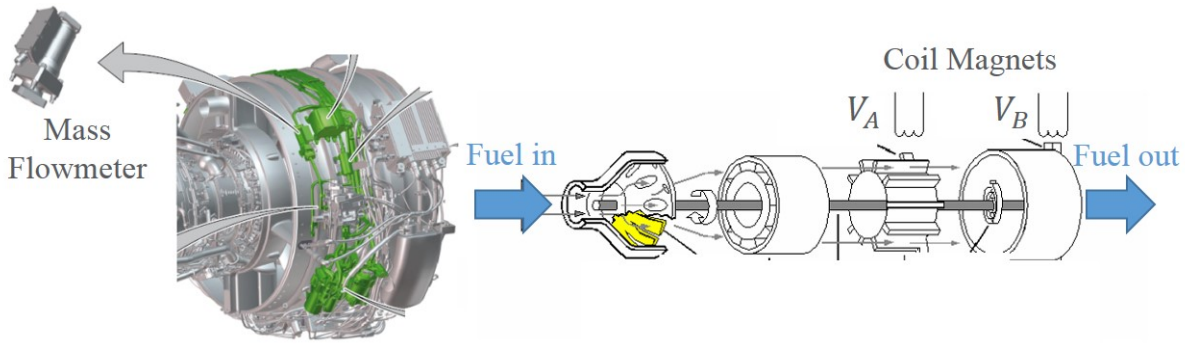


Figure 4.25 *Mechanical structure of the flowmeter.*

4.3 Selection of HIs and CSIs

In this section, the selection process for HIs and CSIs introduced previously is applied to the fuel system. For each functional unit from the highest to lowest level, four types of items are introduced: the targeted compliant service threats (**TCSTs**), the targeted degradation modes (**TDEMs**), the compliant service indicators (**CSIs**) and the health indicators (**HIs**), including both real and virtual ones.

4.3.1 Level 2 subsystems of the fuel system

4.3.1.1 *FMV regulation loop*

- **TCSTs and associated CSIs:** Five TCSTs have been identified for the FMV regulation loop. Three of them are faults: the local sensor, the cross sensor and the actuation faults associated respectively to CSIs. The two others are defects: the null current drift and the internal leakage defects. They are detailed in Appendix VI.

- **Targeted degradation modes:** The list of TDEMs for the FMV loop is given in Table 4.1.

Equipment	Degradation Mode	Equipment	Degradation Mode
Actuator	1. Increase of static friction	**Servovalve**	6. Abrasion of nozzle
Actuator	2. Increase of viscous friction	**LVDT A**	7. Positive drift
Actuator	3. Abrasion of sealing (leakage)	**LVDT A**	8. Negative drift
Servovalve	4. Null current negative drift	**LVDT B**	9. Positive drift
Servovalve	5. Null current positive drift	**LVDT B**	10. Negative drift

Table 4.1 *List of degradation modes for the FMV loop.*

- **Selection of real and virtual HIs:**

To define relevant HIs for monitoring the FMV loop, ATPs are a good source of inspiration. For the servovalve, ATPs are based on the analysis of the flow gain curve, giving the servovalve outlet flow versus the control current. This flow gain curve is a good indicator of the servovalve behavior's conformity, and the first idea is to monitor this flow gain. This operation can effectively be performed during maintenance check-ups with important offline instrumentation to isolate the servovalve and measure the flow. However, when the FMV loop is online, the system is not equipped with a flowmeter, and indirect monitoring means must be found. The proposed solution, which was the subject of a patent (Massé, et al., 2012), is to use the selected cylinder's velocity as an image of the servovalve outlet flow to compute the velocity gain curve. Indeed, for an actuator, the velocity is proportional to the flow according to the following relation:

$$Q = VS \tag{4.1}$$

where Q is the inlet flow; S is the actuator section; V is the actuator speed. Because of the hysteresis, the raw curve has a large dispersion, so a smoothing algorithm based on local means is used to obtain an exploitable curve, as shown in Figure 4.26. Then, 4 HIs are defined from characteristics extracted from this curve: the current hysteresis for points with a null velocity $FmvHyst0$, the slope of the curve computed via main polynomial regression $FmvSlp$, the equilibrium current $FmvCEqu$, equal to the current for which the smoothed curve cross the abscissa axis and the scale of the smoothed curve $FmvScale$. These HIs are defined for the velocities computed from $FMVA$, $FMVB$ and $FMVSEL$. The last three HIs for $FMVSEL$ are presented graphically in Figure 4.27.

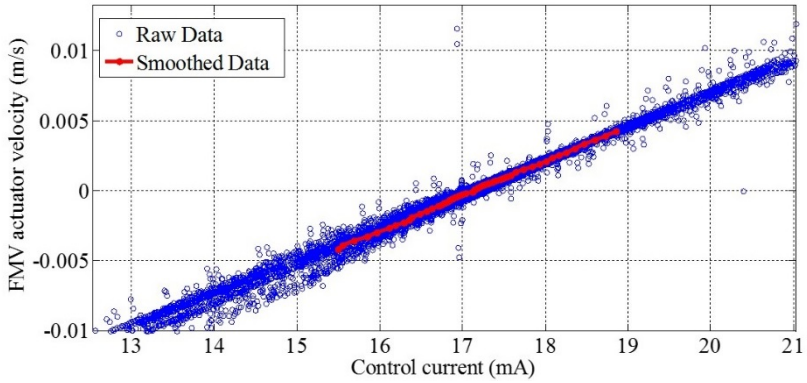


Figure 4.26 *Extraction of the raw and smoothed velocity gain curves for the FMV loop.*

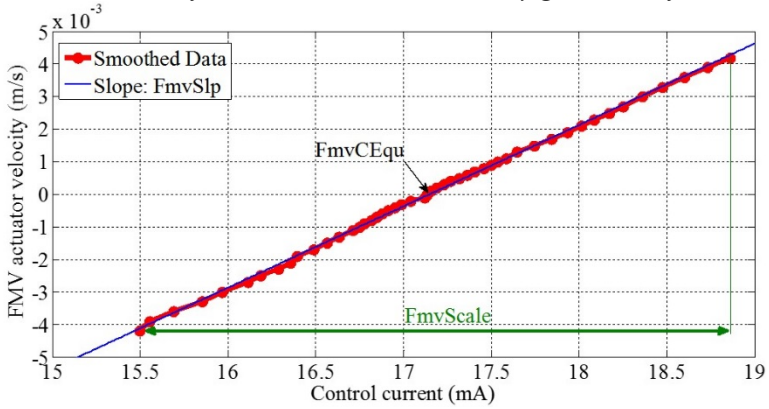


Figure 4.27 *Health Indicators from the smoothed velocity gain curve for the FMV loop.*

Some HIs are also constructed from the positions and velocity measured by redundant LVDTs. Four of them are defined as the maximal and minimal value of position for each LVDT. Four others are defined as standard deviation and mean of the position gaps between the two LVDTs measures. One last HI is defined as the mean of the absolute value of the regulation error over one flight. Finally, the HIs for the FMV loop are listed in Table 4.2, where '$_X$' can be replaced by either $FMVA$, $FMVB$ or $FMVSEL$. Note that all of these HIs are real, as the sensors needed for their construction effectively exist.

Real HIs			
HI	**Description**	**HI**	**Description**
$FmvHyst0_X$	1-3. Hysteresis for null velocity	$FmvminX2$	16. Minimal position LVDTB
$FmvSlp_X$	4-6. Slope of the velocity gain	$FmvmaxGapX$	17. Maximal position gap
$FmvCEqu_X$	7-9. Equilibrium current	$FmvminGapX$	18. Minimal position gap
$FmvScale_X$	10-12. Gain curve scale	$FmvmeanGapX$	19. Mean of position gap
$FmvmaxX1$	13. Maximal position LVDTA	$FmvstdGapX$	20. Deviation of position gap
$FmvmaxX2$	14. Maximal position LVDTB	$MAErrFMV$	21. Mean of absolute error
$FmvminX1$	15. Minimal position LVDTA		

Table 4.2 *List of HIs for the FMV loop.*

4.3.1.2 *High-pressure shut-off valve (SOV)*

- **Targeted compliant service threats and CSIs:** There is no compliant service threat associated with the SOV.

- **Targeted degradation modes:** The list of TDEMs for the SOV is given in Table 4.3.

Equipment	Degradation Mode	Equipment	Degradation Mode
Actuator	1. Increase of static friction	**Proxi A**	6. Positive drift
Actuator	2. Increase of viscous friction	**Proxi A**	7. Negative drift
Actuator	3. Abrasion of sealing (leakage)	**Proxi B**	8. Positive drift
Actuator	4. Decrease of spring force	**Proxi B**	9. Negative drift
Servovalve	5. Response time delay		

Table 4.3 *List of degradation modes for the HPSOV.*

- **Selection of real and virtual HIs:**

For the SOV, the only knowledge available are the signal from the proximeter indicating whether the valve is open or close and the signal from the controller reflecting the positional demand for the SOV. During the start sequence, the opening of the SOV is required to be 5% of the rotation speed $N2$. This action is part of a BITE aimed at verifying the pump efficiency. Then, the closing of the valve is required to be $10\%N2$. The ECU requires then the opening of the SOV to launch the injection at approximately $20\%N2$. Finally, the SOV moves three times between $0\%N2$ and $20\%N2$. Three HIs are then defined as follows: $SOVdelop1$ is the opening delay for the first displacement, $SOVdelclo$ is the closing delay at $10\%N2$ and $SOVdelop2$ is the opening delay for the second displacement (see Figure 4.28).

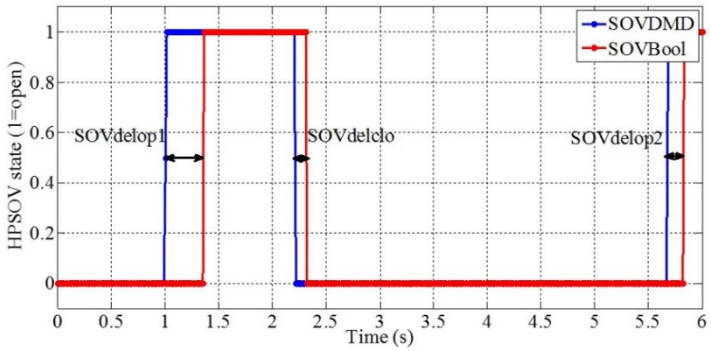


Figure 4.28 *Real HIs for the HPSOV.*

Assuming that proximeters are replaced by LVDTs, three virtual HIs are defined: $VoN2maxSOV$, the maximal value of the valve velocity standardized by the value of $N2$ taken at the same instant and $N2oSOVmean$ and $N2oSOVmax$, respectively, the mean and the maximal value of the ratio between the value of $SOVSEL$ and $N2$ over a complete flight. The final list of HIs is given in Table 4.4.

Real HIs			
HI	**Description**	**HI**	**Description**
$SOVdelop1$	1. First opening delay	$SOVdelop1$	3. Second opening delay
$SOVdelclo$	2. Closing delay		
Virtual HIs			
HI	**Description**	**HI**	**Description**
$VoN2maxSOV$	4. Maximal velocity on N2	$SOVoN2mean$	6. Mean of SOVSEL on N2
$SOVoN2max$	5. Max of SOVSEL on N2		

Table 4.4 *List of HIs for the HPSOV.*

4.3.1.3 *Bypass valve (BYV)*

- **Targeted compliant service threats and CSIs:** There is no TCST, and thus no CSI, associated with the bypass valve.
- **Targeted degradation modes:** The list of TDEMs for the BYV is given in Table 4.5.

Equipment	Degradation Mode	Equipment	Degradation Mode
Actuator	1. Increase of static friction	**Actuator**	3. Decrease of spring force
Actuator	2. Increase of viscous friction	**Actuator**	4. Abrasion of sealing (leakage)

Table 4.5 *List of degradation modes for the bypass valve.*

- **Selection of real and virtual HIs:**

In the current architecture of the fuel system, there is no information associated directly with the bypass valve. Consequently, it is not possible to construct real HIs. Under the assumption that a LVDT sensor measuring the displacement of the valve is available, three virtual HIs are defined: $VoN2maxBYV$, the maximal value of the bypass valve velocity standardized by the value of $N2$ taken at the same instant and $N2oBYVmean$ and $N2oBYVmax$, respectively, the mean and the maximal value of the ratio between the value of $BYVSEL$ and the rotation speed $N2$ over a complete flight. The final list of HIs for the bypass valve is given in Table 4.6.

Virtual HIs			
HI	**Description**	**HI**	**Description**
$VoN2maxBYV$	1. Maximal velocity on N2	$BYVoN2mean$	3. Mean of BYVSEL on N2
$BYVoN2max$	2. Max of BYVSEL on N2		

Table 4.6 *List of HIs for the bypass valve.*

4.3.2 Level 1 subsystems of the fuel system

4.3.2.1 *Fuel metering unit*

- **Targeted compliant service threats and CSIs:** For the FMU, a single TCST has been identified. It is a defect of pressure difference between the FMV inlet and outlet (see Appendix VII). Note that the TCSTs identified for its subsystems (FMV loop, HPSOV and bypass valve) must be added to complete the list.
- **Targeted degradation modes:** There is TDEMs specific to the FMU. The list of TDEMs is thus the fusion of those of the FMV loop, the HPSOV and the bypass valve.
- **Selection of real and virtual HIs:**

In addition to HIs defined for its subsystems, two specific ones are constructed from the relation between $FMVSEL$ and $WFMSEL$. $FmuSlpFW$ is the slope of the curve $log(WFMSEL)$ versus $FMVSEL$, and $FmuR2FW$ the coefficient of determination R^2 of the regression. The complete list of HIs for the FMU is given in Table 4.7.

Real HIs			
HI	**Description**	**HI**	**Description**
$FmvRHIs$	Real HIs of the FMV loop	$FmuSlpFW$	1. Slope FMV=f(log(WFM))

$SovRHIs$	Real HIs of the HPSOV	$FmuR2FW$	2. R^2 of FMV=f(log(WFM))
Virtual HIs			
HI	**Description**	**HI**	**Description**
$SovVHIs$	Virtual HIs of the HPSOV	$ByvVHIs$	Virtual HIs of the Bypass

Table 4.7 *List of HIs for the FMU.*

4.3.2.2 *Low-pressure pump*

- **Targeted compliant service threats and CSIs:** There is no TCST, and thus no CSI, associated with the low-pressure pump.
- **Targeted degradation modes:** The list of TDEMs for the LPP is given in Table 4.8.

Equipment	Degradation Mode
LPP	1. Internal leakage

Table 4.8 *List of degradation modes for the LPP.*

- **Selection of real and virtual HIs:**

In the current architecture of the fuel system, there is no information associated directly with the LPP. Consequently, it is not possible to construct real HIs. Assuming that a sensor measures the pressure difference between the LPP inlet and outlet, it is possible to define virtual HIs and to evaluate their efficiency. From this deltaP sensor, two virtual HIs are defined. $LppSlpN2DP$ is the slope of the curve $\sqrt{DeltaP}$ versus $N2$, and $LppR2N2DP$ is the coefficient of determination R^2 of the regression. The complete list of HIs for the LPP is given in Table 4.9.

Virtual HIs			
HI	**Description**	**HI**	**Description**
$LppSlpN2DP$	1. Slope $\sqrt{\text{DP}}$=f(N2)	$LppR2N2DP$	2. R^2 of $\sqrt{\text{DP}}$=f(N2)

Table 4.9 *List of HIs for the FMU.*

4.3.2.3 *Main fuel pump*

- **Targeted compliant service threats and CSIs:** For the main fuel pump, two TCSTs have been identified: the startup fault and the insufficient flow defect. They are detailed in Appendix IX.
- **Targeted degradation modes:** The list of TDEMs for the MFP is given in Table 4.10.

Equipment	Degradation Mode	Equipment	Degradation Mode
MFP	1. Internal leakage	**MFP**	2. External leakage

Table 4.10 *List of degradation modes for the MFP.*

- **Selection of real and virtual HIs:**

In the present case, there is no direct information on the MFP. To construct a HI capable of reflecting the occurrence of DEMs, the monitoring must be indirect. The idea is to find variables that are images of the hydraulic power gradient over the starting sequence. It appears that the two valves SOV and TBV are in a close position at the beginning of the start sequence ($t = 0$), but their command requires them

to be open. However, as the system is not pressurized at $t = 0$, they cannot move, and their opening occurs only when the hydraulic power has reached a sufficient value. Thus, looking at the evolution of the necessary rotation speed to open the valves appears to be a good way to assess the health status of the pump. Finally, the following HIs, approved by expert knowledge, are defined: ω_{SOV}, the rotation speed $N2$ at the SOV opening, i.e., $\omega_{SOV} = \min\{N2 \,/\, SOVBool = 1\}$ and ω_{TBV}, the rotation speed $N2$ at the TBV opening, i.e., $\omega_{TBV} = \min\{N2 \,/\, TBVBool = 1\}$. The extraction of ω_{SOV} is graphically presented in Figure 4.29.

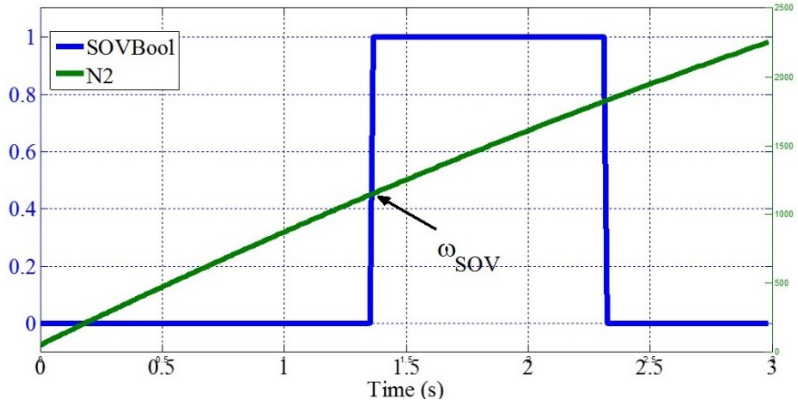


Figure 4.29 *Extraction of ω_{SOV}.*

Moreover, supposing that a sensor measures the pressure difference between the MFP inlet and outlet, it is possible to define virtual HIs and to evaluate their efficiency. From this deltaP sensor, two virtual HIs are defined: $MfpSlpN2DP$ the slope of the curve $\sqrt{DeltaP}$ versus $N2$ and $MfpR2N2DP$, the coefficient of determination R^2 of the regression. The complete list of real and virtual HIs for the MFP is given in Table 4.11.

Real HIs			
HI	**Description**	**HI**	**Description**
ω_{SOV}	1. $N2$ at HPSOV opening	ω_{TBV}	2. $N2$ at TBV opening
Virtual HIs			
HI	**Description**	**HI**	**Description**
$MfpSlpN2DP$	3. Slope $\sqrt{DP}$=f(N2)	$MfpR2N2DP$	4. R^2 of $\sqrt{DP}$=f(N2)

Table 4.11 *List of HIs for the MFP.*

4.3.2.4 *Main fuel filter*

- **Targeted compliant service threats and CSIs:** For the MFF, one TCST has been identified: the incoming bypass fault, presented in Appendix IX.
- **Targeted degradation modes:** The list of TDEMs for the MFF is given in Table 4.12.

Equipment	**Degradation Mode**	**Equipment**	**Degradation Mode**
MFF	1. Filter Clogging	**MFF**	2. Internal leakage

Table 4.12 *List of degradation modes for the MFF.*

- **Selection of real and virtual HIs:**

From the deltaP sensor, two real HIs are defined: $MffSlpN2DP$ the slope of the curve $\sqrt{DeltaP}$ versus $N2$ and $MffR2N2DP$ the coefficient of determination R^2 of the regression. The complete list of real and virtual HIs for the MFF is given in Table 4.13.

Real HIs			
HI	**Description**	**HI**	**Description**
$MffSlpN2DP$	1. Slope $\sqrt{DP}$=f(N2)	$MffR2N2DP$	2. R^2 of $\sqrt{DP}$=f(N2)

Table 4.13 *List of HIs for the MFP.*

4.3.2.5 *VSV regulation loop*

- **Targeted compliant service threats and CSIs:** For the VSV loop, 6 TCSTs have been identified. They are divided into 3 faults (the local sensor, the cross sensor and the actuation faults) and 3 defects (the null current drift and the increase of cooling flow for, respectively, actuator A and actuator B). They are detailed in Appendix X.
- **Targeted degradation modes:** The list of TDEMs for the VSV is given in Table 4.14.

Equipment	Degradation Mode	Equipment	Degradation Mode
Actuator A	1. Increase of static friction	**Servovalve**	11. Clogging of right filter
Actuator A	2. Abrasion of sealing	**Servovalve**	12. Abrasion of the right corner
Actuator A	3. Clogging of cooling orifice	**Servovalve**	13. Abrasion of the right corner
Actuator B	4. Increase of static friction	**Servovalve**	14. Abrasion of sealing
Actuator B	5. Abrasion of sealing	**Kinematic**	15. Increase of dynamic friction
Actuator B	6. Clogging of cooling orifice	**Kinematic**	16. Increase of aerodynamic load
Servovalve	7. Null current negative drift	**LVDT A**	17. Positive drift
Servovalve	8. Null current positive drift	**LVDT A**	18. Negative drift
Servovalve	9. Increase of feedback stiffness	**LVDT B**	19. Positive drift
Servovalve	10. Clogging of left filter	**LVDT B**	20. Negative drift

Table 4.14 *List of degradation modes for the VSV loop.*

- **Selection of real and virtual HIs:**

As for the FMV, the construction of HIs for the VSV loop is based on the velocity gain curve, which is shown in Figure 4.30. In this case, ten HIs are defined: the current hysteresis for points with a null velocity $VsvHyst0$, the slope of the curve computed via main polynomial regression for the left part$VsvSlpLeft$, the null part $VsvSlpNull$ and the right part $VsvSlpRight$, the equilibrium current $VsvCEqu$, the null current coordinates $VsvCNullX$ and $VsvCNullY$, the size of the overlap with respect to abscissa $VsvOverlapX$ and to ordinate $VsvOverlapY$ and the scale of the smoothed curve $VsvScale$. These HIs are defined for the velocities computed from $VSVA$, $VSVB$ and $VSVSEL$. The last nine HIs for $VSVSEL$ are presented graphically in Figure 4.31.

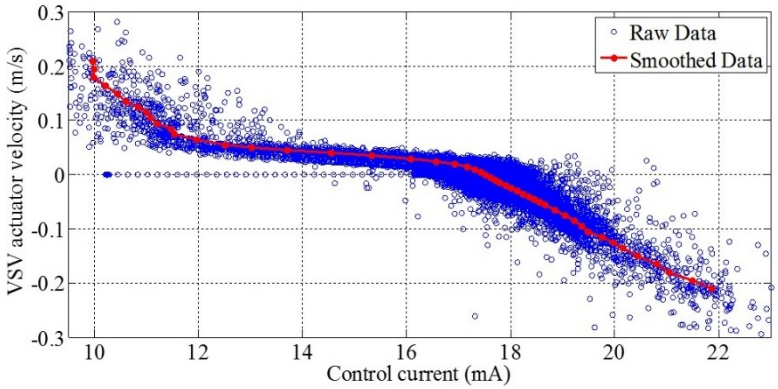


Figure 4.30 *Extraction of the raw and smoothed velocity gain curves for the VSV loop.*

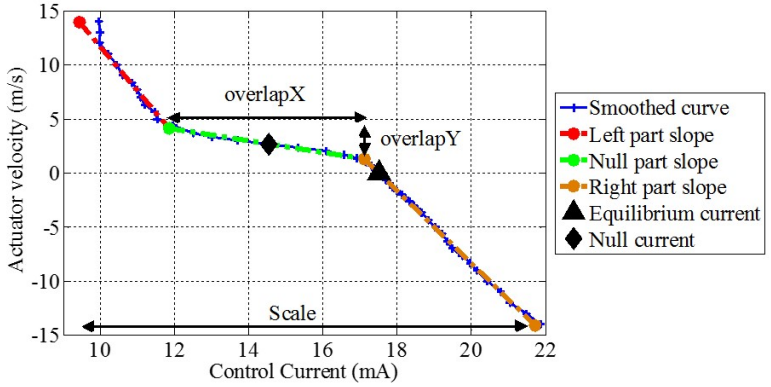


Figure 4.31 *Health Indicators from the smoothed velocity gain curve for the VSV loop.*

Similar to the FMV loop, 8 HIs are also defined from position information from LVDTs, and an additional HI is constructed as the mean of the absolute value of the regulation error. The position-based HIs are very interesting for the VSV loop. Indeed, even if both LVDT measures are identical in cases where the actuators are strictly the same, the cylinders are actually different, and the complexity of the kinematic results in a low stiffness coefficient K bewteen then. As a result, they can move relative to each other. The whole set of real HIs is finally listed in Table 4.15 where '$_X$' can be replaced by either $VSVA$, $VSVB$ or $VSVSEL$.

Real HIs			
HI	**Description**	**HI**	**Description**
$VsvHyst0_X$	1-3. Hysteresis for null velocity	$VsvmaxX1$	31. Maximal position A
$VsvSlpLeft_X$	4-6. Slope of the left part	$VsvmaxX2$	32. Maximal position B
$VsvSlpNull_X$	7-9. Slope of the null part	$VsvminX1$	33. Minimal position A
$VsvSlpRight_X$	10-12. Slope of the right part	$VsvminX2$	34. Minimal position B
$VsvCEqu_X$	13-15. Equilibrium current	$VsvmaxGapX$	35. Maximal position gap
$VsvCNullX_X$	16-18. Abscissa of null point	$VsvminGapX$	36. Minimal position gap
$VsvCNullY_X$	19-21. Ordinate of null point	$VsvmeanGapX$	37. Mean of position gap
$VsvOverlapX_X$	22-24. Abscissa overlap length	$VsvstdGapX$	38. Deviation of position gap
$VsvOverlapY_X$	25-27. Ordinate overlap length	$MAErrVSV$	39. Mean of absolute error
$VsvScale_X$	28-30. Gain curve scale		

Table 4.15 *List of HIs for the VSV loop.*

4.3.2.6 *VBV regulation loop*

- **Targeted compliant service threats and CSIs:** For the VBV, the 6 identified TCSTs are similar to these of the VSV and presented in Appendix XI.

- **Targeted degradation modes:** The list of TDEMs for the VBV is given in Table 4.16.

Equipment	Degradation Mode	Equipment	Degradation Mode
Actuator A	1. Increase of static friction	**Servovalve**	11. Clogging of right filter
Actuator A	2. Abrasion of sealing	**Servovalve**	12. Abrasion of the right corner
Actuator A	3. Clogging of cooling orifice	**Servovalve**	13. Abrasion of the right corner
Actuator B	4. Increase of static friction	**Servovalve**	14. Abrasion of sealing
Actuator B	5. Abrasion of sealing	**Kinematic**	15. Increase of dynamic friction
Actuator B	6. Clogging of cooling orifice	**Kinematic**	16. Increase of aerodynamic load
Servovalve	7. Null current negative drift	**LVDT A**	17. Positive drift
Servovalve	8. Null current positive drift	**LVDT A**	18. Negative drift
Servovalve	9. Increase of feedback stiffness	**LVDT B**	19. Positive drift
Servovalve	10. Clogging of left filter	**LVDT B**	20. Negative drift

Table 4.16 *List of degradation modes for the VBV loop.*

- **Selection of real and virtual HIs:**

Similar to the VSV loop, a part of the HIs is defined from the velocity gain curve. The main difference is that for the VBV, there is no point included in left part (see Figure 4.32). There, the following HIs are defined: the current hysteresis for points with a null velocity $VbvHyst0$, the slope of the curve computed via main polynomial regression for the null part $VbvSlpNull$ and the right part $VbvSlpRight$, the equilibrium current $VbvCEqu$, the slope change point coordinates $VbvXchg$ and $VbvYchg$ and the scale of the smoothed curve $VbvScale$. These HIs are defined for the velocities computed from $VBVA$, $VBVB$ and $VBVSEL$. The last six HIs for $VBVSEL$ are presented graphically in Figure 4.33.

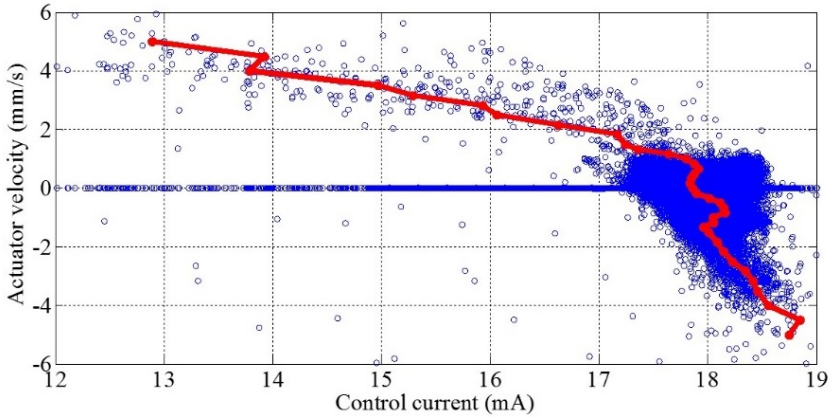


Figure 4.32 *Extraction of the raw and smoothed velocity gain curves for the VBV loop.*

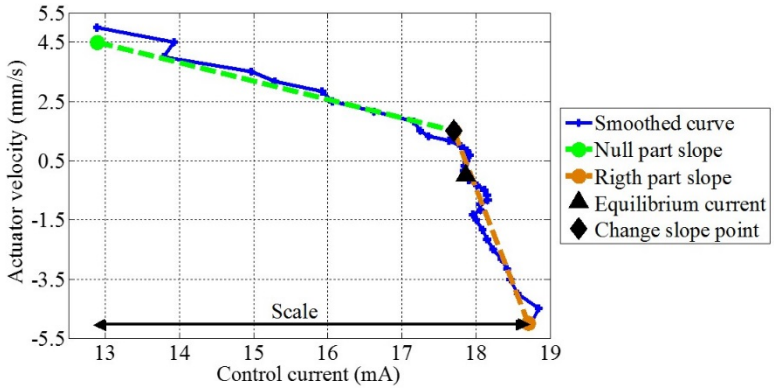


Figure 4.33 *Health Indicators from the smoothed velocity gain curve for the VBV loop.*

Eight HIs are also defined from position information from LVDTs and an additional HI is constructed as the mean of the absolute value of the regulation error. The whole set of real HIs is listed in Table 4.17 where '$_X$' can be replaced by either $VBVA$, $VBVB$ or $VBVSEL$.

Real HIs			
HI	**Description**	**HI**	**Description**
$VbvHyst0_X$	1-3. Hysteresis for null velocity	$VbvmaxX2$	23. Maximal position B
$VbvSlpNull_X$	4-6. Slope of the null part	$VbvminX1$	24. Minimal position A
$VbvSlpRight_X$	7-9. Slope of the right part	$VbvminX2$	25. Minimal position B
$VbvCEqu_X$	10-12. Equilibrium current	$VbvmaxGapX$	26. Maximal position gap
$VbvXchg_X$	13-15. Abscissa of null point	$VbvminGapX$	27. Minimal position gap
$VbvYchg_X$	16-18. Ordinate of null point	$VbvmeanGapX$	28. Mean of position gap
$VbvScale_X$	19-21. Gain curve scale	$VbvstdGapX$	29. Deviation of position gap
$VbvmaxX1$	22. Maximal position A	$MAErrVBV$	30. Mean of absolute error

Table 4.17 *List of HIs for the VBV loop.*

4.3.2.7 *TBV regulation loop*

- **Targeted compliant service threats and CSIs:** There is no compliant service threat associated with the TBV.
- **Targeted degradation modes:** For the TBV, the identified TDEMs are given in Table 4.18.

Equipment	Degradation Mode	Equipment	Degradation Mode
Actuator	1. Increase of static friction	**Actuator**	2. Increase of viscous friction
Actuator	3. Abrasion of sealing (leakage)		

Table 4.18 *List of degradation modes for the bypass valve.*

- **Selection of real and virtual HIs:**

The only information available concerning the TBV is the Boolean $TBVBool$ indicating if the valve is opened or closed. Assuming that a LVDT sensor measuring the displacement of the valve is available, a virtual HI is defined: $VoN2maxTBV$, the maximal value of the TBV velocity standardized by the value of $N2$ taken at the same instant (see Table 4.19).

Virtual HIs	
HI	**Description**
$VoN2maxTBV$	1. Maximal velocity on N2

Table 4.19 *List of HIs for the TBV.*

4.3.2.8 *Flowmeter*

- **Targeted compliant service threats and CSIs:** For the flowmeter, one TCST has been identified: the sensor fault. It is detailed in Appendix XII.
- **Targeted degradation modes:** For the flowmeter, the identified TDEMs are given in Table 4.20.

Equipment	Degradation Mode	Equipment	Degradation Mode
WFM A	1. Sensor positive drift	**WFM A**	4. Sensor negative drift
WFM B	2. Sensor positive drift	**WFM B**	5. Sensor negative drift
Flowmeter	3. Internal leakage		

Table 4.20 *List of degradation modes for the Flowmeter.*

- **Selection of real and virtual HIs:**

From the redundant flow sensors, 8 real HIs are defined, similarly to redundant LVDT sensors. The list of real HIs for the flowmeter is given in Table 4.21.

Real HIs			
HI	**Description**	**HI**	**Description**
$WfmmaxQ1$	1. Maximal flow A	$WfmmaxGapQ$	5. Maximal flow gap
$WfmmaxQ2$	2. Maximal flow B	$WfmminGapQ$	6. Minimal flow gap
$WfmminQ1$	3. Minimal flow A	$WfmmeanGapQ$	7. Mean of flow gap
$WfmminQ2$	4. Minimal flow B	$WfmstdGapQ$	8. Deviation of flow gap

Table 4.21 *List of HIs for the Flowmeter.*

4.3.3 Level 0: fuel system

- **Targeted compliant service threats and CSIs:** The list of TCSTs for the fuel system is the fusion of those of its subsystems.
- **Targeted degradation modes:** One TDEM specific to the fuel system has been identified. It is the abrasion of the min flow orifice (see Table 4.22), linking the HP circuit to the output of the FMV to ensure a minimal flow downstream. It allows the avoidance of coking of the fuel in the piping.

Equipment	Degradation Mode
Fuel system	1. Min flow abrasion

Table 4.22 *List of degradation modes for the fuel system.*

- **Selection of real and virtual HIs:**

The complete list of HIs for the fuel system is given in Table 4.23.

Real HIs			
HI	**Description**	**HI**	**Description**
$FmuRHIs$	Real HIs of the FMU	$LppRHIs$	Real HIs of the LPP
$MfpRHIs$	Real HIs of the MFP	$MffRHIs$	Real HIs of the MFF
$VsvRHIs$	Real HIs of the VSV loop	$VbvRHIs$	Real HIs of the VBV loop
$TbvRHIs$	Real HIs of the TBV loop	$WfmRHIs$	Real HIs of the Flowmeter
Virtual HIs			
HI	**Description**	**HI**	**Description**
$FmuVHIs$	Virtual HIs of the FMU	$LppVHIs$	Virtual HIs of the LPP
$MfpVHIs$	Virtual HIs of the MFP	$TbvVHIs$	Virtual HIs of the TBV loop

Table 4.23 *List of HIs for the fuel system.*

4.3.4 Parameters

4.3.4.1 *Context parameters*

For the fuel system, one context uncertain parameters have been identified as shown in Table 4.24.

Name	**Context Parameter**
T_{fuel}	1. Fuel temperature

Table 4.24 *List of context parameters for the fuel system.*

4.3.4.2 *Epistemic Parameters*

For the fuel system, 12 epistemic uncertain parameters have been identified as shown in Table 4.25.

Name	**Epistemic Parameter**	**Name**	**Epistemic Parameter**
Mfp_{Dis}	1. MFP displacement	Tbv_{Pop}	2. TBV opening pressure
$Tbv_{Ostroke}$	3. TBV opening stroke	Byv_{Drod}	4. Bypass valve rod diameter
Byv_{Dpist}	5. Bypass valve piston diameter	Byv_{Ulp}	6. Bypass valve initial underlap
Sov_{Dpist}	7. HPSOV piston diameter	Sov_{Ulp}	8. HPSOV initial underlap
$Sov_{Ostroke}$	9. HPSOV opening stroke	Fmv_{ChLg}	10. FMV chamber length
Fmv_{Dpist}	11. FMV piston diameter	Sta_{law}	12. Starter control law coefficient

Table 4.25 *List of epistemic parameters for the fuel system.*

Finally, 80 parameters, including a single context, 12 epistemic and 67 degradation parameters, have been identified. They are listed is Appendix XIII. From the 67 degradation parameters, 85 degradation modes (DEMs) are extracted, which means that 18 of them can evolve in two directions. The list of DEMs is given in Appendix XIV. In parallel, a total of 116 His, including 105 real HIs and 11 virtual HIs and 22 CSIs have been defined. The complete lists of HIs and CSIs are given in, respectively, Appendix XV and Appendix XVI.

4.3.4.3 *Initial uncertainties quantification*

Based on engineering judgment, specification documents and experience feedback from other engines, a coarse uncertainties quantification for the 80 uncertain parameters was performed. At this stage, all of these uncertainties are uniform PDFs defined by their parameter vector $[a \quad b]^t$ with a the lower bound and b the upper bound. The values of a and b for the initial parameters are given in Appendix XVII.

4.3.4.4 *Initial sensitivity analysis via the Morris method*

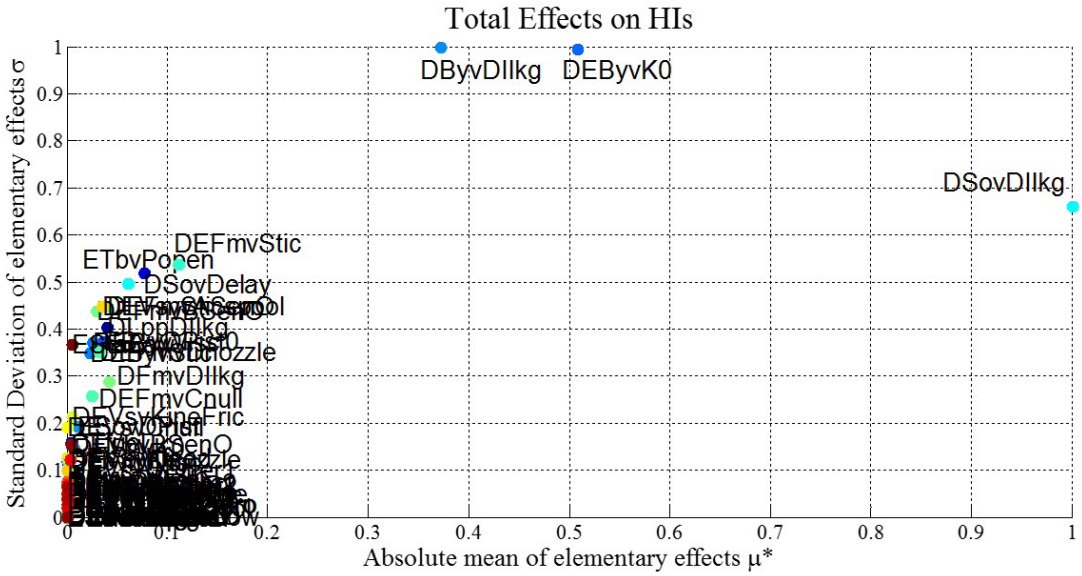
The identification of influential parameters is the first step of the application on the fuel system. This identification is performed through the computation of Morris based sensitivity indices Tot_i and Lin_i. These are computed separately for HIs and CSIs. They are termed, respectively, Tot_i^{HIs} and Lin_i^{HIs} and Tot_i^{CSIs} and Lin_i^{CSIs}. To define influent and linear parameters, two thresholds are defined: Tot_{min} is the minimum value above which parameters are considered influent. Lin_{min} is the minimum value above which parameters are considered linear. For the present application, we use the following:

$$\begin{cases} Tot_{min} = 0.01 \\ Lin_{min} = 0.99 \end{cases} \tag{4.2}$$

Note that it is possible to identify TDEMs associated to each compliant service threat (CST) from Tot_i^{OIs}. These are the degradation parameters i associated to a high value of T_i^{OIs} with a negative direction of variation. Indeed, CST are reached when their related CSI becomes negative.

4.3.4.5 *Health Indicators*

For the sensitivity analysis of HIs, the Morris method was performed with 3 repetitions. The Morris graphical representation is shown in Figure 4.34.



fg

Figure 4.34 *Morris graphical representation for HIs.*

From these results, it appears that of the initial list of 80 parameters, 59 are considered as influential. Moreover, among these influential parameters, 11 are linear. Subsequently, the list of degradation parameters is reduced to 71. The total list of influential parameters is given in Table 4.26 where boxes

with a green background represent linear parameters those with a red background, nonlinear parameters and/or parameters with interactions. The values of Tot_i^{HIs} and Lin_i^{HIs} are given in Appendix XVIII.

HI	HI	HI	HI	HI
$CTfuel$	$DByvDIlkg$	$DEVsvStic1$	$DEVsvDFilter2$	$DEVbvCnull$
$DLppDIlkg$	$ESovDPist$	$DEVsvVisc1$	$DEVsvCorHP1$	$DEVbvDnozzle$
$DMfpDIlkg$	$DESovVisc$	$DEVsvStic2$	$DEVsvCorHP2$	$DEVbvKfeed$
$DEMffFRate$	$DESovStic$	$DEVsvVisc2$	$DEVsvASenO$	$DEVbvSticspool$
$ETbvPopen$	$DSovDIlkg$	$DEVsvDCool1$	$DEVsvBSenO$	$DEVbvDFilter1$
$DTbvDIlkg$	$DSovDelay$	$DEVsvDCool2$	$DEVbvStic1$	$DEVbvDFilter2$
$DEWfmASenO$	$DEFmvStic$	$DEVsvKineFric$	$DEVbvVisc1$	$DEVbvCorHP1$
$DEWfmBSenO$	$DEFmvCnull$	$DEVsvCnull$	$DEVbvStic2$	$DEVbvCorHP2$
$EByvDPist0$	$DEFmvDnozzle$	$DEVsvDnozzle$	$DEVbvVisc2$	$DEVbvASenO$
$DEByvK0$	$DEFmvASenO$	$DEVsvKfeed$	$DEVbvDCool1$	$DEVbvBSenO$
$DEByvVisc$	$DEFmvBSenO$	$DEVsvSticspool$	$DEVbvDCool2$	$EStaLaw$
$DEByvStic$	$DFmvDIlkg$	$DEVsvDFilter1$	$DEVbvKineFric$	

Table 4.26 *List of uncertain parameters.*

4.3.4.6 *Compliant service indicators*

For the sensitivity analysis of CSIs, the parameterization of the Morris method was the same as for the HIs. The result is given in Figure 4.35.

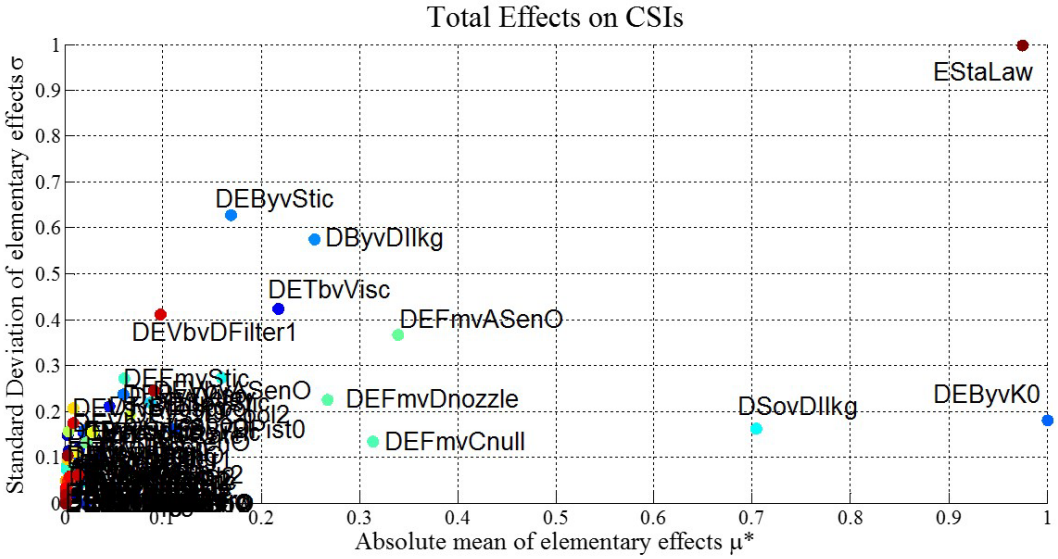


Figure 4.35 *Morris graphical representation for CSIs.*

These results allowed identifying, for each CSIs, the potential cause degradation parameters likely to make the system reach the associated compliant service threat. Table 4.27 shows an example of potential degradation parameters for two CSIs. It shows that an incoming bypass fault of the main fuel filter (MFF), characterized by CSI $DPMFF$, is likely to be provoked by a drift of the MFF difference pressure sensor $DEMffSenO$. Similarly, a null current drift defect of the VBV servovalve ($rVBVCMD0$) can be caused by a drift of the null current $DEVbvCnull$. These results are easily corroborated by physical reasoning. The rest of the results are given in Appendix XIX.

CSIs	Potential cause degradation parameters	CSIs	Potential cause degradation parameters
$DPMFF$	$DEMffSenO$	$rVBVCMD0$	$DEVbvCnull$

Table 4.27 *Example of potential cause degradation parameter for two compliant service indicators (CSIs).*

4.4 Construction and validation of the surrogate model

4.4.1 Designs of experiments

4.4.1.1 *Initial design of experiment*

As presented in Figure 3.22, the initial DOE is composed of the single-dimension learning vectors. For the fuel system, 11 influential parameters with a linear effect have been identified as have 48 with a nonlinear effect. These findings correspond to 11×3 and 48×5 calls for linear and nonlinear parameters, respectively. Finally, the initial DOE is composed of 273 evaluations of the physics-based model.

4.4.1.2 *Test LHSDOE for the computation of Q2 and Sobol indices*

For the computation of the $Q2$ index, a LHSDOE of $4 \times i$ experiments is used, with i the number of influential parameters. Thus, for the 59 uncertain parameters, this DOE represents 236 evaluations of the physics-based model.

4.4.1.3 *Evolutionary DOE for the sequential learning*

For the sequential learning, the maximal number of allowed iterations is limited to 236. The values of validation criteria are chosen as follows:

$$\begin{cases} Q2^{min} = 0.5 \\ \mu_{CV}^{max} = 0.05 \\ \sigma_{CV}^{max} = 0.25 \end{cases} \quad \textbf{(4.3)}$$

In conclusion, considering the model induced by the Morris method, the initial learning DOE, the test LHSDOE and the evolutionary DOE, the maximum number of evaluations of the physics-based model is equal to 973, which is under the specified limit of 1000.

4.4.2 SVR-Kriging modeling and validation

4.4.2.1 *Support vector regression models for HIs and CSIs*

The SVR models are trained based on the initial learning DOE for the 116 HIs and the 22 CSIs. For the individual SVR, the parameters used for the SVR are listed in Table 4.28.

Type of parameters	Learning vector size	Kernel type	Kernel parameters
Linear	3	Linear	No parameter
Nonlinear	5	Radial basis functions	$\gamma = 10$

Table 4.28 *Parameters for the SVR.*

For the evaluation of the models accuracy, the $Q2$ index is computed. Indeed, for the SVR models, the computation of μ_{CV} and σ_{CV} does not have much significance as there is no Gaussian process to calibrate. The results are given in Appendix XX. Table 4.29 is an extract of this appendix. It shows that

whereas the model of HI $FmvHyst0A$ (hysteresis of null speed for the FMV) has a validated value of $Q2$, the model of HI $wTBV$ (engine rotation speed at the TBV opening) needs to be improved.

HIs	$Q2$	HIs	$Q2$
$FmvHyst0A$	0,54	$wTBV$	-0,15

Table 4.29 *Example of performance metrics for the SVR model for HIs.*

In the results of Appendix XX, the value of $Q2$ of the SVR models relate the accuracy of each model with respect to the test LHSDOE. Under the assumption that the individual SVR models are perfectly accurate, the values of $Q2$ give further information about the interaction between parameters. Indeed, if the SVR models flawlessly cover all of the first-order effects, modeling errors come exclusively from interaction effects.

4.4.2.2 *Computation of median limit values*

The SVR models of the CSIs are used to compute the median limit value (MLV), defined in Definition 7. A method for calculating the MLVs from the values of CSIs was proposed in section 0. They indicate, for the 71 degradation modes (**DEMs**), the value for which each compliant service threat (**CST**) is reached. In cases where a CST is never reached for a given DEM, the value is of the MLV is ∞. The values of the MLVs are then used to compute the intensity of DEMs (see Definition 8). The complete results of the MLVs computation for the fuel system are given in Appendix XX. An extract of this appendix is given in Table 4.30. It reveals that DEM $DSovDIlkg_Pos$ (increasing of SOV internal leakage diameter) can lead to two CSTs, namely the MFP startup fault ($XSOV10$) and the VBV actuation fault ($raVBV$). Concerning the DEM $DEFmvASenO_Neg$ (negative drift of FMV sensor A), it can cause either a local FMV sensor fault ($rFMV$) or a cross-sensor fault ($dFMV$). The computation of the vector $\underline{mlv}$ is performed by taking the minimum value of all of the MLVs for each DEM. In the present example, the MLV of $DSovDIlkg_Pos$ and $DEFmvASenO_Neg$ are, respectively, equal to $0{,}59$ and -0.2. One can observe that these values are in consistent with those of Appendix XIX, indicating the potential cause degradation parameters identified from the Morris sensitivity analysis method. Indeed, it reveals that the degradation parameter $DEFmvASenO$ is a potential cause for CSIs $rFMV$ and $dFMV$, which is also a conclusion that can be made from Table 4.30.

Degradation modes	$rFMV$	$dFMV$	...	$XSOV10$	...	$raVBV$	...	$QVBVB$		$\underline{mlv}$
$DSovDIlkg_Pos$	∞	∞	...	0,59	...	0,76	...	∞		0,59
$DEFmvASenO_Neg$	-0,2	-0,6	...	∞	...	∞	...	∞		-0,2

Table 4.30 *Example of MLVs for two degradation modes learning.*

4.4.2.3 *SVR-Kriging models for HIs and CSIs*

First, the SVR-Kriging models are built from the same set of learning points than the SVR models, namely, the monodimensional learning vectors. Table 4.31 shows the parameters used for the training of the SVR-Kriging model.

Type of correlation function	Exponential-Gaussian
Number of $\underline{\theta}$ optimization algorithm iterations	50
Initial values of $\underline{\theta}$: $\underline{\theta}^{init}$	$\underline{\theta_1}^{init} = [1e^{x_1} \quad \cdots \quad 1e^{x_{59}}]^T$; $\underline{\theta_2}^{init} = [y_1 \quad \cdots \quad y_{59}]^T$

	with $x_1 \sim \mathcal{U}(-8\,;2), \dots, x_{59} \sim \mathcal{U}(-8\,;2)$ and $y_1 \sim \mathcal{U}(1\,;2), \dots, y_{59} \sim \mathcal{U}(1\,;2)$
Minimal values of $\underline{\theta}$: $\underline{\theta}^{lb}$	$\underline{\theta_1}^{lb} = [1e^{-8} \quad \cdots \quad 1e^{-8}]^T$; $\underline{\theta_2}^{lb} = [1 \quad \cdots \quad 1]^T$
Maximal values of $\underline{\theta}$: $\underline{\theta}^{ub}$	$\underline{\theta_1}^{ub} = [100 \quad \cdots \quad 100]^T$; $\underline{\theta_2}^{ub} = [2 \quad \cdots \quad 2]^T$
Number of influential parameters included in the DACEFIT algorithm: n_{opt}	$n_{opt} = 5$
Step for the computation of cross-validation error based criteria: n_{CV}	$n_{CV} = 10$

Table 4.31 *Parameters for the SVR-Kriging training.*

The performance metrics computed for this first set of SVR-Kriging models are given in Appendix XXII. They show bad results for $Q2$ but rather good values for the μ_{CV} and σ_{CV} indices. These findings can be explained by the fact that at this point, the training samples are regularly located in the input space and do not model interaction effects. Therefore, it is necessary to add some points.

However, because of limited computational capacities, the sequential learning process presented in section 0 has not been performed yet. To present some results, we chose to add the test LHSDOE to the monodimensional learning vector of the SVR models to construct a global learning DOE with better space-filling properties. It is composed of a set of 509 points. The advantage of this solution is that interaction effects can be modeled, but, in return, the drawback is that the $Q2$ index is not computable anymore. Indeed, as test LHSDOE is part of the training samples, the computed values of $Q2$ are systematically equal to 1. Consequently, only the μ_{CV} and σ_{CV} indices are used as validation criteria (see equation (4.3)). The values of indices μ_{CV} and σ_{CV} computed for this second set of SVR-Kriging models are given in Appendix XXIII. They show that among this set of SVR-Kriging models, 35 are not validated for μ_{CV} , and 35 are not validated for σ_{CV} . For future applications, the sequential training process should allow a complete set of validated models.

4.4.2.4 *Examples of distributions obtained via uncertainty propagation*

Once the SVR-Kriging models are trained, it is possible to compute all of the HIs distributions via uncertainty propagation. Some examples of distributions obtained for Monte Carlo-based uncertainty propagation with 1000 samples and four levels of intensities are given in Figure 4.36 and Figure 4.37. The former represents the distribution of HI $FmvHyst0A$ for DEM $DEFmvStic_Pos$ and the latter the distribution of HI $MffSlpN2DP$ for DEM $DEMffFlowRate_Neg$.

Figure 4.36 shows that the degradation mode $DEFmvStic_Pos$ induces an increase of the HI $FmvHyst0A$. This can be explained physically by the fact that static friction entails delays for displacements that cause a higher hysteresis of the loop. For an intensity of 0.33, the faulty distributions have a significant overlaping area with the healthy distribution, so it will likely not be detectable. On the contrary, distributions corresponding to intensities 0.66 and 1 will most likely be well separated from the healthy distribution. These assumptions will be verified during the computation of NKPIs.

Figure 4.37 shows that the degradation mode $EMffFlowRate_Neg$ induces an increase of the HI $MffSlpN2DP$. Indeed, it is logical, from a physics-based reasoning, that a decrease of the main fuel filter flow rate induces a reduction of $N2$ versus ΔP curve slope. The distributions show that all of the faulty states are easily separable from the healthy state, so they are expected to be detectable. Yet again, these conclusions will be confirmed by NKPIs.

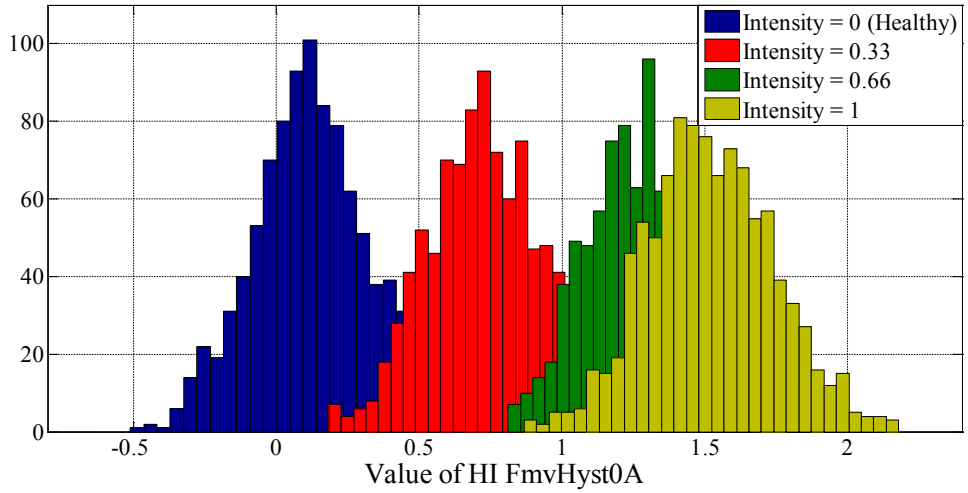


Figure 4.36 *Distribution of HI $FmvHyst0A$ for DEM $DEFmvStic_Pos$.*

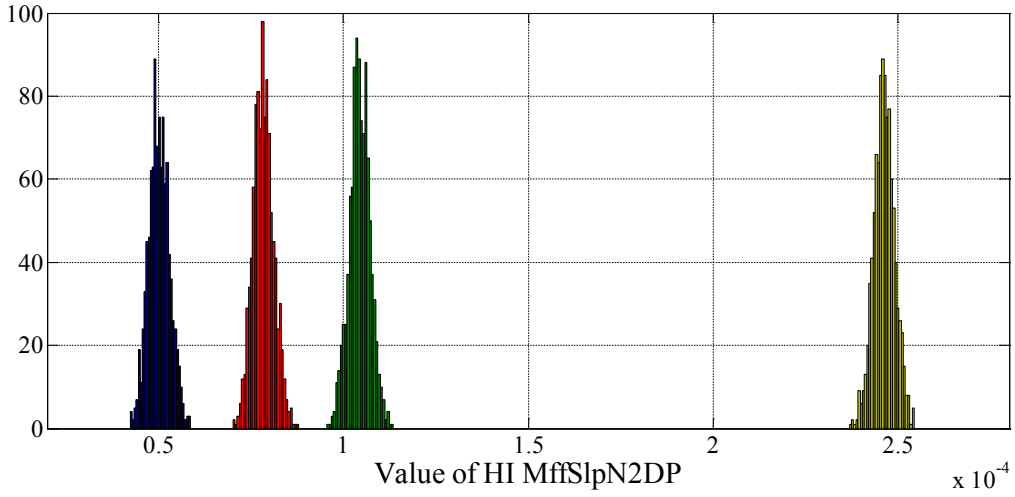


Figure 4.37 *Distribution of HI $MffSlpN2DP$ for DEM $DEMffFlowRate_Neg$.*

4.5 Standardization of HIs

4.5.1 Computation of Sobol indices

The computation of Sobol indices has been performed for the whole set of health indicators via the Monte-Carlo method presented in section 2.3.1.6. For this method, two sets of 10000 points selected via Latin hypercube sampling are used. The results are given in Appendix XXVIII and Appendix XXIX for the first order and the total Sobol indices, respectively.

The remainder of the standardization procedure uses context and epistemic parameters that are known and for which the first-order Sobol index is superior to 0.01 as standardization parameters. In the present application, there is only one known context parameter, $CTfuel$ and one known epistemic parameter $EStaLaw$. For example, considering HI $VsvMAErr$, the first-order Sobol index associated to $EStaLaw$ is equal to 0.31. Thus, it will be a standardization parameter for the model of $VsvMAErr$. Similarly, considering $VbvSlpRightB$, $CTfuel$ will be a standardization parameter as its associated first-order Sobol index is equal to 0.06.

4.5.2 Examples of standardization effects

In terms of proving the efficiency of the standardization procedure, Figure 4.38 shows its effect on the computation of the healthy distribution of HI $VsvMAErr$ (mean regulation error of the VSV loop). It can be clearly observed that the standard deviation of the distribution corresponding to the standardized HI is widely reduced compared with the one associated with the raw HI. The same behavior can be observed for other HI. Thus, the proposed standardization procedure is efficient, at least for simulated data during design stages.

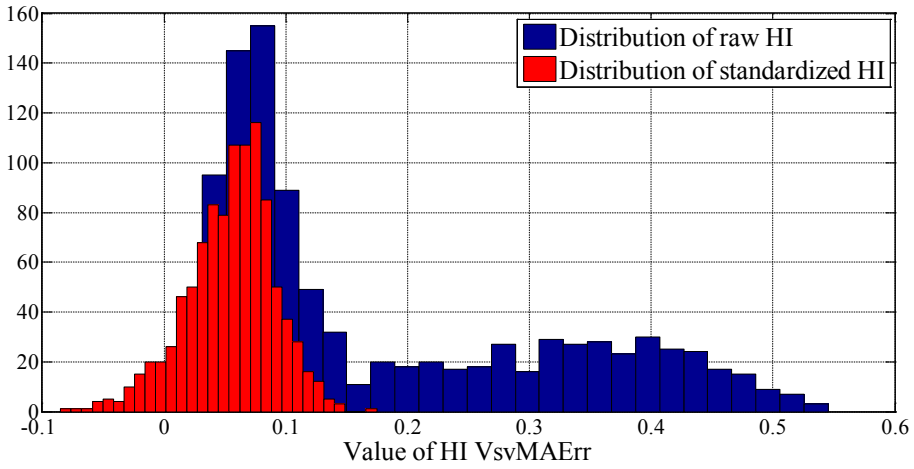


Figure 4.38 *Healthy distribution of HI $VsvMAErr$ for raw and standardized cases.*

4.6 Validation of HIs

4.6.1 Specifications

For the validation of the HIs set, the specifications of Table 4.32 are proposed.

Type	Common Specifications
Targeted system	The targeted system is the fuel system.
Detection performance	Required couple $(TP_{SPEC}, FP_{SPEC}) = (0.80, 0.05)$
	Minimum rate of detectable TDEM: $DTDEM_{\%} = 80\%$
	Minimum rate of relevant detection HIs: $RDHI_{\%} = 50\%$
Identification performance	Required minimal angle $\alpha_{SPEC} = 0.25$
	Minimum rate of identifiable TDEM: $ITDEM_{\%} = 80\%$
	Minimum rate of relevant identification HIs: $RIHI_{\%} = 50\%$
Localization performance	Minimum rate of localizable LRU: $LLRU_{\%} = 80\%$
	Minimum rate of relevant localization HIs: $RLHI_{\%} = 50\%$
Prognostics performance	Minimum rate of prognosticable CSTs: $PCST_{\%} = 25\%$
	Minimum rate of relevant prognostic HIs: $RPHI_{\%} = 50\%$

Table 4.32 *List of specifications for the HIs set.*

4.6.2 NKPIs of real HIs for fleet models

4.6.2.1 *Detection NKPIs*

The detection NKPIs have been computed for each couple degradation mode (DEM)/health indicator (HI). The compliant detectability matrix is given in Appendix XXIV. To recall, it indicates which HI is able to detect each DEM with respect to specified levels of false alarms and good detection (see section 2.4.3.2). The last column gives, for each DEM, the total number of HIs that are able to detect it. A deviation from 0 indicates that the associated DEM is *a priori* detectable. The last line gives, for each HI, the total number of DEMs they are able to detect it. A value other than 0 indicates that the associated HI is *a priori* detection relevant. An extract of this matrix is shown in Table 4.33 for DEMs $DEVbvDCool2_Pos$ and $DEVbvDFilter1_Neg$. The conclusions that can be drawn from this table are as follows:

- $\boldsymbol{DEVbvDCool2_Pos}$ is *a priori* detectable by 10 HIs, which means that its detection potential is theoretically robust to the loss of 9 HIs.
- $\boldsymbol{DEVbvDFilter1_Neg}$ is not *a priori* detectable.
- HIs $\boldsymbol{VbvSlpRightB}$ and $\boldsymbol{VbvSlpRightS}$ are not *a priori* detection relevant so that they can be suppressed from the list of HIs.
- All of he other HIs are *a priori* detection relevant. In particular, $\boldsymbol{VbvXchgS}$ is sensitive to 6 degradation modes.

	$VbvYchgB$	$VbvScaleB$	$VbvSlpLeftB$	$VbvSlpRightB$	$VbvHyst0B$	$VbvCEquS$	$VbvXchgS$	$VbvYchgS$	$VbvScaleS$	$VbvSlpLeftS$	$VbvSlpRightS$	$VbvHyst0S$	$VbvmaxX1$	$VbvmaxX2$	$VbvminX1$	$VbvminX2$	$VbvmaxGapX$	$VbvminGapX$	$VbvmeanGapX$	$VbvstdGapX$	$VbvMAErr$	**TOTAL**
...	.	.	.	.	.	.	.	.	.	.	.	.	.	.	.	.	.	.	.	.	.	...
$DEVbvDCool2_Pos$	0	1	1	0	0	1	1	0	1	1	0	0	0	0	0	0	0	0	0	0	0	10
$DEVbvDFilter1_Neg$	0	0	0	0	0	0	0	0	0	0	0	0	0	0	0	0	0	0	0	0	0	0
...	.	.	.	.	.	.	.	.	.	.	.	.	.	.	.	.	.	.	.	.	.	...
TOTAL	2	3	2	0	3	5	6	3	2	3	0	2	1	1	2	2	4	4	4	4	2	

Table 4.33 *Example of compliant detectability values.*

In conclusion, Appendix XXIV shows that 30 out of 71 degradation modes are not *a priori* detectable with the raw real set of His, so $DTDEM_{\%} = 57.7\%$. The value of $DTDEM_{\%}$ is under the specification (80%), so the current set of HIs is not validated for the detection.

4.6.2.2 *Identification NKPIs*

The compliant identifiability matrix for the set of raw real HIs are listed in Appendix XXV. To recall, it relates, for each couple of DEMs, the identification potential with respect to the specified minimal angle between variation vectors (see section 2.4.3.2). For each line representing a DEM, the last column is the total number of other DEMs with which they are identifiable. If this total is equal to 70, this indicates that the associated DEM is identifiable with respect to the whole set of DEMs. In this case, it is said to be *a priori* identifiable. An extract of this matrix is given in Table 4.34. It reveals that the DEM couples $(DEByvVisc_Pos/DEVbvDnozzle_Pos)$ and $(DEByvVisc_Pos/DEVbvVisc2_Pos)$ are not

identifiable, so DEM $DEByvVisc_Pos$ is not *a priori* identifiable. The DEMs $DByvDIlkg_Pos$, $DEByvK0_Neg$ and $DEByvStic_Pos$ are *a priori* identifiable.

	…	$DEVbvDFilter2_Neg$	$DEVbvDnozzle_Neg$	$DEVbvDnozzle_Pos$	$DEVbvKfeed_Neg$	$DEVbvKineFric_Pos$	$DEVbvStic1_Pos$	$DEVbvStic2_Pos$	$DEVbvSticspool_Pos$	$DEVbvVisc1_Pos$	$DEVbvVisc2_Pos$	…	TOTAL
$DByvDIlkg_Pos$	…	1	1	1	1	1	1	1	1	1	1	…	70
$DEByvK0_Neg$	…	1	1	1	1	1	1	1	1	1	1	…	70
$DEByvStic_Pos$	…	1	1	1	1	1	1	1	1	1	1	…	70
$DEByvVisc_Pos$	…	1	1	0	1	1	1	1	1	1	0	…	67
…	…	.	.	.	.	.	.	.	.	.	.	…	

Table 4.34 *Example of compliant identifiability values.*

In conclusion, Appendix XXV shows that 15 out of 71 degradation modes are not *a priori* identifiable with the raw real set of His, so $ITDEM_{\%} = 78.9\%$. The value of $ITDEM_{\%}$ is then slightly under the specification (80%). Thus, the current set of HIs is not validated for the identification.

4.6.2.3 *Localization NKPIs*

Appendix XXVI presents the complete results of localization NKPIs computation. For each row, a value of the last column inferior to 7 means that the LRU is not *a priori* localizable. Thus, in the present case, 5 out of 8 LRUs are not *a priori* localizable, so $LLRU_{\%} = 37.5\%$. The value of $LLRU_{\%}$ is thus widely under the specification (100%), and the current set of HIs is also not validated for the localization. However, these findings reveal some interesting properties. The ACU is not a priori localizable with respect to neither the FMU nor the variable geometries loops. This can be explained by the fact that the servovalves of the actuation loops are located in the ACU. Moreover, the VSV and VBV loops are not differentiable. However, when analyzing the results more precisely, it appears that this lack of localizability comes from two coupled DEMs that are not identifiable: ($DEVbvDnozzle_Pos/DEVsvDnozzle_Pos$) and ($DEVbvVisc2_Pos/DEVsvVisc2_Pos$). Both are not identifiable because they are not *a priori* detectable, so that their syndrome is close to the null vector. In conclusion, regardless of the existence of the not *a priori* detectable DEMs, the VSV and VBV loops are localizable.

4.6.2.4 *Prognostic NKPIs*

The prognostics NKPIs are listed in Appendix XXVII. They show the values of the detection, identification and localization margins. If the value is equal to 0, the margin is null, so the detection, and identification of localization will occur after the occurrence of a compliant service threat (**CST**). If the value of a margin is equal to ∞, it means that the considered degradation mode is not expected to cause any CST. For a degradation mode (**DEM**) to be said *a priori* prognosticable, its associated detection, identification and localization margin must be different from zero. For the present application, no DEM is *a priori* prognosticable as the value of the localization margin is systematically equal to zero. This phenomenon occurs because the localization performances computed in the previous subsection are far from specifications (25%).

Finally, the raw set of HIs is not validated. Therefore, the standardization procedure is applied from the SVR models trained in section 4.4.2.1 and the values of the Sobol indices computed in section 4.5.1.

4.6.3 NKPIs of standardized HIs for fleet models

The NKPIs for detection, identification, localization and prognostic for the standardized HIs are given, respectively, in Appendix XXX, Appendix XXXI, Appendix XXXII and Appendix XXXIII. They show that after the standardization procedure, 27 out of 71 DEMs are not *a priori* detectable. Thus, the standardization has allowed to detected 3 more DEMs, and the new value of $DTDEM_{\%}$ is 61,9%. However, even if an improvement has been achieved, the specifications are still not reached. Concerning the identification, 14 out of 71 degradation modes are not *a priori* identifiable with the raw real set of His, so $ITDEM_{\%} = 80.3\%$. Consequently, the new set of standardized HIs is compliant with the identification specifications. For the localization performances, they are unchanged after standardization: $LLRU_{\%}$ is still equal to 37.5%. Finally, concerning the prognostics, one DEM is *a priori* prognosticable: 0_Neg ($PCST_{\%} = 1.4\%$), whereas no DEM was for the raw set of HIs. However, the prognostic performances are still far from the specification. Therefore, individual models are constructed by propagating only context-related uncertainties.

4.6.4 NKPIs of real HIs for individual models

For individual models, the NKPIs for detection, identification, localization and prognostics for the standardized HIs are given, respectively, in Appendix XXXIV, Appendix XXXV, Appendix XXXVI and Appendix XXXVII. The detection NKPIs show that for individual models, $DTDEM_{\%} = 85.9\%$ which is compliant with the specifications. Moreover, the results indicate that for each DEM, the number of sensitive HIs is more important than in the fleet model case, which indicates a better robustness to the loss of one HI. Concerning the identification, the increase in the sensitivity of HIs has a negative impact on identifiability performances as the value of $ITDEM_{\%}$ passes from 78.9% to 67,6%. The solution to improve the value of $ITDEM_{\%}$ may be to reduce the number of HIs by eliminating those that are sensitive to a large number of HIs and not determinant for detection performances. For localization NKPIs with individual models, it appears that the criterion $LLRU_{\%}$ improved from 37.5% to 50% from fleet to individual models. Moreover, the VSV and VBV loops are now differentiable. However, the main problem is still that the ACU and particularly the servovalves of the VSV and VBV are not localizable with respect to the rest of their respective actuation loops. Finally, for the prognostics performances, only one DEM is a priori prognosticable, so $PCST_{\%} = 1.4\%$. As the set of HIs is still not validated, the conclusion is that either the set of HIs should be modified, or the specifications should be relaxed. In section 4.3, some virtual HIs were proposed. It is time to evaluate their potential by computing the NKPIs with the set of virtual HIs.

4.6.5 NKPIs of virtual HIs

The NKPIs for virtual HIs are listed in Appendix XXXVIII, Appendix XXXIX, Appendix XL and Appendix XLI for detection, identification, localization and prognostics, respectively. They are to be compared with raw HIs to assess the potential of virtual HIs. Concerning detection, $DTDEM_{\%} = 61.2\%$, which is better than 57.7%. For identification, $ITDEM_{\%} = 76\%$. Thus, the identification performances are worse than for the raw set of HIs for which $ITDEM_{\%} = 78.9\%$. For localization, the criterion $LLRU_{\%}$ is still equal to 37.5%, even if the compliant localizability matrix shows some improvements. Finally, for the prognostics, the performances are not improved.

The final results of the criteria computation are given in Table 4.35. As a conclusion, none of the HI configurations are compliant with the specifications. In particular, the localization performances are far from the required value. Therefore, some modifications to the set of HIs have to be performed. Typically, new HIs capable of differentiating DEMs associated with VSV and VBV servovalves from DEMs associated with the rest of their respective actuation loops could significantly improve identification and localization performance. Concerning the use of individual models, the results have shown a significant improvement of the detection performances but a decrease in identifiability. Thus, the transition to individual models must be accompanied by a reduction of the HI number to maintain identification performance. If the timing is too tight to modify the set of HIs, specifications must be relaxed for the PHM system.

HI configurations	$DTDEM_{\%}$	$ITDEM_{\%}$	$LLRU_{\%}$	$PCST_{\%}$
Raw set of HIs for a fleet model	57.7%	78.9%	37.5%,	0%
Standardized set of HIs for a fleet model	61.9%	80.3%	37.5%,	1.4%
Raw set of HIs for individual models	85.9%	67,6%	50%	1.4%
Virtual set of HIs for a fleet model	61.2%	76%	37.5%,	1.4%

Table 4.35 *Final results of criteria computation for different HI configurations.*

4.7 Conclusion

The main contribution of this chapter was to apply the methodology of IDPHM and the SVR-Kriging tool for the monitoring of a generic aircraft engine fuel system. Aircraft engines are machines that generate thrust via the rotation of a fan; turbines transmit power provided by the combustion of a gas and air mixture, while the compressors increase the upstream air pressure. The mechanical link between turbines and compressors ensures continuous rotation. Within this aircraft engine, the fuel system is in charge of metering the amount of fuel to be injected in the combustor. The functional analysis of the fuel system reveals that it is composed of three level 2 functional units and eight level 1 functional units. They include pumps, filters, fuel metering devices and locally controlled inlet-air variable geometries (fuel metering valve, variable stator vane and variable bleed valve). In parallel, its structure is split into eight LRUs, including the actuation control unit, actuators and several sensors. Some sensors measure the actuators' displacements. Others measure the flow and the fuel differential pressure.

Following the principles of IDPHM, some health indicators (**HIs**) and compliant service indicators (**CSIs**) have been defined hierarchically for each functional unit. The targeted compliant service threats (**TCSTs**) are mostly sensor faults, actuation faults and defects related to important leakages. The targeted degradation modes (**TDEMs**) are principally increases of viscous or static friction, clogging by fuel coking and leakage by erosion for hydraulic parts and sensor drifts or servovalve null currents for electric parts. HIs are then developed from acceptance test procedures, built-in tests and engineering judgment. Some are based on the velocity gain curves for actuation loops of variable geometries. This includes slopes, slope change coordinates and null velocity control current. A second set is devoted to

the sensors. Others are issued from statistical features from redundant sensor information. For the main fuel pump, the desired measurements of flow and pressure are not available. Therefore, the HIs are restricted to the rotation speed of the engine at the opening of the TBV and the SOV. Finally, 105 real HIs have been defined. In parallel, 11 virtual HIs are proposed to improve the complete set if necessary.

The physics-based model of the fuel system is defined using 80 uncertain parameters including one context, 12 epistemic and 67 degradation parameters. From the latter, 85 degradation modes (**DEMs**) are identified. A Morris sensitivity analysis revealed that 59 of the 80 parameters are influent. Among them, 11 are linear with respect to all the HIs. Support vector regression (**SVR**) models have been learnt from mono-dimensional vectors and are used to compute the median limit values (**MLVs**) for each DEM. SVR-Kriging models have finally been constructed by adding a test LHSDOE to the learning samples. The final accuracy was evaluated with respect to criteria issued from the cross-validation error. It appeared that it is not good enough to validate the model, but the future application of the sequential learning is expected to improve it significantly. However, this technique has not been performed because of prohibitive computation time.

The SVR-Kriging models allowed for the use of a Monte Carlo method for the computation of the Sobol sensitivity indices. They revealed that the two potential standardization parameters, namely the fuel temperature and the coefficient of the $N2$ law during the starting sequence, have a significant influence on certain HIs. For those HIs, the efficiency of the standardization procedure is illustrated via the computation of raw and standardized distributions that prove the expected reduction of the standard deviation.

The propagation of uncertainties has finally resulted in the computation of NKPIs for different configurations of the HI sets. It appears that the raw set of real HIs with a fleet model is not validated for detection, identification, localization or prognosticating. The subsequent standardization of HIs results in a specified value for identification but does not significantly improve other criteria because of the limited number of standardization parameters. Therefore, the NKPIs were computed for individual models. For this configuration, the criteria were validated for detection, but the increased sensitivity of HIs resulted in a decrease of identification performance. To illustrate how the IDPHM can benefit the design of the host system, the potential gain for PHM provided by additional sensors is evaluated via the computation of NKPI for virtual HIs. However, the performance gains are not significant. Evidentially, the conclusion is that the set of HIs needs to be changed or the specifications relaxed.

General Conclusion

Conclusions of the PhD thesis work

In the general introduction, the context of the present work was introduced as follows: Snecma is giving increasingly more interest to PHM, but its engineers face many difficulties in defining and applying a suitable development process. A solution to this industrial problem has been developed and illustrated in the four chapters.

The main contribution of the first chapter was to formalize a new development approach, which is called the integrated development of PHM (**IDPHM**). To unfold this new approach on solid foundations, an original terminology that is consistent with current industrial practices was proposed for the PHM items. The main particularity of these definitions is the duality between compliant service threats and physical threats. The former are only available on models, and their evolution is directly characterized by the compliant service indicators (**CSIs**), whereas the latter are actually measurable and characterized by the health indicators (**HIs**). Furthermore, the scope and functional framework of PHM were also defined considering the intended application. The main originality of the proposed scope is to consider the defects that traduce a state of an equipment or a subsystem that is not compliant to its specifications beyond the faults and failures. This consideration can improve the troubleshooting process and reduce the MRO duration. Subsequently, for the functional framework, the original functional and structural hierarchical breakdown representations of the host system were introduced with the standard architecture of the PHM systems based on the segregation between on-board and in-flight tasks. Then, the issue of PHM system development was addressed, and the main shortcoming of the current V-model appears to be a lack of interactions with the lifecycle of the host system. To overcome this weakness, the new approach of IDPHM was proposed based-on the V3-model, which is a declination of the V-model specific to PHM systems, for which the HI extraction is separated from their processing. The V3-model proposes to validate the embedded extraction, processing unit and supervision unit as if they were standalone systems. In particular, the complete V-model of the embedded extraction is performed before the entry into service of the system. This key feature enables an anticipated validation of the HIs, an improved standardization process and an early populating of the precursor database. The main constraint of this approach is that a lot of data are required during the design stages. This requirement is paradoxical because there is no measurement before the entry into service. To overcome this issue, physics-based models were proposed to create the necessary data from simulations.

The second chapter focuses on the issue of the model-based selection and HI validation during the early development stages of the PHM system. The PhD thesis work focuses on this topic because it is not addressed in the scientific community. Moreover, in fields such as aeronautics where controller retrofit costs are often prohibitive and both online storage and computation capabilities are limited, optimizing the set of HIs before the entry into service can be a determinant asset for airline companies. This issue recently becomes more relevant with the progressive appearance of flight hour contracts. In this work, the selection, validation and standardization of HIs were addressed. The first section of

chapter 2 proposes a formalism for the specific modeling framework and formalizes the selection process of HIs. The modeling of aircraft engine systems has three particularities. First, the parameters are organized according to three classes: context, epistemic and degradation parameters. Second, the temporal outputs of the system are transformed into HIs and CSIs using extraction functions. Finally, for the computation complexity matters, the influence of the shape of the temporal input signals is not considered. Consequently, the model is simulated for 1 constant set of input signals, which are retrieved from other engines and transformed to fit to the new application. In the end, the models simulate the behavior of HIs and CSIs in functions of parameters. To select the HIs, a set of key data between the parallel developments of the host and the PHM systems is proposed. This data set is composed of specification documents that contain the functional and structural architecture of the host system, FMEA analysis and the ATP descriptions. The HIs selection is performed following a hierarchical methodology from high to low levels of granularity. We also proposed to define both real HIs, which are issued from the actual sensors, and virtual His, which can be computed using the new potential sensors. The interest is to assess the potential gain of PHM performances that are associated with these new potential sensors. The second section addresses the standardization of HIs. First, two mathematical tools, namely the sensitivity analysis (**SA**) and the support vector regression (**SVR**), were introduced. For the SA, both the Morris method and the Sobol indices were addressed. Moreover, new indices based on the former method were proposed to fit with the multiple-output aspect of the present application. For the SVR, the emphasis was placed on the importance of selecting the kernel function and the learning DOE. The SVR is a well-known and proven technique, and the contribution of this work towards it is to propose to supervise these choices using the results from the SA. For the standardization, a new procedure was proposed, which consists of searching for the standardization parameters using the Sobol indices computation and determining the standardization functions using the single-dimension SVR. The main advantage of this method is its completion before the entry into service, so that the set of HIs is definitely approved before retrofit costs are prohibitive. The last section the HIs validation by proposing new performance metrics, which are called the numerical key performance indicators (**NKPIs**) to evaluate the quality of an HI set based on their distributions. To compute the latter, a methodology based on uncertainty propagation was developed. In addition, validation criteria were proposed with the associated required specifications. The validation process consists of the following steps. First, NKPIs are calculated for only the real raw HIs. If the validation criteria are not satisfied, the HIs are standardized, and the fleet model is replaced by individual engine models. If the results remain unacceptable, either virtual HIs can be added, or the HI set must be reconsidered.

The third chapter focused on the mathematical issues. The NKPIs that were proposed in the second chapter are based on the computation of receiver compliant service characteristic (**ROC**) curves, which is performed using the distributions of two random variables. Hence, the calculation of NKPIs requires a large amount of stochastic data. In the proposed IDPHM framework, it is provided by the uncertainty propagation using Monte-Carlo experiments on physics-based systems. However, the large number of required evaluations of the model makes the simulation time prohibitive. Thus, a surrogate model technique, which is called the Kriging technique, was proposed to reduce the computation load. The first section of this chapter was dedicated to the Kriging technique, by addressing its main issues: the selection of the learning DOE and the estimation of hyperparameters. After presenting a classification of existing Kriging techniques, the chapter focused on the family of non-stationary Kriging, which is *a priori* most related to the present application. However, among various non-stationary Kriging methods,

none can fully manage the specificities of the encountered function shapes. Thus, the second section proposed a new type of Kriging technique, which is named SVR-Kriging, based on the following principle: to keep a strong link with physics, the deterministic part of the Kriging model is built to encompass first-order effects, whereas a Gaussian process is used as a type of error term to account for the interaction effects. To precisely estimate the first-order effects, single-dimension SVRs are used. The advantage of using the SVR is its capability to estimate the nonlinear behavior without *a priori* knowledge about the shape of the functions. The advantage of treating each dimension independently is to better estimate the first-order effects with fewer evaluations of the model. Then, the efficiency of SVR-Kriging was tested on three functions of various dimensions with respect to three different performance metrics: the mean cross-validation error, the standard deviation of the cross-validation error and the Q2 coefficient. This method showed better results than the classical ordinary and universal Kriging methods. The third section proposed a methodology to improve the SVR-Kriging model when its accuracy is not as good as required. This methodology is based on a sequential learning process with a new selection criterion based on a combination of the Kriging variance and the cross-validation error. They provide global and local aspects to select the most relevant new sampling point. This sequential learning is also adapted to the specific multiple-output configuration of the considered models. A probability-assignation step allows one to select the best active model at each iteration.

The fourth chapter applied the methodology of IDPHM and the SVR-Kriging tool to monitor a generic aircraft engine fuel system. In this aircraft engine, the fuel system is in charge of metering the amount of fuel to inject into the combustor. This system has 12 functionnal units and 8 LRUs. Following the IDPHM principles, some health indicators (**HI**) and compliant service indicators (**CSIs**) were hierarchically defined for each functional unit. The targeted compliant service threats (**TCSTs**) are mostly sensor faults, actuation faults and defects that are related to important leakages. The targeted degradation modes (**TDEMs**) are principally increases of viscous or static friction, clogging, leakage and drift of sensors or servovalve null currents. Some HIs are based on the velocity gain curves for the actuation loops of variable geometries. Other HIs are issued from statistical features of redundant sensor information. Finally, 105 real HIs were defined. In parallel, 11 virtual HIs are proposed to improve the complete set if necessary. The physics-based model of the fuel system is defined using 80 uncertain parameters, which include 1 context, 12 epistemic and 67 degradation parameters. A Morris sensitivity analysis allowed us to shorten this list to 59 influential parameters, among which 11 are linear. Support vector regression (**SVR**) models were learnt using monodimensional vectors and used to compute the median limit values (**MLVs**). The SVR-Kriging models were finally constructed by adding a test LHSDOE to the learning samples because a lack of time prevented us from implementing the sequential learning method. This SVR-Kriging model allowed us to perform the Monte-Carlo method to compute the Sobol sensitivity indices, which revealed two potential standardization parameters. The efficiency of the standardization procedure was proven by the computation of raw and standardized distributions. The uncertainty propagation was performed to compute NKPIs. It appeared that the raw set of real HIs with a fleet model was not validated, and the HI standardization and the transition to individual models did not sufficiently improve the performance. Thus, the HIs cannot be implemented in the embedded controller. Either a modification of the HI set or a relaxation of the specifications is required.

Perspectives for future developments

Regarding future academic-related prospects, the first short-term objective is to improve the SVR-Kriging technique on the SVR validation. The sequential learning currently considers only the Gaussian process because the SVR is identical at each iteration. It can be interesting to define a criterion for the validation of the standalone SVR, which can be based on cross-validation errors. The sequential learning process can select the new learning point to improve either the SVR or the Gaussian process hyperparameters estimation. A second short-term improvement of the method is to integrate uncertainties that are related to the temporal input signals. The constant temporal-input model in this work does not integrate this type of uncertainty. For example, instead of using a single profile for each input, for each model evaluation, the input profiles can be randomly drawn from a database of several different profiles. Finally, the last short term objective would be to extend the state of the art about sensitivity analysis. Indeed, as it was not the main topic of this work, some areas for improvement have been left out due to lack of time to implement. For example, it could be interesting to use the Borgonovo's importance measure instead of the Sobol indices. Moreover, a medium-term purpose is to define a methodology to validate and recalibrate the physics-based model. Only the SVR-Kriging model is currently validated in the actual framework. However, if the original physics-based model is not accurate, both the precursor database and the standardization functions may be biased. We can imagine a model recalibration according to a new validation criteria. This recalibration method can be supervised using the SA results to focus on the most influential parameters and subsequently refined with less influential ones. Fortunately, because the NKPIs are based on the difference between the healthy and the degraded distributions, their relevance is not affected, and the global method remains efficient even with this observation. Finally, for the long-term prospects, the main idea is to complete the IDPHM methodology. Indeed, if the basis for the complete development scheme is defined in their outlines, only the first V of the V3-model was almost exhaustively addressed (the validation of the complete model was not). The present work is focused on the development of the monitoring unit is focused because it is the most urgent issue to solve from an industrial viewpoint. Regarding the development of the processing unit, only the main issues and the most common solutions were introduced. Moreover, for the scheduling unit, only the global V-model was proposed, but no solution has been studied. Thus, some performance metrics and validation criteria should be found for these units. Note that another PhD thesis work that was realized at Snecma by Ouadie Hmad addressed the definition of key performance indicators (**KPI**) that would be notably compliant service KPI (**OKPIs**) compared with NKPIs for the validation of the processing unit. Because these OKPIs are computed from the precursors' database, they also require a large amount of data. The simulation results provided by the present work can be useful to perform an earlier computation of these OKPIs. Finally, there remains a lot of work to do regarding the processing and the scheduling units. It was one of the first studies in the field of model-based validation of PHM. Consequently, because physics-based models were not well adapted, a lot of time was spent on the model optimization and the parameterization of the Matlab/AMESim interface. However, for future works on the subject, the models are ready, and they will only be a tool to serve higher PHM purposes.

Regarding the future industrial-related prospects, the first short-term objective is to construct additional HIs to attain the required performances for the detection, identification, localization and prognostics. A second short-term improvement is to apply the fuel system with more iterations for the

Morris method. In this the present application, the number of iterations was reduced to three, whereas it should be ideally equal to 10 to provide relevant results. Moreover, regarding the medium-term objectives, it may be interesting to complete the list of HIs by adding the electrical faults that potentially occur in harnesses and electrical connectors. One of the most common degradation modes is related to the intermittent contacts in the harness connectors. However, this type of degradation and all degradation of an electrical nature except sensor drift were not considered. A considerable evolution is to integrate them in the PHM scope. Similarly, the AMESim model was simplified not to consider the thermal effects on equipment. In fact, only the fuel viscosity is modeled as a function of the temperature. The encompassing of thermal effects would also be interesting. Similarly, the kinematic actuation chains were not completely modeled, so some degradation modes cannot be simulated. Finally, the long-term purpose of the IDPHM is to be applied for other systems. For example, it can be expanded to monitor the vibrations and thermodynamic performances. The next step is to fuse these different solutions to provide broader PHM information for the entire aircraft engine. Then, this same information can be coupled with the PHM of the nacelle. Typically, if the structural monitoring of the nacelle is based on the analysis vibration signals, this information can be transferred to the engine monitoring unit that is in charge of the bearing vibration analysis to improve the diagnostic. It is currently not the case because every supplier is developing its solutions without considering the potential interactions with other equipment or subsystems.

References

Allaire Douglas and Willcox Karen Surrogate modeling for uncertainty assessment with application to aviation environmental system models [Journal] // AIAA journal. - 2010. - 8 : Vol. 48. - pp. 1791-1803.

AMESim User Manual [Report] : Tech. rep.. - 2003.

An Senjian, Liu Wanquan et Venkatesh Svetha Fast cross-validation algorithms for least squares support vector machine and kernel ridge regression [Journal] // Pattern Recognition. - [s.l.] : Elsevier, 2007. - 8 : Vol. 40. - pp. 2154-2162.

Arias-Montano Alfredo, Coello Coello CA and Mezura-Montes Efren Multi-objective airfoil shape optimization using a multiple-surrogate approach [Conference] // Evolutionary Computation (CEC), 2012 IEEE Congress on. - 2012. - pp. 1-8.

Avizienis A. [et al.] Basic concepts and taxonomy of dependable and secure computing [Journal] // Dependable and Secure Computing, IEEE Transactions on. - 2004. - 1 : Vol. 1. - pp. 11-33.

Avizienis A., Laprie J.-C. et Randell B. Fundamental concepts of dependability [Book]. - Boston, Massachusetts, October 24-26 : Third Information Survivability Workshop, 2000.

Baraldi P., Mangili F. and Zio E. Ensemble of Bootstrapped Models for the prediction of the Remaining Useful Life of a Creeping Turbine Blade [Conference] // Proceedings of IEEE PHM. - Denver : [s.n.], 2012.

Barros Anne, Bérenguer Christophe et Grall Antoine Optimization of replacement times using imperfect monitoring information [Paper] // IEEE Transactions on Reliability. - [s.l.] : IEEE, 2003. - 4 : Vol. 52. - pp. 523-533.

Ben-Daya Mohamed [et al.] Handbook of maintenance management and engineering [Book]. - [s.l.] : Springer, 2009. - Vol. 7.

Bérenguer Christophe, Chu Chengbin et Grall Antoine Inspection and maintenance planning: An application of semi-Markov decision processes [Paper] // Journal of Intelligent Manufacturing. - [s.l.] : Springer, 1997. - 5 : Vol. 8. - pp. 467-476.

Bertolino A. [et al.] Dependability and Performance Assessment of Dynamic CONNECTed Systems [Conference] // 11th International School SFM 2011 LNCS 6659. - 2011. - pp. 350-392.

Bichon Barron J [et al.] Efficient global reliability analysis for nonlinear implicit performance functions [Journal] // AIAA journal. - 2008. - 10 : Vol. 46. - pp. 2459-2468.

Bishop Christopher M et Nasrabadi Nasser M Pattern recognition and machine learning [Book]. - [s.l.] : springer New York, 2006. - Vol. 1.

Björkman Mattias et Holmström Kenneth Global optimization using DIRECT algorithm in matlab [Journal]. - [s.l.] : Citeseer, 1999.

Borgonovo Emanuele A new uncertainty importance measure [Paper] // Reliability Engineering & System Safety. - [s.l.] : Elsevier, 2007. - 6 : Vol. 92. - pp. 771-784.

Borgonovo Emanuele Measuring uncertainty importance: investigation and comparison of alternative approaches [Paper] // Risk Analysis. - 2006. - Wiley Online Library. - 5 : Vol. 26. - pp. 1349-1361.

Boufaied Amine Contribution à la Surveillance Distribuée Des Systèmes à Evénements Discrets Complexes [Report] : Ph.D. dissertation / Université Paul Sabatier-Toulouse III. - [s.l.] : Thèse de l'Université Toulouse 3 Paul Sabatier, 2003.

Bradley A. P. The Use of the Area Under the ROC Curve in the Evaluation of Machine Learning Algorithms [Paper] // Pattern Recognition. - 1997. - 7 : Vol. 30. - pp. 1145 – 1159.

Chowdhury Mohammad, Alouani Ali et Hossain Faisal Comparison of ordinary Kriging and artificial neural network for spatial mapping of arsenic contamination of groundwater [Journal] // Stochastic Environmental Research and Risk Assessment. - [s.l.] : Springer, 2010. - 1 : Vol. 24. - pp. 1-7.

Clark J. O. System of Systems Engineering and Family of Systems Engineering From a Standards, V-Model, and Dual-V Model Perspective [Conference] // Systems Conference, 2009 3rd Annual IEEE. - Vancouver : [s.n.], 2009. - pp. 381-387.

Clarke Stella M, Griebsch Jan H et Simpson Timothy W Analysis of support vector regression for approximation of complex engineering analyses [Journal] // Journal of mechanical design. - [s.l.] : American Society of Mechanical Engineers, 2005. - 6 : Vol. 127. - pp. 1077-1087.

Cocheteux Pierre Contribution à la maintenance proactive par la formalisation du processus de pronostic des performances de systèmes industriels [Report] : Ph.D. dissertation / Nancy I University - Henri Poincaré. - [s.l.] : PhD thesis from the Nancy I University - Henri Poincaré, 2010.

Cocheteux Pierre, Voisin Alexandre et Iung Benoît Formalisation du pronostic à base dd'un approche processus [Conference] // 3ème Colloqie Internationnal Francophone Performance et Nouvelles Technologies en Maintenance, PENTOM 2007. - Mons: Belgium : [s.n.], 2007.

Cressie Noel The origins of Kriging [Journal] // Mathematical Geology. - [s.l.] : Springer, 1990. - 3 : Vol. 22. - pp. 239-252.

Davis Bruce M Uses and abuses of cross-validation in geostatistics [Journal] // Mathematical Geology. - [s.l.] : Springer, 1987. - 3 : Vol. 19. - pp. 241-248.

De Rocquigny E. [et al.] Uncertainty in industrial practice: A guide to quantitative uncertainty management [Book]. - [s.l.] : Wiley, 2007.

Den Hertog Dick, Kleijnen Jack PC et Siem AYD The correct Kriging variance estimated by bootstrapping [Journal] // Journal of the Operational Research Society. - [s.l.] : Nature Publishing Group, 2006. - 4 : Vol. 57. - pp. 400-409.

Desforges X. [et al.] A distributed Architecture to implement a Prognostic Function for Complex Systems [Conference] // Proceedings of First European Conference of the Prognostics and Health Management Society. - Dresden : [s.n.], 2012. - pp. 2 - 9.

Diamanti K. et Soutis C. Structural health monitoring techniques for aircraft composite structures [Journal] // Progress in Aerospace Sciences. - November 2010. - 8 : Vol. 46. - pp. 342-352.

Dragomir O. E. [et al.] Review of Prognostic Problem in Condition-Based Maintenance [Conference] // European Control Conference, ECC'09.. - Budapest : [s.n.], 2009. - pp. 1585-1592.

Dzakowic James E. et Valentine Scott G. Advanced Techniques For The Verification And Validation Of Prognostics \& Health Management Capabilities [Journal] // Machinery Failure Prevention Technologies (MFPT 60). - 2007. - Vol. 60. - pp. 1-11.

Echard B, Gayton N et Lemaire M AK-MCS: An active learning reliability method combining Kriging and Monte Carlo Simulation [Journal] // Structural Safety. - [s.l.] : Elsevier, 2011. - 2 : Vol. 33. - pp. 145-154.

Efron Bradley et Tibshirani Robert An introduction to the bootstrap [Book]. - [s.l.] : CRC press, 1993. - Vol. 57.

Fisher James and Bhattacharya Raktim Optimal trajectory generation with probabilistic system uncertainty using polynomial chaos [Journal] // Journal of dynamic systems, measurement, and control. - [s.l.] : American Society of Mechanical Engineers, 2011. - 1 : Vol. 133.

Forrester A. I. J. and Keane A. J. Recent advances in surrogate-based optimization [Journal] // Progress in Aerospace Sciences. - 2009. - 1-3 : Vol. 45. - pp. 50-79.

Friedman Jerome H Multivariate adaptive regression splines [Journal] // The annals of statistics. - [s.l.] : JSTOR, 1991. - pp. 1-67.

Gini C. Concentration and dependency ratios [Journal] // Rivista di Politica Economica. - 1997. - 87. - pp. 769-792.

Goel Tushar [et al.] Ensemble of surrogates [Journal] // Structural and Multidisciplinary Optimization. - [s.l.] : Springer, 2007. - 3 : Vol. 33. - pp. 199-216.

Guo Zhiwei and Bai Guangchen Application of least squares support vector machine for regression to reliability analysis [Journal] // Chinese Journal of Aeronautics. - [s.l.] : Elsevier, 2009. - 2 : Vol. 22. - pp. 160-166.

Hmad Ouadie [et al.] Maturation of Detection Functions by Performances Benchmark. Application to a PHM Algorithm [Journal] // CHEMICAL ENGINEERING. - 2013. - Vol. 33.

Hoeffding W. A class of statistics with asymptotically normal distributions [Journal] // Annals of Mathematical Statistics. - 1948. - Vol. 19. - pp. 293-325.

Homma T. et Saltelli A. Importance measures in global sensitivity analysis of non linear models [Journal] // Reliability Engineering and System Safety. - 1996. - Vol. 52. - pp. 1-17.

Hon Yiu-Chung [et al.] Multiquadric solution for shallow water equations [Journal] // Journal of Hydraulic Engineering. - [s.l.] : American Society of Civil Engineers, 1999. - 5 : Vol. 125. - pp. 524-533.

Hsu Chih-Wei [et al.] A practical guide to support vector classification // A practical guide to support vector classification. - 2003.

Hsu Chih-Wei et Lin Chih-Jen A comparison of methods for multiclass support vector machines [Journal] // Neural Networks, IEEE Transactions on. - [s.l.] : IEEE, 2002. - 2 : Vol. 13. - pp. 415-425.

Hwang Inseok [et al.] A survey of fault detection, isolation, and reconfiguration methods [Journal] // Control Systems Technology, IEEE Transactions on. - [s.l.] : IEEE, 2010. - 3 : Vol. 18. - pp. 636-653.

IATA Airline maintenance costs executive commentary [Report] : Tech. rep.. - 2011.

Iman Ronald L Latin hypercube sampling [Book]. - [s.l.] : Wiley Online Library, 2008.

Iooss B. Revue sur l'Analyse de Sensibilité Globale de Modèles Numériques [Journal] // Journal de la Société Française de Statistique. - 2011. - 1 : Vol. 152. - pp. 3-25.

Isermann R. Model-Based fault-detection and diagnosis - status and applications [Journal] // Annual Reviews in Control. - 2005. - 1 : Vol. 29. - pp. 71-85.

Isermann Rolf Supervision, fault-detection and fault-diagnosis methods - An introduction [Paper] // Control Engineering Practice vol.5. - 1997. - pp. 639-652.

Jamshidi Mohammad System of systems engineering: innovations for the twenty-first century [Book]. - [s.l.] : John Wiley \& Sons, 2011. - Vol. 58.

Jardine Andrew, Lin Daming et Banjevic Dragan A review on machinery diagnostics and prognostics implementing condition-based maintenance [Journal] // Mechanical systems and signal processing. - 2006. - 7 : Vol. 20. - pp. 1483–1510.

Jin Ruichen, Chen Wei and Sudjianto Agus An efficient algorithm for constructing optimal design of computer experiments [Journal] // Journal of Statistical Planning and Inference. - [s.l.] : Elsevier, 2005. - 1 : Vol. 134. - pp. 268-287.

Jin Ruichen, Chen Wei et Simpson Timothy W Comparative studies of metamodelling techniques under multiple modelling criteria [Journal] // Structural and Multidisciplinary Optimization. - [s.l.] : Springer, 2001. - 1 : Vol. 23. - pp. 1-13.

Jin Ruichen, Chen Wei et Sudjianto Agus On sequential sampling for global metamodeling in engineering design [Conference] // ASME 2002 International Design Engineering Technical Conferences and Computers and Information in Engineering Conference. - 2002. - pp. 539-548.

Johnson Mark E, Moore Leslie M and Ylvisaker Donald Minimax and maximin distance designs [Journal] // Journal of statistical planning and inference. - [s.l.] : Elsevier, 1990. - 2 : Vol. 26. - pp. 131-148.

Johnson Stephen B. [et al.] System Health Management with Aerospace Applications [Book]. - [s.l.] : Wiley, 2011.

Jones Donald R, Schonlau Matthias et Welch William J Efficient global optimization of expensive black-box functions [Journal] // Journal of Global optimization. - [s.l.] : Springer, 1998. - 4 : Vol. 13. - pp. 455-492.

Kalgren Patrick W. [et al.] Defining PHM, a Lexical Evolution of Maintenance and Logistics [Conference] // IEEE Autotestcon. - 2006. - pp. 353-358.

Kempowsky T. Surveillance de Procédés à Base de Méthodes de Classification - Conception d'un outil d'Aide pour la Détection et le Diagnostic des Défaillances [Book]. - Toulouse, : PhD thesis from the Institut National des Sciences Appliquées de Toulouse, 2004.

Khalil Wissam [et al.] Hypergraph Models for System of Systems Supervision Design [Journal] // Systems, Man and Cybernetics, Part A: Systems and Humans, IEEE Transactions on. - [s.l.] : IEEE, 2012. - 4 : Vol. 42. - pp. 1005-1012.

Kleijnen J. P. C. Kriging metamodeling in simulation: a review [Journal] // European Journal of Operational Research. - 2009. - 3 : Vol. 192. - pp. 707-716.

Lacaille Jérôme Standardized failure signature for a turbofan engine [Conference] // Aerospace conference, 2009 IEEE. - Big Sky, MT, : [s.n.], 2009. - pp. 1-8.

Lacaille Jérôme, Gerez Valério et Zouari Rafik An Adaptive Anomaly Detector used in Turbofan Test Cells // An Adaptive Anomaly Detector used in Turbofan Test Cells. - [s.l.] : PHM, 2010.

Lacaille Jérôme, Gouby Aurélie et Piol Olivier Wear Prognostic on Turbofan Engines [Conference] // Annual Conference of the Prognostics and Health Management Society. - 2013.

Lamboni Matieyendou [et al.] Derivative-based global sensitivity measures: general links with Sobol'indices and numerical tests [Journal] // Mathematics and Computers in Simulation. - [s.l.] : Elsevier, 2013. - Vol. 87. - pp. 45-54.

Lamoureux B., Massé J. R. et Mechbal N. Improving Aircraft Engines Prognostics and Health Management via Anticipated Model-Based Validation of Health Indicators [Journal] // Prognostics Journal. - 2014. - 1 : Vol. 2. - pp. 18-38.

Lamoureux Benjamin, Mechbal Nazih et Massé Jean-Rémi A Combined Sensitivity Analysis and Kriging Surrogate Modeling for Early Validation of Health Indicators [Journal] // Reliability Engineering and System Safety. - 2014, DOI: 10.1016/j.ress.2014.03.007.

Laprie J.-C. Dependable Computing and Fault Tolerance: Concepts and terminology [Conference] // Proceedings of the 15th IEEE International Symposium on Fault-Tolerant. - 1985.

Li Genyuan, Rosenthal Carey et Rabitz Herschel High dimensional model representations [Journal] // The Journal of Physical Chemistry A. - [s.l.] : ACS Publications, 2001. - 33 : Vol. 105. - pp. 7765-7777.

Li J [et al.] Assessing parameter importance of the Common Land Model based on qualitative and quantitative sensitivity analysis. [Journal] // Hydrology \& Earth System Sciences Discussions. - 2013. - 2 : Vol. 10.

Liefvendahl M et Stocki R A study on algorithms for optimization of Latin hypercubes [Journal] // Journal of Statistical Planning and Inference. - [s.l.] : Elsevier, 2006. - 9 : Vol. 136. - pp. 3231-3247.

Lin Yu-Pin [et al.] Modeling spatial uncertainty of heavy metal content in soil by conditional Latin hypercube sampling and geostatistical simulation [Journal] // Environmental Earth Sciences. - [s.l.] : Springer, 2011. - 2 : Vol. 62. - pp. 299-311.

Liu Weiyu Development of gradient-enhanced Kriging approximations for multidisciplinary design optimization [Report] : Ph.D. dissertation. - 2003.

Lophaven S. N., Nielsen H. B. et Søndergaard J. DACE, a matlab Kriging toolbox [Report] : Tech. rep. / Tech. Rep. IMM-TR-2002-12, IMM. - 2002.

Ly Fatime, Simeu-Abazi Zineb et Leger Jean-Baptiste Terminiologie Maintenance : bilan [Report] / FIMA - Groupement de Recherche en Productique . - Grenoble : [s.n.], 1999.

Marrel A. [et al.] Calculations of Sobol indices for the Gaussian process metamodel [Journal] // Reliability Engineering and System Safety. - 2009. - 3 : Vol. 94. - pp. 742-751.

Marrel Amandine [et al.] An efficient methodology for modeling complex computer codes with Gaussian processes [Journal] // Computational Statistics \& Data Analysis. - [s.l.] : Elsevier, 2008. - 10 : Vol. 52. - pp. 4731-4744.

Marrel Amandine Mise en oeuvre et utilisation du métamodèle processus gaussien pour l'analyse de sensibilité de modèles numériques - Application à un code de transport hydrogéologique [Report] : Ph.D. dissertation / Institut National des Sciences Appliquées de Toulouse. - 2008.

Massé J. R., Hmad O. et Boulet X. System PHM Algorithm Maturation [Conference] // First European Conference of Prognostics and Health Management Society. - Dresden : [s.n.], 2012.

Massé Jean-Rémi [et al.] Method and device for monitoring a feedback loop of a variable-geometry actuator system of a jet engine // Method and device for monitoring a feedback loop of a variable-geometry actuator system of a jet engine. - Geneva, Switzerland: World Intellectual Property Organization, : [s.n.], April 2012.

Massé Jean-Remi Andre [et al.] Method for monitoring a control device of a fuel metering valve of a turbojet engine // Method for monitoring a control device of a fuel metering valve of a turbojet engine. - [s.l.] : Google Patents, #dec#~3 2012. - US Patent App. 13/692,684.

Matheron Georges Principles of geostatistics [Journal] // Economic geology. - [s.l.] : SecG, 1963. - 8 : Vol. 58. - pp. 1246-1266.

McKay MD, Beckman RJ et Conover WJ A comparison of three methods for selecting values of input variables in the analysis of output from a computer code [Journal] // Technometrics. - [s.l.] : Taylor \& Francis Group, 2000. - 1 : Vol. 42. - pp. 55-61.

McRae Gregory J, Tilden James W et Seinfeld John H Global sensitivity analysis—a computational implementation of the Fourier amplitude sensitivity test (FAST) [Journal] // Computers \& Chemical Engineering. - [s.l.] : Elsevier, 1982. - 1 : Vol. 6. - pp. 15-25.

Megill Robert E An introduction to risk analysis [Journal]. - [s.l.] : PennWell Books, Tulsa, OK, 1984.

Metropolis N. et Ulam S. The Monte Carlo Method [Journal] // Journal of the American Statistical Association. - 1949. - 247 : Vol. 44. - pp. 335-341.

Meyer J. F. On Evaluating the Performability of Degradable Computing Systems [Journal] // IEEE Transactions on Computers. - August 1980. - 8 : Vol. C-29. - pp. 720 - 731 .

Meyer J. F. Performability: a retrospective and some pointers to the future [Journal] // Performance evaluation. - 1992. - 3-4 : Vol. 14. - pp. 139-156.

Miao Q. [et al.] Remaining useful life prediction of lithium-ion battery with unscented particle filter technique [Journal] // Microelectronics Reliability. - 2012. - 6 : Vol. 53. - pp. 805-810.

Moir Ian et Seabridge Allan Aircraft Systems: Mechanical, electrical, and avionics subsystems integration [Book]. - [s.l.] : Wiley, 2008.

Mokhtari Aimed Diagnostic des systèmes hybrides: développement d'une méthode associant la détection par classification et la simulation dynamique [Report] : Ph.D. dissertation / INSA de Toulouse. - 2007.

Moore Ramon E et Moore RE Methods and applications of interval analysis [Book]. - [s.l.] : SIAM, 1979. - Vol. 2.

Morris M. D. Factorial sampling plans for preliminary computational experiments [Journal] // Technometrics. - [s.l.] : Taylor \& Francis, 1991. - 2 : Vol. 33. - pp. 161-174.

Moyeed Rana A et Papritz Andreas An empirical comparison of Kriging methods for nonlinear spatial point prediction [Journal] // Mathematical Geology. - [s.l.] : Springer, 2002. - 4 : Vol. 34. - pp. 365-386.

Muller Alexandre Contribution à la maintenance prévisionnelle des systèmes de production par la formalisation d'un processus de pronostic [Report] : Ph.D. dissertation / Université Henri Poincaré, Nancy I. - 2005.

Muller Alexandre, Crespo Marquez Adolfo et Iung Benoît On the concept of e-maintenance: Review and current research [Journal] // Reliability Engineering & System Safety. - [s.l.] : Elsevier, 2008. - 8 : Vol. 93. - pp. 1165-1187.

Myers Donald E Matrix formulation of co-Kriging [Journal] // Journal of the International Association for Mathematical Geology. - [s.l.] : Springer, 1982. - 3 : Vol. 14. - pp. 249-257.

Narvaez Claudia Diagnostic par techniques d'apprentissage floues: conception d'une m{\'e}thode de validation et d'optimisation des partitions [Report] : Ph.D. dissertation / Toulouse, INSA. - 2007.

Nielsen H. B., Lophaven S. N. et Sondergaard J. DACE - A Matlab Kriging Toolbox [Book]. - Lyngby - Denmark : Informatics and Mathematical Modelling, Technical University of Denmark, DTU, 2002.

Omre Henning Bayesian Kriging—merging observations and qualified guesses in Kriging [Journal] // Mathematical Geology. - [s.l.] : Springer, 1987. - 1 : Vol. 19. - pp. 25-39.

OSA-CBM Website [Online]. - http://www.osacbm.org/.

Patterson-Hine Ann [et al.] A Review of Diagnostic Techniques for ISHM Applications // A Review of Diagnostic Techniques for ISHM Applications. - Napa, : [s.n.], 2005. - Vol. 1st Integrated Systems Health Engineering and Management Forum.

Peter J et Marcelet M Comparison of surrogate models for turbomachinery design [Journal] // WSEAS Transactions on Fluid Mechanics. - 2008. - 1 : Vol. 3. - pp. 10-17.

Rajashekhar Malur R et Ellingwood Bruce R A new look at the response surface approach for reliability analysis [Journal] // Structural safety. - [s.l.] : Elsevier, 1993. - 3 : Vol. 12. - pp. 205-220.

Rana S. P. et Taneja S. K. A Distributed Architecture for Automated Manufacturing Systems [Journal] // International Journal of Advanced Manufacturing Technology. - 1988. - 5 : Vol. 3. - pp. 81-98.

Rapajic Jasenka Beyond airline disruptions [Book]. - [s.l.] : Ashgate Publishing, Ltd., 2009.

Rasmussen Carl Edward Gaussian processes for machine learning [Journal]. - [s.l.] : Citeseer, 2006.

Ravalico JK [et al.] A comparison of sensitivity analysis techniques for complex models for environment management [Conference] // International Congress on Modelling and Simulation (2005: Melbourne, Vic.). - 2005.

Rayas-Sanchez José Ernesto EM-based optimization of microwave circuits using artificial neural networks: The state-of-the-art [Journal] // Microwave Theory and Techniques, IEEE Transactions on. - [s.l.] : IEEE, 2004. - 1 : Vol. 52. - pp. 420-435.

Ribot Pauline Vers l'intégration diagnostic/pronostic pour la maintenance des Systèmes Complexes [Book]. - [s.l.] : Thèse de l'Université Toulouse 3 Paul Sabatier, 2009.

Rivoirard Jacques Introduction to disjunctive Kriging and non-linear geostatistics [Journal]. - [s.l.] : Clarendon press, 1994.

Roemer M. J. et Byington C. S. Prognostics and health management software for gas turbine engine bearings [Conference] // Proceedings of the ASME Turbo Expo. - Montreal, : [s.n.], 2007. - pp. 795-802.

Roemer Michael [et al.] An overview of selected prognostic technologies with application to engine health management [Conference] // Proceedings of GT2006 ASME Turbo Expo. - Barcelona : Proceedings of GT2006 ASME Turbo Expo , 2006.

Sacks Jerome [et al.] Design and analysis of computer experiments [Journal] // Statistical science. - [s.l.] : Institute of Mathematical Statistics, 1989. - 4 : Vol. 4. - pp. 409-423.

Saha Bhaskar and Goebel Kai Uncertainty management for diagnostics and prognostics of batteries using Bayesian techniques [Conference] // IEEE Aerospace Conference. - Big Sky : [s.n.], 2008. - pp. 1–8.

Saltelli Andrea [et al.] Sensitivity analysis [Book]. - [s.l.] : Wiley New York, 2000. - Vol. 134.

Samad Abdus [et al.] Multiple surrogate modeling for axial compressor blade shape optimization [Revue] // Journal of Propulsion and Power. - 2008. - 2 : Vol. 24. - pp. 301-310.

Saxena A. [et al.] Metrics for Evaluating Performance of Prognostic Techniques [Conference] // Prognostics and Health Management, 2008. PHM 2008. International Conference on. - 2008. - pp. 1-17.

Saxena A. [et al.] Metrics for Offline Evaluation of Prognostic Performance [Journal] // International Journal of Prognostics and Health Management. - 2010. - 1 : Vol. 1. - p. 20.

Scheidt Céline Analyse statistique d'expériences simulées: Modélisation adaptative de réponses non régulières par krigeage et plans d'expériences, Application à la quantification des incertitudes en ingénierie des réservoirs pétroliers [Report] : Ph.D. dissertation / Université Louis Pasteur-Strasbourg I. - 2006.

Shahsavani Davood et Grimvall Anders Variance-based sensitivity analysis of model outputs using surrogate models [Journal] // Environmental Modelling \& Software. - [s.l.] : Elsevier, 2011. - 6 : Vol. 26. - pp. 723-730.

Sheppard John W, Kaufman Mark A et Wilmer Timothy J IEEE standards for prognostics and health management [Journal] // Aerospace and Electronic Systems Magazine, IEEE. - [s.l.] : IEEE, 2009. - 9 : Vol. 24. - pp. 34-41.

Shu Zhen et Jirutitijaroen Panida Latin hypercube sampling techniques for power systems reliability analysis with renewable energy sources [Journal] // Power Systems, IEEE Transactions on. - [s.l.] : IEEE, 2011. - 4 : Vol. 26. - pp. 2066-2073.

Sick Bernhard On-line and indirect tool wear monitoring in turning with artificial neural networks: a review of more than a decade of research [Journal] // Mechanical Systems and Signal Processing. - [s.l.] : Elsevier, 2002. - 4 : Vol. 16. - pp. 487-546.

Simpson Timothy W [et al.] Kriging models for global approximation in simulation-based multidisciplinary design optimization [Journal] // AIAA journal. - 2001. - 12 : Vol. 39. - pp. 2233-2241.

Simpson Timothy W [et al.] Metamodels for computer-based engineering design: survey and recommendations [Journal] // Engineering with computers. - [s.l.] : Springer, 2001. - 2 : Vol. 17. - pp. 129-150.

Smola Alex J. et Schölkopf Bernhard A tutorial on support vector regression [Journal] // Statistics and computing. - [s.l.] : Springer, 2004. - 3 : Vol. 14. - pp. 199-222.

Sobol I. M. Sensitivity estimates for nonlinear mathematical models [Journal] // Mathematical Modelling and Computational Experiments. - 1993. - Vol. 1. - pp. 407–414.

Sobol Ilya M et Kucherenko Sergei Derivative based global sensitivity measures and their link with global sensitivity indices [Journal] // Mathematics and Computers in Simulation. - [s.l.] : Elsevier, 2009. - 10 : Vol. 79. - pp. 3009-3017.

Swearingen KMWBB [et al.] An open system architecture for condition based maintenance overview [Conference] // Aerospace Conference, 2007 IEEE. - 2007. - pp. 1-8.

Tang Boxin Selecting Latin hypercubes using correlation criteria [Journal] // Statistica Sinica. - [s.l.] : C/O DR HC HO, INST STATISTICAL SCIENCE, ACADEMIA SINICA, TAIPEI 115, TAIWAN, 1998. - 3 : Vol. 8. - pp. 965-977.

Tran V. T. [et al.] Machine performance degradation assessment and remaining useful life prediction using proportional hazard model and support vector machine [Journal] // Mechanical Systems and Signal Processing. - 2012. - Vol. 32. - pp. 320-330.

Vapnik Vladimir, Golowich Steven et Smola Alex Support vector method for function approximation, regression estimation, and signal processing [Journal] // Advances in neural information processing systems. - 1997. - pp. 281-287.

Vazquez Emmanuel et Walter Eric Multi-output support vector regression [Conference] // 13th IFAC Symposium on System Identification. - 2003. - pp. 1820-1825.

Wang H. [et al.] Data Driven Fault Diagnosis and Fault Tolerant Control: Some Advances and Possible New Directions [Journal] // Acta Automatica Sinica. - 2009. - 6 : Vol. 35. - pp. 739–747.

Wickens T. D. Elementary Signal Detection Theory [Book] / éd. Press New York: Oxford University. - 2002.

Ye Kenny Q Orthogonal column Latin hypercubes and their application in computer experiments [Journal] // Journal of the American Statistical Association. - [s.l.] : Taylor \& Francis, 1998. - 444 : Vol. 93. - pp. 1430-1439.

Yee Paul V et Haykin Simon S Regularized radial basis function networks: theory and applications [Book]. - [s.l.] : John Wiley, 2001.

Zemouri R. Contribution à la surveillance des systèmes de production à l'aide des réseaux de neurones dynamiques: Application à la e-maintenance [Book]. - [s.l.] : Thèse de l'Université de Franche-Comté, 2003.

APPENDICES

Overview

Appendix I. Line replaceable units association matrix 234
Appendix II. active channel selection 235
Appendix III. Computation of selected measures 236
Appendix IV. PID controllers for closed-loops 237
Appendix V. Actuation faults detection 238
Appendix VI. Targeted compliant service threats for the fuel metering valve loop 239
Appendix VII. Targeted ompliant service threats for the fuel metering unit 240
Appendix VIII. Compliant service threats for the main fuel pump 241
Appendix IX. Compliant service threats for the main fuel filter 242
Appendix X. Compliant service threats for the variable stator vane 243
Appendix XI. Compliant service threats for the variable stator vane 244
Appendix XII. Compliant service threats for the flowmeter 245
Appendix XIII. Complete list of parameters 246
Appendix XIV. Complete list of degradation modes 248
Appendix XV. Complete list of health indicators 250
Appendix XVI. Complete list of compliant service indicators. 253
Appendix XVII. Initial uncertainties quantification 254
Appendix XVIII. Complete results of the Morris method 255
Appendix XIX. List of potential cause degradation modes 257
Appendix XX. List of degradation modes and associated median limit values. 258
Appendix XXI. Performance metrics for the SVR models of HIs and CSIs 261
Appendix XXII. Performance metrics for the first set of SVR-Kriging models 262
Appendix XXIII. Performance metrics for the second set of SVR-Kriging models 263
Appendix XXIV. Detection NKPIs for the fleet models with real HIs 264
Appendix XXV. Identification NKPIs for the raw set of HIs 268
Appendix XXVI. Localization NKPIs for the raw set of HIs 269
Appendix XXVII. Prognostics NKPIs for the raw set of HIs 270
Appendix XXVIII. List of Sobol indices of order 1 271
Appendix XXIX. List of total Sobol indices 277
Appendix XXX. Detection NKPIs for standardized HIs 283
Appendix XXXI. Identification NKPIs standardized HIs 287
Appendix XXXII. Localization NKPIs for standardized HIs 288
Appendix XXXIII. Prognostics NKPIs for the standardized HIs 289
Appendix XXXIV. Detection NKPIs for individual models 290
Appendix XXXV. Identification NKPIs for individual models 294
Appendix XXXVI. Localization NKPIs for individual models 295
Appendix XXXVII. Prognostics NKPIs for individual models 296
Appendix XXXVIII. Detection NKPIs for virtual HIs 297
Appendix XXXIX. Identification NKPIs for virtual HIs 301
Appendix XL. Localization NKPIs for virtual HIs 302
Appendix XLI. Prognostics NKPIs for virtual HIs 303

Appendix I. Line replaceable units association matrix

	Pumping Unit	Fuel Filter	ACU	FMU	VSV Actuation	VBV Actuation	TBV Actuation	Flowmeter
LPP device	**1**	0	0	0	0	0	0	0
HPP device	**1**	0	0	0	0	0	0	0
Main Fuel Filter device	0	**1**	0	0	0	0	0	0
DP sensor harnesses	0	0	0	0	0	0	0	0
DP sensor device	0	**1**	0	0	0	0	0	0
FMV loop	0	0	0	**1**	0	0	0	0
HPSOV loop	0	0	0	**1**	0	0	0	0
Bypass	0	0	0	**1**	0	0	0	0
VSV servovalve	0	0	**1**	0	0	0	0	0
VSV actuator 1	0	0	0	0	**1**	0	0	0
VSV actuator 2	0	0	0	0	**1**	0	0	0
VSV LVDT A	0	0	0	0	**1**	0	0	0
VSV LVDT B	0	0	0	0	**1**	0	0	0
VSV kinematic chain	0	0	0	0	**1**	0	0	0
VBV servovalve	0	0	**1**	0	0	0	0	0
VBV actuator 1	0	0	0	0	0	**1**	0	0
VBV actuator 2	0	0	0	0	0	**1**	0	0
VBV LVDT A	0	0	0	0	0	**1**	0	0
VBV LVDT B	0	0	0	0	0	**1**	0	0
VBV kinematic chain	0	0	0	0	0	**1**	0	0
TBV servovalve	0	0	**1**	0	0	0	0	0
TBV actuator	0	0	0	0	0	0	**1**	0
TBV LVDT A	0	0	0	0	0	0	**1**	0
TBV LVDT B	0	0	0	0	0	0	**1**	0
WFM flowmeter device	0	0	0	0	0	0	0	**1**

Table A.1 *LRU association matrix for the fuel system.*

Appendix II. active channel selection

The selection of the active channel is performed from the computation of the command fault status. For a given channel, the status is computed in three steps: (1) a range check on the measured command current, consisting in verifying that its values belong to the nominal interval (2) a discrepancy check with respect to wraparound current and (3) a fusion of range check status and discrepancy check status. The wraparound current is the current coming back from the servovalve's torque motor. Theoretically, it is equal to the control current. The discrepancy check consists then in calculating the gap between the control current and the wraparound one. To take into account the delay of the loop, the wraparound current is taken with a delay of 1 RTCs. The block diagram of the fault status calculation is given in Figure A.1, where I_{meas} is the measured command current and I_{wrap} is the measured wraparound current.

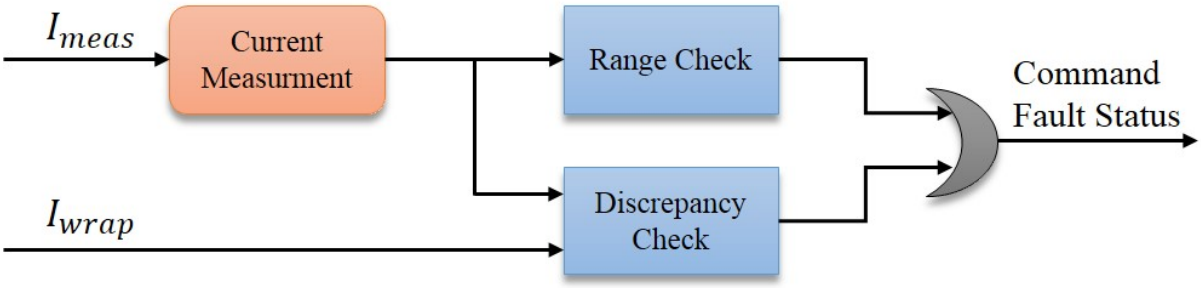


Figure A.1 *Command fault status calculation.*

The command fault status is equal to 0 (no fault) if both the range check and the discrepancy check are equal to 0. The selection of the active channel is performed from the following logic: if the command fault status of the current active channel is equal to 0 (no fault), then no switch occurs and the regulation continues to be done on this channel. If it is equal to 1, then a switch of active channel happens. If the command fault status of the other channel is also equal to 1, then a fault alarm is sent to the pilot.

Appendix III. Computation of selected measures

For the computation of the selected measures for redundant sensors architectures, the logic is the one presented in Figure A.2. It consists of a signal check to verify from the electrical value the absence of shortcuts or open circuits. A range check is also performed to verify that the physical value is in the defined likelihood interval. Finally, a cross check is carried out in parallel to verify that the information given by the redundant sensors are consistent.

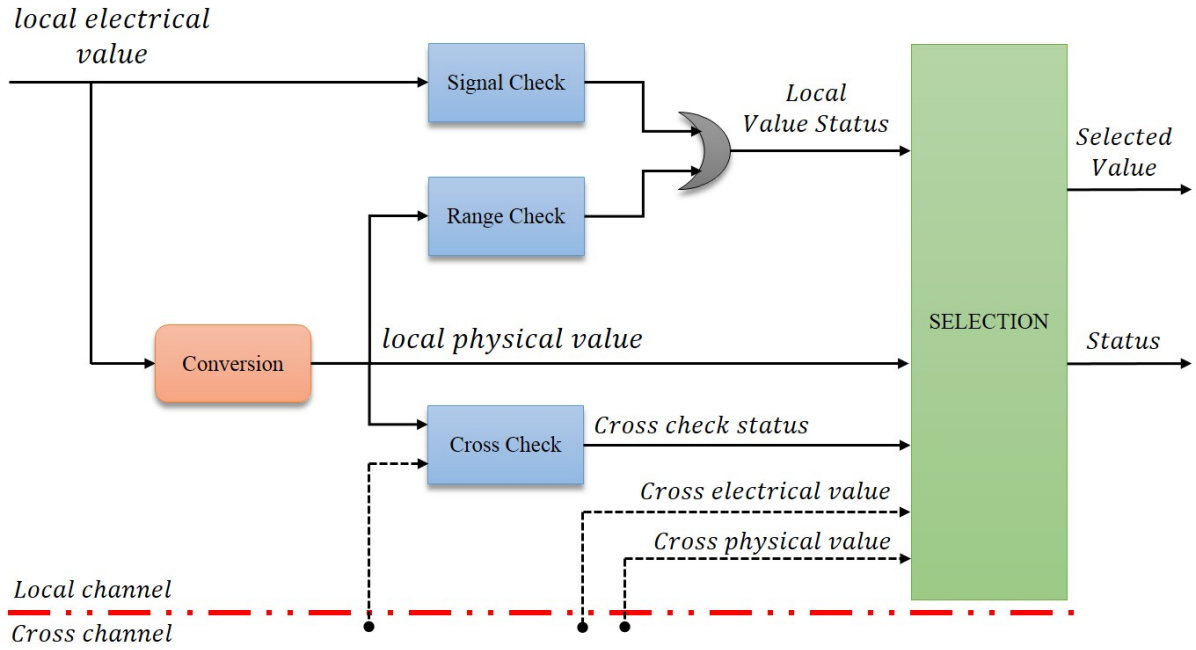


Figure A.2 *Computation of selected measures.*

Appendix IV. PID controllers for closed-loops

For the regulation of the actuators' displacements for variable geometries, the controller is based on a proportional-integral (**PI**) type. To improve the control law, some improvements are defined, as shown in Figure A.3. Indeed, the demanded position (set point) is subjected to a derivative limiter in order to limit the abrupt variations. Moreover, both the proportionnal and the integral actions are multiplied by a coefficient depending on the current hydraulic gain estimated by a model. Thus, the controller is robust with respect to the variations of the hydraulic gain.

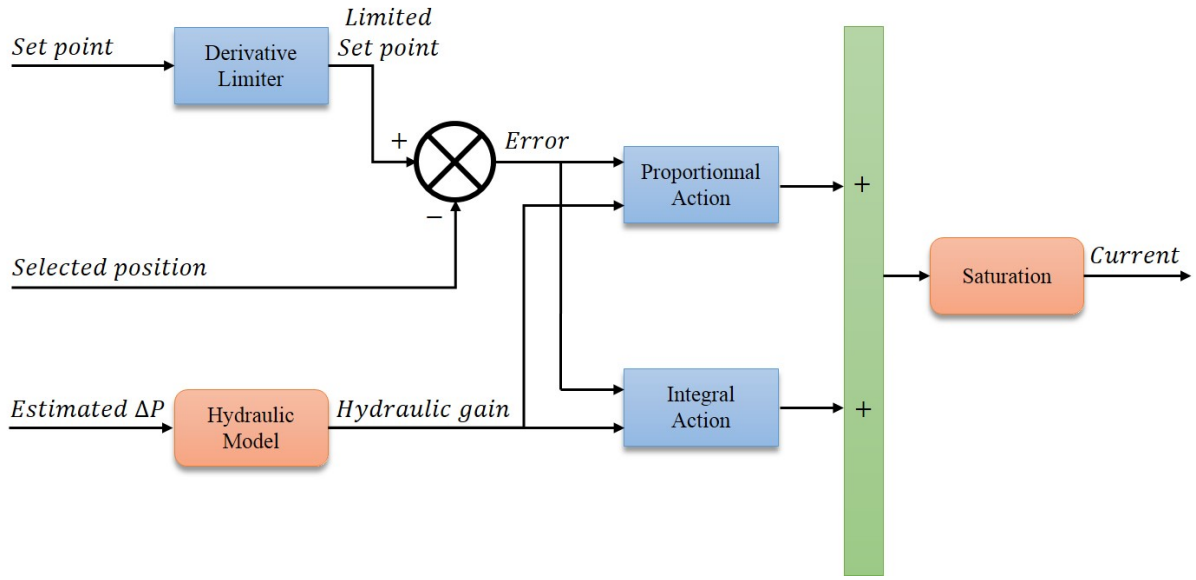


Figure A.3 *Controller logic for actuation loops.*

Appendix V. Actuation faults detection

In the fuel system, the detection of actuation faults is performed via the comparison between the current selected position and theoretical maximum and minimum values (see Figure A.4). These values are computed by a model from the value of the demanded position (set point). If the selected position is outside the theoretical range, an actuation fault is declared.

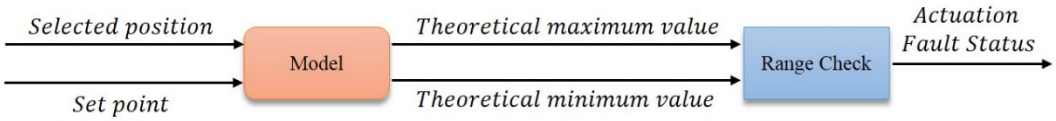


Figure A.4 *Actuation fault status computation.*

The model computing the theoretical maximum and minimum values takes for inputs the selected position and the demanded position. It is defined by five parameters: $N, DTMIN, DTMAX, LSMIN$ and $LSMAX$ whose values are given for the FMV, the VSV and the VBV loops in

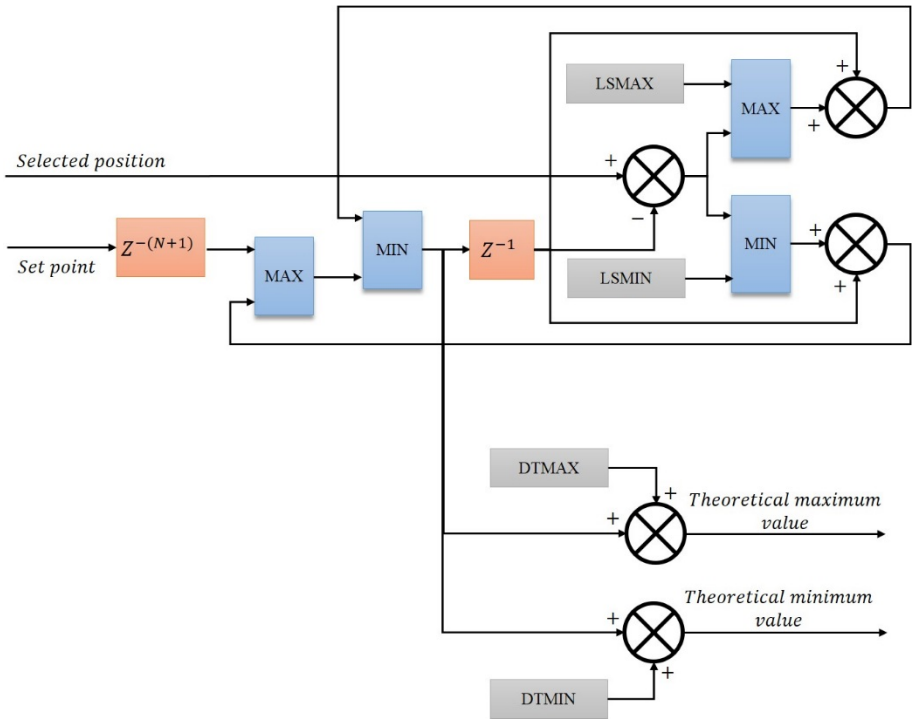


Figure A.5 *Theoretical maximum and minimum values computation.*

	Unit	FMV	VSV	VBV
N	processing cycle	1	2	3
DTMIN	mm	-1.8	-4.67	-3
DTMAX	mm	1.8	4.67	3
LSMIN	mm/processing cycle	-0.05	-0.2	-0.3
LSMAX	mm/processing cycle	0.05	0.2	0.3

Table A.2 *List of models parameters for FMV, VSV and VBV loops.*

Appendix VI. Targeted compliant service threats for the fuel metering valve loop

In the following table, n is the number of samples, $FMVX$ is either $FMVA$ or $FMVB$, $FMVSEL$ is the selected position, $FMVDMD$ is the demanded position, $FMVCMD^0$ is the null control current of the servovalve and Q_{inFMV} and Q_{outFMV} are, respectively, the inlet and outlet flow of the FMV actuator.

Faults			
Name	**Dispatch**	**Description**	**Associated Compliant service indicators (CSIs)**
FMV local sensor	beta	The value of the position from local LVDT is outside $[-1.7mm; 14.2mm]$ during $10RTC$.	$r_{FMV} = \min_{k=1,\dots,n-10}\left\{\max_{i=k,\dots,k+10} r(i)\right\}$ with: $r(i) = \min\{FMVX(i) + 1.7, 14.2 - FMVX(i)\}$
FMV cross sensor	beta	The absolute position gap between sensors is higher than $0.43mm$ during $10RTC$.	$\delta_{FMV} = \min_{k=1,\dots,n-10}\left\{\max_{i=k,\dots,k+10} \delta(i)\right\}$ with: $\delta(i) = 0.43 - \mathrm{abs}\big(FMVA(i) - FMVB(i)\big)$
FMV actuation	A	The value of $FMVSEL$ is outside the range $[X_{min}; X_{max}]$ during $10RTC$.	$ra_{FMV} = \min_{k=1,\dots,n-10}\left\{\max_{i=k,\dots,k+10} ra(i)\right\}$ with: $ra(i) = \min\{FMVSEL(i) - X_{min}, X_{max} - FMVSEL(i)\}$ where X_{min} and X_{max} are computed for $LSMIN = -0.05 = -LSMAX, DTMIN = -1.8 = -DTMAX$ and $N = 1$ from the model of appendix III.
Defects			
Name		**Description**	**Associated Compliant service indicators (CSI)**
FMV null current drift		The value of the null current is outside the range $[11mA; 23mA]$.	$r_{FMVCMD^0} = \underset{k=1,\dots,n}{\mathrm{mean}}\, r^0(k)$ with: $r^0(k) = \min\{FMVCMD^0(k) - 11, 23 - FMVCMD^0(k)\}$
FMV internal leakage		The value of the FMV internal leakage is above $45kg/h$.	$Q_{FMV} = \min_{k=1,\dots,n} Q(k)$ with: $Q(k) = 45 - \mathrm{abs}\big(Q_{inFMV}(k) - Q_{outFMV}(k)\big)$

Table A.3 *List of targeted compliant service threats for the FMV loop.*

Appendix VII. Targeted ompliant service threats for the fuel metering unit

Defects		
Name	**Description**	**Associated Compliant service indicators (CSI)**
FMV delta pressure	The value of the delta pressure for FMV is outside $[3bar; 4bar]$ for $20RTC$ with $N2 > 10000rpm$	$r_{DPFMV} = \min_{k=1,\dots,n-20} \left\{ \max_{i=k,\dots,k+20} r(i) \right\}$ with: $r(i) = \min\{DP(i) - 3{,}4 - DP(i)\}$ where DP is the pressure difference between FMV inlet and outlet

Table A.4 *List of targeted compliant service threats for the FMU.*

Appendix VIII. Compliant service threats for the main fuel pump

Faults			
Name	**Dispatch**	**Description**	**Associated Compliant service indicators (CSI)**
MFP startup fault	A	The MFP is not capable of opening the HPSOV under 10% of N2 rotation speed	$x_{SOV10} = x_{SOV}(k_{10\%}) - Sw_{SOV}$ with: $k_{10\%}$ the sample at which 10% of N2 is reached
Defects			
Name		**Description**	**Associated Compliant service indicators (CSI)**
MFP insufficient flow		The value of the outlet flow is under 443kg/h at 10% of N2 rotation speed	$Q_{10} = Q(k_{10\%}) - 443$ with: $k_{10\%}$ the sample at which 10% of N2 is reached and Q is the MFP outlet flow

Table A.5 *List of targeted compliant service threats for the MFP.*

Appendix IX. Compliant service threats for the main fuel filter

Fault Name	Dispatch	Description	Associated Compliant service indicators (CSI)
MFF Incoming Bypass	A	The MFF is measuring a DeltaP value greater than $0.8bar$	$DP_{MFF} = \max_{k=1,\dots,n} D(k)$ with: $D(k) = 0.8 - DP(k)$

Table A.6 *List of targeted compliant service threats for the MFF.*

Appendix X. Compliant service threats for the variable stator vane

In the following table, n is the number of samples, $VSVX$ is either $VSVA$ or $VSVB$, $VSVSEL$ is the selected position, $VSVDMD$ is the demanded position, $VSVCMD^0$ is the null control current of the servovalve and Q_{leakA} and Q_{leakB} are, respectively, the internal leakage flow of VSV actuators A and B.

Faults			
Name	**Dispatch**	**Description**	**Associated Compliant service indicators (CSI)**
VSV local sensor fault	beta	The absolute value of the position from local LVDT is outside $[-0.2mm; 58mm]$ during $10RTC$.	$r_{VSV} = \min\limits_{k=1,\dots,n-10}\left\{\max\limits_{i=k,\dots,k+10} r(i)\right\}$ with: $r(i) = \min\{VSVX(i) + 0.2, 58 - VSVX(i)\}$
VSV cross sensor fault	beta	The absolute position gap between sensors is greater than $3.5mm$ during $10RTC$.	$\delta_{VSV} = \min\limits_{k=1,\dots,n-10}\left\{\max\limits_{i=k,\dots,k+10} \delta(i)\right\}$ with: $\delta(i) = 3.5 - \mathrm{abs}\big(VSVA(i) - VSVB(i)\big)$
VSV actuation fault	A	The value of $VSVSEL$ is outside $[X_{min}; X_{max}]$ during $10RTC$.	$ra_{VSV} = \min\limits_{k=1,\dots,n-10}\left\{\max\limits_{i=k,\dots,k+10} ra(i)\right\}$ with: $ra(i) = \min\{VSVSEL(i) - X_{min}, X_{max} - VSVSEL(i)\}$ where X_{min} and X_{max} are computed for $LSMIN = -0.2 = -LSMAX, DTMIN = -4.67 = -DTMAX$ and $N = 2$ from the model of appendice III.
Defects			
Name		**Description**	**Associated Compliant service indicators (CSI)**
VSV null current drift		The value of the null current is outside the range $[8.5mA; 20.5mA]$	$r_{VSVCMD^0} = \underset{k=1,\dots,n}{\mathrm{mean}}\, r^0(k)$ with: $r^0(k) = \min\{VSVCMD^0(k) - 8.5, 20.5 - VSVCMD^0(k)\}$
VSV actuator A cooling flow increase		The value of the cooling flow of actuator A is above 9.5 $l/h/\sqrt{bar}$	$Q_{VSVA} = \max\limits_{k=1,\dots,n} Q_{leakA}(k)$ with: Q_{leakA} the flow leaking between the two chambers of actuator A under $1bar$
VSV actuator B cooling flow increase		The value of the cooling flow of actuator B is above 9.5 $l/h/\sqrt{bar}$	$Q_{VSVB} = \max\limits_{k=1,\dots,n} Q_{leakB}(k)$ with: Q_{leakB} the flow leaking between the two chambers of actuator B under $1bar$

Table A.7 *List of targeted compliant service threats for the VSV loop.*

Appendix XI. Compliant service threats for the variable stator vane

In the following table, n is the number of samples, $VBVX$ is either $VBVA$ or $VBVB$, $VBVSEL$ is the selected position, $VBVDMD$ is the demanded position, $VBVCMD^0$ is the null control current of the servovalve and Q_{leakB} and Q_{leakB} are, respectively, the internal leakage flow of VBV actuators A and B.

Faults			
Name	**Dispatch**	**Description**	**Associated Compliant service indicators (CSI)**
VBV local sensor fault	beta	The absolute value of the position from local LVDT is outside $[-0.2mm; 40.7mm]$ during $10RTC$.	$r_{VBV} = \min\limits_{k=1,\dots,n-10}\left\{\max\limits_{i=k,\dots,k+10} r(i)\right\}$ with: $r(i) = \min\{VBVX(i) + 0.2, 40.7 - VBVX(i)\}$
VBV cross sensor fault	beta	The absolute position gap between sensors is greater than $4.05mm$ during $10RTC$.	$\delta_{VBV} = \min\limits_{k=1,\dots,n-10}\left\{\max\limits_{i=k,\dots,k+10} \delta(i)\right\}$ with: $\delta(i) = 4.05 - \mathrm{abs}\big(VBVA(i) - VBVB(i)\big)$
VBV actuation fault	A	The value of $VBVSEL$ is outside $[X_{min}; X_{max}]$ during $10RTC$.	$ra_{VBV} = \min\limits_{k=1,\dots,n-10}\left\{\max\limits_{i=k,\dots,k+10} ra(i)\right\}$ with: $ra(i) = \min\{VBVSEL(i) - X_{min}, X_{max} - VBVSEL(i)\}$ where X_{min} and X_{max} are computed for $LSMIN = -0.3 = -LSMAX, DTMIN = -3 = -DTMAX$ and $N = 2$ from the model of appendice III.
Defects			
Name		**Description**	**Associated Compliant service indicators (CSI)**
VBV null current drift		The value of the null current is outside the range $[8mA; 20mA]$	$r_{VBVCMD^0} = \underset{k=1,\dots,n}{\mathrm{mean}}\, r^0(k)$ with: $r^0(k) = \min\{VBVCMD^0(k) - 8{,}20 - VBVCMD^0(k)\}$
VBV actuator A cooling flow increase		The value of the cooling flow of actuator A is above 9.5 $l/h/\sqrt{bar}$	$Q_{VBVA} = \max\limits_{k=1,\dots,n} Q_{leakA}(k)$ with: Q_{leakA} the flow leaking between the two chambers of actuator A under $1bar$
VBV actuator B cooling flow increase		The value of the cooling flow of actuator B is above 9.5 $l/h/\sqrt{bar}$	$Q_{VBVB} = \max\limits_{k=1,\dots,n} Q_{leakB}(k)$ with: Q_{leakB} the flow leaking between the two chambers of actuator B under $1bar$

Table A.8 *List of targeted compliant service threats for the VBV loop.*

Appendix XII. Compliant service threats for the flowmeter

Fault Name	Dispatch	Description	Associated Compliant service indicators (CSI)
WFM sensor fault	A	The value of the measured flow is under $114kg/h$ at $N2 = 10000\ rpm$	$Q_{wfm} = Q(k_{10000}) - 114$ with: k_{10000} the sample at which $N2 = 10000$ is reached

Table A.9 *List of targeted compliant service threats for the WFM.*

Appendix XIII. Complete list of parameters

Parameter Name	Description	Parameter Name	Description
$CTfuel$	Fuel temperature	$DEFmuDminflow$	Fuel metering unit diameter of min flow diaphragm
$DLppDIlkg$	Diameter of low pressure pump (LPP) internal leakage	$DEVsvStic1$	Static friction of variable stator vane (VSV) actuator 1
$EMfpDis$	Displacement of the main fuel pump (MFP)	$DEVsvVisc1$	Viscous friction of VSV actuator 1
$DMfpDIlkg$	Diameter of MFP internal leakage	$DEVsvStic2$	Static friction of VSV actuator 2
$DEMffFlowRate$	Flow rate into the main fuel filter (MFF)	$DEVsvVisc2$	Viscous friction of VSV actuator 2
$DEMffSenO$	MFF deltaP sensor drift	$DEVsvDCool1$	Cooling orifice diameter of VSV actuator 1
$ETbvPopen$	Opening pressure of the transient bleed valve (TBV)	$DEVsvDCool2$	Cooling orifice diameter of VSV actuator 2
$ETbvOstroke$	Stroke of the opening switch for the TBV	$DEVsvKineFric$	Kinematic friction of the VSV actuation chain
$DETbvVisc$	Viscous friction of the TBV	$DEVsvLoadAero$	Aerodynamic load on the VSV actuation chain
$DETbvStic$	Static friction of the TBV	$DEVsvCnull$	Null current of the VSV servovalve
$DTbvDIlkg$	Diameter of TBV internal leakage	$DEVsvDnozzle$	Nozzle diameter of the VSV servovalve
$DEWfmASenO$	Flowmeter sensor A (WFMA) offset	$DEVsvKfeed$	Feedback stiffness of the VSV servovalve
$DEWfmBSenO$	Flowmeter sensor B (WFMB) offset	$DEVsvSticspool$	Static friction of the VSV servovalve spool
$DWfmDIlkg$	Diameter of flowmeter internal leakage	$DEVsvDFilter1$	Left filter diameter of the VSV servovalve
$EByvDPist0$	Bypass valve (BYV) piston diameter	$DEVsvDFilter2$	Right filter diameter of the VSV servovalve
$EByvDRod$	Bypass valve (BYV) rod diameter	$DEVsvCorHP1$	Left corner radius of the VSV servovalve
$EByvUdlp$	BYV underlap at zero displacement	$DEVsvCorHP2$	Right corner radius of the VSV servovalve
$DEByvK0$	BYV feedback force at zero displacement	$DEVsvASenO$	VSV sensor A (VSVA) offset
$DEByvVisc$	Viscous friction of the BYV	$DEVsvBSenO$	VSV sensor B (VSVB) offset
$DEByvStic$	Static friction of the BYV	$DVsvDIlkg$	Diameter of VSV internal leakage
$DByvDIlkg$	Diameter of BYV internal leakage	$DEVbvStic1$	Static friction of variable bleed valve (VBV) actuator 1
$ESovDPist$	High pressure shut off valve (SOV) piston diameter	$DEVbvVisc1$	Viscous friction of VBV actuator 1
$ESovUdlp$	SOV underlap at zero displacement	$DEVbvStic2$	Static friction of VBV actuator 2
$ESovOstroke$	Stroke of the opening switch for the SOV	$DEVbvVisc2$	Viscous friction of VBV actuator 2
$DESovK0$	SOV feedback force at zero displacement	$DEVbvDCool1$	Cooling orifice diameter of VBV actuator 1
$DESovVisc$	Viscous friction of the SOV	$DEVbvDCool2$	Cooling orifice diameter of VBV actuator 2
$DESovStic$	Static friction of the SOV	$DEVbvKineFric$	Kinematic friction of the VBV actuation chain
$DESovASenO$	SOV sensor A (SOVA) offset	$DEVbvLoadAero$	Aerodynamic load on the VBV actuation chain

$DESovBSenO$	SOV sensor B (SOVB) offset	$DEVbvCnull$	Null current of the VBV servovalve
$DSovDIlkg$	Diameter of SOV internal leakage	$DEVbvDnozzle$	Nozzle diameter of the VBV servovalve
$DSovDelay$	Opening delay of the SOV	$DEVbvKfeed$	Feedback stiffness of the VBV servovalve
$EFmvDPist$	Fuel metering valve (FMV) piston diameter	$DEVbvSticspool$	Static friction of the VBV servovalve spool
$EFmvChLg$	FMV chamber length at zero displacement	$DEVbvDFilter1$	Left filter diameter of the VBV servovalve
$DEFmvStic$	Static friction of the FMV	$DEVbvDFilter2$	Right filter diameter of the VBV servovalve
$DEFmvVisc$	Viscous friction of the FMV	$DEVbvCorHP1$	Left corner radius of the VBV servovalve
$DEFmvCnull$	Null current of the FMV servovalve	$DEVbvCorHP2$	Right corner radius of the VBV servovalve
$DEFmvDnozzle$	Nozzle diameter of the FMV servovalve	$DEVbvASenO$	VBV sensor A (VBVA) offset
$DEFmvASenO$	FMV sensor A (FMVA) offset	$DEVbvBSenO$	VBV sensor B (VBVB) offset
$DEFmvBSenO$	FMV sensor B (FMVB) offset	$DVbvDIlkg$	Diameter of VBV internal leakage
$DFmvDIlkg$	Diameter of FMV internal leakage	$EStaLaw$	Coefficient of the initial starter control law

Table A.10 *Complete list of parameters.*

Appendix XIV. Complete list of degradation modes

Degradation mode name	Description
$DLppDIlkg_Pos$	Increase of the low pressure pump internal leakage diameter
$DMfpDIlkg_Pos$	Increase of the main fuel pump internal leakage diameter
$DEMffFlowRate_Neg$	Decrease of the main fuel filter flow rate (clogging)
$DEMffSenO_Pos$	MFF deltaP sensor positive drift
$DEMffSenO_Neg$	MFF deltaP sensor negative drift
$DETbvVisc_Pos$	Increase of the TBV viscous friction
$DETbvStic_Pos$	Increase of the TBV static friction
$DTbvDIlkg_Pos$	Increase of the transient bleed valve internal leakage diameter
$DEWfmASenO_Pos$	Flowmeter sensor A positive drift
$DEWfmASenO_Neg$	Flowmeter sensor A negative drift
$DEWfmBSenO_Pos$	Flowmeter sensor B positive drift
$DEWfmBSenO_Neg$	Flowmeter sensor B negative drift
$DWfmDIlkg_Pos$	Increase of the flowmeter internal leakage diameter
$DEByvK0_Neg$	Decrease of the bypass valve (BYV) feedback force at zero displacement
$DEByvVisc_Pos$	Increase of the BYV viscous friction
$DEByvStic_Pos$	Increase of the BYV static friction
$DByvDIlkg_Pos$	Increase of the BYV internal leakage diameter
$DESovK0_Neg$	Decrease of the shut off valve (SOV) feedback force at zero displacement
$DESovVisc_Pos$	Increase of the SOV viscous friction
$DESovStic_Pos$	Increase of the SOV static friction
$DSovDIlkg_Pos$	Increase of the SOV internal leakage diameter
$DSovDelay_Pos$	Increase of the SOV opening delay
$DEMffSenO_Pos$	SOV position sensor positive drift
$DEMffSenO_Neg$	SOV position sensor negative drift
$DEFmvStic_Pos$	Increase of the fuel metering valve (FMV) static friction
$DEFmvVisc_Pos$	Increase of the FMV viscous friction
$DEFmvCnull_Pos$	Increase of the null current of the FMV servovalve
$DEFmvCnull_Neg$	Decrease of the null current of the FMV servovalve
$DEFmvDnozzle_Pos$	Increase of the nozzle diameter of the FMV servovalve (erosion)
$DEFmvASenO_Pos$	FMV sensor A positive drift
$DEFmvASenO_Neg$	FMV sensor A negative drift
$DEFmvBSenO_Pos$	FMV sensor B positive drift
$DEFmvBSenO_Neg$	FMV sensor B negative drift
$DFmvDIlkg_Pos$	Increase of the FMV internal leakage diameter
$DEFmuDminflow_Neg$	Decrease of the diameter of the fuel metering unit min flow diaphragm (clogging)
$DEVsvStic1_Pos$	Increase of the variable stator vane (VSV) actuator 1 static friction
$DEVsvVisc1_Pos$	Increase of the VSV actuator 1 viscous friction
$DEVsvStic2_Pos$	Increase of the VSV actuator 2 static friction
$DEVsvVisc2_Pos$	Increase of the VSV actuator 2 viscous friction
$DEVsvDCool1_Pos$	Increase of the cooling orifice diameter of VSV actuator 1 (internal leakage)
$DEVsvDCool1_Neg$	Decrease of the cooling orifice diameter of VSV actuator 1 (clogging)
$DEVsvDCool2_Pos$	Increase of the cooling orifice diameter of VSV actuator 2 (internal leakage)

$DEVsvDCool2_Neg$	Decrease of the cooling orifice diameter of VSV actuator 2 (clogging)
$DEVsvKineFric_Pos$	Increase of the friction in the VSV kinematic chain
$DEVsvLoadAero_Pos$	Increase of the aerodynamic load in the VSV chain
$DEVsvCnull_Pos$	Increase of the null current of the VSV servovalve
$DEVsvCnull_Neg$	Decrease of the null current of the VSV servovalve
$DEVsvDnozzle_Pos$	Increase of the nozzle diameter of the VSV servovalve (erosion)
$DEVsvDnozzle_Neg$	Decrease of the nozzle diameter of the VSV servovalve (clogging)
$DEVsvKfeed_Neg$	Decrease of the VSV servovalve feedback stiffness (wear)
$DEVsvSticspool_Pos$	Increase of the static friction of the VSV servovalve spool
$DEVsvDFilter1_Neg$	Decrease of the diameter of the VSV servovalve left filter (clogging)
$DEVsvDFilter2_Neg$	Decrease of the diameter of the VSV servovalve right filter (clogging)
$DEVsvCorHP1_Pos$	Increase of the left corner radius of the VSV servovalve (erosion)
$DEVsvCorHP2_Pos$	Increase of the right corner radius of the VSV servovalve (erosion)
$DEVsvASenO_Pos$	VSV sensor A positive drift
$DEVsvASenO_Neg$	VSV sensor A negative drift
$DEVsvBSenO_Pos$	VSV sensor B positive drift
$DEVsvBSenO_Neg$	VSV sensor B negative drift
$DVsvDIlkg_Pos$	Increase of the VSV servovalve internal leakage diameter
$DEVbvStic1_Pos$	Increase of the variable bleed valve (VBV) actuator 1 static friction
$DEVbvVisc1_Pos$	Increase of the VBV actuator 1 viscous friction
$DEVbvStic2_Pos$	Increase of the VBV actuator 2 static friction
$DEVbvVisc2_Pos$	Increase of the VBV actuator 2 viscous friction
$DEVbvDCool1_Pos$	Increase of the cooling orifice diameter of VBV actuator 1 (internal leakage)
$DEVbvDCool1_Neg$	Decrease of the cooling orifice diameter of VBV actuator 1 (clogging)
$DEVbvDCool2_Pos$	Increase of the cooling orifice diameter of VBV actuator 2 (internal leakage)
$DEVbvDCool2_Neg$	Decrease of the cooling orifice diameter of VBV actuator 2 (clogging)
$DEVbvKineFric_Pos$	Increase of the friction in the VBV kinematic chain
$DEVbvLoadAero_Pos$	Increase of the aerodynamic load in the VBV chain
$DEVbvCnull_Pos$	Increase of the null current of the VBV servovalve
$DEVbvCnull_Neg$	Decrease of the null current of the VBV servovalve
$DEVbvDnozzle_Pos$	Increase of the nozzle diameter of the VBV servovalve (erosion)
$DEVbvDnozzle_Neg$	Decrease of the nozzle diameter of the VBV servovalve (clogging)
$DEVbvKfeed_Neg$	Decrease of the VBV servovalve feedback stiffness (wear)
$DEVbvSticspool_Pos$	Increase of the static friction of the VBV servovalve spool
$DEVbvDFilter1_Neg$	Decrease of the diameter of the VBV servovalve left filter (clogging)
$DEVbvDFilter2_Neg$	Decrease of the diameter of the VBV servovalve right filter (clogging)
$DEVbvCorHP1_Pos$	Increase of the left corner radius of the VBV servovalve (erosion)
$DEVbvCorHP2_Pos$	Increase of the right corner radius of the VBV servovalve (erosion)
$DEVbvASenO_Pos$	VBV sensor A positive drift
$DEVbvASenO_Neg$	VBV sensor A negative drift
$DEVbvBSenO_Pos$	VBV sensor B positive drift
$DEVbvBSenO_Neg$	VBV sensor B negative drift
$DVbvDIlkg_Pos$	Increase of the VBV servovalve internal leakage diameter

Table A.11 *Complete list of degradation modes.*

Appendix XV. Complete list of health indicators.

HI Name	Description	Real / Virtual
$FmvCEquA$	Equilibrium current from FMV sensor A	Real
$FmvScaleA$	Velocity gain curve scale from FMV sensor A	Real
$FmvSlpA$	Slope of the velocity gain curve from FMV sensor A	Real
$FmvHyst0A$	Hysteresis for null velocity from FMV sensor A	Real
$FmvCEquB$	Equilibrium current from FMV sensor B	Real
$FmvScaleB$	Velocity gain curve scale from FMV sensor B	Real
$FmvSlpB$	Slope of the velocity gain curve from FMV sensor B	Real
$FmvHyst0B$	Hysteresis for null velocity from FMV sensor B	Real
$FmvCEquS$	Equilibrium current from sensor FMV selected measure S	Real
$FmvScaleS$	Velocity gain curve scale from FMV S	Real
$FmvSlpS$	Slope of the velocity gain curve from FMV S	Real
$FmvHyst0S$	Hysteresis for null velocity from FMV S	Real
$FmvmaxX1$	Maximal position from FMV sensor A	Real
$FmvmaxX2$	Maximal position from FMV sensor B	Real
$FmvminX1$	Minimal position from FMV sensor A	Real
$FmvminX2$	Minimal position from FMV sensor B	Real
$FmvmaxGapX$	Maximal position gap between FMV sensors A and B	Real
$FmvminGapX$	Minimal position gap between FMV sensors A and B	Real
$FmvmeanGapX$	Mean of position gap between FMV sensors A and B	Real
$FmvstdGapX$	Standard deviation of position gap between FMV sensors A and B	Real
$FmvMAErr$	Mean of FMV absolute regulation error	Real
$Sovdelop1$	Delay of the first opening of SOV	Real
$Sovdelclo$	Delay of the closing of SOV	Real
$Sovdelop2$	Delay of the second opening of SOV	Real
$VoN2maxSOV$	Maximal SOV velocity standardized by rotation speed N2	Virtual
$SOVoN2max$	Maximal value of the ratio between SOV position and rotation speed N2	Virtual
$SOVoN2mean$	Mean value of the ratio between SOV position and rotation speed N2	Virtual
$VoN2maxBYV$	Maximal BYV velocity standardized by rotation speed N2	Virtual
$BYVoN2max$	Maximal value of the ratio between BYV position and rotation speed N2	Virtual
$BYVoN2mean$	Mean value of the ratio between BYV position and rotation speed N2	Virtual
$LppSlpN2DP$	Slope of the curve √DP=f(N2) for the low pressure pump	Virtual
$LppR2N2DP$	R^2 of the curve √DP=f(N2) for the low pressure pump	Virtual
$wTBV$	Rotation speed N2 at the opening of the transient bleed valve	Real
$wSOV$	Rotation speed N2 at the opening of the shut off valve	Real
$MfpSlpN2DP$	Slope of the curve √DP=f(N2) for the main fuel pump	Virtual
$MfpR2N2DP$	R^2 of the curve √DP=f(N2) for the main fuel pump	Virtual
$MffSlpN2DP$	Slope of the curve √DP=f(N2) for the main fuel filter	Real
$MffR2N2DP$	R^2 of the curve √DP=f(N2) for the main fuel filter	Real
$WfmmaxX1$	Maximal position from flowmeter sensor A	Real
$WfmmaxX2$	Maximal position from flowmeter sensor B	Real

$WfmminX1$	Minimal position from flowmeter sensor A	Real
$WfmminX2$	Minimal position from flowmeter sensor B	Real
$WfmmaxGapX$	Maximal position gap between flowmeter sensors A and B	Real
$WfmminGapX$	Minimal position gap between flowmeter sensors A and B	Real
$WfmmeanGapX$	Mean of position gap between flowmeter sensors A and B	Real
$WfmstdGapX$	Standard deviation of position gap between flowmeter sensors A and B	Real
$VsvCEquA$	Equilibrium current from VSV sensor A	Real
$VsvXnullA$	Abscissa of the null point for the velocity gain curve from VSV sensor A	Real
$VsvYnullA$	Ordinate of the null point for the velocity gain curve from VSV sensor A	Real
$VsvXoverlapA$	Abscissa overlap length for the velocity gain curve from VSV sensor A	Real
$VsvYoverlapA$	Ordinate overlap length for the velocity gain curve from VSV sensor A	Real
$VsvScaleA$	Velocity gain curve scale from VSV sensor A	Real
$VsvSlpLeftA$	Slope of the left part of the velocity gain curve from VSV sensor A	Real
$VsvSlpNullA$	Slope of the null part of the velocity gain curve from VSV sensor A	Real
$VsvSlpRightA$	Slope of the right part of the velocity gain curve from VSV sensor A	Real
$VsvHyst0A$	Hysteresis for null velocity from VSV sensor A	Real
$VsvCEquB$	Equilibrium current from VSV sensor B	Real
$VsvXnullB$	Abscissa of the null point for the velocity gain curve from VSV sensor B	Real
$VsvYnullB$	Ordinate of the null point for the velocity gain curve from VSV sensor B	Real
$VsvXoverlapB$	Abscissa overlap length for the velocity gain curve from VSV sensor B	Real
$VsvYoverlapB$	Ordinate overlap length for the velocity gain curve from VSV sensor B	Real
$VsvScaleB$	Velocity gain curve scale from VSV sensor B	Real
$VsvSlpLeftB$	Slope of the left part of the velocity gain curve from VSV sensor B	Real
$VsvSlpNullB$	Slope of the null part of the velocity gain curve from VSV sensor B	Real
$VsvSlpRightB$	Slope of the right part of the velocity gain curve from VSV sensor B	Real
$VsvHyst0B$	Hysteresis for null velocity from VSV sensor B	Real
$VsvCEquS$	Equilibrium current from VSV selected measure S	Real
$VsvXnullS$	Abscissa of the null point for the velocity gain curve from VSV S	Real
$VsvYnullS$	Ordinate of the null point for the velocity gain curve from VSV S	Real
$VsvXoverlapS$	Abscissa overlap length for the velocity gain curve from VSV S	Real
$VsvYoverlapS$	Ordinate overlap length for the velocity gain curve from VSV S	Real
$VsvScaleS$	Velocity gain curve scale from VSV S	Real
$VsvSlpLeftS$	Slope of the left part of the velocity gain curve from VSV S	Real
$VsvSlpNullS$	Slope of the null part of the velocity gain curve from VSV S	Real
$VsvSlpRightS$	Slope of the right part of the velocity gain curve from VSV S	Real
$VsvHyst0S$	Hysteresis for null velocity from VSV S	Real
$VsvmaxX1$	Maximal position from VSV sensor A	Real
$VsvmaxX2$	Maximal position from VSV sensor B	Real
$VsvminX1$	Minimal position from VSV sensor A	Real
$VsvminX2$	Minimal position from VSV sensor B	Real
$VsvmaxGapX$	Maximal position gap between VSV sensors A and B	Real
$VsvminGapX$	Minimal position gap between VSV sensors A and B	Real
$VsvmeanGapX$	Mean of position gap between VSV sensors A and B	Real
$VsvstdGapX$	Standard deviation of position gap between VSV sensors A and B	Real

$VsvMAErr$	Mean of VSV absolute regulation error	Real
$VbvCEquA$	Equilibrium current from VBV sensor A	Real
$VbvXchgA$	Abscissa of the slope change point for the velocity gain curve from VBV sensor A	Real
$VbvYchgA$	Ordinate of the slope change point for the velocity gain curve from VBV sensor A	Real
$VbvScaleA$	Velocity gain curve scale from VBV sensor A	Real
$VbvSlpLeftA$	Slope of the left part of the velocity gain curve from VBV sensor A	Real
$VbvSlpRightA$	Slope of the right part of the velocity gain curve from VBV sensor A	Real
$VbvHyst0A$	Hysteresis for null velocity from VBV sensor A	Real
$VbvCEquB$	Equilibrium current from VBV sensor B	Real
$VbvXchgB$	Abscissa of the slope change point for the velocity gain curve from VBV sensor B	Real
$VbvYchgB$	Ordinate of the slope change point for the velocity gain curve from VBV sensor B	Real
$VbvScaleB$	Velocity gain curve scale from VBV sensor B	Real
$VbvSlpLeftB$	Slope of the left part of the velocity gain curve from VBV sensor B	Real
$VbvSlpRightB$	Slope of the right part of the velocity gain curve from VBV sensor B	Real
$VbvHyst0B$	Hysteresis for null velocity from VBV sensor B	Real
$VbvCEquS$	Equilibrium current from VBV selected measure S	Real
$VbvXchgS$	Abscissa of the slope change point for the velocity gain curve from VBV S	Real
$VbvYchgS$	Ordinate of the slope change point for the velocity gain curve from VBV S	Real
$VbvScaleS$	Velocity gain curve scale from VBV S	Real
$VbvSlpLeftS$	Slope of the left part of the velocity gain curve from VBV S	Real
$VbvSlpRightS$	Slope of the right part of the velocity gain curve from VBV S	Real
$VbvHyst0S$	Hysteresis for null velocity from VBV S	Real
$VbvmaxX1$	Maximal position from VBV sensor A	Real
$VbvmaxX2$	Maximal position from VBV sensor B	Real
$VbvminX1$	Minimal position from VBV sensor A	Real
$VbvminX2$	Minimal position from VBV sensor B	Real
$VbvmaxGapX$	Maximal position gap between VBV sensors A and B	Real
$VbvminGapX$	Minimal position gap between VBV sensors A and B	Real
$VbvmeanGapX$	Mean of position gap between VBV sensors A and B	Real
$VbvstdGapX$	Standard deviation of position gap between VBV sensors A and B	Real
$VbvMAErr$	Mean of VBV absolute regulation error	Real
$VoN2maxTBV$	Maximal TBV velocity standardized by rotation speed N2	Virtual

Table A.12 *Complete list of health indicators.*

Appendix XVI. Complete list of compliant service indicators.

CSI Name	Associated compliant service threat	Description
$rFMV$	Indicator of FMV local sensor fault	The the position from local LVDT is outside $[-1.7mm; 14.2mm]$ during $10RTC$.
$dFMV$	Indicator of FMV cross sensor fault	The absolute position gap between sensors is higher than $0.43mm$ during $10RTC$.
$raFMV$	Indicator of FMV actuation fault	The value of $FMVSEL$ is outside the range $[X_{min}; X_{max}]$ during $10RTC$.
$rFMVCMD0$	Indicator of FMV null current drift defect	The value of the null current is outside the range $[11mA; 23mA]$.
$QFMV$	Indicator of FMV internal leakage defect	The value of the FMV internal leakage is above $45kg/h$.
$rDPFMV$	Indicator of FMV delta pressure defect	The value of the delta pressure for FMV is outside $[3bar; 4bar]$ for $20RTC$ with $N2 > 10000rpm$
$XSOV10$	Indicator of MFP startup fault	The MFP is not capable of opening the HPSOV under 10% of N2 rotation speed
$Q10$	Indicator of MFP insufficient flow defect	The value of the outlet flow is under 443kg/h at 10% of N2 rotation speed
$DPMFF$	Indicator of incoming bypass of MFF	The MFF is measuring a DeltaP value greater than $0.8bar$
$QWFM$	Indicator of flowmeter sensor fault	The value of the measured flow is under $114kg/h$ at $N2 = 10000\ rpm$
$rVSV$	Indicator of VSV local sensor fault	The absolute value of the position from local LVDT is outside $[-0.2mm; 58mm]$ during $10RTC$.
$dVSV$	Indicator of VSV cross sensor fault	The absolute position gap between sensors is greater than $3.5mm$ during $10RTC$.
$raVSV$	Indicator of VSV actuation fault	The value of $VSVSEL$ is outside $[X_{min}; X_{max}]$ during $10RTC$.
$rVSVCMD0$	Indicator of VSV null current drift defect	The value of the null current is outside the range $[8.5mA; 20.5mA]$
$QVSVA$	Indicator of VSV actuator A cooling flow increase defect	The value of the cooling flow of actuator A is above 9.5 $l/h/\sqrt{bar}$
$QVSVB$	Indicator of VSV actuator B cooling flow increase defect	The value of the cooling flow of actuator B is above 9.5 $l/h/\sqrt{bar}$
$rVBV$	Indicator of VBV local sensor fault	The absolute value of the position from local LVDT is outside $[-0.2mm; 58mm]$ during $10RTC$.
$dVBV$	Indicator of VBV cross sensor fault	The absolute position gap between sensors is greater than $3.5mm$ during $10RTC$.
$raVBV$	Indicator of VBV actuation fault	The value of $VSVSEL$ is outside $[X_{min}; X_{max}]$ during $10RTC$.
$rVBVCMD0$	Indicator of VBV null current drift defect	The value of the null current is outside the range $[8.5mA; 20.5mA]$
$QVBVA$	Indicator of VBV actuator A cooling flow increase defect	The value of the cooling flow of actuator A is above 9.5 $l/h/\sqrt{bar}$
$QVBVB$	Indicator of VBV actuator B cooling flow increase defect	The value of the cooling flow of actuator B is above 9.5 $l/h/\sqrt{bar}$

Table A.13 *Complete list of compliant service indicators.*

Appendix XVII. Initial uncertainties quantification

All the following uncertainties are uniform PDFs defined by their parameter vector $[a \quad b]^t$ with a the lower bound and b the upper bound.

HI	a b	HI	a b	HI	a b	HI	a b
$CTfuel$	30 60	$DByvDIlkg$	0 1	$DEFmuDminf$	0.72 1.4	$DEVbvStic1$	0 100
$DLppDIlkg$	0 1	$ESovDPist$	23.5 26.5	$DEVsvStic1$	0 100	$DEVbvVisc1$	0 5000
$EMfpDis$	$2.2e^{-5}$ $2.5e^{-5}$	$ESovUdlp$	2.05 2.25	$DEVsvVisc1$	0 5000	$DEVbvStic2$	0 100
$DMfpDIlkg$	0 1	$ESovOstroke$	$9e^{-4}$ $1e^{-3}$	$DEVsvStic2$	0 100	$DEVbvVisc2$	0 5000
$DEMffFRate$	0 220	$DESovK0$	250 390	$DEVsvVisc2$	0 5000	$DEVbvDCool1$	0 9
$DEMffSenO$	-4 4	$DESovVisc$	0 5000	$DEVsvDCool1$	0 9	$DEVbvDCool2$	0 9
$ETbvPopen$	7 15	$DESovStic$	0 100	$DEVsvDCool2$	0 9	$DEVbvKineFric$	0.5 1.5
$ETbvOstroke$	0.012 0.013	$DESovASenO$	-5 5	$DEVsvKineFric$	1 2	$DEVbvLoadAero$	0.5 1.5
$DETbvVisc$	0 5000	$DESovBSenO$	-5 5	$DEVsvLoadAero$	1 2	$DEVbvCnull$	9 19
$DETbvStic$	0 100	$DSovDIlkg$	0 1	$DEVsvCnull$	9.5 19.5	$DEVbvDnozzle$	0.36 0.46
$DTbvDIlkg$	0 1	$DSovDelay$	0.015 2	$DEVsvDnozzle$	0.36 0.46	$DEVbvKfeed$	1 1.3
$DEWfmASenO$	-50 50	$EFmvDPist$	21 23	$DEVsvKfeed$	1 1.3	$DEVbvSticspool$	0 100
$DEWfmBSenO$	-50 50	$EFmvChLg$	11.9 13.2	$DEVsvSticspool$	0 100	$DEVbvDFilter1$	1 10
$DWfmDIlkg$	0 2	$DEFmvStic$	0 100	$DEVsvDFilter1$	1 10	$DEVbvDFilter2$	1 10
$EByvDPist0$	28.5 31.5	$DEFmvVisc$	0 5000	$DEVsvDFilter2$	1 10	$DEVbvCorHP1$	0.03 0.05
$EByvDRod$	22.8 25.2	$DEFmvCnull$	12 22	$DEVsvCorHP1$	0.03 0.05	$DEVbvCorHP2$	0.03 0.05
$EByvUdlp$	-4.2 -3.8	$DEFmvDnozzle$	0.3 0.4	$DEVsvCorHP2$	0.03 0.05	$DEVbvASenO$	-2 2
$DEByvK0$	105 225	$DEFmvASenO$	-2 2	$DEVsvASenO$	-2 2	$DEVbvBSenO$	-2 2
$DEByvVisc$	0 5000	$DEFmvBSenO$	-2 2	$DEVsvBSenO$	-2 2	$DVbvDIlkg$	0 1
$DEByvStic$	0 100	$DFmvDIlkg$	0 1	$DVsvDIlkg$	0 1	$EStaLaw$	0.8 1.2

Table A.14 *Initial coarse uncertainties quantification.*

Appendix XVIII. Complete results of the Morris method

	Total index on HIs Tot_i^{HIs}	**Total index on CSIs** Tot_i^{CSIs}	**Linearity index on HIs** Lin_i^{HIs}	**Linearity index on CSIs** Lin_i^{CSIs}
$CTfuel$	0,005	0,023	0,995	0,991
$DLppDIlkg$	0,04	0,035	0,6	0,9
$EMfpDis$	0,002	0,01		
$DMfpDIlkg$	0,001	0,003	0,08	0,89
$DEMffFlowRate$	0	0,002	0,95	0,85
$DEMffSenO$	0	0		
$ETbvPopen$	0,077	0,014	0,48	0,88
$ETbvOstroke$	0	0		
$DETbvVisc$	0	0,003		
$DETbvStic$	0,001	0		
$DTbvDIlkg$	0,001	0,045	0,88	0,79
$DEWfmASenO$	0,217	0,02	1	1
$DEWfmBSenO$	0,018	0,02	1	1
$DWfmDIlkg$	0	0		
$EByvDPist0$	0,036	0,11	0,63	0,84
$EByvDRod$	0	0,01		
$EByvUdlp$	0,001	0		
$DEByvK0$	0,508	1	0,01	0,82
$DEByvVisc$	0,026	0,059	0,63	0,76
$DEByvStic$	0,023	0,169	0,65	0,37
$DByvDIlkg$	0,372	0,254	0	0,42
$ESovDPist$	0,011	0,019	0,81	0,93
$ESovUdlp$	0	0		
$ESovOstroke$	0	0		
$DESovK0$	0,007	0,005		
$DESovVisc$	0,001	0,015	0,95	0,96
$DESovStic$	0	0,087	0,94	0,78
$DESovASenO$	0,001	0		
$DESovBSenO$	0	0		
$DSovDIlkg$	1	0,703	0,34	0,84
$DSovDelay$	0,061	0,159	0,5	0,73
$EFmvDPist$	0,001	0,001		
$EFmvChLg$	0	0,001		
$DEFmvStic$	0,111	0,06	0,46	0,73
$DEFmvVisc$	0,001	0,003		
$DEFmvCnull$	0,025	0,313	0,74	0,87
$DEFmvDnozzle$	0,033	0,267	0,65	0,77
$DEFmvASenO$	0,041	0,339	0,55	0,63
$DEFmvBSenO$	0,031	0,021	0,56	0,87
$DFmvDIlkg$	0,042	0,001	0,71	0,98
$DEFmuDminflow$	0	0		
$DEVsvStic1$	0,028	0,123	1	1
$DEVsvVisc1$	0,01	0,108	1	1
$DEVsvStic2$	0,032	0,005	0,94	0,84
$DEVsvVisc2$	0	0,134	0,97	1
$DEVsvDCool1$	0	0	1	1
$DEVsvDCool2$	0	0,066	0,96	0,81
$DEVsvKineFric$	0,005	0,028	0,79	0,84
$DEVsvLoadAero$	0	0		

DEVsvCnull	0,001	0,011	0,81	0,89
DEVsvDnozzle	0,045	0,001	0,95	0,98
DEVsvKfeed	0,012	0,001	0,87	0,96
DEVsvSticspool	0,036	0,008	0,55	0,79
DEVsvDFilter1	0,001	0,038	0,9	0,9
DEVsvDFilter2	0,001	0,08	0,93	0,95
DEVsvCorHP1	0,082	0,01	0,93	0,99
DEVsvCorHP2	0,098	0,001	0,96	0,95
DEVsvASenO	0,032	0,15	1	1
DEVsvBSenO	0,055	0,116	1	1
DVsvDIlkg	0	0		
DEVbvStic1	0,041	0,156	1	1
DEVbvVisc1	0,01	0,092	1	1
DEVbvStic2	0,022	0,097	0,96	0,96
DEVbvVisc2	0,001	0,174	0,92	0,98
DEVbvDCool1	0,023	0,01	1	1
DEVbvDCool2	0,023	0,037	0,96	0,94
DEVbvKineFric	0,024	0,002	0,95	0,95
DEVbvLoadAero	0	0		
DEVbvCnull	0	0,001	0,93	0,98
DEVbvDnozzle	0,003	0	0,88	0,97
DEVbvKfeed	0	0,004	0,96	0,94
DEVbvSticspool	0	0,008	0,98	0,82
DEVbvDFilter1	0	0,097	0,97	0,59
DEVbvDFilter2	0	0,013	0,93	0,94
DEVbvCorHP1	0,028	0,001	0,95	1
DEVbvCorHP2	0,013	0	0,96	0,98
DEVbvASenO	0	0,09	0,94	0,75
DEVbvBSenO	0,019	0,167	0,85	0,9
DVbvDIlkg	0	0		
EStaLaw	0,005	0,975	0,63	0

Table A.15 *Morris method results.*

Appendix XIX. List of potential cause degradation modes

CSIs	Potential cause degradation parameters	CSIs	Potential cause degradation parameters
$rFMV$	$DEFmvASenO$ $DEFmvBSenO$	$dVSV$	$DEVsvASenO$ $DEVsvBSenO$
$dFMV$	$DEFmvASenO$ $DEFmvBSenO$	$raVSV$	$DTbvDIlkg$ $DEVsvKineFric$ $DEVsvASenO$ $DEVsvBSenO$
$raFMV$	$DEFmvCnull$ $DFmvDIlkg$ $DEByvK0$	$rVSVCMD0$	$DEVsvCnull$
$rFMVCMD0$	$DFmvDnozzle$ $DEFmvCnull$ $DFmvDIlkg$	$QVSVA$	$DEVsvDCool1$
$QFMV$	$DFmvDIlkg$ $DEVsvDFilter1$ $DEVsvDFilter2$	$QVSVB$	$DEVsvDCool2$
$rDPFMV$	$DEByvStic$ $DEByvDIlkg$	$rVBV$	$DEVbvASenO$ $DEVbvBSenO$
$XSOV10$	$DSovDIlkg$	$dVBV$	$DEVbvASenO$ $DEVbvBSenO$
$Q10$	$DEByvK0$ $DESovDelay$ $DTbvVisc$ $ETbvPopen$	$raVBV$	$DTbvDIlkg$ $DEVbvCnull$ $DEVbvASenO$ $DEVbvBSenO$
$DPMFF$	$DEMffSenO$	$rVBVCMD0$	$DEVbvCnull$
$QWFM$	$DEByvK0$ $DSovDIlkg$ $DEFmvCnull$ $DEFmvASenO$ $DEFmvBSenO$ $DEWfmASenO$ $DEWfmBSenO$	$QVBVA$	$DEVbvDCool1$
$rVSV$	$DEVsvASenO$ $DEVsvBSenO$	$QVBVB$	$DEVbvDCool2$

Table A.16 *List of potential cause degradation parameter for each compliant service indicator (CSI).*

Appendix XX. List of degradation modes and associated median limit values.

Degradation modes	$rFMV$	$dFMV$	$raFMV$	$rFMVCMD0$	$QFMV$	$rDPFMV$	$XSOV10$	$Q10$	$DPMFF$	$QWFM$	$rVSV$	$dVSV$	$raVSV$	$rVSVCMD0$	$QVSVA$	$QVSVB$	$rVBV$	$dVBV$	$raVBV$	$rVBVCMD0$	$QVBVA$	$QVBVB$	$\underline{mlv}$
DLppDIlkg_Pos	∞	∞	∞	∞	∞	∞	∞	∞	∞	∞	∞	∞	∞	∞	∞	∞	∞	∞	∞	∞	∞	∞	∞
DMfpDIlkg_Pos	∞	∞	∞	∞	∞	∞	∞	1,64	∞	∞	∞	∞	∞	∞	∞	∞	∞	∞	∞	∞	∞	∞	1,64
DEMffFlowRate_Neg	∞	∞	∞	∞	∞	∞	∞	∞	∞	∞	∞	∞	∞	∞	∞	∞	∞	∞	∞	∞	∞	∞	∞
DTbvDIlkg_Pos	∞	∞	∞	∞	∞	∞	∞	∞	∞	∞	∞	∞	∞	∞	∞	∞	∞	∞	∞	∞	∞	∞	∞
DEWfmASenO_Pos	∞	∞	∞	∞	∞	∞	∞	∞	∞	∞	∞	∞	∞	∞	∞	∞	∞	∞	∞	∞	∞	∞	∞
DEWfmASenO_Neg	∞	∞	∞	∞	∞	∞	∞	∞	∞	∞	∞	∞	∞	∞	∞	∞	∞	∞	∞	∞	∞	∞	∞
DEWfmBSenO_Pos	∞	∞	∞	∞	∞	∞	∞	∞	∞	∞	∞	∞	∞	∞	∞	∞	∞	∞	∞	∞	∞	∞	∞
DEWfmBSenO_Neg	∞	∞	∞	∞	∞	∞	∞	∞	∞	∞	∞	∞	∞	∞	∞	∞	∞	∞	∞	∞	∞	∞	∞
DEByvK0_Neg	∞	∞	∞	∞	∞	-82	∞	∞	∞	∞	∞	∞	∞	∞	∞	∞	∞	∞	∞	∞	∞	∞	-82
DEByvVisc_Pos	∞	∞	∞	∞	∞	∞	∞	∞	∞	∞	∞	∞	∞	∞	∞	∞	∞	∞	∞	∞	∞	∞	∞
DEByvStic_Pos	∞	∞	∞	∞	∞	∞	∞	∞	∞	∞	∞	∞	∞	∞	∞	∞	∞	∞	∞	∞	∞	∞	∞
DByvDIlkg_Pos	∞	∞	∞	∞	∞	0,8	∞	∞	∞	∞	∞	∞	∞	∞	∞	∞	∞	∞	0,77	∞	∞	∞	0,77
DESovVisc_Pos	∞	∞	∞	∞	∞	∞	∞	∞	∞	∞	∞	∞	∞	∞	∞	∞	∞	∞	∞	∞	∞	∞	∞
DESovStic_Pos	∞	∞	∞	∞	∞	∞	∞	∞	∞	∞	∞	∞	∞	∞	∞	∞	∞	∞	∞	∞	∞	∞	∞
DSovDIlkg_Pos	∞	∞	∞	∞	∞	∞	0,59	∞	∞	∞	∞	∞	∞	∞	∞	∞	∞	∞	0,76	∞	∞	∞	0,59
DSovDelay_Pos	∞	∞	∞	∞	∞	∞	0,82	∞	∞	∞	∞	∞	∞	∞	∞	∞	∞	∞	∞	∞	∞	∞	0,82
DEFmvStic_Pos	∞	∞	42,7	∞	∞	∞	∞	∞	∞	∞	∞	∞	∞	∞	∞	∞	∞	∞	∞	∞	∞	∞	42,7
DEFmvCnull_Pos	∞	∞	1,43	∞	∞	∞	∞	∞	∞	∞	∞	∞	∞	∞	∞	∞	∞	∞	∞	∞	∞	∞	1,43
DEFmvCnull_Neg	∞	∞	-1,53	∞	∞	∞	∞	∞	∞	∞	∞	∞	∞	∞	∞	∞	∞	∞	-4,41	∞	∞	∞	-1,53
DEFmvDnozzle_Pos	∞	∞	∞	∞	∞	∞	∞	∞	∞	∞	∞	∞	∞	∞	∞	∞	∞	∞	∞	∞	∞	∞	∞
DEFmvASenO_Pos	∞	0,6	∞	∞	∞	∞	∞	∞	∞	3,31	∞	∞	∞	∞	∞	∞	∞	∞	∞	∞	∞	∞	0,6
DEFmvASenO_Neg	-0,2	-0,6	∞	∞	∞	∞	∞	∞	∞	∞	∞	∞	∞	∞	∞	∞	∞	∞	∞	∞	∞	∞	-0,2
DEFmvBSenO_Pos	∞	0,6	∞	∞	∞	∞	∞	∞	∞	3,31	∞	∞	∞	∞	∞	∞	∞	∞	∞	∞	∞	∞	0,6

DEFmvBSenO_Neg	∞	-0,6	∞	∞	∞	∞	∞	∞	∞	∞	∞	∞	∞	∞	∞	∞	∞	∞	∞	∞	∞	-0,6
DFmvDIlkg_Pos	∞	∞	0,08	0,23	∞	∞	∞	∞	∞	∞	∞	∞	∞	∞	∞	∞	∞	∞	∞	∞	∞	0,08
DEVsvStic1_Pos	∞	∞	∞	∞	∞	∞	∞	∞	∞	∞	∞	∞	∞	∞	∞	∞	∞	∞	∞	∞	∞	∞
DEVsvVisc1_Pos	∞	∞	∞	∞	∞	∞	∞	∞	∞	∞	∞	∞	∞	∞	∞	∞	∞	∞	∞	∞	∞	∞
DEVsvStic2_Pos	∞	∞	∞	∞	∞	∞	∞	∞	∞	∞	∞	∞	∞	∞	∞	∞	∞	∞	∞	∞	∞	∞
DEVsvVisc2_Pos	∞	∞	∞	∞	∞	∞	∞	∞	∞	∞	∞	∞	∞	∞	∞	∞	∞	∞	∞	∞	∞	∞
DEVsvDCool1_Pos	∞	∞	∞	∞	∞	∞	∞	∞	∞	∞	∞	∞	∞	∞	6,3	∞	∞	∞	∞	∞	∞	6,3
DEVsvDCool1_Neg	∞	∞	∞	∞	∞	∞	∞	∞	∞	∞	∞	∞	∞	∞	∞	∞	∞	∞	∞	∞	∞	∞
DEVsvDCool2_Pos	∞	∞	∞	∞	∞	∞	∞	∞	∞	∞	∞	∞	∞	∞	6,3	∞	∞	∞	∞	∞	∞	6,3
DEVsvDCool2_Neg	∞	∞	∞	∞	∞	∞	∞	∞	∞	∞	∞	∞	∞	∞	∞	∞	∞	∞	∞	∞	∞	∞
DEVsvKineFric_Pos	∞	∞	∞	∞	∞	∞	∞	∞	∞	∞	∞	∞	∞	∞	∞	∞	∞	∞	∞	∞	∞	∞
DEVsvCnull_Pos	∞	∞	∞	∞	∞	∞	∞	∞	∞	∞	∞	∞	3,2	∞	∞	∞	∞	∞	∞	∞	∞	3,2
DEVsvCnull_Neg	∞	∞	∞	∞	∞	∞	∞	∞	∞	∞	∞	∞	∞	∞	∞	∞	∞	∞	∞	∞	∞	∞
DEVsvDnozzle_Pos	∞	∞	∞	∞	∞	∞	∞	∞	∞	∞	∞	∞	∞	∞	∞	∞	∞	∞	∞	∞	∞	∞
DEVsvDnozzle_Neg	∞	∞	∞	∞	∞	∞	∞	∞	∞	∞	∞	∞	∞	∞	∞	∞	∞	∞	∞	∞	∞	∞
DEVsvKfeed_Neg	∞	∞	∞	∞	∞	∞	∞	∞	∞	∞	∞	∞	∞	∞	∞	∞	∞	∞	∞	∞	∞	∞
DEVsvSticspool_Pos	∞	∞	∞	∞	∞	∞	∞	∞	∞	∞	∞	∞	∞	∞	∞	∞	∞	∞	∞	∞	∞	∞
DEVsvDFilter1_Neg	∞	∞	∞	∞	∞	∞	∞	∞	∞	∞	∞	∞	∞	∞	∞	∞	∞	∞	∞	∞	∞	∞
DEVsvDFilter2_Neg	∞	∞	∞	∞	∞	∞	∞	∞	∞	∞	∞	∞	∞	∞	∞	∞	∞	∞	∞	∞	∞	∞
DEVsvCorHP1_Pos	∞	∞	∞	∞	∞	∞	∞	∞	∞	∞	∞	∞	∞	∞	∞	∞	∞	∞	∞	∞	∞	∞
DEVsvCorHP2_Pos	∞	∞	∞	∞	∞	∞	∞	∞	∞	∞	∞	∞	∞	∞	∞	∞	∞	∞	∞	∞	∞	∞
DEVsvASenO_Pos	∞	∞	∞	∞	∞	∞	∞	∞	∞	∞	4,3	3,8	∞	∞	∞	∞	∞	∞	∞	∞	∞	3,8
DEVsvASenO_Neg	∞	∞	∞	∞	∞	∞	∞	∞	∞	∞	∞	-3,1	∞	∞	∞	∞	∞	∞	∞	∞	∞	3,1
DEVsvBSenO_Pos	∞	∞	∞	∞	∞	∞	∞	∞	∞	∞	∞	3,8	∞	∞	∞	∞	∞	∞	∞	∞	∞	3,8
DEVsvBSenO_Neg	∞	∞	∞	∞	∞	∞	∞	∞	∞	∞	∞	-3,1	∞	∞	∞	∞	∞	∞	∞	∞	∞	3,1
DEVbvStic1_Pos	∞	∞	∞	∞	∞	∞	∞	∞	∞	∞	∞	∞	∞	∞	∞	∞	∞	∞	∞	∞	∞	∞
DEVbvVisc1_Pos	∞	∞	∞	∞	∞	∞	∞	∞	∞	∞	∞	∞	∞	∞	∞	∞	∞	∞	∞	∞	∞	∞
DEVbvStic2_Pos	∞	∞	∞	∞	∞	∞	∞	∞	∞	∞	∞	∞	∞	∞	∞	∞	∞	∞	∞	∞	∞	∞
DEVbvVisc2_Pos	∞	∞	∞	∞	∞	∞	∞	∞	∞	∞	∞	∞	∞	∞	∞	∞	∞	∞	∞	∞	∞	∞
DEVbvDCool1_Pos	∞	∞	∞	∞	∞	∞	∞	∞	∞	∞	∞	∞	∞	∞	∞	∞	∞	∞	∞	6,3	∞	6,3

DEVbvDCool1_Neg	∞	∞	∞	∞	∞	∞	∞	∞	∞	∞	∞	∞	∞	∞	∞	∞	∞	∞	∞	∞	6,3		6,3
DEVbvDCool2_Pos	∞	∞	∞	∞	∞	∞	∞	∞	∞	∞	∞	∞	∞	∞	∞	∞	∞	∞	∞	∞	∞		∞
DEVbvDCool2_Neg	∞	∞	∞	∞	∞	∞	∞	∞	∞	∞	∞	∞	∞	∞	∞	∞	∞	∞	∞	∞	∞		∞
DEVbvKineFric_Pos	∞	∞	∞	∞	∞	∞	∞	∞	∞	∞	∞	∞	∞	∞	∞	∞	∞	∞	2,7	∞	∞		2,7
DEVbvCnull_Pos	∞	∞	∞	∞	∞	∞	∞	∞	∞	∞	∞	∞	∞	∞	∞	∞	∞	∞	∞	∞	∞		∞
DEVbvCnull_Neg	∞	∞	∞	∞	∞	∞	∞	∞	∞	∞	∞	∞	∞	∞	∞	∞	∞	∞	∞	∞	∞		∞
DEVbvDnozzle_Pos	∞	∞	∞	∞	∞	∞	∞	∞	∞	∞	∞	∞	∞	∞	∞	∞	∞	∞	∞	∞	∞		∞
DEVbvDnozzle_Neg	∞	∞	∞	∞	∞	∞	∞	∞	∞	∞	∞	∞	∞	∞	∞	∞	∞	∞	∞	∞	∞		∞
DEVbvKfeed_Neg	∞	∞	∞	∞	∞	∞	∞	∞	∞	∞	∞	∞	∞	∞	∞	∞	∞	∞	∞	∞	∞		∞
DEVbvSticspool_Pos	∞	∞	∞	∞	∞	∞	∞	∞	∞	∞	∞	∞	∞	∞	∞	∞	∞	∞	∞	∞	∞		∞
DEVbvDFilter1_Neg	∞	∞	∞	∞	∞	∞	∞	∞	∞	∞	∞	∞	∞	∞	∞	∞	∞	∞	∞	∞	∞		∞
DEVbvDFilter2_Neg	∞	∞	∞	∞	∞	∞	∞	∞	∞	∞	∞	∞	∞	∞	∞	∞	∞	∞	∞	∞	∞		∞
DEVbvCorHP1_Pos	∞	∞	∞	∞	∞	∞	∞	∞	∞	∞	∞	∞	∞	∞	∞	∞	∞	∞	∞	∞	∞		∞
DEVbvCorHP2_Pos	∞	∞	0,02	∞	∞	∞	∞	∞	∞	∞	∞	∞	0,02	∞	∞	∞	∞	∞	0,015	∞	∞	∞		0,015
DEVbvASenO_Pos	∞	∞	∞	∞	∞	∞	∞	∞	∞	∞	∞	∞	∞	∞	∞	∞	∞	3,8	1,07	0,71	∞	∞		0,71
DEVbvASenO_Neg	∞	∞	∞	∞	∞	∞	∞	∞	∞	∞	∞	∞	∞	∞	∞	∞	-0,21	-3,9	-4,67	-3,1	∞	∞		-0,21
DEVbvBSenO_Pos	∞	∞	∞	∞	∞	∞	∞	∞	∞	∞	∞	∞	∞	∞	∞	∞	∞	3,8	1,07	0,71	∞	∞		0,71
DEVbvBSenO_Neg	∞	∞	∞	∞	∞	∞	∞	∞	∞	∞	∞	∞	∞	∞	∞	∞	∞	-3,9	-4,67	-3,1	∞	∞		-3,1

Table A.17 *MLV matrix and mlv vector for the degradation modes of the fuel system.*

Appendix XXI. Performance metrics for the SVR models of HIs and CSIs

HIs	$Q2$	HIs	$Q2$	HIs	$Q2$	HIs	$Q2$		CSIs	$Q2$
$FmvCEquA$	0,42	$BYVoN2mean$	0,60	$VsvYnullB$	-0,67	$VbvYchgA$	-8,26		$rFMV$	1,00
$FmvScaleA$	-0,41	$LppSlpN2DP$	0,06	$VsvXoverlapB$	-4,59	$VbvScaleA$	-1,45		$dFMV$	-0,16
$FmvSlpA$	-0,36	$LppR2N2DP$	-0,20	$VsvYoverlapB$	-0,60	$VbvSlpLeftA$	-1,01		$raFMV$	0,13
$FmvHyst0A$	0,54	$wTBV$	-0,15	$VsvScaleB$	0,43	$VbvSlpRightA$	-211		$rFMVCMD0$	-0,03
$FmvCEquB$	0,42	$wSOV$	0,28	$VsvSlpLeftB$	-4,03	$VbvHyst0A$	0,13		$QFMV$	0,35
$FmvScaleB$	-0,41	$MfpSlpN2DP$	-0,34	$VsvSlpNullB$	-0,19	$VbvCEquB$	0,89		$rDPFMV$	-0,61
$FmvSlpB$	-0,36	$MfpR2N2DP$	0,11	$VsvSlpRightB$	0,04	$VbvXchgB$	-3,06		$XSOV10$	-0,72
$FmvHyst0B$	0,54	$MffSlpN2DP$	-1,06	$VsvHyst0B$	0,04	$VbvYchgB$	-5,45		$Q10$	-0,01
$FmvCEquS$	0,45	$MffR2N2DP$	-0,07	$VsvCEquS$	0,99	$VbvScaleB$	-1,55		$DPMFF$	1,00
$FmvScaleS$	-0,26	$WfmmaxX1$	0,39	$VsvXnullS$	-8,41	$VbvSlpLeftB$	-0,88		$QWFM$	0,68
$FmvSlpS$	-0,33	$WfmmaxX2$	0,38	$VsvYnullS$	-22	$VbvSlpRightB$	-1,52		$rVSV$	-5,6
$FmvHyst0S$	0,54	$WfmminX1$	1,00	$VsvXoverlapS$	-145	$VbvHyst0B$	0,13		$dVSV$	-8.7
$FmvmaxX1$	0,53	$WfmminX2$	1,00	$VsvYoverlapS$	-64	$VbvCEquS$	0,88		$raVSV$	-0,79
$FmvmaxX2$	0,49	$WfmmaxGapX$	-0,10	$VsvScaleS$	-1,07	$VbvXchgS$	0,85		$rVSVCMD0$	0,68
$FmvminX1$	0,99	$WfmminGapX$	-0,13	$VsvSlpLeftS$	-305	$VbvYchgS$	-3,39		$QVSVA$	0,99
$FmvminX2$	0,99	$WfmmeanGapX$	1,00	$VsvSlpNullS$	-10,71	$VbvScaleS$	-5,69		$QVSVB$	0,99
$FmvmaxGapX$	0,71	$WfmstdGapX$	-7,80	$VsvSlpRightS$	-7,09	$VbvSlpLeftS$	-0,44		$rVBV$	0,88
$FmvminGapX$	0,68	$VsvCEquA$	0,99	$VsvHyst0S$	0,08	$VbvSlpRightS$	-0,43		$dVBV$	0,04
$FmvmeanGapX$	1,00	$VsvXnullA$	0,37	$VsvmaxX1$	-16,07	$VbvHyst0S$	0,17		$raVBV$	-1,40
$FmvstdGapX$	-0,16	$VsvYnullA$	-0,67	$VsvmaxX2$	-18,08	$VbvmaxX1$	0,97		$rVBVCMD0$	0,28
$FmvMAErr$	-0,23	$VsvXoverlapA$	-4,59	$VsvminX1$	-0,33	$VbvmaxX2$	0,97		$QVBVA$	0,99
$Sovdelop1$	-0,10	$VsvYoverlapA$	-0,60	$VsvminX2$	-0,24	$VbvminX1$	0,81		$QVBVB$	0,99
$Sovdelclo$	-3,57	$VsvScaleA$	0,43	$VsvmaxGapX$	-55	$VbvminX2$	0,80			
$Sovdelop2$	-0,13	$VsvSlpLeftA$	-4,05	$VsvminGapX$	-56	$VbvmaxGapX$	-5,80			
$VoN2maxSOV$	-245	$VsvSlpNullA$	-0,19	$VsvmeanGapX$	-4,70	$VbvminGapX$	-5,27			
$SOVoN2max$	0,53	$VsvSlpRightA$	0,04	$VsvstdGapX$	-73	$VbvmeanGapX$	0,98			
$SOVoN2mean$	0,57	$VsvHyst0A$	0,04	$VsvMAErr$	-0,37	$VbvstdGapX$	0,17			
$VoN2maxBYV$	-7,83	$VsvCEquB$	0,99	$VbvCEquA$	0,88	$VbvMAErr$	-0,83			
$BYVoN2max$	-7,25	$VsvXnullB$	0,37	$VbvXchgA$	-3,01	$VoN2maxTBV$	-14			

Table A.18 *Q2 index of the SVR model for HIs and CSIs.*

Appendix XXII. Performance metrics for the first set of SVR-Kriging models

HIs	$Q2$	μ_{CV}	σ_{CV}	HIs	$Q2$	μ_{CV}	σ_{CV}	HIs	$Q2$	μ_{CV}	σ_{CV}	HIs	$Q2$	μ_{CV}	σ_{CV}
FmvCEquA	0,39	3,10E-06	2,60E-05	*BYVoN2mean*	0,62	1,30E+01	3,80E+01	*VsvYnullB*	-0,69	2,7E-03	1,7E-02	*VbvYchgA*	-7,32	7,70E-03	1,30E-02
FmvScaleA	-0,06	3,90E-04	1,30E-03	*LppSlpN2DP*	-0,04	7,90E-04	2,40E-03	*VsvXoverlapB*	-2,48	1,80E-02	9,80E-02	*VbvScaleA*	-0,81	5,00E+03	2,60E+04
FmvSlpA	-0,39	1,50E-01	7,90E-01	*LppR2N2DP*	-0,2	1,30E-05	9,10E-04	*VsvYoverlapB*	-0,19	4,40E-02	4,90E-01	*VbvSlpLeftA*	-0,97	4,10E-03	7,40E-03
FmvHyst0A	0,41	2,40E-03	4,50E-03	*wTBV*	-0,16	3,80E-03	2,00E-02	*VsvScaleB*	0,18	9,10E-02	9,30E-01	*VbvSlpRightA*	-184,3	6,00E+01	3,90E+02
FmvCEquB	0,38	4,30E-06	3,20E-05	*wSOV*	0,28	1,50E-03	6,60E-03	*VsvSlpLeftB*	-1,59	8,90E+00	4,60E+01	*VbvHyst0A*	0,11	4,00E+12	2,10E+13
FmvScaleB	-0,41	7,60E+01	3,90E+02	*MfpSlpN2DP*	-0,15	1,10E+06	3,80E+06	*VsvSlpNullB*	-0,18	3,10E-03	1,70E-02	*VbvCEquB*	0,9	4,00E+12	1,40E+13
FmvSlpB	-0,39	2,80E-05	1,40E-04	*MfpR2N2DP*	0,12	1,80E-03	3,50E-02	*VsvSlpRightB*	0,04	1,80E-02	7,80E-04	*VbvXchgB*	-2,57	7,10E-02	4,00E-01
FmvHyst0B	0,38	2,00E-03	9,50E-03	*MffSlpN2DP*	-0,27	6,80E+14	3,50E+15	*VsvHyst0B*	0,04	2,00E-03	1,80E-02	*VbvYchgB*	-5,33	1,10E-02	1,80E-02
FmvCEquS	0,42	2,50E+03	1,30E+04	*MffR2N2DP*	-0,07	3,50E-03	1,20E-02	*VsvCEquS*	0,99	4,90E-05	3,10E-04	*VbvScaleB*	-0,93	1,60E+01	8,00E+01
FmvScaleS	-0,19	5,20E-04	2,00E-03	*WfmmaxX1*	0,28	1,40E+02	9,40E+02	*VsvXnullS*	-2,95	2,00E-03	4,40E-03	*VbvSlpLeftB*	-0,88	7,90E-03	1,20E-02
FmvSlpS	-0,37	4,00E-05	3,80E-04	*WfmmaxX2*	0,33	2,10E-03	4,00E-03	*VsvYnullS*	-15,25	3,20E+02	1,60E+03	*VbvSlpRightB*	-1,16	3,30E-03	5,20E-03
FmvHyst0S	0,46	1,70E+03	9,00E+03	*WfmminX1*	1	4,90E-97	2,60E-96	*VsvXoverlapS*	-93,36	2,90E-02	5,10E-02	*VbvHyst0B*	0,1	1,50E-01	8,30E-01
FmvmaxX1	0,53	5,40E-03	2,20E-02	*WfmminX2*	1	3,20E-04	1,70E-03	*VsvYoverlapS*	-61,48	5,10E-02	8,00E-02	*VbvCEquS*	0,88	7,00E-05	1,10E-03
FmvmaxX2	0,51	3,40E+01	3,60E+02	*WfmmaxGapX*	-0,1	0,00E+00	0,00E+00	*VsvScaleS*	-1,07	2,20E-01	2,20E-03	*VbvXchgS*	0,85	3,60E-01	1,90E+00
FmvminX1	0,99	2,20E-04	3,30E-03	*WfmminGapX*	-0,13	0,00E+00	0,00E+00	*VsvSlpLeftS*	-154,3	3,00E-02	5,90E-02	*VbvYchgS*	-3,39	1,00E-02	1,90E-02
FmvminX2	0,99	3,00E-04	1,50E-03	*WfmmeanGapX*	1	2,20E-04	1,10E-03	*VsvSlpNullS*	-8,92	1,20E-02	2,10E-02	*VbvScaleS*	-3,54	1,30E+03	1,10E+05
FmvmaxGapX	0,71	4,20E+00	1,60E+01	*WfmstdGapX*	0,24	3,40E+02	2,50E+03	*VsvSlpRightS*	-7,08	4,40E-01	2,00E-03	*VbvSlpLeftS*	-0,17	1,20E-03	3,50E-03
FmvminGapX	0,67	5,10E+01	2,70E+02	*VsvCEquA*	0,99	3,70E-05	1,90E-04	*VsvHyst0S*	0,08	5,10E-04	1,20E-03	*VbvSlpRightS*	-0,42	7,70E-02	4,70E-01
FmvmeanGapX	1	1,20E-03	4,40E-03	*VsvXnullA*	0,47	1,40E+03	8,40E+03	*VsvmaxX1*	-16,07	0,00E+00	0,00E+00	*VbvHyst0S*	0,14	1,20E-04	2,70E-03
FmvstdGapX	-0,17	1,60E+14	8,70E+14	*VsvYnullA*	-0,67	5,20E-03	1,10E-02	*VsvmaxX2*	-18,08	0,00E+00	0,00E+00	*VbvmaxX1*	0,96	6,70E-05	4,90E-04
FmvMAErr	0,33	2,60E-03	4,30E-03	*VsvXoverlapA*	-4,55	2,50E-03	5,90E-02	*VsvminX1*	-0,41	5,10E-01	2,60E+00	*VbvmaxX2*	0,98	1,90E-04	1,90E-03
Sovdelop1	-0,1	1,10E-03	6,10E-03	*VsvYoverlapA*	-0,6	1,60E-03	3,20E-02	*VsvminX2*	-0,23	4,20E-02	2,20E-02	*VbvminX1*	0,82	2,40E-04	1,00E-03
Sovdelclo	-3,16	1,60E+09	8,30E+09	*VsvScaleA*	0,43	7,60E+14	4,00E+15	*VsvmaxGapX*	-5,86	1,40E+11	4,70E+11	*VbvminX2*	0,8	4,20E-06	2,30E-04
Sovdelop2	-0,13	2,80E-06	9,90E-06	*VsvSlpLeftA*	-3,99	1,80E+03	9,50E+03	*VsvminGapX*	-2,77	8,80E+13	3,10E+14	*VbvmaxGapX*	-4,55	4,00E-04	1,30E-02
VoN2maxSOV	-80	4,50E-02	4,70E-01	*VsvSlpNullA*	-0,19	1,50E-03	1,00E-02	*VsvmeanGapX*	-5,9	9,70E-01	4,80E+00	*VbvminGapX*	-4,1	1,50E-02	7,50E-02
SOVoN2max	0,52	4,60E+01	2,50E+02	*VsvSlpRightA*	0,04	1,80E-02	7,80E-04	*VsvstdGapX*	-4,83	1,40E+31	7,20E+31	*VbvmeanGapX*	0,98	2,40E-04	1,50E-03
SOVoN2mean	0,58	1,00E-03	2,40E-03	*VsvHyst0A*	0,04	3,50E-03	5,10E-02	*VsvMAErr*	-0,36	7,90E-03	1,50E-02	*VbvstdGapX*	0,2	1,40E-02	7,00E-02
VoN2maxBYV	-6,51	4,90E+00	2,50E+01	*VsvCEquB*	0,99	3,80E-05	2,50E-04	*VbvCEquA*	0,89	3,00E-06	1,50E-03	*VbvMAErr*	-0,63	1,80E-03	9,10E-03
BYVoN2max	-6,07	6,80E-04	1,00E-02	*VsvXnullB*	0,48	1,90E-03	1,10E-02	*VbvXchgA*	-1,25	1,70E+03	7,00E+03	*VoN2maxTBV*	-11,87	8,30E-03	4,80E-02

Table A.19 *Performance metrics of the SVR-Kriging model for HIs.*

Appendix XXIII. Performance metrics for the second set of SVR-Kriging models

HIs	μ_{CV}	σ_{CV}	HIs	μ_{CV}	σ_{CV}	HIs	μ_{CV}	σ_{CV}	HIs	μ_{CV}	σ_{CV}
FmvCEquA	1,80E-02	1,18E-01	*BYVoN2mean*	3,75E-03	6,26E-02	*VsvYnullB*	6,26E-02	6,58E-01	*VbvYchgA*	1,78E-01	4,09E-01
FmvScaleA	4,36E-03	1,20E-01	*LppSlpN2DP*	2,58E-03	1,53E-01	*VsvXoverlapB*	5,54E-02	2,67E-01	*VbvScaleA*	2,35E-02	2,76E-01
FmvSlpA	2,05E-02	2,08E-01	*LppR2N2DP*	7,13E-02	2,21E-01	*VsvYoverlapB*	3,56E-02	2,38E-01	*VbvSlpLeftA*	3,12E-02	1,68E-01
FmvHyst0A	8,95E-03	1,44E-01	*wTBV*	9,42E-03	2,42E-01	*VsvScaleB*	7,10E-03	6,85E-02	*VbvSlpRightA*	2,36E-02	9,03E-01
FmvCEquB	3,34E-03	1,22E-01	*wSOV*	1,53E-02	1,97E-01	*VsvSlpLeftB*	1,88E-02	2,44E-01	*VbvHyst0A*	6,46E-03	1,59E-01
FmvScaleB	2,26E-02	1,25E-01	*MfpSlpN2DP*	2,70E-02	1,88E-01	*VsvSlpNullB*	3,11E-02	2,13E-01	*VbvCEquB*	7,31E-03	2,53E-02
FmvSlpB	1,34E-02	2,22E-01	*MfpR2N2DP*	3,17E-03	1,81E-01	*VsvSlpRightB*	1,56E+00	6,48E+00	*VbvXchgB*	2,04E-02	1,08E-01
FmvHyst0B	4,94E-03	1,55E-01	*MffSlpN2DP*	1,46E-03	8,83E-02	*VsvHyst0B*	3,05E-02	1,22E-01	*VbvYchgB*	8,87E-02	3,24E-01
FmvCEquS	1,67E-02	1,47E-01	*MffR2N2DP*	1,19E-02	1,12E-01	*VsvCEquS*	1,15E-03	1,48E-02	*VbvScaleB*	4,56E+01	3,03E+02
FmvScaleS	7,22E-04	1,20E-01	*WfmmaxX1*	2,69E-02	1,93E-01	*VsvXnullS*	1,94E-02	1,19E-01	*VbvSlpLeftB*	7,51E-03	1,39E-01
FmvSlpS	2,67E-03	2,10E-01	*WfmmaxX2*	2,68E-02	1,95E-01	*VsvYnullS*	6,03E-02	2,75E-01	*VbvSlpRightB*	2,84E-02	1,51E-01
FmvHyst0S	1,26E-03	1,63E-01	*WfmminX1*	2,36E-07	1,49E-06	*VsvXoverlapS*	1,23E-01	4,39E-01	*VbvHyst0B*	5,09E-03	1,88E-01
FmvmaxX1	3,09E-02	1,37E-01	*WfmminX2*	4,15E-08	1,17E-06	*VsvYoverlapS*	9,40E-02	3,64E-01	*VbvCEquS*	2,67E-03	2,77E-02
FmvmaxX2	2,74E-02	1,29E-01	*WfmmaxGapX*	1,15E-02	1,38E-01	*VsvScaleS*	1,87E-01	1,00E+00	*VbvXchgS*	3,56E-03	8,86E-02
FmvminX1	2,72E-03	1,86E-02	*WfmminGapX*	9,74E-03	1,66E-01	*VsvSlpLeftS*	9,26E-02	7,98E-01	*VbvYchgS*	4,68E-02	3,01E-01
FmvminX2	8,35E-04	1,31E-02	*WfmmeanGapX*	1,87E-07	1,82E-06	*VsvSlpNullS*	2,63E-02	2,34E-01	*VbvScaleS*	3,14E-02	1,61E-01
FmvmaxGapX	2,79E-02	8,26E-02	*WfmstdGapX*	1,43E-02	1,72E-01	*VsvSlpRightS*	5,64E+03	3,57E+04	*VbvSlpLeftS*	2,70E-02	1,47E-01
FmvminGapX	2,93E-02	8,59E-02	*VsvCEquA*	9,78E+10	6,49E+11	*VsvHyst0S*	1,16E-02	2,71E-01	*VbvSlpRightS*	7,80E-02	2,06E-01
FmvmeanGapX	1,03E-04	9,61E-03	*VsvXnullA*	8,38E-03	1,19E-01	*VsvmaxX1*	3,89E+13	3,75E+14	*VbvHyst0S*	9,04E-03	1,92E-01
FmvstdGapX	6,35E-02	2,15E-01	*VsvYnullA*	5,80E-02	1,64E-01	*VsvmaxX2*	7,68E+13	3,62E+14	*VbvmaxX1*	1,06E-03	2,59E-02
FmvMAErr	9,54E-03	1,36E-01	*VsvXoverlapA*	6,40E-02	2,49E-01	*VsvminX1*	3,70E-02	1,33E-01	*VbvmaxX2*	9,68E-04	2,50E-02
Sovdelop1	4,87E-02	2,93E-01	*VsvYoverlapA*	3,32E-02	2,27E-01	*VsvminX2*	2,39E-02	1,10E-01	*VbvminX1*	1,21E-02	5,41E-02
Sovdelclo	8,34E-03	2,33E-01	*VsvScaleA*	1,00E-01	8,23E-01	*VsvmaxGapX*	8,96E+08	4,34E+09	*VbvminX2*	5,21E-03	4,37E-02
Sovdelop2	5,38E-02	3,04E-01	*VsvSlpLeftA*	6,14E-02	1,96E-01	*VsvminGapX*	1,44E+09	6,74E+09	*VbvmaxGapX*	3,49E-02	2,68E-01
VoN2maxSOV	1,08E-01	6,25E-01	*VsvSlpNullA*	3,25E-02	2,14E-01	*VsvmeanGapX*	7,93E+08	2,51E+09	*VbvminGapX*	4,81E-03	2,48E-01
SOVoN2max	2,51E-02	2,19E-01	*VsvSlpRightA*	7,40E+09	4,57E+10	*VsvstdGapX*	1,85E+08	1,15E+09	*VbvmeanGapX*	5,15E-04	3,99E-02
SOVoN2mean	7,05E-03	1,36E-01	*VsvHyst0A*	8,82E+02	5,64E+03	*VsvMAErr*	6,82E-02	2,22E-01	*VbvstdGapX*	2,11E+00	1,37E+01
VoN2maxBYV	1,12E-01	6,26E-01	*VsvCEquB*	1,78E-04	1,61E-02	*VbvCEquA*	5,58E-03	2,47E-02	*VbvMAErr*	7,90E-02	2,92E-01
BYVoN2max	2,30E-02	2,59E-01	*VsvXnullB*	5,57E-03	1,24E-01	*VbvXchgA*	2,21E-02	6,81E-02	*VoN2maxTBV*	6,32E-02	4,72E-01

Table A.20 *Performance metrics of the SVR-Kriging model for HIs*

Appendix XXIV. Detection NKPIs for the fleet models with real HIs

	FmvCEquA	FmvScaleA	FmvSlpA	FmvHyst0A	FmvCEquB	FmvScaleB	FmvSlpB	FmvHyst0B	FmvCEquS	FmvScaleS	FmvSlpS	FmvHyst0S	FmvmaxX1	FmvmaxX2	FmvminX1	FmvminX2	FmvmaxGapX	FmvminGapX	FmvmeanGapX	FmvstdGapX	FmvMAErr	Sovdelop1	Sovdelclo	Sovdelop2	wTBV	wSOV	MffSlpN2DP	MffR2N2DP
DBvvDIlkg_Pos	0	0	0	0	0	0	0	0	0	0	0	0	0	0	0	0	0	0	0	0	0	0	0	0	0	0	0	0
DEBvvK0_Neg	0	0	0	0	0	0	0	0	0	0	0	0	0	0	0	0	0	0	0	0	0	0	0	0	0	0	0	0
DEBvvStic_Pos	0	0	0	0	0	0	0	0	0	0	0	0	0	0	0	0	0	0	0	0	0	0	0	0	0	0	0	0
DEBvvVisc_Pos	0	0	0	0	0	0	0	0	0	0	0	0	0	0	0	0	0	0	0	0	0	0	0	0	0	0	0	0
DEFmvASenO_Neg	0	0	0	0	0	0	0	0	0	0	0	0	1	0	1	0	0	1	1	1	0	0	0	0	0	0	0	0
DEFmvASenO_Pos	0	0	0	1	0	0	0	1	0	0	0	1	0	1	0	0	1	0	1	1	0	0	0	0	0	0	0	0
DEFmvBSenO_Neg	0	0	0	0	0	0	0	0	0	0	0	0	0	1	0	1	1	0	1	1	0	0	0	0	0	0	0	0
DEFmvBSenO_Pos	0	0	0	1	0	0	0	1	0	0	0	1	1	0	0	0	0	1	1	1	0	0	0	0	0	0	0	0
DEFmvCnull_Neg	1	0	0	0	1	0	0	0	1	0	0	0	1	1	0	0	0	0	0	0	1	0	0	0	0	0	0	0
DEFmvCnull_Pos	1	0	0	0	1	0	0	0	1	0	0	0	1	1	0	0	0	0	0	0	1	0	0	0	0	0	0	0
DEFmvDnozzle_Pos	0	1	0	0	0	1	0	0	0	1	1	0	0	0	0	0	0	0	0	0	0	0	0	0	0	0	0	0
DEFmvStic_Pos	0	0	0	1	0	0	0	1	0	0	0	1	0	1	0	0	0	0	0	0	1	0	0	0	0	0	0	0
DEMffFlowRate_Neg	0	0	0	0	0	0	0	0	0	0	0	0	0	0	0	0	0	0	0	0	0	0	0	0	0	0	1	1
DESovStic_Pos	0	0	0	0	0	0	0	0	0	0	0	0	0	0	0	0	0	0	0	0	0	0	0	0	0	0	0	0
DESovVisc_Pos	0	0	0	0	0	0	0	0	0	0	0	0	0	0	0	0	0	0	0	0	0	0	0	0	0	0	0	0
DEVbvASenO_Neg	0	0	0	0	0	0	0	0	0	0	0	0	0	0	0	0	0	0	0	0	0	0	0	0	0	0	0	0
DEVbvASenO_Pos	0	0	0	0	0	0	0	0	0	0	0	0	0	0	0	0	0	0	0	0	0	0	0	0	0	0	0	0
DEVbvBSenO_Neg	0	0	0	0	0	0	0	0	0	0	0	0	0	0	0	0	0	0	0	0	0	0	0	0	0	0	0	0
DEVbvBSenO_Pos	0	0	0	0	0	0	0	0	0	0	0	0	0	0	0	0	0	0	0	0	0	0	0	0	0	0	0	0
DEVbvCnull_Neg	0	0	0	0	0	0	0	0	0	0	0	0	0	0	0	0	0	0	0	0	0	0	0	0	0	0	0	0
DEVbvCnull_Pos	0	0	0	0	0	0	0	0	0	0	0	0	0	0	0	0	0	0	0	0	0	0	0	0	0	0	0	0
DEVbvCorHP1_Pos	0	0	0	0	0	0	0	0	0	0	0	0	0	0	0	0	0	0	0	0	0	0	0	0	0	0	0	0
DEVbvCorHP2_Pos	0	0	0	0	0	0	0	0	0	0	0	0	0	0	0	0	0	0	0	0	0	0	0	0	0	0	0	0
DEVbvDCool1_Neg	0	0	0	0	0	0	0	0	0	0	0	0	0	0	0	0	0	0	0	0	0	0	0	0	0	0	0	0
DEVbvDCool1_Pos	0	0	0	0	0	0	0	0	0	0	0	0	0	0	0	0	0	0	0	0	0	0	0	0	0	0	0	0
DEVbvDCool2_Neg	0	0	0	0	0	0	0	0	0	0	0	0	0	0	0	0	0	0	0	0	0	0	0	0	0	0	0	0
DEVbvDCool2_Pos	0	0	0	0	0	0	0	0	0	0	0	0	0	0	0	0	0	0	0	0	0	0	0	0	0	0	0	0
DEVbvDFilter1_Neg	0	0	0	0	0	0	0	0	0	0	0	0	0	0	0	0	0	0	0	0	0	0	0	0	0	0	0	0
DEVbvDFilter2_Neg	0	0	0	0	0	0	0	0	0	0	0	0	0	0	0	0	0	0	0	0	0	0	0	0	0	0	0	0
DEVbvDnozzle_Neg	0	0	0	0	0	0	0	0	0	0	0	0	0	0	0	0	0	0	0	0	0	0	0	0	0	0	0	0
DEVbvDnozzle_Pos	0	0	0	0	0	0	0	0	0	0	0	0	0	0	0	0	0	0	0	0	0	0	0	0	0	0	0	0
DEVbvKfeed_Neg	0	0	0	0	0	0	0	0	0	0	0	0	0	0	0	0	0	0	0	0	0	0	0	0	0	0	0	0
DEVbvKineFric_Pos	0	0	0	0	0	0	0	0	0	0	0	1	0	0	0	0	0	0	0	0	0	0	0	0	0	0	0	0
DEVbvStic1_Pos	0	0	0	0	0	0	0	0	0	0	0	0	0	0	0	0	0	0	0	0	0	0	0	0	0	0	0	0
DEVbvStic2_Pos	0	0	0	0	0	0	0	0	0	0	0	0	0	0	0	0	0	0	0	0	0	0	0	0	0	0	0	0
DEVbvSticspool_Pos	0	0	0	0	0	0	0	0	0	0	0	0	0	0	0	0	0	0	0	0	0	0	0	0	0	0	0	0
DEVbvVisc1_Pos	0	0	0	0	0	0	0	0	0	0	0	0	0	0	0	0	0	0	0	0	0	0	0	0	0	0	0	0
DEVbvVisc2_Pos	0	0	0	0	0	0	0	0	0	0	0	0	0	0	0	0	0	0	0	0	0	0	0	0	0	0	0	0
DEVsvASenO_Neg	0	0	0	0	0	0	0	0	0	0	0	0	0	0	0	0	0	0	0	0	0	0	0	0	0	0	0	0
DEVsvASenO_Pos	0	0	0	0	0	0	0	0	0	0	0	0	0	0	0	0	0	0	0	0	0	0	0	0	0	0	0	0
DEVsvBSenO_Neg	0	0	0	0	0	0	0	0	0	0	0	0	0	0	0	0	0	0	0	0	0	0	0	0	0	0	0	0
DEVsvBSenO_Pos	0	0	0	0	0	0	0	0	0	0	0	0	0	0	0	0	0	0	0	0	0	0	0	0	0	0	0	0
DEVsvCnull_Neg	0	0	0	0	0	0	0	0	0	0	0	0	0	0	0	0	0	0	0	0	0	0	0	0	0	0	0	0
DEVsvCnull_Pos	0	0	0	0	0	0	0	0	0	0	0	0	0	0	0	0	0	0	0	0	0	0	0	0	0	0	0	0
DEVsvCorHP1_Pos	0	0	0	0	0	0	0	0	0	0	0	0	0	0	0	0	0	0	0	0	0	0	0	0	0	0	0	0
DEVsvCorHP2_Pos	0	0	0	0	0	0	0	0	0	0	0	0	0	0	0	0	0	0	0	0	0	0	0	0	0	0	0	0
DEVsvDCool1_Neg	0	0	0	0	0	0	0	0	0	0	0	0	0	0	0	0	0	0	0	0	0	0	0	0	0	0	0	0
DEVsvDCool1_Pos	0	0	0	0	0	0	0	0	0	0	0	0	0	0	0	0	0	0	0	0	0	0	0	0	0	0	0	0
DEVsvDCool2_Neg	0	0	0	0	0	0	0	0	0	0	0	0	0	0	0	0	0	0	0	0	0	0	0	0	0	0	0	0
DEVsvDCool2_Pos	0	0	0	0	0	0	0	0	0	0	0	0	0	0	0	0	0	0	0	0	0	0	0	0	0	0	0	0
DEVsvDFilter1_Neg	0	0	0	0	0	0	0	0	0	0	0	0	0	0	0	0	0	0	0	0	0	0	0	0	0	0	0	0
DEVsvDFilter2_Neg	0	0	0	0	0	0	0	0	0	0	0	0	0	0	0	0	0	0	0	0	0	0	0	0	0	0	0	0
DEVsvDnozzle_Neg	0	0	0	0	0	0	0	0	0	0	0	0	0	0	0	0	0	0	0	0	0	0	0	0	0	0	0	0
DEVsvDnozzle_Pos	0	0	0	0	0	0	0	0	0	0	0	0	0	0	0	0	0	0	0	0	0	0	0	0	0	0	0	0
DEVsvKfeed_Neg	0	0	0	0	0	0	0	0	0	0	0	0	0	0	0	0	0	0	0	0	0	0	0	0	0	0	0	0
DEVsvKineFric_Pos	0	0	0	0	0	0	0	0	0	0	0	0	0	0	0	0	0	0	0	0	0	0	0	0	0	0	0	0
DEVsvStic1_Pos	0	0	0	0	0	0	0	0	0	0	0	0	0	0	0	0	0	0	0	0	0	0	0	0	0	0	0	0
DEVsvStic2_Pos	0	0	0	0	0	0	0	0	0	0	0	0	0	0	0	0	0	0	0	0	0	0	0	0	0	0	0	0
DEVsvSticspool_Pos	0	0	0	0	0	0	0	0	0	0	0	0	0	0	0	0	0	0	0	0	0	0	0	0	0	0	0	0
DEVsvVisc1_Pos	0	0	0	0	0	0	0	0	0	0	0	0	0	0	0	0	0	0	0	0	0	0	0	0	0	0	0	0
DEVsvVisc2_Pos	0	0	0	0	0	0	0	0	0	0	0	0	0	0	0	0	0	0	0	0	0	0	0	0	0	0	0	0
DEWfmASenO_Neg	0	0	0	0	0	0	0	0	0	0	0	0	0	0	0	0	0	0	0	0	0	0	0	0	0	0	0	0
DEWfmASenO_Pos	0	0	0	0	0	0	0	0	0	0	0	0	0	0	0	0	0	0	0	0	0	0	0	0	0	0	0	0
DEWfmBSenO_Neg	0	0	0	0	0	0	0	0	0	0	0	0	0	0	0	0	0	0	0	0	0	0	0	0	0	0	0	0
DEWfmBSenO_Pos	0	0	0	0	0	0	0	0	0	0	0	0	0	0	0	0	0	0	0	0	0	0	0	0	0	0	0	0
DFmvDIlkg_Pos	1	1	0	1	1	0	0	1	1	1	1	1	1	1	0	0	0	0	0	0	1	0	0	0	0	0	0	0
DLppDIlkg_Pos	0	0	0	0	0	0	0	0	0	0	0	0	0	0	0	0	0	0	0	0	0	0	0	0	0	0	0	0
DMfpDIlkg_Pos	0	0	0	0	0	0	0	0	0	0	0	0	0	0	0	0	0	0	0	0	0	0	0	0	0	0	0	0
DSovDelay_Pos	0	0	0	0	0	0	0	0	0	0	0	0	0	0	0	0	0	0	0	0	0	0	0	0	1	0	0	0
DSovDIlkg_Pos	0	0	0	0	0	0	0	0	0	0	0	0	0	0	0	0	0	0	0	0	0	0	0	0	1	1	0	0
DTbvDIlkg_Pos	0	0	0	0	0	0	0	0	0	0	0	0	0	0	0	0	0	0	0	0	0	0	0	0	0	0	0	0
TOTAL	3	2	0	4	3	1	0	4	3	2	2	5	4	6	1	1	2	2	4	4	4	0	0	0	2	1	1	1

	WfmmaxX1	WfmmaxX2	WfmminX1	WfmminX2	WfmmaxGapX	WfmminGapX	WfmmeanGapX	WfmstdGapX	VsvCEquA	VsvXnullA	VsvYnullA	VsvXoverlapA	VsvYoverlapA	VsvScaleA	VsvSlpLeftA	VsvSlpNullA	VsvSlpRightA	VsvHyst0A	VsvCEquB	VsvXnullB	VsvYnullB	VsvXoverlapB	VsvYoverlapB	VsvScaleB	VsvSlpLeftB	VsvSlpNullB	VsvSlpRightB	VsvHyst0B	VsvCEquS
DBvvDIlkg_Pos	1	1	0	0	0	0	0	0	0	0	0	0	0	0	0	0	1	0	0	0	0	0	0	1	0	0	1	0	0
DEBvvK0_Neg	1	1	0	0	0	0	0	0	0	0	0	0	0	0	0	0	0	0	0	0	0	0	0	0	0	0	0	0	0
DEBvvStic_Pos	0	0	0	0	0	0	0	0	0	0	0	0	0	0	0	0	0	0	0	0	0	0	0	0	0	0	0	0	0
DEBvvVisc_Pos	0	0	0	0	0	0	0	0	0	0	0	0	0	0	0	0	0	0	0	0	0	0	0	0	0	0	0	0	0
DEFmvASen0_Neg	0	0	0	0	0	0	0	0	0	0	0	0	0	0	0	0	0	0	0	0	0	0	0	0	0	0	0	0	0
DEFmvASen0_Pos	1	0	0	0	0	0	0	0	0	0	0	0	0	0	0	0	0	0	0	0	0	0	0	0	0	0	0	0	0
DEFmvBSen0_Neg	0	0	0	0	0	0	0	0	0	0	0	0	0	0	0	0	0	0	0	0	0	0	0	0	0	0	0	0	0
DEFmvBSen0_Pos	1	0	0	0	0	0	0	0	0	0	0	0	0	0	0	0	0	0	0	0	0	0	0	0	0	0	0	0	0
DEFmvCnull_Neg	0	0	0	0	0	0	0	0	0	0	0	0	0	0	0	0	0	0	0	0	0	0	0	0	0	0	0	0	0
DEFmvCnull_Pos	1	0	0	0	0	0	0	0	0	0	0	0	0	0	0	0	0	0	0	0	0	0	0	0	0	0	0	0	0
DEFmvDnozzle_Pos	0	0	0	0	0	0	0	0	0	0	0	0	0	0	0	0	0	0	0	0	0	0	0	0	0	0	0	0	0
DEFmvStic_Pos	1	0	0	0	0	0	0	0	0	0	0	0	0	0	0	0	0	0	0	0	0	0	0	0	0	0	0	0	0
DEMffFlowRate_Neg	0	0	0	0	0	0	0	0	0	0	0	0	0	0	0	0	0	0	0	0	0	0	0	0	0	0	0	0	0
DESovStic_Pos	0	0	0	0	0	0	0	0	0	0	0	0	0	0	0	0	0	0	0	0	0	0	0	0	0	0	0	0	0
DESovVisc_Pos	0	0	0	0	0	0	0	0	0	0	0	0	0	0	0	0	0	0	0	0	0	0	0	0	0	0	0	0	0
DEVbvASen0_Neg	0	0	0	0	0	0	0	0	0	0	0	0	0	0	0	0	0	0	0	0	0	0	0	0	0	0	0	0	0
DEVbvASen0_Pos	0	0	0	0	0	0	0	0	0	0	0	0	0	0	0	0	0	0	0	0	0	0	0	0	0	0	0	0	0
DEVbvBSen0_Neg	0	0	0	0	0	0	0	0	0	0	0	0	0	0	0	0	0	0	0	0	0	0	0	0	0	0	0	0	0
DEVbvBSen0_Pos	0	0	0	0	0	0	0	0	0	0	0	0	0	0	0	0	0	0	0	0	0	0	0	0	0	0	0	0	0
DEVbvCnull_Neg	0	0	0	0	0	0	0	0	0	0	0	0	0	0	0	0	0	0	0	0	0	0	0	0	0	0	0	0	0
DEVbvCnull_Pos	0	0	0	0	0	0	0	0	0	0	0	0	0	0	0	0	0	0	0	0	0	0	0	0	0	0	0	0	0
DEVbvCorHP1_Pos	0	0	0	0	0	0	0	0	0	0	0	0	0	0	0	0	0	0	0	0	0	0	0	0	0	0	0	0	0
DEVbvCorHP2_Pos	0	0	0	0	0	0	0	0	0	0	0	0	0	0	0	0	0	0	0	0	0	0	0	0	0	0	0	0	0
DEVbvDCool1_Neg	0	0	0	0	0	0	0	0	0	0	0	0	0	0	0	0	0	0	0	0	0	0	0	0	0	0	0	0	0
DEVbvDCool1_Pos	0	0	0	0	0	0	0	0	0	0	0	0	0	0	0	0	0	0	0	0	0	0	0	0	0	0	0	0	0
DEVbvDCool2_Neg	0	0	0	0	0	0	0	0	0	0	0	0	0	0	0	0	0	0	0	0	0	0	0	0	0	0	0	0	0
DEVbvDCool2_Pos	0	0	0	0	0	0	0	0	0	0	0	0	0	0	0	0	0	0	0	0	0	0	0	0	0	0	0	0	0
DEVbvDFilter1_Neg	0	0	0	0	0	0	0	0	0	0	0	0	0	0	0	0	0	0	0	0	0	0	0	0	0	0	0	0	0
DEVbvDFilter2_Neg	0	0	0	0	0	0	0	0	0	0	0	0	0	0	0	0	0	0	0	0	0	0	0	0	0	0	0	0	0
DEVbvDnozzle_Neg	0	0	0	0	0	0	0	0	0	0	0	0	0	0	0	0	0	0	0	0	0	0	0	0	0	0	0	0	0
DEVbvDnozzle_Pos	0	0	0	0	0	0	0	0	0	0	0	0	0	0	0	0	0	0	0	0	0	0	0	0	0	0	0	0	0
DEVbvKfeed_Neg	0	0	0	0	0	0	0	0	0	0	0	0	0	0	0	0	0	0	0	0	0	0	0	0	0	0	0	0	0
DEVbvKineFric_Pos	0	0	0	0	1	0	0	0	0	0	0	0	0	0	0	0	0	0	0	0	0	0	0	0	0	0	0	0	0
DEVbvStic1_Pos	0	0	0	0	0	0	0	0	0	0	0	0	0	0	0	0	0	0	0	0	0	0	0	0	0	0	0	0	0
DEVbvStic2_Pos	0	0	0	0	0	0	0	0	0	0	0	0	0	0	0	0	0	0	0	0	0	0	0	0	0	0	0	0	0
DEVbvSticspool_Pos	0	0	0	0	0	0	0	0	0	0	0	0	0	0	0	0	0	0	0	0	0	0	0	0	0	0	0	0	0
DEVbvVisc1_Pos	0	0	0	0	0	0	0	0	0	0	0	0	0	0	0	0	0	0	0	0	0	0	0	0	0	0	0	0	0
DEVbvVisc2_Pos	0	0	0	0	0	0	0	0	0	0	0	0	0	0	0	0	0	0	0	0	0	0	0	0	0	0	0	0	0
DEVsvASen0_Neg	0	0	0	0	0	0	0	0	0	0	0	0	0	0	0	0	0	0	0	0	0	0	0	0	0	0	0	0	0
DEVsvASen0_Pos	0	0	0	0	0	0	0	0	0	0	0	0	0	0	0	0	0	0	0	0	0	0	0	0	0	0	0	0	0
DEVsvBSen0_Neg	0	0	0	0	0	0	0	0	0	0	0	0	0	0	0	0	0	0	0	0	0	0	0	0	0	0	0	0	0
DEVsvBSen0_Pos	0	0	0	0	0	0	0	0	0	0	0	0	0	0	0	0	0	0	0	0	0	0	0	0	0	0	0	0	0
DEVsvCnull_Neg	0	0	0	0	0	0	0	0	1	1	0	1	1	0	1	0	0	0	1	1	0	1	1	0	0	0	0	0	1
DEVsvCnull_Pos	0	0	0	0	0	0	0	0	1	1	0	0	0	0	0	0	0	0	1	1	0	0	0	0	0	0	0	0	1
DEVsvCorHP1_Pos	0	0	0	0	0	0	0	0	0	0	0	0	0	0	0	0	0	0	0	0	0	0	0	0	0	0	0	0	0
DEVsvCorHP2_Pos	0	0	0	0	0	0	0	0	0	0	0	0	0	0	0	0	0	0	0	0	0	0	0	0	0	0	0	0	0
DEVsvDCool1_Neg	0	0	0	0	0	0	0	0	0	0	0	0	0	0	0	0	0	0	0	0	0	0	0	0	0	0	0	0	0
DEVsvDCool1_Pos	0	0	0	0	0	0	0	0	0	0	0	0	0	0	0	0	0	0	0	0	0	0	0	0	0	0	0	0	0
DEVsvDCool2_Neg	0	0	0	0	0	0	0	0	1	0	1	0	0	0	0	1	0	0	1	0	1	0	0	0	0	1	0	0	1
DEVsvDCool2_Pos	0	0	0	0	0	0	0	0	1	0	1	0	0	0	1	1	0	0	1	0	1	1	0	1	1	1	0	1	1
DEVsvDFilter1_Neg	0	0	0	0	0	0	0	0	0	0	0	0	0	0	0	0	0	0	0	0	0	0	0	0	0	0	0	0	0
DEVsvDFilter2_Neg	0	0	0	0	0	0	0	0	0	0	0	0	0	0	0	0	0	0	0	0	0	0	0	0	0	0	0	0	0
DEVsvDnozzle_Neg	0	0	0	0	0	0	0	0	0	0	0	0	0	0	0	0	0	0	0	0	0	0	0	0	0	0	0	0	0
DEVsvDnozzle_Pos	0	0	0	0	0	0	0	0	0	0	0	0	0	0	0	0	0	0	0	0	0	0	0	0	0	0	0	0	0
DEVsvKfeed_Neg	0	0	0	0	0	0	0	0	0	0	0	0	0	1	1	1	1	0	0	0	0	0	0	1	1	1	1	0	0
DEVsvKineFric_Pos	0	0	0	0	0	0	0	0	1	1	0	1	1	1	1	0	0	0	1	1	0	1	1	1	1	1	0	0	0
DEVsvStic1_Pos	0	0	0	0	0	0	0	0	0	0	0	0	0	0	0	0	0	0	0	0	0	0	0	0	0	0	0	0	0
DEVsvStic2_Pos	0	0	0	0	0	0	0	0	0	0	0	0	0	0	0	0	0	0	0	0	0	0	0	0	0	0	0	0	0
DEVsvSticspool_Pos	0	0	0	0	0	0	0	0	1	0	1	0	1	0	1	1	1	0	1	0	1	0	1	0	1	1	1	1	1
DEVsvVisc1_Pos	0	0	0	0	0	0	0	0	0	0	0	0	0	0	0	0	0	0	0	0	0	0	0	0	0	0	0	0	0
DEVsvVisc2_Pos	0	0	0	0	0	0	0	0	0	0	0	0	0	0	0	0	0	0	0	0	0	0	0	0	0	0	0	0	0
DEWfmASen0_Neg	0	0	1	0	0	1	1	1	0	0	0	0	0	0	0	0	0	0	0	0	0	0	0	0	0	0	0	0	0
DEWfmASen0_Pos	0	0	1	0	1	0	1	1	0	0	0	0	0	0	0	0	0	0	0	0	0	0	0	0	0	0	0	0	0
DEWfmBSen0_Neg	0	0	0	1	1	0	1	1	0	0	0	0	0	0	0	0	0	0	0	0	0	0	0	0	0	0	0	0	0
DEWfmBSen0_Pos	0	0	0	1	0	1	1	1	0	0	0	0	0	0	0	0	0	0	0	0	0	0	0	0	0	0	0	0	0
DFmvDIlkg_Pos	1	0	0	0	0	0	0	0	0	0	0	0	0	0	0	0	0	0	0	0	0	0	0	0	0	0	0	0	0
DLppDIlkg_Pos	0	0	0	0	0	0	0	0	0	0	0	0	0	0	0	0	0	0	0	0	0	0	0	0	0	0	0	0	0
DMfpDIlkg_Pos	0	0	0	0	0	0	0	0	0	0	0	0	0	0	0	0	0	0	0	0	0	0	0	0	0	0	0	0	0
DSovDelay_Pos	0	0	0	0	0	0	0	0	0	0	0	0	0	0	0	0	0	0	0	0	0	0	0	0	0	0	0	0	0
DSovDIlkg_Pos	0	0	0	0	0	0	0	0	0	0	0	0	0	0	0	0	1	0	0	0	0	0	0	0	0	0	1	0	0
DTbvDIlkg_Pos	0	0	0	0	0	0	0	0	0	0	0	0	0	0	0	0	0	0	0	0	0	0	0	0	0	0	0	0	0
TOTAL	7	2	2	2	3	2	4	4	5	3	4	1	3	2	5	5	4	0	5	3	4	2	3	4	4	5	5	2	5

	VsvXnullS	VsvYnullS	VsvXoverlapS	VsvYoverlapS	VsvScaleS	VsvSlpLeftS	VsvSlpNullS	VsvSlpRightS	VsvHyst0S	VsvmaxX1	VsvmaxX2	VsvminX1	VsvminX2	VsvmaxGapX	VsvminGapX	VsvmeanGapX	VsvstdGapX	VsvMAErr	VbvCEquA	VbvXchgA	VbvYchgA	VbvScaleA	VbvSlpLeftA	VbvSlpRightA	VbvHyst0A	VbvCEquB	VbvXchgB
DBvvDIlkg_Pos	0	0	0	0	0	0	0	0	0	0	0	0	0	0	0	0	0	0	0	0	1	0	0	0	0	0	0
DEBvvK0_Neg	0	0	0	0	1	0	0	0	0	0	0	0	0	0	0	0	0	0	0	0	0	0	0	0	0	0	0
DEBvvStic_Pos	0	0	0	0	0	0	0	0	0	0	0	0	0	0	0	0	0	0	0	0	0	0	0	0	0	0	0
DEBvvVisc_Pos	0	0	0	0	0	0	0	0	0	0	0	0	0	0	0	0	0	0	0	0	0	0	0	0	0	0	0
DEFmvASenO_Neg	0	0	0	0	0	0	0	0	0	0	0	0	0	0	0	0	0	0	0	0	0	0	0	0	0	0	0
DEFmvASenO_Pos	0	0	0	0	0	0	0	0	0	0	0	0	0	0	0	0	0	0	0	0	0	0	0	0	0	0	0
DEFmvBSenO_Neg	0	0	0	0	0	0	0	0	0	0	0	0	0	0	0	0	0	0	0	0	0	0	0	0	0	0	0
DEFmvBSenO_Pos	0	0	0	0	0	0	0	0	0	0	0	0	0	0	0	0	0	0	0	0	0	0	0	0	0	0	0
DEFmvCnull_Neg	0	0	0	0	0	0	0	0	0	0	0	0	0	0	0	0	0	0	0	0	0	0	0	0	0	0	0
DEFmvCnull_Pos	0	0	0	0	0	0	0	0	0	0	0	0	0	0	0	0	0	0	0	0	0	0	0	0	0	0	0
DEFmvDnozzle_Pos	0	0	0	0	0	0	0	0	0	0	0	0	0	0	0	0	0	0	0	0	0	0	0	0	0	0	0
DEFmvStic_Pos	0	0	0	0	0	0	0	0	0	0	0	0	0	0	0	0	0	0	0	0	0	0	0	0	0	0	0
DEMffFlowRate_Neg	0	0	0	0	0	0	0	0	0	0	0	0	0	0	0	0	0	0	0	0	0	0	0	0	0	0	0
DESovStic_Pos	0	0	0	0	0	0	0	0	0	0	0	0	0	0	0	0	0	0	0	0	0	0	0	0	0	0	0
DESovVisc_Pos	0	0	0	0	0	0	0	0	0	0	0	0	0	0	0	0	0	0	0	0	0	0	0	0	0	0	0
DEVbvASenO_Neg	0	0	0	0	0	0	0	0	0	0	0	0	0	0	0	0	0	0	0	0	0	0	0	0	0	0	0
DEVbvASenO_Pos	0	0	0	0	0	0	0	0	0	0	0	0	0	0	0	0	0	0	0	0	0	0	0	0	1	0	0
DEVbvBSenO_Neg	0	0	0	0	0	0	0	0	0	0	0	0	0	0	0	0	0	0	0	0	0	0	0	0	0	0	0
DEVbvBSenO_Pos	0	0	0	0	0	0	0	0	0	0	0	0	0	0	0	0	0	0	0	0	0	0	0	0	1	0	0
DEVbvCnull_Neg	0	0	0	0	0	0	0	0	0	0	0	0	0	0	0	0	0	0	1	1	0	0	0	0	0	1	1
DEVbvCnull_Pos	0	0	0	0	0	0	0	0	0	0	0	0	0	0	0	0	0	0	1	1	0	0	0	0	0	1	1
DEVbvCorHP1_Pos	0	0	0	0	0	0	0	0	0	0	0	0	0	0	0	0	0	0	0	0	0	0	0	0	0	0	0
DEVbvCorHP2_Pos	0	0	0	0	0	0	0	0	0	0	0	0	0	0	0	0	0	0	0	0	0	0	0	0	0	0	0
DEVbvDCool1_Neg	0	0	0	0	0	0	0	0	0	0	0	0	0	0	0	0	0	0	0	0	0	0	0	0	0	0	0
DEVbvDCool1_Pos	0	0	0	0	0	0	0	0	0	0	0	0	0	0	0	0	0	0	0	0	0	0	0	0	0	0	0
DEVbvDCool2_Neg	0	0	0	0	0	0	0	0	0	0	0	0	0	0	0	0	0	0	1	0	0	0	0	0	0	1	0
DEVbvDCool2_Pos	0	0	0	0	0	0	0	0	0	0	0	0	0	0	0	0	0	0	1	1	0	0	0	0	0	1	1
DEVbvDFilter1_Neg	0	0	0	0	0	0	0	0	0	0	0	0	0	0	0	0	0	0	0	0	0	0	0	0	0	0	0
DEVbvDFilter2_Neg	0	0	0	0	0	0	0	0	0	0	0	0	0	0	0	0	0	0	0	0	0	0	0	0	0	0	0
DEVbvDnozzle_Neg	0	0	0	0	0	0	0	0	0	0	0	0	0	0	0	0	0	0	0	0	0	0	0	0	0	0	0
DEVbvDnozzle_Pos	0	0	0	0	0	0	0	0	0	0	0	0	0	0	0	0	0	0	0	0	0	0	0	0	0	0	0
DEVbvKfeed_Neg	0	0	0	0	0	0	0	0	0	0	0	0	0	0	0	0	0	0	0	0	0	0	0	0	0	0	0
DEVbvKineFric_Pos	0	0	0	0	0	0	0	0	0	0	0	0	0	0	0	0	0	0	0	0	0	0	0	0	0	0	0
DEVbvStic1_Pos	0	0	0	0	0	0	0	0	0	0	0	0	0	0	0	0	0	0	0	0	0	0	0	0	0	0	0
DEVbvStic2_Pos	0	0	0	0	0	0	0	0	0	0	0	0	0	0	0	0	0	0	0	0	0	0	0	0	0	0	0
DEVbvSticspool_Pos	0	0	0	0	0	0	0	0	0	0	0	0	0	0	0	0	0	0	0	0	0	0	0	0	1	1	0
DEVbvVisc1_Pos	0	0	0	0	0	0	0	0	0	0	0	0	0	0	0	0	0	0	0	0	0	0	0	0	0	0	0
DEVbvVisc2_Pos	0	0	0	0	0	0	0	0	0	0	0	0	0	0	0	0	0	0	0	0	0	0	0	0	0	0	0
DEVsvASenO_Neg	0	0	0	0	0	0	0	0	0	0	0	1	1	0	1	1	1	0	0	0	0	0	0	0	0	0	0
DEVsvASenO_Pos	0	0	0	0	0	0	0	0	1	0	1	1	1	1	1	1	1	0	0	0	0	0	0	0	0	0	0
DEVsvBSenO_Neg	0	0	0	0	0	0	0	0	0	0	1	1	1	1	1	1	1	0	0	0	0	0	0	0	0	0	0
DEVsvBSenO_Pos	0	0	0	0	0	0	0	0	0	1	1	1	0	1	1	1	0	0	0	0	0	0	0	0	0	0	0
DEVsvCnull_Neg	1	0	0	0	0	0	0	0	0	0	0	0	0	0	0	0	0	0	0	0	0	0	0	0	0	0	0
DEVsvCnull_Pos	1	0	0	0	0	0	0	0	0	0	0	0	0	0	0	0	0	0	0	0	0	0	0	0	0	0	0
DEVsvCorHP1_Pos	0	0	0	0	0	0	0	0	0	0	0	0	0	0	0	0	0	0	0	0	0	0	0	0	0	0	0
DEVsvCorHP2_Pos	0	0	0	0	0	0	0	0	0	0	0	0	0	0	0	0	0	0	0	0	0	0	0	0	0	0	0
DEVsvDCool1_Neg	0	0	0	0	0	0	0	0	0	0	0	0	0	0	0	0	0	0	0	0	0	0	0	0	0	0	0
DEVsvDCool1_Pos	0	0	0	0	0	0	0	0	0	0	0	0	0	0	0	0	0	0	0	0	0	0	0	0	0	0	0
DEVsvDCool2_Neg	0	0	0	0	0	0	0	0	0	0	0	0	0	0	0	0	0	0	0	0	0	0	0	0	0	0	0
DEVsvDCool2_Pos	0	0	0	0	1	0	0	0	0	0	0	0	0	0	0	0	0	0	0	0	0	0	0	0	0	0	0
DEVsvDFilter1_Neg	0	0	0	0	0	0	0	0	0	0	0	0	0	0	0	0	0	0	0	0	0	0	0	0	0	0	0
DEVsvDFilter2_Neg	0	0	0	0	0	0	0	0	0	0	0	0	0	0	0	0	0	0	0	0	0	0	0	0	0	0	0
DEVsvDnozzle_Neg	0	0	0	0	0	0	0	0	0	0	0	0	0	0	0	0	0	0	0	0	0	0	0	0	0	0	0
DEVsvDnozzle_Pos	0	0	0	0	0	0	0	0	0	0	0	0	0	0	0	0	0	0	0	0	0	0	0	0	0	0	0
DEVsvKfeed_Neg	0	0	0	0	0	0	0	1	1	0	0	0	0	0	0	0	0	0	0	0	0	0	0	0	0	0	0
DEVsvKineFric_Pos	0	0	0	0	1	0	1	1	0	0	0	0	0	0	0	0	0	0	0	0	0	0	0	0	0	0	0
DEVsvStic1_Pos	0	0	0	0	0	0	0	0	0	0	0	0	0	0	0	0	0	0	0	0	0	0	0	0	0	0	0
DEVsvStic2_Pos	0	0	0	0	0	0	0	0	0	0	0	0	0	0	0	0	0	0	0	0	0	0	0	0	0	0	0
DEVsvSticspool_Pos	0	1	0	0	0	0	0	1	1	0	0	1	0	0	0	0	0	0	0	0	0	0	0	0	0	0	0
DEVsvVisc1_Pos	0	0	0	0	0	0	0	0	0	0	0	0	0	0	0	0	0	0	0	0	0	0	0	0	0	0	0
DEVsvVisc2_Pos	0	0	0	0	0	0	0	0	0	0	0	0	0	0	0	0	0	0	0	0	0	0	0	0	0	0	0
DEWfmASenO_Neg	0	0	0	0	0	0	0	0	0	0	0	0	0	0	0	0	0	0	0	0	0	0	0	0	0	0	0
DEWfmASenO_Pos	0	0	0	0	0	0	0	0	0	0	0	0	0	0	0	0	0	0	0	0	0	0	0	0	0	0	0
DEWfmBSenO_Neg	0	0	0	0	0	0	0	0	0	0	0	0	0	0	0	0	0	0	0	0	0	0	0	0	0	0	0
DEWfmBSenO_Pos	0	0	0	0	0	0	0	0	0	0	0	0	0	0	0	0	0	0	0	0	0	0	0	0	0	0	0
DFmvDIlkg_Pos	0	0	0	0	0	0	0	0	0	0	0	0	0	0	0	0	0	0	0	0	0	0	0	0	0	0	0
DLppDIlkg_Pos	0	0	0	0	0	0	0	0	0	0	0	0	0	0	0	0	0	0	0	0	0	0	0	0	0	0	0
DMfpDIlkg_Pos	0	0	0	0	0	0	0	0	0	0	0	0	0	0	0	0	0	0	0	0	0	0	0	0	0	0	0
DSovDelay_Pos	0	0	0	0	0	0	0	0	0	0	0	0	0	0	0	0	0	0	0	0	0	0	0	0	0	0	0
DSovDIlkg_Pos	0	0	0	0	0	0	0	0	0	0	0	0	0	0	0	0	0	0	0	1	0	0	0	0	0	0	0
DTbvDIlkg_Pos	0	0	0	0	0	0	0	0	0	0	0	0	0	0	0	0	0	0	0	0	0	0	0	0	0	0	0
TOTAL	2	1	0	0	3	0	1	3	2	1	1	5	4	2	4	4	4	0	5	4	1	0	0	0	3	5	3

	VbvYchgB	VbvScaleB	VbvSlpLeftB	VbvSlpRightB	VbvHyst0B	VbvCEquS	VbvXchgS	VbvYchgS	VbvScaleS	VbvSlpLeftS	VbvSlpRightS	VbvHyst0S	VbvmaxX1	VbvmaxX2	VbvminX1	VbvminX2	VbvmaxGapX	VbvminGapX	VbvmeanGapX	VbvstdGapX	VbvMAErr	TOTAL
DBvvDIlkg_Pos	1	1	1	0	0	0	0	0	0	0	0	0	0	0	0	0	0	0	0	0	0	9
DEBvvK0_Neg	0	0	0	0	0	0	0	0	0	0	0	0	0	0	0	0	0	0	0	0	0	3
DEBvvStic_Pos	0	0	0	0	0	0	0	0	0	0	0	0	0	0	0	0	0	0	0	0	0	0
DEBvvVisc_Pos	0	0	0	0	0	0	0	0	0	0	0	0	0	0	0	0	0	0	0	0	0	0
DEFmvASen0_Neg	0	0	0	0	0	0	0	0	0	0	0	0	0	0	0	0	0	0	0	0	0	5
DEFmvASen0_Pos	0	0	0	0	0	0	0	0	0	0	0	0	0	0	0	0	0	0	0	0	0	8
DEFmvBSen0_Neg	0	0	0	0	0	0	0	0	0	0	0	0	0	0	0	0	0	0	0	0	0	5
DEFmvBSen0_Pos	0	0	0	0	0	0	0	0	0	0	0	0	0	0	0	0	0	0	0	0	0	8
DEFmvCnull_Neg	0	0	0	0	0	0	0	0	0	0	0	0	0	0	0	0	0	0	0	0	0	5
DEFmvCnull_Pos	0	0	0	0	0	0	0	0	0	0	0	0	0	0	0	0	0	0	0	0	0	7
DEFmvDnozzle_Pos	0	0	0	0	0	0	0	0	0	0	0	0	0	0	0	0	0	0	0	0	0	4
DEFmvStic_Pos	0	0	0	0	0	0	0	0	0	0	0	0	0	0	0	0	0	0	0	0	0	6
DEMffFlowRate_Neg	0	0	0	0	0	0	0	0	0	0	0	0	0	0	0	0	0	0	0	0	0	2
DESovStic_Pos	0	0	0	0	0	0	0	0	0	0	0	0	0	0	0	0	0	0	0	0	0	0
DESovVisc_Pos	0	0	0	0	0	0	0	0	0	0	0	0	0	0	0	0	0	0	0	0	0	0
DEVbvASen0_Neg	0	0	0	0	0	0	0	0	0	0	0	0	0	0	1	0	1	1	1	1	0	5
DEVbvASen0_Pos	0	0	0	0	1	0	0	0	0	0	0	1	1	0	1	0	1	1	1	1	1	10
DEVbvBSen0_Neg	0	0	0	0	0	0	0	0	0	0	0	0	0	0	0	1	1	1	1	1	0	5
DEVbvBSen0_Pos	0	0	0	0	1	0	0	0	0	0	0	1	0	1	0	1	1	1	1	1	1	10
DEVbvCnull_Neg	0	0	0	0	0	1	1	0	0	0	0	0	0	0	0	0	0	0	0	0	0	6
DEVbvCnull_Pos	0	0	0	0	0	1	1	0	0	0	0	0	0	0	0	0	0	0	0	0	0	6
DEVbvCorHP1_Pos	0	0	0	0	0	0	0	0	0	0	0	0	0	0	0	0	0	0	0	0	0	0
DEVbvCorHP2_Pos	0	0	0	0	0	0	0	0	0	0	0	0	0	0	0	0	0	0	0	0	0	0
DEVbvDCool1_Neg	0	0	0	0	0	0	0	0	0	0	0	0	0	0	0	0	0	0	0	0	0	0
DEVbvDCool1_Pos	0	0	0	0	0	0	0	0	0	0	0	0	0	0	0	0	0	0	0	0	0	0
DEVbvDCool2_Neg	0	0	0	0	0	1	1	1	0	0	0	0	0	0	0	0	0	0	0	0	0	5
DEVbvDCool2_Pos	0	1	1	0	0	1	1	0	1	1	0	0	0	0	0	0	0	0	0	0	0	10
DEVbvDFilter1_Neg	0	0	0	0	0	0	0	0	0	0	0	0	0	0	0	0	0	0	0	0	0	0
DEVbvDFilter2_Neg	0	0	0	0	0	0	0	0	0	0	0	0	0	0	0	0	0	0	0	0	0	0
DEVbvDnozzle_Neg	0	0	0	0	0	0	1	0	0	0	0	0	0	0	0	0	0	0	0	0	0	1
DEVbvDnozzle_Pos	0	0	0	0	0	0	0	0	0	0	0	0	0	0	0	0	0	0	0	0	0	0
DEVbvKfeed_Neg	0	0	0	0	0	0	1	0	0	0	0	0	0	0	0	0	0	0	0	0	0	1
DEVbvKineFric_Pos	0	0	0	0	0	0	0	0	0	0	0	0	0	0	0	0	0	0	0	0	0	2
DEVbvStic1_Pos	0	0	0	0	0	0	0	0	0	0	0	0	0	0	0	0	0	0	0	0	0	0
DEVbvStic2_Pos	0	0	0	0	0	0	0	0	0	0	0	0	0	0	0	0	0	0	0	0	0	0
DEVbvSticspool_Pos	1	1	0	0	1	1	0	1	1	1	0	0	0	0	0	0	0	0	0	0	0	10
DEVbvVisc1_Pos	0	0	0	0	0	0	0	0	0	0	0	0	0	0	0	0	0	0	0	0	0	0
DEVbvVisc2_Pos	0	0	0	0	0	0	0	0	0	0	0	0	0	0	0	0	0	0	0	0	0	0
DEVsvASen0_Neg	0	0	0	0	0	0	0	0	0	0	0	0	0	0	0	0	0	0	0	0	0	5
DEVsvASen0_Pos	0	0	0	0	0	0	0	0	0	0	0	0	0	0	0	0	0	0	0	0	0	7
DEVsvBSen0_Neg	0	0	0	0	0	0	0	0	0	0	0	0	0	0	0	0	0	0	0	0	0	6
DEVsvBSen0_Pos	0	0	0	0	0	0	0	0	0	0	0	0	0	0	0	0	0	0	0	0	0	6
DEVsvCnull_Neg	0	0	0	0	0	0	0	0	0	0	0	0	0	0	0	0	0	0	0	0	0	11
DEVsvCnull_Pos	0	0	0	0	0	0	0	0	0	0	0	0	0	0	0	0	0	0	0	0	0	6
DEVsvCorHP1_Pos	0	0	0	0	0	0	0	0	0	0	0	0	0	0	0	0	0	0	0	0	0	0
DEVsvCorHP2_Pos	0	0	0	0	0	0	0	0	0	0	0	0	0	0	0	0	0	0	0	0	0	0
DEVsvDCool1_Neg	0	0	0	0	0	0	0	0	0	0	0	0	0	0	0	0	0	0	0	0	0	0
DEVsvDCool1_Pos	0	0	0	0	0	0	0	0	0	0	0	0	0	0	0	0	0	0	0	0	0	0
DEVsvDCool2_Neg	0	0	0	0	0	0	0	0	0	0	0	0	0	0	0	0	0	0	0	0	0	7
DEVsvDCool2_Pos	0	0	0	0	0	0	0	0	0	0	0	0	0	0	0	0	0	0	0	0	0	13
DEVsvDFilter1_Neg	0	0	0	0	0	0	0	0	0	0	0	0	0	0	0	0	0	0	0	0	0	0
DEVsvDFilter2_Neg	0	0	0	0	0	0	0	0	0	0	0	0	0	0	0	0	0	0	0	0	0	0
DEVsvDnozzle_Neg	0	0	0	0	0	0	0	0	0	0	0	0	0	0	0	0	0	0	0	0	0	0
DEVsvDnozzle_Pos	0	0	0	0	0	0	0	0	0	0	0	0	0	0	0	0	0	0	0	0	0	0
DEVsvKfeed_Neg	0	0	0	0	0	0	0	0	0	0	0	0	0	0	0	0	0	0	0	0	0	10
DEVsvKineFric_Pos	0	0	0	0	0	0	0	0	0	0	0	0	0	0	0	0	0	0	0	0	0	16
DEVsvStic1_Pos	0	0	0	0	0	0	0	0	0	0	0	0	0	0	0	0	0	0	0	0	0	0
DEVsvStic2_Pos	0	0	0	0	0	0	0	0	0	0	0	0	0	0	0	0	0	0	0	0	0	0
DEVsvSticspool_Pos	0	0	0	0	0	0	0	0	0	0	0	0	0	0	0	0	0	0	0	0	0	18
DEVsvVisc1_Pos	0	0	0	0	0	0	0	0	0	0	0	0	0	0	0	0	0	0	0	0	0	0
DEVsvVisc2_Pos	0	0	0	0	0	0	0	0	0	0	0	0	0	0	0	0	0	0	0	0	0	0
DEWfmASen0_Neg	0	0	0	0	0	0	0	0	0	0	0	0	0	0	0	0	0	0	0	0	0	4
DEWfmASen0_Pos	0	0	0	0	0	0	0	0	0	0	0	0	0	0	0	0	0	0	0	0	0	4
DEWfmBSen0_Neg	0	0	0	0	0	0	0	0	0	0	0	0	0	0	0	0	0	0	0	0	0	4
DEWfmBSen0_Pos	0	0	0	0	0	0	0	0	0	0	0	0	0	0	0	0	0	0	0	0	0	4
DFmvDIlkg_Pos	0	0	0	0	0	0	0	0	0	0	0	0	0	0	0	0	0	0	0	0	0	13
DLppDIlkg_Pos	0	0	0	0	0	0	0	0	0	0	0	0	0	0	0	0	0	0	0	0	0	0
DMfpDIlkg_Pos	0	0	0	0	0	0	0	0	0	0	0	0	0	0	0	0	0	0	0	0	0	0
DSovDelay_Pos	0	0	0	0	0	0	0	0	0	0	0	0	0	0	0	0	0	0	0	0	0	1
DSovDIlkg_Pos	0	0	0	0	0	0	0	1	0	1	0	0	0	0	0	0	0	0	0	0	0	7
DTbvDIlkg_Pos	0	0	0	0	0	0	0	0	0	0	0	0	0	0	0	0	0	0	0	0	0	0
TOTAL	2	3	2	0	3	5	6	3	2	3	0	2	1	1	2	2	4	4	4	4	2	

Table A.21 *Detection NKPIs for the set of raw health indicators.*

Appendix XXV. Identification NKPIs for the raw set of HIs

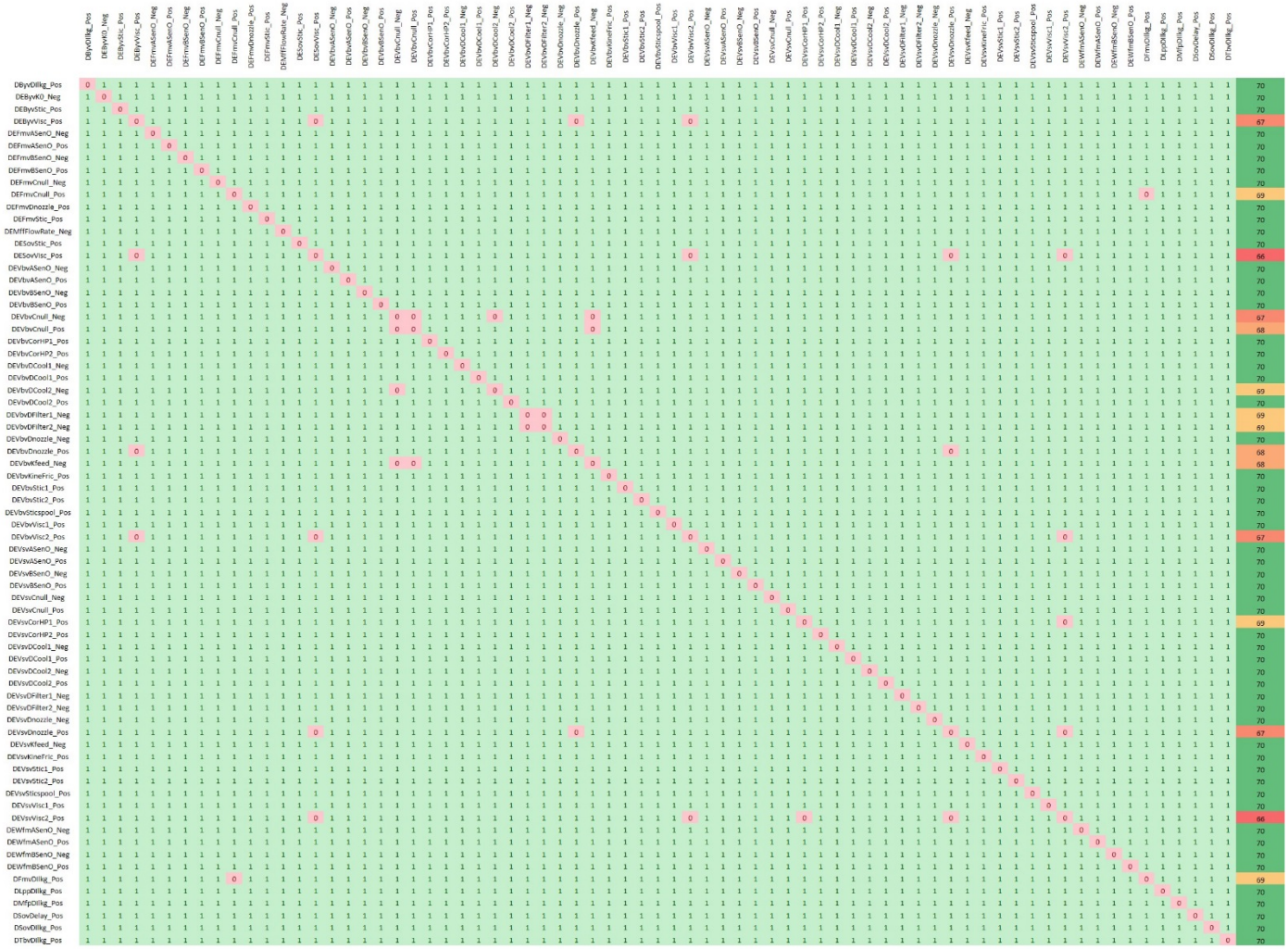


Table A.22 *Identification NKPIs for the set of raw health indicators.*

Appendix XXVI. Localization NKPIs for the raw set of HIs

	Pumping Unit	Fuel Filter	ACU	FMU	VSV Actuation	VBV Actuation	TBV Actuation	Flowmeter	TOTAL
Pumping Unit	0	1	1	1	1	1	1	1	7
Fuel Filter	1	0	1	1	1	1	1	1	7
ACU	1	1	0	0	0	0	0	1	3
FMU	1	1	0	0	0	0	0	1	3
VSV Actuation	1	1	0	0	0	0	0	1	3
VBV Actuation	1	1	0	0	0	0	1	1	4
TBV Actuation	1	1	0	0	0	1	0	1	4
Flowmeter	1	1	1	1	1	1	1	0	7

Table A.23 *Localization NKPIs for the set of raw health indicators.*

Appendix XXVII. Prognostics NKPIs for the raw set of HIs

	DeltaD	DeltaI	DeltaL
DByvDIlkg_Pos	0,23	0	0
DEByvK0_Neg	17,61	0	0
DEByvStic_Pos	0	0	0
DEByvVisc_Pos	0	0	0
DEFmvASenO_Neg	0,75	0,75	0
DEFmvASenO_Pos	0,75	0,75	0
DEFmvBSenO_Neg	0,75	0,75	0
DEFmvBSenO_Pos	0,75	0,75	0
DEFmvCnull_Neg	0	0	0
DEFmvCnull_Pos	17,23	17,23	0
DEFmvDnozzle_Pos	0	0	0
DEFmvStic_Pos	23,98	0	0
DEMffFlowRate_Neg	∞	∞	0
DESovStic_Pos	0	0	0
DESovVisc_Pos	0	0	0
DEVbvASenO_Neg	0	0	0
DEVbvASenO_Pos	0,95	0,95	0
DEVbvBSenO_Neg	0	0	0
DEVbvBSenO_Pos	0,95	0,95	0
DEVbvCnull_Neg	∞	∞	0
DEVbvCnull_Pos	13,43	13,43	0
DEVbvCorHP1_Pos	0	0	0
DEVbvCorHP2_Pos	0	0,021	0
DEVbvDCool1_Neg	0	∞	0
DEVbvDCool1_Pos	0	0	0
DEVbvDCool2_Neg	∞	∞	0
DEVbvDCool2_Pos	1,85	0	0
DEVbvDFilter1_Neg	0	∞	0
DEVbvDFilter2_Neg	0	∞	0
DEVbvDnozzle_Neg	∞	∞	0
DEVbvDnozzle_Pos	0	0	0
DEVbvKfeed_Neg	∞	∞	0
DEVbvKineFric_Pos	0	0	0
DEVbvStic1_Pos	0	0	0
DEVbvStic2_Pos	0	0	0
DEVbvSticspool_Pos	0	0	0
DEVbvVisc1_Pos	0	0	0
DEVbvVisc2_Pos	0	0	0
DEVsvASenO_Neg	0	0	0
DEVsvASenO_Pos	0	0	0
DEVsvBSenO_Neg	0	0	0
DEVsvBSenO_Pos	0	0	0
DEVsvCnull_Neg	∞	∞	0
DEVsvCnull_Pos	12,97	12,97	0
DEVsvCorHP1_Pos	0	0	0
DEVsvCorHP2_Pos	0	0	0
DEVsvDCool1_Neg	0	∞	0
DEVsvDCool1_Pos	0	0	0
DEVsvDCool2_Neg	∞	∞	0
DEVsvDCool2_Pos	0	0	0
DEVsvDFilter1_Neg	0	∞	0
DEVsvDFilter2_Neg	0	∞	0
DEVsvDnozzle_Neg	0	∞	0
DEVsvDnozzle_Pos	0	0	0
DEVsvKfeed_Neg	∞	∞	0
DEVsvKineFric_Pos	0	0	0
DEVsvStic1_Pos	0	0	0
DEVsvStic2_Pos	0	0	0
DEVsvSticspool_Pos	0	0	0
DEVsvVisc1_Pos	0	0	0
DEVsvVisc2_Pos	0	0	0
DEWfmASenO_Neg	∞	∞	0
DEWfmASenO_Pos	0	0	0
DEWfmBSenO_Neg	∞	∞	0
DEWfmBSenO_Pos	0	0	0
DFmvDIlkg_Pos	0,25	0,25	0
DLppDIlkg_Pos	0	0	0
DMfpDIlkg_Pos	0	0	0
DSovDelay_Pos	0	0	0
DSovDIlkg_Pos	0,078	0	0
DTbvDIlkg_Pos	0	0	0

Appendix XXVIII. List of Sobol indices of order 1

	$FmvCEquA$	$FmvScaleA$	$FmvSlpA$	$FmvHyst0A$	$FmvCEquB$	$FmvScaleB$	$FmvSlpB$	$FmvHyst0B$	$FmvCEquS$	$FmvScaleS$	$FmvSlpS$	$FmvHyst0S$	$FmvmaxX1$	$FmvmaxX2$	$FmvminX1$	$FmvminX2$	$FmvmaxGapX$	$FmvminGapX$	$FmvmeanGapX$	$FmvstdGapX$
$CTfuel$	0,02	0,01	0,02	0,01	0,01	0,01	0,03	0,01	0,02	0,01	0,00	0,01	0,00	0,00	0,00	0,00	0,00	0,00	0,00	0,01
$DLppDIlkg$	0,00	0,01	0,01	0,00	0,00	0,01	0,01	0,00	0,00	0,01	0,02	0,01	0,00	0,00	0,00	0,00	0,00	0,00	0,00	0,00
$DMfpDIlkg$	0,00	0,01	0,01	0,00	0,00	0,01	0,00	0,00	0,01	0,01	0,01	0,00	0,00	0,00	0,00	0,00	0,00	0,00	0,00	0,00
$DEMffFlowRate$	0,00	0,03	0,02	0,01	0,00	0,02	0,01	0,01	0,00	0,03	0,00	0,02	0,01	0,00	0,00	0,00	0,00	0,00	0,00	0,00
$ETbvPopen$	0,00	0,01	0,01	0,00	0,00	0,01	0,01	0,00	0,01	0,01	0,00	0,00	0,01	0,01	0,00	0,00	0,00	0,00	0,00	0,00
$DTbvDIlkg$	0,00	0,01	0,03	0,00	0,00	0,01	0,02	0,00	0,00	0,00	0,02	0,00	0,00	0,00	0,00	0,00	0,00	0,00	0,00	0,00
$DEWfmASenO$	0,00	0,01	0,00	0,00	0,00	0,01	0,00	0,00	0,00	0,01	0,00	0,00	0,01	0,00	0,00	0,00	0,00	0,00	0,00	0,00
$DEWfmBSenO$	0,00	0,01	0,03	0,00	0,00	0,00	0,03	0,00	0,00	0,01	0,02	0,00	0,00	0,00	0,00	0,00	0,00	0,00	0,00	0,00
$EByvDPist0$	0,02	0,05	0,03	0,02	0,02	0,04	0,03	0,03	0,02	0,06	0,02	0,03	0,01	0,01	0,00	0,00	0,00	0,00	0,00	0,00
$DEByvK0$	0,05	0,01	0,01	0,00	0,03	0,01	0,01	0,00	0,02	0,01	0,01	0,00	0,01	0,02	0,00	0,00	0,00	0,00	0,00	0,00
$DEByvVisc$	0,01	0,01	0,01	0,00	0,00	0,01	0,01	0,00	0,00	0,01	0,01	0,00	0,01	0,00	0,00	0,00	0,00	0,00	0,00	0,00
$DEByvStic$	0,00	0,02	0,04	0,00	0,00	0,01	0,06	0,00	0,00	0,01	0,08	0,00	0,00	0,00	0,00	0,00	0,00	0,00	0,00	0,00
$DByvDIlkg$	0,09	0,04	0,00	0,00	0,07	0,03	0,00	0,01	0,07	0,05	0,01	0,01	0,01	0,01	0,00	0,00	0,00	0,00	0,00	0,00
$ESovDPist$	0,01	0,01	0,02	0,00	0,01	0,00	0,02	0,00	0,01	0,01	0,02	0,00	0,00	0,00	0,00	0,00	0,00	0,00	0,00	0,00
$DESovVisc$	0,01	0,00	0,02	0,00	0,00	0,00	0,02	0,00	0,01	0,01	0,01	0,00	0,00	0,00	0,00	0,00	0,00	0,00	0,00	0,00
$DESovStic$	0,01	0,01	0,03	0,00	0,01	0,00	0,04	0,00	0,00	0,01	0,02	0,00	0,01	0,00	0,00	0,00	0,00	0,00	0,00	0,00
$DSovDIlkg$	0,00	0,02	0,01	0,01	0,00	0,02	0,00	0,01	0,00	0,01	0,00	0,01	0,00	0,00	0,00	0,00	0,00	0,00	0,00	0,00
$DSovDelay$	0,01	0,01	0,00	0,01	0,01	0,01	0,00	0,01	0,01	0,01	0,00	0,01	0,00	0,00	0,00	0,00	0,00	0,00	0,00	0,00
$DEFmvStic$	0,01	0,26	0,09	0,19	0,01	0,28	0,09	0,18	0,01	0,24	0,16	0,17	0,00	0,00	0,00	0,00	0,00	0,00	0,00	0,00
$DEFmvCnull$	0,20	0,01	0,01	0,00	0,26	0,00	0,01	0,00	0,23	0,01	0,01	0,00	0,07	0,08	0,00	0,00	0,00	0,00	0,00	0,00
$DEFmvDnozzle$	0,07	0,10	0,12	0,00	0,06	0,04	0,06	0,00	0,04	0,10	0,02	0,00	0,00	0,01	0,00	0,00	0,00	0,00	0,00	0,00
$DEFmvASenO$	0,00	0,01	0,00	0,16	0,00	0,04	0,00	0,15	0,00	0,01	0,01	0,15	0,23	0,28	0,98	0,00	0,49	0,49	0,50	0,44
$DEFmvBSenO$	0,00	0,01	0,00	0,16	0,00	0,00	0,00	0,15	0,00	0,01	0,01	0,14	0,24	0,26	0,00	0,99	0,49	0,49	0,50	0,41
$DFmvDIlkg$	0,31	0,09	0,15	0,29	0,34	0,15	0,16	0,28	0,38	0,10	0,26	0,27	0,22	0,21	0,00	0,00	0,00	0,00	0,00	0,01
$DEVsvStic1$	0,00	0,02	0,01	0,00	0,00	0,01	0,02	0,00	0,00	0,02	0,01	0,01	0,01	0,00	0,00	0,00	0,00	0,00	0,00	0,00
$DEVsvVisc1$	0,00	0,01	0,01	0,00	0,00	0,01	0,01	0,00	0,00	0,01	0,00	0,00	0,00	0,00	0,00	0,00	0,00	0,00	0,00	0,00
$DEVsvStic2$	0,00	0,00	0,01	0,00	0,00	0,01	0,01	0,00	0,00	0,00	0,00	0,00	0,00	0,00	0,00	0,00	0,00	0,00	0,00	0,00
$DEVsvVisc2$	0,00	0,00	0,01	0,00	0,01	0,00	0,01	0,00	0,00	0,00	0,01	0,00	0,00	0,00	0,00	0,00	0,00	0,00	0,00	0,01
$DEVsvDCool1$	0,00	0,00	0,00	0,00	0,00	0,00	0,00	0,00	0,00	0,00	0,00	0,00	0,00	0,00	0,00	0,00	0,00	0,00	0,00	0,00
$DEVsvDCool2$	0,00	0,01	0,00	0,00	0,00	0,00	0,00	0,00	0,00	0,00	0,00	0,00	0,00	0,00	0,00	0,00	0,00	0,00	0,00	0,00
$DEVsvKineFric$	0,01	0,01	0,00	0,00	0,01	0,01	0,01	0,00	0,01	0,01	0,02	0,00	0,00	0,00	0,00	0,00	0,00	0,00	0,00	0,00
$DEVsvCnull$	0,01	0,01	0,01	0,00	0,01	0,00	0,01	0,00	0,02	0,02	0,01	0,00	0,00	0,00	0,00	0,00	0,00	0,00	0,00	0,00
$DEVsvDnozzle$	0,01	0,01	0,01	0,00	0,01	0,01	0,01	0,00	0,01	0,00	0,01	0,01	0,00	0,00	0,00	0,00	0,00	0,00	0,00	0,00
$DEVsvKfeed$	0,01	0,02	0,01	0,00	0,01	0,02	0,01	0,00	0,00	0,03	0,00	0,00	0,01	0,00	0,00	0,00	0,00	0,00	0,00	0,01
$DEVsvSticspool$	0,01	0,00	0,01	0,00	0,00	0,00	0,01	0,00	0,01	0,00	0,01	0,00	0,00	0,00	0,00	0,00	0,00	0,00	0,00	0,00
$DEVsvDFilter1$	0,01	0,02	0,01	0,00	0,00	0,01	0,00	0,00	0,01	0,02	0,01	0,00	0,00	0,00	0,00	0,00	0,00	0,00	0,00	0,00
$DEVsvDFilter2$	0,01	0,01	0,01	0,00	0,01	0,00	0,01	0,00	0,01	0,01	0,01	0,00	0,01	0,00	0,00	0,00	0,00	0,00	0,00	0,00
$DEVsvCorHP1$	0,00	0,01	0,01	0,00	0,00	0,01	0,01	0,00	0,01	0,01	0,01	0,00	0,01	0,00	0,00	0,00	0,00	0,00	0,00	0,00
$DEVsvCorHP2$	0,01	0,00	0,02	0,00	0,00	0,00	0,01	0,00	0,01	0,01	0,01	0,00	0,00	0,00	0,00	0,00	0,00	0,00	0,00	0,00
$DEVsvASenO$	0,00	0,01	0,01	0,00	0,00	0,00	0,01	0,00	0,00	0,00	0,01	0,00	0,01	0,00	0,00	0,00	0,00	0,00	0,00	0,00
$DEVsvBSenO$	0,00	0,00	0,00	0,00	0,00	0,00	0,00	0,00	0,00	0,00	0,00	0,00	0,01	0,00	0,00	0,00	0,00	0,00	0,00	0,00
$DEVbvStic1$	0,00	0,00	0,01	0,01	0,00	0,00	0,01	0,01	0,00	0,00	0,00	0,01	0,00	0,00	0,00	0,00	0,00	0,00	0,00	0,00
$DEVbvVisc1$	0,00	0,01	0,01	0,00	0,00	0,01	0,02	0,00	0,00	0,01	0,02	0,00	0,01	0,00	0,00	0,00	0,00	0,00	0,00	0,01
$DEVbvStic2$	0,01	0,00	0,01	0,00	0,00	0,00	0,01	0,00	0,00	0,01	0,01	0,00	0,00	0,00	0,00	0,00	0,00	0,00	0,00	0,00
$DEVbvVisc2$	0,01	0,01	0,01	0,00	0,01	0,00	0,01	0,00	0,01	0,01	0,00	0,00	0,00	0,00	0,00	0,00	0,00	0,00	0,00	0,00
$DEVbvDCool1$	0,00	0,01	0,01	0,00	0,00	0,00	0,00	0,00	0,00	0,01	0,00	0,00	0,00	0,00	0,00	0,00	0,00	0,00	0,00	0,00
$DEVbvDCool2$	0,00	0,03	0,00	0,00	0,00	0,02	0,00	0,00	0,00	0,02	0,00	0,00	0,00	0,00	0,00	0,00	0,00	0,00	0,00	0,00
$DEVbvKineFric$	0,01	0,00	0,01	0,00	0,01	0,00	0,02	0,01	0,01	0,00	0,04	0,02	0,01	0,00	0,00	0,00	0,00	0,00	0,00	0,00
$DEVbvCnull$	0,00	0,01	0,02	0,00	0,00	0,01	0,02	0,01	0,00	0,01	0,01	0,01	0,00	0,00	0,00	0,00	0,00	0,00	0,00	0,00
$DEVbvDnozzle$	0,00	0,01	0,02	0,00	0,00	0,01	0,02	0,01	0,00	0,01	0,00	0,01	0,00	0,00	0,00	0,00	0,00	0,00	0,00	0,00
$DEVbvKfeed$	0,00	0,01	0,01	0,00	0,00	0,01	0,01	0,00	0,00	0,02	0,00	0,00	0,00	0,00	0,00	0,00	0,00	0,00	0,00	0,00
$DEVbvSticspool$	0,01	0,00	0,01	0,01	0,00	0,00	0,01	0,01	0,00	0,00	0,00	0,01	0,00	0,00	0,00	0,00	0,00	0,00	0,00	0,00
$DEVbvDFilter1$	0,00	0,00	0,02	0,01	0,01	0,01	0,02	0,01	0,00	0,00	0,02	0,01	0,00	0,00	0,00	0,00	0,00	0,00	0,00	0,00
$DEVbvDFilter2$	0,00	0,01	0,01	0,01	0,00	0,01	0,01	0,01	0,00	0,01	0,01	0,01	0,01	0,00	0,00	0,00	0,00	0,00	0,00	0,00
$DEVbvCorHP1$	0,00	0,00	0,02	0,00	0,00	0,01	0,03	0,00	0,01	0,00	0,01	0,00	0,00	0,00	0,00	0,00	0,00	0,00	0,00	0,00
$DEVbvCorHP2$	0,00	0,00	0,01	0,00	0,00	0,00	0,01	0,00	0,00	0,00	0,00	0,00	0,01	0,00	0,00	0,00	0,00	0,00	0,00	0,00
$DEVbvASenO$	0,00	0,01	0,01	0,00	0,00	0,01	0,00	0,00	0,00	0,01	0,01	0,00	0,00	0,00	0,00	0,00	0,00	0,00	0,00	0,00
$DEVbvBSenO$	0,00	0,02	0,00	0,00	0,00	0,07	0,00	0,00	0,00	0,01	0,00	0,00	0,00	0,00	0,00	0,00	0,00	0,00	0,00	0,00
$EStaLaw$	0,01	0,00	0,02	0,01	0,00	0,00	0,02	0,01	0,01	0,00	0,02	0,01	0,01	0,00	0,00	0,00	0,00	0,00	0,00	0,00

	FmvMAErr	Sovdelop1	Sovdelclo	Sovdelop2	VoN2maxSOV	SOVoN2max	SOVoN2mean	VoN2maxBYV	BYVoN2max	BYVoN2mean	LppSlpN2DP	LppR2N2DP	wTBV	wSOV	MfpSlpN2DP	MfpR2N2DP	MffSlpN2DP	MffR2N2DP	WfmmaxX1	WfmmaxX2
CTfuel	0,01	0,03	0,00	0,02	0,00	0,00	0,01	0,00	0,00	0,02	0,04	0,02	0,01	0,03	0,03	0,02	0,01	0,03	0,01	0,01
DLppDIlkg	0,00	0,00	0,00	0,00	0,00	0,00	0,01	0,01	0,00	0,01	0,01	0,02	0,00	0,00	0,00	0,00	0,00	0,02	0,00	0,00
DMfpDIlkg	0,00	0,00	0,00	0,00	0,02	0,02	0,01	0,09	0,14	0,03	0,02	0,02	0,02	0,01	0,00	0,00	0,00	0,01	0,00	0,00
DEMffFlowRate	0,00	0,03	0,00	0,02	0,01	0,00	0,01	0,01	0,00	0,00	0,02	0,02	0,00	0,00	0,48	0,13	0,88	0,16	0,00	0,00
ETbvPopen	0,00	0,01	0,00	0,01	0,02	0,04	0,01	0,16	0,14	0,00	0,01	0,01	0,11	0,00	0,01	0,01	0,00	0,01	0,00	0,00
DTbvDIlkg	0,00	0,01	0,02	0,02	0,00	0,00	0,01	0,01	0,03	0,01	0,02	0,01	0,02	0,01	0,00	0,01	0,00	0,01	0,01	0,01
DEWfmASenO	0,00	0,02	0,00	0,02	0,00	0,00	0,01	0,01	0,00	0,01	0,02	0,02	0,01	0,01	0,01	0,02	0,01	0,03	0,00	0,00
DEWfmBSenO	0,00	0,02	0,00	0,02	0,01	0,00	0,01	0,01	0,01	0,00	0,01	0,04	0,02	0,01	0,01	0,00	0,00	0,01	0,01	0,01
EByvDPist0	0,04	0,02	0,02	0,03	0,03	0,00	0,01	0,04	0,00	0,04	0,02	0,02	0,01	0,01	0,01	0,04	0,00	0,02	0,00	0,00
DEByvK0	0,06	0,02	0,00	0,05	0,08	0,02	0,04	0,06	0,04	0,03	0,00	0,00	0,06	0,01	0,01	0,02	0,00	0,01	0,03	0,03
DEByvVisc	0,00	0,01	0,00	0,01	0,04	0,00	0,01	0,06	0,00	0,01	0,02	0,02	0,01	0,00	0,00	0,00	0,00	0,02	0,00	0,00
DEByvStic	0,00	0,00	0,01	0,01	0,04	0,06	0,01	0,11	0,15	0,02	0,02	0,02	0,04	0,00	0,01	0,06	0,00	0,02	0,00	0,00
DByvDIlkg	0,06	0,01	0,02	0,01	0,01	0,14	0,04	0,02	0,31	0,18	0,02	0,01	0,09	0,02	0,02	0,01	0,00	0,01	0,09	0,09
ESovDPist	0,01	0,01	0,00	0,01	0,00	0,00	0,01	0,00	0,00	0,03	0,01	0,02	0,00	0,01	0,07	0,08	0,00	0,02	0,00	0,00
DESovVisc	0,00	0,01	0,01	0,01	0,02	0,00	0,01	0,02	0,00	0,00	0,03	0,02	0,02	0,00	0,00	0,01	0,00	0,01	0,00	0,00
DESovStic	0,00	0,03	0,00	0,03	0,00	0,00	0,01	0,00	0,01	0,01	0,02	0,00	0,00	0,02	0,00	0,26	0,00	0,00	0,01	0,01
DSovDIlkg	0,00	0,14	0,10	0,11	0,10	0,54	0,02	0,13	0,01	0,07	0,01	0,01	0,27	0,54	0,08	0,02	0,00	0,02	0,00	0,00
DSovDelay	0,01	0,01	0,58	0,01	0,25	0,13	0,01	0,01	0,00	0,01	0,02	0,01	0,02	0,01	0,01	0,01	0,00	0,02	0,00	0,00
DEFmvStic	0,01	0,01	0,00	0,00	0,00	0,00	0,00	0,00	0,00	0,03	0,04	0,04	0,02	0,01	0,00	0,00	0,00	0,01	0,02	0,01
DEFmvCnull	0,12	0,02	0,00	0,01	0,00	0,00	0,08	0,00	0,01	0,03	0,01	0,00	0,01	0,01	0,01	0,01	0,00	0,02	0,06	0,06
DEFmvDnozzle	0,07	0,04	0,00	0,07	0,00	0,00	0,01	0,01	0,00	0,01	0,02	0,03	0,02	0,03	0,01	0,01	0,00	0,02	0,00	0,00
DEFmvASenO	0,00	0,00	0,01	0,00	0,01	0,00	0,16	0,00	0,00	0,07	0,01	0,01	0,01	0,00	0,01	0,01	0,00	0,01	0,27	0,27
DEFmvBSenO	0,00	0,00	0,00	0,00	0,00	0,00	0,13	0,00	0,00	0,12	0,03	0,02	0,01	0,00	0,00	0,00	0,00	0,02	0,26	0,26
DFmvDIlkg	0,47	0,07	0,00	0,07	0,00	0,00	0,08	0,00	0,01	0,03	0,02	0,02	0,01	0,01	0,01	0,02	0,00	0,02	0,12	0,12
DEVsvStic1	0,00	0,00	0,00	0,01	0,00	0,00	0,01	0,00	0,00	0,01	0,02	0,00	0,00	0,00	0,01	0,01	0,00	0,00	0,00	0,00
DEVsvVisc1	0,00	0,02	0,00	0,02	0,00	0,00	0,01	0,00	0,00	0,01	0,01	0,01	0,02	0,00	0,01	0,01	0,00	0,01	0,00	0,00
DEVsvStic2	0,00	0,02	0,00	0,01	0,00	0,00	0,01	0,00	0,01	0,01	0,02	0,03	0,00	0,01	0,01	0,01	0,00	0,02	0,00	0,00
DEVsvVisc2	0,00	0,05	0,00	0,05	0,01	0,00	0,01	0,00	0,00	0,01	0,02	0,03	0,00	0,01	0,01	0,01	0,00	0,01	0,00	0,00
DEVsvDCool1	0,00	0,00	0,00	0,00	0,00	0,00	0,01	0,00	0,00	0,01	0,02	0,02	0,00	0,00	0,00	0,00	0,00	0,01	0,00	0,00
DEVsvDCool2	0,01	0,01	0,00	0,01	0,04	0,00	0,01	0,00	0,01	0,00	0,02	0,00	0,01	0,00	0,00	0,00	0,00	0,01	0,00	0,00
DEVsvKineFric	0,00	0,00	0,01	0,00	0,00	0,00	0,01	0,01	0,00	0,01	0,02	0,02	0,00	0,00	0,01	0,01	0,00	0,01	0,00	0,00
DEVsvCnull	0,01	0,02	0,00	0,02	0,00	0,00	0,01	0,00	0,01	0,01	0,02	0,02	0,00	0,01	0,00	0,01	0,00	0,02	0,00	0,00
DEVsvDnozzle	0,01	0,02	0,00	0,02	0,00	0,00	0,01	0,00	0,00	0,00	0,01	0,03	0,00	0,01	0,01	0,01	0,00	0,02	0,00	0,00
DEVsvKfeed	0,00	0,01	0,00	0,01	0,00	0,00	0,01	0,01	0,00	0,00	0,02	0,03	0,01	0,00	0,01	0,03	0,00	0,02	0,00	0,00
DEVsvSticspool	0,01	0,03	0,00	0,03	0,10	0,00	0,01	0,01	0,00	0,01	0,01	0,01	0,00	0,01	0,00	0,01	0,00	0,02	0,00	0,00
DEVsvDFilter1	0,00	0,02	0,00	0,01	0,00	0,00	0,01	0,00	0,00	0,01	0,02	0,02	0,01	0,01	0,00	0,00	0,00	0,01	0,00	0,00
DEVsvDFilter2	0,01	0,01	0,00	0,02	0,00	0,00	0,01	0,00	0,00	0,01	0,02	0,02	0,00	0,01	0,00	0,00	0,00	0,01	0,00	0,00
DEVsvCorHP1	0,00	0,01	0,00	0,01	0,00	0,00	0,01	0,00	0,00	0,00	0,02	0,02	0,00	0,01	0,02	0,01	0,00	0,01	0,00	0,00
DEVsvCorHP2	0,00	0,02	0,01	0,01	0,00	0,00	0,01	0,01	0,00	0,00	0,01	0,01	0,00	0,01	0,00	0,01	0,00	0,00	0,00	0,00
DEVsvASenO	0,00	0,01	0,00	0,01	0,04	0,00	0,01	0,01	0,01	0,01	0,02	0,01	0,01	0,00	0,00	0,00	0,00	0,01	0,01	0,01
DEVsvBSenO	0,00	0,00	0,00	0,00	0,06	0,00	0,01	0,00	0,00	0,01	0,02	0,03	0,01	0,00	0,00	0,00	0,00	0,01	0,00	0,00
DEVbvStic1	0,00	0,03	0,01	0,02	0,00	0,00	0,01	0,00	0,00	0,01	0,01	0,01	0,00	0,01	0,00	0,00	0,00	0,00	0,00	0,00
DEVbvVisc1	0,00	0,00	0,01	0,01	0,00	0,00	0,01	0,01	0,00	0,00	0,01	0,02	0,01	0,00	0,01	0,01	0,00	0,02	0,00	0,00
DEVbvStic2	0,00	0,01	0,00	0,01	0,00	0,00	0,01	0,01	0,01	0,01	0,02	0,01	0,00	0,01	0,02	0,01	0,01	0,02	0,00	0,00
DEVbvVisc2	0,00	0,02	0,00	0,03	0,00	0,00	0,01	0,01	0,01	0,01	0,02	0,01	0,00	0,01	0,00	0,00	0,00	0,01	0,00	0,00
DEVbvDCool1	0,00	0,00	0,00	0,00	0,00	0,00	0,01	0,00	0,00	0,01	0,01	0,01	0,01	0,00	0,00	0,01	0,00	0,01	0,00	0,00
DEVbvDCool2	0,00	0,00	0,00	0,00	0,00	0,00	0,01	0,00	0,00	0,01	0,02	0,02	0,00	0,00	0,00	0,00	0,00	0,01	0,00	0,00
DEVbvKineFric	0,00	0,01	0,00	0,01	0,01	0,00	0,01	0,02	0,01	0,00	0,01	0,01	0,02	0,01	0,00	0,02	0,00	0,01	0,01	0,00
DEVbvCnull	0,00	0,04	0,01	0,04	0,00	0,00	0,01	0,00	0,00	0,01	0,02	0,01	0,00	0,02	0,00	0,01	0,00	0,04	0,00	0,00
DEVbvDnozzle	0,00	0,01	0,01	0,01	0,00	0,00	0,01	0,01	0,00	0,00	0,01	0,01	0,01	0,01	0,01	0,02	0,00	0,02	0,00	0,00
DEVbvKfeed	0,00	0,01	0,00	0,01	0,01	0,00	0,01	0,00	0,00	0,01	0,01	0,02	0,00	0,01	0,01	0,01	0,00	0,02	0,00	0,00
DEVbvSticspool	0,01	0,01	0,00	0,01	0,00	0,00	0,01	0,01	0,00	0,01	0,02	0,03	0,00	0,01	0,00	0,01	0,00	0,00	0,00	0,00
DEVbvDFilter1	0,00	0,01	0,00	0,01	0,00	0,00	0,01	0,00	0,00	0,01	0,02	0,02	0,01	0,00	0,00	0,00	0,00	0,02	0,00	0,00
DEVbvDFilter2	0,00	0,01	0,00	0,01	0,00	0,00	0,01	0,01	0,00	0,00	0,02	0,02	0,01	0,01	0,00	0,00	0,00	0,01	0,00	0,00
DEVbvCorHP1	0,00	0,04	0,01	0,04	0,00	0,00	0,01	0,04	0,00	0,01	0,02	0,01	0,03	0,01	0,01	0,01	0,00	0,02	0,00	0,00
DEVbvCorHP2	0,00	0,02	0,03	0,01	0,00	0,00	0,01	0,01	0,00	0,01	0,02	0,02	0,00	0,01	0,01	0,01	0,00	0,01	0,00	0,00
DEVbvASenO	0,00	0,00	0,00	0,00	0,00	0,00	0,01	0,00	0,00	0,01	0,02	0,02	0,00	0,00	0,00	0,01	0,00	0,01	0,00	0,00
DEVbvBSenO	0,00	0,00	0,00	0,00	0,00	0,00	0,01	0,02	0,00	0,01	0,01	0,02	0,00	0,00	0,00	0,00	0,00	0,01	0,00	0,00
EStaLaw	0,00	0,02	0,08	0,02	0,02	0,03	0,01	0,01	0,02	0,00	0,01	0,01	0,00	0,01	0,01	0,01	0,00	0,01	0,00	0,00

	$Wfmmin X1$	$Wfmmin X2$	$Wfmmax GapX$	$Wfmmin GapX$	$Wfmmean GapX$	$Wfmstd GapX$	$VsvCEquA$	$VsvXnullA$	$VsvYnullA$	$VsvXoverlapA$	$VsvYoverlapA$	$VsvScaleA$	$VsvSlpLeftA$	$VsvSlpNullA$	$VsvSlpRightA$	$VsvHyst0A$	$VsvCEquB$	$VsvXnullB$	$VsvYnullB$	$VsvXoverlapB$
$CTfuel$	0,00	0,00	0,00	0,00	0,00	0,00	0,00	0,00	0,00	0,01	0,00	0,01	0,00	0,00	0,00	0,01	0,00	0,00	0,00	0,01
$DLppDIlkg$	0,00	0,00	0,00	0,00	0,00	0,01	0,00	0,00	0,00	0,01	0,02	0,01	0,00	0,00	0,00	0,02	0,00	0,00	0,00	0,02
$DMfpDIlkg$	0,00	0,00	0,00	0,00	0,00	0,00	0,00	0,01	0,01	0,03	0,00	0,01	0,02	0,00	0,00	0,02	0,00	0,01	0,00	0,01
$DEMffFlowRate$	0,00	0,00	0,00	0,00	0,00	0,00	0,00	0,01	0,00	0,02	0,01	0,01	0,00	0,00	0,00	0,02	0,00	0,01	0,00	0,02
$ETbvPopen$	0,00	0,00	0,00	0,00	0,00	0,01	0,00	0,00	0,00	0,01	0,01	0,00	0,01	0,00	0,00	0,01	0,00	0,00	0,00	0,01
$DTbvDIlkg$	0,00	0,00	0,00	0,00	0,00	0,01	0,00	0,00	0,00	0,01	0,01	0,01	0,01	0,00	0,00	0,01	0,00	0,00	0,00	0,01
$DEWfmASenO$	1,00	0,00	0,45	0,46	0,49	0,28	0,00	0,00	0,00	0,01	0,00	0,01	0,00	0,00	0,00	0,01	0,00	0,00	0,00	0,01
$DEWfmBSenO$	0,00	1,00	0,38	0,44	0,51	0,26	0,00	0,01	0,01	0,02	0,01	0,01	0,00	0,00	0,00	0,02	0,00	0,01	0,00	0,01
$EByvDPist0$	0,00	0,00	0,00	0,00	0,00	0,01	0,00	0,00	0,00	0,00	0,00	0,02	0,01	0,00	0,00	0,01	0,00	0,00	0,00	0,00
$DEByvK0$	0,00	0,00	0,01	0,00	0,00	0,01	0,00	0,00	0,01	0,00	0,00	0,02	0,00	0,00	0,01	0,02	0,00	0,00	0,00	0,00
$DEByvVisc$	0,00	0,00	0,00	0,00	0,00	0,01	0,00	0,01	0,01	0,01	0,01	0,01	0,00	0,00	0,00	0,02	0,00	0,01	0,00	0,01
$DEByvStic$	0,00	0,00	0,00	0,00	0,00	0,02	0,00	0,00	0,01	0,01	0,01	0,01	0,00	0,00	0,00	0,02	0,00	0,00	0,00	0,01
$DByvDIlkg$	0,00	0,00	0,00	0,00	0,00	0,00	0,00	0,01	0,01	0,05	0,02	0,04	0,02	0,00	0,05	0,01	0,00	0,01	0,01	0,04
$ESovDPist$	0,00	0,00	0,00	0,00	0,00	0,00	0,00	0,01	0,01	0,06	0,04	0,02	0,00	0,00	0,03	0,02	0,00	0,01	0,00	0,03
$DESovVisc$	0,00	0,00	0,01	0,00	0,00	0,01	0,00	0,01	0,00	0,00	0,00	0,00	0,00	0,00	0,00	0,01	0,00	0,01	0,00	0,00
$DESovStic$	0,00	0,00	0,00	0,00	0,00	0,01	0,00	0,00	0,00	0,01	0,01	0,01	0,01	0,00	0,00	0,02	0,00	0,00	0,00	0,01
$DSovDIlkg$	0,00	0,00	0,00	0,00	0,00	0,00	0,00	0,00	0,01	0,02	0,01	0,03	0,00	0,00	0,04	0,00	0,00	0,00	0,00	0,01
$DSovDelay$	0,00	0,00	0,00	0,00	0,00	0,01	0,00	0,00	0,00	0,01	0,00	0,01	0,00	0,00	0,00	0,03	0,00	0,00	0,00	0,01
$DEFmvStic$	0,00	0,00	0,00	0,00	0,00	0,00	0,00	0,00	0,00	0,02	0,01	0,01	0,01	0,00	0,00	0,02	0,00	0,00	0,00	0,02
$DEFmvCnull$	0,00	0,00	0,01	0,00	0,00	0,01	0,00	0,00	0,01	0,01	0,01	0,01	0,00	0,00	0,01	0,02	0,00	0,00	0,00	0,00
$DEFmvDnozzle$	0,00	0,00	0,00	0,00	0,00	0,00	0,00	0,01	0,00	0,01	0,00	0,01	0,00	0,00	0,00	0,02	0,00	0,01	0,00	0,01
$DEFmvASenO$	0,00	0,00	0,00	0,00	0,00	0,00	0,00	0,00	0,01	0,00	0,00	0,01	0,00	0,00	0,01	0,01	0,00	0,00	0,00	0,01
$DEFmvBSenO$	0,00	0,00	0,00	0,00	0,00	0,00	0,00	0,00	0,00	0,00	0,02	0,01	0,00	0,00	0,00	0,01	0,00	0,00	0,00	0,00
$DFmvDIlkg$	0,00	0,00	0,00	0,00	0,00	0,00	0,00	0,00	0,00	0,01	0,01	0,01	0,00	0,00	0,00	0,03	0,00	0,01	0,00	0,01
$DEVsvStic1$	0,00	0,00	0,00	0,01	0,00	0,01	0,00	0,00	0,01	0,02	0,00	0,01	0,00	0,00	0,00	0,01	0,00	0,00	0,00	0,02
$DEVsvVisc1$	0,00	0,00	0,00	0,00	0,00	0,00	0,00	0,00	0,00	0,00	0,00	0,01	0,00	0,00	0,00	0,01	0,00	0,00	0,00	0,00
$DEVsvStic2$	0,00	0,00	0,00	0,00	0,00	0,01	0,00	0,00	0,01	0,00	0,00	0,01	0,00	0,00	0,00	0,02	0,00	0,00	0,00	0,00
$DEVsvVisc2$	0,00	0,00	0,01	0,00	0,00	0,01	0,00	0,00	0,00	0,00	0,00	0,01	0,01	0,00	0,00	0,02	0,00	0,00	0,00	0,00
$DEVsvDCool1$	0,00	0,00	0,00	0,00	0,00	0,02	0,00	0,00	0,00	0,00	0,01	0,01	0,00	0,00	0,00	0,01	0,00	0,00	0,00	0,01
$DEVsvDCool2$	0,00	0,00	0,00	0,00	0,00	0,00	0,11	0,04	0,21	0,06	0,02	0,09	0,17	0,01	0,00	0,01	0,11	0,04	0,28	0,07
$DEVsvKineFric$	0,00	0,00	0,00	0,00	0,00	0,01	0,00	0,25	0,39	0,17	0,31	0,32	0,16	0,76	0,48	0,02	0,00	0,26	0,47	0,23
$DEVsvCnull$	0,00	0,00	0,00	0,00	0,00	0,02	0,73	0,49	0,02	0,03	0,01	0,00	0,02	0,00	0,00	0,01	0,71	0,46	0,00	0,02
$DEVsvDnozzle$	0,00	0,00	0,01	0,00	0,00	0,01	0,00	0,01	0,01	0,02	0,00	0,00	0,01	0,00	0,00	0,02	0,00	0,01	0,00	0,01
$DEVsvKfeed$	0,00	0,00	0,00	0,00	0,00	0,00	0,01	0,00	0,01	0,02	0,01	0,05	0,01	0,01	0,07	0,01	0,02	0,00	0,01	0,01
$DEVsvSticspool$	0,00	0,00	0,01	0,00	0,00	0,01	0,00	0,01	0,11	0,16	0,26	0,02	0,33	0,20	0,12	0,02	0,00	0,01	0,13	0,16
$DEVsvDFilter1$	0,00	0,00	0,00	0,00	0,00	0,00	0,00	0,00	0,00	0,03	0,01	0,01	0,00	0,00	0,00	0,03	0,00	0,00	0,00	0,02
$DEVsvDFilter2$	0,00	0,00	0,00	0,00	0,00	0,01	0,00	0,00	0,01	0,01	0,00	0,01	0,01	0,00	0,00	0,02	0,00	0,00	0,01	0,02
$DEVsvCorHP1$	0,00	0,00	0,00	0,00	0,00	0,01	0,00	0,00	0,00	0,00	0,00	0,01	0,00	0,00	0,00	0,02	0,00	0,00	0,00	0,01
$DEVsvCorHP2$	0,00	0,00	0,00	0,00	0,00	0,02	0,00	0,00	0,01	0,02	0,02	0,00	0,01	0,00	0,01	0,01	0,00	0,00	0,00	0,02
$DEVsvASenO$	0,00	0,00	0,00	0,00	0,00	0,00	0,00	0,00	0,00	0,00	0,00	0,01	0,00	0,00	0,00	0,02	0,01	0,00	0,00	0,01
$DEVsvBSenO$	0,00	0,00	0,00	0,00	0,00	0,00	0,00	0,00	0,01	0,02	0,00	0,01	0,02	0,00	0,01	0,02	0,00	0,00	0,00	0,01
$DEVbvStic1$	0,00	0,00	0,01	0,00	0,00	0,00	0,00	0,01	0,00	0,01	0,00	0,02	0,00	0,00	0,00	0,02	0,00	0,01	0,00	0,01
$DEVbvVisc1$	0,00	0,00	0,00	0,00	0,00	0,00	0,00	0,00	0,00	0,00	0,01	0,01	0,01	0,00	0,00	0,02	0,00	0,00	0,00	0,01
$DEVbvStic2$	0,00	0,00	0,00	0,00	0,00	0,00	0,00	0,00	0,01	0,00	0,00	0,01	0,01	0,00	0,00	0,01	0,00	0,00	0,00	0,01
$DEVbvVisc2$	0,00	0,00	0,00	0,00	0,00	0,02	0,00	0,00	0,00	0,01	0,01	0,01	0,00	0,00	0,00	0,02	0,00	0,00	0,00	0,01
$DEVbvDCool1$	0,00	0,00	0,00	0,00	0,00	0,00	0,00	0,00	0,00	0,00	0,00	0,01	0,00	0,00	0,00	0,04	0,00	0,00	0,00	0,00
$DEVbvDCool2$	0,00	0,00	0,00	0,00	0,00	0,01	0,00	0,00	0,00	0,00	0,01	0,01	0,01	0,00	0,00	0,01	0,00	0,00	0,00	0,00
$DEVbvKineFric$	0,00	0,00	0,01	0,00	0,00	0,00	0,00	0,01	0,01	0,00	0,00	0,01	0,00	0,00	0,00	0,01	0,00	0,01	0,01	0,00
$DEVbvCnull$	0,00	0,00	0,00	0,00	0,00	0,00	0,00	0,00	0,00	0,02	0,00	0,01	0,00	0,00	0,00	0,02	0,01	0,00	0,00	0,01
$DEVbvDnozzle$	0,00	0,00	0,01	0,00	0,00	0,03	0,00	0,00	0,01	0,01	0,00	0,01	0,01	0,00	0,00	0,01	0,00	0,00	0,00	0,00
$DEVbvKfeed$	0,00	0,00	0,01	0,00	0,00	0,01	0,00	0,00	0,00	0,02	0,01	0,01	0,00	0,00	0,00	0,03	0,00	0,00	0,00	0,00
$DEVbvSticspool$	0,00	0,00	0,00	0,00	0,00	0,00	0,00	0,00	0,00	0,00	0,00	0,01	0,01	0,00	0,00	0,02	0,00	0,00	0,00	0,01
$DEVbvDFilter1$	0,00	0,00	0,00	0,01	0,00	0,01	0,00	0,01	0,01	0,00	0,00	0,02	0,01	0,00	0,00	0,02	0,00	0,01	0,00	0,00
$DEVbvDFilter2$	0,00	0,00	0,00	0,01	0,00	0,01	0,00	0,00	0,00	0,00	0,00	0,01	0,01	0,00	0,00	0,02	0,00	0,00	0,00	0,00
$DEVbvCorHP1$	0,00	0,00	0,01	0,00	0,00	0,02	0,00	0,01	0,00	0,02	0,01	0,01	0,00	0,00	0,00	0,01	0,00	0,01	0,00	0,01
$DEVbvCorHP2$	0,00	0,00	0,00	0,00	0,00	0,02	0,00	0,00	0,00	0,01	0,00	0,01	0,00	0,00	0,00	0,00	0,00	0,00	0,00	0,01
$DEVbvASenO$	0,00	0,00	0,00	0,00	0,00	0,01	0,00	0,00	0,00	0,01	0,01	0,01	0,00	0,00	0,00	0,02	0,00	0,00	0,00	0,02
$DEVbvBSenO$	0,00	0,00	0,00	0,00	0,00	0,02	0,00	0,00	0,00	0,00	0,02	0,01	0,00	0,00	0,00	0,02	0,00	0,00	0,00	0,00
$EStaLaw$	0,00	0,00	0,00	0,00	0,00	0,00	0,00	0,00	0,00	0,01	0,01	0,01	0,03	0,00	0,00	0,02	0,00	0,00	0,00	0,01

	$VsvYoverlapB$	$VsvScaleB$	$VsvSlpLeftB$	$VsvSlpNullB$	$VsvSlpRightB$	$VsvHyst0B$	$VsvCEquS$	$VsvXnullS$	$VsvYnullS$	$VsvXoverlapS$	$VsvYoverlapS$	$VsvScaleS$	$VsvSlpLeftS$	$VsvSlpNullS$	$VsvSlpRightS$	$VsvHyst0S$	$VsvmaxX1$	$VsvmaxX2$	$VsvminX1$	$VsvminX2$
$CTfuel$	0,01	0,01	0,03	0,00	0,00	0,00	0,00	0,01	0,01	0,02	0,01	0,01	0,01	0,01	0,00	0,00	0,01	0,02	0,01	0,01
$DLppDIlkg$	0,03	0,01	0,01	0,00	0,00	0,00	0,00	0,01	0,00	0,02	0,01	0,01	0,00	0,01	0,00	0,00	0,01	0,02	0,01	0,01
$DMfpDIlkg$	0,00	0,01	0,02	0,00	0,00	0,00	0,00	0,00	0,01	0,00	0,00	0,01	0,00	0,00	0,00	0,00	0,01	0,01	0,01	0,01
$DEMffFlowRate$	0,01	0,01	0,00	0,00	0,00	0,00	0,00	0,00	0,02	0,02	0,02	0,01	0,01	0,02	0,00	0,00	0,00	0,02	0,01	0,01
$ETbvPopen$	0,01	0,00	0,01	0,00	0,00	0,00	0,00	0,00	0,02	0,01	0,01	0,00	0,00	0,01	0,01	0,00	0,01	0,02	0,01	0,02
$DTbvDIlkg$	0,01	0,01	0,01	0,00	0,00	0,00	0,00	0,01	0,02	0,01	0,01	0,01	0,02	0,01	0,01	0,00	0,01	0,01	0,01	0,01
$DEWfmASenO$	0,00	0,01	0,01	0,00	0,00	0,00	0,00	0,02	0,01	0,01	0,00	0,00	0,02	0,01	0,00	0,00	0,02	0,01	0,01	0,01
$DEWfmBSenO$	0,00	0,01	0,01	0,00	0,00	0,00	0,00	0,01	0,01	0,01	0,01	0,01	0,00	0,01	0,00	0,00	0,02	0,00	0,01	0,01
$EByvDPist0$	0,00	0,03	0,01	0,00	0,00	0,01	0,00	0,01	0,01	0,01	0,01	0,01	0,01	0,00	0,00	0,00	0,01	0,00	0,01	0,01
$DEByvK0$	0,00	0,02	0,00	0,00	0,01	0,00	0,00	0,01	0,03	0,03	0,03	0,01	0,01	0,00	0,02	0,00	0,02	0,01	0,01	0,01
$DEByvVisc$	0,01	0,01	0,00	0,00	0,00	0,00	0,00	0,01	0,02	0,03	0,01	0,01	0,01	0,02	0,00	0,00	0,02	0,02	0,01	0,01
$DEByvStic$	0,01	0,01	0,00	0,00	0,00	0,00	0,00	0,01	0,01	0,01	0,02	0,00	0,02	0,01	0,00	0,00	0,02	0,01	0,01	0,01
$DByvDIlkg$	0,02	0,04	0,01	0,00	0,05	0,03	0,00	0,01	0,00	0,01	0,01	0,02	0,01	0,01	0,04	0,00	0,01	0,02	0,01	0,01
$ESovDPist$	0,04	0,02	0,00	0,00	0,03	0,00	0,00	0,02	0,03	0,00	0,01	0,01	0,01	0,01	0,05	0,00	0,02	0,02	0,01	0,01
$DESovVisc$	0,00	0,00	0,00	0,00	0,00	0,00	0,00	0,00	0,03	0,03	0,02	0,00	0,01	0,01	0,00	0,00	0,02	0,00	0,02	0,01
$DESovStic$	0,01	0,01	0,01	0,00	0,00	0,00	0,00	0,01	0,00	0,00	0,00	0,00	0,03	0,01	0,01	0,00	0,02	0,02	0,01	0,01
$DSovDIlkg$	0,01	0,03	0,01	0,00	0,04	0,01	0,00	0,02	0,01	0,01	0,00	0,02	0,01	0,01	0,02	0,00	0,01	0,01	0,01	0,01
$DSovDelay$	0,00	0,01	0,00	0,00	0,00	0,01	0,00	0,01	0,01	0,02	0,01	0,01	0,00	0,01	0,00	0,00	0,01	0,01	0,01	0,01
$DEFmvStic$	0,01	0,01	0,00	0,00	0,00	0,00	0,00	0,01	0,01	0,02	0,01	0,01	0,02	0,02	0,00	0,00	0,01	0,02	0,01	0,02
$DEFmvCnull$	0,01	0,01	0,00	0,00	0,01	0,00	0,00	0,01	0,01	0,02	0,01	0,00	0,02	0,02	0,00	0,00	0,01	0,01	0,01	0,01
$DEFmvDnozzle$	0,00	0,01	0,00	0,00	0,00	0,00	0,00	0,01	0,01	0,00	0,01	0,01	0,00	0,01	0,01	0,00	0,02	0,02	0,01	0,01
$DEFmvASenO$	0,01	0,01	0,00	0,00	0,01	0,00	0,00	0,01	0,00	0,01	0,01	0,01	0,01	0,00	0,00	0,00	0,02	0,01	0,01	0,01
$DEFmvBSenO$	0,02	0,01	0,00	0,00	0,00	0,00	0,00	0,01	0,00	0,00	0,00	0,00	0,01	0,00	0,00	0,00	0,01	0,01	0,01	0,01
$DFmvDIlkg$	0,01	0,01	0,01	0,00	0,00	0,01	0,00	0,00	0,01	0,01	0,01	0,01	0,03	0,00	0,01	0,00	0,02	0,01	0,01	0,01
$DEVsvStic1$	0,00	0,01	0,01	0,00	0,00	0,01	0,00	0,01	0,01	0,01	0,01	0,00	0,00	0,00	0,00	0,00	0,01	0,02	0,01	0,02
$DEVsvVisc1$	0,00	0,00	0,00	0,00	0,00	0,00	0,00	0,01	0,01	0,02	0,02	0,00	0,01	0,01	0,00	0,00	0,01	0,01	0,01	0,01
$DEVsvStic2$	0,00	0,01	0,00	0,00	0,00	0,00	0,00	0,01	0,01	0,00	0,00	0,01	0,01	0,01	0,01	0,00	0,01	0,01	0,01	0,01
$DEVsvVisc2$	0,00	0,01	0,01	0,00	0,00	0,00	0,00	0,01	0,01	0,00	0,00	0,01	0,01	0,00	0,00	0,00	0,01	0,01	0,01	0,01
$DEVsvDCool1$	0,01	0,02	0,00	0,00	0,00	0,01	0,00	0,01	0,00	0,01	0,01	0,00	0,00	0,00	0,00	0,00	0,01	0,01	0,01	0,01
$DEVsvDCool2$	0,02	0,11	0,14	0,01	0,00	0,01	0,12	0,03	0,07	0,07	0,04	0,17	0,06	0,01	0,01	0,03	0,02	0,02	0,00	0,00
$DEVsvKineFric$	0,29	0,29	0,25	0,76	0,48	0,00	0,00	0,12	0,03	0,13	0,33	0,40	0,03	0,48	0,57	0,00	0,01	0,02	0,01	0,01
$DEVsvCnull$	0,01	0,00	0,01	0,00	0,00	0,00	0,74	0,42	0,00	0,00	0,00	0,00	0,01	0,00	0,00	0,00	0,02	0,00	0,01	0,01
$DEVsvDnozzle$	0,00	0,00	0,03	0,00	0,00	0,02	0,00	0,01	0,01	0,00	0,01	0,00	0,02	0,01	0,00	0,00	0,01	0,01	0,01	0,01
$DEVsvKfeed$	0,01	0,05	0,03	0,01	0,07	0,20	0,01	0,01	0,01	0,05	0,01	0,04	0,02	0,03	0,01	0,01	0,02	0,02	0,04	0,03
$DEVsvSticspool$	0,24	0,02	0,16	0,20	0,12	0,55	0,00	0,00	0,22	0,02	0,10	0,05	0,10	0,07	0,08	0,89	0,02	0,02	0,03	0,03
$DEVsvDFilter1$	0,01	0,01	0,00	0,00	0,00	0,00	0,00	0,00	0,01	0,01	0,01	0,01	0,01	0,01	0,01	0,00	0,01	0,02	0,01	0,01
$DEVsvDFilter2$	0,00	0,01	0,01	0,00	0,00	0,00	0,00	0,00	0,02	0,02	0,01	0,01	0,01	0,01	0,01	0,00	0,02	0,02	0,01	0,01
$DEVsvCorHP1$	0,00	0,01	0,01	0,00	0,00	0,00	0,00	0,01	0,01	0,01	0,01	0,01	0,01	0,01	0,00	0,00	0,01	0,02	0,01	0,01
$DEVsvCorHP2$	0,02	0,00	0,01	0,00	0,01	0,00	0,00	0,01	0,01	0,02	0,02	0,00	0,03	0,01	0,01	0,00	0,01	0,02	0,01	0,01
$DEVsvASenO$	0,01	0,01	0,02	0,00	0,00	0,00	0,00	0,01	0,03	0,04	0,01	0,01	0,06	0,01	0,01	0,00	0,18	0,00	0,20	0,17
$DEVsvBSenO$	0,00	0,01	0,00	0,00	0,00	0,00	0,00	0,01	0,01	0,05	0,04	0,00	0,05	0,01	0,00	0,00	0,02	0,17	0,21	0,17
$DEVbvStic1$	0,01	0,02	0,01	0,00	0,00	0,00	0,00	0,01	0,00	0,01	0,00	0,01	0,00	0,01	0,00	0,00	0,02	0,02	0,00	0,00
$DEVbvVisc1$	0,01	0,01	0,01	0,00	0,00	0,00	0,00	0,01	0,01	0,01	0,00	0,01	0,01	0,00	0,00	0,00	0,02	0,01	0,01	0,01
$DEVbvStic2$	0,00	0,01	0,01	0,00	0,00	0,00	0,00	0,01	0,02	0,02	0,01	0,00	0,01	0,01	0,00	0,00	0,01	0,02	0,01	0,01
$DEVbvVisc2$	0,01	0,00	0,01	0,00	0,00	0,00	0,00	0,01	0,00	0,01	0,01	0,00	0,02	0,00	0,00	0,00	0,01	0,01	0,01	0,01
$DEVbvDCool1$	0,00	0,01	0,00	0,00	0,00	0,01	0,00	0,00	0,00	0,00	0,00	0,01	0,00	0,00	0,00	0,00	0,02	0,02	0,01	0,01
$DEVbvDCool2$	0,01	0,01	0,00	0,00	0,00	0,00	0,00	0,02	0,03	0,03	0,02	0,00	0,04	0,00	0,00	0,00	0,01	0,01	0,01	0,01
$DEVbvKineFric$	0,00	0,01	0,02	0,00	0,00	0,00	0,00	0,00	0,04	0,04	0,01	0,00	0,02	0,00	0,00	0,00	0,02	0,02	0,01	0,01
$DEVbvCnull$	0,00	0,01	0,01	0,00	0,00	0,00	0,00	0,01	0,03	0,01	0,00	0,01	0,01	0,00	0,01	0,00	0,01	0,02	0,00	0,00
$DEVbvDnozzle$	0,00	0,01	0,01	0,00	0,00	0,00	0,00	0,01	0,03	0,02	0,01	0,01	0,02	0,02	0,01	0,00	0,01	0,00	0,01	0,02
$DEVbvKfeed$	0,01	0,01	0,02	0,00	0,00	0,00	0,00	0,01	0,01	0,03	0,01	0,00	0,02	0,01	0,00	0,00	0,02	0,02	0,01	0,01
$DEVbvSticspool$	0,00	0,01	0,01	0,00	0,00	0,01	0,00	0,01	0,00	0,02	0,01	0,01	0,02	0,00	0,00	0,00	0,01	0,02	0,01	0,01
$DEVbvDFilter1$	0,00	0,02	0,00	0,00	0,00	0,01	0,00	0,00	0,02	0,01	0,01	0,01	0,00	0,00	0,00	0,00	0,01	0,01	0,01	0,01
$DEVbvDFilter2$	0,00	0,01	0,02	0,00	0,00	0,00	0,00	0,01	0,02	0,00	0,00	0,01	0,00	0,01	0,01	0,00	0,01	0,01	0,01	0,01
$DEVbvCorHP1$	0,01	0,01	0,00	0,00	0,00	0,00	0,00	0,01	0,01	0,00	0,01	0,00	0,00	0,00	0,02	0,00	0,01	0,02	0,01	0,01
$DEVbvCorHP2$	0,00	0,01	0,00	0,00	0,00	0,00	0,00	0,01	0,01	0,01	0,01	0,00	0,01	0,00	0,01	0,00	0,01	0,01	0,01	0,01
$DEVbvASenO$	0,01	0,01	0,00	0,00	0,00	0,00	0,00	0,01	0,01	0,01	0,00	0,00	0,01	0,01	0,00	0,00	0,01	0,02	0,01	0,01
$DEVbvBSenO$	0,03	0,01	0,00	0,00	0,00	0,01	0,00	0,01	0,00	0,01	0,01	0,00	0,02	0,01	0,00	0,00	0,01	0,02	0,01	0,01
$EStaLaw$	0,01	0,01	0,02	0,00	0,00	0,01	0,00	0,00	0,01	0,01	0,01	0,01	0,03	0,01	0,00	0,00	0,01	0,02	0,01	0,01

	$VsvmaxGapX$	$VsvminGapX$	$VsvmeanGapX$	$VsvstdGapX$	$VsvMAErr$	$VbvCEquA$	$VbvXchgA$	$VbvYchgA$	$VbvScaleA$	$VbvSlpLeftA$	$VbvSlpRightA$	$VbvHyst0A$	$VbvCEquB$	$VbvXchgB$	$VbvYchgB$	$VbvScaleB$	$VbvSlpLeftB$	$VbvSlpRightB$	$VbvHyst0B$	$VbvCEquS$
$CTfuel$	0,00	0,00	0,00	0,00	0,01	0,00	0,00	0,02	0,00	0,04	0,04	0,00	0,00	0,00	0,02	0,00	0,00	0,06	0,00	0,01
$DLppDIlkg$	0,00	0,00	0,00	0,00	0,00	0,00	0,00	0,01	0,00	0,01	0,00	0,00	0,00	0,01	0,02	0,00	0,01	0,04	0,00	0,01
$DMfpDIlkg$	0,00	0,00	0,00	0,00	0,00	0,00	0,01	0,01	0,01	0,01	0,01	0,00	0,00	0,01	0,01	0,00	0,00	0,00	0,01	0,01
$DEMffFlowRate$	0,00	0,00	0,00	0,00	0,02	0,00	0,00	0,01	0,00	0,01	0,02	0,00	0,00	0,01	0,01	0,00	0,00	0,02	0,00	0,01
$ETbvPopen$	0,00	0,00	0,00	0,00	0,01	0,00	0,00	0,01	0,00	0,02	0,00	0,00	0,00	0,00	0,01	0,00	0,00	0,03	0,00	0,00
$DTbvDIlkg$	0,00	0,00	0,00	0,00	0,02	0,00	0,00	0,02	0,03	0,04	0,02	0,00	0,00	0,01	0,02	0,00	0,00	0,02	0,00	0,01
$DEWfmASen0$	0,00	0,00	0,00	0,00	0,01	0,00	0,00	0,01	0,01	0,01	0,02	0,00	0,00	0,00	0,02	0,00	0,00	0,05	0,00	0,01
$DEWfmBSen0$	0,00	0,00	0,00	0,00	0,01	0,00	0,01	0,04	0,02	0,03	0,03	0,00	0,01	0,01	0,03	0,00	0,00	0,05	0,00	0,01
$EByvDPist0$	0,00	0,00	0,00	0,00	0,02	0,01	0,00	0,02	0,01	0,01	0,01	0,00	0,01	0,00	0,01	0,01	0,01	0,01	0,00	0,01
$DEByvK0$	0,00	0,00	0,00	0,00	0,01	0,00	0,00	0,01	0,01	0,01	0,01	0,00	0,00	0,01	0,00	0,01	0,00	0,01	0,01	0,00
$DEByvVisc$	0,00	0,00	0,00	0,00	0,00	0,00	0,00	0,01	0,04	0,01	0,02	0,00	0,00	0,00	0,01	0,01	0,00	0,01	0,00	0,01
$DEByvStic$	0,00	0,00	0,00	0,00	0,00	0,00	0,00	0,00	0,01	0,00	0,03	0,00	0,00	0,01	0,00	0,03	0,00	0,02	0,00	0,01
$DByvDIlkg$	0,00	0,00	0,00	0,00	0,02	0,00	0,01	0,09	0,08	0,03	0,06	0,00	0,00	0,01	0,10	0,18	0,08	0,03	0,00	0,01
$ESovDPist$	0,00	0,00	0,00	0,00	0,01	0,00	0,00	0,03	0,02	0,01	0,01	0,00	0,00	0,01	0,02	0,02	0,03	0,01	0,00	0,01
$DESovVisc$	0,00	0,00	0,00	0,00	0,00	0,00	0,00	0,01	0,01	0,01	0,04	0,00	0,00	0,00	0,01	0,01	0,01	0,02	0,00	0,01
$DESovStic$	0,00	0,00	0,00	0,00	0,02	0,00	0,00	0,01	0,01	0,02	0,03	0,00	0,00	0,01	0,01	0,01	0,00	0,03	0,00	0,01
$DSovDIlkg$	0,00	0,00	0,00	0,00	0,01	0,00	0,02	0,03	0,02	0,02	0,04	0,00	0,01	0,02	0,03	0,03	0,03	0,01	0,00	0,01
$DSovDelay$	0,00	0,00	0,00	0,00	0,01	0,00	0,00	0,00	0,00	0,00	0,00	0,00	0,00	0,00	0,00	0,00	0,00	0,01	0,00	0,01
$DEFmvStic$	0,00	0,00	0,00	0,00	0,01	0,00	0,00	0,00	0,00	0,00	0,01	0,00	0,00	0,01	0,01	0,01	0,00	0,01	0,00	0,01
$DEFmvCnull$	0,00	0,00	0,00	0,00	0,04	0,00	0,00	0,02	0,01	0,02	0,01	0,00	0,00	0,01	0,01	0,00	0,00	0,03	0,00	0,01
$DEFmvDnozzle$	0,00	0,00	0,00	0,00	0,01	0,00	0,00	0,00	0,01	0,01	0,01	0,00	0,00	0,01	0,00	0,01	0,00	0,04	0,01	0,01
$DEFmvASen0$	0,00	0,00	0,00	0,00	0,00	0,00	0,00	0,00	0,00	0,00	0,01	0,00	0,00	0,00	0,00	0,00	0,01	0,00	0,01	0,01
$DEFmvBSen0$	0,00	0,00	0,00	0,00	0,01	0,00	0,00	0,00	0,00	0,01	0,01	0,00	0,00	0,01	0,00	0,01	0,01	0,00	0,01	0,01
$DFmvDIlkg$	0,00	0,00	0,00	0,00	0,01	0,00	0,01	0,01	0,03	0,02	0,00	0,00	0,01	0,01	0,01	0,00	0,01	0,03	0,00	0,01
$DEVsvStic1$	0,00	0,00	0,00	0,00	0,01	0,00	0,00	0,00	0,01	0,00	0,00	0,00	0,00	0,00	0,00	0,00	0,00	0,02	0,00	0,01
$DEVsvVisc1$	0,00	0,00	0,00	0,00	0,01	0,00	0,00	0,01	0,00	0,01	0,01	0,00	0,00	0,00	0,01	0,00	0,00	0,01	0,00	0,01
$DEVsvStic2$	0,00	0,00	0,00	0,00	0,00	0,00	0,00	0,00	0,01	0,00	0,00	0,00	0,01	0,01	0,01	0,00	0,00	0,01	0,00	0,00
$DEVsvVisc2$	0,00	0,00	0,00	0,00	0,00	0,00	0,00	0,01	0,01	0,00	0,01	0,00	0,00	0,01	0,01	0,01	0,00	0,01	0,01	0,01
$DEVsvDCool1$	0,00	0,00	0,00	0,00	0,00	0,01	0,00	0,00	0,00	0,00	0,00	0,00	0,01	0,00	0,00	0,00	0,00	0,00	0,00	0,01
$DEVsvDCool2$	0,00	0,00	0,00	0,00	0,01	0,01	0,01	0,00	0,01	0,00	0,01	0,00	0,01	0,00	0,00	0,01	0,00	0,00	0,00	0,01
$DEVsvKineFric$	0,00	0,00	0,00	0,00	0,01	0,00	0,00	0,01	0,01	0,01	0,01	0,00	0,00	0,01	0,01	0,01	0,01	0,00	0,00	0,01
$DEVsvCnull$	0,00	0,00	0,00	0,00	0,01	0,00	0,01	0,02	0,01	0,01	0,00	0,00	0,00	0,01	0,02	0,00	0,00	0,03	0,00	0,01
$DEVsvDnozzle$	0,00	0,00	0,00	0,00	0,01	0,00	0,00	0,03	0,02	0,07	0,03	0,00	0,00	0,01	0,01	0,01	0,00	0,02	0,00	0,01
$DEVsvKfeed$	0,00	0,00	0,00	0,00	0,09	0,00	0,01	0,01	0,02	0,01	0,03	0,00	0,00	0,01	0,00	0,03	0,01	0,02	0,00	0,00
$DEVsvSticspool$	0,00	0,00	0,00	0,00	0,04	0,00	0,00	0,00	0,01	0,01	0,01	0,00	0,00	0,01	0,00	0,02	0,00	0,02	0,00	0,01
$DEVsvDFilter1$	0,00	0,00	0,00	0,00	0,02	0,00	0,00	0,00	0,00	0,01	0,01	0,00	0,00	0,01	0,00	0,00	0,00	0,00	0,00	0,01
$DEVsvDFilter2$	0,00	0,00	0,00	0,00	0,01	0,01	0,00	0,01	0,01	0,01	0,01	0,00	0,01	0,01	0,01	0,00	0,00	0,00	0,00	0,01
$DEVsvCorHP1$	0,00	0,00	0,00	0,00	0,01	0,00	0,00	0,00	0,00	0,01	0,02	0,00	0,00	0,01	0,01	0,00	0,00	0,01	0,00	0,01
$DEVsvCorHP2$	0,00	0,00	0,00	0,00	0,01	0,00	0,01	0,02	0,00	0,02	0,01	0,00	0,00	0,01	0,02	0,01	0,01	0,03	0,00	0,00
$DEVsvASen0$	0,47	0,48	0,50	0,48	0,01	0,01	0,00	0,01	0,01	0,01	0,01	0,00	0,01	0,01	0,00	0,00	0,00	0,00	0,00	0,01
$DEVsvBSen0$	0,50	0,45	0,50	0,48	0,01	0,00	0,00	0,01	0,01	0,01	0,01	0,00	0,00	0,00	0,00	0,00	0,00	0,00	0,01	0,01
$DEVbvStic1$	0,00	0,00	0,00	0,00	0,02	0,01	0,00	0,02	0,04	0,02	0,00	0,00	0,01	0,01	0,01	0,00	0,01	0,02	0,00	0,01
$DEVbvVisc1$	0,00	0,00	0,00	0,00	0,00	0,00	0,00	0,01	0,01	0,02	0,01	0,00	0,00	0,01	0,01	0,00	0,00	0,02	0,00	0,01
$DEVbvStic2$	0,00	0,00	0,00	0,00	0,02	0,00	0,00	0,00	0,01	0,01	0,01	0,00	0,00	0,01	0,00	0,01	0,00	0,01	0,00	0,01
$DEVbvVisc2$	0,00	0,00	0,00	0,00	0,01	0,00	0,01	0,00	0,01	0,01	0,01	0,00	0,00	0,01	0,00	0,01	0,01	0,01	0,00	0,01
$DEVbvDCool1$	0,00	0,00	0,00	0,00	0,01	0,01	0,00	0,01	0,00	0,00	0,00	0,00	0,01	0,01	0,00	0,00	0,01	0,00	0,00	0,01
$DEVbvDCool2$	0,00	0,00	0,00	0,00	0,00	0,04	0,04	0,02	0,08	0,06	0,01	0,00	0,04	0,03	0,02	0,09	0,11	0,00	0,01	0,05
$DEVbvKineFric$	0,00	0,00	0,00	0,00	0,01	0,00	0,00	0,01	0,09	0,03	0,02	0,00	0,00	0,00	0,00	0,12	0,07	0,01	0,00	0,00
$DEVbvCnull$	0,00	0,00	0,00	0,00	0,01	0,75	0,72	0,00	0,03	0,01	0,01	0,04	0,73	0,60	0,01	0,00	0,00	0,01	0,08	0,63
$DEVbvDnozzle$	0,00	0,00	0,00	0,00	0,01	0,00	0,01	0,02	0,01	0,01	0,03	0,00	0,00	0,02	0,02	0,02	0,02	0,03	0,00	0,01
$DEVbvKfeed$	0,00	0,00	0,00	0,00	0,01	0,01	0,01	0,03	0,03	0,03	0,03	0,00	0,01	0,01	0,01	0,02	0,03	0,04	0,01	0,01
$DEVbvSticspool$	0,00	0,00	0,00	0,00	0,00	0,00	0,01	0,30	0,10	0,17	0,19	0,00	0,00	0,01	0,40	0,16	0,44	0,03	0,00	0,00
$DEVbvDFilter1$	0,00	0,00	0,00	0,00	0,01	0,00	0,01	0,01	0,01	0,01	0,01	0,00	0,00	0,01	0,01	0,02	0,00	0,02	0,00	0,01
$DEVbvDFilter2$	0,00	0,00	0,00	0,00	0,00	0,00	0,01	0,01	0,00	0,02	0,01	0,00	0,00	0,01	0,00	0,01	0,00	0,02	0,00	0,01
$DEVbvCorHP1$	0,00	0,00	0,00	0,00	0,01	0,00	0,00	0,01	0,01	0,01	0,01	0,00	0,00	0,01	0,00	0,01	0,00	0,01	0,00	0,01
$DEVbvCorHP2$	0,00	0,00	0,00	0,00	0,06	0,00	0,00	0,00	0,01	0,02	0,01	0,00	0,00	0,00	0,00	0,02	0,00	0,00	0,00	0,01
$DEVbvASen0$	0,00	0,00	0,00	0,00	0,00	0,01	0,01	0,01	0,01	0,01	0,01	0,42	0,01	0,01	0,01	0,03	0,02	0,00	0,33	0,01
$DEVbvBSen0$	0,00	0,00	0,00	0,00	0,00	0,01	0,00	0,02	0,04	0,01	0,02	0,44	0,01	0,00	0,01	0,03	0,01	0,00	0,38	0,00
$EStaLaw$	0,00	0,00	0,00	0,00	0,31	0,00	0,00	0,00	0,01	0,01	0,01	0,00	0,00	0,00	0,00	0,00	0,00	0,03	0,00	0,00

	$VbvXchgS$	$VbvYchgS$	$VbvScaleS$	$VbvSlpLeftS$	$VbvSlpRightS$	$VbvHyst0S$	$VbvmaxX1$	$VbvmaxX2$	$VbvminX1$	$VbvminX2$	$VbvmaxGapX$	$VbvminGapX$	$VbvmeanGapX$	$VbvstdGapX$	$VbvMAErr$	$VoN2maxTBV$
$CTfuel$	0,01	0,00	0,01	0,00	0,03	0,00	0,00	0,00	0,00	0,00	0,00	0,01	0,00	0,00	0,00	0,01
$DLppDIlkg$	0,00	0,00	0,00	0,01	0,00	0,01	0,00	0,00	0,00	0,00	0,00	0,00	0,00	0,00	0,00	0,00
$DMfpDIlkg$	0,00	0,00	0,01	0,01	0,00	0,01	0,00	0,00	0,00	0,00	0,00	0,00	0,00	0,00	0,00	0,02
$DEMffFlowRate$	0,00	0,00	0,02	0,01	0,04	0,00	0,01	0,00	0,00	0,00	0,00	0,00	0,00	0,00	0,00	0,03
$ETbvPopen$	0,00	0,00	0,00	0,00	0,02	0,00	0,00	0,01	0,00	0,00	0,00	0,01	0,00	0,00	0,00	0,03
$DTbvDIlkg$	0,00	0,00	0,01	0,00	0,03	0,00	0,00	0,00	0,00	0,00	0,00	0,01	0,00	0,00	0,00	0,02
$DEWfmASen0$	0,00	0,01	0,01	0,00	0,02	0,00	0,00	0,00	0,00	0,00	0,00	0,00	0,00	0,00	0,00	0,02
$DEWfmBSen0$	0,00	0,01	0,00	0,00	0,03	0,00	0,00	0,00	0,00	0,00	0,00	0,01	0,00	0,00	0,01	0,03
$EByvDPist0$	0,00	0,02	0,01	0,01	0,01	0,00	0,00	0,00	0,00	0,00	0,00	0,00	0,00	0,00	0,00	0,00
$DEByvK0$	0,00	0,01	0,02	0,00	0,01	0,01	0,00	0,00	0,00	0,00	0,00	0,00	0,00	0,00	0,00	0,06
$DEByvVisc$	0,00	0,00	0,01	0,00	0,02	0,00	0,00	0,00	0,00	0,00	0,00	0,00	0,00	0,00	0,00	0,02
$DEByvStic$	0,00	0,00	0,02	0,01	0,02	0,00	0,00	0,00	0,00	0,00	0,00	0,00	0,00	0,00	0,00	0,05
$DByvDIlkg$	0,00	0,00	0,06	0,01	0,02	0,00	0,00	0,00	0,00	0,00	0,00	0,00	0,00	0,00	0,00	0,07
$ESovDPist$	0,00	0,01	0,01	0,01	0,01	0,00	0,00	0,00	0,00	0,00	0,00	0,01	0,00	0,00	0,00	0,00
$DESovVisc$	0,00	0,00	0,01	0,01	0,01	0,00	0,00	0,00	0,00	0,00	0,00	0,00	0,00	0,00	0,00	0,01
$DESovStic$	0,00	0,01	0,01	0,00	0,01	0,00	0,00	0,00	0,00	0,00	0,00	0,00	0,00	0,00	0,00	0,00
$DSovDIlkg$	0,01	0,19	0,02	0,20	0,03	0,00	0,00	0,00	0,00	0,00	0,00	0,00	0,00	0,00	0,00	0,27
$DSovDelay$	0,00	0,00	0,00	0,00	0,02	0,00	0,00	0,00	0,00	0,00	0,00	0,00	0,00	0,00	0,00	0,04
$DEFmvStic$	0,01	0,02	0,00	0,01	0,02	0,00	0,00	0,00	0,00	0,00	0,00	0,00	0,00	0,00	0,00	0,01
$DEFmvCnull$	0,00	0,01	0,02	0,01	0,02	0,00	0,01	0,00	0,00	0,00	0,00	0,01	0,00	0,00	0,00	0,01
$DEFmvDnozzle$	0,00	0,00	0,01	0,00	0,01	0,01	0,00	0,00	0,00	0,00	0,00	0,00	0,00	0,00	0,00	0,00
$DEFmvASen0$	0,00	0,01	0,00	0,00	0,00	0,00	0,00	0,00	0,00	0,00	0,00	0,00	0,00	0,00	0,00	0,00
$DEFmvBSen0$	0,00	0,00	0,00	0,00	0,00	0,00	0,00	0,00	0,00	0,00	0,00	0,00	0,00	0,00	0,00	0,00
$DFmvDIlkg$	0,00	0,03	0,02	0,00	0,01	0,00	0,00	0,00	0,00	0,00	0,00	0,00	0,00	0,00	0,00	0,01
$DEVsvStic1$	0,00	0,00	0,01	0,00	0,01	0,00	0,00	0,00	0,00	0,00	0,01	0,00	0,00	0,00	0,00	0,00
$DEVsvVisc1$	0,00	0,02	0,01	0,00	0,01	0,00	0,00	0,00	0,00	0,00	0,00	0,00	0,00	0,00	0,00	0,01
$DEVsvStic2$	0,00	0,01	0,01	0,00	0,01	0,00	0,00	0,00	0,00	0,00	0,00	0,00	0,00	0,00	0,00	0,01
$DEVsvVisc2$	0,00	0,00	0,00	0,00	0,00	0,00	0,00	0,00	0,00	0,00	0,00	0,00	0,00	0,00	0,00	0,00
$DEVsvDCool1$	0,00	0,00	0,01	0,00	0,00	0,00	0,00	0,00	0,00	0,00	0,01	0,00	0,00	0,00	0,00	0,00
$DEVsvDCool2$	0,00	0,00	0,01	0,01	0,01	0,00	0,00	0,00	0,00	0,00	0,00	0,00	0,00	0,00	0,00	0,00
$DEVsvKineFric$	0,00	0,01	0,01	0,00	0,02	0,00	0,00	0,00	0,00	0,00	0,00	0,00	0,00	0,00	0,00	0,00
$DEVsvCnull$	0,00	0,01	0,01	0,00	0,05	0,01	0,00	0,00	0,00	0,00	0,00	0,00	0,00	0,00	0,00	0,01
$DEVsvDnozzle$	0,00	0,01	0,02	0,00	0,01	0,00	0,00	0,00	0,00	0,00	0,00	0,00	0,00	0,00	0,00	0,01
$DEVsvKfeed$	0,00	0,01	0,01	0,00	0,01	0,00	0,00	0,00	0,00	0,00	0,00	0,01	0,00	0,00	0,00	0,01
$DEVsvSticspool$	0,00	0,00	0,00	0,01	0,01	0,00	0,01	0,00	0,00	0,00	0,00	0,00	0,00	0,00	0,01	0,01
$DEVsvDFilter1$	0,00	0,00	0,01	0,00	0,03	0,00	0,00	0,00	0,00	0,00	0,00	0,00	0,00	0,00	0,00	0,00
$DEVsvDFilter2$	0,01	0,00	0,00	0,01	0,01	0,00	0,00	0,00	0,00	0,00	0,00	0,00	0,00	0,00	0,00	0,00
$DEVsvCorHP1$	0,00	0,00	0,00	0,00	0,02	0,00	0,00	0,00	0,00	0,00	0,01	0,01	0,00	0,00	0,00	0,00
$DEVsvCorHP2$	0,01	0,03	0,00	0,01	0,01	0,00	0,00	0,00	0,00	0,00	0,00	0,00	0,00	0,00	0,00	0,01
$DEVsvASen0$	0,00	0,02	0,00	0,00	0,01	0,00	0,00	0,00	0,00	0,00	0,00	0,00	0,00	0,00	0,00	0,01
$DEVsvBSen0$	0,00	0,00	0,01	0,00	0,00	0,01	0,01	0,00	0,00	0,00	0,00	0,00	0,00	0,00	0,00	0,02
$DEVbvStic1$	0,00	0,00	0,02	0,00	0,03	0,00	0,00	0,00	0,00	0,00	0,00	0,00	0,00	0,00	0,00	0,01
$DEVbvVisc1$	0,00	0,02	0,00	0,01	0,01	0,00	0,00	0,00	0,00	0,00	0,00	0,00	0,00	0,00	0,00	0,01
$DEVbvStic2$	0,00	0,01	0,00	0,00	0,00	0,00	0,00	0,00	0,00	0,00	0,00	0,00	0,00	0,00	0,00	0,01
$DEVbvVisc2$	0,01	0,00	0,01	0,01	0,02	0,01	0,00	0,00	0,00	0,00	0,00	0,00	0,00	0,00	0,00	0,01
$DEVbvDCool1$	0,00	0,01	0,00	0,00	0,00	0,00	0,01	0,00	0,00	0,00	0,00	0,00	0,00	0,00	0,00	0,00
$DEVbvDCool2$	0,03	0,02	0,17	0,14	0,00	0,01	0,01	0,00	0,00	0,00	0,00	0,00	0,00	0,00	0,00	0,01
$DEVbvKineFric$	0,01	0,01	0,05	0,05	0,03	0,00	0,01	0,00	0,00	0,00	0,00	0,00	0,00	0,00	0,00	0,06
$DEVbvCnull$	0,76	0,01	0,01	0,01	0,03	0,07	0,01	0,00	0,00	0,00	0,00	0,01	0,00	0,00	0,00	0,01
$DEVbvDnozzle$	0,01	0,00	0,07	0,00	0,04	0,01	0,01	0,00	0,00	0,00	0,01	0,01	0,00	0,00	0,00	0,02
$DEVbvKfeed$	0,01	0,01	0,02	0,01	0,04	0,01	0,00	0,00	0,00	0,00	0,01	0,01	0,00	0,00	0,00	0,00
$DEVbvSticspool$	0,01	0,40	0,16	0,36	0,15	0,00	0,01	0,00	0,00	0,00	0,00	0,00	0,00	0,00	0,00	0,00
$DEVbvDFilter1$	0,00	0,01	0,00	0,00	0,01	0,00	0,00	0,00	0,00	0,00	0,00	0,00	0,00	0,00	0,00	0,00
$DEVbvDFilter2$	0,00	0,00	0,00	0,00	0,00	0,00	0,00	0,00	0,00	0,00	0,00	0,00	0,00	0,00	0,00	0,00
$DEVbvCorHP1$	0,00	0,01	0,01	0,00	0,01	0,00	0,00	0,00	0,00	0,00	0,00	0,00	0,00	0,00	0,00	0,01
$DEVbvCorHP2$	0,00	0,00	0,01	0,00	0,01	0,00	0,00	0,00	0,00	0,00	0,00	0,00	0,00	0,00	0,00	0,00
$DEVbvASen0$	0,01	0,00	0,01	0,00	0,02	0,35	0,76	0,00	0,91	0,00	0,40	0,39	0,48	0,47	0,42	0,00
$DEVbvBSen0$	0,00	0,00	0,02	0,01	0,02	0,40	0,00	0,86	0,00	0,96	0,42	0,43	0,51	0,53	0,44	0,00
$EStaLaw$	0,00	0,01	0,01	0,01	0,01	0,00	0,01	0,00	0,00	0,00	0,00	0,00	0,00	0,00	0,01	0,01

Appendix XXIX. List of total Sobol indices

	$FmvCEquA$	$FmvScaleA$	$FmvSlpA$	$FmvHyst0A$	$FmvCEquB$	$FmvScaleB$	$FmvSlpB$	$FmvHyst0B$	$FmvCEquS$	$FmvScaleS$	$FmvSlpS$	$FmvHyst0S$	$FmvmaxX1$	$FmvmaxX2$	$FmvminX1$	$FmvminX2$	$FmvmaxGapX$	$FmvminGapX$	$FmvmeanGapX$	$FmvstdGapX$
$CTfuel$	0,02	0,01	0,02	0,01	0,01	0,01	0,03	0,01	0,02	0,02	0,00	0,01	0,00	0,00	0,00	0,00	0,00	0,00	0,00	0,01
$DLppDIlkg$	0,00	0,01	0,01	0,00	0,00	0,01	0,01	0,00	0,00	0,01	0,02	0,01	0,00	0,00	0,00	0,00	0,00	0,00	0,00	0,00
$DMfpDIlkg$	0,00	0,00	0,01	0,00	0,00	0,00	0,00	0,00	0,01	0,00	0,00	0,00	0,00	0,00	0,00	0,00	0,00	0,00	0,00	0,00
$DEMffFlowRate$	0,00	0,02	0,02	0,01	0,00	0,02	0,01	0,01	0,00	0,02	0,00	0,02	0,01	0,00	0,00	0,00	0,00	0,00	0,00	0,00
$ETbvPopen$	0,01	0,00	0,01	0,00	0,00	0,00	0,01	0,00	0,01	0,00	0,00	0,00	0,01	0,01	0,00	0,00	0,00	0,00	0,00	0,00
$DTbvDIlkg$	0,00	0,01	0,03	0,00	0,00	0,01	0,02	0,00	0,00	0,01	0,02	0,00	0,00	0,00	0,00	0,00	0,00	0,00	0,00	0,00
$DEWfmASenO$	0,00	0,01	0,00	0,00	0,00	0,01	0,00	0,00	0,00	0,01	0,00	0,00	0,01	0,00	0,00	0,00	0,00	0,00	0,00	0,00
$DEWfmBSenO$	0,00	0,01	0,03	0,00	0,00	0,00	0,03	0,00	0,00	0,01	0,02	0,00	0,00	0,00	0,00	0,00	0,00	0,00	0,00	0,00
$EByvDPist0$	0,02	0,05	0,03	0,02	0,02	0,03	0,03	0,03	0,02	0,06	0,02	0,03	0,01	0,01	0,00	0,00	0,00	0,00	0,00	0,00
$DEByvK0$	0,05	0,01	0,01	0,00	0,03	0,01	0,01	0,00	0,02	0,01	0,01	0,00	0,01	0,02	0,00	0,00	0,00	0,00	0,00	0,00
$DEByvVisc$	0,01	0,00	0,01	0,00	0,00	0,00	0,01	0,00	0,00	0,00	0,00	0,00	0,01	0,00	0,00	0,00	0,00	0,00	0,00	0,00
$DEByvStic$	0,00	0,01	0,04	0,00	0,00	0,01	0,06	0,00	0,00	0,01	0,08	0,00	0,00	0,00	0,00	0,00	0,00	0,00	0,00	0,00
$DByvDIlkg$	0,09	0,04	0,00	0,00	0,07	0,03	0,00	0,01	0,06	0,05	0,01	0,01	0,01	0,01	0,00	0,00	0,00	0,00	0,00	0,00
$ESovDPist$	0,01	0,02	0,02	0,00	0,01	0,00	0,02	0,00	0,01	0,01	0,01	0,00	0,00	0,00	0,00	0,00	0,00	0,00	0,00	0,00
$DESovVisc$	0,01	0,00	0,02	0,00	0,00	0,00	0,02	0,00	0,01	0,00	0,01	0,00	0,00	0,00	0,00	0,00	0,00	0,00	0,00	0,00
$DESovStic$	0,01	0,01	0,03	0,00	0,00	0,00	0,04	0,00	0,00	0,01	0,02	0,00	0,01	0,00	0,00	0,00	0,00	0,00	0,00	0,00
$DSovDIlkg$	0,00	0,02	0,01	0,01	0,00	0,02	0,00	0,01	0,00	0,01	0,00	0,01	0,00	0,00	0,00	0,00	0,00	0,00	0,00	0,00
$DSovDelay$	0,01	0,00	0,00	0,01	0,00	0,01	0,00	0,01	0,01	0,00	0,00	0,01	0,00	0,00	0,00	0,00	0,00	0,00	0,00	0,00
$DEFmvStic$	0,01	0,26	0,09	0,19	0,01	0,27	0,09	0,18	0,01	0,25	0,16	0,17	0,00	0,00	0,00	0,00	0,00	0,00	0,00	0,00
$DEFmvCnull$	0,20	0,00	0,01	0,00	0,26	0,01	0,01	0,00	0,23	0,00	0,01	0,00	0,07	0,08	0,00	0,00	0,00	0,00	0,00	0,00
$DEFmvDnozzle$	0,07	0,09	0,12	0,00	0,06	0,04	0,06	0,00	0,04	0,10	0,02	0,00	0,00	0,01	0,00	0,00	0,00	0,00	0,00	0,00
$DEFmvASenO$	0,00	0,01	0,00	0,16	0,00	0,04	0,00	0,15	0,00	0,01	0,01	0,15	0,23	0,28	0,98	0,00	0,49	0,49	0,50	0,45
$DEFmvBSenO$	0,00	0,01	0,00	0,16	0,00	0,00	0,00	0,15	0,00	0,01	0,01	0,14	0,24	0,26	0,00	0,99	0,49	0,49	0,50	0,42
$DFmvDIlkg$	0,31	0,10	0,15	0,29	0,35	0,15	0,16	0,28	0,37	0,10	0,26	0,27	0,22	0,21	0,00	0,00	0,00	0,00	0,00	0,00
$DEVsvStic1$	0,00	0,02	0,01	0,00	0,00	0,01	0,02	0,00	0,00	0,02	0,01	0,01	0,01	0,00	0,00	0,00	0,00	0,00	0,00	0,00
$DEVsvVisc1$	0,00	0,01	0,01	0,00	0,00	0,01	0,01	0,00	0,00	0,01	0,00	0,00	0,00	0,00	0,00	0,00	0,00	0,00	0,00	0,00
$DEVsvStic2$	0,00	0,00	0,01	0,00	0,00	0,00	0,01	0,00	0,00	0,00	0,00	0,00	0,00	0,00	0,00	0,00	0,00	0,00	0,00	0,00
$DEVsvVisc2$	0,00	0,01	0,01	0,00	0,00	0,01	0,01	0,00	0,00	0,00	0,01	0,00	0,00	0,00	0,00	0,00	0,00	0,00	0,00	0,01
$DEVsvDCool1$	0,00	0,00	0,00	0,00	0,00	0,00	0,00	0,00	0,00	0,00	0,00	0,00	0,00	0,00	0,00	0,00	0,00	0,00	0,00	0,00
$DEVsvDCool2$	0,00	0,00	0,00	0,00	0,00	0,00	0,00	0,00	0,00	0,00	0,00	0,00	0,00	0,00	0,00	0,00	0,00	0,00	0,00	0,00
$DEVsvKineFric$	0,01	0,02	0,00	0,00	0,01	0,01	0,01	0,00	0,01	0,01	0,01	0,00	0,00	0,00	0,00	0,00	0,00	0,00	0,00	0,00
$DEVsvCnull$	0,01	0,01	0,01	0,00	0,01	0,01	0,01	0,00	0,02	0,02	0,01	0,00	0,00	0,00	0,00	0,00	0,00	0,00	0,00	0,00
$DEVsvDnozzle$	0,01	0,01	0,01	0,00	0,01	0,01	0,01	0,00	0,01	0,01	0,01	0,01	0,00	0,00	0,00	0,00	0,00	0,00	0,00	0,00
$DEVsvKfeed$	0,01	0,02	0,01	0,00	0,00	0,03	0,01	0,00	0,00	0,03	0,00	0,00	0,01	0,00	0,00	0,00	0,00	0,00	0,00	0,01
$DEVsvSticspool$	0,01	0,01	0,01	0,00	0,01	0,01	0,01	0,00	0,01	0,01	0,01	0,00	0,00	0,00	0,00	0,00	0,00	0,00	0,00	0,00
$DEVsvDFilter1$	0,01	0,02	0,01	0,00	0,00	0,01	0,00	0,00	0,01	0,02	0,01	0,00	0,00	0,00	0,00	0,00	0,00	0,00	0,00	0,00
$DEVsvDFilter2$	0,01	0,01	0,01	0,00	0,01	0,01	0,01	0,00	0,01	0,01	0,01	0,00	0,01	0,00	0,00	0,00	0,00	0,00	0,00	0,00
$DEVsvCorHP1$	0,01	0,01	0,01	0,00	0,00	0,01	0,01	0,00	0,01	0,01	0,01	0,00	0,01	0,00	0,00	0,00	0,00	0,00	0,00	0,00
$DEVsvCorHP2$	0,01	0,01	0,02	0,00	0,00	0,01	0,01	0,00	0,01	0,01	0,01	0,00	0,00	0,00	0,00	0,00	0,00	0,00	0,00	0,00
$DEVsvASenO$	0,00	0,00	0,01	0,00	0,00	0,00	0,01	0,00	0,00	0,00	0,01	0,00	0,01	0,00	0,00	0,00	0,00	0,00	0,00	0,00
$DEVsvBSenO$	0,00	0,01	0,00	0,00	0,00	0,00	0,00	0,00	0,00	0,00	0,00	0,00	0,01	0,00	0,00	0,00	0,00	0,00	0,00	0,00
$DEVbvStic1$	0,00	0,00	0,01	0,01	0,00	0,00	0,01	0,01	0,00	0,00	0,00	0,01	0,00	0,00	0,00	0,00	0,00	0,00	0,00	0,00
$DEVbvVisc1$	0,00	0,00	0,01	0,00	0,00	0,01	0,02	0,00	0,00	0,00	0,02	0,00	0,01	0,00	0,00	0,00	0,00	0,00	0,00	0,01
$DEVbvStic2$	0,00	0,00	0,01	0,00	0,00	0,01	0,01	0,00	0,00	0,01	0,01	0,00	0,00	0,00	0,00	0,00	0,00	0,00	0,00	0,00
$DEVbvVisc2$	0,01	0,01	0,01	0,00	0,01	0,00	0,01	0,00	0,01	0,01	0,00	0,00	0,00	0,00	0,00	0,00	0,00	0,00	0,00	0,00
$DEVbvDCool1$	0,00	0,00	0,01	0,00	0,00	0,00	0,00	0,00	0,00	0,00	0,00	0,00	0,00	0,00	0,00	0,00	0,00	0,00	0,00	0,00
$DEVbvDCool2$	0,00	0,02	0,00	0,00	0,00	0,02	0,00	0,00	0,00	0,02	0,00	0,00	0,00	0,00	0,00	0,00	0,00	0,00	0,00	0,00
$DEVbvKineFric$	0,01	0,00	0,01	0,00	0,00	0,00	0,02	0,01	0,01	0,00	0,04	0,02	0,01	0,00	0,00	0,00	0,00	0,00	0,00	0,00
$DEVbvCnull$	0,00	0,00	0,02	0,00	0,00	0,01	0,02	0,01	0,00	0,00	0,01	0,01	0,00	0,00	0,00	0,00	0,00	0,00	0,00	0,00
$DEVbvDnozzle$	0,00	0,00	0,02	0,00	0,00	0,01	0,02	0,01	0,00	0,00	0,01	0,01	0,00	0,00	0,00	0,00	0,00	0,00	0,00	0,00
$DEVbvKfeed$	0,00	0,01	0,01	0,00	0,00	0,02	0,01	0,00	0,00	0,02	0,00	0,00	0,00	0,00	0,00	0,00	0,00	0,00	0,00	0,00
$DEVbvSticspool$	0,00	0,00	0,01	0,01	0,00	0,00	0,01	0,01	0,00	0,00	0,01	0,01	0,00	0,00	0,00	0,00	0,00	0,00	0,00	0,00
$DEVbvDFilter1$	0,00	0,00	0,02	0,01	0,00	0,01	0,02	0,01	0,00	0,00	0,02	0,01	0,00	0,00	0,00	0,00	0,00	0,00	0,00	0,00
$DEVbvDFilter2$	0,01	0,01	0,01	0,01	0,00	0,01	0,01	0,01	0,01	0,01	0,01	0,01	0,01	0,00	0,00	0,00	0,00	0,00	0,00	0,00
$DEVbvCorHP1$	0,00	0,01	0,02	0,00	0,00	0,01	0,03	0,00	0,01	0,01	0,01	0,00	0,00	0,00	0,00	0,00	0,00	0,00	0,00	0,00
$DEVbvCorHP2$	0,00	0,01	0,01	0,00	0,00	0,01	0,01	0,00	0,00	0,00	0,00	0,00	0,01	0,00	0,00	0,00	0,00	0,00	0,00	0,00
$DEVbvASenO$	0,00	0,01	0,01	0,00	0,00	0,00	0,00	0,00	0,00	0,01	0,01	0,00	0,00	0,00	0,00	0,00	0,00	0,00	0,00	0,00
$DEVbvBSenO$	0,00	0,02	0,00	0,00	0,00	0,07	0,00	0,00	0,00	0,01	0,00	0,00	0,00	0,00	0,00	0,00	0,00	0,00	0,00	0,00
$EStaLaw$	0,00	0,00	0,02	0,01	0,00	0,01	0,02	0,01	0,01	0,01	0,02	0,01	0,01	0,00	0,00	0,00	0,00	0,00	0,00	0,00

	$FmvMAErr$	$Sovdelop1$	$Sovdelclo$	$Sovdelop2$	$VoN2maxSOV$	$SOVoN2max$	$SOVoN2mean$	$VoN2maxBYV$	$BYVoN2max$	$BYVoN2mean$	$LppSlpN2DP$	$LppR2N2DP$	$wTBV$	$wSOV$	$MfpSlpN2DP$	$MfpR2N2DP$	$MffSlpN2DP$	$MffR2N2DP$	$WfmmaxX1$	$WfmmaxX2$
$CTfuel$	0,01	0,03	0,00	0,02	0,00	0,00	0,01	0,00	0,00	0,02	0,04	0,02	0,01	0,03	0,03	0,02	0,01	0,03	0,01	0,01
$DLppDIlkg$	0,00	0,00	0,00	0,00	0,00	0,00	0,01	0,01	0,00	0,01	0,01	0,02	0,00	0,00	0,01	0,01	0,00	0,02	0,00	0,00
$DMfpDIlkg$	0,00	0,00	0,00	0,00	0,02	0,02	0,01	0,09	0,14	0,03	0,02	0,02	0,02	0,01	0,00	0,00	0,00	0,01	0,00	0,00
$DEMffFlowRate$	0,00	0,03	0,00	0,01	0,01	0,00	0,01	0,01	0,00	0,00	0,02	0,02	0,00	0,00	0,49	0,14	0,88	0,15	0,00	0,00
$ETbvPopen$	0,00	0,01	0,00	0,01	0,02	0,04	0,01	0,15	0,14	0,01	0,01	0,01	0,11	0,00	0,01	0,01	0,00	0,01	0,00	0,00
$DTbvDIlkg$	0,00	0,01	0,02	0,01	0,00	0,00	0,01	0,01	0,03	0,01	0,02	0,02	0,02	0,01	0,00	0,00	0,00	0,01	0,01	0,01
$DEWfmASenO$	0,00	0,02	0,00	0,02	0,00	0,00	0,01	0,01	0,00	0,01	0,02	0,02	0,01	0,01	0,00	0,02	0,01	0,03	0,00	0,00
$DEWfmBSenO$	0,00	0,02	0,00	0,02	0,01	0,00	0,01	0,01	0,01	0,00	0,01	0,04	0,02	0,01	0,01	0,00	0,00	0,01	0,01	0,01
$EByvDPist0$	0,04	0,02	0,02	0,03	0,03	0,00	0,01	0,04	0,00	0,04	0,02	0,02	0,01	0,01	0,01	0,04	0,00	0,02	0,00	0,00
$DEByvK0$	0,06	0,02	0,00	0,05	0,08	0,02	0,04	0,06	0,04	0,03	0,00	0,00	0,06	0,01	0,01	0,02	0,00	0,01	0,03	0,03
$DEByvVisc$	0,00	0,01	0,00	0,01	0,04	0,00	0,01	0,06	0,00	0,01	0,02	0,02	0,01	0,00	0,00	0,00	0,00	0,02	0,00	0,00
$DEByvStic$	0,00	0,00	0,01	0,01	0,04	0,06	0,01	0,11	0,15	0,02	0,02	0,02	0,04	0,00	0,01	0,06	0,00	0,02	0,00	0,00
$DByvDIlkg$	0,06	0,01	0,02	0,01	0,02	0,14	0,04	0,02	0,31	0,17	0,02	0,02	0,09	0,02	0,02	0,01	0,00	0,01	0,09	0,09
$ESovDPist$	0,01	0,01	0,00	0,01	0,00	0,00	0,01	0,00	0,00	0,03	0,02	0,02	0,00	0,01	0,07	0,09	0,00	0,02	0,00	0,00
$DESovVisc$	0,00	0,01	0,01	0,01	0,02	0,00	0,01	0,02	0,00	0,00	0,03	0,02	0,02	0,00	0,00	0,01	0,00	0,01	0,00	0,00
$DESovStic$	0,00	0,03	0,00	0,03	0,00	0,00	0,01	0,00	0,01	0,01	0,02	0,00	0,00	0,02	0,00	0,26	0,00	0,00	0,01	0,01
$DSovDIlkg$	0,00	0,14	0,10	0,11	0,10	0,54	0,02	0,13	0,01	0,07	0,02	0,01	0,26	0,54	0,08	0,02	0,00	0,02	0,00	0,00
$DSovDelay$	0,01	0,01	0,58	0,01	0,24	0,13	0,01	0,01	0,00	0,01	0,02	0,01	0,03	0,01	0,01	0,01	0,00	0,02	0,00	0,00
$DEFmvStic$	0,01	0,01	0,00	0,00	0,00	0,00	0,00	0,00	0,00	0,03	0,03	0,04	0,02	0,01	0,00	0,00	0,00	0,01	0,02	0,01
$DEFmvCnull$	0,12	0,02	0,00	0,01	0,00	0,00	0,08	0,00	0,01	0,03	0,01	0,00	0,01	0,01	0,01	0,01	0,00	0,02	0,06	0,06
$DEFmvDnozzle$	0,07	0,04	0,00	0,07	0,00	0,00	0,01	0,01	0,00	0,01	0,02	0,03	0,02	0,03	0,01	0,01	0,00	0,02	0,00	0,00
$DEFmvASenO$	0,00	0,00	0,01	0,00	0,01	0,00	0,16	0,00	0,00	0,07	0,02	0,01	0,01	0,00	0,00	0,01	0,00	0,01	0,27	0,27
$DEFmvBSenO$	0,00	0,00	0,00	0,00	0,00	0,00	0,13	0,00	0,00	0,11	0,03	0,02	0,01	0,00	0,00	0,00	0,00	0,02	0,26	0,26
$DFmvDIlkg$	0,47	0,07	0,00	0,07	0,00	0,00	0,08	0,00	0,01	0,03	0,02	0,02	0,01	0,01	0,01	0,02	0,00	0,02	0,12	0,12
$DEVsvStic1$	0,00	0,00	0,00	0,01	0,00	0,00	0,01	0,00	0,00	0,01	0,02	0,00	0,00	0,00	0,01	0,00	0,00	0,00	0,00	0,00
$DEVsvVisc1$	0,00	0,02	0,00	0,02	0,01	0,00	0,01	0,00	0,00	0,01	0,01	0,01	0,02	0,00	0,01	0,01	0,00	0,01	0,00	0,00
$DEVsvStic2$	0,00	0,02	0,00	0,01	0,00	0,00	0,01	0,00	0,01	0,01	0,02	0,02	0,00	0,01	0,01	0,00	0,00	0,02	0,00	0,00
$DEVsvVisc2$	0,00	0,05	0,00	0,05	0,01	0,00	0,01	0,00	0,00	0,01	0,02	0,02	0,00	0,01	0,01	0,01	0,00	0,01	0,00	0,00
$DEVsvDCool1$	0,00	0,00	0,00	0,00	0,00	0,00	0,01	0,00	0,00	0,01	0,02	0,02	0,00	0,00	0,00	0,00	0,00	0,01	0,00	0,00
$DEVsvDCool2$	0,01	0,01	0,00	0,01	0,04	0,00	0,01	0,00	0,01	0,01	0,02	0,00	0,01	0,00	0,00	0,00	0,00	0,01	0,00	0,00
$DEVsvKineFric$	0,00	0,00	0,01	0,00	0,00	0,00	0,01	0,00	0,00	0,01	0,02	0,02	0,00	0,00	0,01	0,01	0,00	0,01	0,00	0,00
$DEVsvCnull$	0,01	0,02	0,00	0,02	0,00	0,00	0,01	0,00	0,01	0,01	0,02	0,02	0,00	0,01	0,00	0,01	0,00	0,02	0,00	0,00
$DEVsvDnozzle$	0,01	0,02	0,00	0,02	0,00	0,00	0,01	0,00	0,00	0,01	0,01	0,03	0,00	0,01	0,01	0,01	0,00	0,02	0,00	0,00
$DEVsvKfeed$	0,00	0,01	0,00	0,00	0,00	0,00	0,01	0,01	0,00	0,00	0,02	0,03	0,01	0,00	0,01	0,03	0,00	0,02	0,00	0,00
$DEVsvSticspool$	0,01	0,03	0,00	0,03	0,09	0,00	0,01	0,01	0,00	0,01	0,01	0,01	0,00	0,01	0,00	0,01	0,00	0,02	0,00	0,00
$DEVsvDFilter1$	0,00	0,02	0,00	0,01	0,00	0,00	0,01	0,00	0,00	0,00	0,02	0,02	0,01	0,01	0,00	0,00	0,00	0,01	0,00	0,00
$DEVsvDFilter2$	0,01	0,01	0,00	0,02	0,01	0,00	0,01	0,00	0,00	0,01	0,01	0,02	0,01	0,01	0,00	0,00	0,00	0,01	0,00	0,00
$DEVsvCorHP1$	0,00	0,01	0,00	0,01	0,00	0,00	0,01	0,00	0,00	0,01	0,02	0,02	0,00	0,01	0,02	0,01	0,00	0,01	0,00	0,00
$DEVsvCorHP2$	0,00	0,02	0,01	0,01	0,00	0,00	0,01	0,01	0,00	0,01	0,01	0,01	0,00	0,01	0,00	0,01	0,00	0,00	0,00	0,00
$DEVsvASenO$	0,00	0,01	0,00	0,01	0,04	0,00	0,01	0,01	0,01	0,01	0,02	0,01	0,01	0,00	0,00	0,00	0,00	0,01	0,01	0,01
$DEVsvBSenO$	0,00	0,00	0,00	0,00	0,06	0,00	0,01	0,00	0,00	0,01	0,02	0,03	0,01	0,00	0,00	0,00	0,00	0,01	0,00	0,00
$DEVbvStic1$	0,00	0,03	0,01	0,02	0,00	0,00	0,01	0,00	0,00	0,01	0,01	0,01	0,00	0,01	0,00	0,00	0,00	0,00	0,00	0,00
$DEVbvVisc1$	0,00	0,00	0,01	0,01	0,00	0,00	0,01	0,01	0,00	0,01	0,02	0,02	0,01	0,00	0,01	0,01	0,00	0,02	0,00	0,00
$DEVbvStic2$	0,00	0,01	0,00	0,01	0,00	0,00	0,01	0,01	0,01	0,00	0,01	0,01	0,00	0,01	0,02	0,01	0,00	0,02	0,00	0,00
$DEVbvVisc2$	0,00	0,02	0,01	0,03	0,00	0,00	0,01	0,01	0,01	0,01	0,02	0,01	0,00	0,01	0,00	0,00	0,00	0,01	0,00	0,00
$DEVbvDCool1$	0,00	0,00	0,00	0,00	0,00	0,00	0,01	0,00	0,00	0,01	0,01	0,01	0,01	0,00	0,00	0,01	0,00	0,01	0,00	0,00
$DEVbvDCool2$	0,00	0,00	0,00	0,00	0,00	0,00	0,01	0,00	0,00	0,01	0,02	0,02	0,00	0,00	0,00	0,00	0,00	0,01	0,00	0,00
$DEVbvKineFric$	0,00	0,01	0,00	0,01	0,01	0,00	0,01	0,02	0,01	0,00	0,01	0,01	0,02	0,01	0,00	0,02	0,00	0,01	0,01	0,00
$DEVbvCnull$	0,00	0,04	0,01	0,04	0,00	0,00	0,01	0,00	0,00	0,01	0,02	0,01	0,00	0,02	0,00	0,01	0,00	0,04	0,00	0,00
$DEVbvDnozzle$	0,00	0,01	0,01	0,01	0,00	0,00	0,01	0,01	0,00	0,00	0,01	0,01	0,00	0,01	0,01	0,02	0,00	0,02	0,00	0,00
$DEVbvKfeed$	0,00	0,01	0,00	0,01	0,01	0,00	0,01	0,00	0,00	0,01	0,01	0,02	0,00	0,01	0,00	0,01	0,00	0,02	0,00	0,00
$DEVbvSticspool$	0,01	0,01	0,00	0,01	0,00	0,00	0,01	0,01	0,00	0,01	0,02	0,03	0,01	0,01	0,00	0,01	0,00	0,01	0,00	0,00
$DEVbvDFilter1$	0,00	0,01	0,00	0,01	0,01	0,00	0,01	0,00	0,00	0,01	0,02	0,02	0,01	0,00	0,01	0,00	0,00	0,02	0,00	0,00
$DEVbvDFilter2$	0,00	0,01	0,00	0,01	0,00	0,00	0,01	0,01	0,00	0,01	0,02	0,02	0,00	0,01	0,00	0,00	0,00	0,01	0,00	0,00
$DEVbvCorHP1$	0,00	0,04	0,01	0,04	0,00	0,00	0,01	0,04	0,00	0,01	0,02	0,01	0,03	0,01	0,01	0,01	0,00	0,02	0,00	0,00
$DEVbvCorHP2$	0,00	0,02	0,02	0,01	0,00	0,00	0,01	0,01	0,00	0,01	0,02	0,02	0,01	0,01	0,00	0,01	0,00	0,01	0,00	0,00
$DEVbvASenO$	0,00	0,00	0,00	0,00	0,00	0,00	0,01	0,00	0,00	0,01	0,02	0,02	0,00	0,00	0,00	0,01	0,00	0,01	0,00	0,00
$DEVbvBSenO$	0,00	0,00	0,00	0,00	0,00	0,00	0,01	0,02	0,00	0,01	0,01	0,02	0,00	0,00	0,00	0,00	0,00	0,01	0,00	0,00
$EStaLaw$	0,00	0,02	0,08	0,02	0,02	0,03	0,01	0,01	0,02	0,01	0,01	0,01	0,01	0,01	0,01	0,01	0,00	0,01	0,00	0,00

	$WfmminX1$	$WfmminX2$	$WfmmaxGapX$	$WfmminGapX$	$WfmmeanGapX$	$WfmstdGapX$	$VsvCEquA$	$VsvXnullA$	$VsvYnullA$	$VsvXoverlapA$	$VsvYoverlapA$	$VsvScaleA$	$VsvSlpLeftA$	$VsvSlpNullA$	$VsvSlpRightA$	$VsvHyst0A$	$VsvCEquB$	$VsvXnullB$	$VsvYnullB$	$VsvXoverlapB$
$CTfuel$	0,00	0,00	0,00	0,00	0,00	0,00	0,00	0,00	0,00	0,01	0,00	0,01	0,00	0,00	0,00	0,01	0,00	0,00	0,00	0,01
$DLppDIlkg$	0,00	0,00	0,00	0,00	0,00	0,01	0,00	0,00	0,00	0,01	0,02	0,01	0,00	0,00	0,00	0,02	0,00	0,00	0,00	0,02
$DMfpDIlkg$	0,00	0,00	0,00	0,00	0,00	0,00	0,00	0,01	0,01	0,03	0,00	0,01	0,02	0,00	0,00	0,03	0,00	0,01	0,00	0,01
$DEMffFlowRate$	0,00	0,00	0,00	0,00	0,00	0,00	0,00	0,01	0,00	0,02	0,00	0,01	0,00	0,00	0,00	0,02	0,00	0,01	0,00	0,01
$ETbvPopen$	0,00	0,00	0,00	0,00	0,00	0,01	0,00	0,00	0,00	0,01	0,01	0,00	0,01	0,00	0,00	0,01	0,00	0,00	0,00	0,01
$DTbvDIlkg$	0,00	0,00	0,00	0,00	0,00	0,01	0,00	0,00	0,00	0,01	0,01	0,01	0,00	0,00	0,00	0,02	0,00	0,00	0,00	0,01
$DEWfmASen0$	1,00	0,00	0,45	0,46	0,49	0,28	0,00	0,00	0,00	0,01	0,00	0,01	0,00	0,00	0,00	0,01	0,00	0,00	0,00	0,01
$DEWfmBSen0$	0,00	1,00	0,38	0,44	0,51	0,26	0,00	0,01	0,01	0,02	0,01	0,01	0,00	0,00	0,00	0,01	0,00	0,01	0,00	0,00
$EByvDPist0$	0,00	0,00	0,00	0,00	0,00	0,01	0,00	0,00	0,01	0,00	0,00	0,02	0,01	0,00	0,00	0,01	0,00	0,00	0,00	0,01
$DEByvK0$	0,00	0,00	0,01	0,00	0,00	0,01	0,00	0,00	0,01	0,01	0,01	0,02	0,00	0,00	0,01	0,03	0,00	0,00	0,00	0,01
$DEByvVisc$	0,00	0,00	0,00	0,00	0,00	0,01	0,00	0,01	0,01	0,01	0,01	0,01	0,00	0,00	0,00	0,02	0,00	0,01	0,00	0,01
$DEByvStic$	0,00	0,00	0,00	0,00	0,00	0,02	0,00	0,00	0,01	0,01	0,00	0,01	0,00	0,00	0,00	0,02	0,00	0,00	0,00	0,01
$DByvDIlkg$	0,00	0,00	0,00	0,00	0,00	0,00	0,00	0,01	0,01	0,04	0,02	0,04	0,01	0,00	0,05	0,02	0,00	0,01	0,01	0,04
$ESovDPist$	0,00	0,00	0,00	0,00	0,00	0,00	0,00	0,01	0,01	0,05	0,04	0,02	0,00	0,00	0,03	0,01	0,00	0,01	0,00	0,03
$DESovVisc$	0,00	0,00	0,01	0,00	0,00	0,01	0,00	0,01	0,00	0,00	0,00	0,00	0,00	0,00	0,00	0,02	0,00	0,01	0,00	0,00
$DESovStic$	0,00	0,00	0,00	0,00	0,00	0,01	0,00	0,00	0,00	0,01	0,01	0,01	0,01	0,00	0,00	0,02	0,00	0,00	0,00	0,00
$DSovDIlkg$	0,00	0,00	0,00	0,00	0,00	0,00	0,00	0,00	0,01	0,02	0,00	0,03	0,00	0,00	0,04	0,01	0,00	0,00	0,00	0,01
$DSovDelay$	0,00	0,00	0,00	0,00	0,00	0,01	0,00	0,00	0,00	0,01	0,01	0,01	0,00	0,00	0,00	0,02	0,00	0,00	0,00	0,01
$DEFmvStic$	0,00	0,00	0,00	0,00	0,00	0,00	0,00	0,00	0,00	0,02	0,01	0,01	0,01	0,00	0,00	0,01	0,00	0,00	0,00	0,02
$DEFmvCnull$	0,00	0,00	0,01	0,00	0,00	0,01	0,00	0,00	0,01	0,01	0,01	0,01	0,00	0,00	0,01	0,01	0,00	0,00	0,00	0,01
$DEFmvDnozzle$	0,00	0,00	0,00	0,00	0,00	0,00	0,00	0,01	0,01	0,01	0,01	0,01	0,00	0,00	0,00	0,03	0,00	0,01	0,00	0,02
$DEFmvASen0$	0,00	0,00	0,00	0,00	0,00	0,00	0,00	0,00	0,01	0,00	0,00	0,01	0,00	0,00	0,01	0,01	0,00	0,00	0,00	0,00
$DEFmvBSen0$	0,00	0,00	0,00	0,00	0,00	0,00	0,00	0,00	0,00	0,00	0,01	0,01	0,00	0,00	0,00	0,01	0,00	0,00	0,00	0,00
$DFmvDIlkg$	0,00	0,00	0,00	0,00	0,00	0,01	0,00	0,01	0,00	0,01	0,01	0,01	0,00	0,00	0,00	0,02	0,00	0,01	0,00	0,01
$DEVsvStic1$	0,00	0,00	0,00	0,01	0,00	0,00	0,00	0,00	0,01	0,02	0,00	0,01	0,00	0,00	0,00	0,03	0,00	0,00	0,00	0,02
$DEVsvVisc1$	0,00	0,00	0,00	0,00	0,00	0,00	0,00	0,00	0,00	0,00	0,00	0,01	0,00	0,00	0,00	0,02	0,00	0,00	0,00	0,00
$DEVsvStic2$	0,00	0,00	0,00	0,00	0,00	0,01	0,00	0,00	0,01	0,00	0,01	0,01	0,00	0,00	0,00	0,03	0,00	0,00	0,00	0,01
$DEVsvVisc2$	0,00	0,00	0,01	0,00	0,00	0,01	0,00	0,00	0,00	0,00	0,00	0,01	0,00	0,00	0,00	0,03	0,00	0,00	0,00	0,00
$DEVsvDCool1$	0,00	0,00	0,00	0,00	0,00	0,02	0,00	0,00	0,00	0,00	0,01	0,01	0,00	0,00	0,00	0,01	0,00	0,00	0,00	0,01
$DEVsvDCool2$	0,00	0,00	0,00	0,00	0,00	0,00	0,11	0,04	0,21	0,05	0,01	0,09	0,17	0,01	0,00	0,02	0,11	0,04	0,29	0,07
$DEVsvKineFric$	0,00	0,00	0,00	0,00	0,00	0,01	0,00	0,25	0,38	0,16	0,31	0,32	0,16	0,76	0,48	0,02	0,00	0,26	0,48	0,23
$DEVsvCnull$	0,00	0,00	0,00	0,00	0,00	0,02	0,76	0,49	0,02	0,02	0,01	0,00	0,02	0,00	0,00	0,01	0,72	0,46	0,00	0,01
$DEVsvDnozzle$	0,00	0,00	0,01	0,00	0,00	0,01	0,00	0,01	0,01	0,02	0,00	0,00	0,01	0,00	0,00	0,01	0,00	0,01	0,00	0,00
$DEVsvKfeed$	0,00	0,00	0,00	0,00	0,00	0,00	0,01	0,00	0,01	0,02	0,02	0,05	0,01	0,01	0,07	0,01	0,02	0,00	0,01	0,02
$DEVsvSticspool$	0,00	0,00	0,01	0,00	0,00	0,01	0,00	0,01	0,11	0,16	0,25	0,01	0,33	0,20	0,12	0,03	0,00	0,01	0,13	0,17
$DEVsvDFilter1$	0,00	0,00	0,00	0,00	0,00	0,00	0,00	0,00	0,00	0,03	0,01	0,01	0,00	0,00	0,00	0,02	0,00	0,00	0,00	0,01
$DEVsvDFilter2$	0,00	0,00	0,00	0,00	0,00	0,01	0,00	0,00	0,02	0,01	0,01	0,01	0,01	0,00	0,00	0,02	0,00	0,00	0,01	0,02
$DEVsvCorHP1$	0,00	0,00	0,00	0,00	0,00	0,01	0,00	0,00	0,00	0,00	0,00	0,01	0,00	0,00	0,00	0,01	0,00	0,00	0,00	0,00
$DEVsvCorHP2$	0,00	0,00	0,00	0,00	0,00	0,02	0,00	0,00	0,01	0,02	0,01	0,00	0,01	0,00	0,01	0,02	0,00	0,00	0,00	0,01
$DEVsvASen0$	0,00	0,00	0,00	0,00	0,00	0,00	0,00	0,00	0,00	0,00	0,00	0,01	0,00	0,00	0,00	0,01	0,01	0,00	0,00	0,01
$DEVsvBSen0$	0,00	0,00	0,00	0,00	0,00	0,00	0,00	0,00	0,01	0,02	0,00	0,01	0,02	0,00	0,01	0,01	0,00	0,00	0,00	0,00
$DEVbvStic1$	0,00	0,00	0,01	0,00	0,00	0,01	0,00	0,01	0,00	0,01	0,01	0,02	0,00	0,00	0,00	0,02	0,00	0,01	0,00	0,01
$DEVbvVisc1$	0,00	0,00	0,00	0,00	0,00	0,00	0,00	0,00	0,00	0,00	0,00	0,01	0,01	0,00	0,00	0,02	0,00	0,00	0,00	0,01
$DEVbvStic2$	0,00	0,00	0,00	0,00	0,00	0,00	0,00	0,00	0,01	0,00	0,00	0,01	0,01	0,00	0,00	0,03	0,00	0,00	0,00	0,00
$DEVbvVisc2$	0,00	0,00	0,00	0,00	0,00	0,02	0,00	0,00	0,01	0,01	0,01	0,01	0,00	0,00	0,00	0,02	0,00	0,00	0,00	0,01
$DEVbvDCool1$	0,00	0,00	0,00	0,00	0,00	0,00	0,00	0,00	0,00	0,00	0,00	0,01	0,00	0,00	0,00	0,01	0,00	0,00	0,00	0,00
$DEVbvDCool2$	0,00	0,00	0,00	0,00	0,00	0,01	0,00	0,00	0,00	0,00	0,00	0,01	0,01	0,00	0,00	0,02	0,00	0,00	0,00	0,00
$DEVbvKineFric$	0,00	0,00	0,01	0,00	0,00	0,00	0,00	0,01	0,01	0,00	0,00	0,01	0,00	0,00	0,00	0,03	0,00	0,01	0,01	0,00
$DEVbvCnull$	0,00	0,00	0,00	0,00	0,00	0,00	0,00	0,00	0,00	0,02	0,00	0,01	0,00	0,00	0,00	0,00	0,00	0,00	0,00	0,01
$DEVbvDnozzle$	0,00	0,00	0,01	0,00	0,00	0,03	0,00	0,00	0,01	0,01	0,00	0,01	0,01	0,00	0,00	0,01	0,00	0,00	0,00	0,00
$DEVbvKfeed$	0,00	0,00	0,01	0,00	0,00	0,01	0,00	0,00	0,01	0,02	0,02	0,01	0,00	0,00	0,00	0,02	0,00	0,00	0,00	0,01
$DEVbvSticspool$	0,00	0,00	0,00	0,00	0,00	0,00	0,00	0,00	0,00	0,00	0,00	0,01	0,01	0,00	0,00	0,02	0,00	0,00	0,00	0,01
$DEVbvDFilter1$	0,00	0,00	0,00	0,01	0,00	0,01	0,00	0,01	0,01	0,00	0,00	0,02	0,01	0,00	0,00	0,03	0,00	0,01	0,00	0,00
$DEVbvDFilter2$	0,00	0,00	0,00	0,01	0,00	0,01	0,00	0,00	0,00	0,00	0,00	0,01	0,01	0,00	0,00	0,02	0,00	0,00	0,00	0,00
$DEVbvCorHP1$	0,00	0,00	0,01	0,00	0,00	0,02	0,00	0,01	0,00	0,02	0,02	0,01	0,00	0,00	0,00	0,01	0,00	0,01	0,00	0,02
$DEVbvCorHP2$	0,00	0,00	0,00	0,00	0,00	0,02	0,00	0,00	0,00	0,01	0,00	0,01	0,00	0,00	0,00	0,02	0,00	0,00	0,00	0,01
$DEVbvASen0$	0,00	0,00	0,00	0,00	0,00	0,00	0,00	0,00	0,00	0,01	0,01	0,01	0,00	0,00	0,00	0,01	0,00	0,00	0,00	0,02
$DEVbvBSen0$	0,00	0,00	0,00	0,00	0,00	0,02	0,00	0,00	0,00	0,00	0,02	0,01	0,00	0,00	0,00	0,00	0,00	0,00	0,00	0,00
$EStaLaw$	0,00	0,00	0,00	0,00	0,00	0,00	0,00	0,00	0,01	0,01	0,01	0,01	0,03	0,00	0,00	0,01	0,00	0,00	0,00	0,02

	$VsvYoverlapB$	$VsvScaleB$	$VsvSlpLeftB$	$VsvSlpNullB$	$VsvSlpRightB$	$VsvHyst0B$	$VsvCEquS$	$VsvXnullS$	$VsvYnullS$	$VsvXoverlapS$	$VsvYoverlapS$	$VsvScaleS$	$VsvSlpLeftS$	$VsvSlpNullS$	$VsvSlpRightS$	$VsvHyst0S$	$VsvmaxX1$	$VsvmaxX2$	$VsvminX1$	$VsvminX2$
$CTfuel$	0,01	0,01	0,03	0,00	0,00	0,00	0,00	0,01	0,01	0,02	0,01	0,01	0,01	0,01	0,00	0,00	0,01	0,02	0,01	0,01
$DLppDIlkg$	0,03	0,01	0,01	0,00	0,00	0,00	0,00	0,01	0,00	0,02	0,01	0,01	0,00	0,01	0,00	0,00	0,01	0,02	0,01	0,01
$DMfpDIlkg$	0,00	0,01	0,02	0,00	0,00	0,00	0,00	0,00	0,01	0,00	0,00	0,01	0,00	0,00	0,00	0,00	0,01	0,01	0,01	0,01
$DEMffFlowRate$	0,00	0,01	0,00	0,00	0,00	0,00	0,00	0,00	0,02	0,02	0,01	0,01	0,01	0,02	0,00	0,00	0,00	0,02	0,01	0,01
$ETbvPopen$	0,01	0,00	0,01	0,00	0,00	0,00	0,00	0,00	0,02	0,00	0,01	0,00	0,00	0,01	0,01	0,00	0,01	0,02	0,01	0,02
$DTbvDIlkg$	0,01	0,01	0,01	0,00	0,00	0,00	0,00	0,01	0,02	0,01	0,01	0,01	0,02	0,01	0,01	0,00	0,01	0,01	0,01	0,01
$DEWfmASenO$	0,00	0,01	0,01	0,00	0,00	0,00	0,00	0,02	0,01	0,01	0,00	0,00	0,02	0,01	0,00	0,00	0,02	0,01	0,01	0,01
$DEWfmBSenO$	0,01	0,00	0,01	0,00	0,00	0,00	0,00	0,01	0,01	0,01	0,01	0,01	0,00	0,01	0,00	0,00	0,02	0,00	0,01	0,01
$EByvDPist0$	0,00	0,03	0,01	0,00	0,00	0,01	0,00	0,01	0,01	0,01	0,01	0,01	0,01	0,00	0,00	0,00	0,01	0,00	0,01	0,01
$DEByvK0$	0,01	0,02	0,00	0,00	0,01	0,00	0,00	0,01	0,03	0,03	0,03	0,01	0,01	0,00	0,01	0,00	0,02	0,01	0,01	0,01
$DEByvVisc$	0,01	0,01	0,00	0,00	0,00	0,00	0,00	0,01	0,02	0,03	0,01	0,01	0,01	0,02	0,00	0,00	0,01	0,02	0,01	0,01
$DEByvStic$	0,00	0,01	0,00	0,00	0,00	0,00	0,00	0,00	0,01	0,01	0,02	0,01	0,02	0,01	0,01	0,00	0,02	0,01	0,01	0,01
$DByvDIlkg$	0,02	0,04	0,01	0,00	0,05	0,03	0,00	0,01	0,00	0,01	0,01	0,02	0,01	0,01	0,04	0,00	0,01	0,02	0,01	0,01
$ESovDPist$	0,05	0,02	0,00	0,00	0,03	0,00	0,00	0,03	0,03	0,00	0,01	0,01	0,01	0,01	0,05	0,00	0,02	0,02	0,01	0,01
$DESovVisc$	0,00	0,00	0,00	0,00	0,00	0,00	0,00	0,00	0,03	0,02	0,02	0,00	0,01	0,01	0,00	0,00	0,02	0,00	0,02	0,01
$DESovStic$	0,01	0,01	0,01	0,00	0,00	0,00	0,00	0,01	0,00	0,00	0,00	0,01	0,03	0,01	0,01	0,00	0,02	0,02	0,01	0,01
$DSovDIlkg$	0,00	0,03	0,01	0,00	0,04	0,01	0,00	0,02	0,01	0,01	0,00	0,02	0,01	0,01	0,02	0,00	0,01	0,01	0,01	0,01
$DSovDelay$	0,01	0,01	0,00	0,00	0,00	0,01	0,00	0,01	0,01	0,02	0,01	0,01	0,00	0,01	0,00	0,00	0,01	0,02	0,01	0,01
$DEFmvStic$	0,01	0,01	0,00	0,00	0,00	0,00	0,00	0,01	0,01	0,02	0,01	0,01	0,02	0,02	0,00	0,00	0,01	0,02	0,01	0,02
$DEFmvCnull$	0,01	0,01	0,00	0,00	0,01	0,00	0,00	0,01	0,01	0,02	0,01	0,00	0,02	0,02	0,00	0,00	0,01	0,01	0,01	0,01
$DEFmvDnozzle$	0,01	0,01	0,00	0,00	0,00	0,00	0,00	0,01	0,01	0,00	0,01	0,01	0,00	0,01	0,01	0,00	0,01	0,02	0,01	0,01
$DEFmvASenO$	0,01	0,01	0,00	0,00	0,01	0,00	0,00	0,01	0,00	0,01	0,01	0,01	0,01	0,00	0,00	0,00	0,02	0,01	0,01	0,01
$DEFmvBSenO$	0,02	0,01	0,00	0,00	0,00	0,00	0,00	0,01	0,00	0,00	0,00	0,01	0,01	0,00	0,00	0,00	0,01	0,01	0,01	0,01
$DFmvDIlkg$	0,01	0,01	0,01	0,00	0,00	0,01	0,00	0,00	0,01	0,01	0,01	0,01	0,03	0,00	0,01	0,00	0,02	0,01	0,01	0,01
$DEVsvStic1$	0,00	0,01	0,01	0,00	0,00	0,01	0,00	0,00	0,01	0,01	0,01	0,01	0,00	0,00	0,00	0,00	0,01	0,02	0,01	0,02
$DEVsvVisc1$	0,00	0,00	0,00	0,00	0,00	0,00	0,00	0,01	0,01	0,02	0,02	0,00	0,01	0,01	0,00	0,00	0,01	0,01	0,01	0,01
$DEVsvStic2$	0,01	0,01	0,00	0,00	0,00	0,00	0,00	0,01	0,01	0,00	0,00	0,01	0,01	0,01	0,01	0,00	0,01	0,01	0,01	0,01
$DEVsvVisc2$	0,00	0,01	0,01	0,00	0,00	0,00	0,00	0,00	0,01	0,00	0,00	0,01	0,01	0,00	0,00	0,00	0,01	0,01	0,01	0,01
$DEVsvDCool1$	0,01	0,02	0,00	0,00	0,00	0,01	0,00	0,01	0,00	0,01	0,01	0,00	0,00	0,00	0,00	0,00	0,01	0,02	0,01	0,01
$DEVsvDCool2$	0,01	0,11	0,14	0,01	0,00	0,01	0,12	0,03	0,07	0,06	0,04	0,16	0,06	0,01	0,01	0,03	0,02	0,02	0,00	0,00
$DEVsvKineFric$	0,28	0,29	0,25	0,76	0,48	0,00	0,00	0,12	0,03	0,13	0,33	0,37	0,03	0,48	0,57	0,00	0,01	0,02	0,01	0,01
$DEVsvCnull$	0,01	0,00	0,01	0,00	0,00	0,00	0,74	0,42	0,00	0,00	0,00	0,00	0,01	0,00	0,00	0,00	0,02	0,00	0,01	0,01
$DEVsvDnozzle$	0,00	0,00	0,03	0,00	0,00	0,02	0,00	0,01	0,02	0,00	0,01	0,00	0,02	0,01	0,00	0,00	0,01	0,01	0,01	0,01
$DEVsvKfeed$	0,02	0,04	0,03	0,01	0,07	0,19	0,01	0,01	0,01	0,04	0,01	0,03	0,02	0,03	0,01	0,01	0,02	0,02	0,03	0,03
$DEVsvSticspool$	0,24	0,02	0,16	0,20	0,12	0,53	0,00	0,00	0,22	0,02	0,10	0,05	0,10	0,07	0,08	0,89	0,02	0,02	0,03	0,03
$DEVsvDFilter1$	0,01	0,01	0,00	0,00	0,00	0,00	0,00	0,00	0,01	0,01	0,01	0,01	0,01	0,01	0,01	0,00	0,01	0,02	0,01	0,01
$DEVsvDFilter2$	0,01	0,01	0,01	0,00	0,00	0,00	0,00	0,00	0,02	0,02	0,01	0,01	0,01	0,01	0,01	0,00	0,02	0,02	0,01	0,01
$DEVsvCorHP1$	0,00	0,01	0,01	0,00	0,00	0,00	0,00	0,01	0,01	0,01	0,01	0,01	0,01	0,01	0,00	0,00	0,01	0,02	0,01	0,01
$DEVsvCorHP2$	0,01	0,00	0,01	0,00	0,01	0,00	0,00	0,01	0,01	0,02	0,02	0,00	0,03	0,01	0,01	0,00	0,01	0,02	0,01	0,01
$DEVsvASenO$	0,00	0,01	0,02	0,00	0,00	0,00	0,00	0,01	0,03	0,04	0,01	0,01	0,06	0,01	0,01	0,00	0,18	0,00	0,20	0,17
$DEVsvBSenO$	0,00	0,01	0,00	0,00	0,00	0,00	0,00	0,01	0,01	0,05	0,03	0,00	0,05	0,01	0,00	0,00	0,02	0,17	0,21	0,17
$DEVbvStic1$	0,01	0,02	0,01	0,00	0,00	0,00	0,00	0,01	0,01	0,01	0,00	0,01	0,00	0,01	0,00	0,00	0,02	0,02	0,00	0,00
$DEVbvVisc1$	0,01	0,01	0,01	0,00	0,00	0,00	0,00	0,01	0,01	0,00	0,00	0,01	0,01	0,00	0,00	0,00	0,02	0,01	0,01	0,01
$DEVbvStic2$	0,00	0,01	0,01	0,00	0,00	0,00	0,00	0,01	0,02	0,02	0,01	0,01	0,01	0,01	0,00	0,00	0,01	0,02	0,01	0,01
$DEVbvVisc2$	0,01	0,01	0,01	0,00	0,00	0,00	0,00	0,01	0,00	0,01	0,01	0,00	0,02	0,00	0,00	0,00	0,01	0,01	0,01	0,01
$DEVbvDCool1$	0,00	0,01	0,00	0,00	0,00	0,01	0,00	0,00	0,00	0,00	0,00	0,01	0,00	0,00	0,00	0,00	0,02	0,02	0,01	0,01
$DEVbvDCool2$	0,00	0,01	0,00	0,00	0,00	0,00	0,00	0,02	0,03	0,03	0,02	0,00	0,04	0,00	0,00	0,00	0,01	0,01	0,01	0,01
$DEVbvKineFric$	0,00	0,01	0,02	0,00	0,00	0,00	0,00	0,00	0,04	0,04	0,01	0,01	0,02	0,00	0,00	0,00	0,02	0,02	0,01	0,01
$DEVbvCnull$	0,01	0,01	0,01	0,00	0,00	0,01	0,00	0,01	0,03	0,01	0,00	0,01	0,01	0,00	0,01	0,00	0,01	0,03	0,00	0,00
$DEVbvDnozzle$	0,00	0,01	0,01	0,00	0,00	0,00	0,00	0,01	0,02	0,02	0,01	0,01	0,02	0,02	0,01	0,00	0,01	0,00	0,01	0,02
$DEVbvKfeed$	0,02	0,01	0,02	0,00	0,00	0,00	0,00	0,01	0,01	0,03	0,01	0,01	0,02	0,01	0,00	0,00	0,02	0,02	0,01	0,01
$DEVbvSticspool$	0,00	0,01	0,01	0,00	0,00	0,01	0,00	0,01	0,00	0,02	0,01	0,01	0,02	0,00	0,00	0,00	0,01	0,02	0,01	0,01
$DEVbvDFilter1$	0,01	0,02	0,00	0,00	0,00	0,01	0,00	0,00	0,02	0,01	0,01	0,01	0,00	0,00	0,00	0,00	0,01	0,02	0,01	0,01
$DEVbvDFilter2$	0,00	0,01	0,02	0,00	0,00	0,00	0,00	0,01	0,02	0,00	0,00	0,01	0,00	0,01	0,01	0,00	0,01	0,02	0,01	0,01
$DEVbvCorHP1$	0,02	0,01	0,00	0,00	0,00	0,00	0,00	0,01	0,01	0,00	0,01	0,00	0,00	0,00	0,02	0,00	0,01	0,02	0,01	0,01
$DEVbvCorHP2$	0,00	0,01	0,00	0,00	0,00	0,00	0,00	0,00	0,01	0,01	0,01	0,00	0,01	0,00	0,01	0,00	0,01	0,01	0,01	0,01
$DEVbvASenO$	0,01	0,01	0,00	0,00	0,00	0,00	0,00	0,01	0,01	0,01	0,00	0,00	0,01	0,01	0,00	0,00	0,01	0,02	0,01	0,01
$DEVbvBSenO$	0,02	0,01	0,00	0,00	0,00	0,01	0,00	0,01	0,00	0,01	0,01	0,00	0,02	0,01	0,00	0,00	0,01	0,02	0,01	0,01
$EStaLaw$	0,01	0,01	0,02	0,00	0,00	0,01	0,00	0,00	0,01	0,01	0,01	0,01	0,03	0,01	0,00	0,00	0,01	0,02	0,01	0,01

	$VsvmaxGapX$	$VsvminGapX$	$VsvmeanGapX$	$VsvstdGapX$	$VsvMAErr$	$VbvCEquA$	$VbvXchgA$	$VbvYchgA$	$VbvScaleA$	$VbvSlpLeftA$	$VbvSlpRightA$	$VbvHyst0A$	$VbvCEquB$	$VbvXchgB$	$VbvYchgB$	$VbvScaleB$	$VbvSlpLeftB$	$VbvSlpRightB$	$VbvHyst0B$	$VbvCEquS$
$CTfuel$	0,00	0,00	0,00	0,00	0,01	0,00	0,00	0,02	0,00	0,04	0,04	0,00	0,00	0,00	0,02	0,00	0,00	0,06	0,00	0,01
$DLppDIlkg$	0,00	0,00	0,00	0,00	0,00	0,00	0,00	0,01	0,00	0,01	0,00	0,00	0,00	0,01	0,02	0,00	0,01	0,04	0,00	0,01
$DMfpDIlkg$	0,00	0,00	0,00	0,00	0,00	0,00	0,00	0,01	0,01	0,01	0,01	0,00	0,00	0,01	0,01	0,00	0,00	0,00	0,01	0,01
$DEMffFlowRate$	0,00	0,00	0,00	0,00	0,02	0,00	0,00	0,01	0,00	0,01	0,02	0,00	0,00	0,01	0,01	0,00	0,00	0,02	0,00	0,01
$ETbvPopen$	0,00	0,00	0,00	0,00	0,01	0,00	0,00	0,01	0,00	0,02	0,00	0,00	0,00	0,00	0,01	0,00	0,00	0,03	0,00	0,01
$DTbvDIlkg$	0,00	0,00	0,00	0,00	0,02	0,00	0,00	0,02	0,04	0,04	0,02	0,00	0,00	0,01	0,02	0,00	0,00	0,02	0,00	0,01
$DEWfmASenO$	0,00	0,00	0,00	0,00	0,01	0,00	0,00	0,01	0,01	0,01	0,02	0,00	0,00	0,00	0,02	0,00	0,00	0,05	0,00	0,01
$DEWfmBSenO$	0,00	0,00	0,00	0,00	0,01	0,00	0,01	0,04	0,02	0,03	0,03	0,00	0,00	0,01	0,03	0,00	0,00	0,05	0,00	0,01
$EByvDPist0$	0,00	0,00	0,00	0,00	0,02	0,00	0,00	0,02	0,01	0,01	0,01	0,00	0,01	0,00	0,01	0,01	0,00	0,01	0,00	0,01
$DEByvK0$	0,00	0,00	0,00	0,00	0,01	0,00	0,00	0,01	0,01	0,01	0,01	0,00	0,00	0,01	0,00	0,01	0,01	0,01	0,01	0,01
$DEByvVisc$	0,00	0,00	0,00	0,00	0,01	0,00	0,00	0,01	0,04	0,01	0,02	0,00	0,00	0,00	0,01	0,01	0,00	0,01	0,00	0,01
$DEByvStic$	0,00	0,00	0,00	0,00	0,01	0,00	0,00	0,00	0,01	0,00	0,03	0,00	0,00	0,01	0,00	0,03	0,00	0,02	0,01	0,01
$DByvDIlkg$	0,00	0,00	0,00	0,00	0,02	0,00	0,01	0,09	0,08	0,03	0,06	0,00	0,00	0,01	0,10	0,18	0,08	0,03	0,00	0,01
$ESovDPist$	0,00	0,00	0,00	0,00	0,01	0,00	0,00	0,03	0,02	0,01	0,01	0,00	0,00	0,01	0,02	0,02	0,03	0,01	0,00	0,01
$DESovVisc$	0,00	0,00	0,00	0,00	0,00	0,00	0,00	0,01	0,01	0,01	0,04	0,00	0,00	0,00	0,01	0,01	0,01	0,02	0,00	0,00
$DESovStic$	0,00	0,00	0,00	0,00	0,02	0,00	0,00	0,01	0,01	0,02	0,03	0,00	0,00	0,01	0,01	0,01	0,00	0,03	0,00	0,01
$DSovDIlkg$	0,00	0,00	0,00	0,00	0,01	0,01	0,02	0,03	0,02	0,02	0,04	0,00	0,01	0,02	0,03	0,02	0,03	0,01	0,00	0,01
$DSovDelay$	0,00	0,00	0,00	0,00	0,01	0,00	0,00	0,00	0,00	0,00	0,00	0,00	0,00	0,00	0,00	0,00	0,00	0,01	0,00	0,01
$DEFmvStic$	0,00	0,00	0,00	0,00	0,01	0,00	0,01	0,00	0,00	0,00	0,01	0,00	0,00	0,01	0,01	0,01	0,00	0,01	0,00	0,01
$DEFmvCnull$	0,00	0,00	0,00	0,00	0,03	0,00	0,00	0,02	0,01	0,02	0,01	0,00	0,00	0,01	0,01	0,00	0,00	0,03	0,00	0,01
$DEFmvDnozzle$	0,00	0,00	0,00	0,00	0,02	0,00	0,00	0,00	0,00	0,01	0,01	0,00	0,00	0,00	0,00	0,01	0,00	0,04	0,01	0,01
$DEFmvASenO$	0,00	0,00	0,00	0,00	0,00	0,00	0,00	0,00	0,01	0,00	0,01	0,00	0,00	0,00	0,00	0,00	0,01	0,00	0,01	0,01
$DEFmvBSenO$	0,00	0,00	0,00	0,00	0,01	0,00	0,00	0,00	0,00	0,01	0,01	0,00	0,00	0,01	0,00	0,01	0,01	0,00	0,01	0,01
$DFmvDIlkg$	0,00	0,00	0,00	0,00	0,01	0,00	0,00	0,01	0,03	0,02	0,00	0,00	0,01	0,01	0,01	0,00	0,01	0,03	0,00	0,01
$DEVsvStic1$	0,00	0,00	0,00	0,00	0,01	0,00	0,00	0,00	0,01	0,00	0,00	0,00	0,00	0,00	0,00	0,00	0,00	0,02	0,00	0,01
$DEVsvVisc1$	0,00	0,00	0,00	0,00	0,01	0,00	0,00	0,01	0,00	0,01	0,01	0,00	0,00	0,00	0,01	0,00	0,00	0,01	0,01	0,01
$DEVsvStic2$	0,00	0,00	0,00	0,00	0,01	0,00	0,00	0,00	0,01	0,00	0,01	0,00	0,01	0,01	0,01	0,00	0,00	0,01	0,00	0,01
$DEVsvVisc2$	0,00	0,00	0,00	0,00	0,01	0,00	0,00	0,01	0,00	0,00	0,01	0,00	0,00	0,01	0,01	0,01	0,00	0,01	0,00	0,01
$DEVsvDCool1$	0,00	0,00	0,00	0,00	0,00	0,01	0,00	0,00	0,00	0,00	0,00	0,00	0,01	0,00	0,00	0,00	0,00	0,00	0,00	0,01
$DEVsvDCool2$	0,00	0,00	0,00	0,00	0,01	0,01	0,01	0,00	0,01	0,00	0,01	0,00	0,01	0,00	0,00	0,01	0,00	0,00	0,00	0,01
$DEVsvKineFric$	0,00	0,00	0,00	0,00	0,01	0,00	0,00	0,01	0,01	0,01	0,01	0,00	0,01	0,01	0,01	0,01	0,01	0,00	0,00	0,01
$DEVsvCnull$	0,00	0,00	0,00	0,00	0,01	0,00	0,01	0,02	0,01	0,01	0,00	0,00	0,00	0,01	0,02	0,00	0,00	0,03	0,00	0,01
$DEVsvDnozzle$	0,00	0,00	0,00	0,00	0,01	0,00	0,00	0,03	0,01	0,07	0,03	0,00	0,00	0,01	0,01	0,01	0,00	0,02	0,00	0,01
$DEVsvKfeed$	0,00	0,00	0,00	0,00	0,08	0,00	0,01	0,01	0,02	0,01	0,03	0,00	0,00	0,01	0,00	0,03	0,01	0,02	0,00	0,00
$DEVsvSticspool$	0,00	0,00	0,00	0,00	0,04	0,00	0,00	0,00	0,01	0,01	0,01	0,00	0,00	0,01	0,00	0,02	0,00	0,02	0,00	0,01
$DEVsvDFilter1$	0,00	0,00	0,00	0,00	0,02	0,00	0,00	0,00	0,00	0,01	0,01	0,00	0,00	0,01	0,00	0,00	0,00	0,00	0,00	0,01
$DEVsvDFilter2$	0,00	0,00	0,00	0,00	0,01	0,01	0,00	0,01	0,01	0,01	0,01	0,00	0,01	0,01	0,01	0,00	0,00	0,00	0,00	0,01
$DEVsvCorHP1$	0,00	0,00	0,00	0,00	0,01	0,00	0,00	0,00	0,01	0,01	0,02	0,00	0,00	0,01	0,01	0,00	0,00	0,01	0,00	0,01
$DEVsvCorHP2$	0,00	0,00	0,00	0,00	0,01	0,00	0,01	0,02	0,00	0,02	0,01	0,00	0,00	0,01	0,02	0,01	0,01	0,03	0,00	0,01
$DEVsvASenO$	0,47	0,48	0,50	0,48	0,01	0,01	0,00	0,01	0,01	0,01	0,01	0,00	0,01	0,01	0,00	0,00	0,00	0,00	0,00	0,01
$DEVsvBSenO$	0,50	0,45	0,50	0,48	0,01	0,00	0,00	0,01	0,01	0,01	0,01	0,00	0,00	0,00	0,00	0,00	0,00	0,00	0,01	0,01
$DEVbvStic1$	0,00	0,00	0,00	0,00	0,02	0,01	0,00	0,02	0,04	0,02	0,00	0,00	0,01	0,01	0,01	0,00	0,01	0,02	0,00	0,01
$DEVbvVisc1$	0,00	0,00	0,00	0,00	0,00	0,00	0,00	0,01	0,00	0,02	0,01	0,00	0,01	0,01	0,01	0,00	0,00	0,02	0,00	0,01
$DEVbvStic2$	0,00	0,00	0,00	0,00	0,02	0,00	0,00	0,00	0,01	0,01	0,01	0,00	0,00	0,01	0,00	0,00	0,00	0,01	0,00	0,01
$DEVbvVisc2$	0,00	0,00	0,00	0,00	0,01	0,00	0,01	0,00	0,01	0,01	0,01	0,00	0,00	0,01	0,00	0,01	0,01	0,01	0,00	0,01
$DEVbvDCool1$	0,00	0,00	0,00	0,00	0,01	0,01	0,00	0,01	0,00	0,00	0,00	0,00	0,01	0,01	0,00	0,00	0,01	0,00	0,00	0,01
$DEVbvDCool2$	0,00	0,00	0,00	0,00	0,00	0,04	0,04	0,02	0,08	0,06	0,01	0,00	0,04	0,03	0,02	0,09	0,11	0,00	0,01	0,05
$DEVbvKineFric$	0,00	0,00	0,00	0,00	0,01	0,00	0,00	0,01	0,09	0,03	0,02	0,00	0,00	0,00	0,00	0,12	0,07	0,01	0,00	0,00
$DEVbvCnull$	0,00	0,00	0,00	0,00	0,01	0,73	0,72	0,00	0,04	0,01	0,01	0,04	0,71	0,61	0,01	0,00	0,00	0,01	0,08	0,62
$DEVbvDnozzle$	0,00	0,00	0,00	0,00	0,01	0,00	0,01	0,02	0,01	0,01	0,03	0,00	0,00	0,02	0,02	0,02	0,02	0,03	0,00	0,01
$DEVbvKfeed$	0,00	0,00	0,00	0,00	0,01	0,01	0,01	0,03	0,03	0,03	0,03	0,00	0,01	0,01	0,01	0,02	0,03	0,04	0,01	0,01
$DEVbvSticspool$	0,00	0,00	0,00	0,00	0,01	0,00	0,01	0,30	0,10	0,17	0,19	0,00	0,00	0,01	0,40	0,16	0,43	0,03	0,00	0,00
$DEVbvDFilter1$	0,00	0,00	0,00	0,00	0,01	0,00	0,01	0,01	0,01	0,01	0,01	0,00	0,00	0,01	0,01	0,02	0,00	0,02	0,00	0,01
$DEVbvDFilter2$	0,00	0,00	0,00	0,00	0,00	0,00	0,01	0,01	0,00	0,02	0,01	0,00	0,00	0,01	0,00	0,01	0,00	0,02	0,00	0,01
$DEVbvCorHP1$	0,00	0,00	0,00	0,00	0,01	0,00	0,00	0,01	0,01	0,01	0,01	0,00	0,00	0,01	0,00	0,01	0,00	0,01	0,00	0,01
$DEVbvCorHP2$	0,00	0,00	0,00	0,00	0,06	0,00	0,00	0,00	0,01	0,02	0,01	0,00	0,00	0,00	0,00	0,02	0,00	0,00	0,00	0,01
$DEVbvASenO$	0,00	0,00	0,00	0,00	0,00	0,01	0,01	0,01	0,01	0,01	0,01	0,42	0,01	0,01	0,01	0,03	0,02	0,00	0,34	0,01
$DEVbvBSenO$	0,00	0,00	0,00	0,00	0,00	0,01	0,00	0,02	0,03	0,01	0,02	0,44	0,01	0,00	0,01	0,03	0,01	0,00	0,40	0,00
$EStaLaw$	0,00	0,00	0,00	0,00	0,27	0,00	0,00	0,00	0,01	0,01	0,01	0,00	0,00	0,00	0,00	0,00	0,00	0,03	0,00	0,01

	$VbvXchgS$	$VbvYchgS$	$VbvScaleS$	$VbvSlpLeftS$	$VbvSlpRightS$	$VbvHyst0S$	$VbvmaxX1$	$VbvmaxX2$	$VbvminX1$	$VbvminX2$	$VbvmaxGapX$	$VbvminGapX$	$VbvmeanGapX$	$VbvstdGapX$	$VbvMAErr$	$VoN2maxTBV$
$CTfuel$	0,00	0,00	0,01	0,00	0,03	0,00	0,00	0,00	0,00	0,00	0,00	0,01	0,00	0,00	0,00	0,01
$DLppDIlkg$	0,00	0,00	0,00	0,01	0,00	0,00	0,00	0,00	0,00	0,00	0,00	0,00	0,00	0,00	0,00	0,00
$DMfpDIlkg$	0,00	0,00	0,01	0,01	0,00	0,01	0,00	0,00	0,00	0,00	0,00	0,00	0,00	0,00	0,00	0,02
$DEMffFlowRate$	0,00	0,00	0,02	0,01	0,04	0,00	0,01	0,00	0,00	0,00	0,00	0,00	0,00	0,00	0,00	0,03
$ETbvPopen$	0,00	0,00	0,00	0,00	0,02	0,00	0,00	0,01	0,00	0,00	0,00	0,01	0,00	0,00	0,00	0,03
$DTbvDIlkg$	0,00	0,00	0,01	0,00	0,02	0,00	0,00	0,00	0,00	0,00	0,00	0,01	0,00	0,00	0,00	0,02
$DEWfmASenO$	0,00	0,01	0,01	0,00	0,02	0,00	0,00	0,00	0,00	0,00	0,00	0,00	0,00	0,00	0,00	0,02
$DEWfmBSenO$	0,00	0,01	0,00	0,00	0,03	0,00	0,00	0,00	0,00	0,00	0,00	0,01	0,00	0,00	0,00	0,03
$EByvDPist0$	0,00	0,02	0,01	0,01	0,01	0,00	0,00	0,00	0,00	0,00	0,00	0,00	0,00	0,00	0,00	0,00
$DEByvK0$	0,00	0,02	0,02	0,01	0,01	0,01	0,00	0,00	0,00	0,00	0,00	0,00	0,00	0,00	0,00	0,06
$DEByvVisc$	0,00	0,00	0,01	0,00	0,02	0,00	0,00	0,00	0,00	0,00	0,00	0,00	0,00	0,00	0,00	0,02
$DEByvStic$	0,00	0,00	0,02	0,00	0,02	0,00	0,00	0,00	0,00	0,00	0,00	0,00	0,00	0,00	0,00	0,05
$DByvDIlkg$	0,00	0,00	0,06	0,01	0,02	0,00	0,00	0,00	0,00	0,00	0,00	0,00	0,00	0,00	0,00	0,07
$ESovDPist$	0,00	0,01	0,01	0,01	0,01	0,00	0,00	0,00	0,00	0,00	0,00	0,01	0,00	0,00	0,00	0,00
$DESovVisc$	0,00	0,01	0,01	0,01	0,01	0,00	0,00	0,00	0,00	0,00	0,00	0,00	0,00	0,00	0,00	0,01
$DESovStic$	0,00	0,01	0,01	0,00	0,01	0,00	0,00	0,00	0,00	0,00	0,00	0,00	0,00	0,00	0,00	0,00
$DSovDIlkg$	0,01	0,18	0,02	0,20	0,03	0,00	0,00	0,00	0,00	0,00	0,00	0,00	0,00	0,00	0,00	0,27
$DSovDelay$	0,00	0,00	0,00	0,00	0,02	0,00	0,00	0,00	0,00	0,00	0,00	0,00	0,00	0,00	0,00	0,04
$DEFmvStic$	0,01	0,02	0,00	0,01	0,02	0,00	0,00	0,00	0,00	0,00	0,00	0,00	0,00	0,00	0,00	0,01
$DEFmvCnull$	0,00	0,01	0,02	0,01	0,02	0,00	0,01	0,00	0,00	0,00	0,00	0,01	0,00	0,00	0,00	0,01
$DEFmvDnozzle$	0,00	0,01	0,01	0,00	0,01	0,00	0,00	0,00	0,00	0,00	0,00	0,00	0,00	0,00	0,00	0,00
$DEFmvASenO$	0,00	0,01	0,00	0,00	0,00	0,00	0,00	0,00	0,00	0,00	0,00	0,00	0,00	0,00	0,00	0,00
$DEFmvBSenO$	0,00	0,00	0,00	0,00	0,00	0,00	0,00	0,00	0,00	0,00	0,00	0,00	0,00	0,00	0,00	0,00
$DFmvDIlkg$	0,00	0,02	0,02	0,00	0,01	0,00	0,00	0,00	0,00	0,00	0,00	0,00	0,00	0,00	0,00	0,01
$DEVsvStic1$	0,00	0,00	0,01	0,00	0,01	0,00	0,00	0,00	0,00	0,00	0,01	0,00	0,00	0,00	0,00	0,00
$DEVsvVisc1$	0,00	0,02	0,01	0,00	0,02	0,00	0,00	0,00	0,00	0,00	0,00	0,00	0,00	0,00	0,00	0,01
$DEVsvStic2$	0,00	0,01	0,01	0,00	0,01	0,00	0,00	0,00	0,00	0,00	0,00	0,00	0,00	0,00	0,00	0,01
$DEVsvVisc2$	0,00	0,00	0,00	0,00	0,00	0,00	0,00	0,00	0,00	0,00	0,00	0,00	0,00	0,00	0,00	0,00
$DEVsvDCool1$	0,00	0,00	0,01	0,00	0,01	0,00	0,00	0,00	0,00	0,00	0,01	0,00	0,00	0,00	0,00	0,00
$DEVsvDCool2$	0,00	0,00	0,01	0,01	0,01	0,00	0,00	0,00	0,00	0,00	0,00	0,00	0,00	0,00	0,00	0,00
$DEVsvKineFric$	0,00	0,01	0,01	0,00	0,02	0,00	0,00	0,00	0,00	0,00	0,00	0,00	0,00	0,00	0,00	0,00
$DEVsvCnull$	0,00	0,01	0,01	0,00	0,04	0,00	0,00	0,00	0,00	0,00	0,00	0,00	0,00	0,00	0,00	0,01
$DEVsvDnozzle$	0,00	0,01	0,02	0,00	0,01	0,00	0,00	0,00	0,00	0,00	0,00	0,00	0,00	0,00	0,00	0,01
$DEVsvKfeed$	0,00	0,01	0,01	0,00	0,01	0,00	0,00	0,00	0,00	0,00	0,00	0,01	0,00	0,00	0,00	0,01
$DEVsvSticspool$	0,00	0,00	0,00	0,01	0,01	0,00	0,01	0,00	0,00	0,00	0,00	0,00	0,00	0,00	0,00	0,01
$DEVsvDFilter1$	0,00	0,00	0,01	0,00	0,03	0,00	0,00	0,00	0,00	0,00	0,00	0,00	0,00	0,00	0,00	0,00
$DEVsvDFilter2$	0,01	0,00	0,00	0,01	0,01	0,00	0,00	0,00	0,00	0,00	0,00	0,00	0,00	0,00	0,00	0,00
$DEVsvCorHP1$	0,00	0,00	0,00	0,00	0,02	0,00	0,00	0,00	0,00	0,00	0,01	0,01	0,00	0,00	0,00	0,00
$DEVsvCorHP2$	0,01	0,03	0,00	0,01	0,01	0,00	0,00	0,00	0,00	0,00	0,00	0,00	0,00	0,00	0,00	0,01
$DEVsvASenO$	0,00	0,02	0,00	0,00	0,01	0,00	0,00	0,00	0,00	0,00	0,00	0,00	0,00	0,00	0,00	0,01
$DEVsvBSenO$	0,00	0,00	0,01	0,00	0,00	0,00	0,01	0,00	0,00	0,00	0,00	0,00	0,00	0,00	0,00	0,02
$DEVbvStic1$	0,00	0,00	0,02	0,00	0,03	0,00	0,00	0,00	0,00	0,00	0,00	0,00	0,00	0,00	0,00	0,01
$DEVbvVisc1$	0,00	0,02	0,00	0,01	0,01	0,00	0,00	0,00	0,00	0,00	0,00	0,00	0,00	0,00	0,00	0,01
$DEVbvStic2$	0,00	0,01	0,00	0,00	0,01	0,00	0,00	0,00	0,00	0,00	0,00	0,00	0,00	0,00	0,00	0,01
$DEVbvVisc2$	0,01	0,00	0,01	0,01	0,02	0,01	0,00	0,00	0,00	0,00	0,00	0,00	0,00	0,00	0,00	0,01
$DEVbvDCool1$	0,00	0,01	0,00	0,01	0,00	0,00	0,01	0,00	0,00	0,00	0,00	0,00	0,00	0,00	0,00	0,00
$DEVbvDCool2$	0,03	0,02	0,17	0,14	0,01	0,01	0,01	0,00	0,00	0,00	0,00	0,00	0,00	0,00	0,00	0,01
$DEVbvKineFric$	0,01	0,01	0,05	0,05	0,03	0,00	0,01	0,00	0,00	0,00	0,00	0,00	0,00	0,00	0,00	0,06
$DEVbvCnull$	0,79	0,01	0,01	0,01	0,03	0,07	0,01	0,00	0,00	0,00	0,00	0,01	0,00	0,00	0,00	0,01
$DEVbvDnozzle$	0,01	0,00	0,07	0,00	0,03	0,01	0,01	0,00	0,00	0,00	0,01	0,01	0,00	0,00	0,00	0,02
$DEVbvKfeed$	0,01	0,01	0,02	0,01	0,04	0,01	0,00	0,00	0,00	0,00	0,01	0,01	0,00	0,00	0,00	0,00
$DEVbvSticspool$	0,00	0,39	0,16	0,37	0,13	0,00	0,01	0,00	0,00	0,00	0,00	0,00	0,00	0,00	0,00	0,00
$DEVbvDFilter1$	0,00	0,01	0,00	0,00	0,01	0,00	0,00	0,00	0,00	0,00	0,00	0,00	0,00	0,00	0,00	0,00
$DEVbvDFilter2$	0,00	0,00	0,00	0,00	0,01	0,00	0,00	0,00	0,00	0,00	0,00	0,00	0,00	0,00	0,00	0,00
$DEVbvCorHP1$	0,00	0,01	0,01	0,00	0,01	0,00	0,00	0,00	0,00	0,00	0,00	0,00	0,00	0,00	0,00	0,01
$DEVbvCorHP2$	0,00	0,00	0,01	0,00	0,01	0,00	0,00	0,00	0,00	0,00	0,00	0,00	0,00	0,00	0,00	0,00
$DEVbvASenO$	0,01	0,00	0,01	0,01	0,02	0,36	0,76	0,00	0,91	0,00	0,41	0,39	0,48	0,47	0,43	0,00
$DEVbvBSenO$	0,00	0,00	0,02	0,01	0,02	0,42	0,00	0,85	0,00	0,96	0,43	0,43	0,51	0,53	0,46	0,00
$EStaLaw$	0,00	0,01	0,01	0,01	0,01	0,00	0,01	0,00	0,00	0,00	0,00	0,00	0,00	0,00	0,01	0,01

Appendix XXX. Detection NKPIs for standardized HIs

	FmvCEquA	FmvScaleA	FmvSlpA	FmvHyst0A	FmvCEquB	FmvScaleB	FmvSlpB	FmvHyst0B	FmvCEquS	FmvScaleS	FmvSlpS	FmvHyst0S	FmvmaxX1	FmvmaxX2	FmvminX1	FmvminX2	FmvmaxGapX	FmvminGapX	FmvmeanGapX	FmvstdGapX	FmvMAErr	Sovdelop1	Sovdelclo	Sovdelop2	wTBV	wSOV	MffSlpN2DP	MffR2N2DP
DBvvDllkg_Pos	0	0	0	0	0	0	0	0	0	0	0	0	0	0	0	0	0	0	0	0	0	0	0	0	0	0	0	0
DEBvvK0_Neg	0	0	0	0	0	0	0	0	0	0	0	0	0	0	0	0	0	0	0	0	0	0	0	0	0	0	0	0
DEBvvStic_Pos	0	0	0	0	0	0	0	0	0	0	0	0	0	0	0	0	0	0	0	0	0	0	0	0	0	0	0	0
DEBvvVisc_Pos	0	0	0	0	0	0	0	0	0	0	0	0	0	0	0	0	0	0	0	0	0	0	0	0	0	0	0	0
DEFmvASenO_Neg	0	0	0	0	0	0	0	0	0	0	0	0	1	0	1	0	0	1	1	1	0	0	0	0	0	0	0	0
DEFmvASenO_Pos	0	0	0	1	0	0	0	1	0	0	0	1	0	1	0	0	1	0	1	1	0	0	0	0	0	0	0	0
DEFmvBSenO_Neg	0	0	0	0	0	0	0	0	0	0	0	0	0	1	0	1	1	0	1	1	0	0	0	0	0	0	0	0
DEFmvBSenO_Pos	0	0	0	1	0	0	0	1	0	0	0	1	1	0	0	0	0	1	1	1	0	0	0	0	0	0	0	0
DEFmvCnull_Neg	1	0	0	0	1	0	0	0	1	0	0	0	0	1	0	0	0	0	0	0	1	0	0	0	0	0	0	0
DEFmvCnull_Pos	1	0	0	0	1	0	0	0	1	0	0	0	1	1	0	0	0	0	0	0	1	0	0	0	0	0	0	0
DEFmvDnozzle_Pos	0	1	0	0	1	0	0	0	1	1	0	0	0	0	0	0	0	0	0	0	1	0	0	0	0	0	0	0
DEFmvStic_Pos	0	0	0	1	0	0	0	1	0	0	0	1	0	1	0	0	0	0	0	0	1	0	0	0	0	0	0	0
DEMffFlowRate_Neg	0	0	0	0	0	0	0	0	0	0	0	0	0	0	0	0	0	0	0	0	0	0	0	0	0	0	1	1
DESovStic_Pos	0	0	0	0	0	0	0	0	0	0	0	0	0	0	0	0	0	0	0	0	0	0	0	0	0	0	0	0
DESovVisc_Pos	0	0	0	0	0	0	0	0	0	0	0	0	0	0	0	0	0	0	0	0	0	0	0	0	0	0	0	0
DEVbvASenO_Neg	0	0	0	0	0	0	0	0	0	0	0	0	0	0	0	0	0	0	0	0	0	0	0	0	0	0	0	0
DEVbvASenO_Pos	0	0	0	0	0	0	0	0	0	0	0	0	0	0	0	0	0	0	0	0	0	0	0	0	0	0	0	0
DEVbvBSenO_Neg	0	0	0	0	0	0	0	0	0	0	0	0	0	0	0	0	0	0	0	0	0	0	0	0	0	0	0	0
DEVbvBSenO_Pos	0	0	0	0	0	0	0	0	0	0	0	0	0	0	0	0	0	0	0	0	0	0	0	0	0	0	0	0
DEVbvCnull_Neg	0	0	0	0	0	0	0	0	0	0	0	0	0	0	0	0	0	0	0	0	0	0	0	0	0	0	0	0
DEVbvCnull_Pos	0	0	0	0	0	0	0	0	0	0	0	0	0	0	0	0	0	0	0	0	0	0	0	0	0	0	0	0
DEVbvCorHP1_Pos	0	0	0	0	0	0	0	0	0	0	0	0	0	0	0	0	0	0	0	0	0	0	0	0	0	0	0	0
DEVbvCorHP2_Pos	0	0	0	0	0	0	0	0	0	0	0	0	0	0	0	0	0	0	0	0	0	0	1	0	0	0	0	0
DEVbvDCool1_Neg	0	0	0	0	0	0	0	0	0	0	0	0	0	0	0	0	0	0	0	0	0	0	0	0	0	0	0	0
DEVbvDCool1_Pos	0	0	0	0	0	0	0	0	0	0	0	0	0	0	0	0	0	0	0	0	0	0	0	0	0	0	0	0
DEVbvDCool2_Neg	0	0	0	0	0	0	0	0	0	0	0	0	0	0	0	0	0	0	0	0	0	0	0	0	0	0	0	0
DEVbvDCool2_Pos	0	0	0	0	0	0	0	0	0	0	0	0	0	0	0	0	0	0	0	0	0	0	0	0	0	0	0	0
DEVbvDFilter1_Neg	0	0	0	0	0	0	0	0	0	0	0	0	0	0	0	0	0	0	0	0	0	0	0	0	0	0	0	0
DEVbvDFilter2_Neg	0	0	0	0	0	0	0	0	0	0	0	0	0	0	0	0	0	0	0	0	0	0	0	0	0	0	0	0
DEVbvDnozzle_Neg	0	0	0	0	0	0	0	0	0	0	0	0	0	0	0	0	0	0	0	0	0	0	0	0	0	0	0	0
DEVbvDnozzle_Pos	0	0	0	0	0	0	0	0	0	0	0	0	0	0	0	0	0	0	0	0	0	0	0	0	0	0	0	0
DEVbvKfeed_Neg	0	0	0	0	0	0	0	0	0	0	0	0	0	0	0	0	0	0	0	0	0	0	0	0	0	0	0	0
DEVbvKineFric_Pos	0	0	0	0	0	0	0	0	0	0	0	1	0	0	0	0	0	0	0	0	0	0	0	0	0	0	0	0
DEVbvStic1_Pos	0	0	0	0	0	0	0	0	0	0	0	0	0	0	0	0	0	0	0	0	0	0	0	0	0	0	0	0
DEVbvStic2_Pos	0	0	0	0	0	0	0	0	0	0	0	0	0	0	0	0	0	0	0	0	0	0	0	0	0	0	0	0
DEVbvSticspool_Pos	0	0	0	0	0	0	0	0	0	0	0	0	0	0	0	0	0	0	0	0	0	0	0	0	0	0	0	0
DEVbvVisc1_Pos	0	0	0	0	0	0	0	0	0	0	0	0	0	0	0	0	0	0	0	0	0	0	0	0	0	0	0	0
DEVbvVisc2_Pos	0	0	0	0	0	0	0	0	0	0	0	0	0	0	0	0	0	0	0	0	0	0	0	0	0	0	0	0
DEVsvASenO_Neg	0	0	0	0	0	0	0	0	0	0	0	0	0	0	0	0	0	0	0	0	0	0	0	0	0	0	0	0
DEVsvASenO_Pos	0	0	0	0	0	0	0	0	0	0	0	0	0	0	0	0	0	0	0	0	0	0	0	0	0	0	0	0
DEVsvBSenO_Neg	0	0	0	0	0	0	0	0	0	0	0	0	0	0	0	0	0	0	0	0	0	0	0	0	0	0	0	0
DEVsvBSenO_Pos	0	0	0	0	0	0	0	0	0	0	0	0	0	0	0	0	0	0	0	0	0	0	0	0	0	0	0	0
DEVsvCnull_Neg	0	0	0	0	0	0	0	0	0	0	0	0	0	0	0	0	0	0	0	0	0	0	0	0	0	0	0	0
DEVsvCnull_Pos	0	0	0	0	0	0	0	0	0	0	0	0	0	0	0	0	0	0	0	0	0	0	0	0	0	0	0	0
DEVsvCorHP1_Pos	0	0	0	0	0	0	0	0	0	0	0	0	0	0	0	0	0	0	0	0	0	0	0	0	0	0	0	0
DEVsvCorHP2_Pos	0	0	0	0	0	0	0	0	0	0	0	0	0	0	0	0	0	0	0	0	0	0	0	0	0	0	0	0
DEVsvDCool1_Neg	0	0	0	0	0	0	0	0	0	0	0	0	0	0	0	0	0	0	0	0	0	0	0	0	0	0	0	0
DEVsvDCool1_Pos	0	0	0	0	0	0	0	0	0	0	0	0	0	0	0	0	0	0	0	0	0	0	0	0	0	0	0	0
DEVsvDCool2_Neg	0	0	0	0	0	0	0	0	0	0	0	0	0	0	0	0	0	0	0	0	0	0	0	0	0	0	0	0
DEVsvDCool2_Pos	0	0	0	0	0	0	0	0	0	0	0	0	0	0	0	0	0	0	0	0	0	0	0	0	0	0	0	0
DEVsvDFilter1_Neg	0	0	0	0	0	0	0	0	0	0	0	0	0	0	0	0	0	0	0	0	0	0	0	0	0	0	0	0
DEVsvDFilter2_Neg	0	0	0	0	0	0	0	0	0	0	0	0	0	0	0	0	0	0	0	0	0	0	0	0	0	0	0	0
DEVsvDnozzle_Neg	0	0	0	0	0	0	0	0	0	0	0	0	0	0	0	0	0	0	0	0	0	0	0	0	0	0	0	0
DEVsvDnozzle_Pos	0	0	0	0	0	0	0	0	0	0	0	0	0	0	0	0	0	0	0	0	0	0	0	0	0	0	0	0
DEVsvKfeed_Neg	0	0	0	0	0	0	0	0	0	0	0	0	0	0	0	0	0	0	0	0	0	0	0	0	0	0	0	0
DEVsvKineFric_Pos	0	0	0	0	0	0	0	0	0	0	0	0	0	0	0	0	0	0	0	0	0	0	0	0	0	0	0	0
DEVsvStic1_Pos	0	0	0	0	0	0	0	0	0	0	0	0	0	0	0	0	0	0	0	0	0	0	0	0	0	0	0	0
DEVsvStic2_Pos	0	0	0	0	0	0	0	0	0	0	0	0	0	0	0	0	0	0	0	0	0	0	0	0	0	0	0	0
DEVsvSticspool_Pos	0	0	0	0	0	0	0	0	0	0	0	0	0	0	0	0	0	0	0	0	0	0	0	0	0	0	0	0
DEVsvVisc1_Pos	0	0	0	0	0	0	0	0	0	0	0	0	0	0	0	0	0	0	0	0	0	0	0	0	0	0	0	0
DEVsvVisc2_Pos	0	0	0	0	0	0	0	0	0	0	0	0	0	0	0	0	0	0	0	0	0	0	0	0	0	0	0	0
DEWfmASenO_Neg	0	0	0	0	0	0	0	0	0	0	0	0	0	0	0	0	0	0	0	0	0	0	0	0	0	0	0	0
DEWfmASenO_Pos	0	0	0	0	0	0	0	0	0	0	0	0	0	0	0	0	0	0	0	0	0	0	0	0	0	0	0	0
DEWfmBSenO_Neg	0	0	0	0	0	0	0	0	0	0	0	0	0	0	0	0	0	0	0	0	0	0	0	0	0	0	0	0
DEWfmBSenO_Pos	0	0	0	0	0	0	0	0	0	0	0	0	0	0	0	0	0	0	0	0	0	0	0	0	0	0	0	0
DFmvDllkg_Pos	1	1	0	1	1	0	0	1	1	1	1	1	1	1	0	0	0	0	0	0	1	0	0	0	0	0	0	0
DLpvDllkg_Pos	0	0	0	0	0	0	0	0	0	0	0	0	0	0	0	0	0	0	0	0	0	0	0	0	0	0	0	0
DMfpDllkg_Pos	0	0	0	0	0	0	0	0	0	0	0	0	0	0	0	0	0	0	0	0	0	0	0	0	0	0	0	0
DSovDelay_Pos	0	0	0	0	0	0	0	0	0	0	0	0	0	0	0	0	0	0	0	0	0	0	0	0	1	0	0	0
DSovDllkg_Pos	0	0	0	0	0	0	0	0	0	0	0	0	0	0	0	0	0	0	0	0	0	0	0	0	1	1	0	0
DTbvDllkg_Pos	0	0	0	0	0	0	0	0	0	0	0	0	0	0	0	0	0	0	0	0	0	0	0	0	0	0	0	0

	WfmmaxX1	WfmmaxX2	WfmminX1	WfmminX2	WfmmaxGapX	WfmminGapX	WfmmeanGapX	WfmstdGapX	VsvCEquA	VsvXnullA	VsvYnullA	VsvXoverlapA	VsvYoverlapA	VsvScaleA	VsvSlpLeftA	VsvSlpNullA	VsvSlpRightA	VsvHyst0A	VsvCEquB	VsvXnullB	VsvYnullB	VsvXoverlapB	VsvYoverlapB	VsvScaleB	VsvSlpLeftB	VsvSlpNullB	VsvSlpRightB	VsvHyst0B	VsvCEquS
DBvvDIlkg_Pos	1	1	0	0	0	0	0	0	0	0	0	0	0	0	0	0	1	0	0	0	0	0	0	1	0	0	1	0	0
DEBvvK0_Neg	1	1	0	0	0	0	0	0	0	0	0	0	0	0	0	0	0	0	0	0	0	0	0	0	0	0	0	0	0
DEBvvStic_Pos	0	0	0	0	0	0	0	0	0	0	0	0	0	0	0	0	0	0	0	0	0	0	0	0	0	0	0	0	0
DEBvvVisc_Pos	0	0	0	0	0	0	0	0	0	0	0	0	0	0	0	0	0	0	0	0	0	0	0	0	0	0	0	0	0
DEFmvASenO_Neg	0	0	0	0	0	0	0	0	0	0	0	0	0	0	0	0	0	0	0	0	0	0	0	0	0	0	0	0	0
DEFmvASenO_Pos	1	1	0	0	0	0	0	0	0	0	0	0	0	0	0	0	0	0	0	0	0	0	0	0	0	0	0	0	0
DEFmvBSenO_Neg	0	0	0	0	0	0	0	0	0	0	0	0	0	0	0	0	0	0	0	0	0	0	0	0	0	0	0	0	0
DEFmvBSenO_Pos	1	1	0	0	0	0	0	0	0	0	0	0	0	0	0	0	0	0	0	0	0	0	0	0	0	0	0	0	0
DEFmvCnull_Neg	0	0	0	0	0	0	0	0	0	0	0	0	0	0	0	0	0	0	0	0	0	0	0	0	0	0	0	0	0
DEFmvCnull_Pos	1	1	0	0	0	0	0	0	0	0	0	0	0	0	0	0	0	0	0	0	0	0	0	0	0	0	0	0	0
DEFmvDnozzle_Pos	0	0	0	0	0	0	0	0	0	0	0	0	0	0	0	0	0	0	0	0	0	0	0	0	0	0	0	0	0
DEFmvStic_Pos	1	1	0	0	0	0	0	0	0	0	0	0	0	0	0	0	0	0	0	0	0	0	0	0	0	0	0	0	0
DEMffFlowRate_Neg	0	0	0	0	0	0	0	0	0	0	0	0	0	0	0	0	0	0	0	0	0	0	0	0	0	0	0	0	0
DESovStic_Pos	0	0	0	0	0	0	0	0	0	0	0	0	0	0	0	0	0	0	0	0	0	0	0	0	0	0	0	0	0
DESovVisc_Pos	0	0	0	0	0	0	0	0	0	0	0	0	0	0	0	0	0	0	0	0	0	0	0	0	0	0	0	0	0
DEVbvASenO_Neg	0	0	0	0	0	0	0	0	0	0	0	0	0	0	0	0	0	0	0	0	0	0	0	0	0	0	0	0	0
DEVbvASenO_Pos	0	0	0	0	0	0	0	0	0	0	0	0	0	0	0	0	0	0	0	0	0	0	0	0	0	0	0	0	0
DEVbvBSenO_Neg	0	0	0	0	0	0	0	0	0	0	0	0	0	0	0	0	0	0	0	0	0	0	0	0	0	0	0	0	0
DEVbvBSenO_Pos	0	0	0	0	0	0	0	0	0	0	0	0	0	0	0	0	0	0	0	0	0	0	0	0	0	0	0	0	0
DEVbvCnull_Neg	0	0	0	0	0	0	0	0	0	0	0	0	0	0	0	0	0	0	0	0	0	0	0	0	0	0	0	0	0
DEVbvCnull_Pos	0	0	0	0	0	0	0	0	0	0	0	0	0	0	0	0	0	0	0	0	0	0	0	0	0	0	0	0	0
DEVbvCorHP1_Pos	0	0	0	0	0	0	0	0	0	0	0	0	0	0	0	0	0	0	0	0	0	0	0	0	0	0	0	0	0
DEVbvCorHP2_Pos	0	0	0	0	0	0	0	0	0	0	0	0	0	0	0	0	0	0	0	0	0	0	0	0	0	0	0	0	0
DEVbvDCool1_Neg	0	0	0	0	0	0	0	0	0	0	0	0	0	0	0	0	0	0	0	0	0	0	0	0	0	0	0	0	0
DEVbvDCool1_Pos	0	0	0	0	0	0	0	0	0	0	0	0	0	0	0	0	0	0	0	0	0	0	0	0	0	0	0	0	0
DEVbvDCool2_Neg	0	0	0	0	0	0	0	0	0	0	0	0	0	0	0	0	0	0	0	0	0	0	0	0	0	0	0	0	0
DEVbvDCool2_Pos	0	0	0	0	0	0	0	0	0	0	0	0	0	0	0	0	0	0	0	0	0	0	0	0	0	0	0	0	0
DEVbvDFilter1_Neg	0	0	0	0	0	0	0	0	0	0	0	0	0	0	0	0	0	0	0	0	0	0	0	0	0	0	0	0	0
DEVbvDFilter2_Neg	0	0	0	0	0	0	0	0	0	0	0	0	0	0	0	0	0	0	0	0	0	0	0	0	0	0	0	0	0
DEVbvDnozzle_Neg	0	0	0	0	0	0	0	0	0	0	0	0	0	0	0	0	0	0	0	0	0	0	0	0	0	0	0	0	0
DEVbvDnozzle_Pos	0	0	0	0	0	0	0	0	0	0	0	0	0	0	0	0	0	0	0	0	0	0	0	0	0	0	0	0	0
DEVbvKfeed_Neg	0	0	0	0	0	0	0	0	0	0	0	0	0	0	0	0	0	0	0	0	0	0	0	0	0	0	0	0	0
DEVbvKineFric_Pos	0	0	0	0	1	0	0	0	0	0	0	0	0	0	0	0	0	0	0	0	0	0	0	0	0	0	0	0	0
DEVbvStic1_Pos	0	0	0	0	0	0	0	0	0	0	0	0	0	0	0	0	0	0	0	0	0	0	0	0	0	0	0	0	0
DEVbvStic2_Pos	0	0	0	0	0	0	0	0	0	0	0	0	0	0	0	0	0	0	0	0	0	0	0	0	0	0	0	0	0
DEVbvSticspool_Pos	0	0	0	0	0	0	0	0	0	0	0	0	0	0	0	0	0	0	0	0	0	0	0	0	0	0	0	0	0
DEVbvVisc1_Pos	0	0	0	0	0	0	0	0	0	0	0	0	0	0	0	0	0	0	0	0	0	0	0	0	0	0	0	0	0
DEVbvVisc2_Pos	0	0	0	0	0	0	0	0	0	0	0	0	0	0	0	0	0	0	0	0	0	0	0	0	0	0	0	0	0
DEVsvASenO_Neg	0	0	0	0	0	0	0	0	0	0	0	0	0	0	0	0	0	0	0	0	0	0	0	0	0	0	0	0	0
DEVsvASenO_Pos	0	0	0	0	0	0	0	0	0	0	0	0	0	0	0	0	0	0	0	0	0	1	0	0	0	0	0	0	0
DEVsvBSenO_Neg	0	0	0	0	0	0	0	0	0	0	0	0	0	0	0	0	0	0	0	0	0	0	0	0	0	0	0	0	0
DEVsvBSenO_Pos	0	0	0	0	0	0	0	0	0	0	0	0	0	0	1	0	0	0	0	0	0	0	0	0	0	0	0	0	0
DEVsvCnull_Neg	0	0	0	0	0	0	0	0	1	1	0	1	1	0	1	0	0	0	1	1	0	1	1	0	0	0	0	0	1
DEVsvCnull_Pos	0	0	0	0	0	0	0	0	1	1	0	0	0	0	0	0	0	0	1	1	0	0	0	0	0	0	0	0	1
DEVsvCorHP1_Pos	0	0	0	0	0	0	0	0	0	0	0	0	0	0	0	0	0	0	0	0	0	0	0	0	0	0	0	0	0
DEVsvCorHP2_Pos	0	0	0	0	0	0	0	0	0	0	0	0	0	0	0	0	0	0	0	0	0	0	0	0	0	0	0	0	0
DEVsvDCool1_Neg	0	0	0	0	0	0	0	0	0	0	0	0	0	0	0	0	0	0	0	0	0	0	0	0	0	0	0	0	0
DEVsvDCool1_Pos	0	0	0	0	0	0	0	0	0	0	0	0	0	0	0	0	0	0	0	0	0	0	0	0	0	0	0	0	0
DEVsvDCool2_Neg	0	0	0	0	0	0	0	0	1	0	1	0	0	0	1	1	0	0	1	0	1	0	0	0	0	1	0	0	1
DEVsvDCool2_Pos	0	0	0	0	0	0	0	0	1	0	1	1	0	0	1	1	0	0	1	0	1	1	0	1	1	1	0	1	1
DEVsvDFilter1_Neg	0	0	0	0	0	0	0	0	0	0	0	0	0	0	0	0	0	0	0	0	0	0	0	0	0	0	0	0	0
DEVsvDFilter2_Neg	0	0	0	0	0	0	0	0	0	0	0	0	0	0	0	0	0	0	0	0	0	1	0	0	0	0	0	0	0
DEVsvDnozzle_Neg	0	0	0	0	0	0	0	0	0	0	0	0	0	0	0	0	0	0	0	0	0	0	0	0	0	0	0	0	0
DEVsvDnozzle_Pos	0	0	0	0	0	0	0	0	0	0	0	0	0	0	0	0	0	0	0	0	0	0	0	0	0	0	0	0	0
DEVsvKfeed_Neg	0	0	0	0	0	0	0	0	0	0	0	0	0	1	1	1	1	0	0	0	0	0	0	1	1	1	1	0	0
DEVsvKineFric_Pos	0	0	0	0	0	0	0	0	1	1	0	1	1	1	1	0	0	0	1	1	0	1	1	1	1	1	0	0	0
DEVsvStic1_Pos	0	0	0	0	0	0	0	0	0	0	0	0	0	0	0	0	0	0	0	0	0	0	0	0	0	0	0	0	0
DEVsvStic2_Pos	0	0	0	0	0	0	0	0	0	0	0	0	0	0	0	0	0	0	0	0	0	0	0	0	0	0	0	0	0
DEVsvSticspool_Pos	0	0	0	0	0	0	0	0	1	0	1	0	1	0	1	1	1	0	1	0	1	0	1	0	1	1	1	1	1
DEVsvVisc1_Pos	0	0	0	0	0	0	0	0	0	0	0	0	0	0	0	0	0	0	0	0	0	0	0	0	0	0	0	0	0
DEVsvVisc2_Pos	0	0	0	0	0	0	0	0	0	0	0	0	0	0	0	0	0	0	0	0	0	0	0	0	0	0	0	0	0
DEWfmASenO_Neg	0	0	1	0	0	1	1	1	0	0	0	0	0	0	0	0	0	0	0	0	0	0	0	0	0	0	0	0	0
DEWfmASenO_Pos	0	0	1	0	1	0	1	1	0	0	0	0	0	0	0	0	0	0	0	0	0	0	0	0	0	0	0	0	0
DEWfmBSenO_Neg	0	0	0	1	1	0	1	1	0	0	0	0	0	0	0	0	0	0	0	0	0	0	0	0	0	0	0	0	0
DEWfmBSenO_Pos	0	0	0	1	0	1	1	1	0	0	0	0	0	0	0	0	0	0	0	0	0	0	0	0	0	0	0	0	0
DFmvDIlkg_Pos	1	1	0	0	0	0	0	0	0	0	0	0	0	0	0	0	0	0	0	0	0	0	0	0	0	0	0	0	0
DLppDIlkg_Pos	0	0	0	0	0	0	0	0	0	0	0	0	0	0	0	0	0	0	0	0	0	0	0	0	0	0	0	0	0
DMfpDIlkg_Pos	0	0	0	0	0	0	0	0	0	0	0	0	0	0	0	0	0	0	0	0	0	1	0	0	0	0	0	0	0
DSovDelay_Pos	0	0	0	0	0	0	0	0	0	0	0	0	0	0	0	0	0	0	0	0	0	0	0	0	0	0	0	0	0
DSovDIlkg_Pos	0	0	0	0	0	0	0	0	0	0	0	0	0	0	0	0	1	0	0	0	0	0	0	0	0	0	1	0	0
DTbvDIlkg_Pos	0	0	0	0	0	0	0	0	0	0	0	0	0	0	0	0	0	0	0	0	0	0	0	0	0	0	0	0	0

	VsvXnullS	VsvYnullS	VsvXoverlapS	VsvYoverlapS	VsvScaleS	VsvSlpLeftS	VsvSlpNullS	VsvSlpRightS	VsvHyst0S	VsvmaxX1	VsvmaxX2	VsvminX1	VsvminX2	VsvmaxGapX	VsvminGapX	VsvmeanGapX	VsvstdGapX	VsvMAErr	VbvCEquA	VbvXchgA	VbvYchgA	VbvScaleA	VbvSlpLeftA	VbvSlpRightA	VbvHyst0A	VbvCEquB	VbvXchgB	VbvYchgB	VbvScaleB
DBvvDIlkg_Pos	0	0	0	0	0	0	0	0	0	0	0	0	0	0	0	0	0	0	0	0	1	0	0	0	0	0	0	1	1
DEBvvK0_Neg	0	0	0	0	1	0	0	0	0	0	0	0	0	0	0	0	0	0	0	0	0	0	0	0	0	0	0	0	0
DEBvvStic_Pos	0	0	0	0	0	0	0	0	0	0	0	0	0	0	0	0	0	0	0	0	0	0	0	0	0	0	0	0	0
DEBvvVisc_Pos	0	0	0	0	0	0	0	0	0	0	0	0	0	0	0	0	0	0	0	0	0	0	0	0	0	0	0	0	0
DEFmvASenO_Neg	0	0	0	0	0	0	0	0	0	0	0	0	0	0	0	0	0	0	0	0	0	0	0	0	0	0	0	0	0
DEFmvASenO_Pos	0	0	0	0	0	0	0	0	0	0	0	0	0	0	0	0	0	0	0	0	0	0	0	0	0	0	0	0	0
DEFmvBSenO_Neg	0	0	0	0	0	0	0	0	0	0	0	0	0	0	0	0	0	0	0	0	0	0	0	0	0	0	0	0	0
DEFmvBSenO_Pos	0	0	0	0	0	0	0	0	0	0	0	0	0	0	0	0	0	0	0	0	0	0	0	0	0	0	0	0	0
DEFmvCnull_Neg	0	0	0	0	0	0	0	0	0	0	0	0	0	0	0	0	0	0	0	0	0	0	0	0	0	0	0	0	0
DEFmvCnull_Pos	0	0	0	0	0	0	0	0	0	0	0	0	0	0	0	0	0	0	0	0	0	0	0	0	0	0	0	0	0
DEFmvDnozzle_Pos	0	0	0	0	0	0	0	0	0	0	0	0	0	0	0	0	0	0	0	0	0	0	0	0	0	0	0	0	0
DEFmvStic_Pos	0	0	0	0	0	0	0	0	0	0	0	0	0	0	0	0	0	0	0	0	0	0	0	0	0	0	0	0	0
DEMffFlowRate_Neg	0	0	0	0	0	0	0	0	0	0	0	0	0	0	0	0	0	0	0	0	0	0	0	0	0	0	0	0	0
DESovStic_Pos	0	0	0	0	0	0	0	0	0	0	0	0	0	0	0	0	0	0	0	0	0	0	0	0	0	0	0	0	0
DESovVisc_Pos	0	0	0	0	0	0	0	0	0	0	0	0	0	0	0	0	0	0	0	0	0	0	0	0	0	0	0	0	0
DEVbvASenO_Neg	0	0	0	0	0	0	0	0	0	0	0	0	0	0	0	0	0	0	0	0	0	0	0	0	0	0	0	0	0
DEVbvASenO_Pos	0	0	0	0	0	0	0	0	0	0	0	0	0	0	0	0	0	0	0	0	0	0	0	0	1	0	0	0	0
DEVbvBSenO_Neg	0	0	0	0	0	0	0	0	0	0	0	0	0	0	0	0	0	0	0	0	0	0	0	0	0	0	0	0	0
DEVbvBSenO_Pos	0	0	0	0	0	0	0	0	0	0	0	0	0	0	0	0	0	0	0	0	0	0	0	0	1	0	0	0	0
DEVbvCnull_Neg	0	0	0	0	0	0	0	0	0	0	0	0	0	0	0	0	0	0	1	1	0	0	0	0	0	1	1	0	0
DEVbvCnull_Pos	0	0	0	0	0	0	0	0	0	0	0	0	0	0	0	0	0	0	1	1	0	0	0	0	0	1	1	0	0
DEVbvCorHP1_Pos	0	0	0	0	0	0	0	0	0	0	0	0	0	0	0	0	0	0	0	0	0	0	0	0	0	0	0	0	0
DEVbvCorHP2_Pos	0	0	0	0	0	0	0	0	0	0	0	0	0	0	0	0	0	1	0	0	0	0	0	0	0	0	0	0	0
DEVbvDCool1_Neg	0	0	0	0	0	0	0	0	0	0	0	0	0	0	0	0	0	0	0	0	0	0	0	0	0	0	0	0	0
DEVbvDCool1_Pos	0	0	0	0	0	0	0	0	0	0	0	0	0	0	0	0	0	0	0	0	0	0	0	0	0	0	0	0	0
DEVbvDCool2_Neg	0	0	0	0	0	0	0	0	0	0	0	0	0	0	0	0	0	0	1	0	0	0	0	0	0	1	0	0	0
DEVbvDCool2_Pos	0	0	0	0	0	0	0	0	0	0	0	0	0	0	0	0	0	1	1	0	0	0	0	0	1	1	0	1	
DEVbvDFilter1_Neg	0	0	0	0	0	0	0	0	0	0	0	0	0	0	0	0	0	0	0	0	0	0	0	0	0	0	0	0	0
DEVbvDFilter2_Neg	0	0	0	0	0	0	0	0	0	0	0	0	0	0	0	0	0	0	0	0	0	0	0	0	0	0	0	0	0
DEVbvDnozzle_Neg	0	0	0	0	0	0	0	0	0	0	0	0	0	0	0	0	0	0	0	0	0	0	0	0	0	0	0	0	0
DEVbvDnozzle_Pos	0	0	0	0	0	0	0	0	0	0	0	0	0	0	0	0	0	0	0	0	0	0	0	0	0	0	0	0	0
DEVbvKfeed_Neg	0	0	0	0	0	0	0	0	0	0	0	0	0	0	0	0	0	0	0	0	0	0	0	0	0	0	0	0	0
DEVbvKineFric_Pos	0	0	0	0	0	0	0	0	0	0	0	0	0	0	0	0	0	0	0	0	0	0	0	0	0	0	0	0	0
DEVbvStic1_Pos	0	0	0	0	0	0	0	0	0	0	0	0	0	0	0	0	0	0	0	0	0	0	0	0	0	0	0	0	0
DEVbvStic2_Pos	0	0	0	0	0	0	0	0	0	0	0	0	0	0	0	0	0	0	0	0	0	0	0	0	0	0	0	0	0
DEVbvSticspool_Pos	0	0	0	0	0	0	0	0	0	0	0	0	0	0	0	0	0	0	1	0	0	0	0	0	1	1	0	1	1
DEVbvVisc1_Pos	0	0	0	0	0	0	0	0	0	0	0	0	0	0	0	0	0	0	0	0	0	0	0	0	0	0	0	0	0
DEVbvVisc2_Pos	0	0	0	0	0	0	0	0	0	0	0	0	0	0	0	0	0	0	0	0	0	0	0	0	0	0	0	0	0
DEVsvASenO_Neg	0	0	0	0	0	0	0	0	0	0	0	1	1	0	1	1	1	0	0	0	0	0	0	0	0	0	0	0	0
DEVsvASenO_Pos	0	0	0	0	0	0	0	0	0	1	0	1	1	1	1	1	1	0	0	0	0	0	0	0	0	0	0	0	0
DEVsvBSenO_Neg	0	0	0	0	0	0	0	0	0	0	0	1	1	1	1	1	1	0	0	0	0	0	0	0	0	0	0	0	0
DEVsvBSenO_Pos	0	0	0	0	0	0	0	0	0	0	1	1	1	0	1	1	1	0	0	0	0	0	0	0	0	0	0	0	0
DEVsvCnull_Neg	1	0	0	0	0	0	0	0	0	0	0	0	0	0	0	0	0	0	0	0	0	0	0	0	0	0	0	0	0
DEVsvCnull_Pos	1	0	0	0	0	0	0	0	0	0	0	0	0	0	0	0	0	0	0	0	0	0	0	0	0	0	0	0	0
DEVsvCorHP1_Pos	0	0	0	0	0	0	0	0	0	0	0	0	0	0	0	0	0	0	0	0	0	0	0	0	0	0	0	0	0
DEVsvCorHP2_Pos	0	0	0	0	0	0	0	0	0	0	0	0	0	0	0	0	0	0	0	0	0	0	0	0	0	0	0	0	0
DEVsvDCool1_Neg	0	0	0	0	0	0	0	0	0	0	0	0	0	0	0	0	0	0	0	0	0	0	0	0	0	0	0	0	0
DEVsvDCool1_Pos	0	0	0	0	0	0	0	0	0	0	0	0	0	0	0	0	0	0	0	0	0	0	0	0	0	0	0	0	0
DEVsvDCool2_Neg	0	0	0	0	0	0	0	0	0	0	0	0	0	0	0	0	0	0	0	0	0	0	0	0	0	0	0	0	0
DEVsvDCool2_Pos	0	0	0	0	1	0	0	0	0	0	0	0	0	0	0	0	0	0	0	0	0	0	0	0	0	0	0	0	0
DEVsvDFilter1_Neg	0	0	0	0	0	0	0	0	0	0	0	0	0	0	0	0	0	0	0	0	0	0	0	0	0	0	0	0	0
DEVsvDFilter2_Neg	0	0	0	0	0	0	0	0	0	0	0	0	0	0	0	0	0	0	0	0	0	0	0	0	0	0	0	0	0
DEVsvDnozzle_Neg	0	0	0	0	0	0	0	0	0	0	0	0	0	0	0	0	0	0	0	0	0	0	0	0	0	0	0	0	0
DEVsvDnozzle_Pos	0	0	0	0	0	0	0	0	0	0	0	0	0	0	0	0	0	0	0	0	0	0	0	0	0	0	0	0	0
DEVsvKfeed_Neg	0	0	0	0	0	0	0	1	1	0	0	0	0	0	0	0	0	0	0	0	0	0	0	0	0	0	0	0	0
DEVsvKineFric_Pos	0	0	0	0	1	0	0	1	0	0	0	0	0	0	0	0	0	0	0	0	0	0	0	0	0	0	0	0	0
DEVsvStic1_Pos	0	0	0	0	0	0	0	0	0	0	0	0	0	0	0	0	0	0	0	0	0	0	0	0	0	0	0	0	0
DEVsvStic2_Pos	0	0	0	0	0	0	0	0	0	0	0	0	0	0	0	0	0	0	0	0	0	0	0	0	0	0	0	0	0
DEVsvSticspool_Pos	0	1	0	0	0	0	0	1	1	0	0	1	0	0	0	0	0	0	0	0	0	0	0	0	0	0	0	0	0
DEVsvVisc1_Pos	0	0	0	0	0	0	0	0	0	0	0	0	0	0	0	0	0	0	0	0	0	0	0	0	0	0	0	0	0
DEVsvVisc2_Pos	0	0	0	0	0	0	0	0	0	0	0	0	0	0	0	0	0	0	0	0	0	0	0	0	0	0	0	0	0
DEWfmASenO_Neg	0	0	0	0	0	0	0	0	0	0	0	0	0	0	0	0	0	0	0	0	0	0	0	0	0	0	0	0	0
DEWfmASenO_Pos	0	0	0	0	0	0	0	0	0	0	0	0	0	0	0	0	0	0	0	0	0	0	0	0	0	0	0	0	0
DEWfmBSenO_Neg	0	0	0	0	0	0	0	0	0	0	0	0	0	0	0	0	0	0	0	0	0	0	0	0	0	0	0	0	0
DEWfmBSenO_Pos	0	0	0	0	0	0	0	0	0	0	0	0	0	0	0	0	0	0	0	0	0	0	0	0	0	0	0	0	0
DFmvDIlkg_Pos	0	0	0	0	0	0	0	0	0	0	0	0	0	0	0	0	0	0	0	0	0	0	0	0	0	0	0	0	0
DLppDIlkg_Pos	0	0	0	0	0	0	0	0	0	0	0	0	0	0	0	0	0	0	0	0	0	0	0	0	0	0	0	0	0
DMfpDIlkg_Pos	0	0	0	0	0	0	0	0	0	0	0	0	0	0	0	0	0	0	0	0	0	0	0	0	0	0	0	0	0
DSovDelay_Pos	0	0	0	0	0	0	0	0	0	0	0	0	0	0	0	0	0	0	0	0	0	0	0	0	0	0	0	0	0
DSovDIlkg_Pos	0	0	0	0	0	0	0	0	0	0	0	0	0	0	0	0	0	0	0	1	0	0	0	0	0	0	0	0	0
DTbvDIlkg_Pos	0	0	0	0	0	0	0	0	0	0	0	0	0	0	0	0	0	0	0	0	0	0	0	0	0	0	0	0	0

	VbvSlpLeftB	VbvSlpRightB	VbvHyst0B	VbvCEquS	VbvXchgS	VbvYchgS	VbvScaleS	VbvSlpLeftS	VbvSlpRightS	VbvHyst0S	VbvmaxX1	VbvmaxX2	VbvminX1	VbvminX2	VbvmaxGapX	VbvminGapX	VbvmeanGapX	VbvstdGapX	VbvMAErr	TOTAL
DByvDIlkg_Pos	1	0	0	0	0	0	0	0	0	0	0	0	0	0	0	0	0	0	1	10
DEByvK0_Neg	0	0	0	0	0	0	0	0	0	0	0	0	0	0	0	0	0	0	0	3
DEByvStic_Pos	0	0	0	0	0	0	0	0	0	0	0	0	0	0	0	0	0	0	0	0
DEByvVisc_Pos	0	0	0	0	0	0	0	0	0	0	0	0	0	0	0	0	0	0	0	0
DEFmvASen0_Neg	0	0	0	0	0	0	0	0	0	0	0	0	0	0	0	0	0	0	0	5
DEFmvASen0_Pos	0	0	0	0	0	0	0	0	0	0	0	0	0	0	0	0	0	0	0	9
DEFmvBSen0_Neg	0	0	0	0	0	0	0	0	0	0	0	0	0	0	0	0	0	0	0	5
DEFmvBSen0_Pos	0	0	0	0	0	0	0	0	0	0	0	0	0	0	0	0	0	0	0	9
DEFmvCnull_Neg	0	0	0	0	0	0	0	0	0	0	0	0	0	0	0	0	0	0	0	5
DEFmvCnull_Pos	0	0	0	0	0	0	0	0	0	0	0	0	0	0	0	0	0	0	0	8
DEFmvDnozzle_Pos	0	0	0	0	0	0	0	0	0	0	0	0	0	0	0	0	0	0	0	4
DEFmvStic_Pos	0	0	0	0	0	0	0	0	0	0	0	0	0	0	0	0	0	0	0	7
DEMffFlowRate_Neg	0	0	0	0	0	0	0	0	0	0	0	0	0	0	0	0	0	0	0	2
DESovStic_Pos	0	0	0	0	0	0	0	0	0	0	0	0	0	0	0	0	0	0	0	0
DESovVisc_Pos	0	0	0	0	0	0	0	0	0	0	0	0	0	0	0	0	0	0	0	0
DEVbvASen0_Neg	0	0	0	0	0	0	0	0	0	0	0	0	1	0	1	1	1	1	0	5
DEVbvASen0_Pos	0	0	1	0	0	0	0	0	0	1	1	0	1	0	1	1	1	1	1	10
DEVbvBSen0_Neg	0	0	0	0	0	0	0	0	0	0	0	0	0	1	1	1	1	1	0	5
DEVbvBSen0_Pos	0	0	1	0	0	0	0	0	0	1	0	1	0	1	1	1	1	1	1	10
DEVbvCnull_Neg	0	0	0	1	1	0	0	0	0	0	0	0	0	0	0	0	0	0	0	6
DEVbvCnull_Pos	0	0	0	1	1	0	0	0	0	0	0	0	0	0	0	0	0	0	0	6
DEVbvCorHP1_Pos	0	0	0	0	0	0	0	0	0	0	0	0	0	0	0	0	0	0	0	0
DEVbvCorHP2_Pos	0	0	0	0	0	0	0	0	0	0	0	0	0	0	0	0	0	0	1	3
DEVbvDCool1_Neg	0	0	0	0	0	0	0	0	0	0	0	0	0	0	0	0	0	0	0	0
DEVbvDCool1_Pos	0	0	0	0	0	0	0	0	0	0	0	0	0	0	0	0	0	0	0	0
DEVbvDCool2_Neg	0	0	0	1	1	1	0	0	0	0	0	0	0	0	0	0	0	0	0	5
DEVbvDCool2_Pos	1	0	0	1	1	0	1	1	0	0	0	0	0	0	0	0	0	0	0	10
DEVbvDFilter1_Neg	0	0	0	0	0	0	0	0	0	0	0	0	0	0	0	0	0	0	0	0
DEVbvDFilter2_Neg	0	0	0	0	0	0	0	0	0	0	0	0	0	0	0	0	0	0	0	0
DEVbvDnozzle_Neg	0	0	0	0	1	0	0	0	0	0	0	0	0	0	0	0	0	0	0	1
DEVbvDnozzle_Pos	0	0	0	0	0	0	0	0	0	0	0	0	0	0	0	0	0	0	0	0
DEVbvKfeed_Neg	0	0	0	0	1	0	0	0	0	0	0	0	0	0	0	0	0	0	0	1
DEVbvKineFric_Pos	0	0	0	0	0	0	0	0	0	0	0	0	0	0	0	0	0	0	0	2
DEVbvStic1_Pos	0	0	0	0	0	0	0	0	0	0	0	0	0	0	0	0	0	0	0	0
DEVbvStic2_Pos	0	0	0	0	0	0	0	0	0	0	0	0	0	0	0	0	0	0	0	0
DEVbvSticspool_Pos	0	0	1	1	0	1	1	1	0	0	0	0	0	0	0	0	0	0	1	11
DEVbvVisc1_Pos	0	0	0	0	0	0	0	0	0	0	0	0	0	0	0	0	0	0	0	0
DEVbvVisc2_Pos	0	0	0	0	0	0	0	0	0	0	0	0	0	0	0	0	0	0	0	0
DEVsvASen0_Neg	0	0	0	0	0	0	0	0	0	0	0	0	0	0	0	0	0	0	0	5
DEVsvASen0_Pos	0	0	0	0	0	0	0	0	0	0	0	0	0	0	0	0	0	0	0	8
DEVsvBSen0_Neg	0	0	0	0	0	0	0	0	0	0	0	0	0	0	0	0	0	0	0	6
DEVsvBSen0_Pos	0	0	0	0	0	0	0	0	0	0	0	0	0	0	0	0	0	0	0	7
DEVsvCnull_Neg	0	0	0	0	0	0	0	0	0	0	0	0	0	0	0	0	0	0	0	11
DEVsvCnull_Pos	0	0	0	0	0	0	0	0	0	0	0	0	0	0	0	0	0	0	0	6
DEVsvCorHP1_Pos	0	0	0	0	0	0	0	0	0	0	0	0	0	0	0	0	0	0	0	0
DEVsvCorHP2_Pos	0	0	0	0	0	0	0	0	0	0	0	0	0	0	0	0	0	0	0	0
DEVsvDCool1_Neg	0	0	0	0	0	0	0	0	0	0	0	0	0	0	0	0	0	0	0	0
DEVsvDCool1_Pos	0	0	0	0	0	0	0	0	0	0	0	0	0	0	0	0	0	0	0	0
DEVsvDCool2_Neg	0	0	0	0	0	0	0	0	0	0	0	0	0	0	0	0	0	0	0	8
DEVsvDCool2_Pos	0	0	0	0	0	0	0	0	0	0	0	0	0	0	0	0	0	0	0	14
DEVsvDFilter1_Neg	0	0	0	0	0	0	0	0	0	0	0	0	0	0	0	0	0	0	0	0
DEVsvDFilter2_Neg	0	0	0	0	0	0	0	0	0	0	0	0	0	0	0	0	0	0	0	1
DEVsvDnozzle_Neg	0	0	0	0	0	0	0	0	0	0	0	0	0	0	0	0	0	0	0	0
DEVsvDnozzle_Pos	0	0	0	0	0	0	0	0	0	0	0	0	0	0	0	0	0	0	0	0
DEVsvKfeed_Neg	0	0	0	0	0	0	0	0	0	0	0	0	0	0	0	0	0	0	0	10
DEVsvKineFric_Pos	0	0	0	0	0	0	0	0	0	0	0	0	0	0	0	0	0	0	0	15
DEVsvStic1_Pos	0	0	0	0	0	0	0	0	0	0	0	0	0	0	0	0	0	0	0	0
DEVsvStic2_Pos	0	0	0	0	0	0	0	0	0	0	0	0	0	0	0	0	0	0	0	0
DEVsvSticspool_Pos	0	0	0	0	0	0	0	0	0	0	0	0	0	0	0	0	0	0	0	18
DEVsvVisc1_Pos	0	0	0	0	0	0	0	0	0	0	0	0	0	0	0	0	0	0	0	0
DEVsvVisc2_Pos	0	0	0	0	0	0	0	0	0	0	0	0	0	0	0	0	0	0	0	0
DEWfmASen0_Neg	0	0	0	0	0	0	0	0	0	0	0	0	0	0	0	0	0	0	0	4
DEWfmASen0_Pos	0	0	0	0	0	0	0	0	0	0	0	0	0	0	0	0	0	0	0	4
DEWfmBSen0_Neg	0	0	0	0	0	0	0	0	0	0	0	0	0	0	0	0	0	0	0	4
DEWfmBSen0_Pos	0	0	0	0	0	0	0	0	0	0	0	0	0	0	0	0	0	0	0	4
DFmvDIlkg_Pos	0	0	0	0	0	0	0	0	0	0	0	0	0	0	0	0	0	0	0	14
DLppDIlkg_Pos	0	0	0	0	0	0	0	0	0	0	0	0	0	0	0	0	0	0	0	0
DMfpDIlkg_Pos	0	0	0	0	0	0	0	0	0	0	0	0	0	0	0	0	0	0	0	1
DSovDelay_Pos	0	0	0	0	0	0	0	0	0	0	0	0	0	0	0	0	0	0	0	1
DSovDIlkg_Pos	0	0	0	0	0	1	0	1	0	0	0	0	0	0	0	0	0	0	1	8
DTbvDIlkg_Pos	0	0	0	0	0	0	0	0	0	0	0	0	0	0	0	0	0	0	0	0

Table A.24 *Detection NKPIs for standardized HIs.*

Appendix XXXI. Identification NKPIs standardized HIs

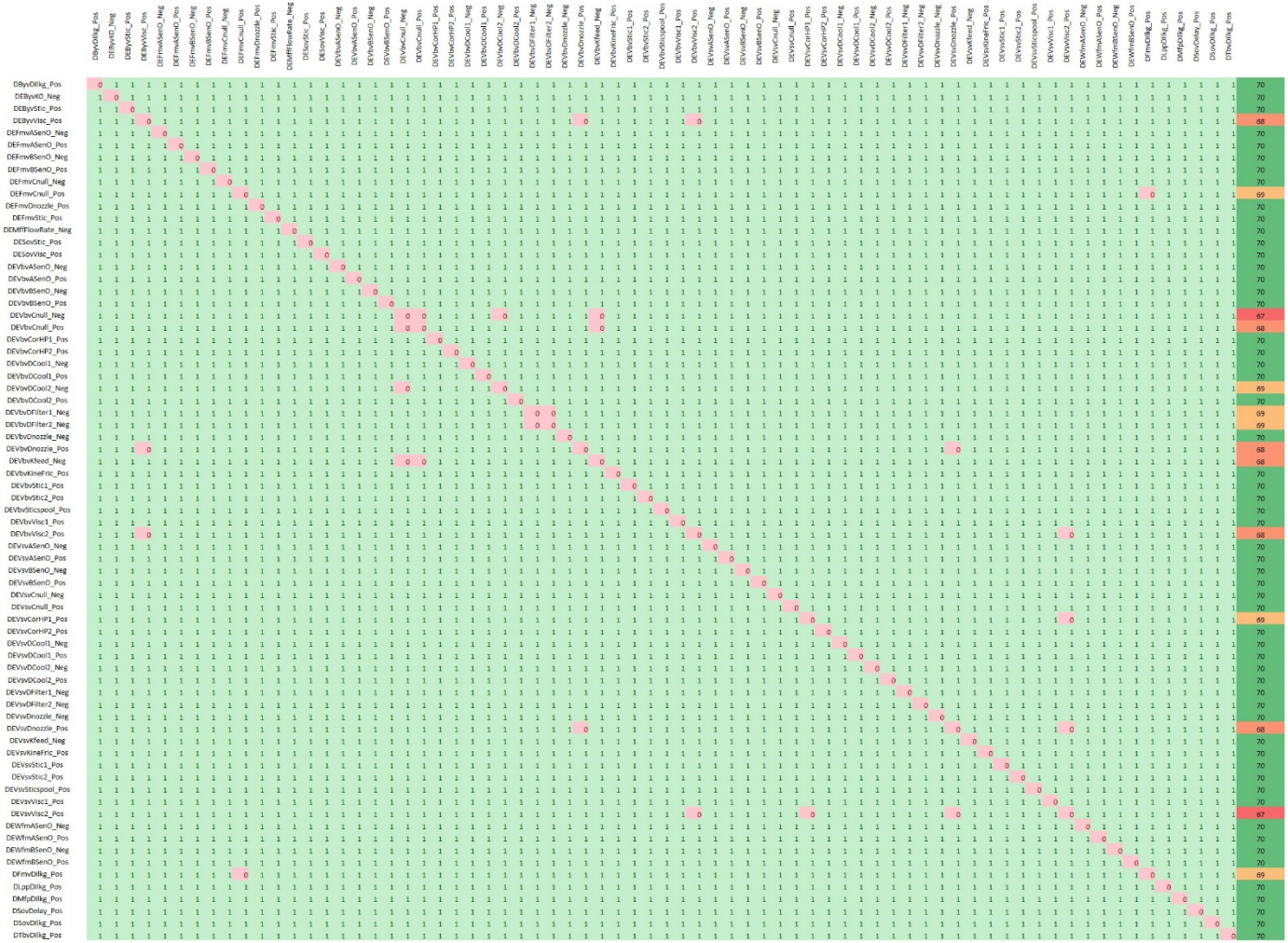


Table A.25 *Identification NKPIs for standardized HIs.*

Appendix XXXII. Localization NKPIs for standardized HIs

	Pumping Unit	Fuel Filter	ACU	FMU	VSV Actuation	VBV Actuation	TBV Actuation	Flowmeter	TOTAL
Pumping Unit	0	1	1	1	1	1	1	1	7
Fuel Filter	1	0	1	1	1	1	1	1	7
ACU	1	1	0	0	0	0	0	1	3
FMU	1	1	0	0	0	1	1	1	5
VSV Actuation	1	1	0	0	0	0	0	1	3
VBV Actuation	1	1	0	1	0	0	1	1	5
TBV Actuation	1	1	0	1	0	1	0	1	5
Flowmeter	1	1	1	1	1	1	1	0	7

Table A.26 *Localization NKPIs for standardized HIs.*

Appendix XXXIII. Prognostics NKPIs for the standardized HIs

	DeltaD	DeltaI	DeltaL
DByvDIlkg_Pos	0	0	0
DEByvK0_Neg	216	149,33	116
DEByvStic_Pos	0	0	0
DEByvVisc_Pos	0	0	0
DEFmvASenO_Neg	0	0	0
DEFmvASenO_Pos	0,75	0,75	0
DEFmvBSenO_Neg	0	0	0
DEFmvBSenO_Pos	0,75	0,75	0
DEFmvCnull_Neg	12,23	12,2	0
DEFmvCnull_Pos	17,23	17,2	0
DEFmvDnozzle_Pos	0	0	0
DEFmvStic_Pos	23,98	0	0
DEMffFlowRate_Neg	76,75	76,7	0
DESovStic_Pos	0	0	0
DESovVisc_Pos	0	0	0
DEVbvASenO_Neg	0	0	0
DEVbvASenO_Pos	0,95	0,95	0
DEVbvBSenO_Neg	0	0	0
DEVbvBSenO_Pos	0,95	0,95	0
DEVbvCnull_Neg	8,43	8,43	0
DEVbvCnull_Pos	13,4	13,43	0
DEVbvCorHP1_Pos	0	0	0
DEVbvCorHP2_Pos	0,03	0,021	0
DEVbvDCool1_Neg	0	0	0
DEVbvDCool1_Pos	0	0	0
DEVbvDCool2_Neg	0	0	0
DEVbvDCool2_Pos	1,85	0	0
DEVbvDFilter1_Neg	0	4	0
DEVbvDFilter2_Neg	0	4	0
DEVbvDnozzle_Neg	0	0	0
DEVbvDnozzle_Pos	0	0	0
DEVbvKfeed_Neg	1,2	1,1	0
DEVbvKineFric_Pos	0	0	0
DEVbvStic1_Pos	0	0	0
DEVbvStic2_Pos	0	0	0
DEVbvSticspool_Pos	0	0	0
DEVbvVisc1_Pos	0	0	0
DEVbvVisc2_Pos	0	0	0
DEVsvASenO_Neg	0	0	0
DEVsvASenO_Pos	0	0	0
DEVsvBSenO_Neg	0	0	0
DEVsvBSenO_Pos	0	0	0
DEVsvCnull_Neg	7,97	7,97	0
DEVsvCnull_Pos	12,9	12,97	0
DEVsvCorHP1_Pos	0	0	0
DEVsvCorHP2_Pos	0	0	0
DEVsvDCool1_Neg	0	0	0
DEVsvDCool1_Pos	0	0	0
DEVsvDCool2_Neg	0	0	0
DEVsvDCool2_Pos	0	0	0
DEVsvDFilter1_Neg	0	4	0
DEVsvDFilter2_Neg	4	4	0
DEVsvDnozzle_Neg	0	0	0
DEVsvDnozzle_Pos	0	0	0
DEVsvKfeed_Neg	1,1	1,1	0
DEVsvKineFric_Pos	0	0	0
DEVsvStic1_Pos	0	0	0
DEVsvStic2_Pos	0	0	0
DEVsvSticspool_Pos	0	0	0
DEVsvVisc1_Pos	0	0	0
DEVsvVisc2_Pos	0	0	0
DEWfmASenO_Neg	0	0	0
DEWfmASenO_Pos	0	0	0
DEWfmBSenO_Neg	0	0	0
DEWfmBSenO_Pos	0	0	0
DFmvDIlkg_Pos	0,25	0,25	0
DLppDIlkg_Pos	0	0	0
DMfpDIlkg_Pos	0,35	0	0
DSovDelay_Pos	0	0	0
DSovDIlkg_Pos	0,07	0	0
DTbvDIlkg_Pos	0	0	0

Appendix XXXIV. Detection NKPIs for individual models

	FmvCEquA	FmvScaleA	FmvSlpA	FmvHyst0A	FmvCEquB	FmvScaleB	FmvSlpB	FmvHyst0B	FmvCEquS	FmvScaleS	FmvSlpS	FmvHyst0S	FmvmaxX1	FmvmaxX2	FmvminX1	FmvminX2	FmvmaxGapX	FmvminGapX	FmvmeanGapX	FmvstdGapX	FmvMAErr	Sovdelop1	Sovdelclo	Sovdelop2	wTBV	wSOV	MffSlpN2DP	MffR2N2DP
DBvvDIlkg_Pos	0	1	0	0	0	1	0	0	0	1	1	0	0	0	0	0	0	0	0	0	0	0	0	0	1	0	0	0
DEBvvK0_Neg	0	1	0	0	0	0	0	0	0	1	0	0	0	0	0	0	0	0	0	0	0	0	0	0	0	0	0	0
DEBvvStic_Pos	0	0	0	0	0	0	0	0	0	1	0	0	0	0	0	0	0	0	0	0	0	0	0	0	1	0	0	0
DEBvvVisc_Pos	0	0	0	0	0	0	0	0	0	0	0	0	0	0	0	0	0	0	0	0	0	0	0	0	0	0	0	0
DEFmvASen0_Neg	0	0	0	0	0	0	0	0	0	0	0	0	1	0	1	0	0	1	1	1	0	0	0	0	0	0	0	0
DEFmvASen0_Pos	0	1	0	1	0	1	0	1	0	1	0	1	0	1	0	0	1	0	1	1	0	0	0	0	0	0	0	0
DEFmvBSen0_Neg	0	0	0	0	0	0	0	0	0	0	0	0	1	0	1	1	0	1	1	0	0	0	0	0	0	0	0	0
DEFmvBSen0_Pos	0	1	0	1	0	1	0	1	0	1	0	1	1	0	0	0	0	1	1	1	0	0	0	0	0	0	0	0
DEFmvCnull_Neg	1	1	0	1	1	0	0	1	1	1	0	1	1	1	0	0	0	0	0	0	1	0	0	0	0	0	0	0
DEFmvCnull_Pos	1	1	0	1	1	0	0	1	1	1	0	1	1	1	0	0	0	0	0	0	1	0	0	0	0	0	0	0
DEFmvDnozzle_Pos	0	1	1	0	0	1	1	0	0	1	1	0	0	0	0	0	0	0	0	0	0	0	0	0	0	0	0	0
DEFmvStic_Pos	0	1	0	1	0	0	0	1	0	1	0	1	1	1	0	0	0	0	0	0	1	0	0	0	0	0	0	0
DEMffFlowRate_Neg	0	0	0	0	0	0	0	0	0	0	0	0	0	0	0	0	0	0	0	0	0	0	0	0	0	0	1	1
DESovStic_Pos	0	1	0	0	0	0	0	0	0	1	0	0	0	0	0	0	0	0	0	0	0	0	0	0	0	0	0	0
DESovVisc_Pos	0	0	0	0	0	0	0	0	0	1	0	0	0	0	0	0	0	0	0	0	0	0	0	0	0	0	0	0
DEVbvASen0_Neg	0	0	0	0	0	0	0	0	0	0	0	0	0	0	0	0	0	0	0	0	0	0	0	0	0	0	0	0
DEVbvASen0_Pos	0	1	0	0	0	0	0	0	0	1	0	0	0	0	0	0	0	0	0	0	0	0	0	0	0	0	0	0
DEVbvBSen0_Neg	0	1	0	0	0	0	0	0	0	1	0	0	0	0	0	0	0	0	0	0	0	0	0	0	0	0	0	0
DEVbvBSen0_Pos	0	1	0	0	0	0	0	0	0	1	0	0	0	0	0	0	0	0	0	0	0	0	0	0	0	0	0	0
DEVbvCnull_Neg	0	0	0	0	0	0	0	0	0	0	0	0	0	0	0	0	0	0	0	0	0	0	0	0	0	0	0	0
DEVbvCnull_Pos	0	0	0	0	0	0	0	0	0	0	0	0	0	0	0	0	0	0	0	0	0	0	0	0	0	0	0	0
DEVbvCorHP1_Pos	0	0	0	0	0	0	0	0	0	0	0	0	0	0	0	0	0	0	0	0	0	0	0	0	0	0	0	0
DEVbvCorHP2_Pos	0	0	0	0	0	0	0	0	0	0	0	0	0	0	0	0	0	0	0	0	0	0	1	0	0	0	0	0
DEVbvDCool1_Neg	0	0	0	0	0	0	0	0	0	0	0	0	0	0	0	0	0	0	0	0	0	0	0	0	0	0	0	0
DEVbvDCool1_Pos	0	0	0	0	0	0	0	0	0	0	0	0	0	0	0	0	0	0	0	0	0	0	0	0	0	0	0	0
DEVbvDCool2_Neg	0	0	0	0	0	0	0	0	0	0	0	0	0	0	0	0	0	0	0	0	0	0	0	0	0	0	0	0
DEVbvDCool2_Pos	0	0	0	0	0	0	0	0	0	0	0	0	0	0	0	0	0	0	0	0	0	0	0	0	0	0	0	0
DEVbvDFilter1_Neg	0	0	0	0	0	0	0	0	0	0	0	0	0	0	0	0	0	0	0	0	0	0	0	0	0	0	0	0
DEVbvDFilter2_Neg	0	0	0	0	0	0	0	0	0	0	0	0	0	0	0	0	0	0	0	0	0	0	0	0	0	0	0	0
DEVbvDnozzle_Neg	0	1	0	0	0	0	0	0	0	1	0	0	0	0	0	0	0	0	0	0	0	0	0	0	0	0	0	0
DEVbvDnozzle_Pos	0	1	0	0	0	0	0	0	0	1	0	0	0	0	0	0	0	0	0	0	0	0	0	0	0	0	0	0
DEVbvKfeed_Neg	0	1	0	0	0	0	0	0	0	1	0	0	0	0	0	0	0	0	0	0	0	0	0	0	0	0	0	0
DEVbvKineFric_Pos	0	1	0	1	0	0	0	1	0	1	0	1	0	0	0	0	0	0	0	0	0	0	0	0	0	0	0	0
DEVbvStic1_Pos	0	0	0	0	0	0	0	0	0	0	0	0	0	0	0	0	0	0	0	0	0	0	0	0	0	0	0	0
DEVbvStic2_Pos	0	0	0	0	0	0	0	0	0	0	0	0	0	0	0	0	0	0	0	0	0	0	0	0	0	0	0	0
DEVbvSticspool_Pos	0	0	0	0	0	0	0	0	0	1	0	0	0	0	0	0	0	0	0	0	0	0	0	0	0	0	0	0
DEVbvVisc1_Pos	0	0	0	0	0	0	0	0	0	0	0	0	0	0	0	0	0	0	0	0	0	0	0	0	0	0	0	0
DEVbvVisc2_Pos	0	1	0	0	0	0	0	0	0	1	0	0	0	0	0	0	0	0	0	0	0	0	0	0	0	0	0	0
DEVsvASen0_Neg	0	0	0	0	0	0	0	0	0	1	0	0	0	0	0	0	0	0	0	0	0	0	0	0	0	0	0	0
DEVsvASen0_Pos	0	0	0	0	0	0	0	0	0	1	0	0	0	0	0	0	0	0	0	0	0	0	0	0	0	0	0	0
DEVsvBSen0_Neg	0	0	0	0	0	0	0	0	0	1	0	0	0	0	0	0	0	0	0	0	0	0	0	0	0	0	0	0
DEVsvBSen0_Pos	0	0	0	0	0	0	0	0	0	1	0	0	0	0	0	0	0	0	0	0	0	0	0	0	0	0	0	0
DEVsvCnull_Neg	0	0	0	0	0	0	0	0	0	1	0	0	0	0	0	0	0	0	0	0	0	0	0	0	0	0	0	0
DEVsvCnull_Pos	0	0	0	0	0	0	0	0	0	0	0	0	0	0	0	0	0	0	0	0	0	0	0	0	0	0	0	0
DEVsvCorHP1_Pos	0	0	0	0	0	0	0	0	0	0	0	0	0	0	0	0	0	0	0	0	0	0	0	0	0	0	0	0
DEVsvCorHP2_Pos	0	0	0	0	0	0	0	0	0	1	0	0	0	0	0	0	0	0	0	0	0	0	0	0	0	0	0	0
DEVsvDCool1_Neg	0	0	0	0	0	0	0	0	0	0	0	0	0	0	0	0	0	0	0	0	0	0	0	0	0	0	0	0
DEVsvDCool1_Pos	0	0	0	0	0	0	0	0	0	0	0	0	0	0	0	0	0	0	0	0	0	0	0	0	0	0	0	0
DEVsvDCool2_Neg	0	0	0	0	0	0	0	0	0	1	0	0	0	0	0	0	0	0	0	0	0	0	0	0	0	0	0	0
DEVsvDCool2_Pos	0	0	0	0	0	0	0	0	0	1	0	0	0	0	0	0	0	0	0	0	0	0	0	0	0	0	0	0
DEVsvDFilter1_Neg	0	0	0	0	0	0	0	0	0	0	0	0	0	0	0	0	0	0	0	0	0	0	0	0	0	0	0	0
DEVsvDFilter2_Neg	0	0	0	0	0	0	0	0	0	0	0	0	0	0	0	0	0	0	0	0	0	0	0	0	0	0	0	0
DEVsvDnozzle_Neg	0	0	0	0	0	0	0	0	0	1	0	0	0	0	0	0	0	0	0	0	0	0	0	0	0	0	0	0
DEVsvDnozzle_Pos	0	0	0	0	0	0	0	0	0	0	0	0	0	0	0	0	0	0	0	0	0	0	0	0	0	0	0	0
DEVsvKfeed_Neg	0	0	0	0	0	0	0	0	0	0	0	0	0	0	0	0	0	0	0	0	0	0	0	0	0	0	0	0
DEVsvKineFric_Pos	0	0	0	0	0	0	0	0	0	1	0	0	0	0	0	0	0	0	0	0	0	0	0	0	0	0	0	0
DEVsvStic1_Pos	0	0	0	0	0	0	0	0	0	0	0	0	0	0	0	0	0	0	0	0	0	0	0	0	0	0	0	0
DEVsvStic2_Pos	0	0	0	0	0	0	0	0	0	0	0	0	0	0	0	0	0	0	0	0	0	0	0	0	0	0	0	0
DEVsvSticspool_Pos	0	0	0	0	0	0	0	0	0	0	0	0	0	0	0	0	0	0	0	0	0	0	0	0	0	0	0	0
DEVsvVisc1_Pos	0	0	0	0	0	0	0	0	0	0	0	0	0	0	0	0	0	0	0	0	0	0	0	0	0	0	0	0
DEVsvVisc2_Pos	0	0	0	0	0	0	0	0	0	0	0	0	0	0	0	0	0	0	0	0	0	0	0	0	0	0	0	0
DEWfmASen0_Neg	0	0	0	0	0	0	0	0	0	0	0	0	0	0	0	0	0	0	0	0	0	0	0	0	0	0	0	0
DEWfmASen0_Pos	0	0	0	0	0	0	0	0	0	0	0	0	0	0	0	0	0	0	0	0	0	0	0	0	0	0	0	0
DEWfmBSen0_Neg	0	0	0	0	0	0	0	0	0	0	0	0	0	0	0	0	0	0	0	0	0	0	0	0	0	0	0	0
DEWfmBSen0_Pos	0	0	0	0	0	0	0	0	0	0	0	0	0	0	0	0	0	0	0	0	0	0	0	0	0	0	0	0
DFmvDIlkg_Pos	1	1	1	1	1	1	1	1	1	1	1	1	1	1	0	0	0	0	0	0	1	0	0	0	0	0	0	0
DLppDIlkg_Pos	0	0	0	0	0	0	0	0	0	0	0	0	0	0	0	0	0	0	0	0	0	0	0	0	0	0	0	0
DMfpDIlkg_Pos	0	0	0	0	0	0	0	0	0	0	0	0	0	0	0	0	0	0	0	0	0	0	0	0	1	0	0	0
DSovDelay_Pos	0	0	0	0	0	0	0	0	0	0	0	0	0	0	0	0	0	0	0	0	0	1	0	1	1	0	0	0
DSovDIlkg_Pos	0	1	0	0	0	1	0	0	0	1	0	0	0	0	0	0	0	0	0	0	0	1	0	1	1	0	0	0
DTbvDIlkg_Pos	0	0	0	0	0	0	0	0	0	0	0	0	0	0	0	0	0	0	0	0	0	0	0	0	0	0	0	0

	WfmmaxX1	WfmmaxX2	WfmminX1	WfmminX2	WfmmaxGapX	WfmminGapX	WfmmeanGapX	WfmstdGapX	VsvCEquA	VsvXnullA	VsvYnullA	VsvXoverlapA	VsvYoverlapA	VsvScaleA	VsvSlpLeftA	VsvSlpNullA	VsvSlpRightA	VsvHyst0A	VsvCEquB	VsvXnullB	VsvYnullB	VsvXoverlapB	VsvYoverlapB	VsvScaleB	VsvSlpLeftB	VsvSlpNullB	VsvSlpRightB	VsvHyst0B	VsvCEquS
DBvvDIlkg_Pos	1	1	0	0	0	0	0	0	1	0	1	0	1	1	0	1	1	0	0	0	1	0	1	1	0	1	1	0	1
DEBvvK0_Neg	1	1	0	0	0	0	0	0	1	0	0	0	0	1	0	0	0	0	0	0	0	0	0	1	0	0	1	0	1
DEBvvStic_Pos	0	0	0	0	0	0	0	0	0	0	0	0	0	0	0	0	0	0	0	0	0	0	0	1	0	0	1	0	1
DEBvvVisc_Pos	0	0	0	0	0	0	0	0	0	0	0	0	0	0	0	0	0	0	0	0	0	0	0	0	0	0	1	0	0
DEFmvASenO_Neg	0	0	0	0	0	0	0	0	0	0	0	0	0	0	0	0	0	0	0	0	0	0	0	0	0	0	0	0	0
DEFmvASenO_Pos	1	1	0	0	0	0	0	0	1	0	0	0	0	0	0	0	0	0	0	0	0	0	0	0	0	0	1	0	1
DEFmvBSenO_Neg	0	0	0	0	0	0	0	0	0	0	0	0	0	0	0	0	0	0	0	0	0	0	0	0	0	0	0	0	0
DEFmvBSenO_Pos	1	1	0	0	0	0	0	0	1	0	0	0	0	0	0	0	0	0	0	0	0	0	0	0	0	0	1	0	1
DEFmvCnull_Neg	1	1	0	0	0	0	0	0	0	0	0	0	0	0	0	0	0	0	0	0	0	0	0	0	0	0	1	0	1
DEFmvCnull_Pos	1	1	0	0	0	0	0	0	0	0	0	0	0	0	0	0	0	0	0	0	0	0	0	0	0	0	1	0	1
DEFmvDnozzle_Pos	0	0	0	0	0	0	0	0	0	0	0	0	0	0	0	0	0	0	0	0	0	0	0	0	0	0	0	0	0
DEFmvStic_Pos	1	1	0	0	0	0	0	0	0	0	0	0	0	0	0	0	0	0	0	0	0	0	0	0	0	0	1	0	1
DEMffFlowRate_Neg	0	0	0	0	0	0	0	0	0	0	0	0	0	0	0	0	0	0	0	0	0	0	0	0	0	0	0	0	0
DESovStic_Pos	0	0	0	0	0	0	0	0	0	0	0	0	0	0	0	0	0	0	0	0	0	0	0	0	0	0	0	0	1
DESovVisc_Pos	0	0	0	0	0	0	0	0	0	0	0	0	0	0	0	0	0	0	0	0	0	0	0	1	0	0	0	0	0
DEVbvASenO_Neg	0	0	0	0	0	0	0	0	0	0	0	0	0	0	0	0	0	0	0	0	0	0	0	0	0	0	0	0	0
DEVbvASenO_Pos	0	0	0	0	0	0	0	0	0	0	0	0	0	0	0	0	0	0	0	0	0	0	0	0	0	0	0	0	0
DEVbvBSenO_Neg	0	0	0	0	0	0	0	0	0	0	0	0	0	0	0	0	0	0	0	0	0	0	0	0	0	0	0	0	0
DEVbvBSenO_Pos	0	0	0	0	0	0	0	0	0	0	0	0	0	0	0	0	0	0	0	0	0	0	0	0	0	0	0	0	0
DEVbvCnull_Neg	0	0	0	0	0	0	0	0	0	0	0	0	0	0	0	0	0	0	0	0	0	0	0	0	0	0	0	0	0
DEVbvCnull_Pos	0	0	0	0	0	0	0	0	0	0	0	0	0	0	0	0	0	0	0	0	0	0	0	0	0	0	0	0	0
DEVbvCorHP1_Pos	0	0	0	0	0	0	0	0	0	0	0	0	0	0	0	0	0	0	0	0	0	0	0	0	0	0	0	0	0
DEVbvCorHP2_Pos	0	0	0	0	0	0	0	0	0	0	0	0	0	0	0	0	0	0	0	0	0	0	0	0	0	0	0	0	0
DEVbvDCool1_Neg	0	0	0	0	0	0	0	0	0	0	0	0	0	0	0	0	0	0	0	0	0	0	0	0	0	0	0	0	0
DEVbvDCool1_Pos	0	0	0	0	0	0	0	0	0	0	0	0	0	0	0	0	0	0	0	0	0	0	0	0	0	0	0	0	0
DEVbvDCool2_Neg	0	0	0	0	0	0	0	0	0	0	0	0	0	0	0	0	0	0	0	0	0	0	0	0	0	0	0	0	0
DEVbvDCool2_Pos	0	0	0	0	0	0	0	0	0	0	0	0	0	0	0	0	0	0	0	0	0	0	0	0	0	0	0	0	0
DEVbvDFilter1_Neg	0	0	0	0	0	0	0	0	0	0	0	0	0	0	0	0	0	0	0	0	0	0	0	0	0	0	0	0	0
DEVbvDFilter2_Neg	0	0	0	0	0	0	0	0	0	0	0	0	0	0	0	0	0	0	0	0	0	0	0	0	0	0	0	0	0
DEVbvDnozzle_Neg	0	0	0	0	0	0	0	0	0	0	0	0	0	0	0	0	0	0	0	0	0	0	0	0	0	0	1	0	0
DEVbvDnozzle_Pos	0	0	0	0	0	0	0	0	0	0	0	0	0	0	0	0	0	0	0	0	0	0	0	0	0	0	0	0	0
DEVbvKfeed_Neg	0	0	0	0	0	0	0	0	0	0	0	0	0	0	0	0	0	0	0	0	0	0	0	0	0	0	1	0	0
DEVbvKineFric_Pos	0	0	0	1	1	0	0	0	0	1	0	0	1	0	0	0	0	0	1	1	1	0	0	0	1	0	0	0	0
DEVbvStic1_Pos	0	0	0	0	0	0	0	0	0	0	0	0	0	0	0	0	0	0	0	0	0	0	0	0	0	0	0	0	0
DEVbvStic2_Pos	0	0	0	0	0	0	0	0	0	0	0	0	0	0	0	0	0	0	0	0	0	0	0	0	0	0	0	0	0
DEVbvSticspool_Pos	0	0	0	0	0	0	0	0	0	0	0	0	0	0	0	0	0	0	0	0	0	0	0	0	0	0	1	0	0
DEVbvVisc1_Pos	0	0	0	0	0	0	0	0	0	0	0	0	0	0	0	0	0	0	0	0	0	0	0	0	0	0	0	0	0
DEVbvVisc2_Pos	0	0	0	0	0	0	0	0	0	0	0	0	0	0	0	0	0	0	0	0	0	0	0	0	0	0	0	0	0
DEVsvASenO_Neg	0	0	0	0	0	0	0	0	0	0	0	0	0	0	0	0	0	0	0	0	0	0	0	0	0	1	0	0	0
DEVsvASenO_Pos	0	0	0	0	0	0	0	0	0	0	0	0	0	0	0	0	0	0	0	0	1	1	1	0	0	1	1	0	1
DEVsvBSenO_Neg	0	0	0	0	0	0	0	0	0	0	0	0	0	0	0	1	0	0	0	0	0	0	0	0	0	0	0	0	0
DEVsvBSenO_Pos	0	0	0	0	0	0	0	0	0	0	1	1	1	0	1	1	0	0	0	0	0	0	0	0	0	0	0	0	1
DEVsvCnull_Neg	0	0	0	0	0	0	0	0	1	1	1	1	1	0	1	1	0	0	1	1	1	1	1	0	1	1	1	0	1
DEVsvCnull_Pos	0	0	0	0	0	0	0	0	1	1	0	0	0	0	0	1	0	0	1	1	0	0	0	0	0	1	0	0	1
DEVsvCorHP1_Pos	0	0	0	0	0	0	0	0	0	0	0	0	0	1	1	0	0	0	0	0	0	0	0	1	0	0	1	0	1
DEVsvCorHP2_Pos	0	0	0	0	0	0	0	0	1	0	1	0	1	0	0	0	0	0	1	0	1	0	1	1	0	0	1	0	1
DEVsvDCool1_Neg	0	0	0	0	0	0	0	0	0	0	0	0	0	0	0	0	0	0	0	0	0	0	0	0	0	0	0	0	0
DEVsvDCool1_Pos	0	0	0	0	0	0	0	0	0	0	0	0	0	0	0	0	0	0	0	0	0	0	0	0	0	0	0	0	0
DEVsvDCool2_Neg	0	0	0	0	0	0	0	0	1	0	1	0	1	1	1	1	0	0	1	0	1	0	1	1	1	1	1	0	1
DEVsvDCool2_Pos	0	0	0	0	0	0	0	0	1	1	1	1	1	1	1	1	0	0	1	1	1	1	1	1	1	1	1	1	1
DEVsvDFilter1_Neg	0	0	0	0	0	0	0	0	0	0	0	0	0	0	0	0	0	0	0	0	0	0	0	0	0	0	0	0	1
DEVsvDFilter2_Neg	0	0	0	0	0	0	0	0	0	0	1	1	1	0	1	1	0	0	0	0	1	1	1	0	0	1	1	0	1
DEVsvDnozzle_Neg	0	0	0	0	0	0	0	0	0	0	0	0	0	0	0	0	0	0	0	0	0	0	0	1	0	0	0	0	0
DEVsvDnozzle_Pos	0	0	0	0	0	0	0	0	0	0	0	0	0	0	0	0	0	0	0	0	0	0	0	1	0	0	1	0	0
DEVsvKfeed_Neg	0	0	0	0	0	0	0	0	1	0	1	1	1	1	1	1	1	0	1	0	1	1	1	1	1	1	1	0	1
DEVsvKineFric_Pos	0	0	0	0	0	0	1	0	0	1	1	1	1	1	1	1	1	0	0	0	1	1	1	1	1	1	1	0	0
DEVsvStic1_Pos	0	0	0	0	0	0	0	0	0	0	0	0	0	0	0	0	0	0	0	0	0	0	0	0	0	0	0	0	0
DEVsvStic2_Pos	0	0	0	0	0	0	0	0	0	0	0	0	0	0	0	0	0	0	0	0	0	0	0	0	0	0	0	0	0
DEVsvSticspool_Pos	0	0	0	0	0	0	0	0	1	0	1	0	1	0	1	1	0	0	1	0	1	0	1	0	1	1	1	1	1
DEVsvVisc1_Pos	0	0	0	0	0	0	0	0	0	0	0	0	0	0	0	0	0	0	0	0	0	0	0	0	0	0	0	0	0
DEVsvVisc2_Pos	0	0	0	0	0	0	0	0	0	0	0	0	0	0	0	0	0	0	0	0	0	0	0	0	0	0	0	0	0
DEWfmASenO_Neg	0	0	1	0	0	1	1	1	0	0	0	0	0	0	0	0	0	0	0	0	0	0	0	0	0	0	0	0	0
DEWfmASenO_Pos	0	0	1	0	1	0	1	1	0	0	0	0	0	0	0	0	0	0	0	0	0	0	0	0	0	0	0	0	0
DEWfmBSenO_Neg	0	0	0	1	1	0	1	1	0	0	0	0	0	0	0	0	0	0	0	0	0	0	0	0	0	0	0	0	0
DEWfmBSenO_Pos	0	0	0	1	0	1	1	1	0	0	0	0	0	0	0	0	0	0	0	0	0	0	0	0	0	0	0	0	0
DFmvDIlkg_Pos	1	1	0	0	0	0	0	0	0	0	0	0	0	0	0	0	0	0	0	0	0	0	0	0	0	0	1	0	1
DLpvDIlkg_Pos	0	0	0	0	0	0	0	0	0	0	0	0	0	0	0	0	0	0	0	0	0	0	0	0	0	0	0	0	1
DMfpDIlkg_Pos	0	0	0	0	0	0	0	0	0	0	1	1	1	0	1	1	0	0	0	0	1	1	1	0	0	1	1	0	1
DSovDelay_Pos	0	0	0	0	0	0	0	0	0	0	0	0	0	0	0	0	0	0	0	0	0	0	0	0	0	0	0	0	0
DSovDIlkg_Pos	0	0	0	0	0	0	0	0	1	0	1	0	1	1	0	1	1	0	0	0	1	0	1	1	0	1	1	0	1
DTbvDIlkg_Pos	0	0	0	0	0	0	0	0	0	0	0	0	0	0	0	0	0	0	0	0	0	0	0	0	0	0	0	0	0

	VsvXnullS	VsvYnullS	VsvXoverlapS	VsvYoverlapS	VsvScaleS	VsvSlpLeftS	VsvSlpNullS	VsvSlpRightS	VsvHyst0S	VsvmaxX1	VsvmaxX2	VsvminX1	VsvminX2	VsvmaxGapX	VsvminGapX	VsvmeanGapX	VsvstdGapX	VsvMAErr	VbvCEquA	VbvXchgA	VbvYchgA	VbvScaleA	VbvSlpLeftA	VbvSlpRightA	VbvHyst0A	VbvCEquB	VbvXchgB	VbvYchgB	VbvScaleB
DBvvDIlkg_Pos	1	1	1	1	1	1	1	1	0	0	0	0	0	0	0	0	0	0	0	1	1	1	1	1	0	0	1	1	1
DEBvvK0_Neg	1	1	1	1	1	0	0	0	0	0	0	0	0	0	0	0	0	0	0	0	0	0	0	0	0	0	0	0	1
DEBvvStic_Pos	1	0	1	1	1	0	0	1	0	0	0	0	0	0	0	0	0	0	0	0	0	1	0	0	0	0	0	0	1
DEBvvVisc_Pos	1	0	1	1	1	0	0	1	0	0	0	0	0	0	0	0	0	0	0	1	0	0	0	0	0	0	0	0	1
DEFmvASenO_Neg	0	0	0	0	0	0	0	0	0	0	0	0	0	0	0	0	0	0	0	0	0	0	0	0	0	0	0	0	0
DEFmvASenO_Pos	1	1	1	1	1	0	0	0	0	0	0	0	0	0	0	0	0	0	0	1	0	0	0	0	0	0	0	0	1
DEFmvBSenO_Neg	0	0	0	0	0	0	0	0	0	0	0	0	0	0	0	0	0	0	0	0	0	0	0	0	0	0	0	0	0
DEFmvBSenO_Pos	1	1	1	1	1	0	0	0	0	0	0	0	0	0	0	0	0	0	0	1	0	0	0	0	0	0	0	0	1
DEFmvCnull_Neg	1	1	1	1	1	0	0	1	0	0	0	0	0	0	0	0	0	0	0	1	0	0	0	0	0	0	0	0	1
DEFmvCnull_Pos	1	0	1	1	1	0	0	1	0	0	0	0	0	0	0	0	0	0	0	1	0	0	0	0	0	0	0	0	1
DEFmvDnozzle_Pos	0	0	0	0	0	0	0	0	0	0	0	0	0	0	0	0	0	0	0	0	0	1	0	0	0	0	0	0	1
DEFmvStic_Pos	1	1	1	1	1	1	1	1	0	0	0	0	0	0	0	0	0	0	0	1	0	1	0	0	0	0	0	0	1
DEMffFlowRate_Neg	0	0	0	0	0	0	0	0	0	0	0	0	0	0	0	0	0	0	0	0	0	0	0	0	0	0	0	0	0
DESovStic_Pos	1	1	1	1	1	1	1	0	0	0	0	0	0	0	0	0	0	1	0	0	1	0	0	0	1	0	0	1	1
DESovVisc_Pos	1	0	1	1	1	0	0	0	0	0	0	0	0	0	0	0	0	0	0	1	0	0	1	0	0	0	0	0	0
DEVbvASenO_Neg	0	0	0	0	0	0	0	0	0	0	0	0	0	0	0	0	0	0	1	0	0	1	0	0	0	0	0	0	1
DEVbvASenO_Pos	1	1	1	1	1	0	0	1	0	0	0	0	0	0	0	0	0	0	1	0	0	1	0	0	1	1	0	0	1
DEVbvBSenO_Neg	0	0	0	0	0	0	0	0	0	0	0	0	0	0	0	0	0	0	1	0	0	1	0	0	0	0	0	0	1
DEVbvBSenO_Pos	1	0	1	1	1	0	0	1	0	0	0	0	0	0	0	0	0	0	1	1	1	1	0	0	1	1	0	0	1
DEVbvCnull_Neg	0	0	0	0	0	0	0	0	0	0	0	0	0	0	0	0	0	0	1	1	0	0	0	0	0	1	1	0	0
DEVbvCnull_Pos	0	0	0	0	0	0	0	0	0	0	0	0	0	0	0	0	0	0	1	1	0	1	0	0	0	1	1	0	1
DEVbvCorHP1_Pos	0	0	0	0	0	0	0	0	0	0	0	0	0	0	0	0	0	0	1	0	0	0	0	0	0	0	0	0	1
DEVbvCorHP2_Pos	0	0	0	0	0	0	0	0	0	0	0	0	0	0	0	0	0	1	1	0	0	1	0	0	0	1	0	0	1
DEVbvDCool1_Neg	0	0	0	0	0	0	0	0	0	0	0	0	0	0	0	0	0	0	0	0	0	0	0	0	0	0	0	0	0
DEVbvDCool1_Pos	0	0	0	0	0	0	0	0	0	0	0	0	0	0	0	0	0	0	0	0	0	0	0	0	0	0	0	0	0
DEVbvDCool2_Neg	0	0	0	0	0	0	0	0	0	0	0	0	0	0	0	0	0	0	1	1	1	0	0	0	1	1	1	1	1
DEVbvDCool2_Pos	1	1	1	1	0	1	1	0	0	0	0	0	0	0	0	0	0	1	1	0	1	1	0	0	1	1	0	1	1
DEVbvDFilter1_Neg	0	0	0	0	0	0	0	0	0	0	0	0	0	0	0	0	0	0	1	0	1	0	0	0	0	0	0	0	1
DEVbvDFilter2_Neg	0	0	0	0	0	0	0	0	0	0	0	0	0	0	0	0	0	0	1	0	1	0	0	0	0	0	0	0	1
DEVbvDnozzle_Neg	1	0	1	1	1	0	0	0	0	0	0	0	0	0	0	0	0	0	1	0	1	0	0	0	0	0	0	0	1
DEVbvDnozzle_Pos	1	1	1	1	0	1	0	1	0	0	0	0	0	0	0	0	0	0	1	0	1	0	0	0	0	0	0	0	1
DEVbvKfeed_Neg	1	0	1	1	1	1	0	0	0	0	0	0	0	0	0	0	0	0	1	1	0	1	0	0	0	1	1	0	1
DEVbvKineFric_Pos	0	0	0	0	1	1	0	0	0	1	0	0	0	0	0	0	0	0	0	1	1	1	0	0	0	0	1	0	1
DEVbvStic1_Pos	0	0	0	0	0	0	0	0	0	0	0	0	0	0	0	0	0	0	0	0	0	0	0	0	0	0	0	0	0
DEVbvStic2_Pos	0	0	0	0	0	0	0	0	0	0	0	0	0	0	0	0	0	0	0	0	0	1	0	0	0	0	0	0	1
DEVbvSticspool_Pos	1	1	1	1	1	1	1	0	0	0	0	0	0	0	0	0	0	0	1	1	1	0	0	0	1	1	0	1	1
DEVbvVisc1_Pos	0	0	0	0	0	0	0	0	0	0	0	0	0	0	0	0	0	0	0	0	0	0	0	0	0	0	0	0	0
DEVbvVisc2_Pos	1	1	1	1	1	1	0	0	0	0	0	0	0	0	0	0	0	0	0	0	0	0	0	0	0	0	0	0	0
DEVsvASenO_Neg	0	0	0	0	1	0	0	0	0	0	0	1	1	0	1	1	1	1	0	0	0	0	0	0	0	0	0	0	0
DEVsvASenO_Pos	1	1	1	1	0	1	1	0	0	1	0	1	1	1	0	1	1	0	0	0	0	0	0	0	0	0	0	0	0
DEVsvBSenO_Neg	0	0	0	0	1	0	0	0	0	0	0	1	1	1	0	1	1	1	0	0	0	0	0	0	0	0	0	0	0
DEVsvBSenO_Pos	1	1	1	1	0	1	1	0	0	0	1	1	1	0	1	1	1	0	0	0	0	0	0	0	0	0	0	0	0
DEVsvCnull_Neg	1	0	0	0	0	0	0	0	0	0	0	0	0	0	0	0	0	0	0	0	0	0	0	0	0	0	0	0	0
DEVsvCnull_Pos	1	1	1	1	0	1	1	0	0	0	0	0	0	0	0	0	0	0	0	0	0	0	0	0	0	0	0	0	0
DEVsvCorHP1_Pos	1	1	1	1	1	0	0	1	0	0	0	0	0	0	0	0	0	0	0	0	0	0	0	0	0	0	0	0	0
DEVsvCorHP2_Pos	1	1	1	1	1	1	1	1	0	0	0	0	0	0	0	0	0	0	0	0	0	1	0	0	0	0	0	0	1
DEVsvDCool1_Neg	0	0	0	0	0	0	0	0	0	0	0	0	0	0	0	0	0	0	0	0	0	0	0	0	0	0	0	0	0
DEVsvDCool1_Pos	0	0	0	0	0	0	0	0	0	0	0	0	0	0	0	0	0	0	0	0	0	0	0	0	0	0	0	0	0
DEVsvDCool2_Neg	1	1	1	1	1	1	1	1	0	0	0	0	1	0	0	0	0	1	0	0	0	0	0	0	0	0	0	0	1
DEVsvDCool2_Pos	0	1	0	1	1	1	1	0	0	0	0	0	0	0	0	0	0	0	0	0	0	1	0	0	0	0	0	0	1
DEVsvDFilter1_Neg	1	1	1	1	1	1	1	0	0	0	0	0	0	0	0	0	0	0	0	0	0	0	0	0	0	0	0	0	0
DEVsvDFilter2_Neg	1	1	1	1	1	1	1	0	0	0	0	0	0	0	0	0	0	0	0	0	0	0	0	0	0	0	0	0	0
DEVsvDnozzle_Neg	1	1	1	1	1	0	0	1	0	0	0	0	0	0	0	0	0	0	0	1	0	1	0	0	0	0	0	0	1
DEVsvDnozzle_Pos	1	1	1	1	1	1	1	1	0	0	0	0	0	0	0	0	0	0	0	1	0	0	0	0	0	0	0	0	1
DEVsvKfeed_Neg	0	1	0	0	1	0	1	1	0	0	0	0	0	0	0	0	0	0	0	1	0	1	0	0	0	0	0	0	1
DEVsvKineFric_Pos	1	1	1	1	1	0	1	1	0	0	0	0	0	0	0	0	0	0	0	0	0	1	0	1	0	0	1	0	1
DEVsvStic1_Pos	0	0	0	0	0	0	0	0	0	0	0	0	0	0	0	0	0	0	0	0	0	0	0	0	0	0	0	0	0
DEVsvStic2_Pos	0	0	0	0	0	0	0	0	0	0	0	0	0	0	0	0	0	0	0	0	0	0	0	0	0	0	0	0	0
DEVsvSticspool_Pos	0	1	0	1	1	1	1	1	0	0	0	1	1	0	0	0	0	1	0	0	0	0	0	0	0	0	0	0	1
DEVsvVisc1_Pos	0	0	0	0	0	0	0	0	0	0	0	0	0	0	0	0	0	0	0	0	0	0	0	0	0	0	0	0	0
DEVsvVisc2_Pos	1	1	1	1	1	0	0	1	0	0	0	0	0	0	0	0	0	0	0	1	0	1	0	0	0	0	0	0	1
DEWfmASenO_Neg	0	0	0	0	0	0	0	0	0	0	0	0	0	0	0	0	0	0	0	0	0	0	0	0	0	0	0	0	0
DEWfmASenO_Pos	0	0	0	0	0	0	0	0	0	0	0	0	0	0	0	0	0	0	0	0	0	0	0	0	0	0	0	0	0
DEWfmBSenO_Neg	0	0	0	0	0	0	0	0	0	0	0	0	0	0	0	0	0	0	0	0	0	0	0	0	0	0	0	0	0
DEWfmBSenO_Pos	0	0	0	0	0	0	0	0	0	0	0	0	0	0	0	0	0	0	0	0	0	0	0	0	0	0	0	0	0
DFmvDIlkg_Pos	1	0	1	1	1	0	0	0	0	0	0	0	0	0	0	0	0	0	0	1	0	0	0	0	0	0	0	0	1
DLppDIlkg_Pos	0	0	0	0	0	0	0	0	0	0	0	0	0	0	0	0	0	0	0	0	0	0	0	0	0	0	0	0	0
DMfpDIlkg_Pos	0	0	0	0	0	0	0	0	0	0	0	0	0	0	0	0	0	0	0	0	0	0	0	0	0	0	0	0	0
DSovDelay_Pos	0	0	0	0	0	0	0	0	0	0	0	0	0	0	0	0	0	0	0	0	0	0	0	0	0	0	0	0	0
DSovDIlkg_Pos	1	1	1	1	1	1	1	1	0	0	0	0	0	0	0	0	0	0	0	1	1	0	0	1	0	0	1	1	1
DTbvDIlkg_Pos	0	0	0	0	0	0	0	0	0	0	0	0	0	0	0	0	0	0	0	0	0	0	0	0	0	0	0	0	0

	VbvSlpLeftB	VbvSlpRightB	VbvHystOB	VbvCEquS	VbvXchgS	VbvYchgS	VbvScaleS	VbvSlpLeftS	VbvSlpRightS	VbvHystOS	VbvmaxX1	VbvmaxX2	VbvminX1	VbvminX2	VbvmaxGapX	VbvminGapX	VbvmeanGapX	VbvstdGapX	VbvMAErr	TOTAL
DBvvDIlkg_Pos	1	0	0	1	1	0	1	1	1	0	0	0	0	0	0	0	0	0	1	42
DEBvvK0_Neg	1	0	0	1	0	0	1	1	0	0	0	0	0	0	0	0	0	0	0	19
DEBvvStic_Pos	0	0	0	1	0	0	1	1	0	0	0	0	0	0	0	0	0	0	0	15
DEBvvVisc_Pos	1	0	0	0	1	0	0	1	0	0	0	0	0	0	0	0	0	0	0	11
DEFmvASen0_Neg	0	0	0	0	0	0	0	0	0	0	0	0	0	0	0	0	0	0	0	5
DEFmvASen0_Pos	1	0	0	1	1	0	0	1	0	0	0	0	0	0	0	0	0	0	0	26
DEFmvBSen0_Neg	0	0	0	0	0	0	0	0	0	0	0	0	0	0	0	0	0	0	0	5
DEFmvBSen0_Pos	1	0	0	1	1	0	0	1	0	0	0	0	0	0	0	0	0	0	0	26
DEFmvCnull_Neg	1	0	0	1	1	0	1	1	0	0	0	0	0	0	0	0	0	0	0	28
DEFmvCnull_Pos	1	0	0	1	1	0	0	1	0	0	0	0	0	0	0	0	0	0	0	25
DEFmvDnozzle_Pos	1	0	0	0	0	0	0	1	0	0	0	0	0	0	0	0	0	0	0	10
DEFmvStic_Pos	1	0	0	1	0	0	1	1	0	0	0	0	0	0	0	0	0	0	0	27
DEMffFlowRate_Neg	0	0	0	0	0	0	0	0	0	0	0	0	0	0	0	0	0	0	0	2
DESovStic_Pos	1	0	0	1	1	0	0	1	0	0	0	0	0	0	0	0	0	0	0	18
DESovVisc_Pos	1	0	0	0	1	0	0	1	0	0	0	0	0	0	0	0	0	0	0	11
DEVbvASen0_Neg	1	0	0	1	0	0	0	1	0	0	0	0	1	0	1	1	1	1	0	11
DEVbvASen0_Pos	1	0	1	1	1	0	0	1	0	1	1	0	1	0	1	1	1	1	1	26
DEVbvBSen0_Neg	1	0	0	1	0	0	0	1	0	0	0	0	0	1	1	1	1	1	1	14
DEVbvBSen0_Pos	1	0	1	1	1	0	0	1	0	1	0	1	0	1	1	1	1	1	1	27
DEVbvCnull_Neg	0	0	0	1	1	0	0	0	0	0	0	0	0	0	0	0	0	0	0	6
DEVbvCnull_Pos	0	0	0	1	1	0	0	0	0	0	0	0	0	0	0	0	0	0	0	8
DEVbvCorHP1_Pos	1	0	0	0	0	0	0	1	0	0	0	0	0	0	0	0	0	0	0	4
DEVbvCorHP2_Pos	1	0	0	1	1	0	0	1	0	0	0	0	0	0	0	0	0	0	1	11
DEVbvDCool1_Neg	0	0	0	0	0	0	0	0	0	0	0	0	0	0	0	0	0	0	0	0
DEVbvDCool1_Pos	0	0	0	0	0	0	0	0	0	0	0	0	0	0	0	0	0	0	0	0
DEVbvDCool2_Neg	1	0	0	1	1	1	0	1	0	0	0	0	0	0	0	0	0	0	0	13
DEVbvDCool2_Pos	1	0	0	1	1	1	1	1	0	0	0	0	0	0	0	0	0	0	0	19
DEVbvDFilter1_Neg	0	0	0	1	0	0	0	1	0	0	0	0	0	0	0	0	0	0	0	5
DEVbvDFilter2_Neg	0	0	0	0	0	0	0	1	0	0	0	0	0	0	0	0	0	0	0	4
DEVbvDnozzle_Neg	1	0	0	1	1	1	1	1	1	0	0	0	0	0	0	0	0	0	0	17
DEVbvDnozzle_Pos	1	0	0	0	0	0	0	0	0	0	0	0	0	0	0	0	0	0	0	12
DEVbvKfeed_Neg	1	0	0	1	1	0	0	1	0	0	0	0	0	0	0	0	0	0	0	18
DEVbvKineFric_Pos	1	0	0	1	0	0	1	1	1	0	0	0	1	0	0	0	0	0	0	27
DEVbvStic1_Pos	0	0	0	0	0	0	0	0	0	0	0	0	0	0	0	0	0	0	0	0
DEVbvStic2_Pos	0	0	0	1	0	0	0	1	0	0	0	0	0	0	0	0	0	0	0	4
DEVbvSticspool_Pos	1	0	1	1	1	1	1	1	1	1	0	0	0	0	0	0	0	0	1	27
DEVbvVisc1_Pos	0	0	0	0	0	0	0	0	0	0	0	0	0	0	0	0	0	0	0	0
DEVbvVisc2_Pos	1	0	0	0	1	0	0	1	0	0	0	0	0	0	0	0	0	0	0	11
DEVsvASen0_Neg	0	0	0	0	0	0	0	0	0	0	0	0	0	0	0	0	0	0	0	9
DEVsvASen0_Pos	0	0	0	0	0	0	0	0	0	0	0	0	0	0	0	0	0	0	0	19
DEVsvBSen0_Neg	0	0	0	0	0	0	0	0	0	0	0	0	0	0	0	0	0	0	0	9
DEVsvBSen0_Pos	0	0	0	0	0	0	0	0	0	0	0	0	0	0	0	0	0	0	0	19
DEVsvCnull_Neg	0	0	0	0	0	0	0	0	0	0	0	0	0	0	0	0	0	0	0	18
DEVsvCnull_Pos	0	0	0	0	0	0	0	0	0	0	0	0	0	0	0	0	0	0	0	13
DEVsvCorHP1_Pos	0	0	0	0	0	0	0	0	0	0	0	0	0	0	0	0	0	0	0	10
DEVsvCorHP2_Pos	0	0	0	0	0	0	0	0	0	0	0	0	0	0	0	0	0	0	0	20
DEVsvDCool1_Neg	0	0	0	0	0	0	0	0	0	0	0	0	0	0	0	0	0	0	0	0
DEVsvDCool1_Pos	0	0	0	0	0	0	0	0	0	0	0	0	0	0	0	0	0	0	0	0
DEVsvDCool2_Neg	0	0	0	0	0	0	0	0	0	0	0	0	0	0	0	0	0	0	0	26
DEVsvDCool2_Pos	0	0	0	0	0	0	0	1	0	0	0	0	0	0	0	0	0	0	0	28
DEVsvDFilter1_Neg	0	0	0	0	0	0	0	0	0	0	0	0	0	0	0	0	0	0	0	8
DEVsvDFilter2_Neg	0	0	0	0	0	0	0	0	0	0	0	0	0	0	0	0	0	0	0	18
DEVsvDnozzle_Neg	0	0	0	0	0	0	0	1	0	0	0	0	0	0	0	0	0	0	0	12
DEVsvDnozzle_Pos	1	0	0	0	0	0	0	1	0	0	0	0	0	0	0	0	0	0	0	14
DEVsvKfeed_Neg	1	0	0	0	1	0	0	1	0	0	0	0	0	0	0	0	0	0	0	27
DEVsvKineFric_Pos	1	0	0	0	0	0	0	1	0	0	0	0	0	0	0	0	0	0	0	30
DEVsvStic1_Pos	0	0	0	0	0	0	0	0	0	0	0	0	0	0	0	0	0	0	0	0
DEVsvStic2_Pos	0	0	0	0	0	0	0	0	0	0	0	0	0	0	0	0	0	0	0	0
DEVsvSticspool_Pos	1	0	0	0	0	0	0	1	0	0	0	0	0	0	0	0	0	0	0	25
DEVsvVisc1_Pos	0	0	0	0	0	0	0	0	0	0	0	0	0	0	0	0	0	0	0	0
DEVsvVisc2_Pos	1	0	0	0	0	0	0	1	0	0	0	0	0	0	0	0	0	0	0	11
DEWfmASen0_Neg	0	0	0	0	0	0	0	0	0	0	0	0	0	0	0	0	0	0	0	4
DEWfmASen0_Pos	0	0	0	0	0	0	0	0	0	0	0	0	0	0	0	0	0	0	0	4
DEWfmBSen0_Neg	0	0	0	0	0	0	0	0	0	0	0	0	0	0	0	0	0	0	0	4
DEWfmBSen0_Pos	0	0	0	0	0	0	0	0	0	0	0	0	0	0	0	0	0	0	0	4
DFmvDIlkg_Pos	1	0	0	1	1	0	0	1	0	0	0	0	0	0	0	0	0	0	0	29
DLpvDIlkg_Pos	1	0	0	0	0	0	0	1	0	0	0	0	0	0	0	0	0	0	0	3
DMfpDIlkg_Pos	0	0	0	0	1	0	0	1	0	0	0	0	0	0	0	0	0	0	0	14
DSovDelay_Pos	0	0	0	0	0	0	0	0	0	0	0	0	0	0	0	0	0	0	0	3
DSovDIlkg_Pos	1	0	0	1	1	1	1	1	1	0	0	0	0	0	0	0	0	0	1	40
DTbvDIlkg_Pos	0	0	0	0	0	0	0	0	0	0	0	0	0	0	0	0	0	0	0	0

Table A.27 *Detection NKPIs for individual models.*

Appendix XXXV. Identification NKPIs for individual models

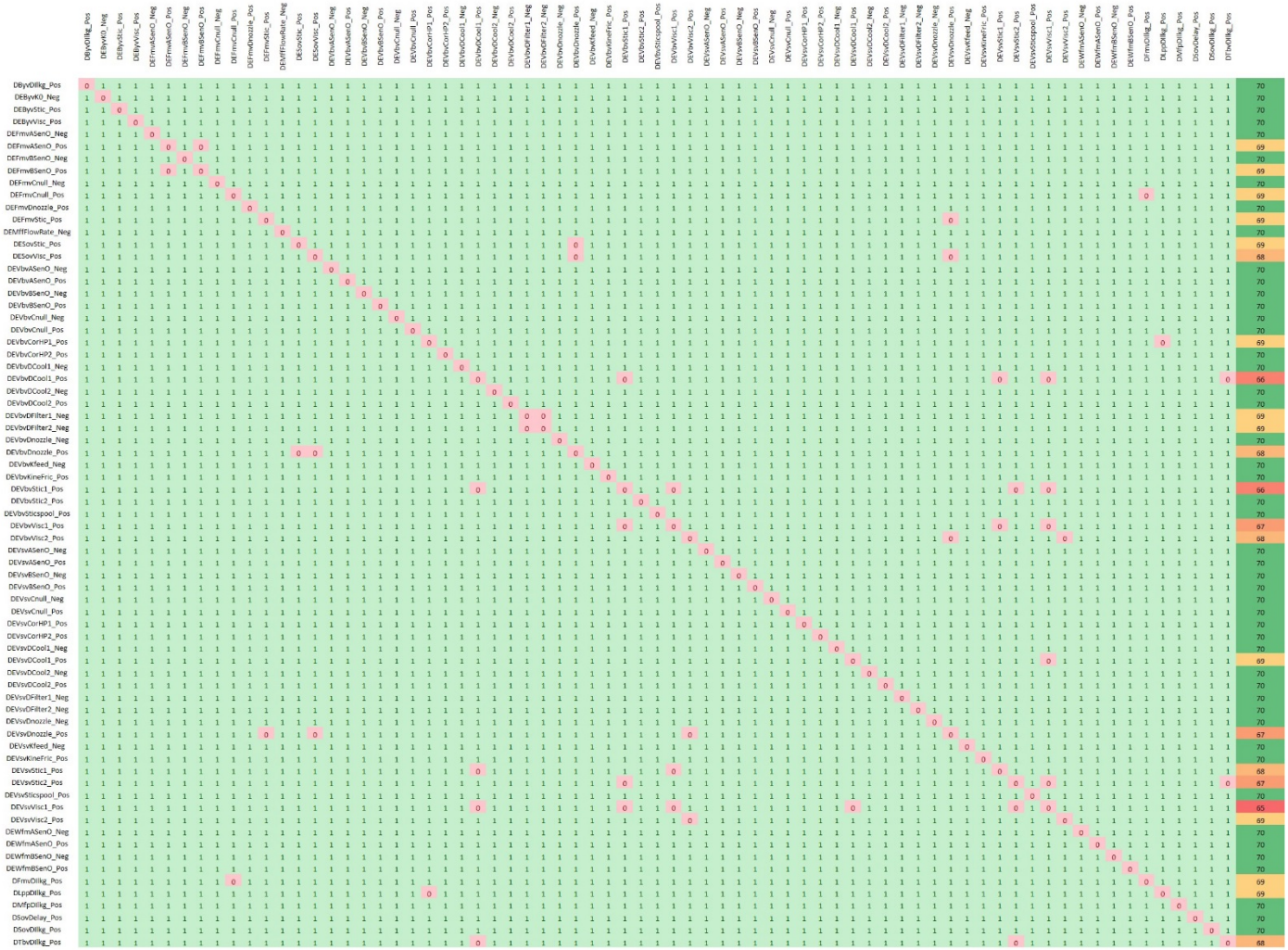


Table A.28 *Identification NKPIs for individual models.*

Appendix XXXVI. Localization NKPIs for individual models

	Pumping Unit	Fuel Filter	ACU	FMU	VSV Actuation	VBV Actuation	TBV Actuation	Flowmeter	TOTAL
Pumping Unit	0	1	1	1	1	1	1	1	7
Fuel Filter	1	0	1	1	1	1	1	1	7
ACU	1	1	0	0	0	0	1	1	4
FMU	1	1	0	0	0	1	1	1	4
VSV Actuation	1	1	0	0	0	1	1	1	5
VBV Actuation	1	1	0	0	1	0	1	1	5
TBV Actuation	1	1	1	1	1	1	0	1	7
Flowmeter	1	1	1	1	1	1	1	0	7

Table A.29 *Localization NKPIs for individual models.*

Appendix XXXVII. Prognostics NKPIs for individual models

	DeltaD	DeltaI	DeltaL
DByvDIlkg_Pos	0	0	0
DEByvK0_Neg	149,33	149,33	116
DEByvStic_Pos	0	0	0
DEByvVisc_Pos	0	0	0
DEFmvASenO_Neg	0	0	0
DEFmvASenO_Pos	0,75	0,75	0
DEFmvBSenO_Neg	0	0	0
DEFmvBSenO_Pos	0,75	0,75	0
DEFmvCnull_Neg	12,2	12,2	0
DEFmvCnull_Pos	17,2	17,2	0
DEFmvDnozzle_Pos	0	0	0
DEFmvStic_Pos	0	0	0
DEMffFlowRate_Neg	76,7	76,7	0
DESovStic_Pos	0	0	0
DESovVisc_Pos	0	0	0
DEVbvASenO_Neg	0	0	0
DEVbvASenO_Pos	0,95	0,95	0
DEVbvBSenO_Neg	0	0	0
DEVbvBSenO_Pos	0,95	0,95	0
DEVbvCnull_Neg	8,43	8,43	0
DEVbvCnull_Pos	13,4	13,4	0
DEVbvCorHP1_Pos	0	0	0
DEVbvCorHP2_Pos	0,02	0,02	0
DEVbvDCool1_Neg	0	0	0
DEVbvDCool1_Pos	0	0	0
DEVbvDCool2_Neg	0	0	0
DEVbvDCool2_Pos	0	0	0
DEVbvDFilter1_Neg	4	4	0
DEVbvDFilter2_Neg	4	4	0
DEVbvDnozzle_Neg	0	0	0
DEVbvDnozzle_Pos	0	0	0
DEVbvKfeed_Neg	1,1	1,1	0
DEVbvKineFric_Pos	0	0	0
DEVbvStic1_Pos	0	0	0
DEVbvStic2_Pos	0	0	0
DEVbvSticspool_Pos	0	0	0
DEVbvVisc1_Pos	0	0	0
DEVbvVisc2_Pos	0	0	0
DEVsvASenO_Neg	0	0	0
DEVsvASenO_Pos	0	0	0
DEVsvBSenO_Neg	0	0	0
DEVsvBSenO_Pos	0	0	0
DEVsvCnull_Neg	7,97	7,97	0
DEVsvCnull_Pos	12,9	12,9	0
DEVsvCorHP1_Pos	0	0	0
DEVsvCorHP2_Pos	0	0	0
DEVsvDCool1_Neg	0	0	0
DEVsvDCool1_Pos	0	0	0
DEVsvDCool2_Neg	0	0	0
DEVsvDCool2_Pos	0	0	0
DEVsvDFilter1_Neg	4	4	0
DEVsvDFilter2_Neg	4	4	0
DEVsvDnozzle_Neg	0	0	0
DEVsvDnozzle_Pos	0	0	0
DEVsvKfeed_Neg	1,1	1,1	0
DEVsvKineFric_Pos	0	0	0
DEVsvStic1_Pos	0	0	0
DEVsvStic2_Pos	0	0	0
DEVsvSticspool_Pos	0	0	0
DEVsvVisc1_Pos	0	0	0
DEVsvVisc2_Pos	0	0	0
DEWfmASenO_Neg	0	0	0
DEWfmASenO_Pos	0	0	0
DEWfmBSenO_Neg	0	0	0
DEWfmBSenO_Pos	0	0	0
DFmvDIlkg_Pos	0,25	0,25	0
DLppDIlkg_Pos	0	0	0
DMfpDIlkg_Pos	0	0	0
DSovDelay_Pos	0	0	0
DSovDIlkg_Pos	0	0	0
DTbvDIlkg_Pos	0	0	0

Appendix XXXVIII. Detection NKPIs for virtual HIs

	FmvCEquA	FmvScaleA	FmvSlpA	FmvHyst0A	FmvCEquB	FmvScaleB	FmvSlpB	FmvHyst0B	FmvCEquS	FmvScaleS	FmvSlpS	FmvHyst0S	FmvmaxX1	FmvmaxX2	FmvminX1	FmvminX2	FmvmaxGapX	FmvminGapX	FmvmeanGapX	FmvstdGapX	FmvMAErr	Sovdelop1	Sovdelclo	Sovdelop2	VoN2maxSOV	SOVoN2max	SOVoN2mean	VoN2maxBYV	BYVoN2max
DBvvDIlkg_Pos	0	0	0	0	0	0	0	0	0	0	0	0	0	0	0	0	0	0	0	0	0	0	0	0	0	1	1	0	1
DEBvvK0_Neg	0	0	0	0	0	0	0	0	0	0	0	0	0	0	0	0	0	0	0	0	0	0	0	0	0	0	1	0	0
DEBvvStic_Pos	0	0	0	0	0	0	0	0	0	0	0	0	0	0	0	0	0	0	0	0	0	0	0	0	0	0	0	0	1
DEBvvVisc_Pos	0	0	0	0	0	0	0	0	0	0	0	0	0	0	0	0	0	0	0	0	0	0	0	0	0	0	0	0	0
DEFmvASenO_Neg	0	0	0	0	0	0	0	0	0	0	0	0	1	0	1	0	0	1	1	1	0	0	0	0	0	0	0	0	0
DEFmvASenO_Pos	0	0	0	1	0	0	0	1	0	0	0	1	0	1	0	0	1	0	1	1	0	0	0	0	0	0	1	0	0
DEFmvBSenO_Neg	0	0	0	0	0	0	0	0	0	0	0	0	0	1	0	1	1	0	1	1	0	0	0	0	0	0	0	0	0
DEFmvBSenO_Pos	0	0	0	1	0	0	0	1	0	0	0	1	1	0	0	0	0	1	1	1	0	0	0	0	0	0	1	0	0
DEFmvCnull_Neg	1	0	0	0	1	0	0	0	1	0	0	0	0	1	0	0	0	0	0	0	1	0	0	0	0	0	1	0	0
DEFmvCnull_Pos	1	0	0	0	1	0	0	0	1	0	0	0	1	1	0	0	0	0	0	0	1	0	0	0	0	0	1	0	0
DEFmvDnozzle_Pos	0	1	0	0	0	1	0	0	0	1	1	0	0	0	0	0	0	0	0	0	0	0	0	0	0	0	0	0	0
DEFmvStic_Pos	0	0	0	1	0	0	0	1	0	0	0	1	0	1	0	0	0	0	0	0	1	0	0	0	0	0	1	0	0
DEMffFlowRate_Neg	0	0	0	0	0	0	0	0	0	0	0	0	0	0	0	0	0	0	0	0	0	0	0	0	0	0	0	0	0
DESovStic_Pos	0	0	0	0	0	0	0	0	0	0	0	0	0	0	0	0	0	0	0	0	0	0	0	0	0	0	0	0	0
DESovVisc_Pos	0	0	0	0	0	0	0	0	0	0	0	0	0	0	0	0	0	0	0	0	0	0	0	0	0	0	0	0	0
DEVbvASenO_Neg	0	0	0	0	0	0	0	0	0	0	0	0	0	0	0	0	0	0	0	0	0	0	0	0	0	0	0	0	0
DEVbvASenO_Pos	0	0	0	0	0	0	0	0	0	0	0	0	0	0	0	0	0	0	0	0	0	0	0	0	0	0	0	0	0
DEVbvBSenO_Neg	0	0	0	0	0	0	0	0	0	0	0	0	0	0	0	0	0	0	0	0	0	0	0	0	0	0	0	0	0
DEVbvBSenO_Pos	0	0	0	0	0	0	0	0	0	0	0	0	0	0	0	0	0	0	0	0	0	0	0	0	0	0	0	0	0
DEVbvCnull_Neg	0	0	0	0	0	0	0	0	0	0	0	0	0	0	0	0	0	0	0	0	0	0	0	0	0	0	0	0	0
DEVbvCnull_Pos	0	0	0	0	0	0	0	0	0	0	0	0	0	0	0	0	0	0	0	0	0	0	0	0	0	0	0	0	0
DEVbvCorHP1_Pos	0	0	0	0	0	0	0	0	0	0	0	0	0	0	0	0	0	0	0	0	0	0	0	0	0	0	0	0	0
DEVbvCorHP2_Pos	0	0	0	0	0	0	0	0	0	0	0	0	0	0	0	0	0	0	0	0	0	0	0	0	0	0	0	0	0
DEVbvDCool1_Neg	0	0	0	0	0	0	0	0	0	0	0	0	0	0	0	0	0	0	0	0	0	0	0	0	0	0	0	0	0
DEVbvDCool1_Pos	0	0	0	0	0	0	0	0	0	0	0	0	0	0	0	0	0	0	0	0	0	0	0	0	0	0	0	0	0
DEVbvDCool2_Neg	0	0	0	0	0	0	0	0	0	0	0	0	0	0	0	0	0	0	0	0	0	0	0	0	0	0	0	0	0
DEVbvDCool2_Pos	0	0	0	0	0	0	0	0	0	0	0	0	0	0	0	0	0	0	0	0	0	0	0	0	0	0	0	0	0
DEVbvDFilter1_Neg	0	0	0	0	0	0	0	0	0	0	0	0	0	0	0	0	0	0	0	0	0	0	0	0	0	0	0	0	0
DEVbvDFilter2_Neg	0	0	0	0	0	0	0	0	0	0	0	0	0	0	0	0	0	0	0	0	0	0	0	0	0	0	0	0	0
DEVbvDnozzle_Neg	0	0	0	0	0	0	0	0	0	0	0	0	0	0	0	0	0	0	0	0	0	0	0	0	0	0	0	0	0
DEVbvDnozzle_Pos	0	0	0	0	0	0	0	0	0	0	0	0	0	0	0	0	0	0	0	0	0	0	0	0	0	0	0	0	0
DEVbvKfeed_Neg	0	0	0	0	0	0	0	0	0	0	0	0	0	0	0	0	0	0	0	0	0	0	0	0	0	0	0	0	0
DEVbvKineFric_Pos	0	0	0	0	0	0	0	0	0	0	0	1	0	0	0	0	0	0	0	0	0	0	0	0	0	0	0	0	0
DEVbvStic1_Pos	0	0	0	0	0	0	0	0	0	0	0	0	0	0	0	0	0	0	0	0	0	0	0	0	0	0	0	0	0
DEVbvStic2_Pos	0	0	0	0	0	0	0	0	0	0	0	0	0	0	0	0	0	0	0	0	0	0	0	0	0	0	0	0	0
DEVbvSticspool_Pos	0	0	0	0	0	0	0	0	0	0	0	0	0	0	0	0	0	0	0	0	0	0	0	0	0	0	0	0	0
DEVbvVisc1_Pos	0	0	0	0	0	0	0	0	0	0	0	0	0	0	0	0	0	0	0	0	0	0	0	0	0	0	0	0	0
DEVbvVisc2_Pos	0	0	0	0	0	0	0	0	0	0	0	0	0	0	0	0	0	0	0	0	0	0	0	0	0	0	0	0	0
DEVsvASenO_Neg	0	0	0	0	0	0	0	0	0	0	0	0	0	0	0	0	0	0	0	0	0	0	0	0	0	0	0	0	0
DEVsvASenO_Pos	0	0	0	0	0	0	0	0	0	0	0	0	0	0	0	0	0	0	0	0	0	0	0	0	1	0	0	0	0
DEVsvBSenO_Neg	0	0	0	0	0	0	0	0	0	0	0	0	0	0	0	0	0	0	0	0	0	0	0	0	0	0	0	0	0
DEVsvBSenO_Pos	0	0	0	0	0	0	0	0	0	0	0	0	0	0	0	0	0	0	0	0	0	0	0	0	1	0	0	0	0
DEVsvCnull_Neg	0	0	0	0	0	0	0	0	0	0	0	0	0	0	0	0	0	0	0	0	0	0	0	0	0	0	0	0	0
DEVsvCnull_Pos	0	0	0	0	0	0	0	0	0	0	0	0	0	0	0	0	0	0	0	0	0	0	0	0	0	0	0	0	0
DEVsvCorHP1_Pos	0	0	0	0	0	0	0	0	0	0	0	0	0	0	0	0	0	0	0	0	0	0	0	0	0	0	0	0	0
DEVsvCorHP2_Pos	0	0	0	0	0	0	0	0	0	0	0	0	0	0	0	0	0	0	0	0	0	0	0	0	0	0	0	0	0
DEVsvDCool1_Neg	0	0	0	0	0	0	0	0	0	0	0	0	0	0	0	0	0	0	0	0	0	0	0	0	0	0	0	0	0
DEVsvDCool1_Pos	0	0	0	0	0	0	0	0	0	0	0	0	0	0	0	0	0	0	0	0	0	0	0	0	0	0	0	0	0
DEVsvDCool2_Neg	0	0	0	0	0	0	0	0	0	0	0	0	0	0	0	0	0	0	0	0	0	0	0	0	1	0	0	0	0
DEVsvDCool2_Pos	0	0	0	0	0	0	0	0	0	0	0	0	0	0	0	0	0	0	0	0	0	0	0	0	0	0	0	0	0
DEVsvDFilter1_Neg	0	0	0	0	0	0	0	0	0	0	0	0	0	0	0	0	0	0	0	0	0	0	0	0	0	0	0	0	0
DEVsvDFilter2_Neg	0	0	0	0	0	0	0	0	0	0	0	0	0	0	0	0	0	0	0	0	0	0	0	0	0	0	0	0	0
DEVsvDnozzle_Neg	0	0	0	0	0	0	0	0	0	0	0	0	0	0	0	0	0	0	0	0	0	0	0	0	0	0	0	0	0
DEVsvDnozzle_Pos	0	0	0	0	0	0	0	0	0	0	0	0	0	0	0	0	0	0	0	0	0	0	0	0	0	0	0	0	0
DEVsvKfeed_Neg	0	0	0	0	0	0	0	0	0	0	0	0	0	0	0	0	0	0	0	0	0	0	0	0	0	0	0	0	0
DEVsvKineFric_Pos	0	0	0	0	0	0	0	0	0	0	0	0	0	0	0	0	0	0	0	0	0	0	0	0	0	0	0	0	0
DEVsvStic1_Pos	0	0	0	0	0	0	0	0	0	0	0	0	0	0	0	0	0	0	0	0	0	0	0	0	0	0	0	0	0
DEVsvStic2_Pos	0	0	0	0	0	0	0	0	0	0	0	0	0	0	0	0	0	0	0	0	0	0	0	0	0	0	0	0	0
DEVsvSticspool_Pos	0	0	0	0	0	0	0	0	0	0	0	0	0	0	0	0	0	0	0	0	0	0	0	0	0	0	0	0	0
DEVsvVisc1_Pos	0	0	0	0	0	0	0	0	0	0	0	0	0	0	0	0	0	0	0	0	0	0	0	0	0	0	0	0	0
DEVsvVisc2_Pos	0	0	0	0	0	0	0	0	0	0	0	0	0	0	0	0	0	0	0	0	0	0	0	0	0	0	0	0	0
DEWfmASenO_Neg	0	0	0	0	0	0	0	0	0	0	0	0	0	0	0	0	0	0	0	0	0	0	0	0	0	0	0	0	0
DEWfmASenO_Pos	0	0	0	0	0	0	0	0	0	0	0	0	0	0	0	0	0	0	0	0	0	0	0	0	0	0	0	0	0
DEWfmBSenO_Neg	0	0	0	0	0	0	0	0	0	0	0	0	0	0	0	0	0	0	0	0	0	0	0	0	0	0	0	0	0
DEWfmBSenO_Pos	0	0	0	0	0	0	0	0	0	0	0	0	0	0	0	0	0	0	0	0	0	0	0	0	0	0	0	0	0
DFmvDIlkg_Pos	1	1	0	1	1	0	0	1	1	1	1	1	1	1	0	0	0	0	0	0	1	0	0	0	0	0	1	0	0
DLvvDIlkg_Pos	0	0	0	0	0	0	0	0	0	0	0	0	0	0	0	0	0	0	0	0	0	0	0	0	0	0	0	0	0
DMfvDIlkg_Pos	0	0	0	0	0	0	0	0	0	0	0	0	0	0	0	0	0	0	0	0	0	0	0	0	0	0	0	0	1
DSovDelay_Pos	0	0	0	0	0	0	0	0	0	0	0	0	0	0	0	0	0	0	0	0	0	0	0	0	0	1	0	0	0
DSovDIlkg_Pos	0	0	0	0	0	0	0	0	0	0	0	0	0	0	0	0	0	0	0	0	0	0	0	0	0	1	1	0	0
DTbvDIlkg_Pos	0	0	0	0	0	0	0	0	0	0	0	0	0	0	0	0	0	0	0	0	0	0	0	0	0	0	0	0	0
TOTAL	3	2	0	4	3	1	0	4	3	2	2	5	4	6	1	1	2	2	4	4	4	0	0	0	3	3	9	0	3

	BYVoN2mean	LppSlpN2DP	LppR2N2DP	wTBV	wSOV	MfpSlpN2DP	MfpR2N2DP	MfSlpN2DP	MfR2N2DP	WfmmaxX1	WfmmaxX2	WfmminX1	WfmminX2	WfmmaxGapX	WfmminGapX	WfmmeanGapX	WfmstdGapX	VsvCEquA	VsvXnullA	VsvYnullA	VsvXoverlapA	VsvYoverlapA	VsvScaleA	VsvSlpLeftA	VsvSlpNullA	VsvSlpRightA	VsvHyst0A	VsvCEquB	VsvXnullB
DBvvDIlkg_Pos	1	0	1	0	0	0	0	0	0	1	1	0	0	0	0	0	0	0	0	0	0	0	0	0	0	1	0	0	0
DEBvvK0_Neg	1	0	0	0	0	0	0	0	0	1	1	0	0	0	0	0	0	0	0	0	0	0	0	0	0	0	0	0	0
DEBvvStic_Pos	0	0	0	0	0	0	0	0	0	0	0	0	0	0	0	0	0	0	0	0	0	0	0	0	0	0	0	0	0
DEBvvVisc_Pos	0	0	0	0	0	0	0	0	0	0	0	0	0	0	0	0	0	0	0	0	0	0	0	0	0	0	0	0	0
DEFmvASenO_Neg	0	0	0	0	0	0	0	0	0	0	0	0	0	0	0	0	0	0	0	0	0	0	0	0	0	0	0	0	0
DEFmvASenO_Pos	1	0	0	0	0	0	0	0	0	1	1	0	0	0	0	0	0	0	0	0	0	0	0	0	0	0	0	0	0
DEFmvBSenO_Neg	0	0	0	0	0	0	0	0	0	0	0	0	0	0	0	0	0	0	0	0	0	0	0	0	0	0	0	0	0
DEFmvBSenO_Pos	1	1	0	0	0	0	0	0	0	1	1	0	0	0	0	0	0	0	0	0	0	0	0	0	0	0	0	0	0
DEFmvCnull_Neg	0	0	0	0	0	0	0	0	0	0	0	0	0	0	0	0	0	0	0	0	0	0	0	0	0	0	0	0	0
DEFmvCnull_Pos	0	0	0	0	0	0	0	0	0	1	1	0	0	0	0	0	0	0	0	0	0	0	0	0	0	0	0	0	0
DEFmvDnozzle_Pos	0	0	0	0	0	0	0	0	0	0	0	0	0	0	0	0	0	0	0	0	0	0	0	0	0	0	0	0	0
DEFmvStic_Pos	0	0	0	0	0	0	0	0	0	1	1	0	0	0	0	0	0	0	0	0	0	0	0	0	0	0	0	0	0
DEMffFlowRate_Neg	0	0	0	0	0	1	1	1	1	0	0	0	0	0	0	0	0	0	0	0	0	0	0	0	0	0	0	0	0
DESovStic_Pos	0	0	0	0	0	0	1	0	0	0	0	0	0	0	0	0	0	0	0	0	0	0	0	0	0	0	0	0	0
DESovVisc_Pos	0	0	0	0	0	0	0	0	0	0	0	0	0	0	0	0	0	0	0	0	0	0	0	0	0	0	0	0	0
DEVbvASenO_Neg	0	0	0	0	0	0	0	0	0	0	0	0	0	0	0	0	0	0	0	0	0	0	0	0	0	0	0	0	0
DEVbvASenO_Pos	0	0	0	0	0	0	0	0	0	0	0	0	0	0	0	0	0	0	0	0	0	0	0	0	0	0	0	0	0
DEVbvBSenO_Neg	0	0	0	0	0	0	0	0	0	0	0	0	0	0	0	0	0	0	0	0	0	0	0	0	0	0	0	0	0
DEVbvBSenO_Pos	0	0	0	0	0	0	0	0	0	0	0	0	0	0	0	0	0	0	0	0	0	0	0	0	0	0	0	0	0
DEVbvCnull_Neg	0	0	0	0	0	0	0	0	0	0	0	0	0	0	0	0	0	0	0	0	0	0	0	0	0	0	0	0	0
DEVbvCnull_Pos	0	0	0	0	0	0	0	0	0	0	0	0	0	0	0	0	0	0	0	0	0	0	0	0	0	0	0	0	0
DEVbvCorHP1_Pos	0	0	0	0	0	0	0	0	0	0	0	0	0	0	0	0	0	0	0	0	0	0	0	0	0	0	0	0	0
DEVbvCorHP2_Pos	0	0	0	0	0	0	0	0	0	0	0	0	0	0	0	0	0	0	0	0	0	0	0	0	0	0	0	0	0
DEVbvDCool1_Neg	0	0	0	0	0	0	0	0	0	0	0	0	0	0	0	0	0	0	0	0	0	0	0	0	0	0	0	0	0
DEVbvDCool1_Pos	0	0	0	0	0	0	0	0	0	0	0	0	0	0	0	0	0	0	0	0	0	0	0	0	0	0	0	0	0
DEVbvDCool2_Neg	0	0	0	0	0	0	0	0	0	0	0	0	0	0	0	0	0	0	0	0	0	0	0	0	0	0	0	0	0
DEVbvDCool2_Pos	0	0	0	0	0	0	0	0	0	0	0	0	0	0	0	0	0	0	0	0	0	0	0	0	0	0	0	0	0
DEVbvDFilter1_Neg	0	0	0	0	0	0	0	0	0	0	0	0	0	0	0	0	0	0	0	0	0	0	0	0	0	0	0	0	0
DEVbvDFilter2_Neg	0	0	0	0	0	0	0	0	0	0	0	0	0	0	0	0	0	0	0	0	0	0	0	0	0	0	0	0	0
DEVbvDnozzle_Neg	0	0	0	0	0	0	0	0	0	0	0	0	0	0	0	0	0	0	0	0	0	0	0	0	0	0	0	0	0
DEVbvDnozzle_Pos	0	0	0	0	0	0	0	0	0	0	0	0	0	0	0	0	0	0	0	0	0	0	0	0	0	0	0	0	0
DEVbvKfeed_Neg	0	0	0	0	0	0	0	0	0	0	0	0	0	0	0	0	0	0	0	0	0	0	0	0	0	0	0	0	0
DEVbvKineFric_Pos	0	0	0	0	0	0	0	0	0	0	0	0	0	1	0	0	0	0	0	0	0	0	0	0	0	0	0	0	0
DEVbvStic1_Pos	0	0	0	0	0	0	0	0	0	0	0	0	0	0	0	0	0	0	0	0	0	0	0	0	0	0	0	0	0
DEVbvStic2_Pos	0	0	0	0	0	0	0	0	0	0	0	0	0	0	0	0	0	0	0	0	0	0	0	0	0	0	0	0	0
DEVbvSticspool_Pos	0	0	0	0	0	0	0	0	0	0	0	0	0	0	0	0	0	0	0	0	0	0	0	0	0	0	0	0	0
DEVbvVisc1_Pos	0	0	0	0	0	0	0	0	0	0	0	0	0	0	0	0	0	0	0	0	0	0	0	0	0	0	0	0	0
DEVbvVisc2_Pos	0	0	0	0	0	0	0	0	0	0	0	0	0	0	0	0	0	0	0	0	0	0	0	0	0	0	0	0	0
DEVsvASenO_Neg	0	0	0	0	0	0	0	0	0	0	0	0	0	0	0	0	0	0	0	0	0	0	0	0	0	0	0	0	0
DEVsvASenO_Pos	0	0	0	0	0	0	0	0	0	0	0	0	0	0	0	0	0	0	0	0	0	0	0	0	0	0	0	0	0
DEVsvBSenO_Neg	0	0	0	0	0	0	0	0	0	0	0	0	0	0	0	0	0	0	0	0	0	0	0	0	0	0	0	0	0
DEVsvBSenO_Pos	0	0	0	0	0	0	0	0	0	0	0	0	0	0	0	0	0	0	0	0	0	0	0	0	0	0	0	0	0
DEVsvCnull_Neg	0	0	0	0	0	0	0	0	0	0	0	0	0	0	0	0	0	1	1	0	1	1	0	1	0	0	0	1	1
DEVsvCnull_Pos	0	0	0	0	0	0	0	0	0	0	0	0	0	0	0	0	0	1	1	0	0	0	0	0	0	0	0	1	1
DEVsvCorHP1_Pos	0	0	0	0	0	0	0	0	0	0	0	0	0	0	0	0	0	0	0	0	0	0	0	0	0	0	0	0	0
DEVsvCorHP2_Pos	0	0	0	0	0	0	0	0	0	0	0	0	0	0	0	0	0	0	0	0	0	0	0	0	0	0	0	0	0
DEVsvDCool1_Neg	0	0	0	0	0	0	0	0	0	0	0	0	0	0	0	0	0	0	0	0	0	0	0	0	0	0	0	0	0
DEVsvDCool1_Pos	0	0	0	0	0	0	0	0	0	0	0	0	0	0	0	0	0	0	0	0	0	0	0	0	0	0	0	0	0
DEVsvDCool2_Neg	0	0	0	0	0	0	0	0	0	0	0	0	0	0	0	0	0	1	0	1	0	0	0	0	1	0	0	1	0
DEVsvDCool2_Pos	0	0	0	0	0	0	0	0	0	0	0	0	0	0	0	0	0	1	0	1	0	0	0	1	1	0	0	1	0
DEVsvDFilter1_Neg	0	0	0	0	0	0	0	0	0	0	0	0	0	0	0	0	0	0	0	0	0	0	0	0	0	0	0	0	0
DEVsvDFilter2_Neg	0	0	0	0	0	0	0	0	0	0	0	0	0	0	0	0	0	0	0	0	0	0	0	0	0	0	0	0	0
DEVsvDnozzle_Neg	0	0	0	0	0	0	0	0	0	0	0	0	0	0	0	0	0	0	0	0	0	0	0	0	0	0	0	0	0
DEVsvDnozzle_Pos	0	0	0	0	0	0	0	0	0	0	0	0	0	0	0	0	0	0	0	0	0	0	0	0	0	0	0	0	0
DEVsvKfeed_Neg	0	0	0	0	0	0	0	0	0	0	0	0	0	0	0	0	0	0	0	0	0	1	1	1	1	0	0	0	0
DEVsvKineFric_Pos	0	0	0	0	0	0	0	0	0	0	0	0	0	0	0	0	0	0	1	1	0	1	1	1	1	0	0	0	1
DEVsvStic1_Pos	0	0	0	0	0	0	0	0	0	0	0	0	0	0	0	0	0	0	0	0	0	0	0	0	0	0	0	0	0
DEVsvStic2_Pos	0	0	0	0	0	0	0	0	0	0	0	0	0	0	0	0	0	0	0	0	0	0	0	0	0	0	0	0	0
DEVsvSticspool_Pos	0	0	0	0	0	0	0	0	0	0	0	0	0	0	0	0	0	1	0	1	0	1	0	1	1	1	0	1	0
DEVsvVisc1_Pos	0	0	0	0	0	0	0	0	0	0	0	0	0	0	0	0	0	0	0	0	0	0	0	0	0	0	0	0	0
DEVsvVisc2_Pos	0	0	0	0	0	0	0	0	0	0	0	0	0	0	0	0	0	0	0	0	0	0	0	0	0	0	0	0	0
DEWfmASenO_Neg	0	0	0	0	0	0	0	0	0	0	0	1	0	0	1	1	1	0	0	0	0	0	0	0	0	0	0	0	0
DEWfmASenO_Pos	0	0	0	0	0	0	0	0	0	0	0	1	0	1	0	1	1	0	0	0	0	0	0	0	0	0	0	0	0
DEWfmBSenO_Neg	0	0	0	0	0	0	0	0	0	0	0	0	1	1	0	1	1	0	0	0	0	0	0	0	0	0	0	0	0
DEWfmBSenO_Pos	0	0	0	0	0	0	0	0	0	0	0	0	1	0	1	1	1	0	0	0	0	0	0	0	0	0	0	0	0
DFmvDIlkg_Pos	1	0	0	0	0	0	0	0	0	1	1	0	0	0	0	0	0	0	0	0	0	0	0	0	0	0	0	0	0
DLppDIlkg_Pos	0	0	0	0	0	0	0	0	0	0	0	0	0	0	0	0	0	0	0	0	0	0	0	0	0	0	0	0	0
DMfpDIlkg_Pos	1	0	0	0	0	0	0	0	0	0	0	0	0	0	0	0	0	0	0	0	0	0	0	0	0	0	0	0	0
DSovDelay_Pos	0	0	0	1	0	0	0	0	0	0	0	0	0	0	0	0	0	0	0	0	0	0	0	0	0	0	0	0	0
DSovDIlkg_Pos	1	0	0	1	1	0	0	0	0	0	0	0	0	0	0	0	0	0	0	0	0	0	0	0	0	1	0	0	0
DTbvDIlkg_Pos	0	0	0	0	0	0	0	0	0	0	0	0	0	0	0	0	0	0	0	0	0	0	0	0	0	0	0	0	0
TOTAL	7	1	1	2	1	1	2	1	1	7	7	2	2	3	2	4	4	5	3	4	1	3	2	5	5	4	0	5	3

	VsvYnullB	VsvXoverlapB	VsvYoverlapB	VsvScaleB	VsvSlpLeftB	VsvSlpNullB	VsvSlpRightB	VsvHyst0B	VsvCEquS	VsvXnullS	VsvYnullS	VsvXoverlapS	VsvYoverlapS	VsvScaleS	VsvSlpLeftS	VsvSlpNullS	VsvSlpRightS	VsvHyst0S	VsvmaxX1	VsvmaxX2	VsvminX1	VsvminX2	VsvmaxGapX	VsvminGapX	VsvmeanGapX	VsvstdGapX	VsvMAErr	VbvCEquA	VbvXchgA
DBvvDIlkg_Pos	0	0	0	1	0	0	1	0	0	0	0	0	0	0	0	0	0	0	0	0	0	0	0	0	0	0	0	0	0
DEBvvK0_Neg	0	0	0	0	0	0	0	0	0	0	0	0	0	1	0	0	0	0	0	0	0	0	0	0	0	0	0	0	0
DEBvvStic_Pos	0	0	0	0	0	0	0	0	0	0	0	0	0	0	0	0	0	0	0	0	0	0	0	0	0	0	0	0	0
DEBvvVisc_Pos	0	0	0	0	0	0	0	0	0	0	0	0	0	0	0	0	0	0	0	0	0	0	0	0	0	0	0	0	0
DEFmvASenO_Neg	0	0	0	0	0	0	0	0	0	0	0	0	0	0	0	0	0	0	0	0	0	0	0	0	0	0	0	0	0
DEFmvASenO_Pos	0	0	0	0	0	0	0	0	0	0	0	0	0	0	0	0	0	0	0	0	0	0	0	0	0	0	0	0	0
DEFmvBSenO_Neg	0	0	0	0	0	0	0	0	0	0	0	0	0	0	0	0	0	0	0	0	0	0	0	0	0	0	0	0	0
DEFmvBSenO_Pos	0	0	0	0	0	0	0	0	0	0	0	0	0	0	0	0	0	0	0	0	0	0	0	0	0	0	0	0	0
DEFmvCnull_Neg	0	0	0	0	0	0	0	0	0	0	0	0	0	0	0	0	0	0	0	0	0	0	0	0	0	0	0	0	0
DEFmvCnull_Pos	0	0	0	0	0	0	0	0	0	0	0	0	0	0	0	0	0	0	0	0	0	0	0	0	0	0	0	0	0
DEFmvDnozzle_Pos	0	0	0	0	0	0	0	0	0	0	0	0	0	0	0	0	0	0	0	0	0	0	0	0	0	0	0	0	0
DEFmvStic_Pos	0	0	0	0	0	0	0	0	0	0	0	0	0	0	0	0	0	0	0	0	0	0	0	0	0	0	0	0	0
DEMffFlowRate_Neg	0	0	0	0	0	0	0	0	0	0	0	0	0	0	0	0	0	0	0	0	0	0	0	0	0	0	0	0	0
DESovStic_Pos	0	0	0	0	0	0	0	0	0	0	0	0	0	0	0	0	0	0	0	0	0	0	0	0	0	0	0	0	0
DESovVisc_Pos	0	0	0	0	0	0	0	0	0	0	0	0	0	0	0	0	0	0	0	0	0	0	0	0	0	0	0	0	0
DEVbvASenO_Neg	0	0	0	0	0	0	0	0	0	0	0	0	0	0	0	0	0	0	0	0	0	0	0	0	0	0	0	0	0
DEVbvASenO_Pos	0	0	0	0	0	0	0	0	0	0	0	0	0	0	0	0	0	0	0	0	0	0	0	0	0	0	0	0	0
DEVbvBSenO_Neg	0	0	0	0	0	0	0	0	0	0	0	0	0	0	0	0	0	0	0	0	0	0	0	0	0	0	0	0	0
DEVbvBSenO_Pos	0	0	0	0	0	0	0	0	0	0	0	0	0	0	0	0	0	0	0	0	0	0	0	0	0	0	0	0	0
DEVbvCnull_Neg	0	0	0	0	0	0	0	0	0	0	0	0	0	0	0	0	0	0	0	0	0	0	0	0	0	0	0	1	1
DEVbvCnull_Pos	0	0	0	0	0	0	0	0	0	0	0	0	0	0	0	0	0	0	0	0	0	0	0	0	0	0	0	1	1
DEVbvCorHP1_Pos	0	0	0	0	0	0	0	0	0	0	0	0	0	0	0	0	0	0	0	0	0	0	0	0	0	0	0	0	0
DEVbvCorHP2_Pos	0	0	0	0	0	0	0	0	0	0	0	0	0	0	0	0	0	0	0	0	0	0	0	0	0	0	0	0	0
DEVbvDCool1_Neg	0	0	0	0	0	0	0	0	0	0	0	0	0	0	0	0	0	0	0	0	0	0	0	0	0	0	0	0	0
DEVbvDCool1_Pos	0	0	0	0	0	0	0	0	0	0	0	0	0	0	0	0	0	0	0	0	0	0	0	0	0	0	0	0	0
DEVbvDCool2_Neg	0	0	0	0	0	0	0	0	0	0	0	0	0	0	0	0	0	0	0	0	0	0	0	0	0	0	0	1	0
DEVbvDCool2_Pos	0	0	0	0	0	0	0	0	0	0	0	0	0	0	0	0	0	0	0	0	0	0	0	0	0	0	0	1	1
DEVbvDFilter1_Neg	0	0	0	0	0	0	0	0	0	0	0	0	0	0	0	0	0	0	0	0	0	0	0	0	0	0	0	0	0
DEVbvDFilter2_Neg	0	0	0	0	0	0	0	0	0	0	0	0	0	0	0	0	0	0	0	0	0	0	0	0	0	0	0	0	0
DEVbvDnozzle_Neg	0	0	0	0	0	0	0	0	0	0	0	0	0	0	0	0	0	0	0	0	0	0	0	0	0	0	0	0	0
DEVbvDnozzle_Pos	0	0	0	0	0	0	0	0	0	0	0	0	0	0	0	0	0	0	0	0	0	0	0	0	0	0	0	0	0
DEVbvKfeed_Neg	0	0	0	0	0	0	0	0	0	0	0	0	0	0	0	0	0	0	0	0	0	0	0	0	0	0	0	0	0
DEVbvKineFric_Pos	0	0	0	0	0	0	0	0	0	0	0	0	0	0	0	0	0	0	0	0	0	0	0	0	0	0	0	0	0
DEVbvStic1_Pos	0	0	0	0	0	0	0	0	0	0	0	0	0	0	0	0	0	0	0	0	0	0	0	0	0	0	0	0	0
DEVbvStic2_Pos	0	0	0	0	0	0	0	0	0	0	0	0	0	0	0	0	0	0	0	0	0	0	0	0	0	0	0	0	0
DEVbvSticspool_Pos	0	0	0	0	0	0	0	0	0	0	0	0	0	0	0	0	0	0	0	0	0	0	0	0	0	0	0	1	0
DEVbvVisc1_Pos	0	0	0	0	0	0	0	0	0	0	0	0	0	0	0	0	0	0	0	0	0	0	0	0	0	0	0	0	0
DEVbvVisc2_Pos	0	0	0	0	0	0	0	0	0	0	0	0	0	0	0	0	0	0	0	0	0	0	0	0	0	0	0	0	0
DEVsvASenO_Neg	0	0	0	0	0	0	0	0	0	0	0	0	0	0	0	0	0	0	0	0	1	1	0	1	1	1	0	0	0
DEVsvASenO_Pos	0	0	0	0	0	0	0	0	0	0	0	0	0	0	0	0	0	0	1	0	1	1	1	1	1	1	0	0	0
DEVsvBSenO_Neg	0	0	0	0	0	0	0	0	0	0	0	0	0	0	0	0	0	0	0	0	1	1	1	1	1	1	0	0	0
DEVsvBSenO_Pos	0	0	0	0	0	0	0	0	0	0	0	0	0	0	0	0	0	0	0	1	1	1	0	1	1	1	0	0	0
DEVsvCnull_Neg	0	1	1	0	0	0	0	0	1	1	0	0	0	0	0	0	0	0	0	0	0	0	0	0	0	0	0	0	0
DEVsvCnull_Pos	0	0	0	0	0	0	0	0	1	1	0	0	0	0	0	0	0	0	0	0	0	0	0	0	0	0	0	0	0
DEVsvCorHP1_Pos	0	0	0	0	0	0	0	0	0	0	0	0	0	0	0	0	0	0	0	0	0	0	0	0	0	0	0	0	0
DEVsvCorHP2_Pos	0	0	0	0	0	0	0	0	0	0	0	0	0	0	0	0	0	0	0	0	0	0	0	0	0	0	0	0	0
DEVsvDCool1_Neg	0	0	0	0	0	0	0	0	0	0	0	0	0	0	0	0	0	0	0	0	0	0	0	0	0	0	0	0	0
DEVsvDCool1_Pos	0	0	0	0	0	0	0	0	0	0	0	0	0	0	0	0	0	0	0	0	0	0	0	0	0	0	0	0	0
DEVsvDCool2_Neg	1	0	0	0	0	1	0	0	1	0	0	0	0	0	0	0	0	0	0	0	0	0	0	0	0	0	0	0	0
DEVsvDCool2_Pos	1	1	0	1	1	1	0	1	1	0	0	0	0	1	0	0	0	0	0	0	0	0	0	0	0	0	0	0	0
DEVsvDFilter1_Neg	0	0	0	0	0	0	0	0	0	0	0	0	0	0	0	0	0	0	0	0	0	0	0	0	0	0	0	0	0
DEVsvDFilter2_Neg	0	0	0	0	0	0	0	0	0	0	0	0	0	0	0	0	0	0	0	0	0	0	0	0	0	0	0	0	0
DEVsvDnozzle_Neg	0	0	0	0	0	0	0	0	0	0	0	0	0	0	0	0	0	0	0	0	0	0	0	0	0	0	0	0	0
DEVsvDnozzle_Pos	0	0	0	0	0	0	0	0	0	0	0	0	0	0	0	0	0	0	0	0	0	0	0	0	0	0	0	0	0
DEVsvKfeed_Neg	0	0	0	1	1	1	1	0	0	0	0	0	0	0	0	0	1	1	0	0	0	0	0	0	0	0	0	0	0
DEVsvKineFric_Pos	1	0	1	1	1	1	1	0	0	0	0	0	0	1	0	1	1	0	0	0	0	0	0	0	0	0	0	0	0
DEVsvStic1_Pos	0	0	0	0	0	0	0	0	0	0	0	0	0	0	0	0	0	0	0	0	0	0	0	0	0	0	0	0	0
DEVsvStic2_Pos	0	0	0	0	0	0	0	0	0	0	0	0	0	0	0	0	0	0	0	0	0	0	0	0	0	0	0	0	0
DEVsvSticspool_Pos	1	0	1	0	1	1	1	1	1	0	1	0	0	0	0	0	1	1	0	0	1	0	0	0	0	0	0	0	0
DEVsvVisc1_Pos	0	0	0	0	0	0	0	0	0	0	0	0	0	0	0	0	0	0	0	0	0	0	0	0	0	0	0	0	0
DEVsvVisc2_Pos	0	0	0	0	0	0	0	0	0	0	0	0	0	0	0	0	0	0	0	0	0	0	0	0	0	0	0	0	0
DEWfmASenO_Neg	0	0	0	0	0	0	0	0	0	0	0	0	0	0	0	0	0	0	0	0	0	0	0	0	0	0	0	0	0
DEWfmASenO_Pos	0	0	0	0	0	0	0	0	0	0	0	0	0	0	0	0	0	0	0	0	0	0	0	0	0	0	0	0	0
DEWfmBSenO_Neg	0	0	0	0	0	0	0	0	0	0	0	0	0	0	0	0	0	0	0	0	0	0	0	0	0	0	0	0	0
DEWfmBSenO_Pos	0	0	0	0	0	0	0	0	0	0	0	0	0	0	0	0	0	0	0	0	0	0	0	0	0	0	0	0	0
DFmvDIlkg_Pos	0	0	0	0	0	0	0	0	0	0	0	0	0	0	0	0	0	0	0	0	0	0	0	0	0	0	0	0	0
DLpvDIlkg_Pos	0	0	0	0	0	0	0	0	0	0	0	0	0	0	0	0	0	0	0	0	0	0	0	0	0	0	0	0	0
DMfpDIlkg_Pos	0	0	0	0	0	0	0	0	0	0	0	0	0	0	0	0	0	0	0	0	0	0	0	0	0	0	0	0	0
DSovDelay_Pos	0	0	0	0	0	0	0	0	0	0	0	0	0	0	0	0	0	0	0	0	0	0	0	0	0	0	0	0	0
DSovDIlkg_Pos	0	0	0	0	0	0	1	0	0	0	0	0	0	0	0	0	0	0	0	0	0	0	0	0	0	0	0	0	1
DTbvDIlkg_Pos	0	0	0	0	0	0	0	0	0	0	0	0	0	0	0	0	0	0	0	0	0	0	0	0	0	0	0	0	0
TOTAL	4	2	3	4	4	5	5	2	5	2	1	0	0	3	0	1	3	2	1	1	5	4	2	4	4	4	0	5	4

	VbvVchgA	VbvScaleA	VbvSlpLeftA	VbvSlpRightA	VbvHystOA	VbvCEquB	VbvXchgB	VbvVchgB	VbvScaleB	VbvSlpLeftB	VbvSlpRightB	VbvHystOB	VbvCEquS	VbvXchgS	VbvVchgS	VbvScaleS	VbvSlpLeftS	VbvSlpRightS	VbvHystOS	VbvmaxX1	VbvmaxX2	VbvminX1	VbvminX2	VbvmaxGapX	VbvminGapX	VbvmeanGapX	VbvstdGapX	VbvMAErr	VoN2maxTBV	TOTAL
DBvvDIlkg_Pos	1	0	0	0	0	0	0	1	1	1	0	0	0	0	0	0	0	0	0	0	0	0	0	0	0	0	0	0	0	14
DEBvvK0_Neg	0	0	0	0	0	0	0	0	0	0	0	0	0	0	0	0	0	0	0	0	0	0	0	0	0	0	0	0	0	5
DEBvvStic_Pos	0	0	0	0	0	0	0	0	0	0	0	0	0	0	0	0	0	0	0	0	0	0	0	0	0	0	0	0	1	2
DEBvvVisc_Pos	0	0	0	0	0	0	0	0	0	0	0	0	0	0	0	0	0	0	0	0	0	0	0	0	0	0	0	0	0	0
DEFmvASenO_Neg	0	0	0	0	0	0	0	0	0	0	0	0	0	0	0	0	0	0	0	0	0	0	0	0	0	0	0	0	0	5
DEFmvASenO_Pos	0	0	0	0	0	0	0	0	0	0	0	0	0	0	0	0	0	0	0	0	0	0	0	0	0	0	0	0	0	11
DEFmvBSenO_Neg	0	0	0	0	0	0	0	0	0	0	0	0	0	0	0	0	0	0	0	0	0	0	0	0	0	0	0	0	0	5
DEFmvBSenO_Pos	0	0	0	0	0	0	0	0	0	0	0	0	0	0	0	0	0	0	0	0	0	0	0	0	0	0	0	0	0	12
DEFmvCnull_Neg	0	0	0	0	0	0	0	0	0	0	0	0	0	0	0	0	0	0	0	0	0	0	0	0	0	0	0	0	0	6
DEFmvCnull_Pos	0	0	0	0	0	0	0	0	0	0	0	0	0	0	0	0	0	0	0	0	0	0	0	0	0	0	0	0	0	9
DEFmvDnozzle_Pos	0	0	0	0	0	0	0	0	0	0	0	0	0	0	0	0	0	0	0	0	0	0	0	0	0	0	0	0	0	4
DEFmvStic_Pos	0	0	0	0	0	0	0	0	0	0	0	0	0	0	0	0	0	0	0	0	0	0	0	0	0	0	0	0	0	8
DEMffFlowRate_Neg	0	0	0	0	0	0	0	0	0	0	0	0	0	0	0	0	0	0	0	0	0	0	0	0	0	0	0	0	0	4
DESovStic_Pos	0	0	0	0	0	0	0	0	0	0	0	0	0	0	0	0	0	0	0	0	0	0	0	0	0	0	0	0	0	1
DESovVisc_Pos	0	0	0	0	0	0	0	0	0	0	0	0	0	0	0	0	0	0	0	0	0	0	0	0	0	0	0	0	0	0
DEVbvASenO_Neg	0	0	0	0	0	0	0	0	0	0	0	0	0	0	0	0	0	0	0	0	0	1	0	1	1	1	1	0	0	5
DEVbvASenO_Pos	0	0	0	0	1	0	0	0	0	0	0	1	0	0	0	0	0	0	1	1	0	1	0	1	1	1	1	1	0	10
DEVbvBSenO_Neg	0	0	0	0	0	0	0	0	0	0	0	0	0	0	0	0	0	0	0	0	0	1	1	1	1	1	1	0	0	5
DEVbvBSenO_Pos	0	0	0	0	1	0	0	0	0	0	0	1	0	0	0	0	0	0	1	0	1	0	1	1	1	1	1	1	0	10
DEVbvCnull_Neg	0	0	0	0	0	1	1	0	0	0	0	0	1	1	0	0	0	0	0	0	0	0	0	0	0	0	0	0	0	6
DEVbvCnull_Pos	0	0	0	0	0	1	1	0	0	0	0	0	1	1	0	0	0	0	0	0	0	0	0	0	0	0	0	0	0	6
DEVbvCorHP1_Pos	0	0	0	0	0	0	0	0	0	0	0	0	0	0	0	0	0	0	0	0	0	0	0	0	0	0	0	0	0	0
DEVbvCorHP2_Pos	0	0	0	0	0	0	0	0	0	0	0	0	0	0	0	0	0	0	0	0	0	0	0	0	0	0	0	0	0	0
DEVbvDCool1_Neg	0	0	0	0	0	0	0	0	0	0	0	0	0	0	0	0	0	0	0	0	0	0	0	0	0	0	0	0	0	0
DEVbvDCool1_Pos	0	0	0	0	0	0	0	0	0	0	0	0	0	0	0	0	0	0	0	0	0	0	0	0	0	0	0	0	0	0
DEVbvDCool2_Neg	0	0	0	0	0	1	0	0	0	0	0	0	1	1	1	0	0	0	0	0	0	0	0	0	0	0	0	0	0	5
DEVbvDCool2_Pos	0	0	0	0	0	1	1	0	1	1	0	0	1	1	0	1	1	0	0	0	0	0	0	0	0	0	0	0	0	10
DEVbvDFilter1_Neg	0	0	0	0	0	0	0	0	0	0	0	0	0	0	0	0	0	0	0	0	0	0	0	0	0	0	0	0	0	0
DEVbvDFilter2_Neg	0	0	0	0	0	0	0	0	0	0	0	0	0	0	0	0	0	0	0	0	0	0	0	0	0	0	0	0	0	0
DEVbvDnozzle_Neg	0	0	0	0	0	0	0	0	0	0	0	0	1	0	0	0	0	0	0	0	0	0	0	0	0	0	0	0	0	1
DEVbvDnozzle_Pos	0	0	0	0	0	0	0	0	0	0	0	0	0	0	0	0	0	0	0	0	0	0	0	0	0	0	0	0	0	0
DEVbvKfeed_Neg	0	0	0	0	0	0	0	0	0	0	0	0	1	0	0	0	0	0	0	0	0	0	0	0	0	0	0	0	0	1
DEVbvKineFric_Pos	0	0	0	0	0	0	0	0	0	0	0	0	0	0	0	0	0	0	0	0	0	0	0	0	0	0	0	0	1	3
DEVbvStic1_Pos	0	0	0	0	0	0	0	0	0	0	0	0	0	0	0	0	0	0	0	0	0	0	0	0	0	0	0	0	0	0
DEVbvStic2_Pos	0	0	0	0	0	0	0	0	0	0	0	0	0	0	0	0	0	0	0	0	0	0	0	0	0	0	0	0	0	0
DEVbvSticspool_Pos	0	0	0	0	1	1	0	1	1	0	0	1	1	0	1	1	1	0	0	0	0	0	0	0	0	0	0	0	0	10
DEVbvVisc1_Pos	0	0	0	0	0	0	0	0	0	0	0	0	0	0	0	0	0	0	0	0	0	0	0	0	0	0	0	0	0	0
DEVbvVisc2_Pos	0	0	0	0	0	0	0	0	0	0	0	0	0	0	0	0	0	0	0	0	0	0	0	0	0	0	0	0	0	0
DEVsvASenO_Neg	0	0	0	0	0	0	0	0	0	0	0	0	0	0	0	0	0	0	0	0	0	0	0	0	0	0	0	0	0	5
DEVsvASenO_Pos	0	0	0	0	0	0	0	0	0	0	0	0	0	0	0	0	0	0	0	0	0	0	0	0	0	0	0	0	0	8
DEVsvBSenO_Neg	0	0	0	0	0	0	0	0	0	0	0	0	0	0	0	0	0	0	0	0	0	0	0	0	0	0	0	0	0	6
DEVsvBSenO_Pos	0	0	0	0	0	0	0	0	0	0	0	0	0	0	0	0	0	0	0	0	0	0	0	0	0	0	0	0	0	7
DEVsvCnull_Neg	0	0	0	0	0	0	0	0	0	0	0	0	0	0	0	0	0	0	0	0	0	0	0	0	0	0	0	0	0	11
DEVsvCnull_Pos	0	0	0	0	0	0	0	0	0	0	0	0	0	0	0	0	0	0	0	0	0	0	0	0	0	0	0	0	0	6
DEVsvCorHP1_Pos	0	0	0	0	0	0	0	0	0	0	0	0	0	0	0	0	0	0	0	0	0	0	0	0	0	0	0	0	0	0
DEVsvCorHP2_Pos	0	0	0	0	0	0	0	0	0	0	0	0	0	0	0	0	0	0	0	0	0	0	0	0	0	0	0	0	0	0
DEVsvDCool1_Neg	0	0	0	0	0	0	0	0	0	0	0	0	0	0	0	0	0	0	0	0	0	0	0	0	0	0	0	0	0	0
DEVsvDCool1_Pos	0	0	0	0	0	0	0	0	0	0	0	0	0	0	0	0	0	0	0	0	0	0	0	0	0	0	0	0	0	0
DEVsvDCool2_Neg	0	0	0	0	0	0	0	0	0	0	0	0	0	0	0	0	0	0	0	0	0	0	0	0	0	0	0	0	0	8
DEVsvDCool2_Pos	0	0	0	0	0	0	0	0	0	0	0	0	0	0	0	0	0	0	0	0	0	0	0	0	0	0	0	0	0	13
DEVsvDFilter1_Neg	0	0	0	0	0	0	0	0	0	0	0	0	0	0	0	0	0	0	0	0	0	0	0	0	0	0	0	0	0	0
DEVsvDFilter2_Neg	0	0	0	0	0	0	0	0	0	0	0	0	0	0	0	0	0	0	0	0	0	0	0	0	0	0	0	0	0	0
DEVsvDnozzle_Neg	0	0	0	0	0	0	0	0	0	0	0	0	0	0	0	0	0	0	0	0	0	0	0	0	0	0	0	0	0	0
DEVsvDnozzle_Pos	0	0	0	0	0	0	0	0	0	0	0	0	0	0	0	0	0	0	0	0	0	0	0	0	0	0	0	0	0	0
DEVsvKfeed_Neg	0	0	0	0	0	0	0	0	0	0	0	0	0	0	0	0	0	0	0	0	0	0	0	0	0	0	0	0	0	10
DEVsvKineFric_Pos	0	0	0	0	0	0	0	0	0	0	0	0	0	0	0	0	0	0	0	0	0	0	0	0	0	0	0	0	0	16
DEVsvStic1_Pos	0	0	0	0	0	0	0	0	0	0	0	0	0	0	0	0	0	0	0	0	0	0	0	0	0	0	0	0	0	0
DEVsvStic2_Pos	0	0	0	0	0	0	0	0	0	0	0	0	0	0	0	0	0	0	0	0	0	0	0	0	0	0	0	0	0	0
DEVsvSticspool_Pos	0	0	0	0	0	0	0	0	0	0	0	0	0	0	0	0	0	0	0	0	0	0	0	0	0	0	0	0	0	18
DEVsvVisc1_Pos	0	0	0	0	0	0	0	0	0	0	0	0	0	0	0	0	0	0	0	0	0	0	0	0	0	0	0	0	0	0
DEVsvVisc2_Pos	0	0	0	0	0	0	0	0	0	0	0	0	0	0	0	0	0	0	0	0	0	0	0	0	0	0	0	0	0	0
DEWfmASenO_Neg	0	0	0	0	0	0	0	0	0	0	0	0	0	0	0	0	0	0	0	0	0	0	0	0	0	0	0	0	0	4
DEWfmASenO_Pos	0	0	0	0	0	0	0	0	0	0	0	0	0	0	0	0	0	0	0	0	0	0	0	0	0	0	0	0	0	4
DEWfmBSenO_Neg	0	0	0	0	0	0	0	0	0	0	0	0	0	0	0	0	0	0	0	0	0	0	0	0	0	0	0	0	0	4
DEWfmBSenO_Pos	0	0	0	0	0	0	0	0	0	0	0	0	0	0	0	0	0	0	0	0	0	0	0	0	0	0	0	0	0	4
DFmvDIlkg_Pos	0	0	0	0	0	0	0	0	0	0	0	0	0	0	0	0	0	0	0	0	0	0	0	0	0	0	0	0	0	16
DLpvDIlkg_Pos	0	0	0	0	0	0	0	0	0	0	0	0	0	0	0	0	0	0	0	0	0	0	0	0	0	0	0	0	0	0
DMfpDIlkg_Pos	0	0	0	0	0	0	0	0	0	0	0	0	0	0	0	0	0	0	0	0	0	0	0	0	0	0	0	0	0	2
DSovDelay_Pos	0	0	0	0	0	0	0	0	0	0	0	0	0	0	0	0	0	0	0	0	0	0	0	0	0	0	0	0	0	2
DSovDIlkg_Pos	0	0	0	0	0	0	0	0	0	0	0	0	0	0	1	0	1	0	0	0	0	0	0	0	0	0	0	0	1	11
DTbvDIlkg_Pos	0	0	0	0	0	0	0	0	0	0	0	0	0	0	0	0	0	0	0	0	0	0	0	0	0	0	0	0	0	0
TOTAL	1	0	0	0	3	5	3	2	3	2	0	3	5	6	3	2	3	0	2	1	1	2	2	4	4	4	4	2	3	

Table A.30 *Detection NKPIs for virtual HIs.*

Appendix XXXIX. Identification NKPIs for virtual HIs

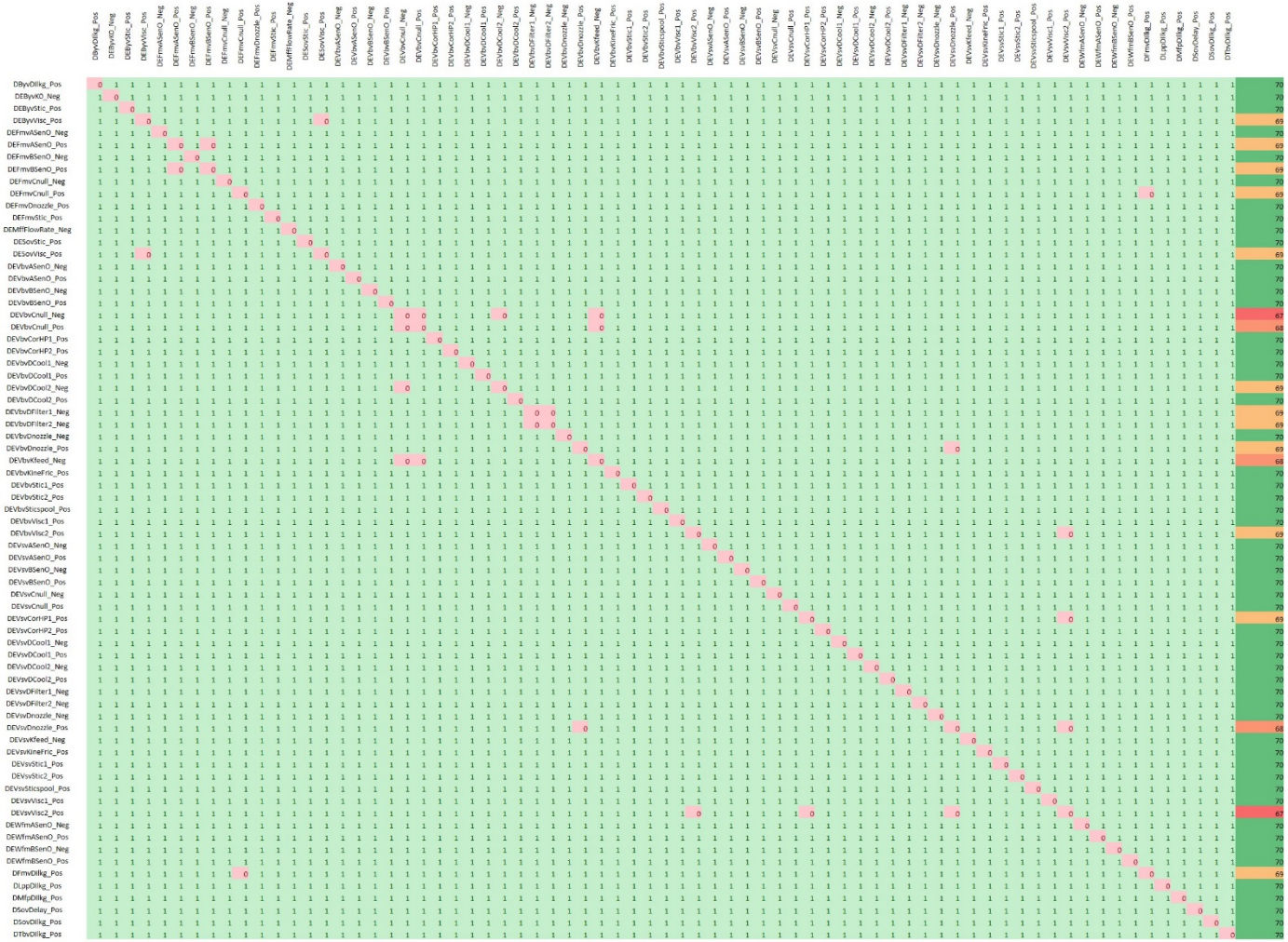


Table A.31 *Identification NKPIs for virtual HIs..*

Appendix XL. Localization NKPIs for virtual HIs

	Pumping Unit	Fuel Filter	ACU	FMU	VSV Actuation	VBV Actuation	TBV Actuation	Flowmeter	TOTAL
Pumping Unit	0	1	1	1	1	1	1	1	7
Fuel Filter	1	0	1	1	1	1	1	1	7
ACU	1	1	0	0	0	0	1	1	4
FMU	1	1	0	0	0	1	0	1	4
VSV Actuation	1	1	0	0	0	0	1	1	4
VBV Actuation	1	1	0	1	0	0	1	1	5
TBV Actuation	1	1	1	0	1	1	0	1	6
Flowmeter	1	1	1	1	1	1	1	0	7

Table A.32 *Localization NKPIs for virtual HIs.*

Appendix XLI. Prognostics NKPIs for virtual HIs

	DeltaD	DeltaI	DeltaL
DByvDIlkg_Pos	0	0	0
DEByvK0_Neg	149,333333	149,333333	116
DEByvStic_Pos	0	0	0
DEByvVisc_Pos	0	0	0
DEFmvASenO_Neg	0	0	0
DEFmvASenO_Pos	0,75617902	0,75617902	0
DEFmvBSenO_Neg	0	0	0
DEFmvBSenO_Pos	0,75617902	0,75617902	0
DEFmvCnull_Neg	12,2338009	12,2338009	0
DEFmvCnull_Pos	17,2338009	17,2338009	0
DEFmvDnozzle_Pos	0	0	0
DEFmvStic_Pos	23,9812959	0	0
DEMffFlowRate_Neg	76,7503333	76,7503333	0
DESovStic_Pos	0	0	0
DESovVisc_Pos	0	0	0
DEVbvASenO_Neg	0	0	0
DEVbvASenO_Pos	0,95524382	0,95524382	0
DEVbvBSenO_Neg	0	0	0
DEVbvBSenO_Pos	0,95524382	0,95524382	0
DEVbvCnull_Neg	8,43119572	8,43119572	0
DEVbvCnull_Pos	13,4311957	13,4311957	0
DEVbvCorHP1_Pos	0	0	0
DEVbvCorHP2_Pos	0	0,02155645	0
DEVbvDCool1_Neg	0	0	0
DEVbvDCool1_Pos	0	0	0
DEVbvDCool2_Neg	0	0	0
DEVbvDCool2_Pos	1,85404142	0	0
DEVbvDFilter1_Neg	0	4	0
DEVbvDFilter2_Neg	0	4	0
DEVbvDnozzle_Neg	0	0	0
DEVbvDnozzle_Pos	0	0	0
DEVbvKfeed_Neg	1,2	1,1	0
DEVbvKineFric_Pos	0	0	0
DEVbvStic1_Pos	0	0	0
DEVbvStic2_Pos	0	0	0
DEVbvSticspool_Pos	0	0	0
DEVbvVisc1_Pos	0	0	0
DEVbvVisc2_Pos	0	0	0
DEVsvASenO_Neg	0	0	0
DEVsvASenO_Pos	0	0	0
DEVsvBSenO_Neg	0	0	0
DEVsvBSenO_Pos	0	0	0
DEVsvCnull_Neg	7,97027388	7,97027388	0
DEVsvCnull_Pos	12,9702739	12,9702739	0
DEVsvCorHP1_Pos	0	0	0
DEVsvCorHP2_Pos	0	0	0
DEVsvDCool1_Neg	0	0	0
DEVsvDCool1_Pos	0	0	0
DEVsvDCool2_Neg	0	0	0
DEVsvDCool2_Pos	0	0	0
DEVsvDFilter1_Neg	0	4	0
DEVsvDFilter2_Neg	0	4	0
DEVsvDnozzle_Neg	0	0	0
DEVsvDnozzle_Pos	0	0	0
DEVsvKfeed_Neg	1,2	1,1	0
DEVsvKineFric_Pos	0	0	0
DEVsvStic1_Pos	0	0	0
DEVsvStic2_Pos	0	0	0
DEVsvSticspool_Pos	0	0	0
DEVsvVisc1_Pos	0	0	0
DEVsvVisc2_Pos	0	0	0
DEWfmASenO_Neg	0	0	0
DEWfmASenO_Pos	0	0	0
DEWfmBSenO_Neg	0	0	0
DEWfmBSenO_Pos	0	0	0
DFmvDIlkg_Pos	0,25417301	0,25417301	0
DLppDIlkg_Pos	0	0	0
DMfpDIlkg_Pos	0,35370541	0	0
DSovDelay_Pos	0	0	0
DSovDIlkg_Pos	0,07848831	0	0
DTbvDIlkg_Pos	0	0	0

Développement d'une approche intégrée de PHM – Prognostics and Health Management - : Application au Circuit Carburant d'un Turboréacteur

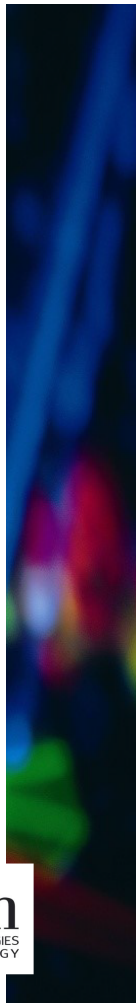
RESUME: Pour les constructeurs de moteurs d'avions comme Snecma, la disponibilité est un des enjeux clés de l'avenir. En effet, la limitation des retards et annulations de vols ainsi que la réduction de la fréquence et de la durée des opérations de maintenance pourrait entraîner des économies importantes. Pour accroître la disponibilité, l'outil le plus utilisé actuellement est le prognostics and health management (PHM). La première contribution de la thèse est de proposer des cadres terminologique et fonctionnel pour le développement du PHM adapté aux spécificités des moteurs d'avions. Par la suite, une approche intégrée basée sur le nouveau modèle en V3 est formalisée. La seconde contribution est un processus basé sur les modèles pour le développement de la partie embarquée chargée de l'extraction des indicateurs de santé. Elle est basée sur l'analyse de sensibilité, la régression par vecteurs supports et des nouveaux indicateurs de performances. Puisque ce processus est réalisé avant l'entrée en service, les données stochastiques sont obtenues par propagation d'incertitudes. Pour surmonter les temps de calcul liés aux évaluations du modèle, des métamodèles sont utilisés. Plus particulièrement, la troisième contribution de la thèse est une technique originale combinant régression par vecteurs supports et Krigeage. L'approche globale est finalement testée sur le système carburant d'un moteur d'avion. Les résultats sont prometteurs, tant au niveau industriel pour les précieuses informations qu'elle fournit sur la qualité du jeu d'indicateurs de santé qu'au niveau académique pour la précision apportée par la nouvelle approche du Krigeage-SVR.

Mots clés : Diagnostic, pronostic, PHM, processus de développement, validation, indicateurs de santé, régression par vecteurs supports, Krigeage, propagation d'incertitudes.

Development of an Integrated Approach for PHM - Prognostics and Health Management - : Application to a Turbofan Fuel System

ABSTRACT: For manufacturers of aircraft engines such as Snecma, the increase of systems availability is one of the key challenges of the future. Indeed, the limitation of delays and cancellations and the reduction of maintenance operations frequency and duration could lead to important costs savings. To improve availability, the most proven tool is currently prognostics and health management (PHM). The first contribution of this thesis work is to propose complete terminological and functional frameworks for the development of PHM adapted to the specific application on aircraft engines. Subsequently, an integrated development approach based on the original V3-model is formalized. The second contribution is an original model-based process for the development of the embedded extraction of health indicators, based on sensitivity analysis, support vector regression and original performance indicators for the validation. Since it is aimed at being performed before the entry into service, the stochastic data are issued from Monte-Carlo based uncertainty propagation. In order to overcome the prohibitive computation time of the model evaluations, surrogate models are used. More particularly, the third contribution of this thesis work is an original technique combining support vector regression with Kriging. The whole approach is finally tested on an aircraft engine fuel system. The results are promising, both at the industrial level with the release of valuable information about the quality of the health indicators set and at the academic level with the proven accuracy of the new SVR-Kriging approach.

Keywords : Diagnostics, prognostics, PHM, development process, validation, health indicators, support vector regression, Kriging, uncertainty propagation.



ARTS ET MÉTIERS ParisTech

ParisTech
INSTITUT DES SCIENCES ET TECHNOLOGIES
PARIS INSTITUTE OF TECHNOLOGY